Bahman Zohuri

Neutronic Analysis For Nuclear Reactor Systems

Springer

Neutronic Analysis For Nuclear Reactor Systems

Bahman Zohuri

Neutronic Analysis For Nuclear Reactor Systems

Springer

Bahman Zohuri
Galaxy Advanced Engineering, Inc.,
University of New Mexico
Albuquerque, NM, USA

ISBN 978-3-319-42962-5 ISBN 978-3-319-42964-9 (eBook)
DOI 10.1007/978-3-319-42964-9

Library of Congress Control Number: 2016948734

Printed on acid-free paper

This Springer imprint is published by Springer Nature
The registered company is Springer International Publishing AG
The registered company address is: Gewerbestrasse 11, 6330 Cham, Switzerland

This book is dedicated to my children,
Natasha, Natalie, and Sasha.

—Zohuri

Preface

This text develops the theory of nuclear reactors from the fundamentals of fission to the operating characteristics of modern reactors. It is aimed at a senior undergraduate or first year graduate student level. It is designed as a two-semester text with the first half emphasizing reactor criticality analysis and all of the physics that goes into modern calculations. It will start with simplified one-group diffusion theory models and extend into sophisticated multigroup transport theory models. Each chapter will have at least one example covering the issues discussed. Desktop calculations will be discussed and demonstrated in examples. A small one-dimensional computer code will be provided to demonstrate the models discussed. Resonance theory, thermal scattering, and heterogeneous effects will be discussed and characterized. Detailed data sets will be provided that will allow two-, three-, and four-group desktop calculations. Additional multigroup data sets will be provided with the computer disk.

The second half of the book will deal with the two main topics of interest to operating reactors—reactor kinetics/dynamics and in-core fuel management. Based on the fundamental physics discussed in the first half of the book, reactivity models will be developed using realistic reactor cross-sectional data and modern analytic tools. Adjoint methods will be explained in detail. Perturbation theory will be used extensively to quantify reactivity effects. Both linear and nonlinear reactor kinetic feedback models are included. Control system models will be mainly based on linearization techniques. Fuel management analysis will be based on a linear reactivity model. Code modeling will be discussed and example problems included that can be addressed with desktop methods. The theory for extending fuel management calculations to modern large-scale computers will be discussed.

Some sections and chapters of the book reflect input from the lecture notes of Professor Emeritus William J. Garland, Department of Engineering Physics, McMaster University, Professor Hiroshi Sekimoto of Tokyo Institute of Technology, and Professor H. Van Dam of Delft University of Technology, as well as some of my own lectures and notes while consulting with the Department of Energy. Some of my lecture notes are from my class notes from when I was taking a related course as a graduate student at the University of Illinois and University of New Mexico.

Many thanks also go to Dr. Stanley Thompson of Oregon State University and his research notes on topics of “unstable nuclear power,” which was available on the Internet.

It is anticipated that the first half of the book will be useful to many professionals in the nuclear industry. The second half of the book should be of use to nuclear engineering professionals concerned with operating nuclear reactors.

Albuquerque, NM Bahman Zohuri

About This Document

This text covers the fundamentals of neutronic analysis for nuclear reactor system required to understand nuclear reactor theory. It then covers the application of these principles to nuclear reactor power systems. With this in mind, this book is written for students who are studying nuclear engineering for the first time.

This book could be pitched at the senior undergraduate level or first year graduate level. It is a two-semester book, to be divided by the start of time-dependent methods in Chap. 11. Both parts should stand on their own. Lecture notes and materials gathered from Professor McDaniel have been taught by him for over 30 years. The material will really build on books by Lamarsh, Henry, Hetrick, and Ott. I hope it will be useful to new students.

I hope that this textbook will stimulate the interest of students in nuclear reactor theory and help them to master the topic within a short period of time.

Acknowledgments

Author would like to thank the following individual for providing their generous information to him

Professor Patrick McDaniel's lecture notes given at the University of New Mexico, Nuclear Engineering Department.

Nuclear Reactor Theory book by Professor Hiroshi Sekimoto of Tokyo Institute of Technology.

Nuclear Reactor Physics lecture notes AP3341: Professor H. Van Dam of Delft University of Technology.

Professor Emeritus William J. Garland, Department of Engineering Physics, McMaster University, who provided me with some of his lectures and class notes and graciously gave me permission to use them in sections or chapters throughout this book where I saw it fit.

I also like to take this opportunity to thank Professor Emeritus Sidney Yip of Massachusetts Institute of Technology for his generous and rich class lectures that he provided me after participating in some of his lecture classes when he was actively teaching in the Nuclear Engineering Department of MIT.

Contents

16 Fuel Burnup and Fuel Management . . . 509

About the Author

Dr. Bahman Zohuri is currently at the Galaxy Advanced Engineering, Inc., a consulting company that he started himself in 1991 when he left both semiconductor and defense industries after many years working as a chief scientist. After graduating from the University of Illinois in the field of physics and applied mathematics, as well as the University of New Mexico from the Nuclear Engineering Department, he joined Westinghouse Electric Corporation where he performed thermal hydraulic analysis and natural circulation for inherent shutdown heat removal system (ISHRS). The study was performed for the core of a liquid metal fast breeder reactor (LMFBR) as a secondary fully inherent shut system for secondary loop heat exchange. All these designs were used for nuclear safety and reliability engineering for self-actuated shutdown system. He designed the mercury heat pipe and electromagnetic pumps for large pool concepts of LMFBR for heat rejection purpose for this reactor in around 1978 where he received a patent for it. He later on was transferred to the defense division of Westinghouse where he was responsible for the dynamic analysis and method of launch and handling of MX missile out of canister. The results are applied to MX launch seal performance and muzzle blast phenomena analysis (i.e., missile vibration and hydrodynamic shock formation). He also was involved in analytical calculation and computation in the study of nonlinear ion wave in rarefying plasma. The results are applied to the propagation of "soliton wave" and the resulting charge collector traces, in the rarefactions characteristic of the corona of the laser-irradiated target pellet. As part of his graduate research work at Argonne National Laboratory, he performed computation and programming of multi-exchange integral in surface physics and solid-state physics. He holds different patents in areas such as diffusion processes and design of diffusion furnace while he was senior process engineer working for different semiconductor industries such as Intel, Varian, and National Semiconductor corporations. Later on he joined Lockheed Missile and Aerospace Corporation as senior chief scientist and was responsible for research and development (R&D) and the study of vulnerability, survivability, and both radiation and laser hardening of different components of the Strategic Defense Initiative known as Star Wars.

This included of payload (i.e., IR sensor) for the Defense Support Program (DSP), Boost Surveillance and Tracking Satellite (BSTS), and Space Surveillance and Tracking Satellite (SSTS) against laser or nuclear threat. While in there, he also studied and performed the analysis of characteristics of laser beam and nuclear radiation interaction with materials, transient radiation effects in electronics (TREE), electromagnetic pulse (EMP), system-generated electromagnetic pulse (SGEMP), single-event upset (SEU), blast and thermomechanics, hardness assurance, maintenance, and device technology.

He did few years of consulting under his company Galaxy Advanced Engineering with Sandia National Laboratories (SNL), where he was supporting the development of operational hazard assessments for the Air Force Safety Center (AFSC) in connection with other interested parties. Intended use of the results was their eventual inclusion in Air Force Instructions (AFIs) specifically issued for directed energy weapon (DEW) operational safety. He completed the first version of a comprehensive library of detailed laser tools for Airborne Laser (ABL), Advanced Tactical Laser (ATL), Tactical High-Energy Laser (THEL), Mobile/Tactical High-Energy Laser (M-THEL), etc.

He also was responsible on SDI computer programs involved with Battle Management C^3 and artificial intelligence and autonomous system. He is the author of few publications and holds various patents such as laser-activated radioactive decay and results of thru-bulkhead initiation.

Recently, he has published two other books with CRC and Francis Taylor on the subject of:

1. *Heat Pipe Design and Technology: A Practical Approach*, published by CRC Publishing Company
2. *Dimensional Analysis and Self-Similarity Methods for Engineers and Scientists*, published by Springer Publishing Company
3. *High Energy Laser (HEL): Tomorrow's Weapon in Directed Energy Weapons Volume I*, published by Trafford Publishing Company
4. *Thermodynamics in Nuclear Power Plant Systems*, published by Springer Publishing Company
5. *Combined Cycle Driven Efficiency for Next Generation Nuclear Power Plants: An Innovative Design Approach 2015 Edition*
6. *Thermal-Hydraulic Analysis of Nuclear Reactors*, published by Springer Publishing Company
7. *Heat Pipe Design and Technology: Modern Applications for Practical Thermal Management*, Springer Publishing Company, 2nd Edition, April 28, 2016
8. *Compact Heat Exchangers: Selection, Application, Design and Evaluation*, Springer Publishing Company, April 20, 2016
9. *Directed Energy Weapons: Physics of High Energy Lasers*, Springer Publishing Company, June 20, 2016
10. *Application of Compact Heat Exchangers for Combined Cycle Driven Efficiency in Next Generation Nuclear Power Plants: A Novel Approach*, Springer Publishing Company, 2015
11. *Nuclear Energy for Hydrogen Generation through Intermediate Heat Exchangers: A Renewable Source of Energy*, Springer Publishing Company, 2016

Chapter 1
Neutron Physics Background

This chapter introduces fundamental properties of the neutron. It covers reactions induced by neutrons, nuclear fission, slowing down of neutrons in infinite media, diffusion theory, the few-group approximation, point kinetics, and fission product poisoning. It emphasizes the nuclear physics bases of reactor design and its relationship to reactor engineering problems.

1.1 Nuclei: Sizes, Composition, and Binding Energies

The diameters of atoms and molecules are of the order of 10^{-10}–10^{-9} m. On the other hand, the diameters of nuclei are small, of the order of 10^{-15}–10^{-14} m. The size of molecules is often measured in Å (angstrom, 1 Å = 10^{-10} m) and nm (1 nm = 10^{-9} m). On the other hand, the size of nuclei is often measured in fm (femtometer, 1 fm = 10^{-15} m). That is, the diameters of atoms and molecules are approximately 0.1–1 nm and the diameters of nuclei are approximately 1^{-10} fm.

Because of the uncertainty principle, a much higher energy is associated with a nucleus than with an atom or a molecule, as it is much smaller. Chemical reactions are measured in the unit of eV (where 1 eV is the energy acquired when a particle with one elementary electric charge is accelerated by a potential difference of 1 V in a vacuum). In contrast, the unit of MeV (1 MeV = 10^6 eV) is usually used for nuclear reactions.

An approximate, but rather more concrete, explanation is given by the following. The nth energy eigenvalue for a particle with mass m trapped inside a potential well of size L is given by the following equation:

$$E_n = N_n \frac{1}{2m}\left(\frac{\pi\hbar}{L}\right)^2 \tag{1.1}$$

B. Zohuri, *Neutronic Analysis For Nuclear Reactor Systems*,
DOI 10.1007/978-3-319-42964-9_1

Table 1.1 Masses of proton, neutron, and electron

Particle	Mass (kg)	Mass (amu)	$\mathrm{MeV/c^2}$
1 atomic mass unit	1.660540×10^{-27}	1.000	931.5016
Proton	1.672623×10^{-27}	1.007276	938.280
Neutron	1.674929×10^{-27}	1.008665	939.573
Electron	9.109390×10^{-31}	0.000549	0.511

Here, N_n is a constant determined by the quantum number n, and $\hbar = 6.582 \times 10^{-16}$ eV s is the value obtained by dividing Planck's constant by 2π. We let $n = 1$ and use the mass of a nucleon and the mass of an electron shown in Table 1.1. For an electron, $(1/2m)(\pi\hbar/L)^2 = 3.8 \times 10^{-15}$ eV if $L = 1$ cm, giving a very small value. For an atom of size 0.1–1 nm, the energy is 38–0.38 eV. In the case of a proton, the energy is 200–2 MeV for a nucleus of size 1^{-10} fm.

The mass of a proton is approximately the same as that of a neutron, whereas the mass of an electron is much smaller than that of a proton or neutron. As a unit for measuring the mass of an atom (the atomic weight), the value obtained by dividing the mass of an atom with its mass number is convenient (this is called the "atomic mass unit" with symbol "amu" or "u"). However, the sum of the masses of a proton and an electron is different from the mass of a neutron.

In addition, when nucleons are bound, the mass will generally decrease from the sum of the masses of the original nucleons (this will be explained later). Thus, it is necessary to use a specific standard nuclide to determine the atomic mass unit. Various nuclides have been proposed for this standard, but from 1962, international consensus has been to use the atomic weight of ${}^{12}_{6}\mathrm{C}$ divided by 12 to obtain the standard 1 amu. The masses of the proton, neutron, and electron using this atomic mass unit are shown in Table 1.1. They are also shown in the unit of $\mathrm{MeV/c^2}$, which will be explained later.

In a nucleus, nucleons are attracted to each other by the nuclear force. Nucleons in such a field try to take as low an energy state as possible. That is, when separate nucleons are combined together, the lowest energy state is taken and the excess energy is released. This energy is called the binding energy. The relationship between the energy E and mass M is the following, derived from Einstein's famous relativity theory with c being speed of light:

$$E = mc^2 \tag{1.2}$$

Equation 1.2 can be used to prove that a mass of 1 amu is equivalent to an energy of 931.5016 MeV.

Something should strike you as strange about Table 1.1. The carbon-12 atom has a mass of 12.000 u, and yet it contains 12 objects (six protons and six neutrons) that each has a mass greater than 1.000 u, not to mention a small contribution from the six electrons.

This is true for all nuclei, that the mass of the nucleus is a little less than the mass of the individual neutrons, protons, and electrons. This missing mass is known as the mass defect and represents the binding energy of the nucleus.

The binding energy is the energy you would need to put in to split the nucleus into individual protons and neutrons. To find the binding energy, add the masses of the individual protons, neutrons, and electrons, subtract the mass of the atom, and convert that mass difference to energy. For carbon-12, this gives

$$\begin{aligned}\text{Mass defect} = \Delta m &= 6{*}1.008664\,\text{u} + 6{*}1.007276\,\text{u} + 6{*}0.00054858\,\text{u} - 12.000\,\text{u}\\ &= 0.098931\,\text{u}\end{aligned}$$

The binding energy in the carbon-12 atom is therefore 0.098931 u * 931.5 MeV/u = 92.15 MeV.

In a typical nucleus the binding energy is measured in MeV, considerably larger than the few eV associated with the binding energy of electrons in the atom. Nuclear reactions involve changes in the nuclear binding energy, which is why nuclear reactions give you much more energy than chemical reactions; those involve changes in electron binding energies.

However, the mass of the atom is smaller than the sum of the masses of nucleons and electrons that constitute the atom. This difference in mass is called the mass defect, $D(Z, N)$ for a nuclide with atomic number Z and neutron number N. For the mass of a hydrogen atom m_{H} and the mass of a neutron m_{N}, the mass of a neutral atom is expressed as follows:

The binding energy can be expressed as follows using Eq. 1.1:

$$B(Z, N) = D(Z, N)c^2 \tag{1.3}$$

The binding energy is equivalent to the mass defect, with the binding energy used when energy is being considered and the mass defect used when mass is being considered. The unit MeV is often used for the energy of nuclear reactions, with mass and energy converted according to the following relationship:

$$1\,\text{amu} = 931.5016\,\text{MeV}/\text{c}^2 \tag{1.4}$$

A term similar to the mass defect is the mass deviation (or mass excess), defined as the difference $M - A$, for M the mass in atomic mass units and A the mass number, which is an integer. It is important to clearly distinguish these terms. Different nuclei have different mass defects. Accordingly, energy is absorbed or released during a nuclear reaction. In addition, it is possible to determine the possibility of a certain reaction occurring by the size of the mass defect. Thus, it is very important to know the mass defect of a nuclide. In this section we are concerned with the state with the lowest internal energy of the nucleus. This state is called the ground state. States with higher internal energy are called excited states.

Bear in mind that in general, species of atoms and nuclei are called elements and nuclides, respectively. An element is determined by its proton number (the number of protons). The proton number is generally called the atomic number and is denoted by Z. A nuclide is determined by both the proton number and the neutron number (the number of neutrons denoted by N). The sum of the proton number and neutron number, namely, the nucleon number, is called the mass number and is denoted by $A(A = Z + N)$. Obviously, a nuclide can also be determined by the atomic number and mass number.

In order to identify a nuclide, A and Z are usually added on the left side of the atomic symbol as superscript and subscript, respectively. For example, there are two representative nuclides for uranium, described as ${}^{235}_{92}\mathrm{U}$ and ${}^{238}_{92}\mathrm{U}$. If the atomic symbol is given, the atomic number can be uniquely determined; thus Z is often omitted like ${}^{235}\mathrm{U}$ and ${}^{238}\mathrm{U}$.

The chemical properties of an atom are determined by the atomic number, so even if the mass numbers of nuclei are different, if the atomic numbers are the same, their chemical properties are the same. These nuclides are called isotopic elements or isotopes. If the mass numbers are the same and the atomic numbers are different, they are called isobars. If the neutron numbers are the same, they are called isotones. The above examples for uranium are isotopes.

Summarizing these and rewriting the constitution of an atom, we obtain the following figure:

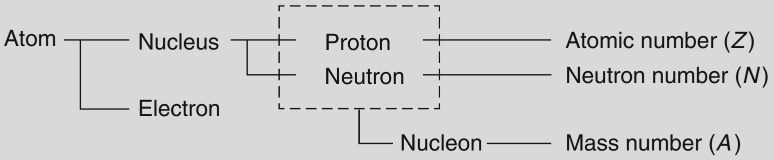

Constitution of an Atom

The most important force in the nucleus is the nuclear force. The nuclear force is a strong interaction, generated by the exchange of pions. The distance of interaction is very short, approximately 2 fm, and thus only neighboring nucleons interact with each other. Therefore, the contribution of the nuclear force to the mass defect is proportional to the mass number. For a_v, a suitable proportionality constant, the contribution is expressed as a_vA. If all the nucleons are surrounded by other nucleons, this expression is satisfactory. However, there are no nucleons outside the surface nucleons, and thus the binding energy is smaller to that extent. This is the so-called surface tension and is expressed as $a_sA^{2/3}$. The second important force in a nucleus is the Coulomb force.

Pion

In particle physics, a pion (short for **pi meson**, denoted with the Greek letter pi: p) is any of three subatomic particles: π^0, π^+, and π^-. Each pion consists of a quark and an antiquark and is therefore a meson. Pions are the lightest mesons and are unstable, with the charged pions π^+ and p-decaying with a mean lifetime of 26 ns (2.6×10^{-8} s) and the neutral pion π^0 decaying with a much shorter lifetime of 8.4×10^{-17} s. Charged pions usually decay into **muons** and **muon** neutrinos and neutral pions into gamma rays.

Note that muon (μ) is an elementary particle similar to the electron, with unitary negative electric charge of -1 and a spin of 1/2, but with a much greater mass (105.7 MeV/c^2) and the three neutrinos.

As is the case with other leptons, the muon is not believed to have any substructure—that is, it is not thought to be composed of any simpler particles.

Inside a nucleus, there are positive charges due to protons, but there are no negative charges. Therefore, a repulsive Coulomb force operates. This force exists among the protons. Its energy is obtained by dividing the product of the electric charges by the distance between them. In this case, the distance may be considered proportional to the size of the nucleus. If the volume of the nucleus is proportional to the mass number, the contribution of the Coulomb force to the mass defect is expressed as $a_c Z^2 A^{-1/3}$. If these were the only forces existing among nucleons, a nucleus containing only neutrons would have strong binding because of the absence of the Coulomb force. However, this is not consistent with experimental results. In reality, in a strongly bound nucleus, the proton number and the neutron number are similar. Thus, there is symmetry between protons and neutrons, and the closer the proton and neutron numbers, the more stable the nucleus is. Thus, the expression $-a_I(N-Z)^2A^{-1}$ is added to the mass defect. In addition to the above important terms, pairs of protons or of neutrons have a stabilizing property. Thus, when the proton number or the neutron number is even, the nucleus is more stable. This effect is expressed as $a_e\delta(Z,N)A^{-1/2}$, with the following function introduced:

$$\delta(Z,N) = \begin{cases} 1: & \rightarrow \text{If both } Z \text{ and } N \text{ are even} \\ 0: & \rightarrow \text{If both } A \text{ is odd} \\ -1 & \rightarrow \text{If both } Z \text{ and } N \text{ are odd} \end{cases} \tag{1.5}$$

Weizsacker and Bethe have proposed the following empirical mass formula by adding these terms together:

$$B(Z,N) = a_v A - a_s A^{/3} - a_c Z^2 A^{-1/3} - a_I (N-Z)^2 A^{-1} + a_e \delta(Z,N) A^{-1/2} \tag{1.6}$$

The terms on the right side are, from the left, the volume term, surface term, Coulomb term, symmetry term, and even–odd term. The coefficients are determined so that the mass defect is consistent with the experimentally determined masses. An example set of coefficients determined by P. E. Hodgson et al. [1] in 1997 is shown below:

$$
\begin{aligned}
a_{\mathrm{v}} &= 15.835\,\mathrm{MeV} \\
a_{\mathrm{s}} &= 18.33\,\mathrm{MeV} \\
a_{\mathrm{c}} &= 0.714\,\mathrm{MeV} \\
a_{\mathrm{I}} &= 23.20\,\mathrm{MeV} \\
a_{\mathrm{e}} &= 11.2\,\mathrm{MeV}
\end{aligned}
$$

This equation is simple, but it nicely reproduces the experimental data, with the errors for heavy nuclei less than 1 %. However, for a detailed analysis of nuclear reactions, more accurate values are often necessary. In that case, please consult reference in footnote.[1] The binding energy per nucleon and contribution of each term will be shown later in Fig. 1.5.

In the derivation of the mass formula, we notice that for suitable values of A and N, there may be a nuclide with the greatest binding energy per nucleon, that is, the most stable nuclide. In fact, 56Fe has the largest binding energy per nucleon of 8.55 MeV. When A and Z depart from the suitable values, the binding energy decreases and the nuclide becomes unstable. When the binding energy is negative, the nucleus cannot exist. However, even when the binding energy is positive, not all nuclides can exist. There are numerous cases where a nuclide will decay to another nuclide with a larger binding energy. However, the number of such decays is limited, and there are numerous nuclides in nature besides the most stable nuclides. This will be explained in a later section.

Nuclei with a neutron number N or proton number Z of 2, 8, 20, 28, 50, 82, or 126 are especially stable compared with nuclei with numbers in the vicinity. These numbers are called magic numbers. They will be shown on the chart of nuclides in Fig. 1.3.

Atom Density

One important property of a material is the atom density. The *atom density* is the number of atoms of a given type per unit volume of the material. To calculate the atom density of a substance, use the following equation:

$$N = \frac{\rho N_{\mathrm{A}}}{M}$$

where:

N = atom density (atoms/cm^3)
ρ = density (g/cm^3)
L_{A} = Avogadro's number (6.022×10^{23} atoms/mol)
M = gram atomic weight

---

[1] You can get the data from http://ie.lbl.gov/toimass.html

1.2 Decay of a Nucleus

Before we start talking about decay of a nucleus, we have to define a value known as Q-value, which in nuclear physics and chemistry counts for a reaction that is the amount of energy released by that reaction. The value relates to the enthalpy of a chemical reaction or the energy of radioactive decay products. It can be determined from the masses of reactants and products. Q-value affects reaction rates. By definition the energy conservation of the simple reaction enables the general definition of Q based on mass–energy equivalence as

$$Q = (m_{\mathrm{Initial}} - m_{\mathrm{Final}})c^2$$

A reaction with a positive Q-value is exothermic, i.e., has a net release of energy, since the kinetic energy of the final state is greater than the kinetic energy of the initial state. A reaction with a negative Q-value is endothermic, i.e., requires a net energy input, since the kinetic energy of the final state is less than the kinetic energy of the initial state.

Example 1.1 If in case of particle physics the Q-value is the kinetic energy released in the decay at rest. Calculate this value for neutron decay.

Solution For neutron decay, some mass disappears as neutrons convert to a proton, electron, and neutrino:

$$Q = \left(m_{\mathrm{n}} - m_{\mathrm{p}} - m_{\overline{\mathrm{v}}} - m_{\mathrm{e}}\right)c^2 = 0.782\,\mathrm{MeV}$$

In this example m_{n} is the mass of the neutron, m_{p} is the mass of the proton, $m_{\overline{\mathrm{v}}}$ is the mass of the electron antineutron, and m_{e} is the mass of the electron. In beta decay a typical Q-value is around 1 MeV.

Now getting back to the discussion of this section on the decay of a nucleus, we can briefly explain as follows. Typical decays are α-decay, β-decay, and γ-decay, which emit α-rays, β-rays, and γ-rays, respectively. An α-ray is a nucleus of 4He, a β-ray is an electron, and a γ-ray is a high-energy photon. In β-decay, a positron may be emitted, which is called β^+-decay. In order to distinguish the two cases, the ordinary decay in which an electron is emitted is sometimes called β^--decay. As a competitive process for β^+-decay, orbital electron capture occurs when a nucleus takes in an orbital electron. As a competitive process for γ-decay, internal conversion occurs, when an orbital electron is ejected, rather than a γ-ray being emitted. By α decay, Z and N both decrease by 2. By β^--decay, Z increases by 1 and N decreases by 1. By β^+-decay and orbital electron capture, Z decreases by 1 and N increases by 1. By γ-decay and the internal conversion, neither Z nor N change.

Some decays take place readily, while other decays rarely occur. The conservation laws for angular momentum, parity, etc. play a great role in this difference. However, we will omit a detailed explanation of this and will instead describe other important matters.

Fig. 1.1 Potential of the Coulomb repulsive force in nuclear decay

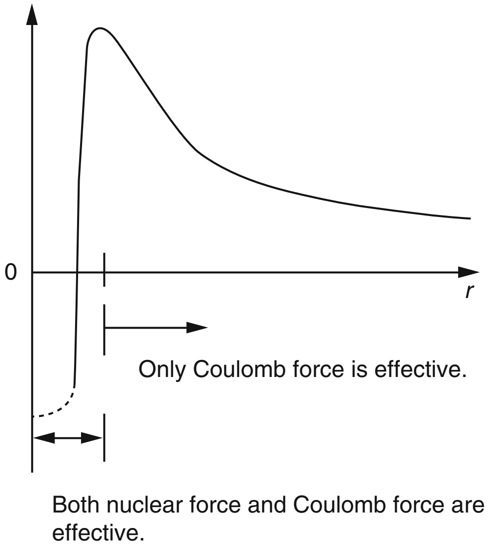

When a positively charged particle is emitted from a nucleus, the particle should normally have to overcome the potential of the Coulomb repulsive force, shown in Fig. 1.1, since the nucleus also has a positive charge. In reality, however, it is not necessary to overcome the potential peak, and a particle with an energy smaller than the peak energy can be emitted by the tunnel effect. However, the probability of this occurring rapidly decreases when the mass of the emitted particle becomes large or the height and thickness of the potential wall increase.

Therefore, the emission of a heavy particle and reactions with low Q-value occur with difficulty. As a result, the α-particle is the only positively charged particle that is regularly emitted and is generally emitted only from nuclei with large atomic numbers Z. However, α-particles can occasionally be emitted from light nuclei, and a nucleus of proton or carbon may occasionally be emitted.

In γ-decay, there is no Coulomb barrier since the emitted particle is a photon. In internal conversion, which competes with γ-decay, there is no barrier since the emitted particle is an electron, which is attracted by the nucleus. In β-decay, there is no barrier for neutrinos, since the interaction of a neutrino with other material can be ignored. When the other emitted particle is an electron, it is attracted by the nucleus, and thus there is also no barrier. In the case of a positron, there is a Coulomb barrier. Nevertheless, the mass of a positron is smaller than that of an α-particle, and thus it can easily pass through the barrier. However, in nuclides with large atomic numbers, β^+-decay with low decay energy rarely takes place since orbital electron capture, which is a competitive process, dominates. Since β-decay is a weak interaction and γ-decay is an electromagnetic interaction, γ-decay takes place more easily than β-decay. Spontaneous fission is another important decay for heavy nuclei. In this case, a Coulomb repulsive force even stronger than for α-decay applies, and the masses of the emitted particles are large; therefore, the parent nucleus must have a sufficiently high energy. Since the neutron has no Coulomb barrier, a neutron can easily jump out of a nucleus if energy permits. Although it is not appropriate to call this a decay, it is important in relation to the later-described delayed neutron, which accompanies nuclear fission. The rate of decay is naturally proportional to the number of nuclides N under consideration and is expressed by the following equation:

$$\frac{dN}{dT} = -\lambda N \tag{1.7}$$

Here, the proportionality constant λ is unique to the particular nuclide and is called the decay constant and its reciprocal of it is called the *mean life of the radioactive species know as* $T_{\mathrm{m}} = 1/\lambda$. If we let the number of nuclides at $t = 0$ be N_0, the following solution is obtained for Eq. 1.7:

$$N = N_0 \exp(-\lambda t) \tag{1.8}$$

The time necessary for N to become half of N_0 is called the half-life, and from Eq. 1.8, the half-life $T_{1/2}$ can be expressed using λ in the following way:

$$T_{1/2} = \frac{1\mathrm{n}\,2}{\lambda} = T_{\mathrm{m}} \cdot 1\mathrm{n}\,2 = (0.69315)T_{\mathrm{m}} = \frac{0.69315}{\lambda} \tag{1.9}$$

The mean life of a nucleus τ is expressed by the following equation:

$$\tau = \frac{1}{N_0}\int_0^{\infty} t\lambda N dt = \frac{1}{\lambda} \tag{1.10}$$

The capability to emit radiation is called radioactivity. Radioactive strength is expressed by the unit Becquerel ($\mathrm{B_q}$), an SI unit. One decay per second is $1\,\mathrm{B_q}$. However, the traditionally used unit, the curie ($\mathrm{C_i}$), is still frequently used. The two units are converted according to the following:

$$1\,\mathrm{C_i} = 3.7 \times 10^{10}\,\mathrm{B_q} \tag{1.11}$$

1.3 Distribution of Nuclides and Nuclear Fission/Nuclear Fusion

In the previous section, it is explained that three kinds of decays can easily take place. The decays are α-decay, β-decay, and γ-decay, but their order of likelihood is γ-decay, β-decay, α-decay. In γ-decay, the nucleus does not change; see the explanation of this statement in the following box.

Gamma Decay

In gamma decay, depicted using the figure below, a nucleus changes from a higher energy state to a lower energy state through the emission of electromagnetic radiation (photons). The number of protons (and neutrons) in the nucleus does not change in this process, so the parent and daughter atoms are the same chemical element. In the gamma decay of a nucleus, the emitted photon and recoiling nucleus each have a well-defined energy after the decay. The characteristic energy is divided between only two particles.

In β-decay, the next most likely decay, the mass number *A* does not change, but the atomic number *Z* changes. Plotting neutron number *Z* against atomic number *Z* following β-decay gives a slope of 45°. On this line, the binding energy (mass defect) changes as shown in Fig. 1.2 (see Eq. 1.6). When *A* is odd, the last term of Eq. 1.6 becomes zero, and the points representing the binding energy for the respective nuclei stay on a parabolic curve. The nuclide at the highest point is a stable nuclide and is generally uniquely determined; nuclides with a higher *Z* than this decay by β^+-decay and nuclides with the lower *Z* decay by β^--decay. When *A* is even, the last term of Eq. 1.6 is positive if *Z* is even and odd if *Z* is negative. Therefore, the points representing the binding energy of respective nuclei are

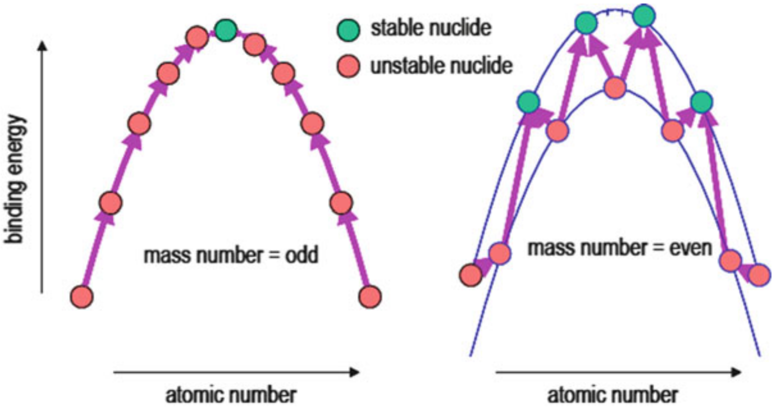

Fig. 1.2 Binding energy change in β-decay and the direction of the decay

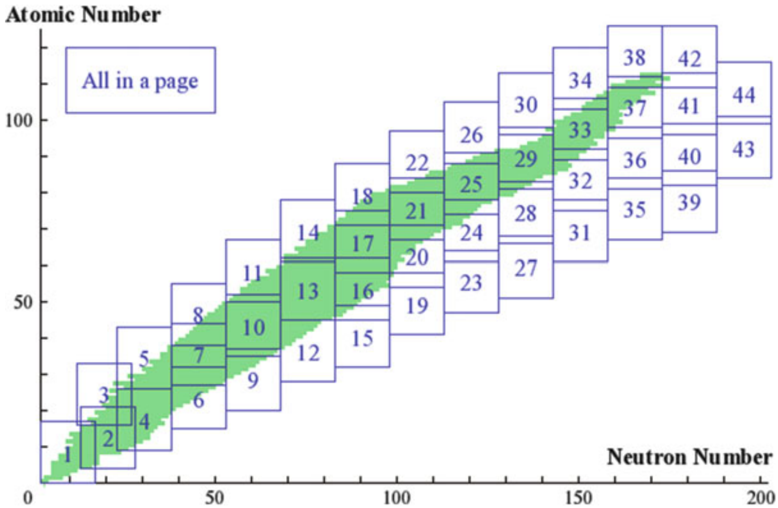

Fig. 1.3 Chart of the nuclides (Nuclear Data Center, JAEA http://wwwndc.tokai-sc.jaea.go.jp/nucldata/index.html, Chart of the Nuclides here is based on the compilation of experimental data until 2008 by H. Koura (JAEA), T. Tachibana (Waseda University), and J. Katakura (JAEA), beta-decay half-lives)

alternately on either of two parabolic curves. Thus, there is a possibility that multiple stable nuclides exist, and these stable nuclides are alternately located between unstable nuclides. Nuclides may also undergo a change in *A*, which is likely to take place through α-decay; however, *A* should be very large in this case. As a result of these decays, the only naturally occurring nuclides are those shown in Fig. 1.3.

In Fig. 1.3, we can see that the curve along the stable nuclides is convex, curving downward at high *A*, because of the balance of the Coulomb and symmetry terms. Therefore, when heavy nuclides fission into two nuclides of approximately equal mass, the resulting nuclides are unstable, having too many neutrons. In reality, two or three neutrons are emitted during fission and most fission products will decay by β-decay.

If the mass number *A* of naturally occurring nuclides is plotted as the abscissa and the binding energy is plotted as the ordinate, Fig. 1.4a is obtained. Where *A* is small, the surface term is large, and where *A* is large, the Coulomb term is large. According to this figure, we can see that a nuclide with small *A* can fuse to a nuclide with a large binding energy and release energy. Similarly, a nuclide with large *A* can fission into nuclides with large binding energies, releasing energy. By nuclear fission, two fission products of approximately equal mass are generated.

One of the most interesting aspects of the nature can be shown in Fig. 1.4b, which shows that the binding energy per nucleon in nuclei of various atoms differs from each other (see Problem 1.3 at the end of this chapter). Sometimes this diagram is referred to as the “most important diagram in the universe.” And in

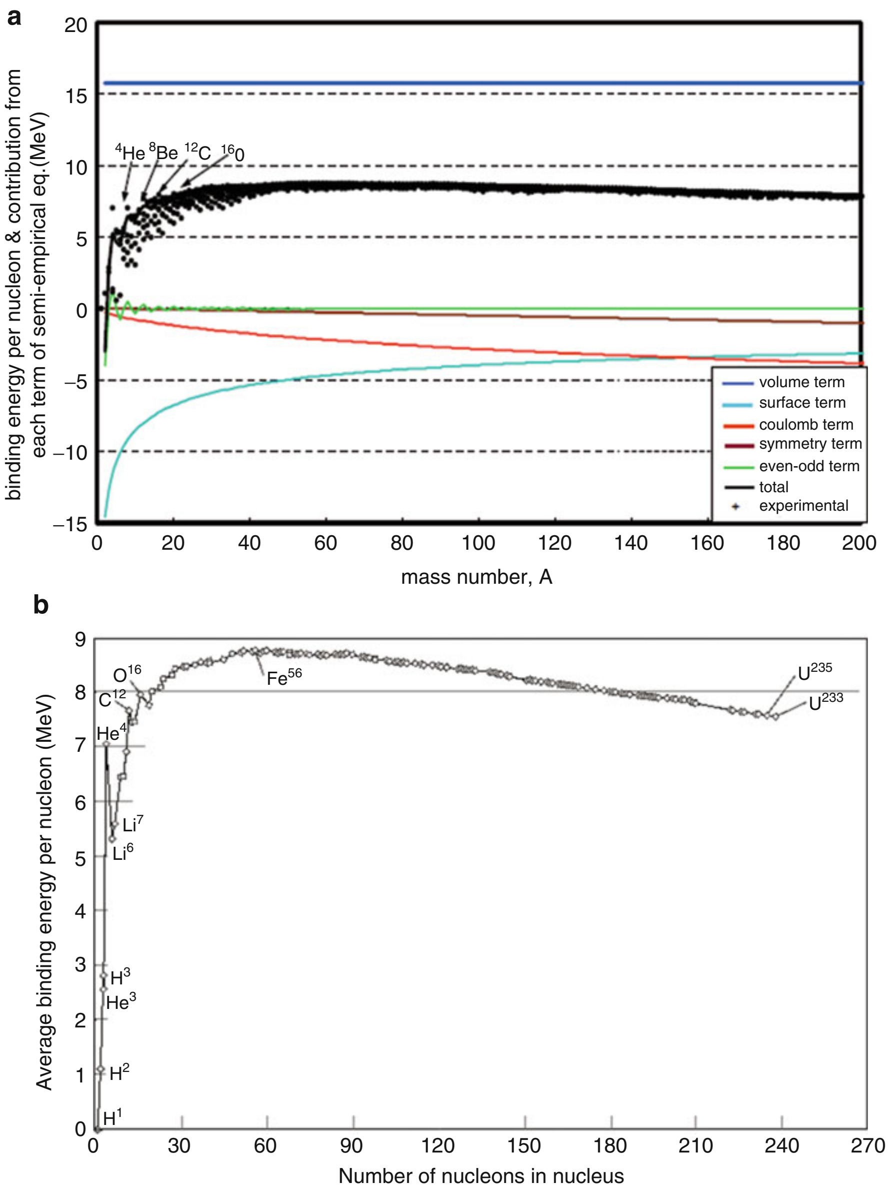

Fig. 1.4 (**a**) Binding energy per nucleon and contribution of each term (Nuclear Data Center, JAEA http://wwwndc.tokai-sc.jaea.go.jp/nucldata/index.html. this is estimated, by T. Tachibana, with the Gross Theory [T. Tachibana, M. Yamada, Proc. Int. Conf. on exotic nuclei and atomic masses, Arles, 1995, p. 763], and alpha-decay half-lives based on the reference of V.E. Vola, Jr. and G.T. Seaborg, J. Inorg. Nucl. Chem., 28, 741 (1966) and newly adjusted parameter values) and (**b**) variation of binding energy per nucleon with mass number (from Wikimedia Commons)

fact, it is difficult to overestimate the importance of that curve. Assume that one uranium nucleus breaks up into two lighter nuclei. For the time being it is assumed that this is possible (this process is called nuclear fission and later on it will be discussed how it can be done).

The total binding energy can be calculated using Eq. 1.6. This equation is very useful since it approximates the binding energy for over 300 stable and non-stable nuclei, but it is applicable for nuclei with large mass numbers only.

1.4 Neutron–Nucleus Interaction

The central problem in nuclear reactor kinetics is to predict the evolution in time of the neutron population in a multiplying medium point reactor kinetics, which allows the study of the global behavior of the neutron population from the average properties of the medium. (This will be explained in later chapter, but for the time being consider that the reactor is viewed as a point, hence the terminology of point reactor kinetics. In this regard, a distinction must be made between the behaviors of the prompt and delayed neutrons. The point kinetics model can be obtained directly from the space- and time-dependent transport equations.) Before tackling the equations governing the time variation of the reactor power (proportional to the total neutron population), we shall discuss briefly the properties of a neutron-multiplying medium after recalling a number of definitions, and we shall give a qualitative description of the principal nuclear reactions at play in a self-sustaining chain reaction and dwell on the source of fission neutrons. Since delayed neutrons play a crucial role in reactor kinetics, we shall describe in detail their production in a reactor.

1.4.1 Nuclear Reaction Rates and Neutron Cross Sections

A neutron is an elementary particle. It is stable when bound to a nucleus by the nuclear force. In its free state, a neutron decays, with a time constant of 12 min, to a proton, accompanied by the emission of a β particle and an antineutrino. In view of the fact that free neutrons in a reactor either are absorbed in matter or escape, on a time scale of less than 10^{-3} s, it is clear that neutron instability is completely negligible in reactor physics.

The power generated in a reactor comes from neutron-induced fissions. It results from the interaction between the neutrons and the nuclei of the physical medium. It is generally possible to neglect neutron–neutron interactions, because the density of neutrons is much smaller than that of nuclei. Free neutrons have a certain speed relative to nuclei. If one neglects the energy of thermal motion of the nuclei, then the kinetic energy E of a neutron represents the energy available to a nuclear reaction in a nucleus. If we denote the relative speed of a neutron by v and its mass by m,[2] then

$$E = \frac{1}{2}mv^2 \tag{1.12}$$

The energy is generally given in units of electron volts ($1\ \text{eV} = 1.6021 \times 10^{-19}$ J).

Interactions of neutrons with matter are described in terms of quantities called cross sections, which can be defined in the following fashion. Imagine a unidirectional neutron beam with a density of n neutrons per cm^3, of speed v, impinging perpendicularly on a thin slice of a target with a density of N identical nuclei per cm^3. Define the neutron flux ϕ by

$$\phi = nv \tag{1.13}$$

Thus, ϕ measures the number of neutrons crossing a unit surface area (1 cm^2) per second. Experiments show that the rate R of interactions of neutrons per cm^2 of target area is proportional to the neutron flux, the density of nuclei, and the target thickness:

$$R = \sigma\phi NV \tag{1.14}$$

where the constant of proportionality σ is called the microscopic cross section. V is the volume of the target per cm^2 (i.e., the target thickness).

The microscopic cross section is a function of the speed of the neutrons relative to the nuclei of the target. It is therefore a function of the kinetic energy available to the reaction. One writes

$$\sigma = \sigma(E) \tag{1.15}$$

Since NV is equal to the total number of nuclei per cm^2 of target area, σ is a measure of the probability that a neutron in the beam will have an interaction per target nucleus. It is to be noted that σ has the dimensions of an area. Microscopic cross sections are usually measured in barns (b), where $1\ \text{b} = 10^{-24}$ cm^2.

Neutrons can interact with nuclei in different ways; each type of interaction will be described in terms of a specific "partial" cross section. Since the probabilities are additive, the sum of the partial cross sections (the total cross section) is a measure of the probability of an interaction of any type when a neutron hits the target.

Let us now consider a physical medium with N nuclei per cm^3. Let us imagine that there exists, within the medium, a density n of free neutrons per cm^3, propagating at a speed v in all directions. The rate of interactions per cm^3 will then be

---

[2] The speed of neutrons in a reactor is sufficiently low that one can neglect relativistic effects therefore $m = m_0$, the neutron rest mass (1.6748×10^{-27} kg).

$$\begin{aligned}\frac{R}{V} &= N\sigma nv \\ &= \Sigma\phi\end{aligned} \tag{1.16a}$$

The constant of proportionality Σ between the rate of interactions and the scalar flux ϕ is called the macroscopic cross section.

In summary, if the total path length of all the neutrons in a cubic centimeter in a second is known (neutron flux (ϕ)) and if the probability of having an interaction per centimeter path length is also known (macroscopic cross section (Σ)), multiply them together to get the number of interactions taking place in that cubic centimeter in one second. This value is known as the reaction rate and is denoted by the symbol R, as we mentioned above. The reaction rate can be calculated by the equation shown below:

$$R = \phi\Sigma \tag{1.16b}$$

where:

R = reaction rate (reactions/s)
ϕ = neutron flux (neutron/cm^2 s)
Σ = macroscopic cross section (cm^{-1})

Substituting $\Sigma N\sigma$ into Eq. 1.16b yields the equation below:

$$R = \phi N\sigma \tag{1.16c}$$

where:

σ = microscopic cross section (cm^2)
N = atom density (atoms/cm^3)

The reaction rate calculated will depend on which macroscopic cross section is used in the calculation. Normally, the reaction rate of greatest interest is the fission reaction rate.

Note that the microscopic cross section σ is a property of each type of nucleus for each type of interaction. If the physical medium contains many types of nuclei, it will be necessary to sum over all types in order to obtain the total macroscopic cross section:

$$\begin{aligned}\sum &= \sum(E) \\ &= \sum_i N_i\sigma_i(E)\end{aligned} \tag{1.17}$$

The macroscopic cross section measures the probability of an interaction for a neutron traveling over a unit distance in the medium under consideration. The units of Σ are therefore cm^{-1}.

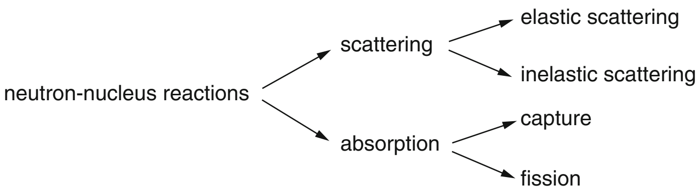

Fig. 1.5 Neutron–nucleus reactions

Each type of interaction has its own particular cross section. The total cross section, σ_{t}, is the sum of the cross sections for scattering, σ_{s}, and for absorption, σ_{a}; thus, we can write

$$\sigma_{\mathrm{t}} = \sigma_{\mathrm{s}} + \sigma_{\mathrm{a}} \tag{1.18}$$

The scattering cross section includes those for elastic scattering, σ_{e}, and for inelastic scattering, σ_{i}. In elastic scattering, the kinetic energy of the incident neutron is shared between the target nucleus and the neutron emerging from the collision. In an inelastic scattering, the kinetic energy is not conserved, the target nucleus being left in an excited state. One has

$$\sigma_{\mathrm{s}} = \sigma_{\mathrm{e}} + \sigma_{\mathrm{i}} \tag{1.19}$$

On the other hand, the absorption cross section includes those for fission, σ_{f}; for radiative capture, σ_{γ}; and for reactions of the type $(n, 2n), (n, 3n)$, etc.:

$$\sigma_{\mathrm{a}} = \sigma_{\mathrm{f}} + \sigma_{\gamma} + \sigma_{n,2n} + \sigma_{n,3n} + \cdots \tag{1.20}$$

In summary, for neutron–nucleus reactions, the following division as shown in Fig. 1.5 is used:

Thus, the concept of the microscopic cross section is introduced to represent the probability of a neutron–nucleus reaction. The cross sections depend on the energy of the incident neutron, and this dependence is very complex. It results from the structure of the target nuclei and the type of interaction. Suppose that a uniform beam of neutrons with intensity $I\,\mathrm{cm}^{-2}\ \mathrm{s}^{-1}$ strikes a thin "film" of atoms (one atomic layer thick) with N_{a} atoms/cm^2. Then the number of interactions C per cm^2 per second will be proportional to the intensity I and the atom density N_{a}. We define the proportionality factor as the microscopic cross section (or just cross section) σ:

$$C = \sigma N_{\mathrm{a}} I \tag{1.21}$$

The microscopic cross section is often expressed in "barns" ($1\ \mathrm{b} = 10^{-24}\ \mathrm{cm}^2$); from this definition, it follows that one can consider ó as the effective "target area" that a nucleus presents to the neutron. The microscopic cross section in general is dependent on the neutron energy and the type of reaction. In accordance with the foregoing scheme, one distinguishes (see Fig. 1.6 below):

Fig. 1.6 Forgoing schema

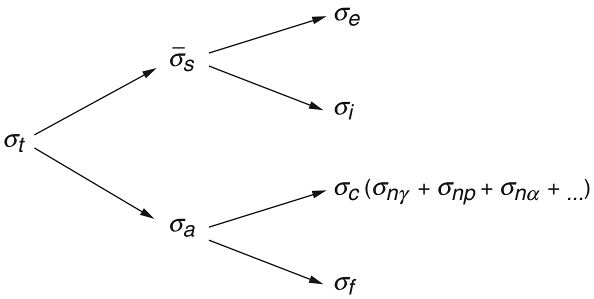

Fig. 1.7 Neutron transmission through a plate

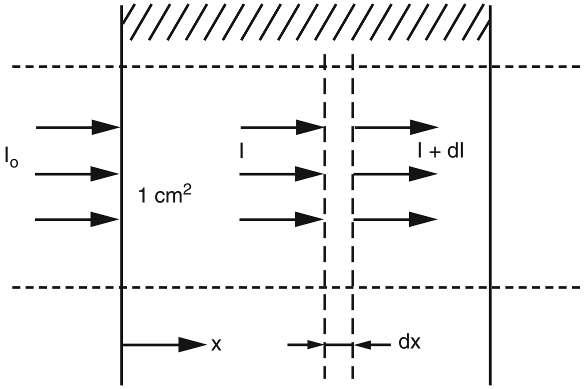

In order to be able to define the concept of the "microscopic cross section," in the foregoing our starting point was a thin film of atoms. In order to be able to determine the microscopic cross section, transmission measurements are performed on plates of materials. Starting from the presumption that no fission or scattering occurs, the neutron attenuation by a plate with thickness x will be calculated (see Fig. 1.7).

Assume that I_0 neutrons per cm^2 and per second perpendicularly strike a plate, the atomic number density of which is N (nuclei per cm^3). Of a layer dx in the plate, the nucleus density per unit area $N_a = Ndx$. Then, according to the definition of the microscopic cross section, the reaction rate per unit area is $N\sigma I(x)dx$. This is equal to the decrease of the beam intensity, so that

$$-dI = N\sigma I dx \tag{1.22}$$

Integration gives

$$I(x) = I_0 e^{-N\sigma x} \tag{1.23}$$

Then the microscopic cross section σ refers to one nucleus. The product

$$\Sigma = N\sigma \tag{1.24}$$

refers to one cm^3 of material and is called the macroscopic cross section, which in fact is an incorrect name, because it is not a cross section (dimension L^{-1}). From Eq. 1.23, it follows that the probability $P(x)$ that a neutron will travel a distance x in the material concerned without becoming involved in a reaction is

$$P(x) = \mathrm{e}^{-\Sigma x} \tag{1.25}$$

The probability that a neutron will be involved in a reaction between x and $x + dx$ is equal to Σdx, so that for the mean free path λ of the neutrons, it follows that

$$\lambda = \int_0^\infty x\mathrm{e}^{-\Sigma x} \sum dx = \frac{1}{\sum} \tag{1.26}$$

whereby one can distinguish λ_s,λ_a, etc. This quantity is also referred to as the *relaxation length*, because it is the distance in which the intensity of the neutrons that have not caused a reaction has decreased with a factor *e*.

If ρ represents the density of material with mass number A, then the following holds:

$$N = \frac{\rho}{A} N_\mathrm{A} \tag{1.27}$$

in which N_A is Avogadro's number = $6.022 \times 10^{23}\ \mathrm{mol}^{-1}$. When one has a mixture of nuclei, it holds that

$$\sum\nolimits_{\mathrm{mixture}} = \sum_i N_i \sigma_i \tag{1.28}$$

which is proof of Eqs. 1.16a, 1.16b, and 1.16c as before and N_i represents the number of nuclei of the ith type per cm^3 in the mixture concerned.

The study of cross sections has been the concern of experimental and of theoretical nuclear physics for many years. Databases of standardized data have been created jointly by several national laboratories. These files, Evaluated Nuclear Data Formats (ENDF), contain an evaluation of all nuclear reactions for each nuclide and include experimental analysis combined with the prediction of theoretical models, in a format allowing electronic processing of the data. Specialized computer programs, such as NJOY of MacFarlane, 1978, allow the preparation of data for neutronics calculations in the form of cross sections as functions of neutron energy. In this monograph, as in most treatises on neutronics, it is assumed that all cross sections $\sigma(E)$ are available.

1.4.2 *Effects of Temperature on Cross Section*

As discussed, the microscopic absorption cross section varies significantly as neutron energy varies. The microscopic cross sections provided on most charts and tables are measured for a standard neutron velocity of 2200 m/s, which corresponds to an ambient temperature of 68 °F. Therefore, if our material is at a higher temperature, the absorption cross section will be lower than the value for 68 °F, and any cross sections which involve absorption (e.g., $\sigma_a, \sigma_c, \sigma_f$) must be corrected for the existing temperature.

The following formula is used to correct microscopic cross sections for temperature. Although the example illustrates absorption cross section, the same formula may be used to correct capture and fission cross sections:

$$\sigma = \sigma_0 \left(\frac{T_0}{T} \right)^{1/2} \tag{1.29}$$

where:

$\sigma =$ microscopic cross section corrected for temperature
$\sigma_0 =$ microscopic cross section at reference temperature (68 °F or 20 °C)
$T_0 =$ reference temperature (68 °F) in degrees Rankine (°R) or Kelvin (°K)
$T =$ temperature for which corrected value is being calculated

Note: when using this formula, all temperatures must be converted to °R or °K per following relationships:

$$
\begin{aligned}
{}^\circ\mathrm{R} &= {}^\circ\mathrm{F} + 460 \\
{}^\circ\mathrm{K} &= {}^\circ\mathrm{C} + 273
\end{aligned}
$$

1.4.3 Nuclear Cross-Sectional Processing Codes

Neutron, gamma ray, and electron interaction cross sections determine the interactions of each of these entities with the atoms and nuclei in the media that they move through. The most complicated interaction cross sections are probably the neutron cross sections. Since these are very important in nuclear reactor design, a great deal of effort has been spent on representing experimental and theoretical data in the most accurate manner possible for neutron transport calculations.

These cross sections are so complicated that it is impossible to go to original publications to obtain data for a design calculation. So the DOE has organized the accumulated data on neutron cross sections into a library called the Evaluated Nuclear Data File. This file is divided into two parts. Part A contains all of the original publications and the raw data. Part B contains the evaluated data and recommended parameters. The data is evaluated by an organization called CSEWG for Cross Section Evaluation Working Group. CSEWG is an almost volunteer informal group with members from a number of DOE labs. It is lead by Brookhaven National Laboratory. Typically, one member of the group will be responsible for a particular nuclide and will follow it for their entire career. Updates to most of the data are not as frequent today as they were in the 1950s and 1960s.

The evaluated data is stored in Evaluated Nuclear Data Formats B (ENDF/B) on an energy grid that represents the best data as accurately as possible, with the fewest number of energy ranges as possible. The overall energy range has always been 10^{-5} eV to 20 MeV. With ENDF/B, release Number VII.1 (or 7), some nuclides have data to much higher energies. There are several interpolation formulas allowed for representing the data over a given energy range in the ENDF rulebook (ENDF-102). The basic idea is to give the energies and values at the ends of an interval and the rule for interpolation as a compact way of representing the data. For a nucleus like H-1, broad ranges can be covered with one interpolation scheme, because the cross section does not vary very rapidly. For a nucleus like U-238, many ranges are required because the cross section does vary quite rapidly.

In fact in the resolved resonance region, from a few eV to several keV, neutron cross sections change so rapidly that it is always impossible to break the data down into a fine enough energy grids to accurately represent the rapidly changing cross section. So some generic formulas are used to represent the resonance cross sections with discrete parameters. The Breit–Wigner formula is an example.

Therefore, to perform a neutron transport calculation with multiple nuclides in a given set of materials, the first processing step that must be taken is to represent all of the cross-sectional data on a grid common to all of the nuclides in the problem. It is easiest to think of this in terms of a multigroup calculation, the approach of breaking the energy range of interest down into a finite set of energy intervals, called groups, over which the cross sections are assumed constant at some average value.

Three major DOE laboratories have developed codes, or code systems, to perform this step of representing the Evaluated Nuclear Data Formats B (ENDF/B) data on a common energy grid. The Los Alamos National Laboratory (LANL) code system is called NJOY, the Oak Ridge National Laboratory (ORNL) code system is called the Standardized Computer Analyses for Licensing Evaluation (SCALE), and the Argonne National Laboratory (ANL) code system is called MC2. They are not all parallel. SCALE does not actually start with ENDF but uses NJOY to preprocess some of the data to a common energy grid. At one time SCALE did it all, but it became too expensive to continue two separate development efforts. MC2 processes from ENDF/B straight through to a finished multigroup set that can immediately be used in a neutron diffusion calculation. Unfortunately, MC2 does not go any further in the neutron transport business than a P1 effort, and so it is not widely used and will not be commented on further. Each of the code systems produces a different format for the final multigroup cross sections that are somewhat incompatible with each other. The only transport code system that reads more than one format multigroup data set is FEMP.[3]

The most comprehensive system is the Nuclear Data Processing System known as NJOY, so it will be followed from here on out (the SCALE approach will be referenced to the NJOY system). After converting all nuclides to a common energy

---

[3] FEMP computer code has been developed by Professor Patrick McDaniel of University of New Mexico, Nuclear Engineering Department.

grid, NJOY generates the actual cross sections in the resonance range from the parametric representation used in ENDF/B. Unfortunately these cross sections depend on two parameters that are usually part of a specific transport calculation. The very sharp resonances in nuclides like U^{238} are broadened by the random motion of the nuclei in a uranium medium because of a nonzero temperature. In fact as the temperature of the medium goes up, the resonances are broadened enough that the absorption in these resonances increases. This gives a negative feedback in low-enrichment reactors that is called the Doppler coefficient.

The second factor that affects the processed cross sections is the actual concentration of the resonance absorber in the media. If the concentration of U-238 is very high, the neutron flux will be severely attenuated at the energies that correspond to the peaks of the U-238 absorption resonances. If the concentration of U^{238} is low, the neutron flux will be only moderately attenuated at the energies of these peaks. Since the actual number of absorption reactions is the product of the flux times the cross section, the average cross section will depend on the ratio of the U^{238} cross section to the cross sections of all of the other materials present in the media. The parameter that is used to characterize this effect is called the background scatter cross section. It is essentially the sum of all of the nuclide scattering cross sections, other than U^{238} (or the resonance nuclide), at the resonance energy per atom of U^{238}.

So when NJOY converts the nuclear data from the random grid in ENDF/B to a common grid for a transport calculation, it generates resonance range cross sections for a two-dimensional matrix of temperature and background scatter cross sections. The number of different temperatures is usually in the range of 3–5. The number of different background scatter cross sections is typically in the range of 5–9. Therefore, for a given problem at a specific temperature and material composition, the code TRANSX (for transport cross-sectional code) can interpolate in the resonance grid that NJOY provides to get a problem-dependent cross section for each material. The output file that NJOY provides with the multiple values of cross sections is called a MATXS (for material cross-sectional library) file. The problem-specific file that TRANSX provides is called a DTF (one-dimensional transport theory code) library. NJOY can produce a DTF library directly, but it assumes one temperature and one concentration of resonance nuclide when it does this. Usually these are room temperature and an infinite dilute resonance nuclide concentration. The cross section of the resonance absorber does not perturb the neutron flux at all in the peak of the resonance. In the SCALE system, the equivalent library to the MATXS data file is the AMPX master library. The equivalent library to the DTF data library in the SCALE system is the AMPX working library. The codes that perform the TRANSX calculation for SCALE are called BONAMI and NITAWL. (Most of the SCALE modules are named after common household products.) SCALE can also produce a data library very similar to the DTF format in what is called ANISN format. DTF and ANISN were early one-dimensional SN transport codes developed by Los Alamos National Laboratory (LANL) and ORNL/Westinghouse, respectively.

The SCALE system has many more modules for manipulating multigroup data libraries than the NJOY–TRANSX system. TRANSX performs multiple functions for NJOY libraries that are performed by separate modules in the SCALE system.

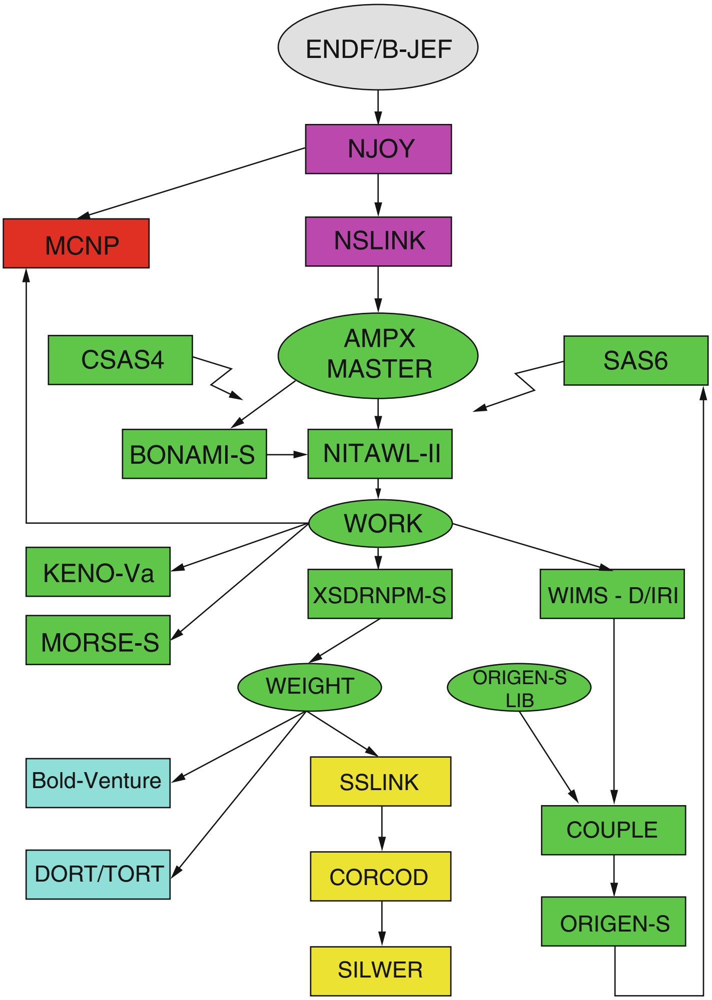

Fig. 1.8 Overview of the INAS code system

The AMPX library formats are much more compact than the MATXS and DTF formats, but both contain comparable data.

In summary then, NJOY converts ENDF/B data to a common energy grid and generates multiple data sets for resonance nuclides for a matrix of temperatures and background scatter cross sections. The output is called a MATXS library. TRANSX reads a MATXS library and generates problem-dependent (temperature and background scatter cross section) DTF cross sections. SCALE uses NJOY to produce an AMPX master library and uses BONAMI/NITAWL to produce an AMPX working library for a specific design problem. FEMP will read either output.

An overview of IRI–NJOY–AMPX–SCALE (INAS) code system is presented in Fig. 1.8.

The NJOY code and ENDF itself are somewhat of an ongoing effort in that the work started here is based on the 1999 version of the NJOY code and ENDF/B-V. But it is desirable that any capability developed should be compatible with the 2005 NJOY version and ENDF/B-VI. In fact, the starting point for code modifications initially was a version of the NJOY-99 code modified at Sandia National Laboratories for enhanced recoil analysis capability. The code at Sandia is maintained with the Update Deck (UPD) processor, so that any modifications generated should be in the form of UPDs that can be incorporated into a UPD input stream to produce a final source code for compilation.[4]

It is important to recognize at the outset that since neutrons are electrically neutral, they are not affected by the electrons in an atom or by the positive charges of the nucleus. Consequently, neutrons pass through the atomic electron cloud and interact directly with the nucleus. In short, neutrons collide with nuclei, not with atoms.

Neutrons may interact with nuclei in one or more of the following ways:

Elastic scattering: In this process, the neutron strikes the nucleus, which is usually in its ground state, the neutron reappears, and the nucleus is left in its ground state. The neutron in this case is said to have been *elastically scattered* by the nucleus. In the notation of nuclear reactions, this interaction is abbreviated by the symbol (n, n).

Inelastic scattering: This process is identical to elastic scattering except that the nucleus is left in an excited state. Because energy is retained by the nucleus, this is clearly an endothermic interaction. Inelastic scattering is denoted by the symbol $(\mathrm{n}, \hat{\mathrm{n}})$. The excited nucleus decays by the emission of γ-rays. In this case, since these γ-rays originate in inelastic scattering, they are called *inelastic* γ-rays.

Radiation capture: Here, the neutron is captured by the nucleus, and one or more γ-rays—called *capture* γ-rays—are emitted. This is an exothermic interaction and is denoted by (n, γ). Since the original neutron is absorbed, this process is an example of a class of interactions known as *absorption reaction*.

Charged particle reaction: Neutron may also disappear as the result of absorption reaction of the type (n, α) and (n, p). Such reactions may be either exothermic or endothermic.

Neutron-producing reaction: Reactions of the type $(\mathrm{n}, 2\mathrm{n})$ and $(\mathrm{n}, 3\mathrm{n})$ occur with energetic neutrons. These reactions are clearly endothermic since in the $(\mathrm{n}, 2\mathrm{n})$ reaction on neutron and in the $(\mathrm{n}, 3\mathrm{n})$ reaction, two neutrons are extracted from the struck nucleus. The $(\mathrm{n}, 2\mathrm{n})$ reaction is especially important in reactors containing heavy water or beryllium since $^{2}\mathrm{H}$ and $^{9}\mathrm{Be}$ have loosely bound neutron which can easily be ejected.

---

[4] This effort was taken in place under contract by McDaniel and Zohuri in time period of 2001–2003 but never was a finished effort, although a lot of work was put into it and somewhat a new modified version NJOY with recoil capability was developed.

Numerical data for microscopic cross sections of many nuclides are available as computer data files (ENDF/B, Evaluated Nuclear Data File, or JEF, Joint Evaluated File). Various computer programs making use of these data files can represent the microscopic cross sections for many nuclides and various reactions graphically.

1.4.4 Energy Dependence of Neutron Cross Sections

Besides a ground state, atomic nuclei also have higher energy levels, which can be excited. The lowest energy levels of the compound nucleus, which is formed in a neutron–nucleus interaction, are relatively far apart, for medium-weighted nuclei ($A = 100$–150) *circa* 0.1 MeV. The high-energy levels become closer and closer to each other. For an excitation energy of about 8 MeV, as is the case after capture of a neutron with low kinetic energy, the separation between the levels is only 1–10 eV. Figure 1.9 schematically indicates the position of the energy levels during the formation of a compound nucleus.

The energy levels of a nucleus are no sharp “lines” but show a certain width Γ, which according to the uncertainty principle of Heisenberg is connected with the average time before a nucleus in an excited state decays by emission of a photon or other particles. If there are several decay possibilities for the compound nucleus (emission of a photon, neutron, etc., or fission), we distinguish partial level widths $\Gamma_\gamma, \Gamma_n, \Gamma_f$, etc., which summed yield the total level width Γ.

If the excitation energy of the compound nucleus corresponds with one of the level energies, the probability of an interaction is large: resonance occurs. As the excitation, energy depends on the kinetic energy of the neutron and the probability of an interaction, and thus the microscopic cross section varies strongly with the energy of the neutron. Breit and Wigner, on the ground of quantum mechanical

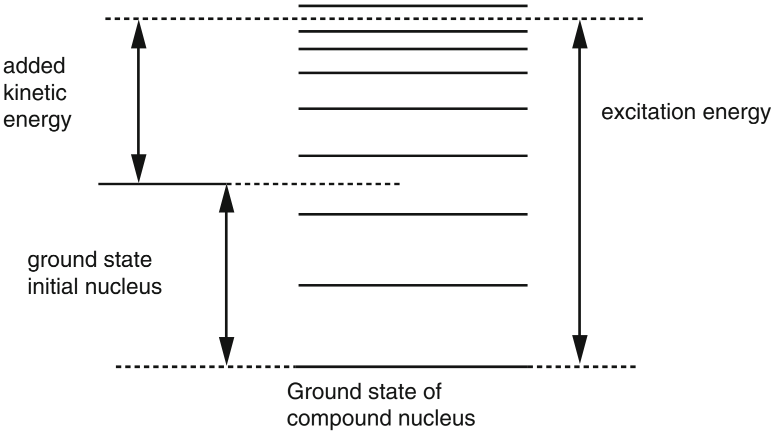

Fig. 1.9 Energy diagram of a neutron–nucleus interaction

considerations, have derived the following expression for the microscopic cross section σ_{na} for an interaction whereby the neutron is included in the nucleus and a particle a (possibly the same neutron again) is emitted:

$$\sigma_{\mathrm{na}}(E) = \frac{\lambda^2}{4\pi}\frac{\Gamma_{\mathrm{n}}\Gamma_{\mathrm{a}}}{(E-E_{\mathrm{r}})^2 + (\Gamma/2)^2} \tag{1.30}$$

in which $\lambda = h/p = h/mv$ (where p is the neutron momentum, h is Planck's constant, m is mass of neutron, and v is the presentation of neutron velocity) is the de Broglie wavelength of the neutron and E_{r} the resonance energy. The microscopic cross section shows a maximum if the kinetic energy E of the neutron equals E_{r}. If $E = E_{\mathrm{r}} \pm \Gamma/2$, the value of the microscopic cross section is halved, so that Γ indicates the width of the resonance peak at half height. As the level widths are often small, the resonance peaks can be very sharp. Figure 1.10 gives an example.

Accordingly, as the neutron energy increases, the peak height of the resonance decreases, and the resonances become relatively closer to each other, so that they finally cannot be distinguished anymore (see Fig. 1.11).

Note that the resonances bunch together because the energy scale is drawn in logarithmic scale in Fig. 1.10. Normally, resonances are processed with a constant average energy spacing in the unresolved resonance region.

For the derivation of the Breit–Wigner equation, the starting point is an unmoving nucleus, which is struck by a neutron. In reality, the nucleus will also

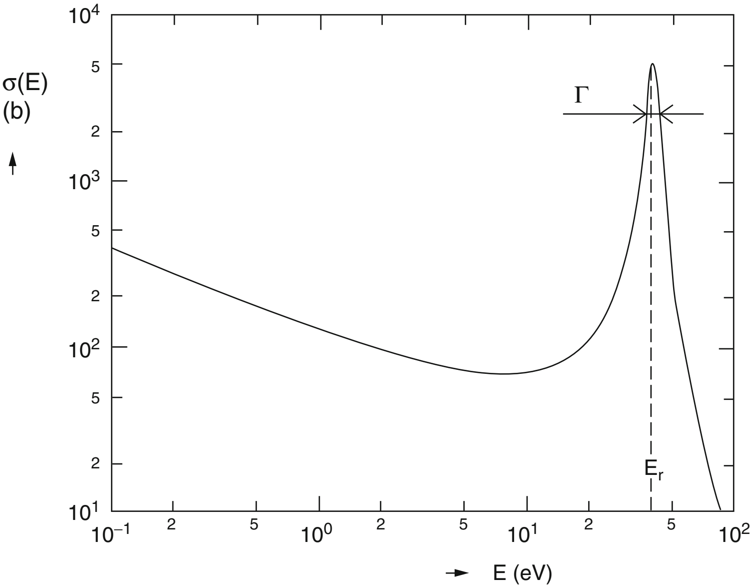

Fig. 1.10 Microscopic cross section at a resonance

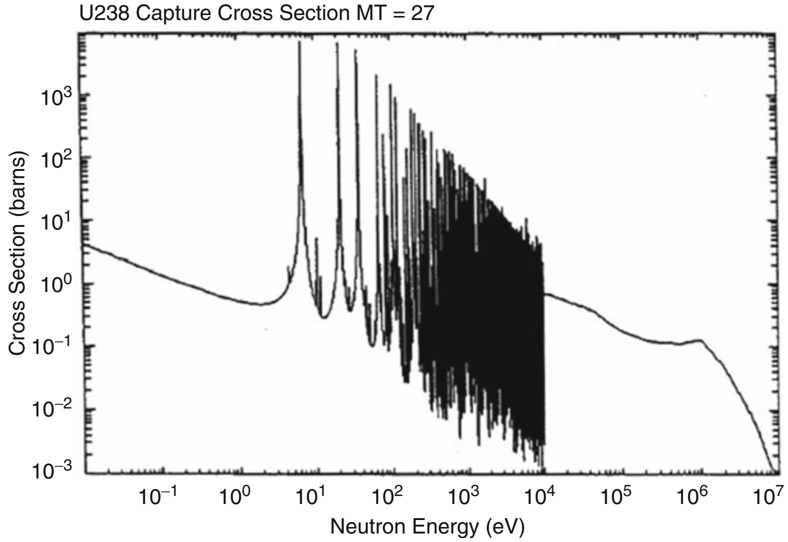

Fig. 1.11 Microscopic cross section of a U^{238} nucleus for neutron capture

have a kinetic energy as a result of thermal excitation. This expresses itself in the microscopic cross section, because averaging over the energy distribution of the nuclei must take place. Although the average energy of the nuclei is small, at room temperature 0.025 eV, this averaging still has noticeable consequences for the resonances, because the width of the resonances can be of the same order of magnitude. This leads to broadening of the resonances and lowering of the top value. This so-called Doppler effect is thus temperature dependent and plays an important role in reactors.

The microscopic cross section outside the resonance is also determined by the behavior of the level widths $\Gamma_\gamma, \Gamma_\mathrm{n}, \Gamma_\mathrm{f}, \ldots$ as a function of the neutron energy. The level widths Γ_γ and Γ_f appear to be rather constant, whereas Γ_n increases approximately proportional to $\sqrt{E}$. From this, it can be derived that for energies much lower than the lowest resonance energy, the capture and fission cross sections behave as follows:

$$\sigma_\gamma, \sigma_\mathrm{f}(E) \div \frac{1}{\sqrt{E}} \div \frac{1}{v} \tag{1.31}$$

One finds this "$\frac{1}{v}$ relation" for many nuclides, and it means that the probability of such a reaction is proportional to the time that the incident neutron spends in the proximity of the nucleus.

For scattering, the microscopic cross section decreases sharply outside the resonance, and the so-called potential scattering will predominate, whereby the neutron is scattered by the potential field of the nucleus and does not form a compound nucleus. The potential scattering cross section is constant over a large energy range, but decreases at high energies. For light nuclides, at low energies, chemical bonding effects can occur, by which the microscopic cross section is larger than that of the free atomic nucleus (e.g., H in H_2O).

In addition to elastic scattering, whereby the total kinetic energy of the particles is conserved, also inelastic scattering can occur. In that case, the nucleus remains in an excited state after emission of the neutron and rapidly decays to the ground state under emission of a photon. The incident neutron then must have sufficient energy to be able to excite this level, so that inelastic scattering is a threshold reaction.

The energy dependence of the microscopic cross section can be summarized as

Capture and fission	$\frac{1}{v}$ + resonances
Elastic scattering	Constant/decreasing + resonances
Inelastic scattering	Threshold reaction; for light nuclides, a few MeV; for heavy nuclides, 10–100 keV
Resonances	Width Γ_γ, Γ_f constant; $\Gamma_n \div \sqrt{E}$ peak width decreasing with E for light nuclides $E_\gamma > 1$ MeV; for heavy nuclides, $E_\gamma > 1$ eV as a result of resonances at very low energy, e.g., 0.1 eV deviations occur in the $1/v$ relation

1.4.5 Types of Interactions

When a neutron comes into collision with a nucleus, three types of interaction are possible and they are as follows:

1. Formation of a compound nucleus
2. Potential scattering
3. Direct interaction

Each of these three above possibilities is described in detail below.

1. **Compound Nucleus**
   In compound nucleus formation, the incident neutron is absorbed by the target nucleus, and a system called compound nucleus is formed. The neutron's kinetic energy is shared among all nucleons. If the target nucleus is ${}_Z X^A$, where Z is the number of protons, A the number of nucleons (also called the "mass number"), and X the chemical symbol of the element, then the compound nucleus formation can be represented as

$$ {}_Z X^A + {}_0 n^1 \rightarrow \left({}_Z X^{A+1}\right)^* \tag{1.32}$$

The energy of excitation (i.e., above the ground state) of the compound nucleus E^* is, however, larger than the incident neutron's kinetic energy (much larger if the incident neutron is in the thermal energy range). This is so for the following reason. The binding energy of a nucleon in a nucleus is the

Table 1.2 De-excitation pathways for the compound nucleus

Elastic resonant scattering (n, n)	$\left({}_z\mathrm{X}^{A+1}\right)^* \rightarrow {}_z\mathrm{X}^A + {}_0\mathrm{n}^1$
Inelastic resonant scattering (n, n ’)	$\left({}_z\mathrm{X}^{A+1}\right)^* \rightarrow {}_z\mathrm{X}^A + {}_0\mathrm{n}^1 + \gamma$
Radiative capture (n, g)	$\left({}_z\mathrm{X}^{A+1}\right)^* \rightarrow {}_z\mathrm{X}^A + \gamma$
Fission (n, f)	$\left({}_z\mathrm{X}^{A+1}\right)^* \rightarrow {}_c\mathrm{PF}_1^B + {}_{z-c}\mathrm{PF}_1^{A+1-B-v} + \mathrm{v}_0\mathrm{n}^1 + \gamma$
Transmutation (n, p)	$\left({}_z\mathrm{X}^{A+1}\right)^* \rightarrow {}_{z-1}\mathrm{Y}^A + {}_1\mathrm{H}^1$
(n, a) reaction	$\left({}_zX^{A+1}\right)^* \rightarrow {}_{z-1}\mathrm{Y}^{A-3} + {}_2\mathrm{He}^4$
(n, 2n), (n, 3n)…reactions	–

energy which must be supplied to the nucleon to free it from the nucleus. In the reverse process, this energy reappears when the neutron is captured into the nucleus.[5] Therefore, when the incident neutron is absorbed into the target nucleus to form the compound nucleus, it contributes its binding energy E_b to the compound nucleus. The energy of excitation of the compound nucleus is consequently the sum of the incident neutron’s kinetic energy and its binding energy in the compound nucleus:

$$E^* = E + E_\mathrm{b} \tag{1.33}$$

The compound nucleus is highly unstable. It is in an excited state and lives only about $10^{-14}\,\hat{E}$ s before de-excitation. This occurs by particle and/or photon emission. The type of nuclear reaction allowing the compound nucleus to reach stability is called a de-excitation pathway. The main de-excitation pathways of the compound nucleus are shown in Table 1.2.

The compound nucleus can also de-excite by reemitting a neutron. If the residual nucleus ${}_z\mathrm{X}^A$ is in its ground state, the process is called elastic scattering. More often the residual nucleus is left in an excited state (later de-exciting by emitting a photon), and the kinetic energy of the emitted neutron is smaller than that of the incident neutron: this is inelastic scattering.

The compound nucleus can also de-excite to the ground state of the nuclide ${}_z\mathrm{X}^{A+1}$ by emitting one or more γ rays. This is called radiative capture. In addition, depending on the random collisions between nucleons in the highly excited compound nucleus, one or more nucleons (a proton, a deuteron, two or three neutrons, an α particle, …) can be ejected. These reactions generally require that the kinetic energy E supplied be above a minimum value. These are termed threshold-type reactions.

In general, cross sections involving the capture or absorption of the neutron vary inversely with the neutron speed. This illustrated the fact that it is generally

---

[5] One can calculate the total binding energy of a nucleus from the mass defect, Δm which is the difference between the mass of the bound nucleus and the sum of the masses of the nucleons, using Einstein’s equation $E_{\mathrm{b}_{\mathrm{Total}}} = \Delta mc^2$.

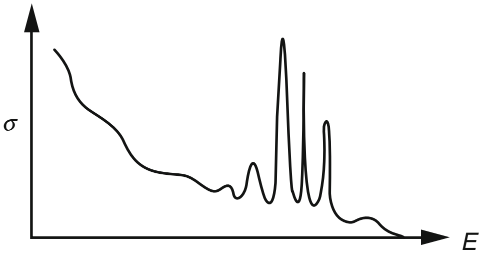

Fig. 1.12 Nuclear cross section with resonances

more difficult to hit a moving target than a stationary one. Also, according to quantum mechanics, a nucleus can exist only in certain states called quantum states. For a compound nucleus to be formed, it must be in an allowed intermediate state. If there is an excited state of the nucleus ${}_{z}X^{A+1}$ in the vicinity of $E^{*} = E + E_{\mathrm{b}}$, the probability of compound nucleus formation will be great, and the cross section for the reaction will be large. But if there is no allowed level close to $E*$, the cross section will be much smaller. The dependence of the cross sections on the kinetic energy of the incident neutron will therefore exhibit resonances, which lead to sudden variations of the cross sections with neutron energy. The presence of resonances is illustrated in Fig. 1.12.

2. **Potential Scattering**

While the cross section for elastic scattering is significant only near a resonance, potential scattering is a type of elastic scattering which can take place for any energy of the incident neutron.

This mode of interaction does not involve the formation of a compound nucleus. It appears simply as a result of the presence of the nucleus. It is a collision of the "billiard ball" type, in which the total energy is conserved. Potential scattering is a function only of the forces which act on the neutron in the vicinity of the target nucleus, and these fames depend on the dimensions and the shape of the nucleus.

If we assume the target nucleus to be at rest, energy conservation can be shown to imply that the kinetic energy E' of the neutron after the collision is always smaller than the incident energy E and must be in the range

$$\alpha E \leq E' \leq E \tag{1.34a}$$

where:

$$\alpha \approx \left(\frac{A-1}{A+1}\right)^{2} \tag{1.34b}$$

The neutron loses therefore a fraction of its energy in each collision: we have neutron moderation (slowing down). We further discuss this under slowing down of neutron due to scattering.

3. **Direct Interaction**

High-energy neutrons can also interact with nuclei by direct interaction. In this type of interaction, a direct collision between the neutron and the nucleus results in the ejection of one or more nucleons (protons or neutrons) and in the absorption of the incident neutron. However, very few neutrons in a reactor possess sufficient energy to enter into direct interaction. This type of interaction is thus of little interest in reactor physics.

1.5 Mean Free Path

We proved this by Eq. 1.26. Now, if a neutron has a certain probability of undergoing a particular interaction in one centimeter of travel, then the inverse of this value describes how far the neutron will travel (in the average case) before undergoing an interaction. This average distance traveled by a neutron before interaction is known as the *mean free path* for that interaction and is represented by the symbol λ. The relationship between the mean free path (λ) and the macroscopic cross section (Σ) is shown below.

$$\lambda = \frac{1}{\Sigma} \tag{1.35}$$

1.6 Nuclear Cross Section and Neutron Flux Summary

The important information so far is summarized below:

- Atom density (N) is the number of atoms of a given type per unit volume of a material.
- Microscopic cross section (Σ) is the probability of a given reaction occurring between a neutron and a nucleus.
- Microscopic cross sections are measured in units of barns, where 1 barn $= 10^{-24}$ cm^2.
- Macroscopic cross section (Σ) is the probability of a given reaction occurring per unit length of travel of the neutron. The unit Σs for macroscopic cross section are cm^{-1}.
- The mean free path (λ) is the average distance that a neutron travels in a material between interactions.
- Neutron flux (ϕ) is the total path length traveled by all neutrons in one cubic centimeter of a material during one second.
- The macroscopic cross section for a material can be calculated using the equation below.

$$\Sigma = N\sigma$$

- The absorption cross section for a material usually has three distinct regions. At low neutron energies (<1 eV), the cross section is inversely proportional to the neutron velocity.

- Resonance absorption occurs when the sum of the kinetic energy of the neutron and its binding energy is equal to an allowed nuclear energy level of the nucleus.
- Resonance peaks exist at intermediate energy levels. For higher neutron energies, the absorption cross section steadily decreases as the neutron energy increases.
- The mean free path equals $1/\Sigma$.
- The macroscopic cross section for a mixture of materials can be calculated using the equation below.

$$\sum = N_1\sigma_1 + N_2\sigma_2 + \cdots + N_n\sigma_n \tag{1.36}$$

- Self-shielding is where the local neutron flux is depressed within a material due to neutron absorption near the surface of the material.

1.7 Fission

To make sense of nuclear reactor design in general and any reactor design in particular, the reader needs to have some familiarity with a few key nuclear concepts and phenomena. In a nutshell, slow neutrons (called thermal neutrons) can initiate a fission of uranium-235 (U-235), an isotope of uranium that occurs in nature. Natural uranium that is mined from the ground is 0.7 % U-235 and 99.3 % U-238. The result of fission is fission products that are radioactive, radiation, fast (or energetic) neutrons, and heat as shown in Fig. 1.13. The fast neutrons have a low

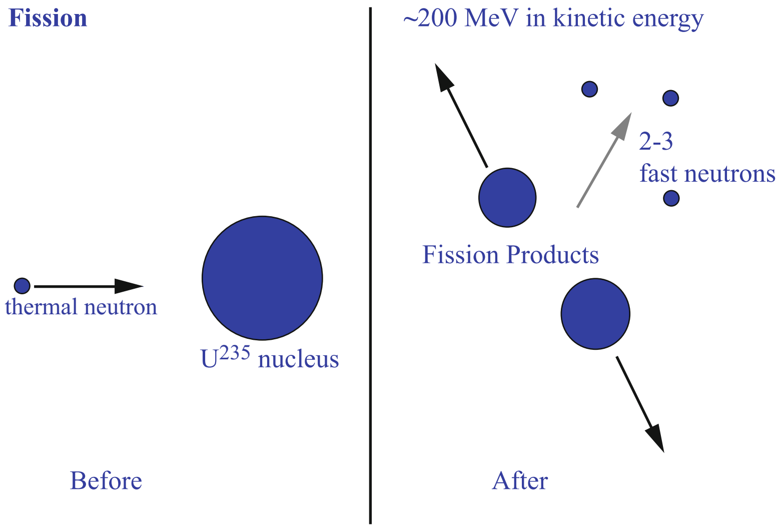

Fig. 1.13 A fission process

probability of inducing further fissions and hence have a low probability of generating more neutrons and thus sustaining a chain reaction. So we need to slow down the neutrons (i.e., thermalize or moderate them), which we do by using a moderator such as water. We also need to remove the heat generated. We control the process by controlling the number of neutrons since the number of fissions per second (and hence the heat produced) is proportional to the number of neutrons present to induce the fissions.

From this we can directly derive the basic functional requirements of a reactor. We need:

- A fuel such as U-235
- A moderator to thermalize (i.e., slow down) the fast neutrons
- A coolant to remove the heat
- A control system to control the number of neutrons
- A shielding system to protect equipment and people from radiation
- A system that pulls all this together into a workable device

1.8 Fission Spectra

The nuclear fission process is the fundamental reason that nuclear reactors can produce energy. It also determines all of the characteristics of a reactor from criticality to control to control to waste disposal. Understanding fission is fundamental to understanding reactor design, operation, and licensing. Fission occurs when a neutron enters the nucleus and forms a compound nucleus. The compound nucleus divides into two unsymmetrical parts about two magic number kernels. These kernels “bounce” apart until they are far enough apart to separate based on the Coulomb repulsion of their respective protons. Once the split occurs, the newly formed fission products are rich in energy and neutrons. They boil off 1~6 neutrons until there is not enough excitation energy left to release another neutron with its binding energy. The remaining excitation energy is released as prompt gamma rays. The fission products are still rich in neutrons having approximately six excess neutrons between them. These two nuclei then beta decay back to stability. This process can take a long time and is the reason that radioactive waste takes a long time to give up its energy. Associated with most beta decays are several gamma decays. Some of the beta decays produce residual nuclei that have enough energy to release another neutron, thus a neutron is then promptly released. Therefore, the half-life for delayed neutrons is determined by the intermediate beta decay.

1. Neutron contributes 6.0–7.5 MeV excitation energy.
2. Two magic number kernels form.

MAGIC NUMBERS

Protons	Neutrons
2	2
8	8
20	20
28	28
50	50
82	82
114	126

Light kernel: 28 protons, 50 neutrons; $A = 78$
Heavy kernel: 50 protons, 82 neutrons; $A = 132$
$U^{235} = 92$ protons, 143(+1) neutrons; $A = 235(+1)$
Excess protons = 14
Excess neutrons = 12

Consider a Typical Fission Product Split

Xe^{140}: 54 protons, 86 neutrons
Sr^{96}: 38 protons, 58 neutrons

Average Binding Energies

U^{235}: 7.6 MeV/nucleon
Xe^{140}: 8.4 MeV/nucleon
Sr^{96}: 8.7 MeV/nucleon

Binding energy available from thermal neutron fission		
U^{236} 7.6 MeV/nucleon × 236 nucleons	=	−1793.6 MeV
Xe^{140} 8.4 MeV/nucleon × 140 nucleons	=	1176.0 MeV
Sr^{96} 8.7 MeV/nucleon × 96 nucleons	=	835.2 MeV
Energy available from incoming neutron	=	7.6 MeV
Net binding energy released	=	225.2 MeV

Prompt Emissions

Nucleus Splits into Two Fission Products

1. Kernels repel each other due to Coulomb energy.
2. Each kernel is neutron rich.
3. The stable nuclides are determined by

$Z_{st} = 0.5 * A_{st}/(1.0 + 0.007826 * A_{st}{}^{2/3})$
$A_{st}(54) = 130$, $N_{st} = 76$, 10 excess neutrons
$A_{st}(38) = 88$, $N_{st} = 50$, 8 excess neutrons

Prompt Neutrons Boil Off

1. Neutrons evaporate until excitation energy is too low.
2. Remaining energy released as prompt gammas.
3. Evaporation spectrum

$$\chi(E) \sim E^{1/2}\mathrm{e}^{-E/T} \quad [E \text{ in MeV}] \quad \text{In the center of mass (CM) system}$$

Maxwellian spectrum—A fit in the laboratory reference system to the correct shape for a single fission product in the center of mass system.

The excitation energy of the nucleons in the two fission fragments can be given by

$$E^{*} = E_{\mathrm{r}} + B_{\mathrm{n}} + E_{\mathrm{n}} - \langle E_{\mathrm{f}} \rangle^{\mathrm{tot}}$$

E^* = energy available for internal excitation of fission products
E_{r} = total difference in binding energies of the fissioning nucleus and the two fission products
B_{n} = binding energy of neutron added to nucleus to cause fission
E_{n} = kinetic energy of neutron added to nucleus to cause fission
$\langle E_{\mathrm{f}} \rangle^{\mathrm{tot}}$ = total kinetic energy of fission products

The expected kinetic energy per nucleon of the light fission fragment is given by

$$\langle E_{\mathrm{f}} \rangle^{\mathrm{L}} = (A_{\mathrm{H}}/A_{\mathrm{L}})*\left(\langle E_{\mathrm{f}} \rangle^{\mathrm{tot}}/A\right)$$

A_{L} = mass number of light fission fragment
A_{H} = mass number of heavy fission fragment
A = mass number of compound nucleus undergoing fission

The kinetic energy of the heavy fragment is given by the converse relation.

Inside the nucleus, we assume a Fermi gas model for the statistical distribution of nucleon energies,

$$T_{\mathrm{m}} = \left(E^{*}/a\right)^{1/2}$$

where a is the nuclear-level density parameter, nominally A/11 MeV^{-1} to A/8 MeV^{-1}, and E^* is the residual energy of the nucleus after fission.

We can then estimate an average Maxwellian temperature given by

$$T_{\mathrm{M}} = \frac{1}{3}\left(\langle E_{\mathrm{f}} \rangle^{\mathrm{H}} + \langle E_{\mathrm{f}} \rangle^{\mathrm{L}}\right) + 8/9T_{\mathrm{m}}$$

If we use the same average kinetic energy per nucleon for both the heavy and light fragments and neglect the center of mass to lab transformation, we have a laboratory Maxwellian spectrum given by

$$\chi(E) = 2E^{1/2}*\mathrm{e}^{-E/T_{\mathrm{M}}}/\left(\pi^{1/2}T_{\mathrm{M}}^{3/2}\right) \quad [E \text{ in MeV}]$$

The following parameters (in MeV) are extracted from the paper by Madlang and Nix [2] for a value of **a** = A/9.

Nuclide	E_r	B_n	$\langle E_f \rangle^{tot}$	T_m	T_M	T_w
U^{233}	188.971	6.844	172.1	0.955	1.339	0.849
U^{235}	186.980	6.546	171.8	0.910	1.294	0.809
Pu^{239}	198.154	6.534	177.1	1.017	1.396	0.904

For ^{235}U this gives

$$\chi(E) = 0.7665E^{1/2}\mathrm{e}^{-E/1.293} \quad [E \text{ in MeV}]$$

Watt spectrum—If we use the calculated T_m for both nuclei and transform the Maxwellian from the center of mass to the laboratory system for the average fission fragment, we obtain the Watt spectrum:

$$T_w = 8/9T_m$$

$$\langle E_f \rangle^{ave} = \left(\langle E_f \rangle^H + \langle E_f \rangle^L\right)/2$$

$$\chi(E) = \mathrm{e}^{-(E+\langle E_f \rangle^{ave})/T_W} \sinh\left((2\langle E_f \rangle^{ave} E)^{1/2}/T_W\right)/(\pi \langle E_f \rangle^{ave} T_W)^{1/2} \quad [E \text{ in MeV}]$$

For U^{235} this gives

$$\chi(E) = 0.271\mathrm{e}^{-E/0.809}\sinh(2.38E)^{1/2} \quad [E \text{ in MeV}]$$

A better fit to the experimental data gives

$$\chi(E) = 0.4527\mathrm{e}^{-5/0.965}\sinh(2.29E)^{1/2} \quad [E \text{ in MeV}]$$

Madlang–Nix spectrum—The Madlang–Nix spectrum [2] is the most accurate spectrum used today and can be obtained from their paper referenced at the end of these notes. It computes average light and average heavy nuclei from fission and calculates an evaporation spectrum for each in the center of mass system. Then it translates both to the laboratory system and averages them. However, there is not a closed form representation, which is easily computable on a hand calculator. It is given by

$$\chi(E) = \frac{1}{2}\left\{N\left(E, E_f^L\right) + N\left(E, E_f^H\right)\right\}$$

where

$$N(E, E_f) = \frac{1}{3(E_f T_m)^{1/2}}\left\{u_2^{3/2}E_1(u_2) - u_1^{3/2}E(u_1) + \gamma\left(\frac{3}{2}, u_2\right) - \gamma\left(\frac{3}{2}, u_1\right)\right\}$$

and

E_f = average kinetic energy of the fission product in MeV
T_m = Fermi gas model temperature of the nucleus
$E_1(x)$ = the exponential integral of x

$$E_1(x) = \int_x^\infty \frac{\exp(-u)}{u} du$$

$\gamma(a, x)$ = the incomplete gamma function of order a

$$\gamma(a,x) = \int_0^x u^{a-1} \exp(-u) du$$

$$u_1 = \left(E^{1/2} - E_f^{1/2}\right)^2 / T_m$$

$$u_2 = \left(E^{1/2} + E_f^{1/2}\right)^2 / T_m$$

Average energy of neutrons released in fission ~2.0 MeV
Average number of prompt neutrons ~2.5
Most probable energy ~0.8 MeV

The average number of neutrons increases with the energy of the neutron causing fission.

Nuclide	N_{thermal}	dN/dE	N (14 MeV)
U^{233}	2.493	0.136	4.393
U^{235}	2.425	0.150	4.525
Pu^{239}	2.877	0.133	4.737

Prompt gammas boil off

Prompt gamma spectrum

$$\begin{aligned} N_\gamma(E) &= 6.6\gamma'\text{s/MeV}, & 0.1\,\text{MeV} < E < 0.6\,\text{MeV} \\ &= 20.2\text{e}^{-1.78\text{E}}\gamma'\text{s/MeV}, & 0.6\,\text{MeV} < E < 1.5\,\text{MeV} \\ &= 7.2\text{e}^{-1.09\text{E}}\gamma'\text{s/MeV}, & 1.5\,\text{MeV} < E < 10.5\,\text{MeV} \\ &\quad [E\,\text{in}\,\text{MeV}] \end{aligned}$$

Approximately 7.4 prompt gammas per fission
Approximately 7.2 MeV in prompt gammas per fission

This corresponds to about 3.6 MeV per fission product, which is about half the binding energy of a neutron. When the neutrons finish boiling off, each fission product is left with some residual energy. If the actual energy left is randomly distributed in value between its peak (the energy required to release another neutron) and zero, then the average energy left per fission product will be about half the binding energy of the last neutron or 7.0–8.5 MeV.

Decay Emissions

Delayed Betas

Assume that two neutrons are boiled off from Sr^{96} and one neutron is boiled off from Xe^{140}. To estimate the number of beta decays required to reach stability, assume that each neutron converted to a proton moves the nucleus toward the stability line. This means that each beta, decay, reduces the number of excess neutrons and increases the number of protons in the fission products. This gives

Number of excess neutrons remaining		
Beta decays	Sr^{94}	Xe^{139}
1	3.72 (Y^{94})	6.64 (Cs^{139})
2	1.16 (Zr^{94})	3.93 (Ba^{139})
3	−1.40 (Nb^{94})	1.20 (La^{139})
4		–1.53 (Ce^{139})

For this case, Zr^{94} and La^{139} are stable. Five beta decays will be required to reach stability. The three neutrons boiled off meant fewer than average beta decays were required. Of course, fewer or more neutrons could have been boiled off. On the average, considering all fission products, there are nominally six beta decays per fission required to reach two stable fission products.

Beta Decay

Beta decay occurs in groups of reactions given by Sagan's equation:

$$\log_{10}(f^*\tau) = C_\beta \quad \text{or} \quad \tau = \frac{10^{C_\beta}}{f_o E_\beta^5}$$

where:

$$f = f_0 (E_\beta)^5$$

$f_0 = 0.676$
$E_\beta =$ maximum decay energy in MeV
$\tau =$ mean life in seconds = (half-life)/0.693
$C_\beta =$ a constant associated with the forbiddingness of the beta (β)-decay
$C_\beta \sim$ 2.0–3.0 for super allowed decays

~4.0–6.0 for allowed decays
~6.0–8.0 for first-level forbidden decays
~8.0–10.0 for second-level forbidden decays

Note for neutron decay, we have:

$E_\beta = 0.782$ MeV
$t_{1/2} = 624$ s
$\tau = 900$ s
$C_\beta = 2.25$

The total energy released in beta decay is approximately 8.0 MeV per fission.

Delayed Neutrons

Delayed neutrons are given off some time after fission and have decay e-folding times in the range of ~0.25 to ~80.0 s (half-lives from ~0.17 to ~55 s). In order for a delayed neutron to be given off, a beta decay must occur first, and the beta decay must leave the new compound nucleus with enough excitation energy to emit a neutron. This is possible due to the difference in binding energy required between even–even and odd–odd nuclei. The beta decays that offer this possibility fall into the "allowed" decay category. Even if they were to be "super allowed" decays, the shortest possible mean lifetime would be about 3–3.5 ms. This corresponds to a maximum beta decay energy of 8.4–8.7 MeV or roughly the binding energy of an additional neutron in the fission product nucleus. If the nucleus had more energy than this, it would emit another neutron rather than waiting for a beta decay to occur. The fact that we have not measured decay constants shorter than this is probably not due to a lack of fast instrumentation but rather due to the physics of the decay process.

Nominally, six families of delayed neutrons can be measured. There are far more than six delayed neutron precursors, but their decay constants can be conveniently represented by no more than six decay constants that vary slightly with the fissioning species. The following data are taken from the text by Lewins: [3]

The data for thermal fission of U^{235}, $\beta = 0.00700$, $\beta/\lambda = 0.089$ s

Family	Yield fraction (β_I)	Decay constant (λ_I)
1	0.000266	0.0127
2	0.001492	0.0317
3	0.001317	0.115
4	0.002851	0.311
5	0.000897	1.40
6	0.000182	3.87

for thermal fission of Pu^{239}, $\beta = 0.00227$, $\beta/\lambda = 0.033$ s

Family	Yield fraction (β_I)	Decay constant (λ_I)
1	0.000086	0.0129
2	0.000637	0.0311
3	0.000491	0.134
4	0.000746	0.331
5	0.000234	1.26
6	0.000080	3.21

for thermal fission of U^{233}, $\beta = 0.00281$, $\beta/\lambda = 0.050$ s

Family	Yield fraction (β_I)	Decay constant (λ_I)
1	0.000241	0.0126
2	0.000769	0.0334
3	0.000637	0.131
4	0.000890	0.302
5	0.000205	1.27
6	0.000065	3.13

Unfortunately, in real reactors, there are usually several species of delayed neutrons present and trying to predict time-dependent reactor behavior by keeping track of each fissioning nuclide, and its measured delay families can get very messy. Ott and Neuhold [4] has presented a convenient scheme for presenting effective delayed yields based on the decay constants of Pu^{239} that matches the experimental curves very accurately. However, assuming the following sets of decay constants

Family	Decay constant (s^{-1})	e-Folding (s)	Half-life (s)
1	0.0129 ± 0.0002	77.5	53.7
2	0.0311 ± 0.0005	32.2	22.3
3	0.134 ± 0.003	7.5	5.2
4	0.331 ± 0.012	3.0	2.1
5	1.26 ± 0.12	0.8	0.6
6	3.21 ± 0.26	0.3	0.2

The yields for each of the delay families by nuclide are

Family	U^{233}	U^{235}	U^{238}	Th^{232}
1	0.00053	0.00060	0.00049	0.00143
2	0.00197	0.00364	0.00540	0.00776
3	0.00175	0.00349	0.00681	0.00843
4	0.00212	0.00628	0.01526	0.02156
5	0.00047	0.00179	0.00836	0.00838
6	0.00016	0.00070	0.00488	0.00204

	Pu^{239}	Pu^{240}	Pu^{241}	Pu^{242}
1	0.00024	0.00028	0.00019	0.00036
2	0.00176	0.00237	0.00369	0.00263
3	0.00136	0.00162	0.00276	0.00270
4	0.00207	0.00314	0.00534	0.00607
5	0.00065	0.00106	0.00310	0.00279
6	0.00022	0.00039	0.00032	0.00145

The average number of delayed neutrons given off varies with the fissioning species. Some typical numbers for thermal fission are

Nuclide	Delayed yield	Total yield	Delayed fraction
U^{233}	0.000698	2.493	0.0028
U^{235}	0.00170	2.425	0.0070
Pu^{239}	0.000662	2.877	0.0023

The delayed yield is fairly constant from thermal energies up to about 4 MeV, and then it falls off to about 50 % of its thermal value by 14 MeV. Since the total yield and prompt yield increase as a function of the fissioning neutron energy, β actually decreases slightly as energy increases. However, this is such a small effect that it is neglected and β is assumed constant for most neutronics calculations.

The delayed neutron energy spectrum actually varies with the delayed family under consideration, but a convenient average spectrum can be calculated by using a Maxwellian at a lower temperature than the prompt spectrum temperature.

$$\chi_{\mathrm{d}}(E) \sim E^{1/2}\mathrm{e}^{-E/T} \quad [E \text{ in MeV}]$$

$T(U^{235}) \sim 0.29$ MeV	$T(Pu^{239}) \sim 0.27$ MeV	$T(U^{233}) \sim 0.26$ MeV

The energy carried away by the delayed neutrons is negligible compared to the accuracy of the other energies generated during fission.

Delayed Gammas

The spectrum of delayed gammas is generally assumed to be similar to the prompt gamma spectrum.

The energy carried away by the delayed gammas is also about 7.0 MeV.

Fission energy summary

Total energy available	225.2 MeV
Neutron binding energy (2.43 * 7.5)	18.3
Neutron kinetic energy (2.43 * 2.0)	4.9
Fission product kinetic energy	172.0
Prompt gammas	6.0
Delay gammas	6.0
Decay betas	6.0
Neutrinos	12.0
	225.2 MeV
Less neutrinos and binding energy	30.2
Sensible energy	195.0 MeV

Average energies available from fission (MeV)

Nuclide	Thermal	Fast	14 MeV
Th^{232}	–	196.98	216.75
Pa^{233}	–	200.27	–
U^{233}	200.32	200.91	225.06
U^{234}	–	202.14	–

(continued)

Nuclide	Thermal	Fast	14 MeV
U^{235}	202.64	203.41	228.47
U^{236}	–	205.14	–
U^{238}	–	−208.96	229.77
Np^{237}	–	203.93	–
Pu^{238}	208.88	–	–
Pu^{239}	211.44	212.26	237.67
Pu^{240}	–	211.21	–
Pu^{241}	213.44	214.38	–
Pu^{242}	–	215.50	–
Am^{241}	213.62	–	–
Am^{242}	213.62	–	–
Am^{243}	–	221.25	–
Cm^{243}	218.65	–	–
Cm^{244}	218.03	–	–

Time History of Decay Energy Release

Traditionally, the decay energy release has been described by formulas of the form

$$P_{\text{decay}} = 2.66/t^{1/2}\,\text{MeV/Fiss/s}, \quad [\,t \text{ in s}], \quad 1.0 < t < 10^6\,\text{s}$$

This gives a total decay energy release from 1 s on of 13.3 MeV per fission.

A more recent formula that is somewhat more accurate is given by the work of R. J. LaBauve, T. R. England, and D. C. George of the Los Alamos National Laboratory [5]:

$$P_{\text{decay}} = \sum\nolimits_i \alpha_i e^{-\beta_i t}\,\text{MeV/Fiss/s}, \quad [t \text{ in s}], \quad 0 < t < 10^9\,\text{s}$$

where the α_i's and β_i's for ^{235}U are given by

Beta decays			Gamma decays		
α_i	β_i	α_i/β_i	α_i	β_i	α_i/β_i
6.169E−11	7.953E−10	7.757E−02	2.808E−11	7.332E−10	3.830E−02
2.249E−09	2.758E−08	8.154E−01	6.038E−10	4.335E−08	1.393E−02
2.365E-08	2.082E−07	1.136E−01	3.227E−08	1.932E−07	1.670E−01
2.194E−07	1.846E−06	1.189E−01	4.055E−07	1.658E−06	2.446E−01
1.140E−05	2.404E−05	4.742E−01	8.439E−06	2.147E−05	3.931E−01
1.549E−04	2.337E−04	6.628E−01	2.421E−04	2.128E−04	1.138E+00
1.991E−03	1.897E−03	1.050E+00	1.792E−03	1.915E−03	9.358E−01
3.256E−02	1.926E−02	1.691E+00	2.810E−02	1.769E−02	1.588E+00
2.227E−01	1.573E−01	1.416E+00	1.516E−01	1.652E−01	9.177E−01
5.381E−01	1.264E+00	4.257E−01	4.162E−01	1.266E+00	3.288E−01
1.282E−01	5.196E+00	2.481E−02	1.053E−01	5.222E+00	2.016E−02
	Total	6.869 MeV			5.785 MeV

This method gives a total decay energy per fission of 12.654 MeV per fission.

1.9 The Nuclear Fuel

When we start talking about fuel for nuclear power reactor as a source of fissile material for starting the reactor, we encounter some ambiguity since actual fissile material is mixed with some fertile material or diluents (see next section for the definition of fertile material), and normally this is the mixture that is referred to as fuel. Therefore, this provides fuels of 15 % $Pu^{49}O_2$ in natural form of UO_2, or "slightly enriched" UO_2 where uranium oxide has a content of 2 or 3 % U25 rather than 0.7 % in the natural ore, or "highly enriched" uranium–zirconium alloy with uranium being in 93 % U^{25} included [6].

The chemical property of uranium isotopes such as U^{238} cannot alone be used as fissionable source with energetic neutron for fuel of nuclear reactors. It is the fissile isotopes U^{233}, U^{235}, and Pu^{239} that are practical enough to be used for nuclear power plant fuels. Among all these nuclei, only U^{235} can be found as ore in nature, does exist as 0.71 at.% in natural uranium, and can be extracted by various means of separation processes in the related industries to bring it to the level of desired enrichment [7], which is any specified atom percent of U^{235}. The isotope U^{233} can be produced by the absorption of neutrons by Th^{232}.

The reactions involved are

$$\mathrm{Th}^{232}(\mathrm{n},\gamma)\mathrm{Th}^{232} \xrightarrow[22\mathrm{m}]{\beta^-} \mathrm{Pa}^{233} \xrightarrow[27.4\mathrm{d}]{\beta^-} \mathrm{U}^{233}$$

U^{233} holds considerable potential for fueling certain advanced types of reactors, in particular as part of Generation IV (GEN-IV) reactors. Molten salt reactor (MSR) uses nuclear fuel, which is dissolved in the molten fluoride salt as uranium tetrafluoride (UF_4) or thorium tetrafluoride (ThF_4), where also part of this fuel can be used as primary coolant in the form of molten salt mixture. GEN-IV is playing a big role in future existence of nuclear power plants, and it is a very promising technological approach to replace the existing old operational and experimental plants. In some cases such as gas-cooled fast reactor (GFR), providing the high temperature output of 850 °C justifies better thermal efficiencies using a direct Brayton cycle gas turbine [8–13]. For more details of each GEN-IV reactor, refer to Chap. 17 of this book.

The fuel for a nuclear power reactor is the source of energy by the fission process. The probability of neutron capture leading to fission is larger for slow neutrons than for fast neutrons. Hence, most practical reactors are "thermal" reactors, that is, they utilize the higher thermal cross sections. Possible fuels include some of the various isotopes of uranium (U) and plutonium (Pu). The only naturally occurring fuel with suitable properties of significant quantities is U^{235}; hence, most reactors use this fuel (see Fig. 1.14), 0.7 % U-235. The rest is U^{238}. This percentage is too low to sustain a chain reaction when combined with most practical moderators. Hence, either the probability of fission must be enhanced or the moderator effectiveness must be enhanced. One group of reactor types (PWR, BWR, and HTGR) enriches the fuel (a costly task) and uses a cheap moderator (ordinary water or graphite).

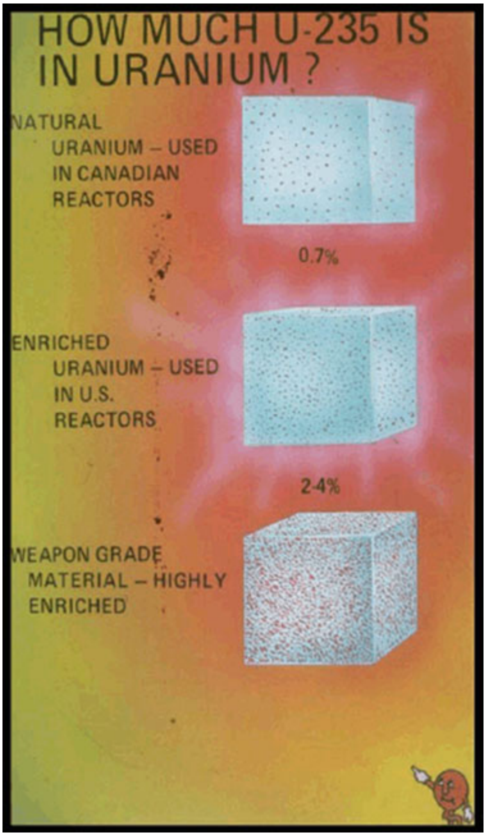

Fig. 1.14 Uranium enrichment

It should be mentioned that isotopes such as Th^{232} which are not themselves fissile (though they may be fissionable) but which can be used as the raw materials for production of fissile isotopes are called *fertile*. See next section for the definition of fertile material.

Pu^{239} is produced by the absorption of neutrons by U^{235} via the following reactions:

$$U^{238}(n,\gamma)Th^{232} \xrightarrow[23\mathrm{m}]{\beta^-} Pa^{233} \xrightarrow[2.3\mathrm{d}]{\beta^-} Pu^{239}$$

The Manhattan Project during World War II and for nuclear weapon rushed production of plutonium, and it has been continued since the war on an even greater scale. For the following reasons, plutonium production is still very active, although comparatively has little application as a fuel reactor. The reasons are [7]:

1. Pu^{239} is more expensive to produce than U^{235}.
2. It is less satisfactory than U^{235} for fueling most of reactors built since World War II, because of its high value α.

3. The physical and chemical properties of plutonium make it a difficult material to work with.
4. Little Pu^{239} has been available because of the competing demand of the weapons program.

Nevertheless, as in the case of U^{233}, Pu^{239} appears to be a far better fuel than U^{235} for certain advanced types of reactor, and the future will undoubtedly see an increased use of this isotope.

Note that a certain amount of Pu^{239} accumulates in any reactor containing U^{238}, as the result of neutron absorption. In a similar fashion the fissile isotope Pu^{241} accumulates in reactors containing Pu^{239} by the absorption of two additional neutrons, and bear in your mind that at this point, the absorption of a neutron by Pu^{239} does not always lead to fission. The reactions involved are [7]

$$\mathrm{Pu}^{239} + \mathrm{n}\begin{array}{l} \nearrow \text{fission} \\ \searrow \mathrm{Pu}^{240}(\mathrm{n},\gamma)\mathrm{Pu}^{241} \end{array}$$

Note that the operation of a reactor certainly will be impacted by the presence of Pu^{241}, and therefore it should be taken into account in the design of Pu^{239}-fueled reactor or reactors containing large amounts of U^{238}.

1.9.1 Fertile Material

All of the neutron absorption reactions that do not result in fission lead to the production of new nuclides through the process known as *transmutation*. These nuclides can, in turn, be transmuted again or may undergo radioactive decay to produce still different nuclides. The nuclides that are produced by this process are referred to as transmutation products. Because several of the fissile nuclides do not exist in nature, they can only be produced by nuclear reactions (transmutation).

The target nuclei for such reactions are said to be fertile. *Fertile materials* are materials that can undergo transmutation to become fissile materials. Figure 1.15 traces the transmutation mechanism by which two fertile nuclides, thorium-232 and uranium-238, produce uranium-233 and plutonium-239, respectively; see Fig. 1.15.

If a reactor contains fertile material in addition to its fissile fuel, some new fuel will be produced as the original fuel is burned up. This is called conversion. Reactors that are specifically designed to produce fissionable fuel are called "breeder" reactors. In such reactors, the amount of fissionable fuel produced is greater than the amount of fuel burnup. If less fuel is produced than used, the process is called conversion, and the reactor is termed a "converter."

It is important to remember that the "fuel" generally refers to a mixture of fissile material with fertile or diluents.

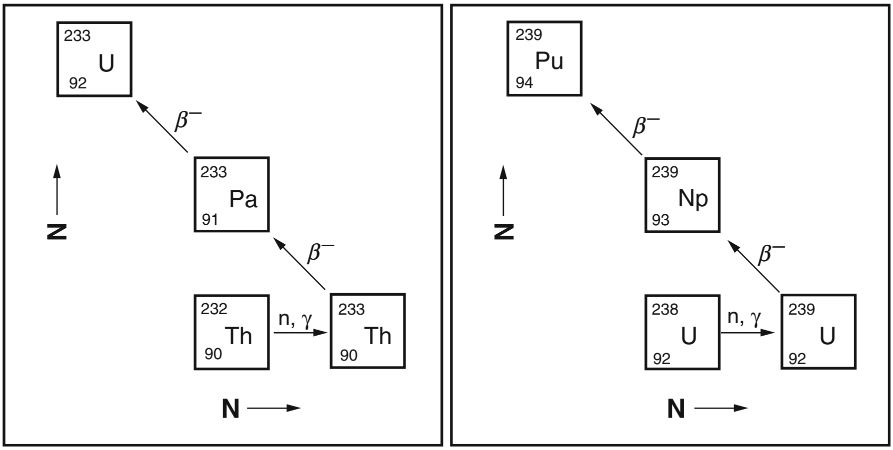

Fig. 1.15 Conversion of fertile nuclides to fissile nuclides

1.10 Liquid Drop Model of a Nucleus

The nucleus is held together by the attractive nuclear force between nucleons, which was discussed in the previous chapter. The characteristics of the nuclear force are listed below:

(a) Very short range, with essentially no effect beyond nuclear dimensions (10^{-13} cm)
(b) Stronger than the repulsive electrostatic forces within the nucleus
(c) Independent of nucleon pairing, in that the attractive forces between pairs of neutrons are no different than those between pairs of protons or a neutron and a proton
(d) Saturable, that is, a nucleon can attract only a few of its nearest neighbors

One theory of fission considers the fissioning of a nucleus similar in some respect to the splitting of a liquid drop. This analogy is justifiable to some extent by the fact that a liquid drop is held together by molecular forces that tend to make the drop spherical in shape and that try to resist any deformation in the same manner as nuclear forces are assumed to hold the nucleus together. By considering the nucleus as a liquid drop, the fission process can be described.

Referring to Fig. 1.16a, the nucleus in the ground state is undistorted, and its attractive nuclear forces are greater than the repulsive electrostatic forces between the protons within the nucleus.

When an incident particle (in this instance a neutron) is absorbed by the target nucleus, a compound nucleus is formed. The compound nucleus temporarily contains all the charge and mass involved in the reaction and exists in an excited state. The excitation energy added to the compound nucleus is equal to the binding energy contributed by the incident particle plus the kinetic energy possessed by that

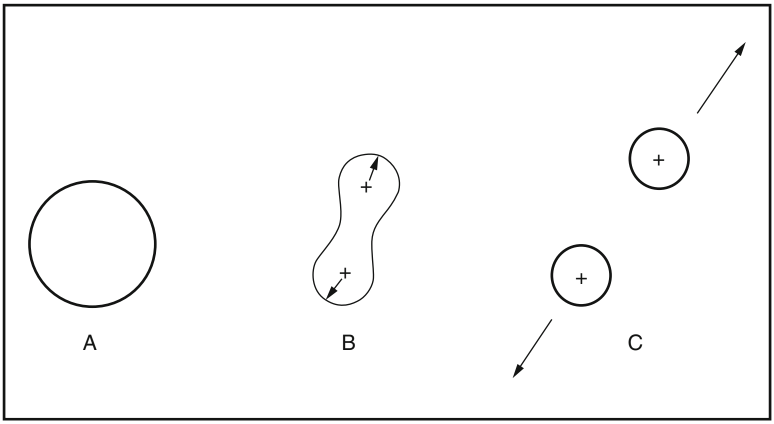

Fig. 1.16 Liquid drop model of fission

particle. Figure 1.16b illustrates the excitation energy thus imparted to the compound nucleus, which may cause it to oscillate and become distorted. If the excitation energy is greater than a certain critical energy, the oscillations may cause the compound nucleus to become dumbbell-shaped. When this happens, the attractive nuclear forces (short range) in the neck area are small due to saturation, while the repulsive electrostatic forces (long range) are only slightly less than before. When the repulsive electrostatic forces exceed the attractive nuclear forces, nuclear fission occurs, as illustrated in Fig. 1.16c.

1.11 Summary of Fission Process

The important information for nuclear fission is summarized as follows:

- The fission process can be explained using the liquid drop model of a nucleus. In the ground state the nucleus is nearly spherical in shape. After the absorption of a neutron, the nucleus will be in an excited state and start to oscillate and become distorted. If the oscillations cause the nucleus to become shaped like a dumbbell, the repulsive electrostatic forces will overcome the short-range attractive nuclear forces, and the nucleus will split in two.
- Excitation energy is the amount of energy a nucleus has above its ground state.
- Critical energy is the minimum excitation energy that a nucleus must have before it can fission.
- Fissile material is a material for which fission is possible with neutrons that have zero kinetic energy. Fissionable material is a material for which fission caused by neutron absorption is possible provided the kinetic energy added with the binding energy is greater than the critical energy. Fertile material is material that can undergo transmutation to become fissile material.

- Transmutation is the process of neutron absorption and subsequent decay, which changes one nuclide to another nuclide. Conversion is the process of transmuting fertile material into fissile material in a reactor, where the amount of fissile material produced is less than the amount of fissile material consumed. Breeding is the same as conversion, except the amount of fissile material produced is more than the amount of fissile material consumed.
- The curve of binding energy per nucleon increases quickly through the light nuclides and reaches a maximum at a mass number of about 56. The curve decreases slowly for mass numbers greater than 60.
- The heaviest nuclei are easily fissionable because they require only a small distortion from the spherical shape to allow the Coulomb forces to overcome the attractive nuclear force, forcing the two halves of the nucleus apart.
- Uranium-235 fissions with thermal neutrons because the binding energy released by the absorption of a neutron is greater than the critical energy for fission. The binding energy released by uranium-238 absorbing a neutron is less than the critical energy; therefore, additional kinetic energy must be possessed by the neutron for fission to be possible.

1.12 Reactor Power Calculation

Multiplying the reaction rate per unit volume by the total volume of the core results in the total number of reactions occurring in the core per unit time. If the amount of energy involved in each reaction were known, it would be possible to determine the rate of energy release (power) due to a certain reaction.

In a reactor where the average energy per fission is 200 MeV, it is possible to determine the number of fissions per second that are necessary to produce one watt of power using the following conversion factors.

1 fission = 200 MeV
1 MeV = 1.602×10^{-6} ergs
1 erg = 1×10^{-7} W s

$$1\,\mathrm{W}\left(\frac{1\,\mathrm{erg}}{1\times10^{-7}\,\mathrm{W\,s}}\right)\left(\frac{1\,\mathrm{MeV}}{1.602\times10^{-6}\,\mathrm{erg}}\right)\left(\frac{1\,\mathrm{fission}}{200\,\mathrm{MeV}}\right)=3.12\times10^{10}\,\frac{\mathrm{fission}}{\mathrm{s}}$$

This is equivalent to stating that 3.12×10^{10} fissions release 1 W s of energy.

The power released in a reactor can be calculated based on relation of $R = \phi\Sigma$; here, R is the reaction rate (reactions/s), ϕ the neutron flux (neutron/cm^2 s), and Σ the macroscopic cross section (cm^{-1}). Multiplying the reaction rate by the volume of the reactor results in the total fission rate for the entire reactor. Dividing by the number of fissions per watt second results in the power released by fission in the reactor in units of watts. This relationship is shown mathematically in Eq. 1.37:

$$P = \frac{\phi_{\text{th}} \sum_{\text{f}} V}{3.12 \times 10^{10} \frac{\text{fission}}{\text{s}}} \tag{1.37}$$

where:

$P =$ power (W)
$\phi_{\text{th}} =$ thermal neutron flux (neutron/cm^2-s)
$\Sigma_{\text{f}} v =$ macroscopic cross section for fission (cm^{-1})
$V =$ volume of core (cm^3)

1.13 Relationship Between Neutron Flux and Reactor Power

In an operating reactor, the volume of the reactor is constant. Over a relatively short period of time (days or weeks), the number density of the fuel atoms is also relatively constant. Since the atom density and microscopic cross section are constant, the macroscopic cross section must also be constant. Examining Eq. 1.35, it is apparent that if the reactor volume and macroscopic cross section are constant, then the reactor power and the neutron flux are directly proportional. This is true for day-to-day operation. The neutron flux for a given power level will increase very slowly over a period of months due to the burnup of the fuel and resulting decrease in atom density and macroscopic cross section.

In summary:

- The reaction rate is the number of interactions of a particular type occurring in a cubic centimeter of material in a second.
- The reaction rate can be calculated by the equation below.

$$R = \phi\Sigma$$

- Over a period of several days, while the atom density of the fuel can be considered constant, the neutron flux is directly proportional to the reactor power.

Problems

Problem 1.1 If atomic mass unit is designated by u, where 1 u is exactly one-twelfth of the mass of the ^{12}C atom, equal to 1.661×10^{-27} kg, then calculate the energy equivalent to a conventional mass equal to 1 u.

Problem 1.2 Calculate the energy as Problem 1.1 using MeV as units.

Problem 1.3 (a) Calculate the mass defect and the binding energy for a nucleus of an isotope of tin ^{120}Sn (atomic mass $M = 119.9022$ u) and for an isotope of uranium ^{235}U (atomic mass $M = 235.0439$). Assume the measured mass of the atom is M; the mass defect ΔM is given by

$$\Delta M = Z \cdot \left(m_p + m_e\right) + (A - Z) \cdot m_n - M$$

$Z \cdot m_p =$ total mass of proton
$Z \cdot m_e =$ total mass of electron
$(A - Z) \cdot m_n =$ total mass of neutrons

(b) Assume the total binding energy for uranium is approximately the same as tin; what would be the total energy that will be released after fission of a single U^{235} nucleus?

Problem 1.4 Calculate the mass defect for lithium-7. The mass of lithium-7 is 7.016003 amu. Assuming that:

$m_p =$ mass of a proton (1.007277 amu)
$m_n =$ mass of neutron (1.008665 amu)
$m_e =$ mass of an electron (0.000548597 amu)

Problem 1.5 Consider that 1 amu is equivalent to 931.5 MeV of energy; the binding energy can be calculated using the following relationship:

$$\text{Binding energy} = \Delta m\left(\frac{931.5\,\text{MeV}}{1\,\text{amu}}\right)$$

Then calculate the mass defect and binding energy for uranium235. One uranium235 atom has a mass of 235.043924 amu.

Problem 1.6 Calculate the decay constant, mean life, and half-life of a radioactive isotope which radioactivity after 100 days is reduced 1.07 times.

Problem 1.7 A block of aluminum has a density of 2.699 g/cm^3. If the gram atomic weight of aluminum is 26.9815 g, then calculate the atom density of aluminum.

Problem 1.8 Since the activity and the number of atom are always proportional, they may be used interchangeably to describe any given radionuclide population. Therefore, the following is true.

$$A = A_0 e^{-\lambda t}$$

where

$A =$ activity present at time t
$A_0 =$ activity initially present
$\lambda =$ decay constant (time^{-1})
$t =$ time

Assuming a sample of material contains 20 μg of californium-252 and this element has a half-life of 2.638 years; then calculate:

(a) The number of californium-252 atoms initially present
(b) The activity of californium-252 in curies, assuming the relationship between the activity, number of atoms, and decay constant is shown in $A = \lambda N$, where A is the activity of nuclide (disintegrations/s), λ-decay constant of the nuclide (1/s), and finally N the number of atoms of the nuclide in the sample
(c) The number of californium-252 atoms that will remain in 12 years
(d) The time it will take for the activity to reach 0.001 curies

Problem 1.9 Plot the radioactive decay curve for nitrogen-16 over a period of 100 s. The initial activity is 142 curies and the half-life of nitrogen-16 is 7.13 s. Plot the curve on both linear rectangular coordinates and a semilog scale.

Problem 1.10 Find the macroscopic thermal neutron absorption cross section for iron, which has a density of 7.86 g/cm. The microscopic cross section for absorption of iron is 2.56 barns, and the gram atomic weight is 55.847 g.

Problem 1.11 An alloy is composed of 95 % aluminum and 5 % silicon (by weight). The density of the alloy is 2.66 g/cm. Properties of aluminum and silicon are shown below.

Element	Gram atomic weight	σ_a(barns)	σ_s(barns)
Aluminum	26.9815	0.23	1.49
Silicon	28.0855	0.16	2.20

1. Calculate the atom densities for the aluminum and silicon.
2. Determine the absorption and scattering macroscopic cross sections for thermal neutrons.
3. Calculate the mean free paths for absorption and scattering.

Problem 1.12 What is the value of σ_f for uranium-235 for thermal neutrons at 500 °F? Uranium-235 has σ_f of 583 barns at 68 °F.

Problem 1.13 If a one cubic centimeter section of a reactor has a macroscopic fission cross section of 0.1 cm^{-1}, and if the thermal neutron flux is 10^{13} neutrons/cm^2 s, what is the fission rate in that cubic centimeter?

Problem 1.14 A reactor operating at a flux level of 3×10^{13} neutrons/cm^2 s contains 10^{20} atoms of uranium-235 per cm^3. The reaction rate is 1.29×10^{12} fission/cm^3. Calculate Σ_f and σ_f.

Problem 1.15 The microscopic cross section for the capture of thermal neutrons by hydrogen is 0.33 barn and for oxygen 2×10^{-4} barn. Calculate the macroscopic capture cross section of the water molecule for thermal neutrons.

Problem 1.16 Calculate the minimum energy that a neutron with energy 1 MeV can be reduced to after collision with:

(a) Nucleus of hydrogen
(b) Nucleus of carbon

References

1. P.E. Hodgson, E. Gadioli, E. Gadioli Erb, *Introductory Nuclear Physics* (Oxford Science Publications, Oxford, 1997)
2. D.G. Madland, J. Rayford Nix, New calculation of prompt fission neutron spectra and average prompt neutron multiplicities. Nucl. Sci. Eng. **81**, 213–271 (1982)
3. J. Lewins, *Nuclear Reactor Kinetics and Control* (Pergamon Press, Oxford, 1978)
4. K. Ott, R.J. Neuhold, *Nuclear Reactor Dynamics* (American Nuclear Society, LaGrange Park, 1985)
5. R.J. LaBauve, T.R. England, D.C. George, C.W. Maynard, Fission product analytic impulse source functions. Nucl. Technol. **56**, 332–339 (1982)
6. A.F. Henry, *Nuclear Reactor Analysis* (The MIT Press, Cambridge, 1975)
7. J.R. Lamarsh, *Introduction to Nuclear Reactor Theory* (Addison Wesley, Boston, 1966)
8. B. Zohuri, *Combined Cycle Driven Efficiency for Next Generation Nuclear Power Plants: An Innovative Design Approach* (Springer, New York, 2015)
9. B. Zohuri, P. McDaniel, A comparison of a recuperated open cycle (air) brayton power conversion system with the traditional steam rankine cycle for the next generation nuclear power plant. Nucl. Sci., October 2015
10. B. Zohuri, *Innovative Open Air Brayton Combined Cycle Systems for the Next Generation Nuclear Power Plants* (University of New Mexico Publications, Albuquerque, 2014)
11. P.J. McDaniel, B. Zohuri, C.R.E. de Oliveira, in *A Combined Cycle Power Conversion System for Small Modular LMFBRs*, ANS Transactions, September 2014
12. *Cycle Power Conversion System for the Next Generation Nuclear Power Plan*, ANS Transactions, November 2012
13. C. Forsberg, P. McDaniel, B. Zohuri, Variable electricity and steam from salt, helium, and sodium cooled base-load reactors with gas turbines and heat storage, in *Proceedings of ICAPP* 2015

Chapter 2
Modeling Neutron Transport and Interactions

It is essential to know the spatial and energy distributions of the neutrons in a field in a nuclear fission reactor, D–T (or D–D) fusion reactor, or other nuclear reactors populated with large numbers of neutrons. It is obvious why the spatial distribution should be known, and because neutron reactions vary widely with energy, the energy distribution is also a critical parameter. The neutron energy distribution is often called the neutron spectrum. The neutron distribution satisfies transport equation. It is usually difficult to solve this equation, and often approximated equation so-called diffusion equation is solved instead. In this chapter only overview of transport equation and diffusion equation of neutrons is presented, and methods for solving these equations are presented in the following sections.

2.1 Transport Equations

In order to predict the reaction rates in a nuclear reactor, we need to know two entities. We need to know the nuclear cross sections as a function of space and position, and we need to know the neutron population as a function of time, space, and position. We can calculate this neutron population if we can develop a balance equation, or conservation equation, to describe the neutron population. Actually, there are two approaches to derive the balance or conservation equation. There is the integrodifferential equation approach and the complete integral equation approach. We will use the integrodifferential approach for most of this class because with suitable approximations it reduces to the multigroup diffusion equations or simply the diffusion equation. The complete integral equation is the equation solved by Monte Carlo transport codes and therefore is used in more advanced analyses. Further discussion of transport equations will take place in Chap. 3 of the book.

B. Zohuri, *Neutronic Analysis For Nuclear Reactor Systems*,
DOI 10.1007/978-3-319-42964-9_2

Before we move on further, we need to define few concepts in neutronic analysis which falls under category of *neutron transport analysis* concept and reactor design process that one should know, and they are as follows.

2.2 Reaction Rates

It is possible to determine the rate at which a nuclear reaction will take place based on the neutron flux, cross section for the interaction, and atom density of the target. This relationship illustrates how a change in one of these items affects the reaction rate.

If the total path length of all the neutrons in a cubic centimeter in a second is known, neutron flux (ϕ), and if the probability of having an interaction per centimeter path length is also known, which we called it macroscopic cross section (Σ), multiply them together to get the number of interactions taking place in that cubic centimeter in one second. This value is known as the reaction rate and is denoted by the symbol R. The reaction rate can be calculated by the equation shown below:

$$R = \phi\Sigma \tag{2.1}$$

where

R = reaction rate (reactions/s)
ϕ = neutron flux (neutron/cm^2 s)
Σ = macroscopic cross section (cm^{-1})

Substituting the fact that $\Sigma = N\sigma$ into Eq. 2.1 yields the following equation as

$$R = \phi N\sigma \tag{2.2}$$

where

σ = microscopic cross section (cm^2)
N = atom density (atoms/cm^3)

The reaction rate calculated will depend on which macroscopic cross section is used in the calculation. Normally, the reaction rate of greatest interest is the fission reaction rate.

In addition to using Eq. 2.1 to determine the reaction rate based on the physical properties of material, it is also possible to algebraically manipulate the equation to determine physical properties if the reaction rate is known.

2.3 Reactor Power Calculation

Multiplying the reaction rate per unit volume by the total volume of the core results in the total number of reactions occurring in the core per unit time. If the amount of energy involved in each reaction were known, it would be possible to determine the rate of energy release (power) due to a certain reaction.

In a reactor where the average energy per fission is 200 MeV, it is possible to determine the number of fissions per second that are necessary to produce one watt of power using the following conversion factors:

$$\begin{aligned} 1\ \text{fission} &= 200\,\text{MeV} \\ 1\ \text{MeV} &= 1.602 \times 10^{-6}\,\text{ergs} \\ 1\ \text{erg} &= 1 \times 10^{-7}\,\text{W s} \end{aligned}$$

$$1\,\text{W}\left(\frac{1\,\text{erg}}{1 \times 10^{-7}\,\text{W s}}\right)\left(\frac{1\,\text{MeV}}{1.602 \times 10^{-6}\,\text{erg}}\right)\left(\frac{1\,\text{fission}}{200\,\text{MeV}}\right) = 3.12 \times 10^{10}\,\frac{\text{fission}}{\text{s}}$$

This is equivalent to stating that 3.12×10^{10} fissions release 1 W s of energy.

The power released in a reactor can be calculated based on Eq. 2.1. Therefore, multiplying the reaction rate by the volume of the reactor would result in the total fission rate for the entire reactor. Dividing by the number of fissions per watt second would result in the power released by fission in the reactor in units of watts. This relationship is shown mathematically in Eq. 2.3:

$$P = \frac{\phi_{\text{th}} \Sigma_{\text{f}} V}{3.12 \times 10^{10}\,\frac{\text{fissions}}{\text{W s}}} \tag{2.3}$$

where

P = power (W)
ϕ_{th} = thermal neutron flux (neutrons/cm^2 s)
Σ_{f} = macroscopic cross section for fission (cm^{-1})
V = volume of core (cm^3)

2.4 Relationship Between Neutron Flux and Reactor Power

In an operating reactor, the volume of the reactor is constant. Over a relatively short period of time (days or weeks), the number density of the fuel atoms is also relatively constant. Since the atom density and microscopic cross section are constant, the macroscopic cross section must also be constant. Examining Eq. 2.3, it is apparent that if the reactor volume and macroscopic cross section are constant, then the reactor power and the neutron flux are directly proportional. This is true for day-to-day operation. The neutron flux for a given power level will increase very slowly over a period of months due to the burnup of the fuel and resulting decrease in atom density and macroscopic cross section.

2.5 Neutron Slowing Down and Thermalization

In thermal reactors, the neutrons that cause fission are at a much lower energy than the energy level at which they were born from fission. In this type of reactor, specific materials must be included in the reactor design to reduce the energy level of the neutrons in an efficient manner.

Fission neutrons are produced at an average energy level of 2 MeV and immediately begin to slow down as the result of numerous scattering reactions with a variety of target nuclei. After a number of collisions with nuclei, the speed of a neutron is reduced to such an extent that it has approximately the same average kinetic energy as the atoms (or molecules) of the medium in which the neutron is undergoing elastic scattering. This energy, which is only a small fraction of an electron volt at ordinary temperatures (0.025 eV at 20 °C), is frequently referred to as the thermal energy, since it depends upon the temperature. Neutrons whose energies have been reduced to values in this region (less than 1 eV) are designated thermal neutrons. The process of reducing the energy of a neutron to the thermal region by elastic scattering is referred to as *thermalization*, slowing down, or moderation. The material used for the purpose of thermalizing neutrons is called a moderator. A good moderator reduces the speed of neutrons in a small number of collisions, but does not absorb them to any great extent. Slowing the neutrons in as few collisions as possible is desirable in order to reduce the amount of neutron leakage from the core and also to reduce the number of resonance absorptions in nonfuel materials. Neutron leakage and resonance absorption will be discussed in the next module.

The ideal moderating material (moderator) should have the following nuclear properties:

- Large scattering cross section
- Small absorption cross section
- Large energy loss per collision

A convenient measure of energy loss per collision is the logarithmic energy decrement. The *average logarithmic energy decrement* is the average decrease per collision in the logarithm of the neutron energy. This quantity is represented by the symbol ξ (Greek letter xi) and it is shown as

$$\begin{aligned} \xi &= \ln E_{\mathrm{i}} - \ln E_{\mathrm{f}} \\ \xi &= \ln\left(\frac{E_{\mathrm{i}}}{E_{\mathrm{f}}}\right) \end{aligned} \tag{2.4}$$

where

ξ = average logarithmic energy decrement
E_{i} = average initial neutron energy
E_{f} = average final neutron energy

The symbol ξ is commonly called the average logarithmic energy decrement because of the fact that a neutron loses, on the average, a fixed fraction of its energy per scattering collision. Since the fraction of energy retained by a neutron in a single elastic collision is a constant for a given material, it is also a constant. Because it is a constant for each type of material and does not depend upon the initial neutron energy, it is a convenient quantity for assessing the moderating ability of a material.

The values for the lighter nuclei are tabulated in a variety of sources. The following commonly used approximation may be used when a tabulated value is not available:

$$\xi = \frac{2}{A + \frac{2}{3}} \tag{2.5}$$

This approximation is relatively accurate for mass numbers (A) greater than 10, but for some low values of A, it may be in error by over three percent.

Since ξ represents the average logarithmic energy loss per collision, the total number of collisions necessary for a neutron to lose a given amount of energy may be determined by dividing into the difference of the natural logarithms of the energy range in question. The number of collisions (N) to travel from any energy, E_{high}, to any lower energy, E_{low}, can be calculated as shown below:

$$\begin{aligned} N &= \frac{\ln E_{\text{high}} - \ln E_{\text{low}}}{\xi} \\ &= \frac{\ln\left(\frac{E_{\text{high}}}{E_{\text{low}}}\right)}{\xi} \end{aligned} \tag{2.6}$$

Sometimes it is convenient, based upon the information known, to work with an average fractional energy loss per collision as opposed to an average logarithmic fraction. If the initial neutron energy level and the average fractional energy loss per collision are known, the final energy level for a given number of collisions may be computed using the following formula:

$$E_N = E_0(1 - x)^N \tag{2.7}$$

where

E_0 = initial neutron energy
E_N = neutron energy after N collisions
x = average fractional energy loss per collision
N = number of collision

2.6 Macroscopic Slowing Down Power

Although the logarithmic energy decrement is a convenient measure of the ability of a material to slow neutrons, it does not measure all necessary properties of a moderator. A better measure of the capabilities of a material is the macroscopic slowing down power. The *macroscopic slowing down power* (MSDP) is the product of the logarithmic energy decrement and the macroscopic cross section for scattering in the material. Equation 2.8 illustrates how to calculate the macroscopic slowing down power:

$$\mathrm{MSDP} = \xi \Sigma_\mathrm{s} \tag{2.8}$$

2.7 Moderate Ratio

Macroscopic slowing down power indicates how rapidly a neutron will slow down in the material in question, but it still does not fully explain the effectiveness of the material as a moderator. An element such as boron has a high logarithmic energy decrement and a good slowing down power, but it is a poor moderator because of its high probability of absorbing neutrons.

The most complete measure of the effectiveness of a moderator is the moderating ratio. The *moderating ratio* is the ratio of the macroscopic slowing down power to the macroscopic cross section for absorption. The higher the moderating ratio, the more effectively the material performs as a moderator. Equation 2.9 shows how to calculate the moderating ratio of a material:

$$\mathrm{MR} = \frac{\xi \Sigma_\mathrm{s}}{\Sigma_\mathrm{a}} \tag{2.9}$$

Moderating properties of different materials are compared in Table 2.1.

Table 2.1 Moderating properties of materials

Material	ξ	Number of collision thermalized	Macroscopic slowing down power	Moderating ratio
H_2O	0.927	19	1.425	62
D_2O	0.510	35	0.177	4830
Helium	0.427	42	9×10^{-6}	51
Beryllium	0.207	86	0.154	126
Boron	0.171	105	0.092	0.00086
Carbon	0.158	114	0.083	216

2.8 Integrodifferential Equation (Maxwell–Boltzmann Equation)

The integrodifferential equation is also called the Maxwell–Boltzmann equation after its original developers. However, they developed it in its most complete nonlinear form wherein each particle could interact with every other particle in the solution space. Here, we will only deal with the linear form, wherein we only consider neutron interactions with nuclei. We will not consider nuclei interactions with other nuclei or neutron interactions with other neutrons. There are, on the order of 10^{21-22}, nuclei per cubic centimeter in a typical reactor and on the order of 10^{13-15} neutrons in the same reactor. The interactions of neutrons with themselves are very low probability events compared with their interactions with nuclei. In addition, nuclei are held in place and do not interact with each other except as characterized by an equilibrium temperature mode4l.

Consider Fig. 2.1.

Now define

$n\left(\vec{\boldsymbol{r}}, \vec{\boldsymbol{\Omega}}, E, t\right) d^3r\, d\vec{\boldsymbol{\Omega}}\, dE\, dt$ = the number of neutrons in a differential spatial volume $d^3r = d\vec{\boldsymbol{r}}$ about $\vec{\boldsymbol{r}}$, moving in direction $d\vec{\boldsymbol{\Omega}}$ about direction $\vec{\boldsymbol{\Omega}}$ with an energy within dE about E, in a time interval dt about time t. This quantity will be called the neutron angular density. Note bold quantities indicate a vector. Thus, n is dependent on seven variables.

Now we can write a balance equation for n as simply

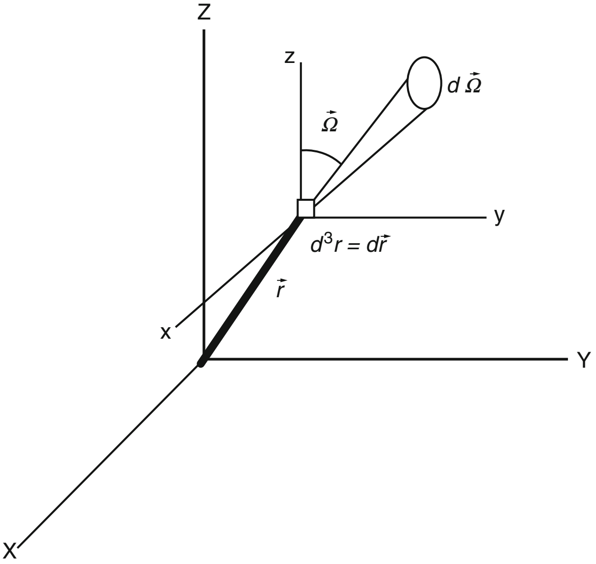

Fig. 2.1 Solid angle

$$\frac{dn}{dt} = \text{Gains} - \text{Losses} \tag{2.10}$$

The principle gains will be composed of three terms. These are

1. Inhomogeneous sources or direct production of neutrons
2. In-scatter sources where at a point a neutron shows up with energy E and going in direction $\vec{\boldsymbol{\Omega}}$ as the result of scattering $\vec{\boldsymbol{r}}$
3. Fission sources that are the result of a fission occurring at **r**

The inhomogeneous source is given by

$$IS = q\left(\vec{\boldsymbol{r}}, \vec{\boldsymbol{\Omega}}, E, t\right) d\vec{\boldsymbol{r}}\, d\vec{\boldsymbol{\Omega}}\, dE \tag{2.11}$$

The in-scatter source term is given by

$$SS = \int_{E'} \int_{\vec{\boldsymbol{\Omega}}'} \Sigma_{\mathrm{s}}\left(E', \boldsymbol{\Omega}' \to E, \vec{\boldsymbol{\Omega}}\right) v(E') n\left(\vec{\boldsymbol{r}}, E', \vec{\boldsymbol{\Omega}}', t\right) dE'\, d\vec{\boldsymbol{\Omega}}'\, d\vec{\boldsymbol{r}}\, d\vec{\boldsymbol{\Omega}}\, dE \tag{2.12}$$

And the fission source is given by

$$\int_{E'} \int_{\vec{\boldsymbol{\Omega}}'} \chi(E) \frac{\nu(E')}{4\pi} \Sigma_{\mathrm{f}}(E') v(E') n\left(\vec{\boldsymbol{r}}, E', \vec{\boldsymbol{\Omega}}', t\right) dE'\, d\vec{\boldsymbol{\Omega}}'\, d\vec{\boldsymbol{r}}\, dE\, d\vec{\boldsymbol{\Omega}} \tag{2.13}$$

The two loss terms correspond to particles that have a collision at $\vec{\boldsymbol{r}}$ or leak out of $d\vec{\boldsymbol{r}}$. The collision term is

$$\mathrm{CL} = \Sigma_{\mathrm{T}}(\vec{\boldsymbol{r}}, E) v(E) n\left(\vec{\boldsymbol{r}}, E, \vec{\boldsymbol{\Omega}}, t\right) d\vec{\boldsymbol{r}}\, d\vec{\boldsymbol{\Omega}}\, dE \tag{2.14}$$

And the leakage term is

$$\mathrm{LL} = \vec{\mathbf{v}}(E) n\left(\vec{\boldsymbol{r}}, E, \vec{\boldsymbol{\Omega}}, t\right) \cdot d\vec{\boldsymbol{S}}\, d\vec{\boldsymbol{\Omega}}\, dE \tag{2.15}$$

where $d\vec{\boldsymbol{S}}$ is the surface area of the differential volume $d\vec{\boldsymbol{r}}$ and the vector dot product of $\vec{\mathbf{v}}(E)$ with $d\vec{\boldsymbol{S}}$ gives the net leakage through the surface surrounding $d\vec{\boldsymbol{r}}$.

Note that in order to get reaction rates per unit time, each of the cross sections with units of 1/cm had to be multiplied by $\vec{\mathbf{v}}(E)$ to get units of 1/s. It is easier to group the $\vec{\mathbf{v}}(E)$ with $n\left(\vec{\boldsymbol{r}}, E, \vec{\boldsymbol{\Omega}}, t\right)$ and call the new quantity $\psi = \left(\vec{\boldsymbol{r}}, E, \vec{\boldsymbol{\Omega}}, t\right) = \vec{\mathbf{v}}(E) n\left(\vec{\boldsymbol{r}}, E, \vec{\boldsymbol{\Omega}}, t\right)$ the neutron angular flux density.

Now note that we can apply Gauss theorem to the leakage loss term to get

$$\vec{\boldsymbol{\psi}}\left(\vec{\boldsymbol{r}},E,\vec{\boldsymbol{\Omega}},\ t\right)\cdot d\vec{\boldsymbol{S}}=\nabla\cdot\vec{\boldsymbol{\Omega}}\psi\left(\vec{\boldsymbol{r}},E,\vec{\boldsymbol{\Omega}},\ t\right)d\vec{\boldsymbol{r}} \tag{2.16}$$

This allows us to delete the $d\vec{\boldsymbol{S}}d\vec{\boldsymbol{\Omega}}dE$ factor from each term. The complete equation then becomes

$$\begin{aligned}\frac{1}{v(E)}\frac{\partial\psi\left(\vec{\boldsymbol{r}},E,\vec{\boldsymbol{\Omega}},t\right)}{\partial t}= {} & q\left(\vec{\boldsymbol{r}},E,\vec{\boldsymbol{\Omega}},t\right)+\int_{E'}\int_{\vec{\boldsymbol{\Omega}}'}\Sigma_{\mathrm{s}}\left(\vec{\boldsymbol{r}},E',\vec{\boldsymbol{\Omega}}'\rightarrow E,\vec{\boldsymbol{\Omega}}\right)\psi\left(\vec{\boldsymbol{r}},E',\vec{\boldsymbol{\Omega}}',t\right)dE'd\vec{\boldsymbol{\Omega}}'\\ & +\int_{E'}\int_{\vec{\boldsymbol{\Omega}}'}\chi(E)\frac{v(E')}{4\pi}\Sigma_{\mathrm{f}}(\vec{\boldsymbol{r}},E')\psi\left(\vec{\boldsymbol{r}},E',\vec{\boldsymbol{\Omega}}',t\right)dE'd\vec{\boldsymbol{\Omega}}'\\ & -\Sigma_{\mathrm{T}}(\vec{\boldsymbol{r}},E)\psi\left(\vec{\boldsymbol{r}},E,\vec{\boldsymbol{\Omega}},t\right)-\nabla\cdot\vec{\boldsymbol{\Omega}}\psi\left(\vec{\boldsymbol{r}},E,\vec{\boldsymbol{\Omega}},t\right)\end{aligned} \tag{2.17}$$

Now note that $\nabla\cdot\vec{\boldsymbol{\Omega}}\psi\left(\vec{\boldsymbol{r}},E,\vec{\boldsymbol{\Omega}},\ t\right)=\psi\left(\vec{\boldsymbol{r}},E,\vec{\boldsymbol{\Omega}},\ t\right)\nabla\cdot\vec{\boldsymbol{\Omega}}+\vec{\boldsymbol{\Omega}}\ \nabla\psi\left(\vec{\boldsymbol{r}},E,\vec{\boldsymbol{\Omega}},\ t\right)$. In addition, the first term on the left-hand side is zero due to the constancy of $\vec{\boldsymbol{\Omega}}$. Thus, the divergence term is often written as $\vec{\boldsymbol{\Omega}}\cdot\nabla\psi\left(\vec{\boldsymbol{r}},E,\vec{\boldsymbol{\Omega}},\ t\right)$. However, for many numerical schemes, it is conservative to keep it in its original form. If we move the two loss terms to the left-hand side of the equation, we can write it as

$$\begin{aligned}&\frac{1}{v(E)}\frac{\partial\psi\left(\vec{\boldsymbol{r}},E,\vec{\boldsymbol{\Omega}},\ t\right)}{\partial t}+\nabla\cdot\vec{\boldsymbol{\Omega}}\psi\left(\vec{\boldsymbol{r}},E,\vec{\boldsymbol{\Omega}},\ t\right)+\Sigma_{\mathrm{T}}(\vec{\boldsymbol{r}},E)\psi\left(\vec{\boldsymbol{r}},E,\vec{\boldsymbol{\Omega}},\ t\right)\\ &\quad=q\left(\vec{\boldsymbol{r}},E,\vec{\boldsymbol{\Omega}},\ t\right)+\int_{E'}\int_{\vec{\boldsymbol{\Omega}}'}\Sigma_{\mathrm{S}}\left(\vec{\boldsymbol{r}},E',\vec{\boldsymbol{\Omega}}'\rightarrow E,\ \vec{\boldsymbol{\Omega}}\right)\psi\left(\vec{\boldsymbol{r}},E',\vec{\boldsymbol{\Omega}}',\ t\right)dE'd\vec{\boldsymbol{\Omega}}'\\ &\quad+\chi(E)\int_{E'}\int_{\vec{\boldsymbol{\Omega}}'}\frac{v(E')}{4\pi}\Sigma_{\mathrm{f}}(\vec{\boldsymbol{r}},E')\psi\left(\vec{\boldsymbol{r}},E,\vec{\boldsymbol{\Omega}}',\ t\right)dE'd\vec{\boldsymbol{\Omega}}'\end{aligned} \tag{2.18}$$

The time-independent form can be obtained by dropping the derivative term with respect to time. Then, if the inhomogeneous term is omitted, we will have the term of most interest for reactor analysis. However, in this form, the equation becomes homogenous, and every term depends on the angular flux density. So in order to obtain a solution, an eigenvalue, $1/k$, has to be introduced. This gives the following equation:

$$\begin{aligned}\nabla\cdot\boldsymbol{\Omega}\psi(\boldsymbol{r},E,\boldsymbol{\Omega})+\Sigma_{\mathrm{T}}(\boldsymbol{r},E)\psi(\boldsymbol{r},E,\boldsymbol{\Omega})= {} & \int_{E'}\int_{\vec{\boldsymbol{\Omega}}'}\Sigma_{\mathrm{S}}(\boldsymbol{r},E',\boldsymbol{\Omega}'\rightarrow E,\ \boldsymbol{\Omega})\psi(\boldsymbol{r},E',\boldsymbol{\Omega}')dE'd\boldsymbol{\Omega}''\\ & +\frac{\chi(E)}{k}\int_{E'}\int_{\vec{\boldsymbol{\Omega}}'}\frac{v(E')}{4\pi}\Sigma_{\mathrm{f}}(\boldsymbol{r},E')\psi(\boldsymbol{r},E',\boldsymbol{\Omega}')dE'd\boldsymbol{\Omega}'\end{aligned} \tag{2.19}$$

which is the version of the transport equation that is of most concern for reactor criticality analyses.

2.9 Integral Equation

Consider now the following Fig. 2.2:

We have

$$\vec{\boldsymbol{R}} = R\vec{\boldsymbol{\Omega}}$$

$$\frac{d\psi\left(\vec{\boldsymbol{r}}, E, \vec{\boldsymbol{\Omega}},\ t\right)}{dR} = \frac{\partial x}{\partial R}\frac{\partial \psi}{\partial x} + \frac{\partial y}{\partial R}\frac{\partial \psi}{\partial y} + \frac{\partial z}{\partial R}\frac{\partial \psi}{\partial z} + \frac{\partial t}{\partial R}\frac{\partial \psi}{\partial t}$$

$$\frac{\partial x}{\partial R} = \vec{\boldsymbol{\Omega}}_x$$

$$\frac{\partial y}{\partial R} = \vec{\boldsymbol{\Omega}}_y$$

$$\frac{\partial z}{\partial R} = \vec{\boldsymbol{\Omega}}_z$$

$$\vec{\mathbf{v}} = \frac{\partial \vec{\boldsymbol{R}}}{\partial t}$$

or

$$\frac{d\psi\left(\vec{\boldsymbol{r}}, E, \vec{\boldsymbol{\Omega}},\ t\right)}{dR} = -\vec{\boldsymbol{\Omega}} \cdot \nabla\psi\left(\vec{\boldsymbol{r}}, E, \vec{\boldsymbol{\Omega}},\ t\right) - \frac{1}{v}\frac{\partial \psi\left(\vec{\boldsymbol{r}}, E, \vec{\boldsymbol{\Omega}},\ t\right)}{\partial t} \tag{2.20}$$

Substituting this into the integrodifferential form gives

$$\begin{aligned} -\frac{d\psi(r,E,\Omega,\ t)}{dR} &+ \Sigma_{\mathrm{t}}(r,E)\psi(r,E,\Omega,\ t) = q(r,E,\Omega,\ t) \\ &+ \int_{E'}\int_{\Omega'} \Sigma_{\mathrm{s}}(r,E',\Omega' \rightarrow\ E,\Omega)\psi(r,E',\Omega',t)dE'\,d\Omega' \\ &+ \frac{\chi(E)}{4\pi}\int_{E'}\int_{\Omega'} \nu(E')\Sigma_{\mathrm{f}}(r,E')\psi(r,E',\Omega',t)dE'\,d\Omega \end{aligned} \tag{2.21}$$

Now with the integrating factor

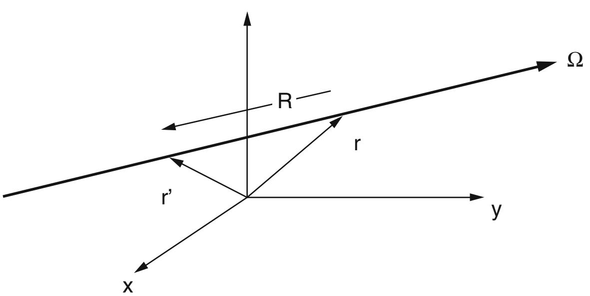

Fig. 2.2 Three-dimensional configuration for integral equation derivations

$$\mathrm{e}^{-\int_0^R \Sigma_{\mathrm{t}}(r-R'\Omega,\, E)\, dR'} \tag{2.22}$$

the equation becomes

$$\begin{aligned}
&\frac{d}{dR}\left\{\psi\left(\vec{\boldsymbol{r}},E,\vec{\boldsymbol{\Omega}},t\right)\mathrm{e}^{-\int_0^R \Sigma_{\mathrm{t}}\left(\vec{\boldsymbol{r}}-R'\vec{\boldsymbol{\Omega}},E\right)d\vec{\boldsymbol{r}}'}\right\} \\
&=\mathrm{e}^{-\int_0^R \Sigma_{\mathrm{t}}\left(\vec{\boldsymbol{r}}-R'\vec{\boldsymbol{\Omega}},E\right)dR'}\left\{\begin{array}{l}
q\left(\mathbf{r},E,\vec{\boldsymbol{\Omega}},t\right) \\
+\displaystyle\int_{E'}\int_{\Omega'}\Sigma_{\mathrm{s}}\left(\vec{\boldsymbol{r}},E',\vec{\boldsymbol{\Omega}}'\to E,\vec{\boldsymbol{\Omega}}\right)\psi\left(\vec{\boldsymbol{r}},E',\vec{\boldsymbol{\Omega}}',t\right)dE'\,d\vec{\boldsymbol{\Omega}}' \\
+\dfrac{\chi(E)}{4\pi}\displaystyle\int_{E'}\int_{\vec{\Omega}'}\nu(E')\Sigma_{\mathrm{f}}(\vec{\boldsymbol{r}},E')\psi\left(\vec{\boldsymbol{r}},E',\vec{\boldsymbol{\Omega}}',t\right)dE'\,d\vec{\boldsymbol{\Omega}}'
\end{array}\right\}
\end{aligned} \tag{2.23}$$

Integrating over R gives the following equation. (Note the equation $R = vt$ must be satisfied at all points along the ray defined by $\vec{\boldsymbol{R}}=R\vec{\Omega}$.)

$$\begin{aligned}
&\psi\left(\vec{\boldsymbol{r}},E,\vec{\boldsymbol{\Omega}},t\right)-\psi\left(\infty,E,\vec{\boldsymbol{\Omega}},t\right)\mathrm{e}^{-\int_0^\infty \Sigma_{\mathrm{t}}\left(\vec{\boldsymbol{r}}-R'\vec{\boldsymbol{\Omega}},E\right)dR'} \\
&=\int_0^\infty dR\,\mathrm{e}^{-\int_0^R \Sigma_{\mathrm{t}}\left(\vec{\boldsymbol{r}}-R'\vec{\boldsymbol{\Omega}},E\right)dR'}\left\{\begin{array}{l}
q\left(\vec{\boldsymbol{r}},E,\vec{\boldsymbol{\Omega}},t\right) \\
+\displaystyle\int_{E'}\int_{\Omega'}\Sigma_{\mathrm{s}}\left(\vec{\boldsymbol{r}},E',\vec{\boldsymbol{\Omega}}'\to E,\vec{\boldsymbol{\Omega}}\right)\psi\left(\vec{\boldsymbol{r}},E',\vec{\boldsymbol{\Omega}}',t\right)dE'\,d\vec{\boldsymbol{\Omega}}' \\
+\dfrac{\chi(E)}{4\pi}\displaystyle\int_{E'}\int_{\Omega'}\nu(E')\Sigma_{\mathrm{f}}(\vec{\boldsymbol{r}},E')\psi\left(\vec{\boldsymbol{r}},E',\vec{\boldsymbol{\Omega}}',t\right)dE'\,d\vec{\boldsymbol{\Omega}}'
\end{array}\right\}
\end{aligned} \tag{2.24}$$

Hoping that we can find a location at infinity along the ray such that $\psi = \left(\vec{\boldsymbol{r}},E',\vec{\boldsymbol{\Omega}},t\right)$ can be neglected and defining the optical thickness as

$$\beta\left(\vec{\boldsymbol{r}},R,E,\vec{\boldsymbol{\Omega}},t\right)=\int_0^R \Sigma_{\mathrm{t}}\left(\vec{r}-R'\vec{\boldsymbol{\Omega}},E\right)dR' \tag{2.25}$$

we have

$$\psi\left(\vec{\boldsymbol{r}},E,\vec{\boldsymbol{\Omega}},t\right)=\int_0^\infty dR\,\mathrm{e}^{-\beta\left(\vec{r},R,E,\vec{\boldsymbol{\Omega}},t\right)}\left\{\begin{array}{l}
q\left(\vec{\boldsymbol{r}},E,\vec{\boldsymbol{\Omega}},t\right) \\
+\displaystyle\int_{E'}\int_{\Omega'}\Sigma_{\mathrm{s}}\left(\vec{\boldsymbol{r}},E',\vec{\boldsymbol{\Omega}}'\to E,\vec{\boldsymbol{\Omega}}\right)\psi\left(\vec{\boldsymbol{r}},E',\vec{\boldsymbol{\Omega}}',t\right)dE'\,d\vec{\boldsymbol{\Omega}}' \\
+\dfrac{\chi(E)}{4\pi}\displaystyle\int_{E'}\int_{\Omega'}\nu(E')\Sigma_{\mathrm{f}}(\vec{\boldsymbol{r}},E')\psi\left(\vec{\boldsymbol{r}},E',\vec{\boldsymbol{\Omega}}',t\right)dE'\,d\vec{\boldsymbol{\Omega}}'
\end{array}\right\} \tag{2.26}$$

Note that the time dependence is tied up in β, and the equation $R = vt$ must still be satisfied. However, this is a purely integral equation. It can be multigrouped simply by integrating over a set of energy group intervals. We can also find the isotropic flux simply by integrating ψ over $\vec{\boldsymbol{\Omega}}$. That is

$$\phi(r, E, t) = \int_{\Omega} \psi(r, E, \Omega, t) d\Omega \tag{2.27}$$

2.10 Multigroup Diffusion Theory

In this section, the multigroup form of the neutron diffusion equation is developed and explored with the aim to relate the mathematics to the physical meaning. Keep in your mind that the diffusion theory model of neutron transport has a crucial input and plays a major role in reactor theory since its simplification allows scientific insight, and it is sufficiently realistic enough to study many important design problems in real world of reactor design and manufacturing. In order to simplify the complex mathematics of multigroup diffusion theory, one can assume neutrons can be characterized by a single energy or speed if need be, and a model then allows preliminary design problem estimations. In that case, the mathematical methods used to analyze such a model are the same as those applied in more sophisticated methods that are applied in multigroup diffusion theory and transport theory which are our intention in this section and chapter. There are enough literature and notes of references that can be found on the Internet, which shows the derivation of such a simple diffusion equation which depends on Fick's law, even though a direct derivation from the transport equation is also possible, and as result the Helmholtz equation can easily be derived in this simple case. In this simple case approach, the limitation on diffusion equation as well as the boundary conditions can be applied in its application to realistic engineering and physics problem of reactor theory [1].

Back to our subject of multigroup diffusion theory, we start by asking question of why we need the *multigroup model* to start with. In order to answer this question, we know that neutrons have a wide energy spectrum, ranging from a fraction of an eV to a few MeV. The cross sections vary over decades in this range so we can hardly expect the one-group approximation to be very accurate. To illustrate this, consider a simple cell model as shown in Fig. 2.3 for a tank-type experimental reactor as

The height, H, of the D_2O moderator was varied to achieve criticality. Then, a void was introduced in the coolant by bubbling air into it. The height, H, of the moderator was again varied to keep the reactor critical. A range of void fraction was introduced. Figure 2.4 gives the experimental results (buckling $(\pi/H)^2$ vs. void fraction, α) and the predictions of a number of simple reactor models. One-group theory does not come close to predicting the buckling, even if the cross sections are

Fig. 2.3 Schematic of the nuclear reactor model showing the top view of the lattice structure of fuel bundles and a side view of the two-region cell

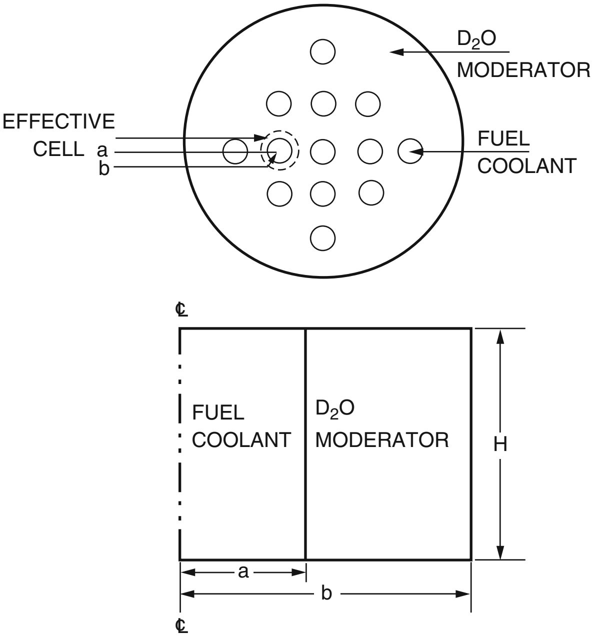

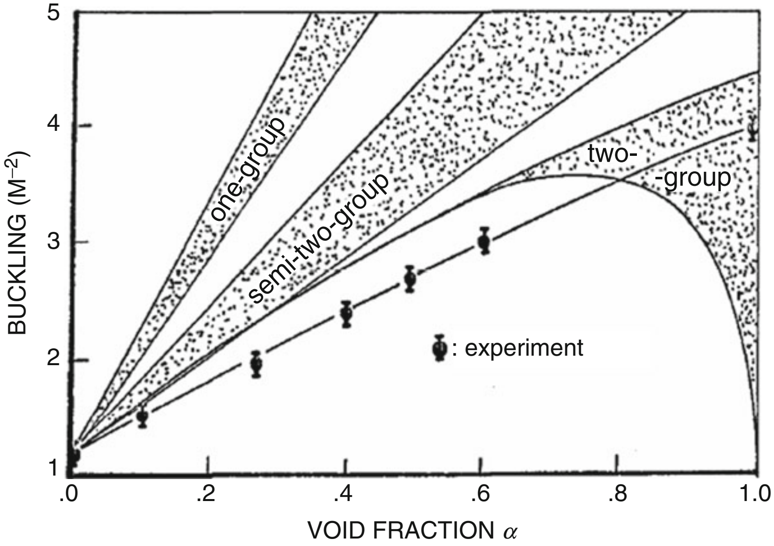

Fig. 2.4 Comparison between experimentally observed and calculated buckling

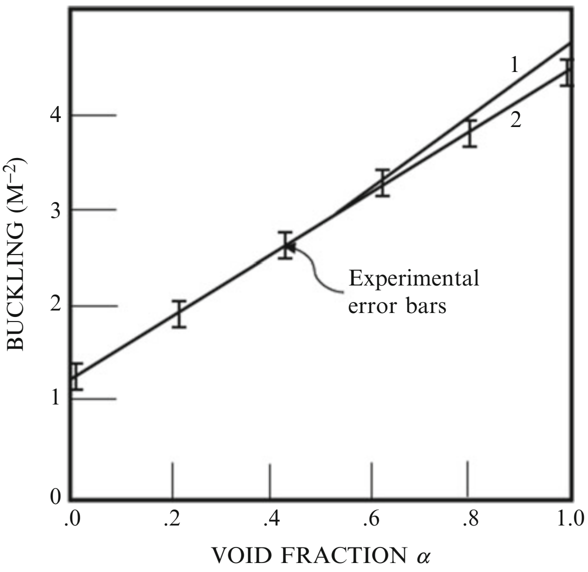

Fig. 2.5 Comparison of experimentally observed buckling and predictions of the two-group model using adjusted parameters

varied within their experimental error. The semi-two-group theory does better and the two-group model does better still.

The two-group model can be further improved by using energy-averaged cross sections obtained by a comprehensive cell code that employs a detailed energy structure. The improved comparison shown in Fig. 2.5 shows what can be achieved with a few-group model (in this case, two) if the "appropriate" average cross sections can be found that represent the cell in question. We shall see that we can only get good values if we first perform a many-group model calculation.

This work is detailed in B. Garland (1975) [2], but for the present discussion, the main point to note is the inadequacy of the one-group model or even the two-group model since the appropriate cross sections are not explicitly available and since these low-order models do not come close to capturing the energy structure. Accurate cell calculations are done typically with up to 150 neutron energy groups to obtain cell-averaged cross sections. Then, few-group approximations are used for the full-core calculation based on the cell-averaged cross sections. Few-group calculations can be successfully done but only if they are backed up by detailed multigroup cell calculations.

This chapter is all about the governing equations for the multigroup model that are the essence of all these calculations.

2.11 The Multigroup Equations

To form the multigroup neutron diffusion equations, we first divide the energy range for the neutrons up into groups as shown in Fig. 2.6.

Thus, we have

$$\phi_g(\overline{r},t) \text{ for } E \in \left(E_g, E_{g-1}\right) \text{ where } E_g < E < E_{g-1} \tag{2.28}$$

The multigroup form of the neutron diffusion equation is then given by

$$\begin{aligned}\frac{1}{v_g}\frac{\partial}{\partial t}\phi_g(\overline{r},t) = {} & \underbrace{\nabla \bullet D_g(r)\phi_g(\overline{r},t)}_{\text{leakage}} \underbrace{-\Sigma_{\text{ag}}(r)\phi_g(\overline{r},t)}_{\text{loss by absorption}} - \underbrace{\Sigma_{\text{sg}}(r)\phi_g(\overline{r},t)}_{\text{removal by scattering}} \\ & \underbrace{+\sum_{g'=1}^{G}\Sigma_{\text{s}g'g}(r)\phi_{g'}(\overline{r},t)}_{\text{scattering into group } g} + \underbrace{\chi_g}_{\substack{\text{fission}\\ \text{appearing}\\ \text{group } g}} \underbrace{\sum_{g'=1}^{G}\nu_{g'}\Sigma_{\text{f}g'}(r)\phi_{g'}(\overline{r},t)}_{\text{total fission production}} + \underbrace{S_g^{\text{ext}}}_{\text{external source}}\end{aligned} \tag{2.29}$$

Note that the neutrons are born with no knowledge of their parents. Thus, we write the total fission production as a sum that is independent of the index g. From there, we split out the fraction, χ_g, that appears in group g.

As we know, the cross sections and flux can vary greatly as a function of neutron energy, E. Figure 2.7 shows an illustrative five-group approximation. So we will have to use some average flux and cross section that have been averaged over the property in the group energy range in question.

We will see how to do this soon, but for now, we want to concentrate on each of the terms in Eq. 2.20 to make sure you understand what each term represents in a physical sense.

The fission terms are as follows:

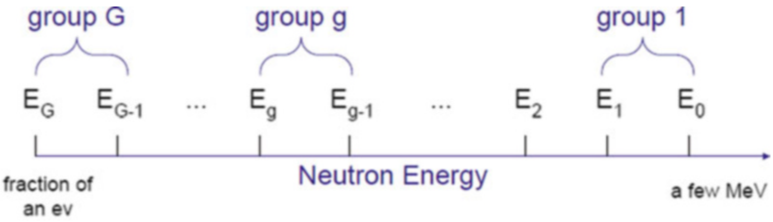

Fig. 2.6 Neutron energy group numbering schema

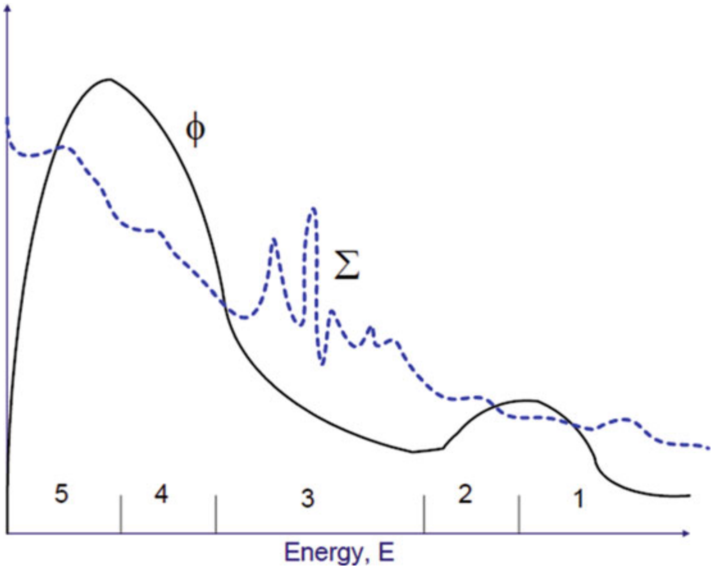

Fig. 2.7 Illustrative flux and cross-sectional variation with energy

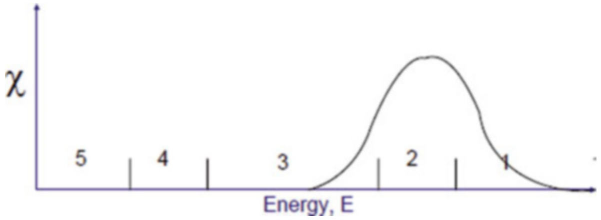

Fig. 2.8 Fission neutron energy spectrum

$$\underbrace{\sum_{g'=1}^{G} \nu_g \Sigma_{\mathrm{f}g'}(r)\phi_{g'}(\bar{r},t)}_{\text{total fission production}} = \underbrace{\nu_5\sum\nolimits_{\mathrm{f}5}\phi_5+\nu_4\sum\nolimits_{\mathrm{f}4}\phi_4}_{\text{thermal fission (about 97 \%)}} + \underbrace{\nu_3\sum\nolimits_{\mathrm{f}3}\phi_3+\nu_2\sum\nolimits_{\mathrm{f}2}\phi_2+\nu_1\sum\nolimits_{\mathrm{f}1}\phi_1}_{\text{fast fission (about 3 \%)}} \tag{2.30}$$

These fission neutrons, arising mostly from the fissions that are induced by thermal neutrons, have energies in the MeV range, for the most part. Figure 2.8 illustrates this.

So, for the illustrated five-group example, $\chi_5 = \chi_4 = 0$, and the other χ's are nonzero. So, for the thermal groups (i.e., groups 5 and 4), there are no fission source neutrons. The summation term contains contributions from all five fission terms, but the biggest contributors are from the thermal group. This sum of fission neutrons will only show up as sources for groups 1, 2, and 3.

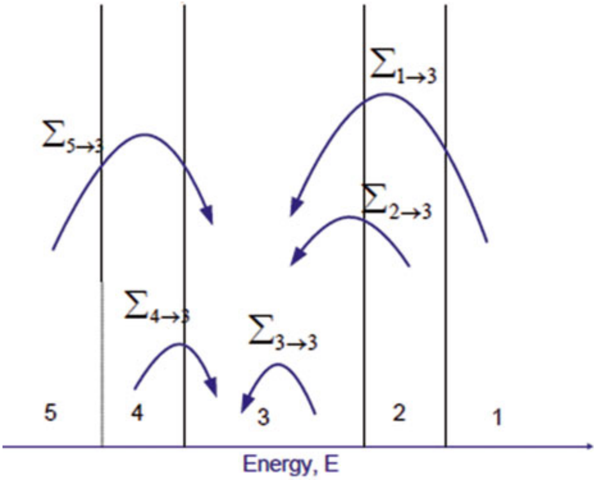

Fig. 2.9 Scattering into group (WIMS can provide simple pin cell calculations of reactivity to whole core estimates of power and flux distributions. The user can benefit from the flexibility of using predefined calculation routes or providing customized methods of solution using diffusion theory, discrete-ordinates, collision probability, characteristics or Monte Carlo methods)

Now would be a good time to look back at the governing equations and write them out for the five-group case. It is important that you get it right.

Now, let us look at the scattering terms. These are new. They add complexity but, taken step by step, they are not that hard to understand. In previous chapters, which assumed monoenergetic neutrons, we did not have to consider the loss and gain of neutrons by the scattering process because when a scattering event occurs, the neutron is simply deflected. It is not absorbed; hence, there is no gain or loss of neutrons **in total** because of scattering. However, now that we have subdivided the neutrons up into groups, the scattered neutrons emerge from the scattering process at some energy different, in all likelihood, from the incident energy.

The scattering removal term in Eq. 2.29 is straightforward. It says that all the neutrons in group g scatter to some other energy and, so, disappear from the gth neutron balance equation. Some of the scattered neutrons will emerge with a new energy that is within the range of the energies represented by group g. Therefore, we have to add those back in. We'll do that via the scattering in term, discussed next, and that is as follows:

The scattering in term is given as

$$\sum_{g'=1}^{G} \sum\nolimits_{sg'g}(r)\phi_{g'}(\bar{r},t) = \sum\nolimits_{s1g}\phi_1 + \sum\nolimits_{s2g}\phi_2 + \sum\nolimits_{s3g}\phi_3 + \sum\nolimits_{s4g}\phi_4 + \sum\nolimits_{s5g}\phi_5 \tag{2.31}$$

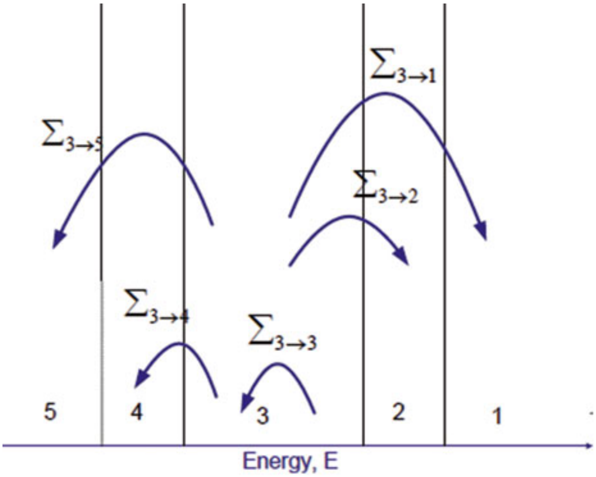

Fig. 2.10 Scattering out of group (WIMS can provide simple pin cell calculations of reactivity to whole core estimates of power and flux distributions. The user can benefit from the flexibility of using predefined calculation routes or providing customized methods of solution using diffusion theory, discrete-ordinates, collision probability, characteristics or Monte Carlo methods)

that is, neutrons are scattered into group g from all the five groups. Note that we have a term representing scattering from group *g* to group *g*, i.e., the ones that stay in the group even after scattering. This effectively adds back in the neutrons that were erroneously subtracted by the scattering removal term of the previous paragraph. Figure 2.9 illustrates the process.

Of course, the total scattering out of group 3 is just the sum total of all the scattering-out processes, i.e.,

$$\begin{aligned}\sum\nolimits_{s3}\phi_3 &= \sum\nolimits_{s31}\phi_3 + \sum\nolimits_{s32}\phi_3 + \sum\nolimits_{s33}\phi_3 + \sum\nolimits_{s34}\phi_3 + \sum\nolimits_{s35}\phi_3 \\ &= \left(\sum_{g'=1}^{G}\sum\nolimits_{s3g'}(r)\right)\phi_3(\bar{r},t)\end{aligned} \tag{2.32}$$

or for the general group *g*, we can write

$$\begin{aligned}\sum\nolimits_{sg}\phi_g &= \sum\nolimits_{sg1}\phi_g + \sum\nolimits_{sg2}\phi_g + \sum\nolimits_{sg3}\phi_g + \sum\nolimits_{sg4}\phi_g + \sum\nolimits_{sg5}\phi_g \\ &= \left(\sum_{g'=1}^{G}\sum\nolimits_{sgg'}(r)\right)\phi_g(\bar{r},t)\end{aligned} \tag{2.33}$$

This is illustrated in Fig. 2.10 as

Now we can plug Eqs. 2.31 and 2.33 into Eq. 2.29, using group 3 as an example to obtain the following relationship as

$$\begin{aligned}\frac{1}{v_3}\frac{\partial}{\partial t}\phi_3(\bar{r},t) = {} & \underbrace{\nabla\cdot D_3(r)\nabla\phi_3(\bar{r},t)}_{\text{leakage}} \; -\underbrace{\sum\nolimits_{a3}(r)\phi_3(\bar{r},t)}_{\text{loss by absorption}} \\ & -\underbrace{\sum\nolimits_{s31}(r)\phi_3(\bar{r},t)+\sum\nolimits_{s32}(r)\phi_3(\bar{r},t)+\cancel{\sum\nolimits_{s33}(r)\phi_3(\bar{r},t)}+\sum\nolimits_{s34}(r)\phi_3(\bar{r},t)+\sum\nolimits_{s35}(r)\phi_3(\bar{r},t)}_{\text{scattering out}} \\ & +\underbrace{\sum\nolimits_{s13}(r)\phi_3(\bar{r},t)+\sum\nolimits_{s23}(r)\phi_3(\bar{r},t)+\cancel{\sum\nolimits_{s33}(r)\phi_3(\bar{r},t)}+\sum\nolimits_{s43}(r)\phi_3(\bar{r},t)+\sum\nolimits_{s53}(r)\phi_3(\bar{r},t)}_{\text{scattering in}} \\ & + \underbrace{\chi_g}_{\substack{\text{fission}\\ \text{appearing}\\ \text{group in } g}} \underbrace{\sum_{g'=1}^{G}\nu_{g'}\sum\nolimits_{fg'}(\boldsymbol{r})\phi_{g'}(\bar{r},t)}_{\text{total fission production}} + \underbrace{S_3^{\text{ext}}}_{\text{external source}}\end{aligned} \tag{2.34}$$

Notice how the "in-group" scattering terms cancel.

Just to confuse matter a bit more, the **removal cross section** is often used. It is defined for group 3 as

$$\begin{aligned}\sum\nolimits_{r3} &\equiv \sum\nolimits_{a3}+\sum\nolimits_{s3}-\sum\nolimits_{s33} = \sum\nolimits_{a3}+\sum\nolimits_{s31}+\sum\nolimits_{s32}+\sum\nolimits_{s34}+\sum\nolimits_{s35} \\ &= \sum\nolimits_{a3} = \sum_{\substack{g'=1\\ g'\neq 3}}^{G}\sum\nolimits_{s3g'}(r)\end{aligned} \tag{2.35}$$

i.e., it is the net removal of neutron from group 3 by scattering and absorption. If we use this definition, the governing equation becomes

$$\begin{aligned}\frac{1}{v_g}\frac{\partial}{\partial t}\phi_g(\bar{r},t) = {} & \underbrace{\nabla\cdot D_g(r)\nabla\phi_g(\bar{r},t)}_{\text{leakage}} - \underbrace{\Sigma_{\text{rg}}(r)\phi_g(\bar{r},t)}_{\text{removal}} \underbrace{-\Sigma_{sgg}(r)\phi_g(\bar{r},t)}_{\text{in-group scattering}} + \underbrace{\sum_{g'=1}^{G}\Sigma_{sg'g}(r)\phi_{g'}(\bar{r},t)}_{\text{net scattering into group g}} \\ & + \underbrace{\chi_g}_{\substack{\text{fission}\\ \text{appearing}\\ \text{group in } g}} \underbrace{\sum_{g'=1}^{G}\nu_{g'}\Sigma_{\text{f}g'}(\boldsymbol{r})\phi_{g'}(\bar{r},t)}_{\text{total fission production}} + \underbrace{S_g^{\text{ext}}}_{\text{external source}} \quad g=1,2,\ldots,G\end{aligned} \tag{2.36}$$

or more simply

$$\begin{aligned}\frac{1}{v_g}\frac{\partial}{\partial t}\phi_g(\bar{r},t) &= \underbrace{\nabla\cdot D_g(r)\nabla\phi_g(\bar{r},t)}_{\text{leakage}} - \underbrace{\sum\nolimits_{\text{r}g}(r)\phi_g(\bar{r},t)}_{\text{removal}} - \underbrace{\sum\nolimits_{\text{s}gg}(r)\phi_g(\bar{r},t)}_{\text{in-group scattering}} \\ &+ \underbrace{\sum_{\substack{g'=1\\ g\neq g}}^{G}\sum\nolimits_{\text{s}g'g}(r)\phi_{g'}(\bar{r},t)}_{\text{net scattering into group g}} + \underbrace{\chi_g}_{\substack{\text{fission}\\ \text{appearing}\\ \text{in group } g}} \underbrace{\sum_{g'=1}^{G}\nu_{g'}\Sigma_{\text{f}g'}(\mathbf{r})\phi_{g'}(\bar{r},t)}_{\text{total fission production}} + \underbrace{S_g^{\text{ext}}}_{\text{external source}}\end{aligned} \tag{2.37}$$

May be the use of the removal form is unnecessary and a bit confusing, and some folks like to use and remember just the relationship in Eq. 2.29. Everything else discussed above flows readily from that equation. There is no need to memorize any of this. If you take the time to visualize the processes that are occurring, then you should be able to state Eq. 2.29 as you go through the accounting of the sinks and sources of neutrons. **Try it**! **Do not be afraid to spend some time making sure that you have it clear in your mind. It is a milestone concept in reactor physics and the subject won't make sense unless you grasp it**.

2.12 Generating the Coefficients

The raw cross-sectional data is available in libraries like ENDF/B in the public domain. This data gives the experimental values as a function of energy in far too much detail for our multigroup model. We need to come up with good estimates of the group-averaged cross sections. To do that we step back and use the more general form of the neutron diffusion equation, one that has energy represented as a continuum rather than as discrete bins:

$$\begin{aligned}\frac{1}{v}\frac{\partial\phi}{\partial t} &= \underbrace{\nabla\cdot D(r)\nabla\phi}_{\text{leakage}} - \underbrace{\sum\nolimits_{\text{a}}(r)\phi}_{\text{loss by absorption}} - \underbrace{\sum\nolimits_{\text{s}}(r)\phi}_{\text{removal by scattering}} \\ &+ \underbrace{\int_0^\infty \sum\nolimits_{\text{s}}(E'\to E)\phi(r,E',t)dE'}_{\text{scattering into } E\to E+dE \text{ range}} + \underbrace{\chi(E)}_{\substack{\text{fission}\\ \text{appearing}\\ E\to E+dE\\ \text{range}}} \underbrace{\int_0^\infty \nu(E')\sum\nolimits_{\text{f}}(E')\phi(\bar{r},E',t)}_{\text{total fission production}} \\ &+ \underbrace{S^{\text{ext}}}_{\text{external source}}\end{aligned} \tag{2.38}$$

Note that $\phi = \phi(\bar{r},E',t)$

The term $\sum_{\mathrm{s}}(E' \rightarrow E)dE'$ is the cross section for neutrons at energy E' scattering to energy E. Note that $\sum_{\mathrm{s}}(E' \rightarrow E)dE'$ has units of cm^{-1} so $\sum_{\mathrm{s}}(E' \rightarrow E)$ as units of cm^{-1} eV^{-1}.

We define the group flux as

$$\phi_g(\bar{r}, t) = \int_{E_g}^{E_{g-1}} \phi(\bar{r}, E, t)dE \tag{2.39}$$

This prompts us to perform the same integral for each term of Eq. 2.38 and to equate what we get to Eq. 2.29 to generate a rigorous definition of the group-averaged cross sections. Thus, Eq. 2.38 becomes term by term:

$$\frac{\partial}{\partial t}\left(\int_{E_g}^{E_{g-1}} \frac{1}{v(E)}\phi(\bar{r}, E, t)dE\right) = \frac{\partial}{\partial t}\left(\frac{\phi_g}{v_g}\right) = \frac{1}{v_g}\frac{\partial \phi_g}{\partial t} \tag{2.40}$$

$$\text{where} \quad \frac{1}{v_g} \equiv \frac{\displaystyle\int_{E_g}^{E_{g-1}} \frac{1}{v(E)}\phi(\bar{r}, E, t)dE}{\displaystyle\int_{E_g}^{E_{g-1}} \phi(\bar{r}, E, t)dE}$$

Notice how the coefficient, $1/v_g$, is determined simply as the flux-weighted integral over the group energy range. As we go through the integral term by term, we will see the same pattern.

Now for the diffusion coefficient,

$$\nabla \cdot \left(\int_{E_g}^{E_{g-1}} D(E)\nabla\phi(\bar{r}, E, t)dE\right) \equiv \nabla \cdot D_g \nabla \phi_g \tag{2.41}$$

$$\text{i.e.,} \quad D_g \equiv \frac{\displaystyle\int_{E_g}^{E_{g-1}} D(E)\nabla\phi(\bar{r}, E, t)dE}{\displaystyle\int_{E_g}^{E_{g-1}} \nabla\phi(\bar{r}, E, t)dE}$$

This time, the weighting is $\nabla\phi(\bar{r}, E, t)$ since that is how the flux factor appears in the term.

The absorption term is just

$$\int_{E_g}^{E_{g-1}} \sum\nolimits_{\mathrm{a}}(E)\phi(\bar{r}, E, t)dE \equiv \sum\nolimits_{\mathrm{ag}}\phi_g \tag{2.42}$$

$$\text{i.e.,}\quad \sum\nolimits_{\mathrm{a}g} \equiv \frac{\int_{E_g}^{E_{g-1}} \Sigma_{\mathrm{a}}(E)\phi(\bar{r},E,t)dE}{\int_{E_g}^{E_{g-1}} \phi(\bar{r},E,t)dE}$$

The scattering removal term is similar.

The scattering down term is a bit messier:

$$\begin{aligned}\int_{E_g}^{E_{g-1}}\left(\int_0^{\infty}\sum\nolimits_{\mathrm{s}}(E'\to E)\phi(\bar{r},E',t)dE'\right)dE &= \int_{E_g}^{E_{g-1}}\left(\sum_{g'=1}^{G}\int_{E_{g'}}^{E_{g'-1}}\sum\nolimits_{\mathrm{s}}(E'\to E)\phi(\bar{r},E',t)dE'\right)dE\\ &= \sum_{g'=1}^{G}\int_{E_{g'}}^{E_{g'-1}}\left(\int_{E_{g'}}^{E_{g'-1}}\sum\nolimits_{\mathrm{s}}(E'\to E)\phi(\bar{r},E',t)dE'\right)dE\\ &\equiv \sum_{g'=1}^{G}\sum\nolimits_{sg'g}\phi_{g'}\end{aligned} \tag{2.43}$$

So we have

$$\sum\nolimits_{sg'g} = \frac{1}{\phi_{g'}}\int_{E_{g'}}^{E_{g'-1}}\left(\int_{E_{g'}}^{E_{g'-1}}\sum\nolimits_{\mathrm{s}}(E'\to E)\phi(\bar{r},E',t)dE'\right)dE \tag{2.44}$$

The fission term is

$$\begin{aligned}\int_{E_g}^{E_{g-1}}\chi(E)\int_0^{\infty}\nu(E')\Sigma_{\mathrm{f}}(E')\phi(\bar{r},E',t)dE'dE &= \int_{E_g}^{E_{g-1}}\chi(E)dE\int_0^{\infty}\nu(E')\Sigma_{\mathrm{f}}(E')\phi(\bar{r},E',t)dE'\\ &= \chi_g\int_0^{\infty}\nu(E')\Sigma_{\mathrm{f}}(E')\phi(\bar{r},E',t)dE'\\ &= \chi_g\sum_{g'=1}^{G}\int_{E_g}^{E_{g-1}}\nu(E')\Sigma_{\mathrm{f}}(E')\phi(\bar{r},E',t)dE'\\ &= \chi_g\sum_{g'=1}^{G}\nu_{g'}\Sigma_{fg'}\phi_{g'}\end{aligned} \tag{2.45}$$

$$\text{where}\quad \chi_g \equiv \int_{E_g}^{E_{g-1}}\chi(E)dE$$

Dropping the summation, we finally arrive at

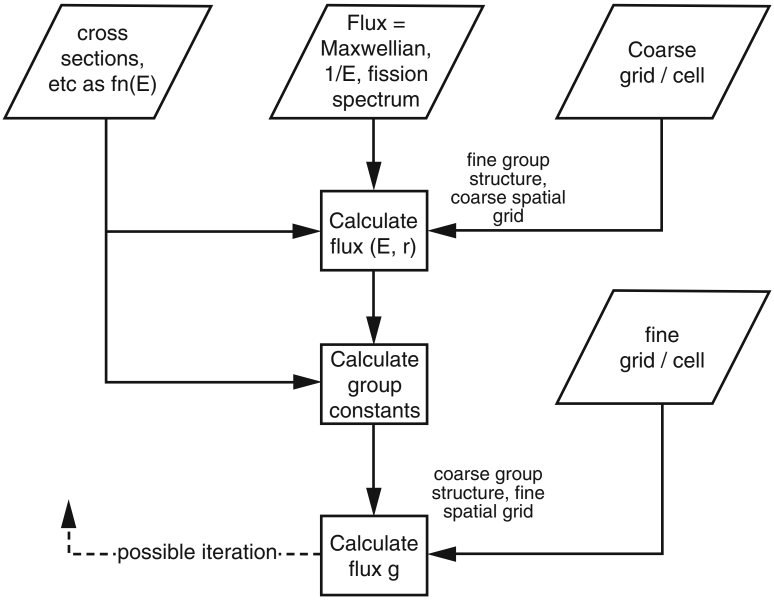

Fig. 2.11 Typical calculation schema

$$\begin{aligned} v_{g'}\sum\nolimits_{\mathrm{f}g'} &\equiv \frac{1}{\phi_{g'}}\int_{E_g}^{E_{g-1}} v(E')\sum\nolimits_{\mathrm{f}}(E')\phi(\bar{r},E',t)dE' \\ \chi_g &\equiv \int_{E_g}^{E_{g-1}} \chi(E)dE \end{aligned} \tag{2.46}$$

The accuracy of the multigroup model depends very much on the group constants chosen.

Note that the constants depend on ϕ which depends on the constants. This is a circular argument. To compensate, the typical practice is to follow a scheme as outlined in Fig. 2.11.

A fine energy structure (many groups, perhaps of the order of 100 or more) is assumed by taking the flux as Maxwellian in the thermal range, $1/E$ in the midrange, and a fission spectrum for the high end. A coarse spatial grid is assumed or a small representative region is chosen (usually a representative cell). The multigroup equations can then be solved numerically (high G, small number of spatial mesh points). This yields ϕ_g for the cell, $g=1$, 100 (say). This flux can be used to calculate weighted cross sections and other constants for a coarse energy structure, perhaps $G=5$ or so. Now, with a manageable number of neutron equations per spatial mesh point, the whole core (or a typical cell) can numerically be solved with a large number of spatial mesh points, giving good spatial detail, albeit with a coarse energy resolution. Once these calculations are done, there is the possibility that a reweighting of the group constants might have to be done to account for flux-dependent effects like Xe, burnup, temperature, control rod position, etc. Therefore, iteration might be required.

We could use the same basic equation (i.e., Eq. 2.29) for both the fine energy calculation and the fine spatial mesh calculation. The more typical route, however, is to not use diffusion-based calculation for the fine energy mesh/cell calculation because diffusion theory is not accurate near interfaces that involve large changes in cross sections (like water/control rod interfaces). Rather, a transport-based code such as *WIMS*[3] is used (i.e., VIMS is a general purpose reactor physics program for core physics calculations). The fine spatial mesh/core calculations typically do use the diffusion approximation propped up by the group-averaged coefficients based on transport calculations. Herein, we will assume that the proper flux-weighted coefficients have been found, and we explore some simplifications and criticality calculations.

2.13 Simplifications

Most neutrons lose energy when they scatter. Only the low-energy thermal neutrons experience any significant upscatter (that's what the Maxwellian is all about, after all). Therefore, it is a reasonable approximation to assume that all groups do not upscatter if the thermal breakpoint is kept above ~1 eV. That will keep the thermal upscatter restricted to itself. Thus,

$$\sum\nolimits_{sg'g}(r) \approx 0 \quad \text{for} \quad g' > g \quad \text{No up-stream assumption}$$

This simplifies the group in-scattering term:

$$\underbrace{\sum_{g'=1}^{G}\sum\nolimits_{sg'g}(r)\phi_{g'}(\bar{r},t)}_{\text{scattering into group g}} \rightarrow \sum_{g'=1}^{g-1}\sum\nolimits_{sg'g}(r)\phi_{g'}(\bar{r},t) + \underbrace{\sum\nolimits_{sgg}(r)\phi_{g}(\bar{r},t)}_{\substack{\text{can lump this into}\\ \text{the removal term}}} \tag{2.47}$$

We can also sometimes assume that scattering down is to the next lowest group only, i.e., no groups are skipped when scattering down. Thus,

$$\underbrace{\sum_{g'=1}^{G}\sum\nolimits_{sg'g}(r)\phi_{g'}(\bar{r},t)}_{\text{scattering into group g}} \rightarrow \sum\nolimits_{sg-1g}(r)\phi_{g-1}(\bar{r},t) + \sum\nolimits_{sgg}(r)\phi_{g}(\bar{r},t) \tag{2.48}$$

This is called "directly coupled."

Consider that in a scattering event,

$$E_{\mathrm{f}} = \alpha E_{\mathrm{i}} \quad \text{where} \quad \alpha \equiv \left(\frac{A-1}{A+1}\right)^2 \tag{2.49}$$

Therefore, if we maintain a group separation such that

$$\frac{E_g}{E_{g-1}} \leq \alpha \tag{2.50}$$

then the scattered neutron cannot have a final energy that is below the next group down. For hydrogen, which has $A = 1$, there is a problem because $\alpha = 0$. But it can be shown that, even then, the error is <1 % if $E_g/E_{g-1} < 1/150$.

2.14 Nuclear Criticality Concepts

A nuclear reactor works on the principle of a chain reaction. An initial neutron is absorbed by a fissile nuclide, and during the process of fission, additional neutrons are released to replace the neutron that was consumed. If more neutrons are produced than are consumed, then the neutron population grows. If fewer neutrons are produced than are consumed, the neutron population shrinks. The number of fissions caused by the neutron population determines the energy released.

In order to quantify this concept, let us define a multiplication factor k. We will define k as the ratio of the production to consumption of neutrons:

$$k = \text{Multiplication Factor} = \frac{\text{Production}}{\text{Consumption}} \tag{2.51}$$

Now both production and consumption are reaction rates. Reaction rates are products of neutron fluxes and nuclide cross sections. And since the neutrons are produced at high energies (~2 MeV) and are consumed at thermal energies (~0.05 eV) at least in light-water reactors (LWRs), it is important to integrate these reaction rates over all energies. Consider the neutron flux spectrum in a typical LWR, as plotted in Fig. 2.12 here:

It is basically composed of three main functions. At the high end, it looks like a fission spectrum; in the intermediate range (0.25 MeV to 0.25 eV), it looks like a $1/E$ spectrum, and in the thermal range, it looks like a Maxwellian. Since cross sections also vary significantly as a function of energy, the true production and destruction rates must be integrals over energy. In real reactors, some neutrons are destroyed by absorption in the fuel, moderator, and structure, and some leak out. All of these processes depend on the energy distribution of the neutrons within the reactor.

Fig. 2.12 LWR neutron flux spectrum

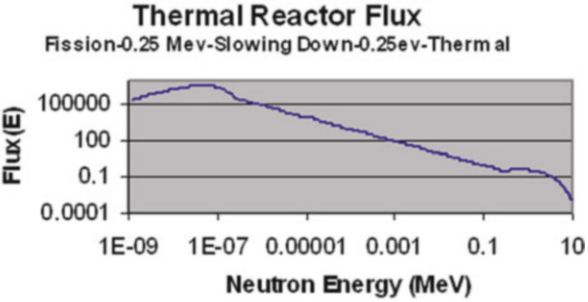

2.15 Criticality Calculation

The criticality calculation follows the same itinerary as the one-speed neutron case except that we now have to sweep through the energy groups as well as through space. The basic steady-state equation to solve is (assuming no upscatter)

$$-\nabla\cdot D_g(r)\nabla\phi_g(\bar{r},t)+\underbrace{\Sigma_{\mathrm{r}g}(r)\phi g(\bar{r},t)}_{\text{removal}}+\sum_{g'=1}^{G}\Sigma_{\mathrm{s}g'g}(r)\phi_{g'}(\bar{r},t)$$

$$=\frac{1}{k}\chi_g\sum_{g'=1\ g'\neq 1\,.}^{G}\nu_{g'}\Sigma_{\mathrm{f}g'}(r)\times\phi_{g'}(\bar{r},t) \tag{2.52}$$

Note that $\sum_{\mathrm{r}g}=\sum_{\mathrm{t}g}-\sum_{\mathrm{s}g'g}=\sum_{\mathrm{a}g}+\sum_{\mathrm{s}g}+\sum_{\mathrm{s}g'g}$. We can write this in a matrix form:

$$M\phi=\frac{1}{k}F\phi \tag{2.53}$$

where

$$\underline{\underline{M}}=\begin{pmatrix}-\nabla\cdot D_1\nabla+\sum_{\mathrm{r}1} & 0 & 0\\ -\sum_{\mathrm{s}12} & -\nabla\cdot D_2\nabla+\sum_{\mathrm{r}2} & 0\\ -\sum_{\mathrm{s}13} & & -\nabla\cdot D_3\nabla+\sum_{\mathrm{r}3}\\ \vdots & \vdots & \vdots\end{pmatrix} \tag{2.54}$$

$$\underline{\phi}=\begin{bmatrix}\phi_1\\ \phi_2\\ \phi_3\\ \vdots\end{bmatrix} \tag{2.55}$$

$$\underline{\underline{F}} = \begin{pmatrix} \chi_1 \nu_1 \sum_{\mathrm{f}1} & \chi_1 \nu_2 \sum_{\mathrm{f}2} & \chi_1 \nu_3 \sum_{\mathrm{f}3} & \cdots \\ \chi_2 \nu_1 \sum_{\mathrm{f}1} & \chi_2 \nu_2 \sum_{\mathrm{f}2} & \chi_2 \nu_3 \sum_{\mathrm{f}3} & \cdots \\ \chi_3 \nu_1 \sum_{\mathrm{f}1} & \chi_3 \nu_2 \sum_{\mathrm{f}2} & \chi_3 \nu_2 \sum_{\mathrm{f}3} & \cdots \\ \vdots & \vdots & \vdots & \end{pmatrix} \tag{2.56}$$

Please note that the span is over the groups, not space. Imbedded in the diffusion term is the space mesh. Two-dimensional papers cannot do justice to the complexity of the structure in matrix form. With the assumption of no upscatter, the *M* matrix is lower triangular. If we further assume that the neutrons are directly coupled, *M* would be two striped, i.e.,

$$M = \underbrace{\begin{pmatrix} \mathrm{X} & & & \\ \mathrm{X} & \mathrm{X} & & \\ \mathrm{X} & \mathrm{X} & \mathrm{X} & \\ \mathrm{X} & \mathrm{X} & \mathrm{X} & \mathrm{X} \end{pmatrix}}_{\text{no up-scatter}} = \underbrace{\begin{pmatrix} \mathrm{X} & & & \\ \mathrm{X} & \mathrm{X} & & \\ & \mathrm{X} & \mathrm{X} & \\ & & \mathrm{X} & \mathrm{X} \end{pmatrix}}_{\text{directly coupled}} \tag{2.57}$$

Solution, numerically, proceeds are for the one-speed case. The right-hand side (RHS) of Eq. 2.53 is evaluated from a guess at the flux in space and energy. The RHS is the source term. The flux is found using Gauss–Seidel or SOR to complete the inner iteration for the first iteration. Typically, the spatial grid is swept sequentially, starting with the equation for group 1, then 2, etc. *G* since the faster neutrons are essentially the source terms for the slower neutrons, but we suspect that it really does not matter what order the equations are swept.

Next, the source terms and *k* are updated and the iteration is repeated until both *k* and the flux have converged. It is a straightforward procedure; just be careful to properly account for all the scattering terms.

2.16 The Multiplication Factor and a Formal Calculation of Criticality

We are now at the point that we need to pay some attention to the calculation of *k* or four-factor formula that allows the analysis of the multiplication factor for pile of uranium that is possibly used in a nuclear reactor. In order to hold the core of reactor together, we probably need to add some coolant to remove fission-produced heat and maybe some structural materials as well. We also need to define *multiplication factor k* that characterized the chain reaction in reactor core as

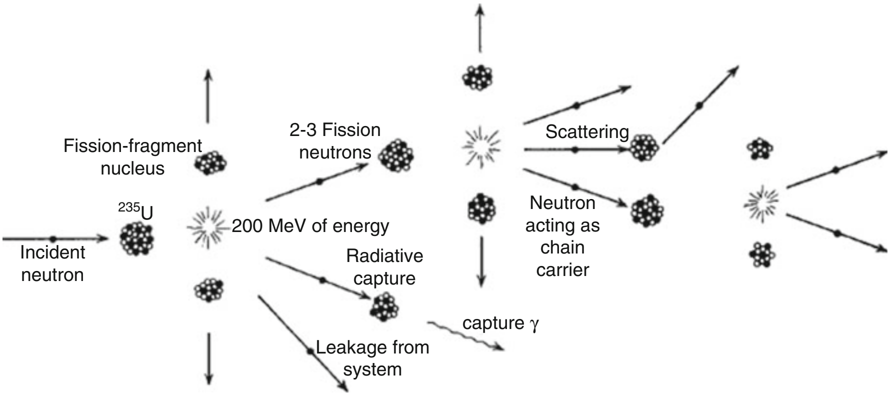

Fig. 2.13 A simple schematic of fission chain reaction for ^{235}U (Courtesy of Duderstadt and Hamilton) [3]

$$k \equiv \text{Multiplication Factor} \equiv \frac{\text{Number of neutron in one generation}}{\text{Number of neutron in preceding generation}}$$

A simple chain reaction also can schematically be depicted in Fig. 2.13.

Using the definition of multiplication factor k above, then we can declare the chain reaction is time independent, if $k = 1$, where the number of neutrons in any two consecutive fission generations is the same, and at this point the reactor is in critical mode. By the same talking if $k < 1$, then the reactor is in subcritical condition, and similarly if $k > 1$, the core is under supercritical operating mode.

In summary reactor core can operate under three following conditions:

$k < 1$ Subcritical
$k = 1$ Critical
$k > 1$ Supercritical

For purpose of reactor design, all the chosen materials and related subsystem within core (i.e., fuel rods) should be considered as part of criticality analysis so we can meet our primary objective of reactor design, which is having a reactor that can be in critical mode. Sometimes we need to reiterate our analysis and material that reactor finally goes critical as part of design and criticality condition is met, where $k = 1$.

Note that sometimes the multiplication factor k in terms of successive fission neutron generation is called and known as *life cycle*. Also bear in your mind that in the process of a chain reaction, some neutrons may not induce fission reactions at all, but instead are absorbed in a nonproductive capture or leak out of the core system; under these conditions we can somewhat have a better definition for multiplication factor k in order to have a neutron balance, as follows:

$$
\begin{aligned}
k &\equiv \text{Multiplication Factor} \\
&\equiv \frac{\text{Rate of neutron production in reactor}}{\text{Rate of neutron loss or absorption plus capture in reactor}}
\end{aligned}
$$

The above definition is explicitly indicating that the production and loss rate are a function of time due to fuel consumption, and they may vary accordingly [3].

We can also at this stage define the neutron lifetime l is as follows:

$$l = \frac{N(t)}{L(t)} \tag{2.58}$$

where $N(t)$ is the total neutron population or the number of neutron count and $L(t)$ is the loss rate in reactor at time t. And in order to have a better understanding of $N(t)$ in a nuclear reactor at a time t, we can take under consideration a simple *kinetics of chain reactions*, using the following analysis as

$$\frac{dN(t)}{dt} = \text{Production Rate} - \text{Loss Rate} = P(t) - L(t) \tag{2.59}$$

By the definition of multiplication factor k for balancing neutron, Eq. 2.59 further can be expanded to the following form of Eq. 2.60 as

$$\frac{dN(t)}{dt} = \left[\frac{P(t)}{L(t)} - 1\right] L(t) = (k-1)L(t) \tag{2.60}$$

To proceed further, we can write

$$\frac{dN(t)}{dt} = \frac{(k-1)}{l} N(t) \tag{2.61}$$

If we set an initial condition for the above ordinary differential Eq. 2.61 that there are N_0 neutrons in the reactor at time $t=0$ and assume that both k and l are time independent and in general they are not, we write a solution for Eq. 2.61 as

$$N(t) = N_0 \exp\left[\left(\frac{k-1}{l}\right)t\right] \tag{2.62}$$

The above simple approach to model a nuclear reactor kinetic agrees with reactor criticality in terms of k and depicted in Fig. 2.14 as well:

Note that the power level of a nuclear reactor is proportional to its neutron population; therefore, we are in position to regard the time behavior of the reactor power level as an exponential with a time constant or *reactor period* T given by

Fig. 2.14 Time behavior of the neutrons in a reactor

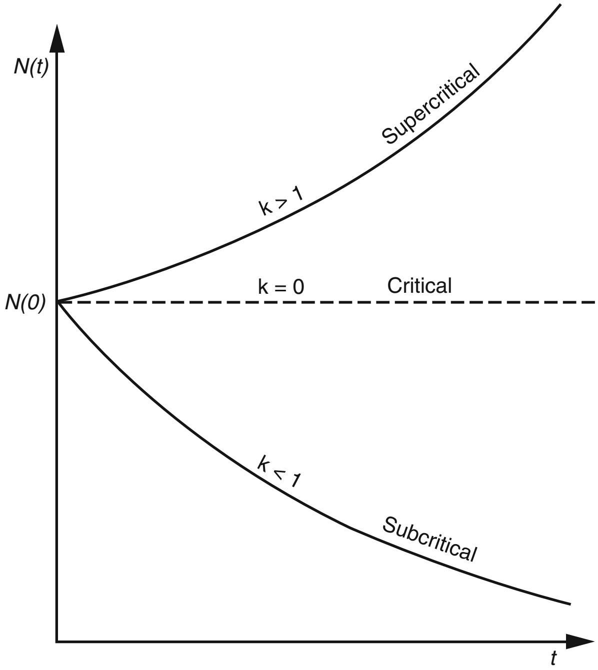

$$T = \frac{l}{k - 1} \tag{2.63}$$

Analyzing Eq. 2.63, we can observe if $k \rightarrow$ and then $T \rightarrow \infty$, which corresponds to a time-independent neutron population or reactor power level and is in agreement with our previous arguments above. However, if we want to expand our simple kinetics model, then we need to study the subject of nuclear reactor kinetic analysis which is beyond the scope of this book.

Before we continue with our analysis to calculate k, we need to investigate what is going with the neutrons in a given fission reaction or generation. Such fission neutron and probabilities for each of these possible events such as leak out of the reactor and be lost to the chain reaction and eventually absorbed that might be due to nonproductive capture event in either fuel or other materials can be depicted as shown in Fig. 2.15.

To make it more formal, we define the probabilities for each of these possible events presented in Fig. 2.15 as follows [3]:

$P_{\mathrm{NL}} \equiv$ probability that neutron will not leak out of the system before absorption

$P_{\mathrm{AF}} \equiv$ conditional probability that *if* neutron is absorbed, it will be absorbed in the fuel

$P_{\mathrm{f}} \equiv$ conditional probability that *if* neutron is absorbed in fuel, it will induce a fission reaction

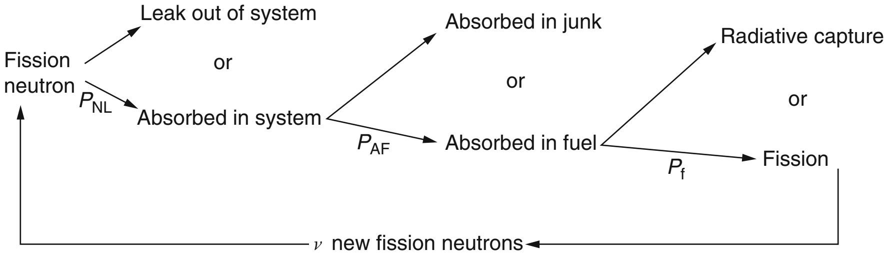

Fig. 2.15 Schematic of new fission neutron generation and possible event sequence (Courtesy of Duderstadt and Hamilton) [3]

We can easily calculate the last two probability conditions, and the conditional probability for absorption in the fuel P_{AF} can be expressed as the ratio of the macroscopic absorption cross section for the fuel $\sum_a^F$ and for the fuel plus the rest of the material in the core $\sum_a$ [3].

Note that, in Chap. 1, we defined the general form of macroscopic cross section as $\sum$. However, here we show the superscript to refer to material which we are concerned with (i.e., fuel), and the absence of the superscript will indicate that the macroscopic cross section is the total for all of the material in the system, and we use the symbol $\sum_t$ thus, for the probability of absorption, we can write

$$P_{AF} = \frac{\sum_a^F}{\sum_a} \tag{2.64}$$

Equation 2.64 holds only for the situation where the reactor has a uniform composition. Although in reality most the reactor design engineers encounter nonuniform compositions with modern reactor analysis, which varies from point to point due to fuel elements, coolant channels, support structure, etc., but usage macroscopic cross sections that is shown as symbol $\sum_a$ in respect to spatial average over all the reactor in more general case. Considering that we need to evaluate neutron energy at which these cross sections are under consideration, so Eq. 2.55 is valid for appropriately averaged over energy, just as they are over space.

It is where common knowledge that the probability of absorption to be called as *thermal utilization factor* of reactor and denote it by f as below and will be discussed further in section "References":

$$P_{AF} \equiv f \tag{2.65}$$

The term in Eq. 2.65 historically comes from the early analysis of thermal reactors in which essentially all fissions in the fuel were induced by thermal neutrons. Under these circumstances, the cross sections in f would be evaluated at thermal neutron energies and would represent the effectiveness of the fuel in competing with other materials in the reactor. For the absorption of thermal neutrons, that is, the effectiveness with which the reactor utilized the thermal neutrons in the fuel, Eq. 2.64 usually holds for any type of reactor [3].

Now, we are getting back to our definition above about conditional probability for inducing a fission reaction in the fuel. Thus, we can express it in terms of cross sections, which in that case we simply take the ratio of the fission cross section to that of the absorption cross section due to both fission and radiative capture in the fuel material as

$$P_{\mathrm{f}} = \frac{\sum_{\mathrm{f}}^{\mathrm{F}}}{\sum_{\mathrm{a}}^{\mathrm{F}}} = \frac{\sigma_{\mathrm{f}}^{\mathrm{F}}}{\sigma_{\mathrm{a}}^{\mathrm{F}}} \tag{2.66}$$

Now we are at the stage where we can utilize all these probabilities in order to determine the multiplication factor k defined above in order to follow the neutrons.

We start with N_1 neutrons present in the reactor in a given fission generation process; then, using Eq. 2.66 along with Fig. 2.15, we can compute the number of neutrons N_2 in the next step generation as

$$N_2 = \nu P_{\mathrm{f}} P_{\mathrm{AF}} P_{\mathrm{NL}} N_1 \tag{2.67}$$

So if substituting both Eqs. 2.65 and 2.66 into Eq. 2.67 and using the definition of the number of fission neutrons produced per absorption in the fuel as $\eta = \nu\left(\sigma_{\mathrm{t}}^{\mathrm{F}}/\sigma_{\mathrm{a}}^{\mathrm{F}}\right)$, then we get

$$N_2 = \eta f P_{\mathrm{NL}} N_1 \tag{2.68}$$

Note that η is also known as reproduction factor, and most of the neutrons absorbed in the fuel cause fission, but some do not. The reproduction factor η is defined as the ratio of the number of fast neutrons produced by thermal fission to the number of thermal neutrons absorbed in the fuel. The reproduction factor is shown below as

$$\eta = \frac{\text{number of fast neutrons produced by thermal fission}}{\text{number of thermal neutrons absorbed in the fuel}}$$

The reproduction factor can also be stated as the ratio of rated as shown below as well:

$$\eta = \frac{\text{rate of production of fast neutrons by thermal fission}}{\text{rate of absorption of thermal neutrons by the fuel}}$$

The rate of production of fast neutrons by thermal fission can be determined by the product of the fission reaction rate ($\sum_{\mathrm{f}}^{\mathrm{U}}\phi^{\mathrm{U}}$) and the average number of neutrons produced per fission (n). The average number of neutrons released in thermal fission of uranium-235 is 2.42. The rate of absorption of thermal neutrons by the fuel is $\sum_{\mathrm{f}}^{\mathrm{U}}\phi^{\mathrm{U}}$. Substituting these terms into the definition above results in the following equation:

Table 2.2 Average number of neutrons liberated in fission

Fissile nucleus	Thermal neutrons		Fast neutrons	
	v	η	v	η
Uranium-233	2.49	2.29	2.58	2.40
Uranium-235	2.42	2.07	2.51	2.35
Uranium-239	2.93	2.15	3.04	2.90

$$\eta = \frac{\sum_{\mathrm{f}}^{\mathrm{U}} \phi^{\mathrm{U}} v}{\sum_{\mathrm{f}}^{\mathrm{U}} \phi^{\mathrm{U}}} \tag{2.69}$$

Table 2.2 lists values of v and η for fission of several different materials by thermal neutrons and fast neutrons.

In the case where the fuel contains several fissionable materials, it is necessary to account for each material. In the case of a reactor core containing both uranium-235 (**^{235}U**) and uranium-238 (**^{238}U**), the reproduction factor would be calculated as shown below:

$$\eta = \frac{N^{\mathrm{U-235}} \sigma_{\mathrm{f}}^{\mathrm{U-235}} v^{\mathrm{U-235}}}{N^{\mathrm{U-235}} \sigma_{\mathrm{a}}^{\mathrm{U-235}} + N^{\mathrm{U-238}} \sigma_{\mathrm{a}}^{\mathrm{U-238}}} \tag{2.70}$$

To determine the reproduction factor for a single nuclide rather than for a mixture, the calculation may be further simplified to the one shown below:

$$\eta = v\left(\sigma_{\mathrm{t}}^{\mathrm{F}} / \sigma_{\mathrm{a}}^{\mathrm{F}}\right) \tag{2.71}$$

Note that the superscript is referring to uranium.

Now again utilizing the definition of multiplication factor k as being the ratio of the number of neutrons in two successive fission generations,

$$k = \frac{N_2}{N_1} = \frac{\eta f P_{\mathrm{NL}} N_1}{N_1} = \eta f P_{\mathrm{NL}} \tag{2.72}$$

In this equation the non-leakage probability P_{NL} and characterizing neutron leakage from the core of the reactor are very difficult to compare, and it will require more accurate analysis, and further analysis should be in place. However, since no neutrons could leak out, we can immediately come to conclusion that we should set the non-leakage probability $P_{\mathrm{NL}} = 1$, and therefore, the corresponding multiplication factor is then known as the *infinite-medium multiplication factor* and expressed by the following form of equation by substituting this value of P_{NL} in Eq. 2.69:

$$k_{\infty} = \eta f \tag{2.73}$$

However, we have to bear in mind that no reactor is of infinite size, but k_{∞} is a useful parameter in reactor analysis since it characterizes the multiplication properties of the *material* used in the reactor as distinct from the *geometry* of the reactor core. Of course since $P_{\mathrm{NL}} < 1$ more generally for a finite reactor from which some neutron leakage can occur, then we must have $k_\infty > 1$ in order to have any chance for critical chain reaction in reactor, which is in agreement with what we expressed previously.

2.17 Fast Fission Factor $\boldsymbol{\varepsilon}$ Definition

Another definition that we need to know for our further discussion in neutronic analysis *fast fission factor* $\boldsymbol{\varepsilon}$ as part of the first process that the neutron of one generation may undergo is fast fission. Fast fission is fission caused by neutrons that are in the fast energy range and slowing down to thermal energies. Fast fission results in the net increase in the fast neutron population of the reactor core. This factor as part of four-factor formula takes into account of the fact that, although most fission will be induced in fissile materials by thermal neutrons, some fissions will be induced in both fissile and fissionable materials by fast neutrons and will be related to multiplication factor k as shown in Eq. 2.72. The cross section for fast fission in uranium-235 ($^{\mathbf{235}}\mathbf{U}$) or uranium-238 ($^{\mathbf{238}}\mathbf{U}$) is small; therefore, only a small number of fast neutrons cause fission. The fast neutron population in one generation is therefore increased by a factor called the *fast fission factor*. The fast fission factor ($\boldsymbol{\varepsilon}$) is defined as the ratio of the net number of fast neutrons produced by all fissions to the number of fast neutrons produced by thermal fissions. The mathematical expression of this ratio is shown below:

$$\boldsymbol{\varepsilon} = \frac{\text{Total number of fission neutrons (from both fast and thermal fission)}}{\text{Number of fission neutrons from thermal fissions}}$$

Furthermore, the above definition can be presented by the following equation as

$$\boldsymbol{\varepsilon} \equiv \frac{\displaystyle\int_{\mathrm{fuel}} dV \int_0^\infty \nu \sum\nolimits_{\mathrm{f}}(\vec{\boldsymbol{r}}, E)\, dE}{\displaystyle\int_{\mathrm{fuel}} dV \int_0^{E_2} \nu \sum\nolimits_{\mathrm{f}}(\vec{\boldsymbol{r}}, E)\phi_1(\vec{\boldsymbol{r}}, E)\, dE} \tag{2.74}$$

where $\Phi(\boldsymbol{r}, E)$ is a flux and will be presented for infinite lattice of cells, where these cells are for given square shape fuel rod and its associated moderator and will be the same as that for any other cell. Thus, if we know $\Phi(\boldsymbol{r}, E)$ for one cell, we know it for all [4].

Note that, just as, if we know $\Phi(E)$ at one *point* in and infinite homogeneous medium, we know it for all points. The relationship that is given by fraction in Eq. 2.74 is the definition of fast fission factor $\boldsymbol{\varepsilon}$. The above relation is the ratio of the total rate of production of fission neutrons in the lattice to the rate of production due to fission in the thermal energy range, and with what is presented in Eq. 2.70, it is clear from the definition that $\boldsymbol{\varepsilon}$ depends directly only on $\mathrm{v}^j\sigma_f^j(E)n^j(\vec{\boldsymbol{r}},E)$ of the various fissionable isotopes contained in the fuel rod [4].

Also in order for a neutron to be absorbed by a fuel nucleus as a fast neutron, it must pass close enough to a fuel nucleus while it is a fast neutron. The value of $\boldsymbol{\varepsilon}$ will be affected by the arrangement and concentrations of the fuel and the moderator. The value of $\boldsymbol{\varepsilon}$ is essentially 1.00 for a homogenous reactor where the fuel atoms are surrounded by moderator atoms. However, in a heterogeneous reactor, all the fuel atoms are packed closely together in elements such as pins, rods, or pellets. Neutrons emitted from the fission of one fuel atom have a very good chance of passing near another fuel atom before slowing down significantly. The arrangement of the core elements results in a value of about 1.03 for $\boldsymbol{\varepsilon}$ in most heterogeneous reactors. The value of $\boldsymbol{\varepsilon}$ is not significantly affected by variables such as temperature, pressure, enrichment, or neutron poison concentrations. Poisons are nonfuel materials that easily absorb neutrons and will be discussed in more detail later.

To further enhance our analysis, we need to introduce a second factor in the next section that will characterize the possibility, where neutron might be absorbed while slowing down from fission to thermal energies.

2.18 Resonance Escape Probability *p*

After increasing in number as result of some fast fission, the neutrons continue to diffuse through the reactor. As the neutrons move, they collide with nuclei of fuel and nonfuel material and moderator in the reactor losing a part of their energy in each collision and slowing down. While they are slowing down through the resonance region of uranium-238, which extends from about 6 to 200 eV, there is a chance that some neutrons will be captured. The probability that a neutron will not be absorbed by a resonance peak is called the resonance escape probability. The *resonance escape probability* (p) is defined as the ratio of the number of neutrons that reach thermal energies to the number of fast neutrons that start to slow down. This ratio is shown below:

$$p = \frac{\text{number of neutron that reach thermal energy}}{\text{number of fast neutrons that start to slow down}}$$

The value of the resonance escape probability is determined largely by the fuel–moderator arrangement and the amount of enrichment of uranium-235 ($^{235}\mathbf{U}$) (if any is used). To undergo resonance absorption, a neutron must pass close enough to a uranium-238 ($^{238}\mathbf{U}$) nucleus to be absorbed while slowing down. In a homogeneous reactor, the neutron does its slowing down in the region of the fuel nuclei, and this condition is easily met. This means that a neutron has a high probability of being absorbed by uranium-238 ($^{238}\mathbf{U}$) while slowing down; therefore, its escape probability is lower. In a heterogeneous reactor, however, the neutron slows down in the moderator where there are no atoms of uranium-238 ($^{\mathbf{238}}\mathbf{U}$) present. Therefore, it has a low probability of undergoing resonance absorption, and its escape probability is higher.

The value of the resonance escape probability is not significantly affected by pressure or poison concentration. In water-moderated, low-uranium-235 ($^{\mathbf{235}}\mathbf{U}$) enrichment reactors, raising the temperature of the fuel will raise the resonance absorption in uranium-238 ($^{\mathbf{238}}\mathbf{U}$) due to the Doppler effect (an apparent broadening of the normally narrow resonance peaks due to thermal motion of nuclei). The increase in resonance absorption lowers the resonance escape probability, and the fuel temperature coefficient for resonance escape is negative (explained in detail later). The temperature coefficient of resonance escape probability for the moderator temperature is also negative. As water temperature increases, water density decreases. The decrease in water density allows more resonance energy neutrons to enter the fuel and be absorbed. The value of the resonance escape probability is always slightly less than one (normally 0.95–0.99).

The product of the fast fission factor and the resonance escape probability ($\boldsymbol{\varepsilon p}$) is the ratio of the number of fast neutrons that survive slowing down (thermalization) compared to the number of fast neutrons originally starting the generation.

Finally, as a useful step, we modify our definition of the non-leakage probability to take under consideration the fact that there would be two distinct phases of neutron leakage that will require two rather different types of analysis in our later work. First, the neutron may leak out while slowing down. In reality the neutron mean free path is relatively large for high energies; such fast neutron leakage may be quite slow down to thermal energies. After slowing down, the neutron may continue to scatter and eventually leak out before it has had an opportunity to be absorbed. To take account of these two processes, we will break up our earlier non-leakage probability P_{NL} as follows [3]:

$$P_{\mathrm{NL}} = P_{\mathrm{FNL}} P_{\mathrm{TNL}} \tag{2.75}$$

where P_{FNL} and P_{TNL} are defined below as

$P_{\mathrm{FNL}} \equiv$ probability that fast neutron will not leak out (fast non-leakage)
$P_{\mathrm{TNL}} \equiv$ probability that thermal neutron will not leak out (thermal non-leakage)

Inserting these two above definitions in Eq. 2.71 along with Eqs. 2.72 and 2.74, we get a new form for infinite-medium multiplication factor as follows:

$$k_{\infty} = \eta f p \varepsilon \tag{2.76}$$

This equation is known as the *four-factor formula* that is defined before in Sect. 2.16 of this book, and furthermore, one can write multiplication factor k of Eq. 2.69 in the following form:

$$k_\infty = \eta f p \varepsilon P_{\mathrm{FNL}} P_{\mathrm{TNL}} \tag{2.77}$$

which, this form of Eq. 2.77, is surprisingly known as the *six-factor formula*.

Note that one can vary the non-leakage probability P_{NL} by changing the geometry of the reactor or changing the materials surrounding the reactor with larger scattering cross section so that some of the neutrons leaking out will scatter back into the reactor [3].

As a matter of fact, when leakage is changed, there will be some changes in the parameters that consist of a four-factor formula as well since these are actually averages over the various neutron energies in the reactor, and this causes distribution of energies to vary with the amount of leakage. Thus, such consideration deduces somewhat different notation for multiplication factor characterizing a finite system which is occasionally referred to as the *effective multiplication factor* and denoted by k_{eff} and written as

$$k_{\mathrm{eff}} = k_\infty P_{\mathrm{FNL}} P_{\mathrm{TNL}} \tag{2.78}$$

More details and mathematical analysis can be found in Henry [4], and we encourage the reader to refer to that book.

2.19 Group Collapsing

Herein we will collapse the multigroup equations to one group just to show that the two forms are consistent with each other. Then, we will look at the two-group approximation because it is commonly used and it is illustrative without being overly complex.

2.19.1 Multigroup Collapsing to One Group

We have the general multigroup equation as

$$\frac{1}{v_g}\frac{\partial}{\partial t}\phi_g = \nabla\cdot D_g\nabla\phi_g - \sum\nolimits_{\mathrm{a}g}\phi_g - \sum\nolimits_{\mathrm{s}g}\phi_g + \sum_{g'=1}^{G}\sum\nolimits_{\mathrm{s}g'g}\phi_{g'} + \chi_g\sum_{g'=1}^{G}\nu_{g'}\sum\nolimits_{\mathrm{f}g'}\phi_{g'} + S_g^{\mathrm{ext}} \tag{2.79}$$

And we have the definitions of the coefficients as well in the form of

$$\phi_g(\vec{\boldsymbol{r}},t) \equiv \int_{E_g}^{E_{g-1}} \phi(\vec{\boldsymbol{r}},E,\, t)\, dE \Rightarrow \phi(\vec{\boldsymbol{r}},t) \equiv \int_0^\infty \phi(\vec{\boldsymbol{r}},E,\, t)\, dE \tag{2.80}$$

But in one group, we can write

$$\frac{1}{v_g} \equiv \frac{\displaystyle\int_{E_g}^{E_{g-1}} \frac{1}{v(E)}\phi(\vec{\boldsymbol{r}},E,t)dE}{\displaystyle\int_{E_g}^{E_{g-1}} \phi(\vec{\boldsymbol{r}},E,t)dE} \Rightarrow \frac{1}{v} \equiv \frac{\displaystyle\int_0^\infty \frac{1}{v(E)}\phi(\vec{\boldsymbol{r}},E,t)dE}{\displaystyle\int_0^\infty \phi(\vec{\boldsymbol{r}},E,t)dE} \tag{2.81}$$

and we can claim as well that

$$D_g \equiv \frac{\displaystyle\int_{E_g}^{E_{g-1}} D(E)\phi(\vec{\boldsymbol{r}},E,t)dE}{\displaystyle\int_{E_g}^{E_{g-1}} \nabla\phi(\vec{\boldsymbol{r}},E,t)dE} \Rightarrow D \equiv \frac{\displaystyle\int_0^\infty D(E)\nabla\phi(\vec{\boldsymbol{r}},E,t)dE}{\displaystyle\int_0^\infty \nabla\phi(\vec{\boldsymbol{r}},E,t)dE} \tag{2.82}$$

$$\sum\nolimits_{\mathrm{a}g} \equiv \frac{\displaystyle\int_{E_g}^{E_{g-1}} \sum\nolimits_{\mathrm{a}}(E)\phi(\overline{r},E,t)dE}{\displaystyle\int_{E_g}^{E_{g-1}} \phi(\overline{r},E,t)dE} \Rightarrow \sum\nolimits_{\mathrm{a}} \equiv \frac{\displaystyle\int_0^\infty \sum\nolimits_{\mathrm{a}}(E)\phi(\overline{r},E,t)dE}{\displaystyle\int_0^\infty \phi(\vec{\boldsymbol{r}},E,t)dE} \tag{2.83}$$

The scattering terms are

$$-\sum\nolimits_{\mathrm{s}g}\phi_g + \sum_{g'=1}^{G} \sum\nolimits_{\mathrm{s}g'g}(r)\phi_{g'}(\vec{\boldsymbol{r}},t) \rightarrow \sum\nolimits_{\mathrm{s}}\phi_g + \sum\nolimits_{\mathrm{s}}\phi_g = 0 \tag{2.84}$$

Note that Eq. 2.83 holds when $G = 1$.

The fission term is

$$\begin{gathered} \chi_g \equiv \int_{E_g}^{E_{g-1}} \chi(E)dE \Rightarrow \chi \equiv \int_0^\infty \chi(E)dE = 1 \\ \sum_{g'=1}^{G} v_{g'}\sum\nolimits_{\mathrm{f}g'}\phi_{g'} \Rightarrow v\sum\nolimits_{\mathrm{f}}\phi \end{gathered} \tag{2.85}$$

Putting all these terms together, we get back the one-group equation:

$$\frac{1}{v}\frac{\partial}{\partial t}\phi(\vec{\boldsymbol{r}},t) = \nabla \cdot D(r)\nabla\phi(\vec{\boldsymbol{r}},t) - \sum\nolimits_{\mathrm{a}}(r)\phi(\vec{\boldsymbol{r}},t) + v\sum\nolimits_{\mathrm{f}}\phi(\vec{\boldsymbol{r}},t) \tag{2.86}$$

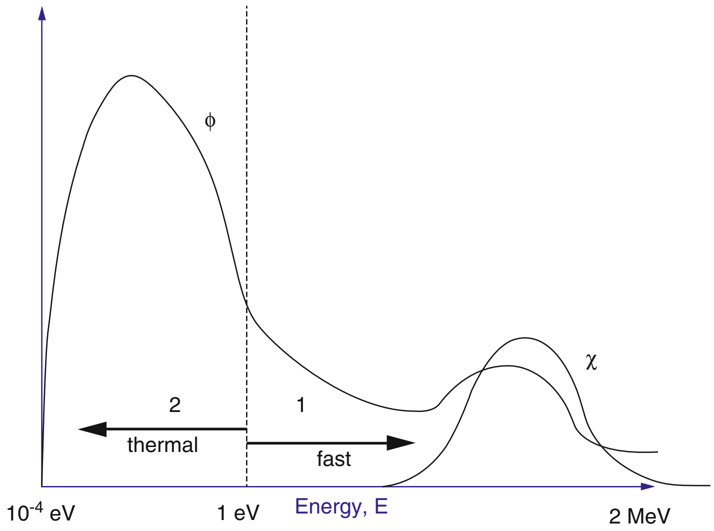

Fig. 2.16 Two-group approximation

2.19.2 Multigroup Collapsing to Two Group

The two-group approximation is a common and illustrative one. We divide the neutrons into a thermal group and a fast group with the division at 1 eV, as shown in Fig. 2.16.

Note that

$$\chi_2 = \int_0^{1\ \mathrm{eV}} \chi(E)dE = 0 \quad \text{and} \quad \chi_1 = 1 \tag{2.87}$$

Thus, the general fission source term is

$$S_g = \underbrace{\chi_g}_{\substack{\text{fission}\\ \text{appearing}\\ \text{in group } g}} \underbrace{\sum_{g'=1}^{G} \nu_{g'} \sum\nolimits_{\mathrm{f}g'}(\vec{\boldsymbol{r}})\phi_{g'}(\vec{\boldsymbol{r}},t)}_{\text{total fission production}} \tag{2.88}$$

For the simple two-group case,

$$\begin{aligned} S_1 &= \nu_1 + \textstyle\sum_{\mathrm{f}1}\phi_1 + \nu_2\textstyle\sum_{\mathrm{f}2}\phi_2 \\ S_2 &= 0 \end{aligned} \tag{2.89}$$

There is no upscattering so

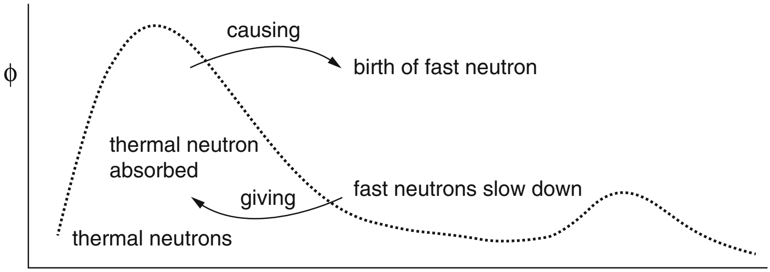

Fig. 2.17 Thermal fast exchange

$$\sum\nolimits_{s21} = 0 \Rightarrow \sum\nolimits_{s2} + \sum\nolimits_{s22} \Rightarrow \sum \mathrm{S}_{s2} = \sum\nolimits_{s22} \tag{2.90}$$

Therefore,

$$\sum\nolimits_{s21} = \sum\nolimits_{t2} - \sum\nolimits_{s22} = \sum\nolimits_{a2} \tag{2.91}$$

Thus, the two-group equations are

$$\begin{aligned} \frac{1}{v_1}\frac{\partial \phi_1}{\partial t} &= \nabla \cdot D_1 \phi_1 - \sum\nolimits_{r1} \phi_1 + v_1 \sum\nolimits_{f1} \phi_1 + v_2 \sum\nolimits_{f2} \phi_2 \ \text{ no up} - \text{scatter} \\ \frac{1}{v_1}\frac{\partial \phi_1}{\partial t} &= \nabla \cdot D_2 \phi_2 - \sum\nolimits_{a2} \phi_2 + \sum\nolimits_{s12} \phi_1 \ \text{ no direct fission source} \end{aligned} \tag{2.92}$$

In a steady state, adding the *k* fudge factor, we have

$$\begin{aligned} -\nabla \cdot D_1 \phi_1 - \sum\nolimits_{r1} \phi_1 &= \frac{1}{k}\left[v_1 \sum\nolimits_{f1} \phi_1 + v_2 \sum\nolimits_{f2} \phi_2 \right] \ \text{ no up} - \text{scatter} \\ -\nabla \cdot D_2 \phi_2 - \sum\nolimits_{a2} \phi_2 &= \sum\nolimits_{s12} \phi_1 \ \text{ no direct fission source} \end{aligned} \tag{2.93}$$

Notice how the fast flux is the source term for the thermal neutrons (by scattering down in energy), while the thermal flux is the source for the fast neutrons by the fission event. This is illustrated in Fig. 2.17.

So, it follows that you would expect to see an abundance or peak of fast neutrons in the fuel region (because that is where the fissions take place). They diffuse to the moderator where there is a high probability of slowing down (because of the materials used there for just that purpose). Hence, you would expect to see a peak of thermal neutrons in the moderator. This is illustrated in Fig. 2.18.

Thus, the fast and thermal neutrons not only have a vastly different energy distribution; they have different spatial distributions in general.

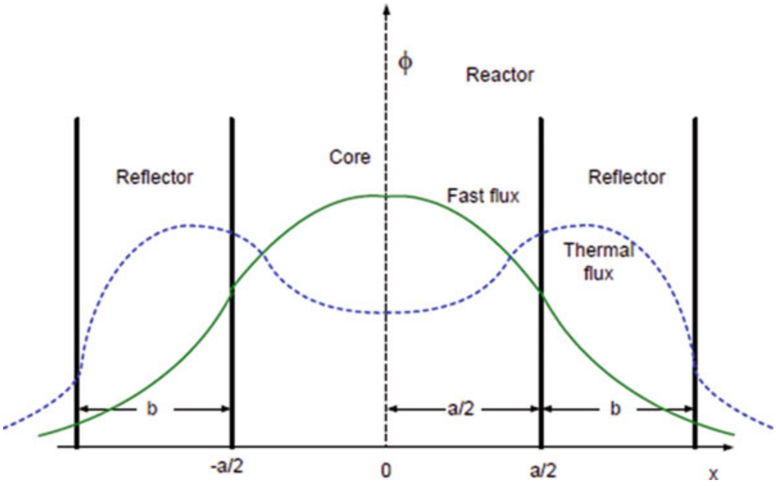

Fig. 2.18 Spatial distribution of flux

2.19.3 Two-Group Criticality

We consider the case of a bare (i.e., unreflected) reactor so that we can develop the criticality condition for the two-group case and compare it to the one-speed case developed earlier. Because the moderator and fuel are mixed together, the thermalization and fission processes are not physically separated. We can expect that both the fast and the thermal fluxes will have the same fundamental cosine shape for a simple slab reactor. The basic equations are

$$\begin{aligned} -\nabla \cdot D_1\phi_1 - \textstyle\sum_{\mathrm{r}1}\phi_1 &= \frac{1}{k}\left[\nu_1\textstyle\sum_{\mathrm{f}1}\phi_1 + \nu_2\textstyle\sum_{\mathrm{f}2}\phi_2\right] \\ -\nabla \cdot D_2\phi_2 - \textstyle\sum_{\mathrm{a}2}\phi_2 &= \textstyle\sum_{\mathrm{s}12}\phi_1 \end{aligned} \tag{2.94}$$

We write the flux as a product of an amplitude factor and a shape factor:

$$\phi_1(\bar{r}) = \varphi_1\psi(\bar{r}) \quad \text{and} \quad \phi_2(\bar{r}) = \varphi_2\psi(\bar{r}) \tag{2.95}$$

Defining the buckling for homogeneous reactor as usual:

$$\nabla^2\psi(\bar{r}) + B^2\psi(\bar{r}) = 0 \tag{2.96}$$

We find that Eq. 2.95 becomes

$$\begin{aligned} &+D_1B^2\varphi_1+\sum\nolimits_{r1}\varphi_1=\frac{1}{k}\left[\nu_1\sum\nolimits_{f1}\varphi_1+\nu_2\sum\nolimits_{f2}\varphi_2\right] \\ &+D_2B^2\varphi_2-\sum\nolimits_{a2}\varphi_2=\sum\nolimits_{s12}\varphi_1 \end{aligned} \tag{2.97}$$

Or in matrix form Eq. 2.97 can be written as

$$\begin{pmatrix} \left(D_1B^2-\sum_{r1}-\frac{\nu_1\sum_{f1}}{k}\right) & -\frac{\nu_2\sum_{f2}}{k} \\ -\sum_{s12} & \left(D_2B^2+\sum_{a2}\right) \end{pmatrix}=0 \tag{2.98}$$

$$\text{i.e.,}\quad \overline{\overline{A}}\,\overline{\varphi}=0 \tag{2.99}$$

which has a nontrivial solution for the flux amplitudes only if the following relationship is imposed

$$\left|\overline{\overline{A}}\right|=0 \tag{2.100}$$

Thus:

$$\left(D_1B^2-\sum\nolimits_{r1}-\frac{\nu_1\sum_{f1}}{k}\right)\left(D_2B^2+\sum\nolimits_{a2}\right)-\frac{\nu_2\sum_{f2}\sum_{s12}}{k}=0 \tag{2.101}$$

Solving for the multiplication factor k, we get

$$\begin{aligned} k&=\underbrace{\frac{\nu_1\sum_{f1}}{\sum_{r1}+D_1B^2}}_{\text{fast fission}}+\frac{\sum_{s12}}{\left(\sum_{r1}+D_1B^2\right)}\,\frac{\nu_2\sum_{s12}}{\left(\sum_{a2}+D_2B^2\right)} \\ &=1\quad\text{at criticality} \end{aligned} \tag{2.102}$$

The first term on the right-hand side (RHS) is the fast fission contribution. We can lump it into the second term via the fast fission factor ε which is defined below and recognize that:

- The resonance escape probability is just the ratio of the number of neutrons that successfully scatter down to group 2 over the number that leave group 1.
- Likewise, ηf is just the ratio of neutrons born to the number of thermal absorbed, and further discussion is given in Sect. 2.9 as well.

Thus, we can reconstruct the four-factor formula, with additional factors for fast and thermal leakage:

$$\begin{aligned} k &= \frac{\sum_{\mathrm{s}12}}{\left(\sum_{\mathrm{r}1} + D_1 B^2\right)} \frac{\nu_2 \sum_{\mathrm{f}2}}{\left(\sum_{\mathrm{a}2} + D_2 B^2\right)} \\ &= \frac{\sum_{\mathrm{s}12} / \sum_{\mathrm{r}1}}{\left(1 + L_1^2 B^2\right)} \frac{\nu_2 \sum_{\mathrm{f}2} / \sum_{\mathrm{a}2}}{\left(1 + L_2^2 B^2\right)} = \frac{p}{\left(1 + L_1^2 B^2\right)} \frac{\eta f}{\left(1 + L_2^2 B^2\right)} \\ &= p \eta f P_{\mathrm{NL}1} P_{\mathrm{NL}2} \end{aligned} \tag{2.103}$$

where $L^2 \equiv D / \sum_{\mathrm{a}2}$.

Note that as again we mentioned previously, the fast fission factor $\boldsymbol{\varepsilon}$ is usually quite close to unity in a thermal reactor with typical values ranging between $\boldsymbol{\varepsilon} = 1.03$ and $\boldsymbol{\varepsilon} = 1.15$.

2.20 The Infinite Reactor

To simplify analysis and separate effects, begin by considering an infinitely large reactor. This means that leakage could be ignored for the moment. The above spectrum is a characteristic of such a reactor. The multiplication factor can be written as

$$k = \frac{\int \nu \Sigma_{\mathrm{f}}(E) \phi(E) dE}{\int \Sigma_{\mathrm{a}}(E) \phi(E) dE} = \frac{\text{Production}}{\text{Absorption}} \tag{2.104}$$

Now if we define an average fission production rate as

$$\nu \Sigma_{\mathrm{f}} = \frac{\int \nu \Sigma_{\mathrm{f}}(E) \phi(E) dE}{\int \phi(E) dE} \tag{2.105}$$

and an average consumption rate as

$$\Sigma_{\mathrm{a}} = \frac{\int \Sigma_{\mathrm{a}}(E) \phi(E) dE}{\int \phi(E) dE} \tag{2.106}$$

we can write k as

$$k_{\infty} = \frac{v\Sigma_{\mathrm{f}}}{\Sigma_{\mathrm{a}}} \tag{2.107}$$

where k is identified with the subscript for infinity to identify this multiplication factor as applying to an infinitely large reactor.

2.21 Finite Reactor

In order to consider a finite reactor, we must introduce the concept of leakage out of the reactor as a destruction process. This can be written as

$$k = \frac{\text{Production}}{\text{Absorption } + \text{Leakage}} \tag{2.108}$$

or

$$\begin{aligned} k &= \frac{\int v\Sigma_{\mathrm{f}}(E)\ \varphi(E)dE}{\int \Sigma_{\mathrm{a}}(e)\ \varphi(e)dE + \int L(E)\ dE} \\ &= \frac{\int v\Sigma_{\mathrm{f}}(E)\ \varphi(E)dE}{\int \Sigma_{\mathrm{a}}(E)\ \varphi(E)dE} \frac{1}{1 + \dfrac{\int L(E)\ dE}{\int \Sigma_{\mathrm{a}}(E)\ \varphi(E)dE}} \end{aligned} \tag{2.109}$$

$$k = k_{\infty} P_{\mathrm{NL}} \tag{2.110}$$

or the multiplication factor with leakage is equal to the infinite multiplication factor times the probability of non-leakage. This multiplication factor is called k_{eff}, which is in agreement with what we presented before.

2.22 Time Dependence

These are static concepts. In order to make it more realistic, we need to introduce time dependence. To introduce time dependence, we need some estimate of how long it takes a generation to be produced or consumed. This concept can be defined as the average neutron lifetime and given in the symbol l. Then, a simple balance equation can be written as

$$\frac{d\phi(t)}{dt}=\frac{\text{Differential Production}}{\text{Consumption Rate}}=\frac{\nu\sum_{\mathrm{f}}\phi-\sum_{\mathrm{a}}\phi}{\sum_{\mathrm{a}}l}=\frac{(k-1)\sum_{\mathrm{a}}}{\sum_{\mathrm{a}}l}\phi \tag{2.111}$$

$$\frac{d\phi(t)}{dt}=\frac{(k-1)}{l}\phi(t) \tag{2.112}$$

whose solution is

$$\phi(t)=\phi(0)\mathrm{e}^{-\frac{k-1}{l}t} \tag{2.113}$$

Thus, the flux level in a reactor (and therefore the power level) will exponentially increase or decrease depending on the sign of $k-1$. The following table applies

$k>1$, flux exponentially increases
$k=0$, flux is stable
$k<1$, flux exponentially decreases

Since even thermal neutrons move at speeds over a thousand meters per second, neutron lifetimes are very short. A typical lifetime in a thermal reactor is on the order of tenths of a millisecond. In a fast reactor, lifetimes can be as short as tenths of a microsecond. If there were no delayed neutrons, these short time constants would make a nuclear reactor almost uncontrollable. However, delayed neutrons add a significant delay to control actions so that most reactors are easily controllable by human manipulation. The time required, for reactor power (or neutron flux) to increase or decrease by a factor of exponential, is called the reactor "period." For this simple model, this is given by $l/k-1$.

The four-, five-, or six-factor formulas can give a slightly more detailed model of the chain reaction process. The four-factor formula breaks down the chain reaction into a factor that takes into account the efficiency of the fuel nuclide itself, called η and defined by

$$\eta=\frac{\nu\sigma_{\mathrm{f}}^{\mathrm{F}}}{\sigma_{\mathrm{a}}^{\mathrm{F}}}$$

Again, this is in agreement with the previous discussion and presented in Eq. 2.71.

A second factor quantifies the ratio of the absorption of thermal neutrons in the fuel to the absorption of thermal neutrons in the fuel and moderator. This factor is called thermal utilization factor and given by f as

$$f=\frac{\sum_{\mathrm{a}}^{\mathrm{F}}}{\sum_{\mathrm{a}}^{\mathrm{F}}+\sum_{\mathrm{a}}^{\mathrm{M}}} \tag{2.114}$$

This factor is defined in more detail in section "References".

In a homogeneous reactor, the neutron flux seen by the fuel, moderator, and poison will be the same. In addition, since they are spread throughout the reactor, they all occupy the same volume. This allows the previous equation to be rewritten as shown below:

$$f = \frac{\sum_{\mathrm{a}}^{\mathrm{F}}}{\sum_{\mathrm{a}}^{\mathrm{F}} + \sum_{\mathrm{a}}^{\mathrm{M}} + \sum_{\mathrm{a}}^{\mathrm{P}}} \tag{2.115}$$

The superscripts F, M, and P refer to fuel such as uranium, moderator, and poison, respectively.

A third factor takes into account the fraction of fast neutrons that slow down from fission energies to thermal energies without being absorbed. This factor is called the probability of resonance escape and given in the symbol p_{re}. The fourth factor takes into account the fact that not all fissions are caused by thermal neutrons. It is simply called the fast fission factor and is given the symbol ε. The four-factor formula is then written as

$$k_{\infty} = \eta f p_{\mathrm{re}} \varepsilon \tag{2.116}$$

For a finite reactor, this must be modified by including the probability of leakage. We get five terms if an integral non-leakage probability is considered. If we separate out fast and thermal leakage, then we get two non-leakage terms. This is often done to emphasize the fast leakage, as thermal leakage is usually insignificant for a large reactor. The formula for k_{eff} becomes

$$k_{\mathrm{eff}} = \eta f p_{\mathrm{re}} \varepsilon P_{\mathrm{NL}} = \eta f p_{\mathrm{re}} \varepsilon P_{\mathrm{NL}}^{\mathrm{F}} P_{\mathrm{NL}}^{\mathrm{Th}} \tag{2.117}$$

Perhaps the real reasons for trying to understand the four- or six-factor formulas are historical ones. They were an attempt to isolate effects, so that they could be measured separately. Typical values for any of the parameters are no longer tabulated for any of these quantities. Their values can be obtained from multigroup calculations for specific configurations. And multigroup calculations are so inexpensive today that tabulating these parameters does not produce a useful analysis approach.

2.23 Thermal Utilization Factor f

Once thermalized, the neutrons continue to diffuse throughout the reactor and are subject to absorption by other materials in the reactor as well as the fuel. The thermal utilization factor describes how effectively thermal neutrons are absorbed by the fuel or how well they are utilized within the reactor. The *thermal utilization factor* (f) is defined as the ratio of the number of thermal neutrons absorbed in the fuel to the number of thermal neutrons absorbed in any reactor material. This ratio is shown below:

$$f = \frac{\text{number of thermal neutrons absorbed in the fuel}}{\text{number of thermal neutrons absorbed in all reactor materials}}$$

The thermal utilization factor will always be less than one, because some of the thermal neutrons that are absorbed within the reactor will be absorbed by atoms of nonfuel materials.

An equation can be developed for the thermal utilization factor in terms of reaction rates as follows:

$$f = \frac{\text{rate of absorption of thermal neutrons by the fuel}}{\text{rate of absorption of thermal neutrons by all reactor materials}}$$

or in general mathematically can be written as

$$f = \frac{\sum_{\mathrm{a}}^{\mathrm{F}} \phi^{\mathrm{F}} V^{\mathrm{F}}}{\sum_{\mathrm{a}}^{\mathrm{F}} \phi^{\mathrm{F}} V^{\mathrm{F}} + \sum_{\mathrm{a}}^{\mathrm{M}} \phi^{\mathrm{M}} V^{\mathrm{M}} + \sum_{\mathrm{a}}^{\mathrm{P}} \phi^{\mathrm{P}} V^{\mathrm{P}}} \tag{2.118}$$

The superscripts F, M, and P refer to fuel, moderator, and poison, respectively. In a heterogeneous reactor, the flux will be different in the fuel region than in the moderator region due to the high absorption rate by the fuel. Also, the volumes of fuel, moderator, and poison will be different. Although not shown in the above equation, other nonfuel materials, such as core construction materials, may absorb neutrons in a heterogeneous reactor. These other materials are often lumped together with the superscript designation OS, for "other stuff." To be completely accurate, the above equation for the thermal utilization factor should include all neutron-absorbing reactor materials when dealing with heterogeneous reactors. However, for the purposes of this text, the above equation is satisfactory.

However, as we said before, in a homogeneous reactor, the neutron flux seen by the fuel, moderator, and poison will be the same. In addition, since they are spread throughout the reactor, they all occupy the same volume. This allows Eq. 2.116 to reduce to Eq. 2.115.

Equation 2.118 gives an approximation for a heterogeneous reactor if the fuel and moderator are composed of small elements distributed uniformly throughout the reactor.

Since absorption cross sections vary with temperature, it would appear that the thermal utilization factor would vary with a temperature change. But substitution of the temperature correction formulas in Eq. 2.115 will reveal that all terms change by the same amount, and the ratio remains the same. In heterogeneous water-moderated reactors, there is another important factor. When the temperature rises, the water moderator expands, and a significant amount of it will be forced out of the reactor core. This means that N^{M}, the number of moderator atoms per cm^3, will be reduced, making it less likely for a neutron to be absorbed by a moderator atom. This reduction in Nm results in an increase in thermal utilization as moderator temperature increases because a neutron now has a better chance of hitting a fuel atom. Because of this effect, the temperature coefficient for the thermal utilization factor is positive. The amount of enrichment of uranium-235 and the poison concentration will affect the thermal utilization factor in a similar manner as can be seen from the equation above.

Problems

Problem 2.1 If a one cubic centimeter section of a reactor has a macroscopic fission cross section of 0.1 cm^{-1} and if the thermal neutron flux is 10^{13} neutrons/cm^2 s, what is the fission rate in that cubic centimeter?

Problem 2.2 A reactor operating at a flux level of 3×10^{13} neutrons/cm^2 s contains 1020 atoms of uranium-235 per cm^3. The reaction rate is 1.29×10^{12} fission/cm^3. Calculate $\sum_f$ and σ_f, assuming 1 barn $= 10^{-24}$ cm^2.

Problem 2.3 How many collisions are required to slow a neutron from energy of 2 MeV to a thermal energy of 0.025 eV, using water as the moderator. Water has a value of 0.948 for M.

Problem 2.4 If the average fractional energy loss per collision in hydrogen is 0.63, what will be the energy of a 2 MeV neutron after (a) five collisions and (b) ten collisions?

Problem 2.5 A block of aluminum has a density of 2.699 g/cm^3. If the gram atomic weight of aluminum is 26.9815 g, calculate the atom density of the aluminum.

Problem 2.6 How long will it be on average for a given nuclei to suffer a neutron interaction?

Problem 2.7 Find the macroscopic thermal neutron absorption cross section for iron, which has a density of 7.86 g/cm^3. The microscopic cross section for absorption of iron is 2.56 barns and the gram atomic weight is 55.847 g.

Problem 2.8 Calculate the reproduction factor for a reactor that uses 10 % enriched uranium fuel. The microscopic absorption cross section for uranium-235 is 694 barns. The cross section for uranium-238 is 2.71 barns. The microscopic fission cross section for uranium-235 is 582 barns. The atom density of uranium-235 is 4.83×10^{21} atoms/cm^3. The atom density of uranium-238 is 4.35×10^{22} atoms/cm^3. N is 2.42.

Problem 2.9 Calculate the thermal utilization factor for a homogeneous reactor. The macroscopic absorption cross section of the fuel is 0.3020 cm^{-1}, the macroscopic absorption cross section of the moderator is 0.0104 cm^{-1}, and the macroscopic absorption cross section of the poison is 0.0118 cm^{-1}.

Problem 2.10 Determine the infinite multiplication factor k_∞ for a uniform mixture of uranium-235 and beryllium oxide in the atomic or molecular ratio of 1–10,000. The value of absorption cross section for beryllium is

$\sigma_a = 0.010$ (barn) and for uranium is $\sigma_U = 683$ (barn). Assume the resonance escape probability and the fast fission factor may be taken to be unity and ratio of average number of neutrons librated per neutron absorbed for uranium-235 at thermal (2200 m/s) is $\eta = 2.06$.

References

1. M. Ragheb, *Neutron Diffusion Theory,* http://mragheb.com/NPRE%20402%20ME%20405%20Nuclear%20Power%20Engineering/Neutron%20Diffusion%20Theory.pdf
2. B. Garland, http://www.nuceng.ca/ep4d3/ep4d3home.htm
3. J. Duderstadt, L. Hamilton, *Nuclear Reactor Analysis* (Wiley, New York, 1976)
4. A. Henry, *Nuclear Reactor Analysis* (The MIT Press, Cambridge, 1975)

Chapter 3
Spatial Effects in Modeling Neutron Diffusion: One-Group Models

The fundamental aspect of keeping a reactor critical was discussed in Chap. 2, and we found out that the most principal evaluation quantity of the nuclear design calculation is the effective multiplication factor ($\overline{\sigma}(v,T) = \frac{1}{v}\int d^3V|v-V|\ \sigma(|v-V|)M(V,T)$) and neutron flux distribution. We also so far have noticed that the excess reactivity, control rod worth, reactivity coefficient, power distribution, etc., are undoubtedly inseparable from the nuclear design calculation. Some quantities among them can be derived by secondary calculations from the effective multiplication factor or neutron flux distribution that was also discussed in Sect. 2.15 of Chap. 2. In this chapter we treat the theory and mechanism to be able to analysis and calculate the effective multiplication factor and neutron flux distribution and possibly show numerical analysis and computer codes involved with solving the diffusion equation in a one-dimensional and one-group models. The goal of this chapter is also for readers to understand simple reactor systems, the notion of criticality, what it means both physically and mathematically, how to analytically solve steady-state flux for simple geometries, and finally how to numerically solve the steady state for more arbitrarily complex geometries.

3.1 Nuclear Reactor Calculations

The fundamental tool for reactor design analyses is multigroup diffusion theory. The ability of Monte Carlo methods to accurately calculate criticality in complex geometry has grown significantly with the advent of very high-speed computers with megabytes of fast memory. However, improved computing capability means that multigroup deterministic methods also run faster, and more questions can be asked during the design process. The design process really is one of synthesis, and therefore a deterministic method guides the thought patterns required to understand the complex interplay of materials and physical processes. Monte Carlo methods

B. Zohuri, *Neutronic Analysis For Nuclear Reactor Systems*,
DOI 10.1007/978-3-319-42964-9_3

perform the analysis task very well but often do not provide this insight into the interplay of the physical processes involved. In addition, there is always the concern that the effects observed by varying a design parameter are not really real but rather the result of some unlucky statistical occurrence due to the random numbers chosen. Running enough histories can always minimize this, but it is sometimes hard to determine the required number ahead of time. Finally, deterministic multigroup calculations are based on a set of tested cross sections that behave the same way every time. Monte Carlo cross sections can also be tested multiple times, but they never give exactly the same answer for the same problem starting with different random numbers.

A well-thought-out process has been developed over the years for performing high-quality multigroup diffusion calculations for reactor design. The **ENDF/B** pointwise data is processed through a number of steps to obtain problem-dependent "group constants" appropriate for the design of the reactor under consideration. This process goes as follows:

1. The pointwise **ENDF/B data** is processed to a set of many (~200–1000) group cross sections so that every material has the same group boundaries for its linear and two-dimensional arrays. The within-group weighting spectrum for this processing is normally chosen to be either the fission slowing down thermal Maxwellian asymptotic spectrum or a constant.
2. An infinite medium or zero-dimensional calculation is performed for all core compositions of interest. The individual group fluxes from this calculation are used as the within-group spectrum to collapse the material cross sections to a broad group set typically in the range of 10–50 groups.
3. These cross sections are then used in a cell calculation to determine spatial self-shielding factors for various geometric configurations within the reactor assembly. The cell fluxes are used for this collapse and self-shielding subject to the requirement to match reaction rates as closely as possible in going from broad groups to few groups.
4. Finally, the multidimensional reactor design calculations are performed with the few-group cross sections.

In some cases, steps 2 and 3 can be combined, but they will be dealt with separately in this book to demonstrate the difference between spatial and energy-dependent effects.

The nuclear reactor calculation is classified broadly into the reactor core calculation and the nuclear plant characteristic calculation. The former is done to clarify nuclear, thermal, or their composite properties. The latter is done to clarify dynamic and control properties, start-up and stability, and safety by modeling pipes and valves of the coolant system, coolant pump, their control system, steam turbine and condenser, etc., connected with the reactor pressure vessel as well as the reactor core. The reactor core, plant dynamics, safety analysis, and fuel rod analysis are described in later part of this book.

The collective behavior of neutrons in a reactor core is described by the neutron transport equation presented in Eq. 3.1 which is also referred to as the Boltzmann equation.

$$\frac{1}{v(E)}\frac{\partial}{\partial t}\phi\left(\vec{\boldsymbol{r}},\vec{\boldsymbol{\Omega}},E,t\right)=S\left(\vec{\boldsymbol{r}},\vec{\boldsymbol{\Omega}},E,t\right)-\vec{\boldsymbol{\Omega}}\cdot\nabla\phi\left(\vec{\boldsymbol{r}},\vec{\boldsymbol{\Omega}},E,t\right)-\Sigma_{\mathrm{t}}(\vec{\boldsymbol{r}},E,t)\phi\left(\vec{\boldsymbol{r}},\vec{\boldsymbol{\Omega}},E,t\right) \tag{3.1}$$

Here, S is the neutron source, Σ_{t} is the macroscopic total cross section, and ϕ is the angular neutron flux being calculated. And finally $v(E)$ is the neutron velocity corresponding to energy, E. This equation represents the balance between gain and loss in the unit volume of neutrons that are characterized by a specific kinetic energy E with velocity v and are traveling in a specific direction $\vec{\boldsymbol{\Omega}}$ at a time t and a position $\vec{\boldsymbol{r}}$. That is, the time change of the target neutrons which is the first term in the *left-hand side* (LHS) is given by the balanced relation among the gain of neutrons appearing from the neutron source S, which is the first term in the *right-hand side* (RHS). The net loss of neutrons traveling is the second term in the RHS, and the loss of neutrons due to nuclear collisions is the third term in the RHS. It should be noted that the changes in angle and energy of neutrons are also included in the gain and loss.

We expand upon this equation in Chap. 2 and the target neutrons are gained from three mechanisms: scattering, fission, and external neutron sources. Each gain is represented as follows:

$$\begin{aligned}S\left(\vec{\boldsymbol{r}},\vec{\boldsymbol{\Omega}},E,t\right)=&\int_0^\infty dE'\int_{4\pi}\Sigma_{\mathrm{s}}\left(\vec{\boldsymbol{r}},\vec{\boldsymbol{\Omega}}'\to\vec{\boldsymbol{\Omega}},E'\to E,t\right)\phi\left(\vec{\boldsymbol{r}},\vec{\boldsymbol{\Omega}}',E',t\right)d\boldsymbol{\Omega}'\\&+\frac{\chi(E)}{4\pi}\int_0^\infty dE'\int_{4\pi}\chi(E)\upsilon\Sigma_{\mathrm{f}}(\vec{\boldsymbol{r}},E',t)\phi\left(\vec{\boldsymbol{r}},\vec{\boldsymbol{\Omega}}',E',t\right)d\boldsymbol{\Omega}'\\&+S_{\mathrm{ex}}\left(\vec{\boldsymbol{r}},\vec{\boldsymbol{\Omega}},E,t\right)\end{aligned} \tag{3.2}$$

A very similar form of Eq. 3.2 was also presented in Chap. 2, where Σ_{s} and Σ_{f} are the macroscopic scattering and fission cross sections, respectively, and υ is the average number of neutrons released per fission and the product $v\Sigma_{\mathrm{f}}$ is treated as a production cross section. The cross sections were described in Chap. 2 of this book.

The first term in the RHS of Eq. 3.2 is called the *scattering source*, and it totals the number of the target neutrons scattering into E and $\vec{\Omega}$ from another energy E and direction $\vec{\Omega}$ by integrating the number for E and $\vec{\Omega}$. The second term is the fission source, and it indicates that the neutrons produced by fission over the whole range of energies are distributed with the isotropic probability in direction ($1/4\pi$) and the probability $\chi(E)$ in energy. $\chi(E)$ is called the *fission spectrum*, and it is dependent on the nuclide undergoing fission and the energy of incident neutrons. For instance, the fission spectrum in an enriched uranium-fueled light-water reactor (LWR) is well described by the function of Eq. 3.3 below.

$$\chi(E) = \sinh\left(\sqrt{2.29E}\right)\mathrm{e}^{(-E/0.965)} \tag{3.3}$$

Since $\chi(E)$ is a probability distribution function, it is normalized so that we can write the following form:

$$\int_0^\infty \chi(E)dE = 1.0 \tag{3.4}$$

The third term in the RHS of Eq. 3.2, S_{ex}, expresses the external neutron source for reactor start-up which may be such species as ^{252}Cf or Am-Be. Therefore, it is not used in the nuclear design calculation of a reactor in operation.

More details of the neutron transport equation are not handled here. If the cross-sectional data (Σ_t, Σ_s, and $\nu\Sigma_f$) in Eqs. 3.1 and 3.2 are provided, the angular neutron flux $\phi\left(\vec{r}, \vec{\boldsymbol{\Omega}}, E, t\right)$, which depends on location, traveling direction, energy, and time, can be calculated by properly solving the equation.

The information on traveling direction of neutrons is finally unimportant in the nuclear design calculation. The scalar neutron flux integrated over the angle is rather meaningful and presented as

$$\phi(\vec{r}, E, t) = \int_0^{4\pi} \phi\left(\vec{r}, \vec{\boldsymbol{\Omega}}, E, t\right) d\boldsymbol{\Omega} \tag{3.5}$$

3.1.1 Neutron Spectrum

The function characterizing the energy dependence of neutron flux $\phi(\vec{r}, E, t)$ is called the *neutron spectrum*, and it varies with fuel enrichment, moderator density, void fraction, burnup, and so on. Figure 3.1 shows a neutron spectrum of a thermal reactor. The neutron spectrum of thermal reactors is divided into three distinct energy regions. In the high-energy region above 105 eV, since the prompt neutrons released by fission are dominant, the neutron spectrum is approximately proportional to the fission spectrum $\chi(E)$. In the energy region below several hundreds of keV, the fast neutrons from fission lose their energies mainly through *elastic scattering* reaction with light moderator nuclides such as hydrogen. According to neutron slowing down theory [1], when fast neutron sources are in an infinite homogeneous medium which is an ideal moderator with negligible absorption, the neutron energy spectrum behaves as $1/E$.

The above definition proportionality can be presented as

$$\phi(E) \propto \frac{1}{E} \tag{3.6}$$

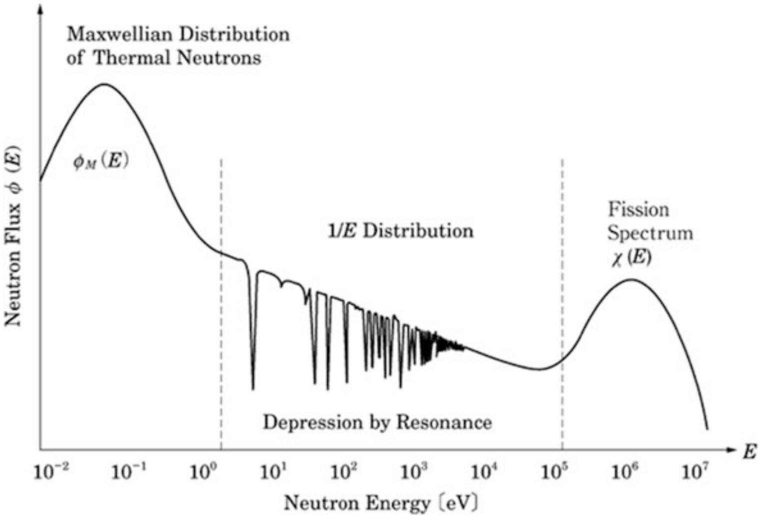

Fig. 3.1 Neutron spectrum of a thermal reactor

In the practical medium of fuel and moderator, the $1/E$ distribution is characterized by the occurrence of fairly sharp depressions due to the resonance absorption of U^{238}, etc., as shown in Fig. 3.1.

Moreover, if the resonance absorption is large, the neutron flux becomes somewhat smaller than the $1/E$ distribution in the low energy region [1].

If neutrons are moderated below several eV of kinetic energy, the kinetic energy by thermal vibration of nuclei cannot be ignored. In other words, if kinetic energies of neutrons become appropriately small, the neutrons collide with thermally vibrating moderator nuclei, and their kinetic energies become reversely large. This is called *upscattering* against moderation which is called the *downscattering*. In this energy region, the neutron spectrum is characterized in a thermal equilibrium at a temperature T by a balance between downscattering and upscattering. Further, in the ideal infinite medium without absorption, the thermal equilibrium neutron spectrum is described by the following Maxwellian distribution function:

$$\phi_M(E) \propto E\exp\left(-\frac{E}{kT}\right) \tag{3.7}$$

where k is the Boltzmann constant. At room temperature ($T = 300$ K), $\phi_M(E)$ is maximized at $E = 0.0253$ eV for which the corresponding velocity is 2200 m/s. On being absorbed, the thermal neutron spectrum deviates a little from $\phi_M(E)$ to the high-energy region because absorption cross sections are larger in lower energies. This is called *absorption hardening*. To compensate the Maxwellian distribution for the absorption hardening, neutron temperature, which is a little higher than moderator temperature, is used as T in Eq. 3.7 [1].

3.2 Control Rods in Reactors

Early approach to nuclear industry and making the reactor going critical were designed around controlling comparatively few rods, and naturally they were around invariable cylindrical shape made of a strong thermal neutron absorber such as cadmium with absorption cross section of $\sigma_{\mathrm{a}} = 0.025\ \mathrm{eV} = 245\ \mathrm{b}$. These cylindrical rods were called *black rods* and had a substantial diameter greater than the absorption mean free path of thermal neutrons, and all thermal neutrons striking the rod were thus absorbed [2].

In today's nuclear reactor design technologies, these black rods are not utilized as frequent because of the following reasons:

(a) Strong absorbing rods are having undesirable distorting flux in their vicinity, and this gives rise to undesirable power and temperature distributions.
(b) Less strong absorbing materials such as hafnium with absorbing cross section of $\sigma_{\mathrm{a}} = 0.025\ \mathrm{eV} = 105\ \mathrm{b}$ or steel containing small amount of boron are therefore used for the rods in most modern reactors. These rods are also comparatively thin, so that while they are providing a good neutron absorbent conditions, all their thermal neutrons striking them are not absorbed and these rods are called *gray rods*.

In today's modern reactors the control rods no longer are in cylindrical shape but are fabricated in various shapes such as the cruciform or cross-like rods, and they fit closely into an array of fuel assemblies and widely used in reactors of water, moderated reactors in particular that have tight fuel lattices. As results proper lattice calculation and analysis are desired using high-performance computer codes, and a direct core calculation with several tens of thousands of fuel pins is difficult to perform in its heterogeneous geometry model form, where one needs to use fine-group analysis to prepare a reactor constant library. The gray rods have additional advantages over the cylindrical rod in that they can be cooled more easily. This is particularly important in power reactors where a rod may become very hot unless properly cooled [2].

When we remove the rods from a solid-moderated reactor, the region originally occupied by the rod remains behind as space vacancy, while in a liquid-moderated reactor, the region may be filled with moderator. In either case when the void is replacing the strongly absorbing rod or a weak absorber tends to peak the flux in this region. To avoid this situation, it is common practice to attach a region of fuel or mildly absorbing structural material to the end of the rod [1].

Such rod *followers*, as these extensions to a control rod are called, reduce the peaking of the flux, and if the followers are fueled, they may substantially increase the reactivity equivalent of the rod, and then under this condition, the fuel is simultaneously introduced into the system as the rod is extracted.

When we insert the control rod in a reactor, it changes its multiplication factor in two possible ways as follows:

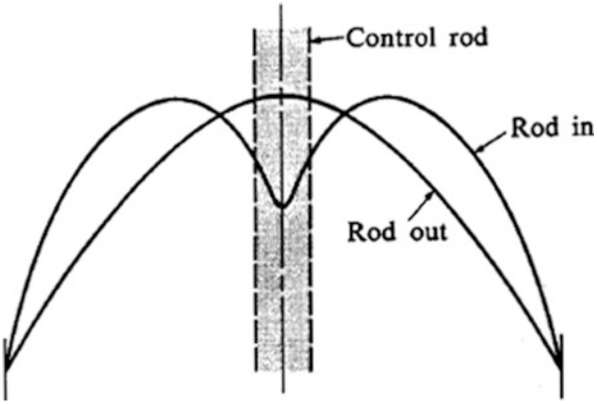

Fig. 3.2 Flux in a reactor with and without central control rod [1]

1. The rod simply absorbs neutrons, while simultaneously the rod distorts the flux such that the leakage of neutrons from the system is increased. Figure 3.2 demonstrates these processes where the flux is presented in the bare cylindrical reactor before and after insertion of a single rod takes place.
2. Observation of the curvature or buckling of the flux is *greater* when the rod is present and the gradient of the flux at the surface of the reactor is greater and so is the leakage current.

With many reactors these two above effects of a control rod increasing absorption and leakage are very important and play important roles in determining the impact of the rod upon the multiplication factor of the system [1].

In summary the effectiveness of a control rod totally depends mainly upon the value of the ratio of the neutron flux of the location of the rod to the average neutron flux ϕ in the reactor. The control rod has maximum effect, which inserts the most negative reactivity, if it is placed in the reactor where the flux has maximum value. If the reactor has only one control rod, the rod must be placed in the center of the reactor core as shown in Figs. 3.2 and 3.3. The effect of such a rod on the flux is illustrated in Fig. 3.3.

In the case of additional rod scenario, if they are added to such simple reactor, the most effective location is where the flux is maximum, which is shown as point A in Fig. 3.3. Numerous control rods are required for a reactor that has a large amount of excessive reactivity necessary for reactor to go critical. The exact amount of reactivity that each control rod inserts depends upon the reactor design and core shape. The change in reactivity caused by control rod motion is referred to as control rod worth. Note that the exact effect of control rods on reactivity can be determined via experiment such that a control rod can be withdrawn in small increments, for example, about 0.5 in., and the change in reactivity can be determined following each increment of withdrawal. Consequently, by plotting the resulting reactivity versus the rod position as shown in Fig. 3.4, one can illustrate the integral control rod worth over the full range of withdrawal. This way we can define the *integral control rod worth* as the total reactivity worth of the rod at that

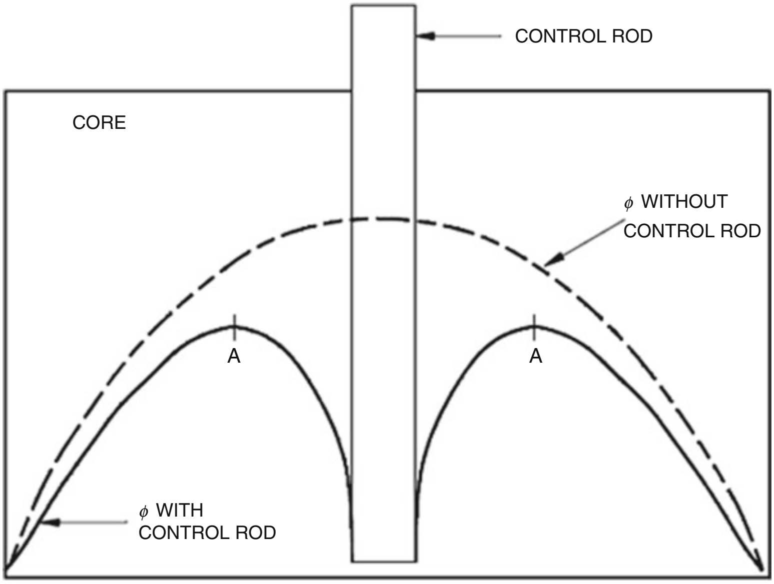

Fig. 3.3 Effect of control rod on radial flux distribution

Fig. 3.4 Integral control rod worth

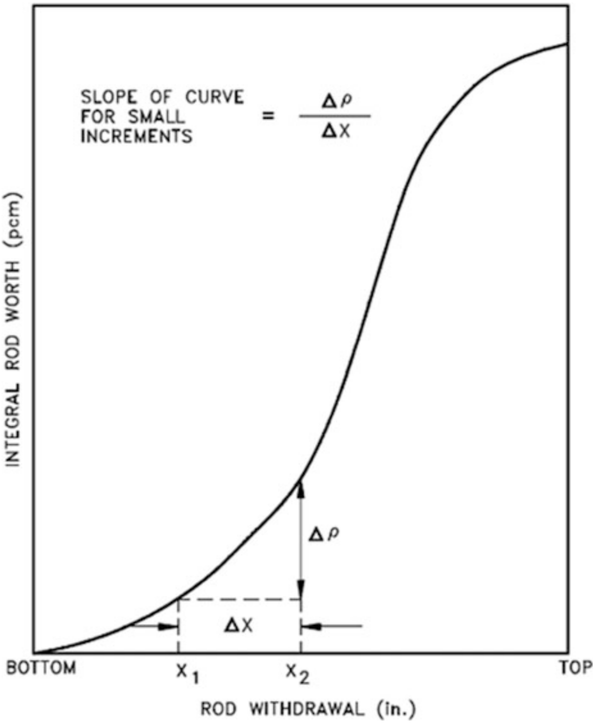

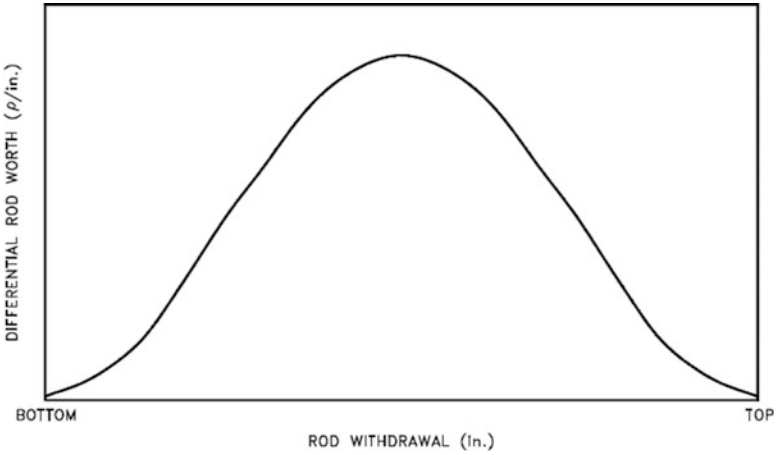

Fig. 3.5 Differential control rod worth

particular degree of withdrawal and is usually defined to be greatest when the rod is fully withdrawn.

As it can be seen in Fig. 3.4, the slope of the curve $\Delta\rho/\Delta x$, and hence the amount of reactivity inserted per unit of withdrawal, is greatest when the control rod is midway out of the core of the reactor. This situation takes place due to the area of greatest neutron flux, which is near the center of the core; therefore, the amount of change in neutron absorption is greatest in this area. If the slope of the curve for integral rod worth in Fig. 3.4 is taken, the result is a value for change rate of control rod worth as a function of control rod position.

A plot of the slope of the integral rod worth curve is also known as the *differential control rod worth*, which is illustrated in Fig. 3.5. As one can see, in this figure at the bottom of the core, where there are few neutrons, rod movement has little effects so the change in rod worth per inch varies a little. As the rod approaches the center of the core, its effect becomes greatest, and the change in rod worth per inch is greater. At the center of the core, the differential rod worth is greatest and varies a little with rod motion. From the center of the core to the top, the rod worth per inch is basically the inverse of the rod worth per inch from the center to the bottom.

Based in the above discussion, we now can define *differential control rod worth* as the reactivity change per unit movement of a rod and is normally expressed as ρ/in., $\Delta k/k$ per inch, or pcm/in. The integral rod worth at a given withdrawal is merely the summation of the entire differential rod worth up to that point of withdrawal. It is also the area under the differential rod worth curve at any given withdrawal position.

Some classes of power reactors contain space for the control rods as channels reserved for them within designated fuel assemblies; the assemblies shown in Fig. 3.6a, b fall into this category. In other systems, the control rods are inserted between the fuel assemblies. For a better understanding of the above issues, refer to Problems 3.3 and 3.4 at the end of this chapter.

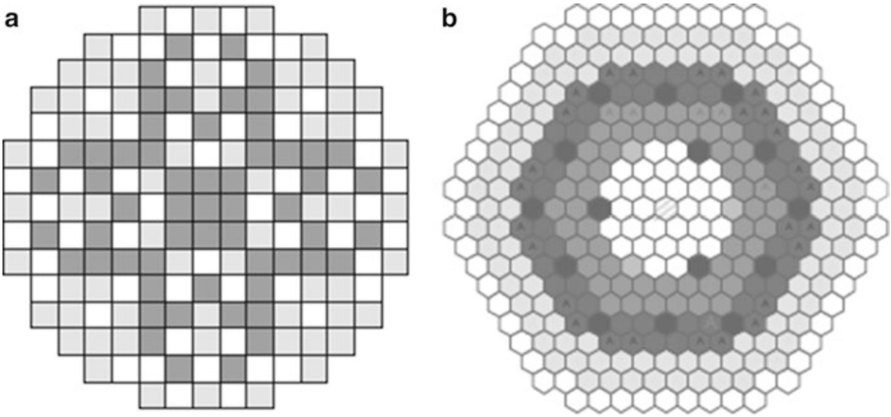

Fig. 3.6 Reactor cores consisting of square and hexagonal fuel assemblies. (**a**) Square fuel assemblies, (**b**) hexagonal fuel assemblies (Courtesy of W. S. Yang, Argonne National Laboratory)

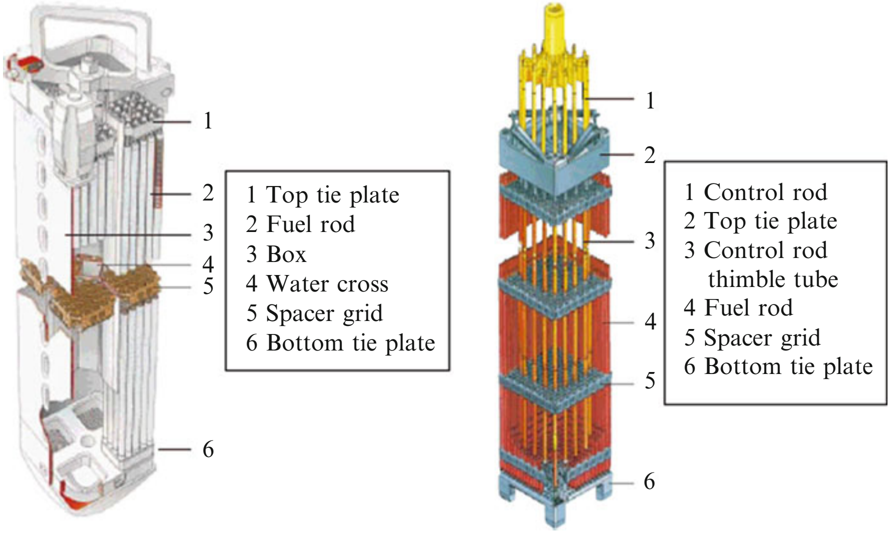

Fig. 3.7 Typical fuel assemblies used in BWRs (*left*) and PWRs (*right*)

Control rods with cruciform cross sections may be placed at the intersections of square assemblies or control rods may be inserted into moderator regions between assemblies.

Typical reactor core and fuel assemblies consist of a number of fuel assemblies fixed in the pressure vessel between the lower and the upper core support plates. Fuel assemblies typical for pressurized water reactors (PWRs) and boiling water reactors (BWRs) are shown in Fig. 3.7.

Bear in your mind that the control rods are manufactured from materials that are strong absorbers of neutrons. These are usually special alloys, for example, 80 % silver, 15 % indium, and 5 % cadmium. Generally, the material selected should have a good absorption cross section for neutrons and have a long lifetime as an absorber (not burn out rapidly).

The ability of a control rod to absorb neutrons can be adjusted during manufacture. A control rod that is referred to as a *black absorber* absorbs essentially all incident neutrons. A gray absorber absorbs only a part of them. While it takes more *gray rods* than black rods for a given reactivity effect, the gray rods are often preferred because they cause smaller depressions in the neutron flux and power in the vicinity of the rod.

This leads to a flatter neutron flux profile and more even power distribution in the core.

If gray rods are desired, the amount of material with a high absorption cross section that is loaded in the rod is limited. A material with a very high absorption cross section may not be desired for use in a control rod, because it will burn out rapidly due to its high absorption cross section. The same amount of reactivity worth can be achieved by manufacturing the control rod from a material with a slightly lower cross section and by loading more of the material. This also results in a rod that does not burn out rapidly.

Another factor in control rod material selection is that materials that are resonantly absorbing neutrons are often preferred to those that merely have high thermal neutron absorption cross sections. Resonance neutron absorbers absorb neutrons in the epithermal energy range. The path length traveled by the epithermal neutrons in a reactor is greater than the path length traveled by thermal neutrons. Therefore, a resonance absorber absorbs neutrons that have their last collision farther (on the average) from the control rod than a thermal absorber. This has the effect of making the area of influence around a resonance absorber larger than around a thermal absorber and is useful in maintaining a flatter flux profile.

In summary, the control rod insertion rates on a reactor scram situation for a reactor operation that encounter such circumstances are designed to be sufficient to protect the reactor against damage in all transients modes that are expected to occur during the life cycle of the reactor.

During a normal reactor operation, the control rods must be able to move fast enough to compensate for the most rapid rate at which positive reactivity is expected to build within the reactor in order to provide positive control. The transient that is normally considered when setting this minimum rod speed is the burnout of maximum peak xenon while at full power. Xenon burnout is usually the most rapid, non-accident transient circumstances expected. The maximum rod speed is normally limited in order to reduce the severity of a reactor accident involving the continuous withdrawal of control rods.

3.2.1 Lattice Calculation Analysis

The purpose of lattice calculation as we mentioned above is to use a high-performance computer. A direct core calculation with several tens of thousands of fuel pins is difficult to perform in its heterogeneous geometry model form. Using finite groups (e.g., 107 groups in **SRAC** which is a Japanese Atomic Energy Agency (JAEA) code for Research Group for Reactor Physics and Standard Nuclear Code System using **NJOY 99** to produce cross-sectional library for thermal reactor analysis) of a prepared reactor constant library.

To do lattice calculation analysis, the Monte Carlo method can handle such a core calculation, but it is not easy to obtain enough accuracy for a local calculation or small reactivity because of accompanying statistical errors. Hence, the Monte Carlo method is not employed for nuclear design calculations requiring a fast calculation time. Instead, the nuclear design calculation is performed in two steps: lattice calculation in a two-dimensional (2D) infinite arrangement of fuel rods or assemblies and core calculation in a three-dimensional (3D) whole core. The lattice calculation prepares few-group homogenized cross sections, which maintain the important energy dependence (neutron spectrum) of nuclear reactions, as shown in Fig. 3.8, and this reduces the core calculation cost in terms of time and memory. Since final design parameters in the core calculation are not concerned with the energy dependence, the spatial dependence such as for the power distribution is important.

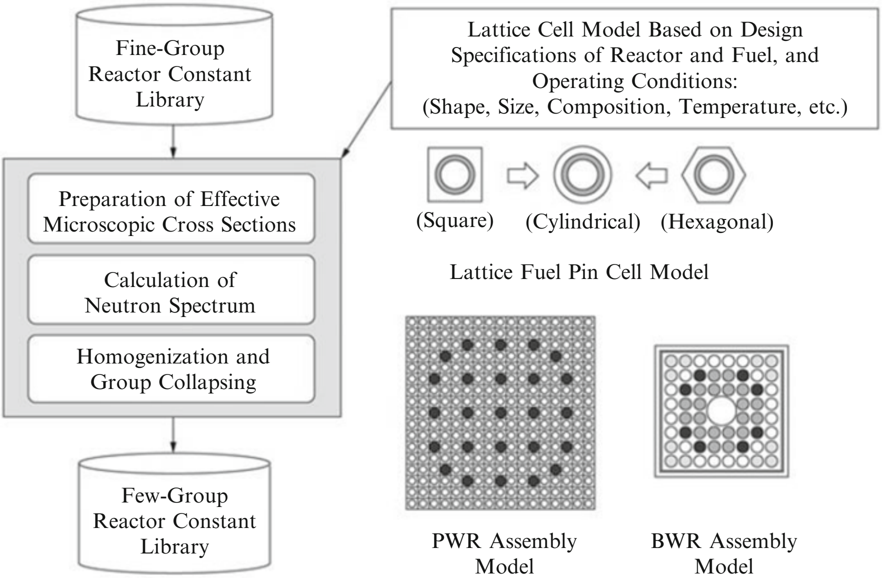

Fig. 3.8 Lattice calculation flow

Multigroup neutron transport equation is also playing an important role where the neutron transport equation in the lattice calculation is a steady-state equation without the time differential term in Boltzmann Equation 3.1. Further, the neutron energy variable is discretized in the equation, and therefore a multigroup form is used in design computer codes as presented below

$$-\vec{\boldsymbol{\Omega}}\cdot\nabla\phi_g\left(\vec{\boldsymbol{r}},\vec{\boldsymbol{\Omega}}\right)-\Sigma_{\mathrm{t},g}(\vec{\boldsymbol{r}})\phi_g\left(\vec{\boldsymbol{r}},\vec{\boldsymbol{\Omega}}\right)+S_g\left(\vec{\boldsymbol{r}},\vec{\boldsymbol{\Omega}}\right)=0 \tag{3.8}$$

The neutron source of Eq. 3.9 is the multigroup form without the external neutron source of Eq. 3.2 at the critical condition.

$$\begin{aligned} S_g\left(\vec{\boldsymbol{r}},\vec{\boldsymbol{\Omega}}\right)=&\int_{4\pi}d\Omega'\sum_{g'}\Sigma_{\mathrm{s},g'\to g}\left(\vec{\boldsymbol{r}},\vec{\boldsymbol{\Omega}}'\to\vec{\Omega}\right)\phi_{g'}\left(\vec{\boldsymbol{r}},\vec{\boldsymbol{\Omega}}\right)\\ &+\frac{\chi_g}{4\pi}\sum_{g'}\nu\Sigma_{\mathrm{f},g'}(\vec{\boldsymbol{r}})\int_{4\pi}\phi_{g'}\left(\vec{\boldsymbol{r}},\vec{\Omega}\right)d\boldsymbol{\Omega}' \end{aligned} \tag{3.9}$$

The system to which the multigroup transport equation is applied is an infinite lattice system of a two-dimensional fuel assembly (including assembly gap) with a reflective boundary condition. For a complicated geometry, two lattice calculations corresponding to a single fuel rod and a fuel assembly are often combined.

In practically solving Eq. 3.8 in the lattice model, the space variable ($\vec{r}$) is also discretized in the equation, and each material region is divided into several subregions where the neutron flux is regarded to be flat. In liquid metal-cooled fast reactors (LMFRs), neutron flux in each energy group has an almost flat spatial distribution within the fuel assembly because the mean free path of the fast neutrons is long. A simple hexagonal lattice model covering a single fuel rod or its equivalent cylindrical model simplified to one dimension is used in the design calculation of LMFRs. The spatial division can also be simplified by assigning the macroscopic cross section by material.

On the other hand, thermal reactors have a highly nonuniform distribution (called the spatial self-shielding effect) of neutron flux in a fuel assembly as thermal neutron flux rises in the moderator region or steeply falls in the fuel and absorber as shown in Fig. 3.9. Moreover, control rod guide tubes or water rods are situated within fuel assemblies, and differently enriched fuels or burnable poison (Gd_2O_3) fuels are loaded. In such a lattice calculation, therefore, it is necessary to make an appropriate spatial division in the input data predicting spatial distribution of thermal neutron flux and its changes with burnup.

In lattice calculation codes, effective microscopic cross sections are first prepared from fine-group infinite dilution cross sections based on input data such as material compositions, dimensions, temperatures, and so on. The effective cross sections are provided in solving Eqs. 3.8 and 3.9 by the use of the collision probability method, etc., and then multigroup neutron spectra are obtained in each divided region (neutron spectrum calculation).

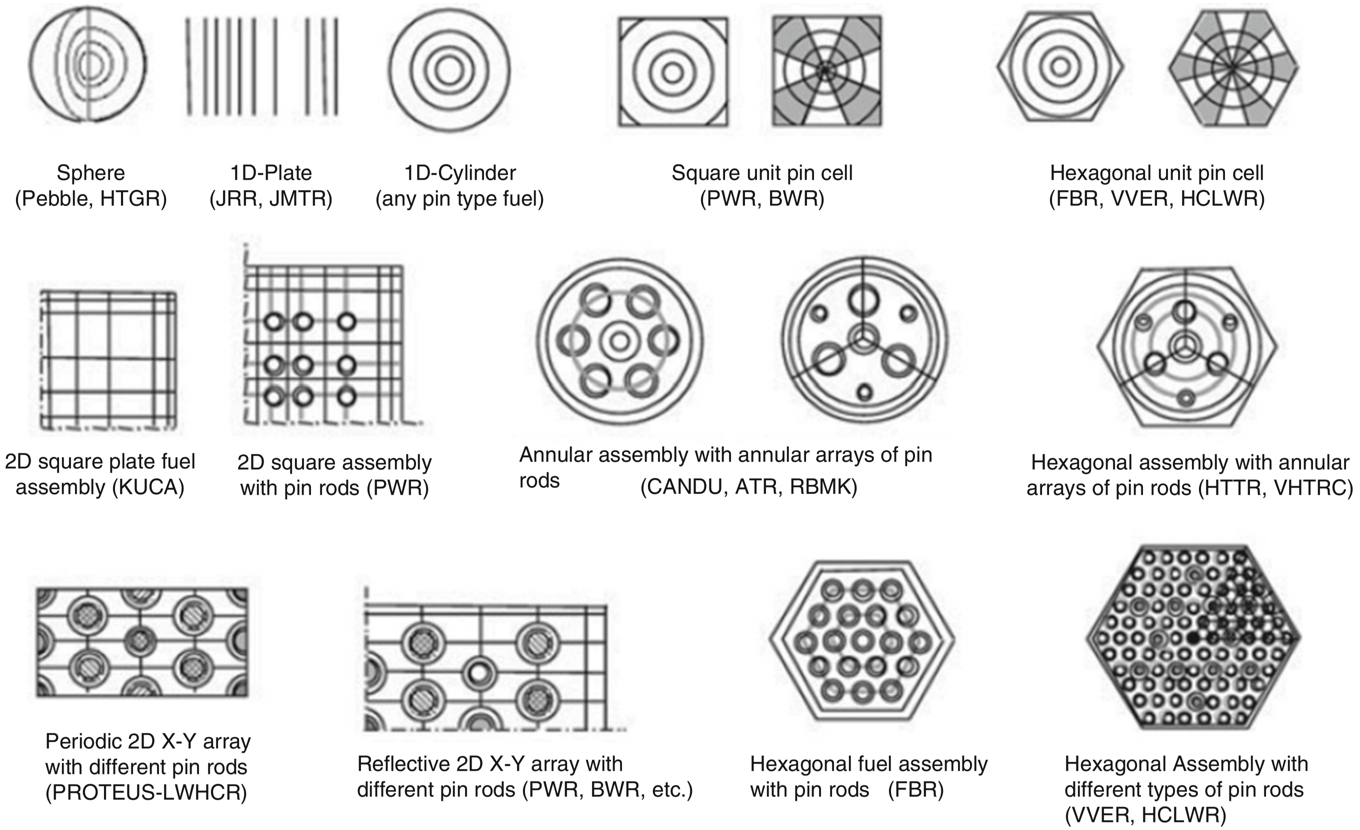

Fig. 3.9 Lattice models of SRAC [6]

3.3 An Introduction to Neutron Transport Equation

Now if we turn our attention to the original subject of this chapter and to the central issue of nuclear reactor theory, including the determination of the neutron distribution in the reactor as well as the rate at which various nuclear reactions take place within core of reactor. In that case, one needs then to understand the fundamental of *neutron transport equation* as indicated in this section of this chapter. This way we are able to investigate the process and the motion of the neutrons as they stream about the reactor core and frequently scatter off from the atomic nuclei and eventually either are absorbed or leak out of the reactor. Neutrons have a tendency to diffuse from regions of high to low temperature, analogous to how gas molecules would diffuse through another to reduce spatial variations in concentration. However, in the case of neutrons, they have the tendency to travel or stream for a large distance between interactions, which is typically called the *mean free path* (MFP) characterized by fast neutrons on order of centimeters. This is where the dimensions characterizing changes in the reactor core composition are comparable to a neutron MFP, knowing that a reactor fuel pin or rod is typically about 1 cm in diameter. Ultimately our goal is to determine the distribution of neutrons in a nuclear reactor core, which also requires the understanding of the neutron motion about the core and neutron interactions with nuclei in the core.

The most fundamental equation in the study of neutron interactions and migration in any media is the neutron transport equation. This equation has as its solution the time-dependent distribution function for neutrons in configuration–velocity (phase) space. Knowledge of this distribution function is sufficient to solve almost all problems of interest in reactor theory. However, most of the time, one does not need to know the distribution function itself; the integrals over some of the phase space coordinates such as velocity direction, energy, or position are usually sufficient.

We consider a brief derivation of the transport equation to show that it is just a balance relation. One can give a more elaborate derivation than what we do here, including a quantum mechanical formulation, but we believe this is not necessary for the basic understanding of the physical content of the equation. To start with, statistically speaking, we define the number density at any point $\vec{\boldsymbol{r}}$ in the reactor core as follows using Fig. 3.10 which is the depiction of the neutron density $\boldsymbol{N}(\vec{\boldsymbol{r}}, \boldsymbol{t})$:

$$\left[N(\vec{\boldsymbol{r}}, \vec{\mathbf{v}}, t)d^3r\right]\vec{\mathbf{v}} = N(\vec{\boldsymbol{r}}, \vec{\mathbf{v}}, t)d^3rd^3v \equiv \left|\begin{array}{l}\text{expected number of neutrons in } d^3r \\ \text{about } \vec{\boldsymbol{r}}, \text{ with velocities in } d^3v \\ \text{about } \vec{\mathbf{v}} \text{ at time } t\end{array}\right. \tag{3.10}$$

Note that the vector variable $\vec{\mathbf{v}}$ for velocity has been used, and it is often more convenient to use the scalar variable for neutron energies E where we will further analyze the reaction rate density $F(\vec{\boldsymbol{r}}, E, t)$. This is taking place in both space and energy for a given neutron nuclear reaction in terms of macroscopic cross section

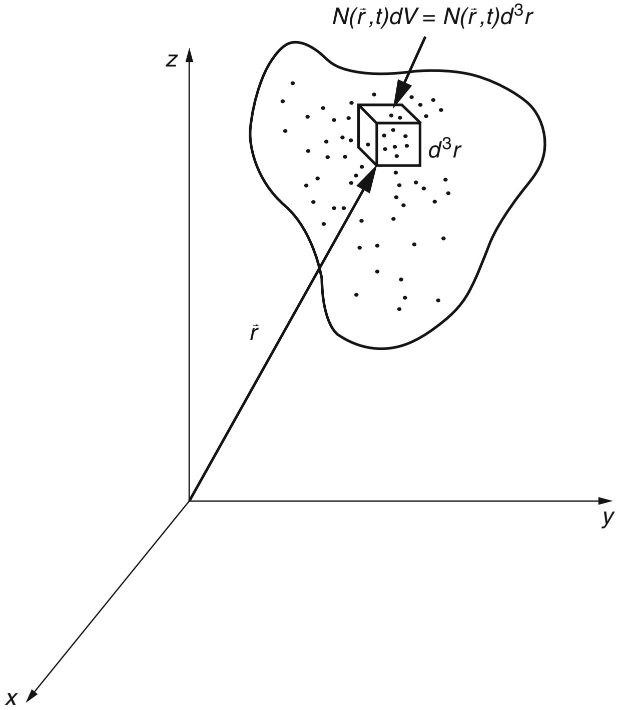

Fig. 3.10 The neutron density $N(\vec{r}, t)$

characterizing the reaction Σ_f and the neutron speed v to further define the neutron flux $\phi\left(\vec{r}, \vec{\Omega}, E, t\right)$ in the same domain. This also leads to the vector solid angle $\vec{\Omega}$, so that the vector velocity $\vec{\mathbf{v}}$ of neutron can be presented as $\vec{\mathbf{v}} = \left(v_x, v_y, v_z\right) \rightarrow (v, \theta, \varphi) \rightarrow (E, \theta, \varphi)$. Correspondingly, $d^3v = v^2 dv d\Omega$ with $d\Omega = \sin\theta d\theta d\varphi$.

As one notices, the word "expected" has been applied in Eq. 3.10. This is simply because the definition of this equation on the right-hand side (RHS) indicates that it falls into the statistical theory concept in which only mean or average values for neutron density can be calculated when we deal with masses as small as neutron at velocity $\vec{\mathbf{v}}$ and volume dV. In reality one is able to measure through a series of events where such measurements are fluctuating around the mean values. By measuring the neutron density $N(\vec{r}, \vec{\mathbf{v}}, t)$ or calculating it, we are able to analyze the *rate* at which nuclear reactions are taking place at any point in the space core of the reactor.

Now recall from the above that the frequency of neutron encountering a given neutron nuclear reaction in terms of the macroscopic cross section and neutron speed can be expressed as

$$v\Sigma_{\mathrm{f}} = \text{Interaction Frequency} \tag{3.11}$$

Thus the reaction rate density $F(\vec{\boldsymbol{r}}, t)$ at any point in the system space in the absence of energy can be defined by merely multiplying the neutron density $N(\vec{\boldsymbol{r}}, t)$ with no energy involved by the interaction frequency of Eq. 3.11, using Fig. 3.10 again, as

$$F(\vec{\boldsymbol{r}}, t)d^3r \equiv v\Sigma_{\mathrm{f}}N(\vec{\boldsymbol{r}}, t)d^3r \equiv \left|\begin{array}{l}\text{expected rate at which} \\ \text{interactions are occuring} \\ \text{in } d^3r \text{ about } \vec{\boldsymbol{r}} \text{ at time } t\end{array}\right. \tag{3.12}$$

This concept easily can be extended to the case in which the neutron density is different for various neutron energies E by defining Eq. 3.11 as

$$N(\vec{\boldsymbol{r}}, E, t)d^3r d^3\mathrm{v} \equiv \left|\begin{array}{l}\text{expected number of neutrons in } d^3r \\ \text{about } \vec{\boldsymbol{r}}, \text{ energies in } dE \text{ about } E \\ \text{at time } t\end{array}\right. \tag{3.13}$$

And again note here that neutron density is expressed as function of space and energy as well as time, and we can generalize this concept of reaction rate density to include energy dependency as we showed in the form $F(\vec{\boldsymbol{r}}, E, t)$; thus, we can establish Eq. 3.14 by utilizing Eq. 3.12 as

$$F(\vec{\boldsymbol{r}}, E, t)d^3r dE = v\Sigma_{\mathrm{f}}N(\vec{\boldsymbol{r}}, E, t)d^3r dE \tag{3.14}$$

The product of $\mathrm{v}N(\vec{\boldsymbol{r}}, dE, t)$ in terms of generalizing neutron of various energies shown in Eqs. 3.12 and 3.14 takes place more often in reactor theory analysis, and therefore it can be assigned a special name as *neutron flux* and in terms of energy can be defined as

$$\phi(\vec{\boldsymbol{r}}, E, t) \equiv vN(\vec{\boldsymbol{r}}, E, t) \equiv \text{ neutron flux} \tag{3.15}$$

and in the absence of energy is written as

$$\phi(\vec{\boldsymbol{r}}, t) \equiv vN(\vec{\boldsymbol{r}}, t) \equiv \text{ neutron flux } \left[\mathrm{cm}^2 s^{-1}\right] \tag{3.16}$$

which will prove to be very convenient to work with either form of neutron flux $\phi(\vec{\boldsymbol{r}}, E, t)$ for further analysis in reactor theory rather than neutron density $N(\vec{\boldsymbol{r}}, E, t)$.

If we now take the solid angle $\vec{\boldsymbol{\Omega}}$ into consideration and establish Fig. 3.11 below for driving Fick's law later on, then Eq. 3.13 can have a new form generalization as

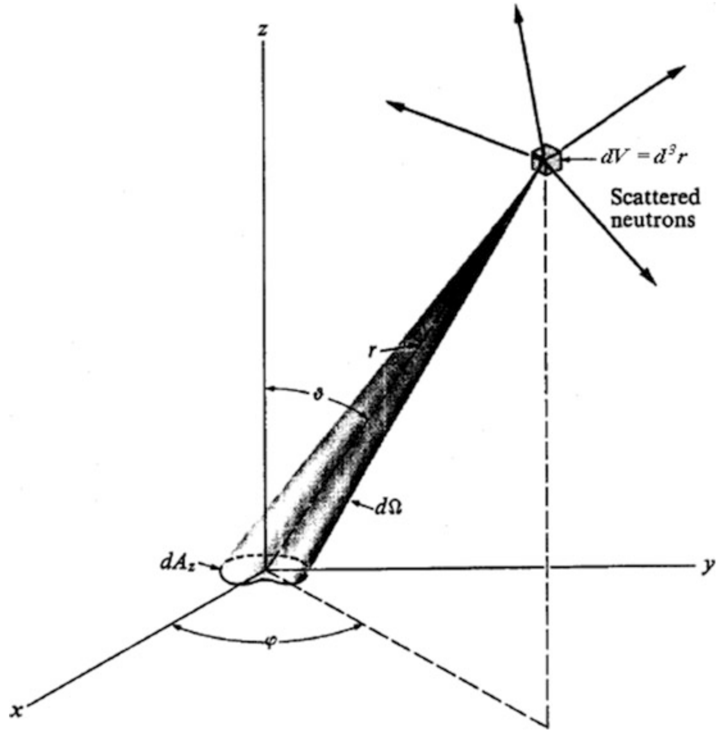

Fig. 3.11 Schematic for deriving Fick's law

$$N(\vec{\boldsymbol{r}}, \vec{v}, t)d^3rd^3v \equiv N\left(\vec{\boldsymbol{r}}, E, \vec{\boldsymbol{\Omega}}, t\right)d^3rdEd\Omega = \left|\begin{array}{l}\text{expected number of neutrons in } d^3r\\ \text{about } \vec{\boldsymbol{r}},\ \text{with energies in } dE \text{ about } E\\ \text{and going in direction in } d\Omega\\ \text{about } \vec{\Omega} \text{ at time } t\end{array}\right. \tag{3.17}$$

Consider a subsystem of volume V and surface S. Suppose we want to calculate the change in the number of neutrons in V with energies in dE about E and direction in $d\Omega$ about $\vec{\boldsymbol{\Omega}}$ during a time interval Δt. This is given by

$$\int_V N\left(\vec{\boldsymbol{r}}, E, \vec{\boldsymbol{\Omega}}, t + \Delta t\right) - N\left(\vec{\boldsymbol{r}}, E, \vec{\boldsymbol{\Omega}}, t\right)d^3rdEd\Omega = \text{ Gains} - \text{Losses} \tag{3.18}$$

There are two contributions to gains as follows:

1. ***Fission and External Source***

$$\frac{\nu\chi(E)dEd\Omega}{4\pi}\iiint\limits_{V,E',\vec{\boldsymbol{\Omega}}'}\Sigma_{\mathrm{f}}(E')\phi\left(\vec{\boldsymbol{r}},\vec{\boldsymbol{\Omega}}',E',t\right)dE'd\Omega'd^3r\Delta t \\ +\int_V S\left(\vec{\boldsymbol{r}},E,\vec{\boldsymbol{\Omega}},t\right)d^3rdEd\Omega\Delta t \tag{3.19}$$

where $\chi(E)$ is the fission spectrum as is defined before, $\phi\left(\vec{\boldsymbol{r}},E,\vec{\boldsymbol{\Omega}},t\right)\equiv vN\left(\vec{\boldsymbol{r}},E,\vec{\boldsymbol{\Omega}},t\right)$ is the *neutron flux*, and S is the external source distribution.

2. ***Scattering***

$$\iiint\limits_{V,\vec{E}',\vec{\Omega}'}\Sigma_{\mathrm{s}}(E')\phi\left(\vec{\boldsymbol{r}},\vec{\boldsymbol{\Omega}}',E',t\right)dE'd\Omega'd^3r\Delta tF\left(E'\vec{\boldsymbol{\Omega}}'\to E\vec{\boldsymbol{\Omega}}\right)dEd\Omega \tag{3.20}$$

where $F\left(E'\vec{\boldsymbol{\Omega}}'\to E\vec{\boldsymbol{\Omega}}\right)$ is the conditional probability that a neutron is scattered at $\left(E'\vec{\boldsymbol{\Omega}}'\right)$; its energy will be in dE about E and its direction will be in $d\Omega$ about $\vec{\boldsymbol{\Omega}}$. For losses, there are also two terms, one for collisions and the other for convective flow.

3. ***Collisions***

$$\int_V\Sigma_{\mathrm{t}}(E)S\left(\vec{\boldsymbol{r}},E,\vec{\boldsymbol{\Omega}},t\right)d^3rdEd\Omega\Delta t \tag{3.21}$$

4. ***Net Flow Outward***

$$\int_S\vec{\boldsymbol{\Omega}}\cdot\hat{n}N\left(\vec{\boldsymbol{r}},E,\vec{\boldsymbol{\Omega}},t\right)dsdEd\Omega\Delta t=\int_V\vec{\boldsymbol{\Omega}}\cdot\nabla\phi\left(\vec{\boldsymbol{r}},E,\vec{\boldsymbol{\Omega}},t\right)d^3rdsdEd\Omega\Delta t \tag{3.22}$$

where $\hat{\vec{N}}$ is the outward normal at $\vec{\boldsymbol{r}}$ and the divergence theorem $\int_S d\vec{s}\cdot\vec{F}=\int_V\left(\nabla\cdot\vec{F}\right)d^3r$ has been applied. Putting together the gains and losses, dividing by Δt, and taking the limit of $\Delta t\to 0$, we can write the balance, Eq. 3.18, as $\int_V[]=0$. Since volume V can be any arbitrary part of the system, the integral $\int_V[]$ must vanish identically if the integral is to vanish for any V. Thus, we can write the following relationship:

$$\begin{aligned}\frac{\partial N\left(\vec{\boldsymbol{r}},E,\vec{\boldsymbol{\Omega}},t\right)}{\partial t}&=\frac{v\chi(E)}{4\pi}\int_{E',\vec{\Omega}}dEd\Omega'\Sigma_{\mathrm{f}}(E')\phi\left(\vec{\boldsymbol{r}},E,\vec{\boldsymbol{\Omega}},t\right)+S\left(\vec{\boldsymbol{r}},E,\vec{\boldsymbol{\Omega}},t\right)\\&+\int_{E',\vec{\Omega}}dE'd\Omega'\Sigma_{\mathrm{s}}(E')\phi\left(\vec{\boldsymbol{r}},E',\vec{\boldsymbol{\Omega}}',t\right)F\left(E'\vec{\boldsymbol{\Omega}}'\to E\vec{\boldsymbol{\Omega}}\right)\\&+\Sigma_{\mathrm{t}}(E)\phi\left(\vec{\boldsymbol{r}},E,\vec{\boldsymbol{\Omega}},t\right)-\vec{\boldsymbol{\Omega}}\cdot\nabla\phi\left(\vec{\boldsymbol{r}},E,\vec{\boldsymbol{\Omega}},t\right)\end{aligned}\tag{3.23}$$

Equation 3.23 is what is known as the neutron transport equation for a homogeneous medium. For a heterogeneous system, we simply let $\Sigma(E)\to\Sigma(\vec{\boldsymbol{r}},E)$. Notice that this is a *linear* equation because we have ignored the neutron–neutron interaction (the mean free path for such events is 10^8 cm or greater). Sometimes the neutron transport equation is also called the Boltzmann equation; one should be careful when using this terminology since the Boltzmann equation in kinetic theory of gases treats explicitly the collisions among the particles and is in general *nonlinear*.

The transport equation is an integrodifferential equation in seven variables. While it is much too complicated for us to attempt any kind of solution directly, either as a boundary value or initial value problem, all the equations in the reactor theory that we will encounter can be derived from the transport equation in one approximation or another.

3.4 Neutron Current Density Concept in General

The term current has been used to denote a stream of particles flowing in a certain direction; it frequently appears in discussions of scattering of a particle beam or some kind of transport process. To be precise, one should begin with the definition in terms of the neutron flux $\phi\left(\vec{\boldsymbol{r}},E,\vec{\boldsymbol{\Omega}},t\right)$, which as we have just seen is the solution to the neutron transport equation, which will be discussed in the next section. Since the current and the flux have the same dimensions, what then are the differences between these two quantities? Let

$$\begin{aligned}\vec{\boldsymbol{J}}(\vec{\boldsymbol{r}},E,t)&=\int_{\vec{\Omega}}\vec{\boldsymbol{\Omega}}\phi\left(\vec{\boldsymbol{r}},E,\vec{\boldsymbol{\Omega}},t\right)d\Omega\\&=\int_{\vec{\Omega}}vN\left(\vec{\boldsymbol{r}},E,\vec{\boldsymbol{\Omega}},t\right)d\Omega\end{aligned}\tag{3.24}$$

If we recall the meaning of a particle flux from the previous section as

$$vN\left(\vec{\boldsymbol{r}}, E, \vec{\boldsymbol{\Omega}}, t\right) dEd\Omega\Delta tdA\cos\theta = \left|\begin{array}{l}\text{expected number in } dE \text{ about } E \text{ and } d\Omega \\ \text{about } \vec{\boldsymbol{\Omega}} \text{ crossing } dA \text{ during } \Delta t\end{array}\right. \tag{3.25}$$

Let

$$\begin{aligned} J_+(\vec{\boldsymbol{r}}, E, t)dEdA\Delta t &= \text{expected number in } dE \text{ about } E \text{ crossing } dA \text{ during } \Delta t \\ &\quad \text{from } '-' \text{ to } '+' \text{ in the sence of a normal vector } \hat{n} \\ &= \int_{\hat{n}\,,\,\vec{\boldsymbol{\Omega}}>0} \hat{n}\cdot\vec{\boldsymbol{\Omega}}\phi\left(\vec{\boldsymbol{r}}, E, \vec{\boldsymbol{\Omega}}, t\right) dEd\Omega\Delta tdA \end{aligned} \tag{3.26}$$

or

$$J_+(\vec{\boldsymbol{r}}, E, t) = \int_{\hat{N}\,,\,\vec{\boldsymbol{\Omega}}>0} \hat{n}\cdot\vec{\boldsymbol{\Omega}}\phi\left(\vec{\boldsymbol{r}}, E, \vec{\boldsymbol{\Omega}}, t\right) d\Omega \tag{3.27}$$

Similarly, those going in the opposite direction become

$$J_-(\vec{\boldsymbol{r}}, E, t) = \int_{\hat{n}\,,\,\vec{\boldsymbol{\Omega}}<0} \left(-\hat{n}\cdot\vec{\boldsymbol{\Omega}}\right)\phi\left(\vec{\boldsymbol{r}}, E, \vec{\boldsymbol{\Omega}}, t\right) d\Omega \tag{3.28}$$

We can define the vector $\vec{\boldsymbol{J}}(\vec{\boldsymbol{r}}, E, t)$ such that

$$\hat{n}\cdot\vec{\boldsymbol{J}}(\vec{\boldsymbol{r}}, E, t) = J_+(\vec{\boldsymbol{r}}, E, t) - J_-(\vec{\boldsymbol{r}}, E, t) = \hat{n}\cdot\int_{\vec{\boldsymbol{\Omega}}} \vec{\boldsymbol{\Omega}}\phi\left(\vec{\boldsymbol{r}}, E, \vec{\boldsymbol{\Omega}}, t\right) d\Omega \tag{3.29}$$

As one can see, Eq. 3.29 is consistent with Eq. 3.24 and allows us to arrive at the interpretation.

$$\begin{aligned} \hat{n}\cdot\vec{\boldsymbol{J}}(\vec{\boldsymbol{r}}, E, t)dEdA\Delta t &= \textit{net} \text{ number neutron in } dE \text{ about } E \text{ crossing } dA \text{ during } \Delta t \\ &\quad \text{from } '-' \text{ to } '+' \text{ during } \Delta t \end{aligned} \tag{3.30}$$

The difference between $\hat{n}\cdot\vec{\boldsymbol{J}}$ and J_+ lies in the word *net*.

3.5 Neutron Current Density and Fick's Law

In order to have a better understanding of the nuclear reactor theory filed where one should deal with the general and very complicated problem of neutron transport in it. In order to do that, first, we can show that the neutron flux ϕ and current $\vec{\boldsymbol{J}}$ are associated with each other in a simple manner if certain conditions could be met. When such conditions are established, then it is possible to obtain very elementary solutions to neutron transport problem, and this is where we lay the ground in order to be able to deal with this complicated problem.

Fick's law is establishing the relationship between neutron flux ϕ and current $\vec{J}$, which is known for many years and is used in order to describe diffusion phenomena in fluid dynamics of liquid and gas analyses. Similarly in reactor theory, Fick's law leads to understand what is known as the *diffusion approximation*, which will be the subject of our discussion in the following sections of this chapter.

However, in order to be able to derive and apply Fick's law in the reactor theory, a simple number of simplification assumptions need to take place, where the neutron current density at any point in core of reactor or medium where the neutrons do exist. For that matter at minimum, the following assumption will be made:

1. We assume that the medium is finite and uniform; thus, all the cross sections are constants and independent of position.
2. There exist no neutron sources in the medium.
3. In the *laboratory coordinate system*, the neutron scattering is isotropic.
4. The neutron flux is a function of time and yet slowly varying function of position.

For us to continue with derivation Fick's law, it would be possible to relax certain of these above restrictions in future discussion. We start our computation of the current density vector $\vec{J}$ at the center of the laboratory coordinate system as it was shown in Fig. 3.11, where we can identify the three components of current density vector as J_x, J_y, and J_z, so we are able to evaluate them as well. To begin with we take the component of J_x into consideration where the neutron current flow rate through cross-sectional area dA_z laying in the xy-plane at the origin can be evaluated. Based on our above assumptions, it is very clear that there are no neutron sources present in the medium and every neutron which passes through dA_z has just arrived from a scattering collision event and as result the neutrons flow downstream through dA_z above the xy-plane and they flow upstream through dA_z from these collisions below the xy-plane.

Before we go on with further discussion of the problem in hand, consider the following statement in the following box:

Note that:

The central problem of reactor physics can be stated quite simply. It is to compute, for any time t, the characteristics of the free neutron population throughout an extended region of space containing an arbitrary, but known, mixture of materials. Specifically we wish to know the number of neutrons in any infinitesimal volume dV that have kinetic energies between E and $E + \Delta E$ *and are traveling in directions within an infinitesimal solid angle of a fixed direction specified by the unit vector* $\vec{\Omega}$.

Considering Fig. 3.11 and volume element dV located at the point $\vec{\boldsymbol{r}}$ and the number of scattering collisions per second that takes place in it presented as $\Sigma_{\mathrm{s}}\phi(\vec{\boldsymbol{r}})$, where Σ_{s} is the macroscopic scattering cross section and $\phi(\vec{\boldsymbol{r}})$ is the neutron flux at point $\vec{\boldsymbol{r}}$, then scattering in this case is assumed to be isotopic in the laboratory coordinate system. However, the fraction of these neutrons that are scattered in the direction of the surface element dA_z in xy-plane is just the fraction of the total solid angle $\vec{\boldsymbol{\Omega}}$ subtended by surface element dA_z at volume element dV, and from the definition of solid angle, one can write the following equation for this fraction as

$$\text{Fraction of Neutrons Occupied in Solid Angle } \vec{\boldsymbol{\Omega}} = \frac{dA_z \cos\vartheta}{4\pi r^2} \tag{3.31}$$

From this equation the number of neutrons scattered per second in volume element dV which headed toward surface element dA_z is then demonstrated by the following:

$$\frac{\Sigma_{\mathrm{s}}\phi(\vec{\boldsymbol{r}})\cos\vartheta dA_z dV}{4\pi r^2} \tag{3.32}$$

Not all of these neutrons reach the surface element dA_z; some are scattered or absorbed in the process, and the number of those that reach dA_z per second is expressed as

$$\frac{\mathrm{e}^{-\Sigma_{\mathrm{t}} r}\Sigma_{\mathrm{s}}\phi(\vec{\boldsymbol{r}})\cos\vartheta dA_z dV}{4\pi r^2} \tag{3.33}$$

where Σ_{t} is the macroscopic total cross section of the medium. For convenience we take into consideration the contributions of current neutrons of J_z separately, which are passing downward through dA_z, and those which pass upward through the same surface element as well. With volume element dV written in spherical coordinates and using Fig. 3.11 as $dV = r^2 \sin\vartheta dr d\vartheta$, the total number of neutrons which flow downward through dA_z per second is written as

$$\frac{\Sigma_{\mathrm{s}} dA_z}{4\pi}\int_{\varphi=0}^{2\pi}\int_{\vartheta=0}^{\pi/2}\int_{r=0}^{\infty}\mathrm{e}^{-\Sigma_{\mathrm{t}} r}\phi(\vec{\boldsymbol{r}})\cos\vartheta\sin\vartheta dr d\vartheta d\varphi \tag{3.34}$$

Now if we take into consideration the number of neutrons passing per second in the negative direction of z coordinate through a unit and denote it with J_z^-, which is just Eq. 3.34 divided by the surface element dA_z, then we get the following mathematical form:

$$J_z^- = \frac{\Sigma_{\mathrm{s}}}{4\pi}\int_{\varphi=0}^{2\pi}\int_{\vartheta=0}^{\pi/2}\int_{r=0}^{\infty}\mathrm{e}^{-\Sigma_{\mathrm{t}} r}\phi(\vec{\boldsymbol{r}})\cos\vartheta\sin\vartheta dr d\vartheta d\varphi \tag{3.35}$$

Since the flux $\phi(\vec{r})$ is unknown function in Eq. 3.35, the integral in that equation cannot be evaluated as it stands in the above form. In order to perform this integral, we fall on our assumption that this flux varies slowly with position as we expressed before as part of our assumption above. Thus, we can use Taylor's series properties, and we expand $\phi(\vec{r})$ in the following form:

$$\phi(\vec{r}) = \phi_0 + x\left(\frac{\partial \phi}{\partial x}\right)_0 + y\left(\frac{\partial \phi}{\partial y}\right)_0 + z\left(\frac{\partial \phi}{\partial z}\right)_0 + \dots, \tag{3.36}$$

In Eq. 3.35 the subscripts zero is an indication of that ϕ, and its derivatives are going to be evaluated at the origin. However, considering the spherical coordinate and writing the component of x, y, and z in that coordinate, we have

$$x = r\sin\vartheta\cos\varphi \quad y = r\sin\vartheta\sin\varphi \quad z = r\cos\vartheta$$

Now by inserting Eq. 3.36 into Eq. 3.35, it can easily be found that the terms containing $\cos\varphi$ and $\sin\varphi$ immediately integrate to zero; hence, the J_z^- reduces to the following form:

$$J_z^- = \frac{\Sigma_s}{4\pi}\int_{\varphi=0}^{2\pi}\int_{\vartheta=0}^{\pi/2}\int_{r=0}^{\infty} e^{-\Sigma_t r}\left[\phi_0 + \left(\frac{\partial \phi}{\partial z}\right)_0 r\cos\vartheta\sin\vartheta dr d\vartheta d\varphi\right] \tag{3.37}$$

where the evaluation of integral in Eq. 3.37 results in J_z^- as

$$J_z^- = \frac{\Sigma_s\phi_0}{4\Sigma_t} + \frac{\Sigma_s}{6\Sigma_t^2}\left(\frac{\partial \phi}{\partial z}\right)_0 \tag{3.38}$$

Similarly we can evaluate the J_z^+, which is the number of neutrons moving per second in the positive z-direction through a unit area in the xy-plane as

$$J_z^+ = \frac{\Sigma_s\phi_0}{4\Sigma_t} - \frac{\Sigma_s}{6\Sigma_t^2}\left(\frac{\partial \phi}{\partial z}\right)_0 \tag{3.39}$$

Then the z-component of current density $\vec{J}$ which refers to the *net flow* of neutrons per unit area can be expressed as

$$\begin{aligned} J_z = J_z^+ - J_z^- &= \left\{\frac{\Sigma_s\phi_0}{4\Sigma_t} - \frac{\Sigma_s}{6\Sigma_t^2}\left(\frac{\partial \phi}{\partial z}\right)_0\right\} - \left\{\frac{\Sigma_s\phi_0}{4\Sigma_t} + \frac{\Sigma_s}{6\Sigma_t^2}\left(\frac{\partial \phi}{\partial z}\right)_0\right\} \\ &= -\frac{\Sigma_s}{3\Sigma_t^2}\left(\frac{\partial \phi}{\partial z}\right)_0 \end{aligned} \tag{3.40}$$

We performed the above analysis for the z-component of current density vector $\vec{J}$, and since the orientation of the coordinate system is purely arbitrary, thus the component $\vec{J}$ in both x and y directions can be analyzed the same way and the results are as follows:

$$J_x = -\frac{\Sigma_s}{3\Sigma_t^2}\left(\frac{\partial \phi}{\partial x}\right)_0 \tag{3.41}$$

and

$$J_y = -\frac{\Sigma_s}{3\Sigma_t^2}\left(\frac{\partial \phi}{\partial y}\right)_0 \tag{3.42}$$

Based on Eqs. 3.40, 3.41, and 3.42, the current density vector $\vec{\boldsymbol{J}}$ is now written as

$$\begin{aligned}\vec{\boldsymbol{J}} &= J_x\hat{i} + J_y\hat{j} + J_z\hat{k} \\ &-\frac{\Sigma_s}{3\Sigma_t^2}\left[\left(\frac{\partial \phi}{\partial x}\right)_0\hat{i} + \left(\frac{\partial \phi}{\partial y}\right)_0\hat{j} + \left(\frac{\partial \phi}{\partial z}\right)_0\hat{k}\right] \\ &-\frac{\Sigma_s}{3\Sigma_t^2}\mathrm{grad}\phi\end{aligned}$$

or in a final form is given as

$$\vec{\boldsymbol{J}} = -\frac{\Sigma_s}{3\Sigma_t^2}\,\mathrm{grad}\phi = D\mathrm{grad}\phi \tag{3.43}$$

As we note the subscript of zero has been dropped in Eq. 3.43 since the location of the origin of coordinates in this derivation is also arbitrary, so this indicates that Eq. 3.43 is valid at any point in the medium where the initial assumption at the begging of this discussion is a valid one as well.

Equation 3.43 is known as Fick's law, which states that *the current density vector* $\vec{\boldsymbol{J}}$ *is proportional to the negative gradient of the flux* $\phi(\vec{\boldsymbol{r}})$. The proportionality constant $D = \Sigma_s/3\Sigma_t^2$ is called the *diffusion constant* and is denoted by the symbol D, and this final form of Fick's law becomes

$$\vec{\boldsymbol{J}} = -D\mathrm{grad}\phi \tag{3.44}$$

3.6 Problem Classification and Neutron Distribution

To understand this problem better, we classify the neutron distribution as function of seven variables, where three of these variables are associated with neutron position $\vec{\boldsymbol{r}}$ at any point in space of medium, while the other three variables are representing the velocity of neutron in three-dimensional space and finally the last variable can count for neutron energy. We can consider one for energy and two for direction of travel in the laboratory coordinate system as it was describe under

Fick's law assumption in the previous section, and last but not the least, statistically speaking, time is playing as another variable in neutron distribution if we want to be more accurate.

One can define several reduced distributions by integrating out one or more of the variables or by setting a variable such as the energy at a particular value. By doing this we can break down the transport problem into several simpler problems such as:

1. **Neutron slowing down**
2. **Neutron diffusion**
3. **Neutron thermalization and one-speed neutron transport**

Each then can be studied separately with further simplifying approximations. Not only does each problem have physical interest by itself but also the problems can be combined to give understanding of the essence of neutron transport phenomena.

For steady-state problems one simply postulates that the neutron distribution and the external source are both time-independent. The left-hand side of Eq. 3.23 vanishes; what is left is the time-independent neutron transport equation. Two kinds of problems can be investigated, one with an external source and the other without. The former corresponds to a subcritical reactor system since a source is needed to maintain a steady-state neutron density. The latter describes a critical reactor, a system in which one can have steady-state neutron density in the absence of a source.

Suppose one is not interested in the neutron direction of travel, then in that case Eq. 3.23 can be integrated over $\vec{\boldsymbol{\Omega}}$. In steady state and in the absence of a source, this gives

$$\begin{aligned}&-\nabla\cdot\vec{\boldsymbol{J}}(\vec{\boldsymbol{r}},E)+\int dE'\Sigma_{\mathrm{s}}(E')\phi(\vec{\boldsymbol{r}},E)F(E'\rightarrow E)\\&+\nu\chi(E)\int dE\Sigma_{\mathrm{f}}(E')\phi(\vec{\boldsymbol{r}},E')-\Sigma_{\mathrm{t}}(E)\phi(\vec{\boldsymbol{r}},E)=0\end{aligned}\tag{3.45}$$

where we have used Eq. 3.24. The equation describes the distribution of neutrons in configuration space and energy. It is not a closed equation in that it involves two unknown quantities, the neutron flux and the net current. To take another step in simplification, one commonly makes the approximation that the current is related to the flux by Fick's law of diffusion, which was proven as presented in Eq. 3.44

$$\vec{\boldsymbol{J}}=-D\vec{\nabla}\phi$$

which then leads to the diffusion equation for a multiplying system in steady state

$$
\begin{aligned}
&\left[D\nabla^2 - \Sigma_t\right]\phi(\vec{\boldsymbol{r}}, E) + \nu\chi(E)\int dE'\Sigma_\mathrm{f}(E')\phi(\vec{\boldsymbol{r}}, E') \\
&\quad + \int dE'\Sigma_\mathrm{s}(E')\phi(\vec{\boldsymbol{r}}, E')F(E' \to E) = 0
\end{aligned}
\tag{3.46}
$$

This is the energy-dependent diffusion equation, and still it is not the simplest diffusion equation that one can solve. Since this equation also treats the process of neutron energy moderation where neutron slowing down and further reductions can be considered.

At this stage, one can go in two directions of simplification. One is to get rid of the energy dependence by integrating over E. The result is then the problem of neutron diffusion

$$
\vec{D}\nabla^2\vec{\phi}(\vec{\boldsymbol{r}}) + \left[\nu\overline{\Sigma}_\mathrm{f} - \overline{\Sigma}_\mathrm{a}\right]\vec{\phi}(\vec{\boldsymbol{r}}) = 0 \tag{3.47}
$$

where using the overhead bar denotes two kinds of energy-integrated quantities, an effective flux-averaged cross section and the integrated flux.

$$
\overline{\Sigma} = \frac{\int dE\Sigma(E)\phi(\vec{\boldsymbol{r}}, E)}{\int dE\phi(\vec{\boldsymbol{r}}, E)} \quad \text{and} \quad \vec{\phi}(\vec{\boldsymbol{r}}) = \int \phi(\vec{\boldsymbol{r}}, E)dE \tag{3.48}
$$

This is the starting point for the discussion of neutron diffusion. For simplicity we will not bother to write out explicitly the overhead bar, but the origin of Eq. 3.47 should be kept in mind. We will return later on to consider the different solutions to this equation, including the treatment of boundary conditions. Notice that Eq. 3.47 is still a balance relation—the difference between what flows into and out of a volume element where by diffusion is balanced by the difference between production and absorption in the volume element dV. The other simplification of Eq. 3.46 is to get rid of the spatial dependence by integrating over the volume of the system. The first term in Eq. 3.46 then vanishes because the integral gives

$$
\int_V D\nabla^2\phi(\vec{\boldsymbol{r}}, E)d^3r = -D\int_V \nabla \cdot \vec{\boldsymbol{J}}(\vec{\boldsymbol{r}}, E)d^3r = -D\int_V \vec{\boldsymbol{J}}(\vec{\boldsymbol{r}}, E) \cdot d\vec{\boldsymbol{S}} \tag{3.49}
$$

which is proportional to the current integrated over the surface of the system. The latter is taken to be zero for large or infinite systems. The remaining terms in Eq. 3.46 become

$$
[\nu\Sigma_\mathrm{f}(E) - \Sigma_\mathrm{t}(E)]\phi(E) + \int \Sigma_\mathrm{s}(E')\phi(E')F(E' \to E)dE' = 0 \tag{3.50}
$$

where we continue to use the same symbol for the spatially integrated flux,

$$\phi(E) = \int_V \phi(\vec{\boldsymbol{r}}, E) d^3 r \tag{3.51}$$

For further discussion of neutron slowing down, we can use Eq. 3.50 as starting point, which is a balance in energy space—the loss of neutrons at energy E by all kinds of interactions, represented by Σ_t, is balanced by gains from neutrons produced directly from fission and neutrons which scatter into energy E from some other energy. We will analyze the various solutions of Eq. 3.50 later in this chapter.

In addition to Eqs. 3.47 and 3.50 and two other equations can be derived from the transport equation, Eq. 3.23. Suppose we assume that all neutrons can have only energy, E_0. This is tantamount to setting the following:

$$\phi\left(\vec{\boldsymbol{r}}, E, \vec{\boldsymbol{\Omega}}\right) = \phi\left(\vec{\boldsymbol{r}}, \vec{\boldsymbol{\Omega}}\right)\delta(E - E_0) \tag{3.52}$$

$$F\left(E' \vec{\boldsymbol{\Omega}}' \to E, \vec{\boldsymbol{\Omega}}\right) = F\left(\vec{\boldsymbol{\Omega}}' \to \vec{\boldsymbol{\Omega}}\right)\delta(E - E_0) \tag{3.53}$$

$$\chi(E) = \delta(E - E_0) \tag{3.54}$$

$$\Sigma(E) = \Sigma \quad \text{a constant} \tag{3.55}$$

Here $\delta(x)$ is the Dirac delta function—it is zero everywhere except at the point where its argument vanishes, and there its value is infinite. Note that the integral of the delta function is unity provided the point where it is infinite lies within the range of integration. Some properties of $\delta(x)$ are

$$\int_{a-\delta}^{a+\delta} \delta(x-a)dx = 1 \quad \int_{a-\delta}^{a+\delta} f(x)\delta(x-a)dx = f(a) \tag{3.56}$$

$$\delta(x) = \delta(-x) \quad x\delta(x) = 0 \quad \delta(ax) = \frac{1}{a}\delta(x) \tag{3.57}$$

Inserting Eq. 3.52 through Eq. 3.55 into Eq. 3.23 and integrating over E, we obtain

$$\left[\Sigma_t + \vec{\boldsymbol{\Omega}} \cdot \vec{\nabla}\right]\phi\left(\vec{\boldsymbol{r}}, \vec{\boldsymbol{\Omega}}\right) = \frac{\nu\Sigma_f}{4\pi}\int_{\vec{\boldsymbol{\Omega}}'} \phi\left(\vec{\boldsymbol{r}}, \vec{\boldsymbol{\Omega}}\right) d\Omega + S\left(\vec{\boldsymbol{r}}, \vec{\boldsymbol{\Omega}}\right) + \Sigma_s \int_{\vec{\boldsymbol{\Omega}}'} \phi\left(\vec{\boldsymbol{r}}, \vec{\boldsymbol{\Omega}}'\right) d\Omega F\left(\vec{\boldsymbol{\Omega}}' \to \vec{\boldsymbol{\Omega}}\right) \tag{3.58}$$

This is the one-speed, time-independent transport equation. It can be simplified further if we restrict our attention to a slab system (system is infinite in two directions and finite in the third, or x, direction). Let the angle between $\vec{\boldsymbol{\Omega}}$ and the x-axis be the polar angle θ. Then,

$$\vec{\boldsymbol{\Omega}} \cdot \vec{\nabla}\phi = \mu\frac{\partial\phi}{\partial x} + \sin\theta\cos\varphi\frac{\partial\phi}{\partial y} + \sin\theta\sin\varphi\frac{\partial\phi}{\partial z} \tag{3.59}$$

We then integrate over y and z and the azimuthal angle φ to obtain

$$\left[\mu\frac{\partial}{\partial x} + \Sigma_{\mathrm{t}}\right]\phi(x,\mu) = \frac{\nu\Sigma_{\mathrm{f}}}{4\pi}\int_{-1}^{1} d\mu'\phi(x,\mu') + \Sigma_{\mathrm{s}}\int_{-1}^{1} d\mu'\phi(x,\mu')F(\mu_0) + S(x,\mu) \tag{3.60}$$

where

$$\phi(x,\mu) = \iint dydz\int_{0}^{2\pi}\phi(xyz\mu\varphi)d\varphi \tag{3.61}$$

and $\mu = \cos\theta$, and we have put $F\left(\vec{\boldsymbol{\Omega}}' \rightarrow \vec{\boldsymbol{\Omega}}\right) = F\left(\vec{\boldsymbol{\Omega}} \cdot \vec{\boldsymbol{\Omega}}'\right) \equiv F(\mu_0)/2\pi$. Equation 3.60 is the one-speed transport equation for a slab. It is the simplest transport equation which one can consider. It is however still as rigorous as the original transport equation since we have made *no approximations* in the reduction. Equation 3.60 can be solved in an infinite medium problem or in problems involving boundaries. These solutions are useful mainly for checking approximate solutions and also in cases where energy dependence is of no interest.

3.7 Neutron Slowing Down

We are at the point to tackle neutron slowing down subject before we go on with the rest of this chapter and the following sections. In order to understand this matter, we now turn our attention to the topic of neutron energy moderation, the slowing down of a fast neutron to the thermal energy region. The equation that describes the slowing down process, as we can expect by now, can be obtained by reducing the transport equation, Eq. 3.23 in Sect. 3.4. There are two simple ways to get rid of the spatial dependence of the flux. One is to integrate the transport equation over a large system and then take the system size to be infinite; thus we can write the following relationship:

$$\phi(E) = \int\phi(\vec{\boldsymbol{r}},E)d^3r \tag{3.62}$$

and

$$\int \vec{\nabla} \cdot \vec{\boldsymbol{J}} d^3 r = \int_s \left(\hat{n} \cdot \vec{\boldsymbol{J}} \right) dS \to 0 \tag{3.63}$$

The other situation we need to pay attention and take into consideration is "point reactor" condition defined as

$$\phi(\vec{\boldsymbol{r}}, E) = \phi(E)\delta(\vec{\boldsymbol{r}}) \tag{3.64}$$

Here again we integrate over space along with invoking help from Fick's law above to obtain the following result:

$$\int_{-\infty}^{+\infty} \frac{\partial^2}{\partial x^2} \delta(x) dx = \frac{1}{2\pi} \int_{-\infty}^{+\infty} \frac{\partial^2}{\partial x^2} dx \int_{-\infty}^{+\infty} \mathrm{e}^{ikx} dk = -\int_{-\infty}^{+\infty} k^2 \delta(k) dk = 0 \tag{3.65}$$

In either, we get the equivalent result of Eq. 3.50 as

$$\Sigma_{\mathrm{t}}(E)\phi(E) = S(E) + \int \Sigma_{\mathrm{s}}(E')\phi(E') dE' F(E' \to E) \tag{3.66}$$

which is known as the slowing down equation for an infinite medium. In writing Eq. 3.66, we have combined the external source with the fission source in $S(E)$. Without specifying the scattering kernel F, an equation having the same form as Eq. (5.66) is also applicable to the thermal energy region, where upscattering of the neutron must be considered. In that case the energy balance problem would be called neutron thermalization, which will be discussed later.

Further study of Eq. 3.65 reveals that using the energy transfer kernel, we have previously derived under the conditions of elastic scattering, target nucleus at rest, and isotropic scattering in center of mass coordinate system (CMCS). [3]. This kernel is perfectly valid in the slowing down region where the neutron loses energy every time it is scattered by the nucleus. Then we can recall the following relation:

$$\begin{aligned} F(E' \to E) &= \frac{1}{E'(1-\alpha)} \quad \text{for} \quad \alpha E' \le E \le E' \\ F(E' \to E) &= 0 \qquad\qquad \text{otherwise} \end{aligned} \tag{3.67}$$

where $\alpha = (A-1)^2/(A+1)^2$ and $A = M/m$.

Isotropic Source and Scattering [4]

Note that one major simplification that can be introduced into the neutron transport equation arises when one assumes both isotropic neutron sources as

$$s\left(\vec{\boldsymbol{r}}, \vec{\boldsymbol{\Omega}}, t\right) = \frac{1}{4\pi} S(\vec{\boldsymbol{r}}, t) \tag{1}$$

and isotropic scattering in laboratory frame system

$$\Sigma_{\mathrm{s}}\left(\vec{\boldsymbol{\Omega}}' \to \vec{\boldsymbol{\Omega}}\right) = \frac{1}{4\pi} \Sigma_{\mathrm{s}} \tag{2}$$

The assumption of isotropic neutron source is usually not too restrictive since most source such as fission is indeed essentially isotropic. Unfortunately although neutron scattering is usually isotropic in the center of mass (CM) system, it is far from isotropic in the laboratory system, particularly for low mass numbers scatters such as hydrogen. Undeterred by such physical considerations, we will assume for the moment that isotropic scattering is present. Then the one-speed transport equation simplifies still further to

$$\frac{1}{v}\frac{\partial \phi}{\partial t} + \vec{\boldsymbol{\Omega}} \cdot \nabla \phi + \Sigma_{\mathrm{t}}\left(\vec{\boldsymbol{r}}, \vec{\boldsymbol{\Omega}}, t\right) = \frac{\Sigma_{\mathrm{s}}}{4\pi} \int_{4\pi} d\vec{\boldsymbol{\Omega}}' \phi\left(\vec{\boldsymbol{r}}, \vec{\boldsymbol{\Omega}}', t\right) + \frac{S(\vec{\boldsymbol{r}}, t)}{4\pi} \tag{3}$$

However, even this equation is extremely difficult to solve in general.

Before discussing the solution of Eq. 3.66, we first consider the problem of estimating the escape probability $P(E' \to E)$ that a neutron, scattered at E', will cross E, with no restriction on how large is the interval from E' to E and how many collisions are involved. Notice that $P(E' \to E)$ differs from $P(E' \to E)$ in that the latter is for one collision and is a distribution function in the variable E. (In contrast P is not a distribution function, although it is a probability.) The exercise of estimating $P(E' \to E)$ will also help to make clear this distinction. Since the energy range (E', E) is arbitrary, we divide this interval into a number of subintervals, ΔE_j where $j = 1, \ldots,$ such that for each subinterval we can write

$$\begin{aligned} \left\{p_{\mathrm{a}}\left(\Delta E_j\right)\right\} = {} & [\text{Average Number Collision Required to Cross}] \\ & \times [\text{Probability Absorb per Cell}] \end{aligned} \tag{3.68}$$

where $p_{\mathrm{a}}(\Delta E_j)$ is the probability of neutron absorption while crossing ΔE_j. The second term in Eq. 3.68 is the probability of absorption each time the neutron collides

$$[\text{Probability Absorb per Cell}] = \Sigma_{\mathrm{a}}\left(\Delta E_j\right) = \Sigma_{\mathrm{t}}\left(\Delta E_j\right) \tag{3.69}$$

Equation is an indication of the strategy we are following in making our estimate of P. To find the probability of no absorption while crossing the interval (E', E), we write it as a product of probabilities, in a format as below:

$$P(E' \to E) = \prod_j \left[1 - p_{\mathrm{a}}\left(\Delta E_j\right)\right] \tag{3.70}$$

where $p_{\mathrm{a}}(\Delta E_j)$ is to be obtained according to Eqs. 3.68 and 3.69. The advantage of doing this is that once we have Eq. 3.70, we can rewrite it as follows:

$$\ln(P) = -\sum_{j=1,\ldots} p_{\mathrm{a}}\left(\Delta E_j\right) \to \int_E^{E'} p_{\mathrm{a}}\left(E''\right) dE'' \tag{3.71}$$

using the logarithmic properties of $\ln(ab) = \ln(a) + \ln(b)$ and $\ln(1-x) \approx -x$ for $x \ll 1$. Now we see the condition on the subinterval division, ΔE_j, has to be small enough to make $p_{\mathrm{a}}(\Delta E_j)$ small compared to unity. Equation 3.71 means the probability we are seeking is given by the expression

$$P(E' \to E) = \exp\left(-\int_E^{E'} p_{\mathrm{a}}\left(E''\right) dE''\right) \tag{3.72}$$

To turn this into an explicit expression, we can use Eqs. 3.68 and 3.69 to find $p_a(\Delta E_j)$, which means we need to make an estimate of the average number of collisions a neutron should make in going from energy E' to energy E.

A simple way to estimate the number of collisions a neutron should make, on average, in crossing an energy interval, we need only the average energy that a neutron will lose in a collision at a given energy. Suppose the neutron collision occurs at energy E' and the neutron has energy E after the collision. The probability of such an event is just given by the energy transfer kernel $F \to (E' \to E)$. The energy the neutron would have, on average, after a collision at E' then becomes

$$\overline{E} = \int E F(E' \to E) dE = (1+\alpha)E'/2 \tag{3.73}$$

where we have used Eq. 3.67. The energy loss per collision is $E' - \overline{E} = (1+\alpha)E'/2$. Thus the average number of collisions required to cross an interval ΔE is

$$[\text{Average Number Collision Required to Cross}] = \frac{2}{1-\alpha}\frac{\Delta E}{E} \tag{3.74}$$

With this result, we have an explicit expression for the escape probability $P(E' \to E)$ from Eq. 3.72, and then we can write the following relation:

$$P(E' \to E) = \exp\left(-\frac{2}{1-\alpha}\int_{E}^{E'} \frac{\Sigma_{\mathrm{a}}\left(E''\right)}{\Sigma_{\mathrm{t}}\left(E''\right)} \frac{dE''}{E''}\right) \tag{3.75}$$

This expression contains the parameter α whose numerical value depends on the mass number of the target nucleus A. In the case of a hydrogenous medium, $A = 1$ and $\alpha = 0$.

Note that for a heavy target nucleus, $A \gg 1$, then $\alpha \approx 1 - (4/A)$, and the coefficient in front of the integral in Eq. 3.74 becomes $A/2$.

Before closing this discussion, we take the opportunity to introduce another energy-like quantity, called the lethargy in the reactor physics literature,

$$u = \ln(E_0/E) \tag{3.76}$$

where E_0 is some constant energy. Notice that there is a one-to-one correspondence between energy and lethargy, the two variables moving in opposite directions in that when the energy decreases the lethargy would increase. Given that we have just calculated the average energy loss per collision, it is perhaps not surprising that the corresponding average lethargy increase per collision turns out to be a rather useful quantity,

$$\begin{aligned}\langle \Delta u \rangle &= \langle u - u' \rangle = \langle \ln(E'/E) \rangle \\ &= \int_{\alpha E'}^{E'} \ln(E'/E) F(E' \to E) dE = 1 + \frac{\alpha \ln \alpha}{1-\alpha} \equiv \xi \end{aligned} \tag{3.77}$$

In the two limits which are always of interest,

$$\begin{array}{lll} A = 1 & \alpha = 1 & \xi = 1 \\ A \gg 1 & \alpha \approx 1 & \xi = 2/(A + 2/3) \approx 2/A \end{array} \tag{3.78}$$

Now we can use Eq. 3.77 to estimate the average number of collisions to cross an interval ΔE and write the following relationship:

$$\begin{aligned}&[\text{Number Collisions Required to Cross } \Delta E] \\ &= \frac{\ln(E) - \ln(E - \Delta E)}{\xi} = \frac{1}{\xi}\ln\left(\frac{E}{E - \Delta E}\right) = \frac{1}{\xi}\ln\left(1 + \frac{\Delta E}{E}\right) \approx \frac{1}{\xi}\frac{\Delta E}{E}\end{aligned} \tag{3.79}$$

Notice that if we insert the estimate as Eq. 3.79 into Eq. 3.68, we would arrive at the estimate for P as

$$P(E' \to E) = \exp\left(-\int_E^{E'} \frac{\Sigma_a(E'')}{\Sigma_t(E'')} \frac{dE''}{\xi E''} \right) \tag{3.80}$$

In which it agrees with Eq. 3.74 in the case of heavy target nucleus, but not when $A = 1$. We conclude that when $A > 1$, one can use either Eq. 3.74 or Eq. 3.80, whereas for $A = 1$ our present discussion indicates that Eq. 3.74 should be preferred since it involves fewer approximations.

We now turn our attention to the solution of the slowing down equation, Eq. 10.5, for the special case of hydrogenous medium, $A = 1$, a monoenergetic source at E_0, $S(E) = S_0 \delta(E - E_0)$, and furthermore we neglect absorption. Equation 3.66 then reads

$$\Sigma_s(E)\phi(E) = \frac{S_0}{E_0} + \int_E^{E_0} \Sigma_s(E')\phi(E') \frac{dE'}{E'} \tag{3.81}$$

This is a simple integral equation, which can be solved readily. Let $G(E) = \Sigma_s(E)\phi(E)$; Eq. 3.66 is then of the following form:

$$G(E) = \text{constant} + \int_E^{E_0} G(E') \frac{dE'}{E'} \tag{3.82}$$

Now differentiating both sides of Eq. 3.82 with respect to E gives the following:

$$\frac{dG(E)}{dE} = -\frac{G(E)}{E} \quad \text{Or} \quad \frac{dG}{G} = -\frac{dE}{E} \tag{3.83}$$

Therefore, we can write that

$$G(E) = \text{cte}/E = c/E \tag{3.84}$$

where c is an integration constant. To find c, take the limit as E approaches E_0 in which case $G(E)$ should approach S_0; thus $c = S_0$.

We have shown that in the energy region of neutron slowing down, the flux is given by the following relationship:

$$\phi(E) = \frac{S_0}{\Sigma_s(E)E} \tag{3.85}$$

The $1/E$ behavior of the flux is very characteristic of the neutron distribution during energy moderation by elastic collisions with the target nuclei. Equation 3.85 has been obtained for the case of the hydrogenous medium. We can extend it to an arbitrary medium, $A > 1$, by writing in the same spirit as Eqs. 3.79 and 3.80, where for flux $\phi(E)$ we can write

$$\phi(E) \simeq \frac{1}{\Sigma_s(E)\xi E} \tag{3.86}$$

In summary, we have obtained an expression for the probability that a neutron will undergo energy moderation by elastic scattering across an arbitrary interval in the form of Eq. 3.80, which involves the quantity ξ, the average lethargy increase per collision. We have also shown that the flux in the slowing down region, the region of energy below the fission spectrum and above thermal energy where neutrons can be upscattered, is $1/E$.

3.8 Neutron Diffusion Concept

To study neutron diffusion, we go back to the neutron transport equation and obtain an equation only in the spatial variable. We first eliminate the $\vec{\boldsymbol{\Omega}}$ dependence by integrating the transport equation over $\vec{\boldsymbol{\Omega}}$, getting an equation with two unknowns

$$\phi(\vec{\boldsymbol{r}}, E, t) = \int \phi\left(\vec{\boldsymbol{r}}, E, \vec{\boldsymbol{\Omega}}, t\right) d\boldsymbol{\Omega} \tag{3.87}$$

$$\vec{\boldsymbol{J}}(\vec{\boldsymbol{r}}, E, t) = \int \phi\left(\vec{\boldsymbol{r}}, E, \vec{\boldsymbol{\Omega}}, t\right) \vec{\boldsymbol{\Omega}} d\boldsymbol{\Omega} \tag{3.88}$$

Then we invoke Fick's law to eliminate $\vec{\boldsymbol{J}}$, thus obtaining

$$\begin{aligned} \frac{1}{v}\frac{\partial \phi(\vec{\boldsymbol{r}}, E, t)}{\partial t} &= \left[D(E)\nabla^2 - \Sigma_t(E)\right]\phi(\vec{\boldsymbol{r}}, E, t) + S(\vec{\boldsymbol{r}}, E, t) \\ &\quad + vf(E)\int \Sigma_f(E')\phi(\vec{\boldsymbol{r}}, E', t)dE' \\ &\quad + \int \Sigma_s(E')\phi(\vec{\boldsymbol{r}}, E', t)dE'(E' \to E) \end{aligned} \tag{3.89}$$

To reduce further, we consider only steady-state solutions and integrate over all energy to arrive at the following results:

$$\left[\overline{D}\nabla^2 + \left(v\overline{\Sigma}_f - \overline{\Sigma}_a\right)\right]\phi(\vec{\boldsymbol{r}}) = -S(\vec{\boldsymbol{r}}) \tag{3.90}$$

where

$$\phi(\vec{\boldsymbol{r}}) = \int \phi(\vec{\boldsymbol{r}}, E)dE \tag{3.91}$$

$$\overline{D} \equiv \frac{\int D(E)\phi(\vec{\mathbf{r}}, E)dE}{\int \phi(\vec{\mathbf{r}}, E)dE} \tag{3.92}$$

and a similar expression like Eq. 3.92 for the macroscopic cross section $\overline{\Sigma}$. The overhead denotes energy average weighed by the flux as indicated in Eq. 3.92 (recall also Eq. 3.48). In writing Eq. 3.90, we have made use of the statement of neutron conservation as follows:

$$\int F(E' \to E)dE = 1 \tag{3.93}$$

We need to keep in mind that in Eq. 3.90, we are also assuming that the external source is time-independent and more significantly that D is independent of position, which would be the case if $\phi(\vec{\mathbf{r}}, E)$ were separable in r and E (this is not true in general).

Equation 3.90 is a second-order differential equation with constant coefficients. Since the *Schrödinger equation*, in the case of constant potential, is also of this form, it is worthwhile to make note of the analogy between the problem of neutron diffusion and the problem of a particle confined in a potential well, particularly in the role of the boundary conditions.

To keep the notations simple, we will drop the overhead bar on the material constants with the understanding that they are to be regarded as energy-averaged quantities.

3.9 The One-Group Model and One-Dimensional Analysis

In the beginning of this chapter, we talked about control rod in reactor and discussed. When we insert the control rod in a reactor, it changes its multiplication factor in two possible ways, and further we pointed out that for many reactors these two effects of a control rod, increases in absorption and increases in leakage, play important roles in determining the impact of the rod upon the multiplication factor of system [1]. However, in summary, we took under consideration that the effectiveness of a control rod totally depends mainly upon the value of the ratio of the neutron flux of the location of the rod to the average neutron flux ϕ in the reactor. We also said that the control rod has maximum effect, which inserts the most negative reactivity, if it is placed in the reactor where the flux has maximum value. Now, we will further talk about the one-group model and the one-dimensional analysis of the problem in hand, so we can lay out the foundation for the diffusion theory and boundary conditions associated with it. To do so, we pay our attention to a simple reactor system as before and take the notion of criticality under consideration. In this case we have a better understanding of what it means from the point of view of both physics and mathematics of the problem, and then we see how we can solve analytically the steady-state flux for simple geometries and present the numerical solution for steady state for a more arbitrary complex form of these geometries.

Therefore, we start our opening discussion with the time-dependent, one-speed model where we ignore the delay neutrons with *source distribution function* $S_f(\vec{\boldsymbol{r}}, t)$, which is equal to the number of neutrons emitted per cm^3/s by sources at the point $\vec{\boldsymbol{r}}$ and the time t, along with its associated *fuel fusion cross section* $\Sigma_{\mathrm{f}}(\vec{\boldsymbol{r}})$. Thus, the diffusion equation in the following forms:

$$S_f(\vec{\boldsymbol{r}}, t) \Rightarrow \nu\Sigma_{\mathrm{f}}(\vec{\boldsymbol{r}})\phi(\vec{\boldsymbol{r}}, t) \tag{3.94}$$

$$\frac{1}{v}\frac{\partial}{\partial t}\phi(\vec{\boldsymbol{r}}, t) = \nabla \cdot D(\vec{\boldsymbol{r}})\nabla\phi(\vec{\boldsymbol{r}}, t) - \Sigma_{\mathrm{a}}(\vec{\boldsymbol{r}})\phi(\vec{\boldsymbol{r}}, t) + \nu\Sigma_{\mathrm{f}}(\vec{\boldsymbol{r}})\phi(\vec{\boldsymbol{r}}, t) \tag{3.95}$$

In the above relationship, the absorption term $\Sigma_{\mathrm{a}}(\vec{\boldsymbol{r}})$ is a local parameter that may vary in space, depending on the material at hand (moderator, structure, coolant, fuel, etc.), and the fuel fission cross section $\Sigma_{\mathrm{f}}(\vec{\boldsymbol{r}})$ is part of the fuel absorption cross section as

$$\Sigma_{\mathrm{a}}^{\mathrm{fuel}}(\vec{\boldsymbol{r}}) = \Sigma_{\gamma}^{\mathrm{fuel}}(\vec{\boldsymbol{r}}) + \Sigma_{\mathrm{f}}^{\mathrm{fuel}}(\vec{\boldsymbol{r}}) \tag{3.96}$$

where $\Sigma_{\gamma}^{\mathrm{fuel}}(\vec{\boldsymbol{r}})$ is the neutron capture cross section for radiative capture reaction as it was defined previously [2].

Note that we also treat both $\Sigma_{\mathrm{a}}^{\mathrm{fuel}}(\vec{\boldsymbol{r}})$ and $D(\vec{\boldsymbol{r}})$ as constant over time since typically they do not vary substantially over the short time span that the flux can vary significantly in time. The details of the problem in hand will guide you. As example of the above consideration, we look at a simple one-dimensional slab reactor as demonstrated in Fig. 3.12, a case that readily yields an analytical solution. The reactor is composed of a homogeneous mixture of fuel and moderator. The slab

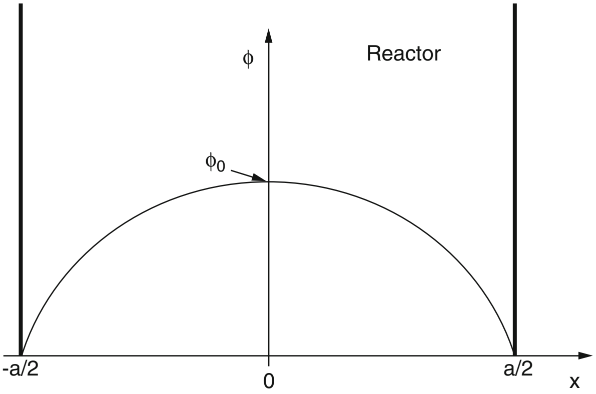

Fig. 3.12 A simple slab reactor

thickness is at centimeters. We assume the dimensions represent the extrapolated distances at which the flux goes to zero.

The steady-state equation for constant coefficients is

$$D\frac{\partial^2\phi(x)}{\partial x^2} + (-\Sigma_\mathrm{a} + \nu\Sigma_\mathrm{f})\phi(x) = 0 \tag{3.97}$$

The solution to the one-dimensional partial differential equation will be of the form

$$\phi(x) = \phi_0 \cos(Bx) \tag{3.98}$$

and for the flux to go to zero at the extrapolated boundaries, we must have

$$B = \frac{\pi}{a} \tag{3.99}$$

Substituting Eq. 3.98 with Eq. 3.97 and after dropping the common $\phi_0\cos(Bx)$ factor, we find that

$$\begin{aligned} &-DB^2 - \Sigma_\mathrm{a} + \nu\Sigma_\mathrm{f} = 0 \Rightarrow DB^2 = \nu\Sigma_\mathrm{f} - \Sigma_\mathrm{a} \\ \text{and}\quad &B_\mathrm{g}^2 = \left(\pi/a\right)^2 = \frac{\nu\Sigma_\mathrm{f} - \Sigma_\mathrm{a}}{D} = B_\mathrm{m}^2 \end{aligned} \tag{3.100}$$

where the subscript *g* refers to the geometric buckling and the subscript *m* refers to the material buckling.

The Criticality Condition

Referring back to Eq. 3.97 and using $\frac{\nu\Sigma_\mathrm{f} - \Sigma_\mathrm{a}}{D} = B^2$, we find that

$$\frac{\partial^2\phi(x)}{\partial x^2} + B^2\phi(x) = 0 \tag{3.101}$$

As we can see this form of equation is used quite often, and in a three-dimensional form Eq. 3.101 can be written as

$$D\left(\frac{\partial^2\phi}{\partial x^2} + \frac{\partial^2\phi}{\partial y^2} + \frac{\partial^2\phi}{\partial z^2}\right) + (-\Sigma_\mathrm{a} + \nu\Sigma_\mathrm{f})\phi(x) = 0 \tag{3.102}$$

and general solution to Eq. 3.102 is in the following form:

$$\phi(x) = \phi_0 \cos(B_x x)\cos\left(B_y y\right)\cos(B_z z) \tag{3.103}$$

which leads to the criticality condition as

$$B_{\mathrm{g}}^2 = B_x^2 + B_y^2 + B_z^2 = \left(\frac{\pi}{a}\right)^2 + \left(\frac{\pi}{b}\right)^2 + \left(\frac{\pi}{c}\right)^2 = \frac{\nu\Sigma_{\mathrm{f}} - \Sigma_{\mathrm{a}}}{D} = B_{\mathrm{m}}^2 \tag{3.104}$$

where a, b, and c are the slab dimensions in the three directions. Note that the basic equality of geometric and material buckling holds even though the exact form of the equality is case dependent.

It is important to stop for a moment and reflect on what this means. This is a statement of the balance between neutron production by fission and neutron loss by leakage and absorption. A unique slab thickness ensures that the ratio of net production to loss (i.e., production/loss) is zero for the given material properties. Any other size will result in a net loss of gain of neutrons over time.

It is also important to realize that this critical size is the size that is **predicted** by the model. Reality will be something else. For the remainder of this section, we spend some of our effort to establish a way of solving the diffusion equation as we started at the beginning of this section as well as with subsections below. We also deal with boundary conditions related to the steady-state diffusion equation for simple slab geometry as part of our opening discussion in this chapter. These include sections and then extend to more complex geometries and include the time variable with more sophisticated boundary conditions that handle both space and time as derivatives to diffusion theory and neutron diffusion equation.

3.9.1 Boundary Conditions for the Steady-State Diffusion Equation

As we have seen so far, the neutron diffusion equation is a type of partial diffusion equation that has derivatives in both space $\vec{r}$ and time t. Since the steady-state diffusion equation is a *partial differential equation* (PDE) as function of space t only, then infinite numbers of solutions can be found for such form of PDEs, or basically there are an infinite number of functions which satisfy the partial differential equation in hand, but in our case there is just *one* function that correctly represents the neutron flux given boundary conditions corresponding to the problem of interest. These boundary conditions are restrictions that must be imposed on the solution of the problem or differential equation by nature of a physical problem. In other words the boundary conditions cannot be imposed arbitrarily; however, it can be demonstrated that for each or every differential equation or partial differential equation, a corresponding set of boundary conditions will help to find a reasonable solution. For a typical Helmholtz scalar-type equation, the following can be stated as [5]:

> *On the boundaries of a region in which ϕ satisfies the differential equation, either ϕ, or the normal derivative of ϕ, or a linear combination of the two must be specified; both ϕ and its normal derivative cannot be specified independently.*

Therefore, for any imposing boundary conditions based on physical argument, the above definition or requirements must not and will not be violated under any circumstances, given the physical problem in hand. Now if we assume a boundary condition *at the surface* of the medium of the form:

$$\frac{1}{\phi}\frac{d\phi}{dn}=-\frac{1}{d} \tag{3.105}$$

where $d\phi/dn$ is the normal derivative of the neutron flux and d is a parameter known as the *reciprocal logarithm derivative* considering that Eq. 3.104 can be written as $d/dn(\ln\phi)=-1/d$ which sometimes is referred to as logarithmic boundary condition. Normally, these types of boundary conditions apply in reactor problems that are comparatively dense and essentially vacuous media [2].

In the above case, the exterior surface of a reactor represents a situation that the surrounding atmosphere is a vacuum in reality and the mean free path of neutrons in air is much larger than in nongaseous materials. It is usually possible to treat it as a vacuum in reactor analysis, and we have to bear in mind that as we mentioned before, the related diffusion theory is not valid near such a surface and it is required to for our further analysis of such problem to take special care and handling of the solution.

In the case of special handling, the value of distance d that is also known as the *extrapolation distance* or *extrapolation length* can be chosen so that the solution to the diffusion equation satisfies the boundary condition given in Eq. 3.105. This solution can be as close as possible to the rigorous solution that is given by neutron transport theory in the interior of the reactor media. It should be also noted that when Eq. 3.105 is written as

$$\frac{d\phi}{dn}+\frac{\phi}{d}=0 \tag{3.106}$$

then this boundary condition is of the form required by the above theorem at hand [2].

To find an appropriate value for d that is also shown in Fig. 3.14, we need to apply the condition that is necessary to take under consideration two types of surfaces that are known as *reentrant* and *non-reentrant*, respectively, and they are demonstrated in Fig. 3.13 as well.

Each of these surfaces is described as follows:

1. **Reentrant Surface**
   A surface is called reentrant if it is possible to draw, through any point on the surface, one straight line outward, which eventually reenters the medium.
2. **Non-reentrant Surface**
   A surface is called non-reentrant if no straight line that reenters the medium can be drawn through the surface

The essential differences between these two surfaces are that a neutron leaving a reentrant surface may *reappear* elsewhere in the system, whereas a neutron that passes through a non-reentrant surface is *permanently* lost from the same system [2].

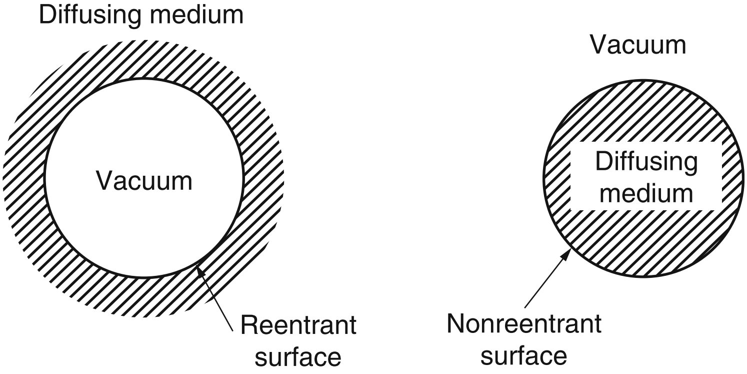

Fig. 3.13 Simple reentrant and non-reentrant surface [2]

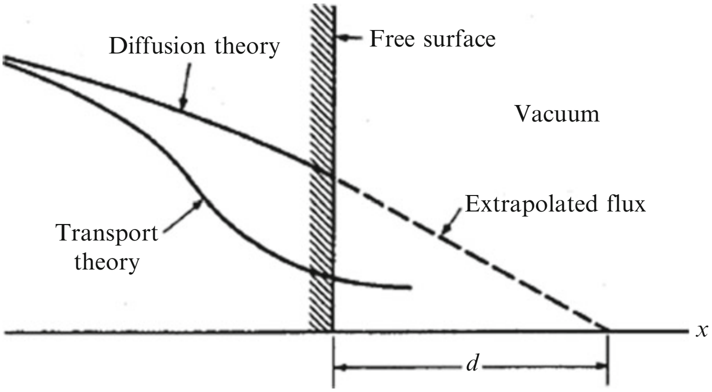

Fig. 3.14 Neutron flux as a function of position near a free surface according to diffusion theory and transport theory [2]

Note that the value of extrapolation distance/length d at a reentrant depends in a complicated way upon the size and the shape of the space adjacent to the surface, which is by far simpler in a non-reentrant surface situation, identically known as a *free surface* in a reactor analysis or theory. In a particular planner free surface, it can be demonstrated by transport theory that for the value of d as per the following equation

$$d = 0.7\lambda_{\text{Tran.}} \tag{3.107}$$

where $\lambda_{\text{Tran.}}$ is the *transport mean free path* of the medium, the solution of neutron flux diffusion equation will be subject to the above boundary condition that provides a good approximation to the actual flux ϕ everywhere within the medium except near the surface of the reactor, in which the situation is plotted in Fig. 3.14.

Further analysis of Fig. 3.14 reveals that the flux ϕ is shown near a free surface as calculated by the exact transport theory and by diffusion theory using similar boundary conditions as above. It also demonstrates that, while the two solutions are very nearly the same in the interior of the reactor, they also differ from each other. This difference is quite of bid in the immediate vicinity of the surface and with curved free surface as it can be found for the outer edge of a cylindrical or spherical shape of simple reactor case. The extrapolation distance d is given by a somewhat more complex formula than the one we see in Eq. 3.107 and that depends on the radius of curvature R of the reactor surface. However, for extrapolation distance d approaching the planar value for the larger limit of curvature radius of reactor surface, i.e., $d/R \rightarrow 0$, it is possible to use Eq. 3.107. This situation can be implemented at the surface of cylindrical and spherical reactors providing that $d \ll R$ [2].

In quest of simple solution for diffusion equation using the condition provided in Eq. 3.106, we notice this solution does vanish at the extrapolation distance d from the surface if the solution gets extended beyond the surface of the reactor by means of linear extrapolation. However, such approach for the quest of the solution for flux ϕ does introduce negligible error into diffusion equation solution, and it can be shown that ordinarily the extrapolation distance d is very small compared with the dimensions of practical reactor design system. In that case, it is possible to replace the above boundary condition to be a simple statement as below:

> *The solution to the diffusion equation vanishes at the extrapolation distance d beyond the edge of a free surface.*

We use this simple statement as a mathematical tool to be able to simplify the neutron diffusion equation for quest of simpler solutions. Note that the neutron flux *does not* ϕ vanish at the extrapolation distance anymore, and solutions of this type of approach do not provide the correct flux near the boundary. If we use the diffusion coefficient D that is validating Fick's law for its value of $D = \lambda_{\text{Tran.}}/3$, the extrapolation distance is then about $d = 2D$ [2].

Lamarsh [2] further makes a statement that for most diffusing media in a reactor, diffusion coefficient D is in the order of 1 cm or less and consequently the extrapolation distance d is never more than 2 cm. He also indicates that the most reactors, however, are of the order of meters in size, so that in many reactor analyses and calculations, the extrapolation distance d can be neglected altogether; thus the neutron flux ϕ presumably will vanish at the actual surface of the reactor of concern.

Further boundary condition types for different circumstances such as multilayer of materials at the interface for handling the problems involving neutron diffusion can be found in Lamarsh [2]. Interface boundary condition is discussed in details in that reference, and an elementary solution of the steady-state diffusion equation is provided as follows given the modified version of neutron diffusion of Eq. 2.96 that is satisfying the preceding boundary conditions.

$$D\nabla^2\phi - \Sigma_a\phi + S = 0 \qquad (3.108)$$

We can rewrite Eq. 3.107 in the form of

$$\nabla^2\phi - \frac{1}{L^2}\phi + S = -\frac{S}{D} \qquad (3.109)$$

where the constant L^2 is defined as

$$L^2 = \frac{D}{\Sigma_a} \qquad (3.110)$$

The constant quantity L appears very frequently in the equations of reactor theory and is known as the *diffusion length*, and the dimension of it is in centimeter range based on the dimension of D and Σ_a being in range of cm and cm^{-1}, respectively. Again, we encourage readers to refer to Lamarsh‘s [2] book for more details; however, in summary the steady-state solution is of linear type:

$$\phi(x) = A\mathrm{e}^{-x/L} + C\mathrm{e}^{-x/L} \qquad (3.111)$$

This solution is provided based on the following limitation current density $J(x)$ in x-direction and utilizing Fig. 3.15:

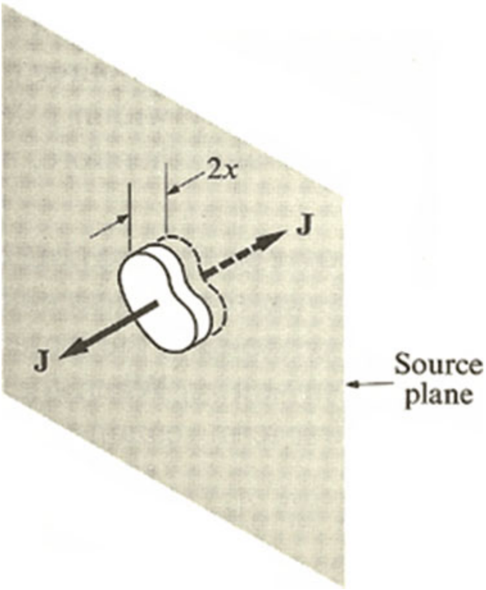

Fig. 3.15 Construction to drive the planar source condition

$$\lim_{x\to 0} J(x) = \frac{S}{2} \tag{3.112}$$

Note that A and C are constants that need to be determined for the given boundary conditions, and we purposely did not use letter B since it has a different meaning and designation in the reactor theory as it was demonstrated in Eq. 3.105.

3.9.2 Boundary Conditions: Consistent and Approximate

In general, in a three-dimensional space, a nonsteady-state diffusion equation has a derivative of both space $\vec{r} = x\hat{\boldsymbol{i}} + x\hat{\boldsymbol{j}} + z\hat{\boldsymbol{k}}$ and time t (see Fig. 3.16) as we have indicated in the previous section, and one must assign the proper boundary and initial conditions to complete the specification of any particular problem. To solve such general problem in hand knowing that the diffusion equation itself is only approximation to the more exact neutron transport equation in our case, we might expect that we can use the transport theory boundary conditions as a direction to our development for appropriate diffusion boundary conditions. However, in the previous section, we saw it was sufficient to consider this development in a one-speed (one-dimensional) or one-group approximation, and we can express that the neutron transport theory boundary condition can be defined as

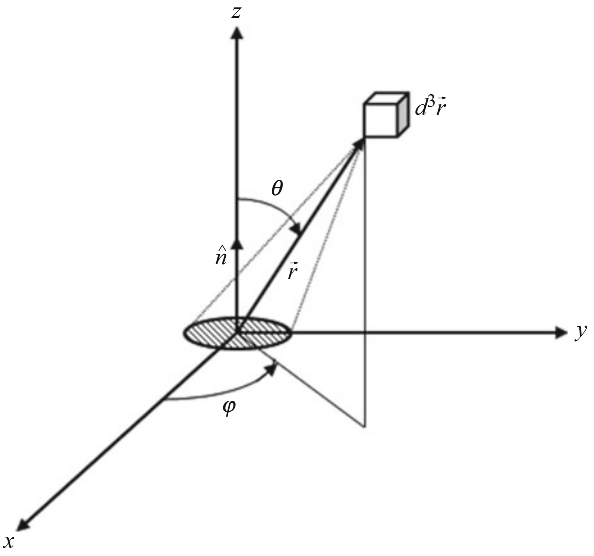

Fig. 3.16 Three-dimensional space presenting diffusion equation problem

$$\text{Initial Condition}: \quad \varphi\left(\vec{r}, \vec{\Omega}, 0\right)\Big|_{t=0} = \varphi_0\left(\vec{r}, \vec{\Omega}\right) \tag{3.113}$$

$$\text{Boundary Condition}: \quad \varphi\left(\vec{r}, \vec{\Omega}, t\right) = 0 \quad \text{for} \quad \vec{\Omega}\cdot\hat{n}_{\mathrm{s}} \ \text{ all } \ \vec{r}_{\mathrm{s}} \text{ on } S \tag{3.114}$$

We are able to obtain the appropriate initial condition for the diffusion equation by merely integrating the transport condition over solid angle $\vec{\Omega}$ to have the following initial condition:

$$\text{Initial Condition}: \quad \phi(\vec{r}, 0)\big|_{t=0} = \phi_0(\vec{r}) \tag{3.115}$$

As we mentioned in the previous section, the boundary conditions are getting set up for a specific problem in the reactor theory, and several types of them are discussed by Lamarsh [2] as well as Duderstadt and Hamilton [4].

Depending on the particular physics problem of interest in nuclear reactor analysis, these boundary conditions can be grouped in several classes, but as we have said, the boundary conditions to be imposed on $\phi(\vec{r})$ are quite similar to those imposed on the wave function in solving the Schrödinger equation. Because we are dealing with a physical quantity, the neutron distribution in space $\phi(\vec{r})$ must be positive and finite everywhere or zero. In addition, the distribution must reflect the symmetry of the problem, such as $\phi(x) = \phi(-x)$ in a slab system with $x = 0$ being at the center of the slab. Then there are the usual boundary conditions at a material interface; flux and currents must be continuous since there are no sources or sinks at such interfaces. All these conditions have counterparts in solving the wave equation.

The one boundary condition, which requires some discussion, is the statement of no reentrant current across the boundary between a medium and a vacuum. Let this surface be located at the position $x = x_0$ in slab geometry. The physical condition is $J_-(x_0) = 0$. While the definition of J_- is given in Eq. 3.28 and Sect. 3.4 is perfectly correct, we can evaluate J_- according to its physical meaning and by making the assumptions that the scattering is isotropic in *laboratory coordinate system* (LCS), the medium is nonabsorbing, and the flux is slowly varying. Then J_- is approximately given by the following integral (see Fig. 3.16). In this figure the geometrical setup for estimating the current of neutrons crossing a unit area A shown as shaded area at the origin with normal unit $\hat{\boldsymbol{n}}$ after scattering isotropically in the volume element d^3r about the vector space $\vec{\boldsymbol{r}}$ is given by [2]

$$\hat{z}\cdot\boldsymbol{J}_- = \int_{\mathrm{UHS}} \Sigma_{\mathrm{s}}\boldsymbol{\phi}(\vec{r})\left(\frac{A\cos\theta}{4\pi r^2}\right)\mathrm{e}^{-\Sigma_{\mathrm{t}}r}d^3r \tag{3.116}$$

where the integral extends over the upper half space (UHS) of the medium because we are interested in all those neutrons which can cross the unit area A from above (in the direction opposite to the unit normal). The part of the integrand in the parenthesis is the fraction of the neutron going through the unit area A if there were no collisions along the way, with A being subtended at an angle θ from the elemental volume d^3r at $\vec{r}$. The fact that neutrons can collide on the way to the unit area is taken into account by the factor $\exp(-\Sigma_t r)$. To carry out the indicated integral, we need to know $\phi(\vec{r})$, and since we have assumed the flux is slowly varying, we can expand the origin (the location of the unit area) and keep only the first term in the expansion.

$$\boldsymbol{\phi}(\vec{\boldsymbol{r}}) \simeq \phi(0) + \vec{\boldsymbol{r}} \cdot \vec{\nabla}\phi|_{x=0} \tag{3.117}$$

Then,

$$J_{-}^{z}(0) = \frac{\Sigma_s}{4\pi}\int_{\varphi=0}^{2\pi} d\varphi \int_{\theta=0}^{\pi/2} \cos\theta \sin\theta d\theta \int_{r=0}^{\infty} dr e^{-\Sigma_t r}\left[\phi_0 + x(\partial\phi/\partial x)_{x=0} + y(\partial\phi/\partial y)_{y=0} + z(\partial\phi/\partial z)_{z=0}\right] \tag{3.118}$$

where we have taken $A = 1$. Writing out the Cartesian component x, y, and z in terms of the spherical coordinates (r, θ, φ), $x = r\sin\theta\cos\varphi$, $y = r\sin\theta\sin\varphi$, and $z = r\cos\theta$ as before, we find the ϕ-integration renders the terms containing x or y equal to zero. The term containing z can be easily integrated to give the following forms after shifting the unit area from being at the origin as in Fig. 3.16 to a slab geometry with the unit area on the surface at $x = x_0$.

$$J_{-}(x_0) = \frac{\phi(x_0)}{4} + \frac{D}{2}\left(\frac{d\phi}{dx}\right)_{x_0} \tag{3.119}$$

or

$$\left(\frac{d\phi}{dx}\right)_{x_0} = -\frac{1}{2D}\phi(x_0) \tag{3.120}$$

Equation 3.120 is not really a bona fide condition on $\phi(x_0)$ because the gradient $d\phi/dx$ is not known. To find another relation between the flux and gradient, we interpret the latter as a finite difference

$$\left(\frac{d\phi}{dx}\right)_{x_0} = -\frac{\phi(x_0) - \phi(x')}{x' - x_0} \quad x' > x_0 \tag{3.121}$$

where we use the negative sign because we know the gradient must be negative. Now we choose x' such that we know the value of the flux at this position. How is this possible? Suppose we choose x' to be the distance where the flux linearly extrapolates from $x = x_0$ to zero. Calling this distance $x' = x_0 + \delta$ (see Fig. 3.17), we then have from Eq. 3.121.

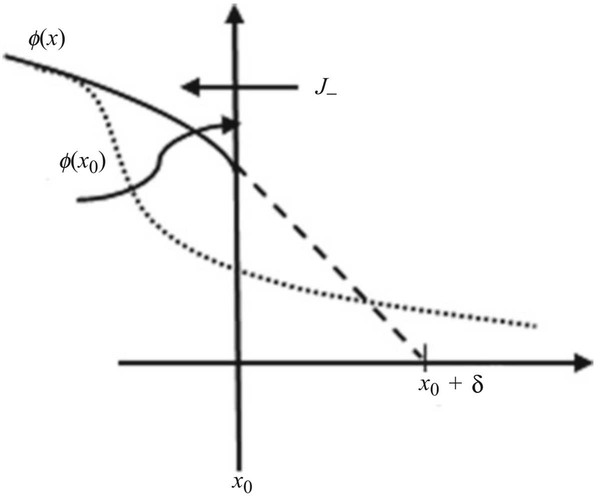

Fig. 3.17 Schematic of the extrapolated boundary condition

Figure 3.17 shows a schematic of the extrapolated boundary condition, with δ being the distance beyond the actual boundary where a linear extrapolation of the flux at $x = x_0$ would vanish as it was explained in the previous section and the dotted curve showing the variation of the flux that would be obtained from transport theory [2].

$$\left(\frac{d\phi}{dx}\right)_{x=x_0} = -\frac{1}{\delta}\phi(x_0) \tag{3.122}$$

Combining this with Eq. 3.117, we obtain for the extrapolated distance $\delta = 2D$. Conventionally instead of the physical condition of no reentrant current, one often applies the simpler mathematical (and approximate) condition of the following form:

$$\phi(x_0 + 2D) = \phi(\widetilde{x}_0) = 0 \tag{3.123}$$

where$\widetilde{x}_0 = x_0 + 2D$. Equation 3.12 is called the extrapolated boundary condition; it is commonly adopted because of its simplicity. One can use transport theory to do a better calculation of the extrapolated distance δ. We have seen that in simple diffusion theory, this turns out to be $2D$ or $2/3\Sigma_\alpha$. The transport theory result, when there is no absorption, is $0.71/\Sigma_{\text{tran.}}$, where again $\Sigma_{\text{tran.}}$ is transport mean free path. The rather small difference between diffusion theory and transport theory should not be taken to mean that the flux near the surface is always accurately given by diffusion theory. As can be seen in Fig. 3.17, diffusion theory typically overestimates the flux at the surface relative to transport theory. All these were discussed differently in the previous section.

Note that as part of the infinite planner source which emits at a constant rate of neutrons per second per unit area into an infinite homogeneous medium, where the source plane and medium are both infinite, the flux at any point in the medium can be a function of distance explicitly from the plane, and we can write Eq. 3.108 as

$$\frac{d^2\phi}{dx^2} - \frac{1}{L^2}\phi = -\frac{s(x)}{D} \tag{3.124}$$

In this equation the source density function $s(x)$ is an orthodox function of x, and since there are no sources present in the medium itself, then $s(x)$ is zero everywhere in that medium. However, at $x = 0$, the source density function $s(x)$ is infinite. This is because the source density function is the number of neutrons emitted per plane, and thus the source density is necessarily infinite at the plane, simply because a finite number of neutrons are produced in zero volume [2].

Functions such as $s(x)$, which are zero everywhere except at $x = 0$, can be represented in terms of the *Dirac delta function* $\delta(x)$, which is defined by

$$\begin{aligned} &\delta(x) = 0 \qquad\qquad x \neq 0 \\ &\int_a^b \delta(x) = \begin{cases} 1 & a < 0 < b \\ 0 & \text{otherwise} \end{cases} \end{aligned} \tag{3.125}$$

In any case, $s(x)$ can be written as

$$s(x) = S\delta(x) \tag{3.126}$$

In view of Eq. 3.125, the total number of neutrons emitted per second per unit area of the source plane is just in the form of the following, where ε has any value [2]:

$$\int_{-\varepsilon}^{+\varepsilon} s(x)dx = S\int_{-\varepsilon}^{+\varepsilon} \delta(x)dx = S \tag{3.127}$$

Inserting Eq. 3.126 into diffusion Eq. 3.124, we get the following result:

$$\frac{d^2\phi}{dx^2} - \frac{1}{L^2}\phi = -\frac{S\delta(x)}{D} \tag{3.128}$$

The above equation is an ordinary, inhomogeneous, linear differential equation which easily can be solved by all the known methods of solving differential equation in mathematics, and for all the value of x, except for $x = 0$, the above equation can be converted to a simple equation of homogeneous form as

$$\frac{d^2\phi}{dx^2} - \frac{1}{L^2}\phi = 0 \quad \text{for} \quad x \neq 0 \tag{3.129}$$

Note that at $x = 0$ can now be taken into account by means of a *source condition* rather than using the source density function directly.

3.9.3 An Approximate Method for Solving the Diffusion Equation

Now let us consider an approximate method for solving the diffusion equation for an inhomogeneous problem in slab geometry. We know that the eigenfunctions for this problem are the *exponentials* or the sinh and cosh. But suppose we didn't know this or that the actual eigenfunctions were unknown. Let us try an approximate approach that often gives very good answers.

Let us choose a set of functions that satisfy the boundary conditions automatically. The easiest set to choose, because most people are familiar with them, is the sin and cos functions. However, since we will put the plane source at the middle of our inhomogeneous slab and require the solution to be symmetric, the sin functions are not acceptable. This leaves only the cos functions.

Now in order for the $\cos(\alpha z)$ to be zero at the boundary where $z = H/2$, we must have the following,

$$\frac{\alpha H}{2} = \frac{(2k+1)\pi}{2} \quad \text{or} \quad \alpha = \frac{(2k+1)\pi}{H} \tag{3.130}$$

Now since the cos functions are not eigenfunctions of the operator for an attenuation problem, we will want to use more than one of them in our approximate solution. We might even want to use an infinite number if we are mathematicians and want the best accuracy. However, since we are engineers, we will only take a few if they work. So we can choose for our solution

$$\phi(z) = \sum_{k=0}^{N} C_k \cos\left(\frac{(2k+1)\pi}{H} z\right) \tag{3.131}$$

If we substitute this equation into our differential equation, we obtain

$$\sum_{k=0}^{N} \left(\frac{(2k+1)\pi}{H}\right)^2 C_k \cos\left(\frac{(2k+1)\pi}{H} z\right) + \frac{1}{L^2} \sum_{k=0}^{N} C_k \cos\left(\frac{(2k+1)\pi}{H} z\right) = \frac{S_D}{D} \delta(0) \tag{3.132}$$

So now we would like to choose the C_k in such a way that we get the best solution we can get with the fewest terms. What we will do is to require the equation to be satisfied in an integral sense. However if we want to use N terms to approximate our solution, we must have N equations to solve for the N coefficients. Therefore, to get

N equations, we will multiply the equation by each of the solution functions, one at a time. This will give us N equations, and luckily since the cos functions are orthogonal on the interval of our problem, we will get a simple equation for each coefficient. Thus, we have

$$\begin{aligned}&\int_{-H/2}^{H/2} \cos\left(\frac{(2n+1)\pi}{H}z\right)\sum_{k=0}^{N}\left(\left[\frac{(2n+1)\pi}{H}\right]^2+\frac{1}{L^2}\right)C_k\cos\left(\frac{(2k+1)\pi}{H}z\right)dz\\ &\quad=\int_{-H/2}^{H/2}\frac{S_D}{D}\delta(0)\cos\left(\frac{(2n+1)\pi}{H}z\right)dz\end{aligned} \tag{3.133}$$

$$\begin{aligned}\int_{-H/2}^{H/2}\cos^2\left(\frac{(2n+1)\pi}{H}z\right)dz &= \frac{H}{(2n+1)\pi}\int_{-H/2}^{H/2}\cos^2\beta d\beta\\ &=\frac{H}{(2n+1)\pi}(2n+1)\int_{-H/2}^{H/2}\cos^2\beta d\beta=\frac{H}{\pi}\frac{1}{2}\pi\end{aligned} \tag{3.134}$$

or

$$\int_{-H/2}^{H/2}\frac{S_D}{D}\delta(0)\cos\left(\frac{(2n+1)\pi}{H}z\right)dz=\frac{S_D}{D} \tag{3.135}$$

So each of the coefficients must satisfy

$$\left(\left[\frac{(2n+1)\pi}{H}\right]^2+\frac{1}{L^2}\right)C_n\frac{H}{2}=\frac{S_D}{D} \tag{3.136}$$

or

$$C_n=\frac{2S_D}{HD\left(\frac{1}{L^2}+\left[\frac{(2n+1)\pi}{H}\right]^2\right)} \tag{3.137}$$

So we have an approximate solution that satisfies the differential equation in an integral sense. Let us see how good it is. Consider a stainless steel slab that has a planar source at its center. Let the slab be 60 cm thick, and we will use the one-group fast energy spectrum cross sections.

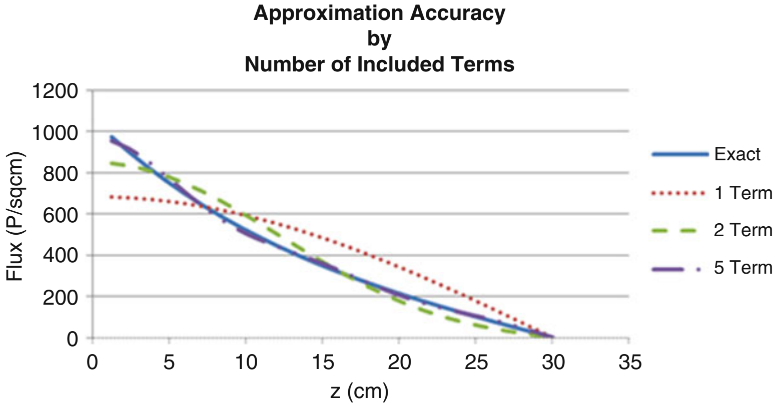

Fig. 3.18 Approximation accuracy by number of included terms

$$\Sigma_a = 0.002963\ \text{cm}^{-1}$$
$$D = 0.6962\ \text{cm}$$
$$L^2 = 234.96\ \text{cm}^2$$

and let $S_D = 100$ particles/s/cm^2

In Fig. 3.18, the exact solution, the approximate solution with one term, the approximate solution with two terms, and the approximate solution with five terms are plotted. Two terms give a solution that looks close, and five terms cannot be distinguished from the exact solution on this chart.

Of course all approximate solutions match the exact solution at the boundary because each of the terms is exactly equal to zero at the boundary. However, if the slab thickness is broken up into 26 mesh points or 25 intervals, the largest difference between the exact solution and the five term approximate solution occurs at the last mesh point in the slab, and at this point the approximate solution is off by 21 % of the exact value, which is pretty small.

If ten terms are used, the largest difference also occurs at the same mesh point, and the difference is 8 %. If 25 terms are used, the largest difference is 0.2 %, and it occurs at the first mesh point near the center of the slab.

We now continue with further analysis approximation in transport theory.

3.9.4 The $\mathbf{P}_1$ Approximate Methods in Transport Theory

Referring to Eq. 3.60 we see that this equation is still an integrodifferential equation that cannot be solved easily. One of the most common methods of extracting a more tractable description of transport is to expand the distribution function in a series of angular functions and then truncate the series. This is reminiscent of the use of partial wave expansion as a means of reducing the Schrödinger equation to a more manageable form. For this discussion we can ignore the fission without any loss of generality. We write the following relationship:

$$\phi(x,\mu) = \sum_{t=0}^{\infty} \frac{2\ell+1}{2} \phi_\ell(x) P_\ell(\mu) \tag{3.138}$$

$$F(\mu_0) = \sum_{t=0}^{\infty} \frac{2\ell+1}{2} F_\ell P_\ell(\mu_0) \tag{3.139}$$

where $P_\ell(\mu)$ is the ℓth-order Legendre polynomial. This expansion leads to an infinite set of coupled equations for the functions

$$\phi_\ell(x) = \int_{-1}^{+1} P_\ell(\mu) \phi_\ell(x,\mu) d\mu \tag{3.140}$$

$$F_\ell = \int_{-1}^{+1} P_\ell(\mu) F(\mu) d\mu \tag{3.141}$$

The first two such equations are

$$\frac{d\phi_1(x)}{dx} + \Sigma_{\mathrm{t}} \phi_0(x) = \Sigma_{\mathrm{s}} F_0 \phi_0(x) + S_0(x) \tag{3.142}$$

$$\frac{2}{3} \frac{d\phi_2(x)}{dx} + \frac{1}{3} \frac{d\phi_0}{dx} + \Sigma_{\mathrm{t}} \phi_1(x) = \Sigma_{\mathrm{s}} F_1 \phi_1(x) \tag{3.143}$$

If somehow we are justified in ignoring the term containing $\phi_2(x)$, then we would have a closed set of equations in which we can solve for the flux coefficients, ϕ_0 and ϕ_1,

$$\frac{d\phi_1(x)}{dx} + (\Sigma_{\mathrm{t}} - \Sigma_{\mathrm{s}} F_0) \phi_0(x) = S_0(x) \tag{3.144}$$

$$\frac{1}{3} \frac{d\phi_0(x)}{dx} + (\Sigma_{\mathrm{t}} - \Sigma_{\mathrm{s}} F_1) \phi_1(x) = 0 \tag{3.145}$$

The truncation of the Legendre polynomial expansion at $\ell = 1$ is called the P_1 approximation. In general, retaining the $N+1$ terms in the series leads to a coupled set of $N+1$ equations—the P_N approximation.

The two scattering kernel coefficients, which appear in the P_1 equations, have quite simple meanings,

$$F_0 = \int_{-1}^{+1} F(\mu) d\mu = 1 \quad \text{(Particle Conservation)} \tag{3.146}$$

$$F_1 = \int_{-1}^{+1} F(\mu) \mu d\mu = \langle \mu \rangle \tag{3.147}$$

An immediate consequence of the P_1 approximation is that we obtain a relation between the current and the gradient of the flux from Eq. 3.145 as

$$\phi_1(x) = -\frac{1}{3}[\Sigma_t - \Sigma_s\langle\mu\rangle]^{-1}\frac{d\phi_0(x)}{dx} \tag{3.148}$$

where ϕ_0 and ϕ_1 are the neutron flux distribution in position space (position flux) and the neutron net current, respectively. Such a relation defines a transport coefficient, in this case the neutron diffusion coefficient

$$D = [3(\Sigma_t - \Sigma_s)\langle\mu\rangle]^{-1} \tag{3.149}$$

Equation 3.148 is the P_1 approximation to Fick's law of diffusion, generally written as

$$\vec{J} = -D\vec{\nabla}\phi \tag{3.150}$$

As we said in previous sections, this relation is also well known in the kinetic theory of gases, with one difference. In neutron transport, the diffusion coefficient has a dimension of cm, whereas in kinetic theory its dimension would be cm^2/s. This distinction arises from a factor of the thermal speed, that is, in kinetic theory one uses number density rather than flux.

If absorption is weak, $(\Sigma_a/\Sigma_t) \ll 1$, the diffusion coefficient simplifies to

$$D \simeq \frac{1}{3\Sigma_s(1-\langle\mu\rangle)} \equiv \frac{1}{3\Sigma_{\text{tran.}}} \tag{3.151}$$

with $\Sigma_{\text{tran.}}$ being an effective "transport cross section." Since $\langle\mu\rangle$ is average of the cosine of the scattering angle in the laboratory coordinate system (LCS), it would have a larger value if the scattering were preferentially biased in the forward direction. Then D and the net current would increase as one would intuitively expect. If the medium has a large scattering cross section, D would decrease since the neutron would be scattered more frequently thus impeding its forward progress. These simple physical interpretations apply to neutron diffusional transport as well as particle diffusion in general. Another remark is that we can go back to the transport equation without making the P_1 approximation and derive Fick's law relation between the current and the flux gradient. This however would take us to Sect. 3.5 discussion.

Further discussion of this topic and derivation of the one-dimensional multigroup P_N equations will be discussed later in this book.

3.10 Further Analysis Methods for One Group

Now let us try to perform a little more sophisticated analysis of the spatial variation, of the flux, in a nuclear reactor. To make things simple and focus on one part of the problem at a time, assume that a suitable within-group spectrum can be found such that the multigroup equations can be reduced to one equivalent group and reasonable estimates of reaction rates can be obtained. We will assume that this spectrum can vary with material, but within a given material, it is constant across all space. The one-group diffusion equation becomes

$$-\frac{\partial}{\partial z}D\frac{\partial}{\partial z}\phi(z)+\Sigma_{\mathrm{a}}\varphi(z)=\frac{1}{k}\nu\Sigma_{\mathrm{f}}\phi(z) \tag{3.152}$$

Since we have assumed that the spectrum is constant for any given material, then each of the coefficients appearing in the equation will be constant, and in particular the diffusion coefficient will not change with location and it can be brought out of the first derivative operation. This will give

$$-D\frac{\partial^2}{\partial z^2}\phi(z)+\Sigma_{\mathrm{a}}\phi(z)=\frac{1}{k}\nu\Sigma_{\mathrm{f}}\phi(z) \tag{3.153}$$

Now the second derivative with respect to z in the first term is the same as the $-\nabla^2$ operator in one spatial dimension. In fact if the multigroup diffusion equations were derived in three dimensions or in any other coordinate system, this first term would always come out to be the $-\nabla^2$ operator. So let us write the equation as

$$-D\nabla^2\phi(z)+\Sigma_{\mathrm{a}}\phi(z)=\frac{1}{k}\nu\Sigma_{\mathrm{f}}\phi(z) \tag{3.154}$$

We will deal with the changes in group cross sections across different materials by applying boundary, or interface, conditions at those boundaries. This simplifies the analysis somewhat and allows some problems to be solved analytically.

Note that this equation is still a homogeneous equation as the flux, $\phi(z)$, appears in every term. If the flux is exactly zero at every point, then the equation is completely satisfied. However, this is a very uninteresting result. Therefore, in order for the flux to nonzero, a unique relationship must exist between the operators and constants in the equation. Note the equation can be rewritten in the following fashion:

$$-\nabla^2\phi(z)=\frac{\frac{1}{k}\nu\Sigma_{\mathrm{f}}-\Sigma_{\mathrm{a}}}{D}\phi(z) \tag{3.155}$$

This is the form of

$$-\nabla^2\phi(z) = \lambda\phi(z), \quad \lambda = \frac{\frac{1}{k}\nu\Sigma_\mathrm{f} - \Sigma_\mathrm{a}}{D}$$

a classic eigenvalue problem. The question becomes "does a set of functions exist that will satisfy this equation such that operating on the functions with the $-\nabla^2$ operator will reproduce the same functions multiplied by a constant?" It is also worth noting that the constant, λ, can be either positive or negative depending on the relative values of Σ_a and $\nu\Sigma_\mathrm{f}$. Of course there exist functions that will replicate themselves multiplied by a nonzero constant when operated on by the $-\nabla^2$ operator. These functions will depend on exactly how the $-\nabla^2$ operator is expressed.

We will deal with the $-\nabla^2$ operator in three one-dimensional geometries, two two-dimensional geometries, and one three-dimensional geometry all together. There are an infinite variety of ways that three-dimensional space can be measured, and just because we do not address a three-dimensional spherical coordinate system, geometry does not mean that it would not be appropriate for certain problems. The coordinate systems that we will use one-dimensional problems and the appropriate expression of the $-\nabla^2$ operator are

(1) **Infinite Slab**

$$-\nabla^2\phi(z) = -\frac{\partial^2}{\partial z^2}\phi(z) \tag{3.156}$$

(2) **Infinite Cylinder**

$$-\nabla^2\phi(\rho) = -\frac{1}{\rho}\frac{\partial}{\partial\rho}\rho\frac{\partial}{\partial\rho}\phi(\rho) \tag{3.157}$$

(3) **Sphere**

$$-\nabla^2\phi(r) = -\frac{1}{r^2}\frac{\partial}{\partial r}r^2\frac{\partial}{\partial r}\phi(r) \tag{3.158}$$

The two-dimensional coordinate systems and the appropriate $-\nabla^2$ operators are

(4) **Finite Cylinder**

$$-\nabla^2\phi(\rho,z) = -\frac{1}{\rho}\frac{\partial}{\partial\rho}\rho\frac{\partial}{\partial\rho}\phi(\rho,z) - \frac{\partial^2}{\partial z^2}\phi(\rho,z) \tag{3.159}$$

(5) **Infinite Rectangular Column**

$$-\nabla^2\phi(x,y) = -\frac{\partial^2}{\partial x^2}\phi(x,y) - \frac{\partial^2}{\partial y^2}\phi(x,y) \tag{3.160}$$

We will consider two three-dimensional $-\nabla^2$ operators, the rectilinear one based on Cartesian coordinates (x, y, z) and the spherical coordinate one based on the (r, θ, φ) system.

(6) **Rectangular Parallelepiped**

$$-\nabla^2\phi(x,y,z) = -\frac{\partial^2}{\partial x^2}\phi(x,y,z) - \frac{\partial^2}{\partial y^2}\phi(x,y,z) - \frac{\partial^2}{\partial z^2}\phi(x,y,z) \tag{3.161}$$

(7) **Nonhomogeneous Sphere**

$$\begin{aligned}-\nabla^2\phi(r,\theta,\varphi) = &-\frac{\partial}{\partial r}\left(r^2\frac{\partial}{\partial r}\phi(r,\theta,\varphi)\right)\\ &+\frac{1}{\sin\theta}\frac{\partial}{\partial\theta}\left(\sin\theta\frac{\partial}{\partial\theta}\phi(r,\theta,\varphi)\right)+\frac{1}{\sin^2\theta}\frac{\partial^2}{\partial\varphi^2}\phi(r,\theta,\varphi)\end{aligned} \tag{3.162}$$

Each of these coordinate systems and $-\nabla^2$ operators will have different eigenfunctions that will satisfy the above homogeneous equation. Note that the one-dimensional spherical system is a way of representing a physically realizable object, as are the two-dimensional finite cylinder and three-dimensional box. Ultimately, these two coordinate systems will allow us to build simple models that can be used in real experiments to test our mathematical theories.

3.10.1 Slab Geometry

Now consider the eigenfunctions that will satisfy the one-dimensional slab problem. The simplest case corresponds to when λ is a negative constant. Note that the units on λ are (length)$^{-2}$. So the physical constant that will nondimensionalize our solutions should really be the square root of λ. We will use a different symbol for this constant depending on whether λ is positive or negative. If λ is negative, the constant will be imaginary, and we will give it a different interpretation than if λ were positive. Consider first the case where λ is negative. We will let our fundamental constant be the square root of $1/|\lambda|$. Thus we will write $|\lambda| = 1/L^2$. We will call L the diffusion length. For this case the eigenfunctions are the exponential functions with positive or negative exponents.

$$\hat{\Phi}_1(z) = \mathrm{e}^{z/L}, \quad \hat{\Phi}_2(z) = \mathrm{e}^{-z/L} \tag{3.163}$$

These functions can also be expressed as the hyperbolic sine and cosine functions such that both representations are equivalent, and the one that we will choose to solve a given problem will depend on the geometry and boundary conditions for the problem. The exponentials are often easier to use if one boundary condition is at infinity; the hyperbolic functions are often easier to use if symmetry about the origin is a natural boundary condition. Either set will work in all cases, but the solutions are usually simpler if the appropriate basis set is chosen.

Next consider the case where λ is a positive number. We can still set it equal to the square of another number, but now this number is imaginary. We will let $\lambda = B^2$ where we will call B the buckling and its nominal units will be 1/cm. If we use the exponential functions for the eigenfunctions (we will talk about the eigenfunctions expansion in the next section) for this case, they replicate themselves but their arguments must be imaginary. This really does not present a problem, as the exponential of an imaginary argument can be transformed to the trigonometric functions, sin and cosine, by the De Moivre identities as below:

$$\hat{\Phi}_1(z) = \sin Bz = \frac{\mathrm{e}^{iBz} - \mathrm{e}^{-iBz}}{2i}, \quad \hat{\Phi}_2(z) = \cos Bz = \frac{\mathrm{e}^{iBz} + \mathrm{e}^{-iBz}}{2} \tag{3.164}$$

Thus any time we have $-\nabla^2$ operator operating on a single Cartesian dimension, the eigenfunctions will be either the exponential functions or the trigonometric functions depending on the sign of the constant, λ.

3.10.2 Cylindrical Geometry

For the cylindrical geometry, $-\nabla^2$ operator, consider the case of a positive λ first. The eigenfunctions for a positive λ are the Bessel functions. The first and most common of these is the $J_0(\rho)$ function. It is called the Bessel function of the first kind of order zero. It has a value of 1.0 at $\rho = 0$ and has a value of 0.0 at $\rho = 2.4048255577\ldots$. After that, it goes negative and continues to oscillate with a slightly decreasing period out to infinity. It is a solution to Bessel's equation,

$$\frac{\partial^2}{\partial \rho^2}\phi(\rho) + \frac{1}{\rho}\frac{\partial}{\partial \rho}\phi(\rho) + \left(1 - \frac{n^2}{\rho^2}\right)\phi(\rho) = 0 \tag{3.165}$$

for $n = 0$. Moreover, it can be computed from the general series expansion form as

$$\hat{\Phi}_1(\rho) = \mathrm{J}_n(B\rho) = \frac{\left(\frac{B\rho}{2}\right)^n}{\Gamma(n+1)}\left\{1 - \frac{\left(\frac{B\rho}{2}\right)^2}{1\cdot(n+1)} + \frac{\left(\frac{B\rho}{2}\right)^4}{1\cdot 2\cdot(n+1)(n+2)}\cdots\right\} \tag{3.166}$$

where the only case of interest is $n = 0$ case. Note $\Gamma(n+1)$ is the gamma function of order n. It is given by

$$\Gamma(n) = \int_0^\infty t^{n-1}\mathrm{e}^{-t}dt \tag{3.167}$$

and when n is an integer, $\Gamma(n+1) = n!$, i.e., $\Gamma(5) = 5 * 4 * 3 * 2 * 1$.

Since, we have a second-order differential equation, then there must be a second solution that also satisfies it. This solution in our notation will be called $Y_0(\rho)$ or Neumann's function, and it is negative infinity for $\rho = 0$ and it passes through zero at $\rho = 0.89357697\ldots$.

It continues to oscillate out to infinity interlacing its zeroes with $J_0(\rho)$. An expansion for $J_0(\rho)$ is given by

$$\hat{\Phi}_2(\rho) = Y_0(B\rho) = J_0(B\rho)\log(B\rho) + \left\{\left(\frac{B\rho}{2}\right)^2 - \frac{\left(\frac{B\rho}{2}\right)^4}{2!}\left(1+\frac{1}{2}\right) + \frac{\left(\frac{B\rho}{2}\right)^6}{3!}\left(1+\frac{1}{2}+\frac{1}{3}\right)\cdots\right\} \tag{3.168}$$

For the case of a negative λ in our original differential equation, we will obtain the modified Bessel functions of integer order. These are identified as $I_n(\rho)$ and $K_n(\rho)$. $I_0(\rho)$ starts at 1.0 for $\rho = 0.0$ and increases without bound, much as a positive exponential function. It is given by

$$\hat{\Phi}_1(\rho) = I_n(B\rho) = \frac{\left(\frac{B\rho}{2}\right)^n}{\Gamma(n+1)}\left\{1 + \frac{\left(\frac{B\rho}{2}\right)^2}{1\cdot(n+1)} + \frac{\left(\frac{B\rho}{2}\right)^4}{1\cdot 2\cdot(n+1)(n+2)}\cdots\right\} \tag{3.169}$$

$I_n(\rho)$ starts at 0.0 and increases without bound in a similar fashion.

All of the $K_n(\rho)$ start at a positive infinity and decrease to zero as their argument goes from 0.0 to infinity, paralleling the behavior of a negative exponential. $K_0(\rho)$ is given by

$$\hat{\Phi}_2(\rho) = K_0(B\rho) = -\left\{\gamma + \log\left(\frac{B\rho}{2}\right)\right\}I_0(B\rho) + \left(\frac{B\rho}{2}\right)^2 + \frac{\left(\frac{B\rho}{2}\right)^4}{2!}\left(1+\frac{1}{2}\right) + \frac{\left(\frac{B\rho}{2}\right)^6}{3!}\left(1+\frac{1}{2}+\frac{1}{3}\right)\dots \tag{3.170}$$

where γ is Euler's constant ($\gamma = 0.5772156649\dots$). Probably the only real thing to remember about the Bessel functions for this course is that they are the eigensolutions in cylindrical geometry for the $-\nabla^2$ operator and that the first zero of $J_0(\rho)$ is 2.4048.... Most students are not that facile with Bessel functions for solving differential equations, and they are only useful when exact analytic solutions can be obtained. Unfortunately, in nuclear engineering, most solutions wind up being numerical and trying to compute Bessel functions numerically is the *wrong* way to solve the problem.

3.10.3 Spherical Geometry

Moving on to spherical geometry, the one-dimensional eigenfunctions for the $-\nabla^2$ operator with a negative λ are the exponential functions divided by the radius variable

$$\hat{\Phi}_1(r) = \frac{e^{r/L}}{r}, \quad \hat{\Phi}_2(r) = \frac{e^{-r/L}}{r} \tag{3.171}$$

These can be shown to be the eigenfunctions by simply plugging them into the differential equation and verifying that they repeat themselves multiplied by a constant when operated on by the $-\nabla^2$ operator.

$$\begin{aligned}\frac{1}{r^2}\frac{\partial}{\partial r}r^2\frac{\partial}{\partial r}\frac{e^{r/L}}{r} &= \frac{1}{r^2}\frac{\partial}{\partial r}r^2\left(\frac{1}{L}\frac{e^{r/L}}{r} - \frac{e^{r/L}}{r^2}\right) = \frac{1}{r^2}\frac{\partial}{\partial r}\left(\frac{r}{L}e^{r/L} - e^{r/L}\right)\\ &= \frac{1}{r^2}\left\{\frac{e^{r/L}}{L} + \frac{1}{L^2}re^{r/L} - \frac{e^{r/L}}{L}\right\} = \frac{1}{L^2}\frac{e^{r/L}}{r}\end{aligned} \tag{3.172}$$

Equation 3.172 is a quod erat demonstrandum, meaning “which is what had to be proven.”

Of course the hyperbolic functions can be substituted for the exponential functions by using linear combinations of exponential functions as for the slab geometry case

$$\hat{\Phi}_1(r) = \frac{\sinh^{r}/_{L}}{r}, \quad \hat{\Phi}_2(r) = \frac{\cosh^{r}/_{L}}{r} \tag{3.173}$$

This is particularly useful when the problem under consideration contains the origin, as both the positive and negative exponential functions divided by the radius give an unbounded answer at the origin. The hyperbolic sine function, however, goes to zero at the origin and therefore produces a bounded eigenfunction at the origin for this operator.

The spherical geometry case for a positive λ parallels the slab geometry case, and the standard trigonometric functions are substituted for the exponential functions to give the eigenfunctions for this operator.

$$\hat{\Phi}_1(r) = \frac{\sin Br}{r}, \quad \hat{\Phi}_2(r) = \frac{\cos Br}{r} \tag{3.174}$$

3.11 Eigenfunction Expansion Methods and Eigenvalue Equations

For solving the linear but nonhomogeneous ordinary differential equation (ODE), one can use the method of variation that helps to determine the constants, and it will be useful for finding the solution in more general problems of that sort. Using this method allows one to find both auxiliary and particular solution of nonlinear differential equation solution. (See Problems 3.19 and 3.20 at the end of this chapter.) In this case one must be able to guess the particular solution for such ODEs by inspection; hence for most problems, Green's function techniques is more convenient.

Green's functions are particularly helpful in quest of the solution of partial differential equations. However, they can be used to solve ordinary differential equations. Few examples here can briefly show the ideas that are extended to solve partial differential equations.

Example 3.1 Let us reconsider the following linear nonhomogeneous differential equation, namely,

$$y'' + \omega^2 y = f(t) \quad \text{with boundary condition} \quad y_0 = y'_0 = 0 \tag{1}$$

Note that this equation might describe the oscillations of a mass suspended by a spring, or a simple series electric circuit with negligible resistance.

Solution Considering the differential equation given by the example, we can write

$$f(t) = \int_0^x f(t')\delta(t' - t)dt' \tag{2}$$

This is based on thoughts that the force $f(t)$ is a whole sequence of impulses. You might reflect that, on the molecular level, air pressure is the force per unit area to a tremendous number of impacts of individual molecules. Now suppose that we have solved the given differential equation with $f(t)$ replaced by $\delta(t' - t)$, that is, we find the response of the system to a unit impulse at $G(t, t')$. Let us call this response $G(t, t')$, that is, t' is the solution of

$$\frac{d^2}{dt^2} G(t, t') + \omega^2 G(t, t') = \delta(t' - t) \tag{3}$$

Then, given some forcing function $f(t)$, we try to find a solution of the differential equation of the example by "adding up" the responses of many such impulses. We shall show that this solution is

$$y(t) = \int_0^x G(t, t') f(t') dt' \tag{4}$$

Substituting Eq. 4 into differential Eq. 1 of the problem in hand provides the following results:

$$\begin{aligned} y'' + \omega^2 y &= \left(\frac{d^2}{dt^2} + \omega^2\right) y = \left(\frac{d^2}{dt^2} + \omega^2\right) \int_0^\infty G(t, t') f(t') dt' \\ &= \int_0^\infty \left(\frac{d^2}{dt^2} + \omega^2\right) G(t, t') f(f') dt' \\ &= \int_0^\infty \delta(t' - t) f(t') dt' = f(t) \end{aligned} \tag{5}$$

Thus, the function $G(t, t')$ is called a *Green's function*. Green's function is the response of the system to a unit impulse at $t = t'$. Solving Eq. 3 with initial conditions $G = 0$ and $(dG/dt) = 0$ at $t = 0$, we find that

$$G(t, t') = \begin{cases} 0 & 0 < t < t' \\ (1/\omega) \sin \omega(t - t') & 0 < t' < t \end{cases} \tag{6}$$

Then Eq. 4 gives the solution of Eq. 1 with $y_0 = y_0^{'} = 0$, namely,

$$y(t) = \int_0^t \left(\frac{1}{\omega}\right) \sin \omega(t - t') f(t') dt' \tag{7}$$

The upper limit is $t = t'$ since $G = 0$ for $t' > t$; thus, given a forcing function $f(t)$, we can find the response $y(t)$ of the system Eq. 1 by increasing Eq. 7 to Eq. 6. Similarly, for other differential equations, we can find the solution in terms of an appropriate Green's function.

Note that in general, once a Green's function has been obtained for a given ordinary differential equation of $d^2y/dx^2 + y = f(x)$ and boundary conditions, one can apply Eq. 4 to provide the solution for the problem in hand.

One of the most powerful methods available for solving boundary value problems is to search the right solution as an expansion in the set of *normal modes* or *eigenfunctions* characterizing the geometry of interest. The problem of finding the solution of a given differential equation subject to given boundary conditions is called a *boundary value problem* (BVP). Such problems often lead to *eigenvalue problems* or *characteristic value problem*. Under these conditions, there are parameters that their values are to be selected so that the solutions of boundary value problems of these ODEs could meet the given requirements, and these parameters could be separation constants that we need in order to solve our BVPs. Then their values are determined by demanding that the solutions satisfy some of the boundary conditions (BCs). The resulting values of the separation constants are called *eigenvalues*, and the basic solutions of the differential equation corresponding to the eigenvalues are called *eigenfunctions*.

To further enhance the understanding of the boundary value and eigenvalue problems, we continue to look at the solutions of second-order ordinary differential equations of the following form that exist under general conditions.

$$y'' = f(t, y, y') \tag{3.175}$$

It becomes unique if we specify initial values for $y(t_0)$ and $y'(t_0)$, which is the foundation of *initial value problem* (IVP).

In many applications, we are seeking a solution for Eq. 3.175, in which one specifies the *values* of the solution $y(t)$ at two separate points $t_0 < t_1$ rather than specifying the value of $y(t)$ and its derivative at a single point.

This leads to the subject of boundary value problems, a very large and important area of mathematics dealing with differential equation of different subjects such as heat transfer, fluid mechanics, reactor theory, and diffusion equations. The subject is studied for both ordinary and partial differential equations. In the case of partial differential equations, one deals with solutions which are defined on subsets of various Euclidean spaces, and hence there are many interesting regions for which boundary conations can be specified.

In most applications, the independent variable of the differential equation represents a spatial condition along a real interval rather than time, so we use x for the independent variable of our functions instead of t. The general linear second-order boundary value problems have the following form:

$$\begin{cases} \dfrac{d^2y}{dx^2} + p(x)\dfrac{dy}{dx} + q(x)y = h(x) \\ y'' + p(x)y' + q(x)y = h(x) \end{cases} \quad \text{including boundary conditions} \tag{3.176}$$

Here, x is in some interval $I = (a, b) \subset \Re$, and $p(x)$, $q(x)$, and $h(x)$ are continuous real-valued functions on I with $\alpha < \beta$ the two fixed real numbers in I, and boundary condition (BC) refers to specific boundary conditions.

Let us use the letters BVP to denote *boundary value problem*. We wish to study all solutions of such a problem. In the cases considered here, we can replace x by $x + a$ if necessary and assume that $\alpha = 0$. We will denote the right boundary point by L.

For the purpose and further study of this subject, we will consider four types of boundary conditions, which we denote by the expressions 00, 01, 10, and 11. These are defined by

$$\begin{cases} \text{type}\,00: & y(0) = 0, y(L) = 0 \\ \text{type}\,01: & y(0) = 0, y'(L) = 0 \quad \text{where} \quad L > 0 \\ \text{type}\,10: & y'(0) = 0, y(L) = 0 \end{cases} \tag{3.177}$$

Then the boundary value problem of the form

$$y'' + p(x)y' + q(x)y = 0 \quad \text{with} \quad \text{BC}\,y(0) = 0,\ y(L) = 0 \tag{3.178}$$

is called a *homogeneous boundary value problem* (HBVP); thus any BVP which is not homogeneous will be called a nonhomogeneous boundary value problem (NHBVP).

Given a BVP as Eq. 3.176 of type 00, 01, or 10, there is an associated HBVP of type 00 obtained by replacing $h(x)$ by the zero function and replacing the boundary conditions by $y(0) = 0$, $y(L) = 0$.

From our experience with initial value problems (IVPs), we might expect that the solutions to a general NHBVP are related to those of its associated HBVP. It turns out that BVPs behave very differently than IVPs. For instance, a BVP may have no solution at all, may have infinitely many solutions, or may have a unique solution. In a certain sense, BVPs behave more like systems of linear algebraic equations than IVPs.

For comparison, let us recall some general properties of linear algebraic equations. Consider the matrix equation

$$Ax = b \tag{3.179}$$

where A is an $n \times n$ matrix and x is $n \times 1$ matrices, which we think of as column vectors. Here, A and b are known, and we wish to find x.

Based on the given situation, we have the following facts:

1. If $\det(A) \neq 0$, then
   (a) $Ax = 0$ has only the trivial solution.
   (b) $Ax = b$ has a unique solution for every b.
2. If $\det(A) = 0$, then
   (a) $Ax = 0$ has infinitely many solutions.

(b) $Ax = b$ has either no solutions at all or infinitely many solutions.

Now if we impose a constraint on our study of BVPs upon the case where $p(x) = p$ and $q(x) = q$ are constants (i.e., not function of variable x) and the boundary conditions are of the types 00, 01, and 11, then we can begin with HBVP of the following form:

$$y''(x) + py'(x) + qy(x) = 0 \quad \text{for boundary conditions} \quad y(0)\,\text{and}\,y(L) = 0 \tag{3.180}$$

If Eq. 3.180 has a *nontrivial* solution, then $p^2 - 4q < 0$, which is the *characteristic polynomial* $z(r) = r^2 + pr + q$ with no real roots. Under these conditions of the assumption that by way of contradiction $z(r)$ has real roots, then the following two cases can be considered for the purpose of our analysis:

1. **Case 1:** $z(r) = (r - r_1)(r - r_2) \quad \text{where} \quad r_1 \neq r_2\,.$
   In this case the general solution to the differential equation of Eq. 3.180 has the form:

   $$y(x) = c_1 e^{r_1 x} + c_2 e^{r_2 x}$$

   Assume that it is a nontrivial solution, so that either $c_1 \neq 0$ or $c_2 \neq 0$.
   The first BC $y(0) = 0$ gives $c_1 + c_2 = 0$, so that $c_1 = -c_2$.
   The second BC $y(L) = 0$ gives

   $$e^{r_1 L} + e^{r_2 L}$$

   But the function $x \to e^x$ is strictly increasing, so this implies that $r_1 = r_2$, which is a contradiction.
2. **Case 2:** $z(r) = (r - r_1)^2$
   Here, the general solution is in the form:

   $$y(x) = c_1 e^{r_1 x} + c_2 x e^{r_2 x}$$

   The first BC, $y(0) = 0$, gives $c_1 = 0$.
   Then, the second BC, $y(L) = 0$, gives $c_2 L e^{r_1 L} = 0$. But since $L > 0$, we have that $L e^{r_1 L} > 0$, so $c_2 = 0$ also. This is a contradiction and the above proposition is proved.

Remark: In a similar manner, one can prove that the BVPs $y'' + py' + qy = 0$ of types 01, 10, and 11 only have nontrivial solutions if $z(r)$ has no real roots. We leave the proof as an exercise; see Problem 3.7 at the end of this chapter. Thus, in considering constant coefficient BVPs of type 00, 01, 10, and 11, we might as well assume that $p^2 - 4q < 0$. The quadratic formula gives that the roots have the form

$$r = -p/2 \pm \sqrt{p^2 - 4q}/2$$

Letting $a = -p/2$ and $b = \sqrt{p^2 - 4q}/2$, we get the general solution to the differential equation as

$$y(x) = \mathrm{e}^{ax}[c_1 \cos{(bx)} + c_2 \sin{(bx)}]$$

It turns out that the methods and ideas in the study of this expression with BCs of types 00, 01, 10, and 11 are not much different when a $a \neq 0$ or $a = 0$. So, for simplicity, we only consider the case when $a = 0$. That is, the case in which $z(r)$ has purely imaginary roots.

This can be interpreted as that our differential equation has the form

$$y''(x) + qy(x) = 0 \tag{3.181}$$

where $q > 0$. It will simplify things if we follow books on other differential equations and boundary value problems to write $q > \lambda^2$, where $\lambda > 0$.

Thus, we consider the boundary value problem as

$$y''(x) + \lambda^2 y(x) = 0 \tag{3.182}$$

where the boundary condition is one of the four types, 00, 01, 10, and 11.

3.11.1 Eigenvalue and Eigenfunction Problems

As we did in the previous section, we need to again note that we are only going to give a brief look at the topic of eigenvalues and eigenfunctions for boundary value problems. Generally speaking again, for a given matrix A, if we could find values for λ for which we could find nonzero solutions, i.e., $\vec{x} = 0$, to the following relation

$$A\vec{x} = \lambda\vec{x} \tag{3.183}$$

then we call λ an eigenvalue of A and $\vec{x}$ is its corresponding eigenvector. It is important to recall here that in order for λ to be an eigenvalue, then we had to be able to find nonzero solutions to the equation.

So, just what does this have to do with boundary value problems? We'll go back to the previous section and look at Examples 3.2 and 3.3. In these two examples, we solved homogeneous BVPs in the form

$$y'' + \lambda y = 0 \quad y(0) \quad \text{and} \quad y(2\pi) = 0 \tag{3.184}$$

Example 3.2 Solve the following BVP along with its boundary conditions:

$$y'' + 4y = 0 \quad y(0) \quad \text{and} \quad y(2\pi) = 0$$

Solution Here, the general solution is of the following form:

$$y(x) = c_1 \cos(2x) + c_2 \sin(2x)$$

Applying the boundary conditions gives

$$\begin{aligned} c_1 &= y(0) = 0 \\ c_1 &= y(2\pi) = 0 \end{aligned}$$

Thus, c_2 is arbitrary and the solution is as

$$y(x) = c_2 \sin(2x)$$

and in this case we will get infinitely many solutions.

Example 3.3 Solve the following BVP along with its boundary conditions:

$$y'' + 3y = 0 \quad y(0) \quad \text{and} \quad y(2\pi) = 0$$

Solution Here, the general solution is of the following form:

$$y(x) = c_1 \cos\left(\sqrt{3}x\right) + c_2 \sin\left(\sqrt{3}x\right)$$

Applying the boundary conditions gives

$$\begin{aligned} &c_1 = y(0) = 0 \\ &c_2 \sin\left(2\sqrt{3}x\right) = y(2\pi) = 0 \Rightarrow c_2 = 0 \end{aligned}$$

In this case, we will have both constants as zero and so the solution is of the following form:

$$y(x) = 0$$

To further analyze the two above examples, we can see that we have solved the homogeneous boundary value problem (HBVP) as in Eq. 3.182, where in Example 3.1 we had $\lambda = 4$ and we found nontrivial (i.e., nonzero) solutions to BVP. However, in Example 3.2, we use $\lambda = 3$ and the only solution was the trivial solution (i.e., $y(x)=0$), so that the homogeneous BVP seems to exhibit similar behavior to the behavior in the matrix equation given in Eq. 3.180. Recall that it also means the boundary conditions are zero as well. There are values of λ that will give nontrivial solutions to this BVP and values of λ and will only admit the trivial solutions.

From what we have learned so far, those values of λ that give nontrivial solutions will be called λ, and the **eigenvalue** for the BVP and the nontrivial solutions will be called **eigenfunctions** for the BVP corresponding to the given eigenvalue.

We know by now that for homogeneous boundary value problem in Eq. 3.182, $\lambda=4$ is an eigenvalue with eigenfunction $y(x)=c_2\sin(2x)$ and $\lambda=3$ is not an eigenvalue.

Eventually, we will try to determine if there are any other eigenvalues for Eq. 3.182; however, before we do that, let us comment briefly on why it is so important for the BVP to be homogeneous in this discussion. In Examples 3.4 and 3.5, we solve the homogeneous differential equation as in Eq. 3.182 with two boundary conditions, $y(0)=a$ and $y(2\pi)=b$.

Example 3.4 Solve the BVP of the following form along with its given boundary conditions:

$$y''+4y=0 \quad y(0)=-2 \quad \text{and} \quad y(2\pi)=-2$$

Solution We are working with the same differential equation that is given in Eq. 3.182 with eigenvalue of $\lambda=4$, so we have a general solution of the following form:

$$y(x)=c_1\cos(2x)+c_2\sin(2x)$$

Upon applying the given boundary conditions, we get

$$\begin{cases} y(0)=-2=c_1 \\ y(2\pi)=-2=c_1 \end{cases}$$

So in this case, unlike in the previous example, both boundary conditions tell us that we have to have $c_1=-2$ and neither one of them tells us anything about them. Remember however that all we are asking for is a solution to the differential equation that satisfies the two given boundary conditions and the following function will do that:

$$y(x)=-2\cos(2x)+c_2\sin(2x)$$

In other words, regardless of the value of c_2, we get a solution, and so in this case we get infinitely many solutions to the boundary value problem.

Example 3.5 Solve the BVP of the following form along with its given boundary conditions:

$$y'' + 4y = 0 \quad y(0) = -2 \quad \text{and} \quad y(2\pi) = 3$$

Solution Again, we have the following general solution as below, given an eigenvalue of $\lambda = 4$:

$$y(x) = c_1 \cos(2x) + c_2 \sin(2x)$$

However, this time the boundary conditions are providing the following result:

$$\begin{cases} y(0) & = -2 = c_1 \\ y(2\pi) & = 3 = c_1 \end{cases}$$

In this case, we have a set of boundary conditions each of which requires a different value of c_1 in order to be satisfied. This, however, is not possible and so in this case have **no solution**.

If we now introduce the boundary value problem of Example 3.6 and its associated boundary conditions, we get a totally different eigenfunction as its solution. The only difference between this example and the other two examples of 3.4 and 3.5 is the boundary conditions.

Example 3.6 Solve the BVP of the following form along with its given boundary conditions:

$$y'' + 4y = 0 \quad y(0) = -2 \quad \text{and} \quad y(\pi/4) = 10$$

Solution Again, given the eigenvalue of $\lambda = 4$ is

$$y(x) = c_1 \cos(2x) + c_2 \sin(2x)$$

and applying the two boundary conditions provided, the general solution to this differential equation is the following eigenfunction solution:

$$\begin{cases} y(0) = -2 = c_1 \\ y(\pi/4) = 10 = c_2 \end{cases}$$

With final solution of

$$y(x) = -2\cos(2x) + 10\sin(2x)$$

In Examples 3.3 and 3.4, we saw that by simply changing the value of a and/or b, we were able to either get nontrivial solutions or force no solution at all. In the discussion of eigenvalues and associated eigenfunctions, we need solutions to exist, and the only way to assure this behavior is to require that the boundary conditions also be homogeneous. In other words, we need for the BVP to be homogeneous.

There is one final topic that we need to discuss before we move into the topic of eigenvalues and eigenfunctions, and this is more of a notational issue that will help us with some of the work that we'll need to do.

Let us suppose that we have second-order differential equations and its characteristic polynomial has two real distinct roots and that they are in the form of

$$\left| \begin{aligned} & r_1 = \alpha \\ & r_2 = -\alpha \end{aligned} \right. \tag{3.185}$$

Then we know that the solution is

$$y(x) = c_1 \mathrm{e}^{r_1 x} + c_2 \mathrm{e}^{r_2 x} = c_1 \mathrm{e}^{\alpha x} + c_2 \mathrm{e}^{-\alpha x} \tag{3.186}$$

While there is nothing wrong with this solution, let us do a little rewriting. We will start by splitting up the terms as follows:

$$\begin{aligned} y(x) &= c_1 \mathrm{e}^{\alpha x} + c_2 \mathrm{e}^{-\alpha x} \\ &= \frac{c_1}{2}\mathrm{e}^{\alpha x} + \frac{c_1}{2}\mathrm{e}^{\alpha x} + \frac{c_2}{2}\mathrm{e}^{-\alpha x} + \frac{c_2}{2}\mathrm{e}^{-\alpha x} \end{aligned} \tag{3.187}$$

Now we will add and subtract the following terms as well as notice we are "mixing" the c_i for $i = 1, 2$ and $\pm\alpha$ up in the new terms to obtain the following mathematical relationship for the general solution of our boundary value problem:

$$y(x) = \frac{c_1}{2}\mathrm{e}^{\alpha x} + \frac{c_1}{2}\mathrm{e}^{\alpha x} + \frac{c_2}{2}\mathrm{e}^{-\alpha x} + \frac{c_2}{2}\mathrm{e}^{-\alpha x} + \left(\frac{c_1}{2}\mathrm{e}^{\alpha x} - \frac{c_1}{2}\mathrm{e}^{\alpha x}\right) + \left(\frac{c_2}{2}\mathrm{e}^{\alpha x} + \frac{c_2}{2}\mathrm{e}^{\alpha x}\right) \tag{3.188}$$

Next, rearrange terms around a little with the help of mathematical manipulation, and we have

$$y(x) = \frac{1}{2}\left(c_1 \mathrm{e}^{\alpha x} + c_1 \mathrm{e}^{-\alpha x} + c_2 \mathrm{e}^{\alpha x} + c_2 \mathrm{e}^{-\alpha x}\right) + \frac{1}{2}\left(c_1 \mathrm{e}^{\alpha x} - c_1 \mathrm{e}^{-\alpha x} - c_2 \mathrm{e}^{\alpha x} + c_2 \mathrm{e}^{-\alpha x}\right) \tag{3.189}$$

Finally, the quantities in parenthesis factor and we will move the location of the fraction as well. Doing this, as well as renaming the new constants, we get

$$\begin{aligned} y(x) &= (c_1 + c_2)\left[\frac{e^{\alpha x} + e^{-\alpha x}}{2}\right] + (c_1 - c_2)\left[\frac{e^{\alpha x} - e^{-\alpha x}}{2}\right] \\ &= A\left[\frac{e^{\alpha x} + e^{-\alpha x}}{2}\right] + B\left[\frac{e^{\alpha x} - e^{-\alpha x}}{2}\right] \end{aligned} \tag{3.190}$$

All this work probably seems very mysterious and unnecessary. However, there really was a reason for it. In fact, you may have already seen the reason, at least in part. The two "new" very well-known hyperbolic functions that we have in our solution are in fact two of the hyperbolic functions that we discussed previously as sinh(x) and cosh(x). In particular, they can be mathematically presented as

$$\left[\begin{aligned} \sinh(\alpha x) &= \frac{e^{\alpha x} - e^{-\alpha x}}{2} \\ \cosh(\alpha x) &= \frac{e^{\alpha x} + e^{-\alpha x}}{2} \end{aligned}\right. \tag{3.191}$$

So, another way to write the solution to a second-order differential equation presented in Eq. 3.184 whose characteristic polynomial has two real, distinct roots in the form $r_1 = \alpha$ and $r_2 = -\alpha$ is

$$y(x) = c_1 \cosh(\alpha x) + c_2 \sinh(\alpha x) \tag{3.192}$$

Note that we switched both constants A and B back to c_1 and c_2, which totally is acceptable.

Having the solution in this form for some or actually in most of the problems we will be looking would make our life a lot easier. The hyperbolic functions have some very nice properties that we can and will take advantage of the two forms of trigonometric relationships in differential calculus. Since we are going to need these forms, we write the derivative of the two hyperbolic functions as

$$\left[\begin{aligned} \frac{d}{dx}[\cosh(x)] &= \sinh(x) \\ \frac{d}{dx}[\sinh(x)] &= \cosh(x) \end{aligned}\right. \tag{3.193}$$

Next, let us take a quick look at the graphical depiction of these two functions given in Eq. 3.191 with the value of $\alpha = 1$ (Fig. 3.19).

Note that $\cosh(0) = 1$ and $\sinh(0) = 0$. Since most of the time in reactor analysis and neutron diffusion equations we will be working with boundary conditions at the edge of reactor core for distance $x = 0$, these figures will be useful evaluations.

Now if also look at possibility more important case such, as when $\cosh(x) > 0$ for all value of x and so the hyperbolic cosine will never be zero. Similarly, we can see that $\sinh(x) = 0$ only if $x = 0$. We will be using both of these facts in some of our work so we should not forget them.

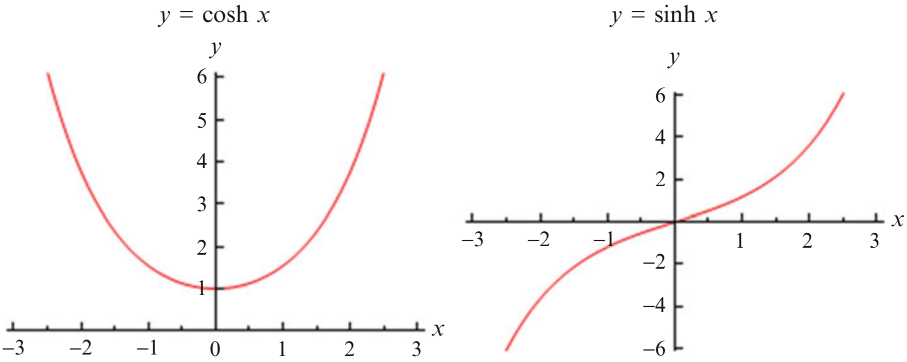

Fig. 3.19 Depiction of hyperbolic cosine and sine functions

Only, we have all we need to understand all the above examples and be able to work on some of the boundary value problems that are provided at the end of this chapter.

3.12 Multidimensional Models and Boundary Conditions

The basic multidimensional neutron kinetics model that is currently the state of the art and is expected to be applicable to LWR applications for the expected future is based on the three-dimensional neutron diffusion equation for two neutron energy groups and with six groups of delayed neutron precursors. Several solution methods are considered state of the art, although those that are expected to be most applicable in the future utilize a nodal method to handle the spatial dependence and direct integration to handle the temporal dependence.

For light-water reactors (LWRs), a two-group diffusion theory approach has proven to be adequate for steady-state applications, and, for those transient applications where direct validation is possible, it also has been found to be adequate. One could argue that more energy groups or a higher-order approximation to the angular dependence of the neutron flux (i.e., a more rigorous approximation to the transport equation than diffusion theory) might improve the rigor of the methodology. However, since there is an interest in making the transient analysis compatible with steady-state core calculations and since there is no direct evidence that these higher-order methods give more accurate results for two-group diffusion theory and should continue to be the standard approach.

Six delayed neutron precursor groups are the standard for treating LWRs, and no change should be made in this area either. However, it should be noted that these properties should be defined for each computational cell throughout the core. Although this is the practice in some state-of-the-art codes, some transient codes currently use global averages for the delayed neutron parameters.

Computer codes such as NESTLE solves a few-group neutron diffusion equations utilizing the nodal expansion method (NEM) for eigenvalue adjoint and fixed source steady-state and transient problems.

The NESTLE code can solve the eigenvalue (criticality), eigenvalue adjoint, external fixed source steady-state, and external fixed source or eigenvalue-initiated transient problems. The eigenvalue problem allows criticality searches to be completed, and the external fixed source steady-state problem can search to achieve a specified power level. Transient problems model delayed neutrons via precursor groups. Several core properties can be input as time dependent. Two- or four-energy groups can be utilized, with all energy groups being thermal groups (i.e., upscatter exists) if desired. Core geometries modeled include Cartesian and hexagonal. Three-, two-, and one-dimensional models can be utilized with various symmetries. The thermal conditions predicted by the thermal–hydraulic model of the core are used to correct cross sections for temperature and density effects. Cross sections are parameterized by color, control rod state (i.e., in or out), and burnup, allowing fuel depletion to be modeled. Either a macroscopic or a microscopic model may be employed.

The nonlinear iterative strategy associated with the NEM method is employed. An advantage of the nonlinear iterative strategy is that NESTLE can be utilized to solve either the nodal or finite difference method representation of the few-group neutron diffusion equation. Thermal–hydraulic feedback is modeled employing a homogeneous equilibrium mixture (HEM) model, which allows the two-phase flow to be treated. However, only the continuity and energy equations for the coolant are solved, so they are implying a constant pressure treatment.

The slip is assumed to be one in the HEM model. A lumped parameter model is employed to determine the fuel temperature. Decay heat groups are used to model decay heat. All cross sections are expressed in terms of Taylor's series expansion in coolant density, coolant temperature, effective fuel temperature, and soluble poison number density.

Note that this does not preclude the use of point kinetics models when the neutronic response of the core is not of primary importance. A code which models the nuclear steam supply system (NSSS) should have the ability to use point kinetics with parameters supplied by the user or calculated from the three-dimensional neutronics model—an approach not conducive to automation. One aspect of the point model mat is easy to relate to the multidimensional core model.

The equations are to be solved in three dimensions using rectangular or hexagonal geometry. Multidimensional kinetics should be equated with three-dimensional kinetics for the simple reason that there is no need to consider one-dimensional or two-dimensional models. The latter two approximations are only applicable for certain transients when there is separation between the axial and radial changes during a transient. Furthermore, both of these approximations require considerable analysis in order to obtain nuclear data that have been properly averaged over the remaining dimensions (e.g., over the radial plane when the axial direction is explicitly modeled). This complicates the analysis and negates any simplification that might result from using a lower-order spatial representation. Hence, it has became well established that only three-dimensional methods are of interest.

The treatment of multidimensional systems, other than the spherical geometry, is an important topic since reactor systems normally have finite cylinder geometry. Two approaches are possible: numerical methods and, in the simplest case, the separation of variable method that can be used for homogeneous systems. The method of separation of variables is then used to study the criticality and the flux distribution for the parallelepiped reactor geometry, of which the cube is a special case, and the finite cylinder reactor core, which is the geometric configuration of most existing nuclear power reactors.

Hence, in the following content of this section, we deal with this kind of geometry for reactor core and show the related analysis using the separation of variable method, as well as taking orthogonal and orthonormal functions under consideration where we are going to use their advantages.

First, we look at two simple functions $\phi_m(x)$ and $\phi_n(x)$ which are said to be orthogonal over an interval $[a, b]$ if the integral of the product of two functions over that interval vanishes where it can be seen mathematically as

$$\int_a^b \phi_m(x)\phi_n(x)dx = 0 \tag{3.194}$$

Or generally speaking, the two functions $\phi_m(x)$ and $\phi_n(x)$ are said to be orthogonal with respect to a weighting function $r(x)$, over an interval $[a, b]$ if the following equation is satisfied.

$$\int_a^b r(x)\phi_m(x)\phi_n(x)dx = 0 \tag{3.195}$$

So in summary, a set of functions is said to be orthogonal in interval $[a, b]$ if all pairs of distinct functions in the set are orthogonal in same interval $[a, b]$.

In the previous section we fairly discussed the eigenvalues and eigenfunction solution of general one-dimensional differential equation of form such as Eq. 3.182, and now we write the same equation in the following form to later on match it with our separation of variable method of solving these types of ordinary differential equations. Hence, as an application of one-dimensional problem, we can write

$$\frac{d^2X(x)}{dx^2} + \alpha^2 X(x) = 0 \tag{3.196}$$

with the boundary conditions such as 00 in the form of $X(0) = X(a) = 0$ having the eigenvalues or characteristic values of

$$\alpha_n^2 = \left(\frac{n\pi}{\alpha}\right)^2 \tag{3.197}$$

with corresponding characteristic functions or eigenfunctions of the following form:

$$X_n(x) = \sin\left(\frac{n\pi x}{\alpha}\right) \tag{3.198}$$

where in this case the weighting function $r(x) = 1$; thus, it follows the orthogonality of the following form:

$$\int_0^a X_m(x)X_n(x)dx = \int_0^a \sin\left(\frac{m\pi x}{a}\right)\sin\left(\frac{n\pi x}{a}\right)dx = 0 \quad \text{for} \quad m \neq n \tag{3.199}$$

where m and n are positive integers, and the weighted integral of the square of characteristic function $\varphi_n(x)$ has a positive numerical value as follows:

$$C_n = \int_a^b r(x)[\varphi_n(x)]^2 dx \tag{3.200}$$

If the arbitrary multiplicative factor involved in the definition of $\varphi_n(x)$ is so chosen that this integral has the value unity, the function $\varphi_n(x)$ is said to be normalized with respect to the weighting function $r(x)$; hence, a set of normalized orthogonal functions is said to be orthonormal.

By direct integration of Eq. 3.200, we get the following:

$$C_n = \int_0^a X_n^2(x)dx = \int_0^a \sin^2\left(\frac{n\pi x}{a}\right)dx = \frac{a}{2} \tag{3.201}$$

Thus in order to normalize the functions $\sin(n\pi x/a)$ over the interval [0, a], we would divide them by the normalizing factor $\sqrt{a/2}$, and the set of eigenfunction will yield as

$$X_n(x) = \sqrt{\frac{a}{2}\sin\left(\frac{n\pi x}{a}\right)} \tag{3.202}$$

Equation 3.202 is an orthonormal set in the interval [0, a].

3.12.1 The Unreflected Reactor Parallelepiped Core

The unreflected reactor parallelepiped core geometry configuration as depicted in Fig. 3.20 is the simplest possible model of a nuclear fission reactor, where a reflector is not used and the coordinate axes are $2a$, $2b$, and $2c$, respectively. The diffusion equation to be solved is the eigenvalue equation of the following form:

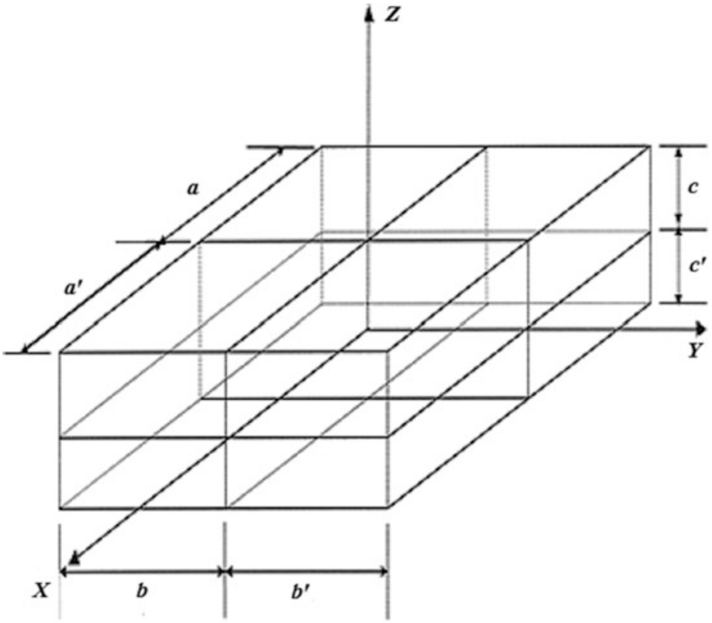

Fig. 3.20 Unreflected or bare parallelepiped reactor core

$$\frac{\partial^2\phi(x,y,z)}{\partial x^2}+\frac{\partial^2\phi(x,y,z)}{\partial y^2}+\frac{\partial^2\phi(x,y,z)}{\partial z^2}+B_{\mathrm{g}}^2\phi(x,y,z)=0 \tag{3.203}$$

The boundary conditions associated with this partial differential equation are in form of

$$\phi(\pm a,y,z)=\phi(x,\pm b,z)=\phi(x,y,\pm c)=0 \tag{3.204}$$

To solve the partial differential Eq. 3.203 via the separation of variable methods assuming the equation

$$\phi(x,y,z)=X(x)Y(y)Z(z) \tag{3.205}$$

and substituting Eq. 3.205 with Eq. 3.203 will yield

$$Y(y)Z(z)\frac{\partial^2X(x)}{\partial x^2}+X(x)Z(z)\frac{\partial^2Y(y)}{\partial y^2}+X(x)Y(y)\frac{\partial^2Z(z)}{\partial z^2}+B_{\mathrm{g}}^2X(x)Y(y)Z(z)=0 \tag{3.206}$$

Or simply we can write Eq. 3.206 as

$$YZ\frac{\partial^2 X}{\partial x^2}+XZ\frac{\partial^2 Y}{\partial y^2}+XY\frac{\partial^2 Z}{\partial z^2}+B_{\mathrm{b}}^2 XYZ=0 \tag{3.207}$$

We should replace the partial derivatives by total derivatives. Dividing by XYZ yields

$$\frac{1}{X}\frac{d^2X}{dx^2}+\frac{1}{Y}\frac{d^2Y}{dy^2}+\frac{1}{Z}\frac{d^2Z}{dz^2}=-B_{\mathrm{g}}^2 \tag{3.208}$$

Each term must be separately equal to a constant if it is to hold for all allowed values of x, y, z. This results in three ordinary rather than partial differential equations:

$$\begin{cases}\dfrac{1}{X}\dfrac{d^2X}{dx^2}=-\alpha^2\\ \dfrac{1}{Y}\dfrac{d^2Y}{dy^2}=-\beta^2\\ \dfrac{1}{Z}\dfrac{d^2Z}{dz^2}=-\gamma^2\end{cases} \tag{3.209}$$

With the condition

$$\alpha^2+\beta^2+\gamma^2=B_{\mathrm{g}}^2 \tag{3.210}$$

Considering the first ordinary second-order differential equation in variable x:

$$\frac{d^2X(x)}{dx^2}=-\alpha^2 X(x) \tag{3.211}$$

Equation 3.211 is known to have the solution of the following form as we have seen in the previous section.

$$X(x)=A\cos(\alpha x)+C\sin(\alpha x) \tag{3.212}$$

Note again in Eq. 3.211, we purposely have not used the constant, since it has a special meaning in the reactor theory and it is usually reserved for that purpose as demonstrated in Eq. 3.104.

Applying the boundary condition $X(\pm a)=0$ enforces that

$$A\cos(\alpha a)\pm C\sin(\alpha a)=0 \tag{3.213}$$

Since we are not interested in the trivial solution $A=C=0$, this can be satisfied if

$$C = 0 \rightarrow \alpha a = \frac{n\pi}{2} \quad \text{for all } n \text{ odd}$$

Or by

$$A = 0 \rightarrow \alpha a = \frac{n\pi}{2} \quad \text{for all } n \text{ even}$$

Therefore

$$\alpha^2 = \left(\frac{n\pi}{2a}\right)^2 \tag{3.214}$$

The even and odd solutions can be taken as members of the normalized set:

$$\begin{aligned} X_n(x) &= \frac{1}{\sqrt{a}} \cos\left(\frac{n\pi x}{2a}\right) \quad \text{for all } n \text{ odd} \\ X_n(x) &= \frac{1}{\sqrt{a}} \sin\left(\frac{n\pi x}{2a}\right) \quad \text{for all } n \text{ even} \end{aligned} \tag{3.215}$$

Similarly, for the variables y and z cases, we can write the following results:

$$\begin{aligned} Y_p(y) &= \frac{1}{\sqrt{b}} \cos\left(\frac{p\pi x}{2b}\right) \quad \text{for all } p \text{ odd} \\ Y_p(y) &= \frac{1}{\sqrt{b}} \sin\left(\frac{p\pi x}{2b}\right) \quad \text{for all } p \text{ even} \end{aligned} \tag{3.216}$$

Therefore

$$\beta^2 = \left(\frac{p\pi}{2b}\right)^2 \tag{3.217}$$

and

$$\begin{aligned} Z_q(z) &= \frac{1}{\sqrt{c}} \cos\left(\frac{q\pi z}{2c}\right) \quad \text{for all } q \text{ odd} \\ Z_q(z) &= \frac{1}{\sqrt{c}} \sin\left(\frac{q\pi z}{2c}\right) \quad \text{for all } q \text{ even} \end{aligned} \tag{3.218}$$

Therefore

$$\gamma^2 = \left(\frac{q\pi}{2c}\right)^2 \tag{3.219}$$

The geometric buckling is the sum of the $B^2_{\mathrm{g}(npq)}$ given by Eqs. 3.214, 3.217, and 3.219, which matches what we expressed in Eq. 3.104:

$$B^2_{\mathrm{g}(npq)} = \left(\frac{n\pi}{2a}\right)^2 + \left(\frac{p\pi}{2b}\right)^2 + \left(\frac{q\pi}{2c}\right)^2 \tag{3.220}$$

and the corresponding eigenfunction solution is

$$\phi_{npq}(x,y,z) = X_n(x)Y_p(y)Z_q(z) \tag{3.221}$$

The only choice of n, p, and q which gives a nonnegative flux over the whole core is

$$n = p = q = 1 \tag{3.222}$$

Thus for a solution, we use

$$B^2_{\mathrm{g}} = B^2_{\mathrm{g}(1,1,1)} = \left(\frac{\pi}{2a}\right)^2 + \left(\frac{\pi}{2b}\right)^2 + \left(\frac{\pi}{2c}\right)^2 \tag{3.223}$$

Since B^2_{g} is fixed by the medium, there are many choices of the dimensions of the medium to reach criticality, but these dimensions much satisfy the condition presented in Eq. 3.223.

Finally, the solution for the critical system from Eqs. 3.215, 3.216, 3.218, and 3.221 becomes

$$\phi(x,y,z) = A\phi_{111}(x) = A\frac{1}{\sqrt{abc}}\cos\left(\frac{\pi x}{2a}\right)\cos\left(\frac{\pi y}{2b}\right)\cos\left(\frac{\pi z}{2c}\right) \tag{3.224}$$

3.12.2 The Minimum Volume of the Critical Parallelepiped

Let us minimize the volume V of the parallelepiped as below subject to the condition presented in Eq. 3.223:

$$V = 8abc \tag{3.225}$$

To introduce the constraint, let us solve for one of the dimensions in terms of B_{g} and the other two dimensions:

$$a' = a + d = \left[\left(\frac{2B_{\mathrm{g}}}{\pi}\right)^2 - \frac{1}{b^2} - \frac{1}{c^2}\right]^{-\frac{1}{2}} \tag{3.226}$$

where d is the extrapolation distance. On substitution for "a" into the expression of volume V given in Eq. 3.225, we get

$$V=8\left\{\left[\left(\frac{2B_{\mathrm{g}}}{\pi}\right)^2-\frac{1}{(b+d)^2}-\frac{1}{(c+d)^2}\right]-d\right\}\cdot bc \tag{3.227}$$

The minimization is processed by setting

$$\frac{\partial V}{\partial b}=\frac{\partial V}{\partial c}=0 \tag{3.228}$$

This results in two equation in the two unknown b and c:

$$\begin{aligned}\frac{\partial V}{\partial b}=8c&\left\{\left[\left(\frac{2B_{\mathrm{g}}}{\pi}\right)^2-\frac{1}{(b+d)^2}-\frac{1}{(c+d)^2}\right]^{-\frac{1}{2}}-d\right\}\\&-\frac{8cb}{(b+d)^3}\left(\frac{1}{2}\right)(2)\left[\left(\frac{2B_{\mathrm{g}}}{\pi}\right)^2-\frac{1}{(b+d)^2}-\frac{1}{(c+d)^2}\right]^{\frac{3}{2}}=0\end{aligned} \tag{3.229}$$

$$\begin{aligned}\frac{\partial V}{\partial c}=8b&\left\{\left[\left(\frac{2B_{\mathrm{g}}}{\pi}\right)^2-\frac{1}{(b+d)^2}-\frac{1}{(c+d)^2}\right]^{-\frac{1}{2}}-d\right\}\\&-\frac{8cb}{(c+d)^3}\left(\frac{1}{2}\right)(2)\left[\left(\frac{2B_{\mathrm{g}}}{\pi}\right)^2-\frac{1}{(b+d)^2}-\frac{1}{(c+d)^2}\right]^{\frac{3}{2}}=0\end{aligned} \tag{3.230}$$

Using Eq. 3.226 and applying the above two equations will yield the following result:

$$\begin{aligned}a&=\frac{b}{(b+d)^3}(a+d)^3\\a&=\frac{c}{(c+d)^3}(a+d)^3\end{aligned} \tag{3.231}$$

Equating the two above expressions presented in Eq. 3.231 for a, we get

$$\frac{b}{(b+d)^3}=\frac{c}{(c+d)^3} \tag{3.232}$$

Equation 3.141 implies that

$$b=c \tag{3.233}$$

If we would have started by eliminating b instead of a, we would have obtained $a=c$; thus, we can say that

$$a = b = c \tag{3.234}$$

The critical parallelepiped with minimum volume is found to be a cube with

$$a = b = c = \sqrt{3}\frac{\pi}{2B_{\mathrm{g}}} \tag{3.235}$$

3.12.3 The Peak-to-Average Flux Ratio

This is an important quantity for heat transfer and fuel management design considerations. This ratio should be as small as possible in order to make the heat generation and the fuel burnup as uniform as possible. Otherwise, larger cooling ducts or orifices must be used in the central parts of the reactor core, and shorter refueling and fuel shuffling times will ensue. However, the average flux is given by

$$\begin{aligned}\overline{\phi} &= \frac{A}{V}\int_{-c}^{+c}\int_{-b}^{+b}\int_{-a}^{+a}\cos\left(\frac{\pi x}{2a'}\right)\cos\left(\frac{\pi y}{2b'}\right)\cos\left(\frac{\pi z}{2c'}\right)dxdydz\\ &= A\cdot\left(\tfrac{2}{\pi}\right)^3\frac{a'b'c'}{8abc}\left[\sin\left(\frac{\pi x}{2a'}\right)\right]_{-a}^{a}\left[\sin\left(\frac{\pi y}{2b'}\right)\right]_{-b}^{b}\left[\sin\left(\frac{\pi z}{2c'}\right)\right]_{-c}^{c}\\ &= A\cdot\left(\tfrac{4}{\pi}\right)^3\frac{a'b'c'}{8abc}\left[\sin\left(\frac{\pi x}{2a'}\right)\right]\left[\sin\left(\frac{\pi y}{2b'}\right)\right]\left[\sin\left(\frac{\pi z}{2c'}\right)\right]\end{aligned} \tag{3.236}$$

Then the maximum flux is as follows:

$$\phi_{\max} = \phi(x = y = z = 0) = A \tag{3.237}$$

Thus, we can write

$$\frac{\phi_{\max}}{\phi} = \left(\frac{\pi}{2}\right)^3\frac{abc}{a'b'c'}\sqrt{\left[\sin\left(\frac{\pi a}{2a'}\right)\right]\left[\sin\left(\frac{\pi b}{2b'}\right)\right]\left[\sin\left(\frac{\pi c}{2c'}\right)\right]} \tag{3.238}$$

If d is small, then $a' \approx a$, $b' \approx b$, $c' \approx c$ and Eq. 3.146 becomes

$$\frac{\phi_{\max}}{\overline{\phi}} = \left(\frac{\pi}{2}\right)^3 \tag{3.239}$$

which is a quantity that is independent of the values of a, b, and c.

3.12.4 The Finite Height Cylindrical Core

This is the geometry adopted by most reactor nuclear power plants in today's fission reactors. In this case the equation to be solved is

$$\frac{1}{r}\frac{\partial}{\partial r}\left[r\frac{\partial\phi(r,z)}{\partial r}\right]+\frac{\partial^2\phi(r,z)}{\partial z^2}+B_{\mathrm{g}}^2\phi(r,z)=0 \tag{3.240}$$

Assume a separable solution of the form

$$\phi(r,z)=R(r)Z(z) \tag{3.241}$$

Substitution of Eq. 3.241 with Eq. 3.240 would yield

$$\frac{1}{R}\frac{1}{r}\frac{\partial}{\partial r}\left(r\frac{\partial R}{\partial r}\right)+\frac{1}{Z}\frac{\partial^2 Z}{\partial z^2}+B_{\mathrm{g}}^2=0 \tag{3.242}$$

In Eq. 3.242, each term must be a constant; therefore, we can conclude the following relationships:

$$\frac{1}{R}\frac{1}{r}\frac{d}{dr}\left(r\frac{\partial R}{\partial r}\right)=-\gamma^2 \tag{3.243}$$

$$\frac{1}{Z}\frac{d^2Z}{dz^2}=-\delta^2 \tag{3.244}$$

with the constraint of the following form:

$$\gamma^2+\delta^2=B_{\mathrm{g}}^2 \tag{3.245}$$

Equation 3.244 has a solution for $Z(z)$ as follows:

$$Z(z)=A\cos(\delta z)+C\sin(\delta z) \tag{3.246}$$

At the extrapolated height of the cylinder and then with the help from Fig. 3.21, we can write the following relationship:

$$Z\left(\pm\frac{h'}{2}\right)=A\cos\left(\frac{\delta h'}{2}\right)\pm C\sin\left(\frac{\delta h'}{2}\right)=0 \tag{3.247}$$

Because of the symmetry around $z=0$, the terms with C are ruled out; thus $C=0$, and we have

Fig. 3.21 The unreflected finite height cylindrical reactor core

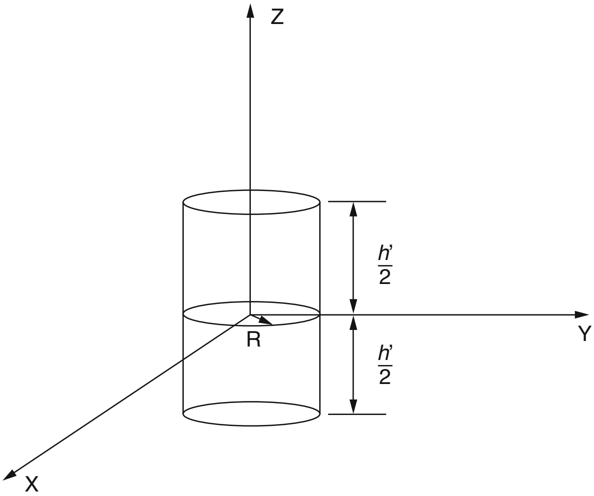

$$Z(z) = A\cos(\delta z) \tag{3.248}$$

and

$$\frac{\delta h'}{2} = \frac{n\pi}{2} \quad \text{for all} \quad n = 1, 2, 5, \cdots \quad \text{being odd} \tag{3.249}$$

or:

$$\delta^2 = \left(\frac{n\pi}{h'}\right)^2 \quad \text{for all } n \text{ odd} \tag{3.250}$$

The equation for R is then going to be

$$\frac{d^2R}{dr^2} + \frac{1}{r}\frac{dR}{dr} = -\gamma^2 R \tag{3.251}$$

which is a Bessel equation of order zero.

This equation derives its name from the German mathematician and astronomer Friedrich Bessel (1784–1846) who reported it while studying planetary motions. In modern engineering practice and analysis, it is encountered whenever cylindrical geometry arises.

The general form of the Bessel equation of order n, which is a variable coefficient equation, is written as

$$x^2\frac{d^2y}{dx^2} + x\frac{dy}{dx} + \left(x^2 - n^2\right)y = 0 \tag{3.252}$$

where n is a constant.

Equation 3.160 has a general solution as

$$y(x) = EJ_n(x) + FY_n(x) \tag{3.253}$$

where E and F are constants of integration to be determined by the boundary conditions and $J_n(x)$ is the Bessel function of the first kind of order n, while $Y_n(x)$ is the Bessel function of the second kind of order n which is also designated as the Neumann function.

If x is replaced by jx where $j = \sqrt{-1}$, Bessel's equation modifies into the form

$$x^2\frac{d^2y}{dx^2} + x\frac{dy}{dx} + \left(x^2 + n^2\right)y = 0 \tag{3.254}$$

This in turn has a general solution as

$$y(x) = E'I_n(x) + F'K_n(x) \tag{3.255}$$

where E' and F' are constants of integration to be determined by the boundary conditions and $I_n(x)$ is the modified Bessel function of the first kind of order n, while $K_n(x)$ is the modified Bessel of the second kind of order n.

The four Bessel functions of zero order are shown in Fig. 3.22 and are compared to the cos(x) function. It can be noticed that both $J_0(x)$ and $Y_0(x)$ are oscillatory. The distance between the roots, or the values at which the functions have a value of zero when they cross the x-axis, becomes larger and approaches the value of π as x increases. The amplitudes of these two functions decrease as x increases, and they are bounded and not infinite everywhere except for $Y_0(x)$ at $x = 0$, which reaches $-\infty$. It is of interest to note that the first root or zero of the function J_0 occurs at $x = 2.405$.

The two functions, $I_0(x)$ and $K_0(x)$, are non-oscillatory and unbounded, the former going to infinity at $x = \infty$ and the latter at $x = 0$.

Per our discussion so far, the general solution of Eq. 3.39 in terms of the Bessel functions of the first and second kind of zeroth order is

$$R(r) = EJ_0(\gamma r) + FY_0(\gamma r) \tag{3.256}$$

For the flux to be finite, $F = 0$, and thus Eq. 3.256 reduces to the following form:

$$R(r) = EL_0(\gamma r) \tag{3.257}$$

For the flux to vanish at the extrapolated $EJ_0(\gamma a') = 0$, we must have the following relation:

$$\gamma_p a' = j_{0,p} \quad \text{for all} \quad p = 1, 2, 3, \cdots \tag{3.258}$$

where $j_{0,p}$ is the argument at which J_0 becomes zero at the pth time.

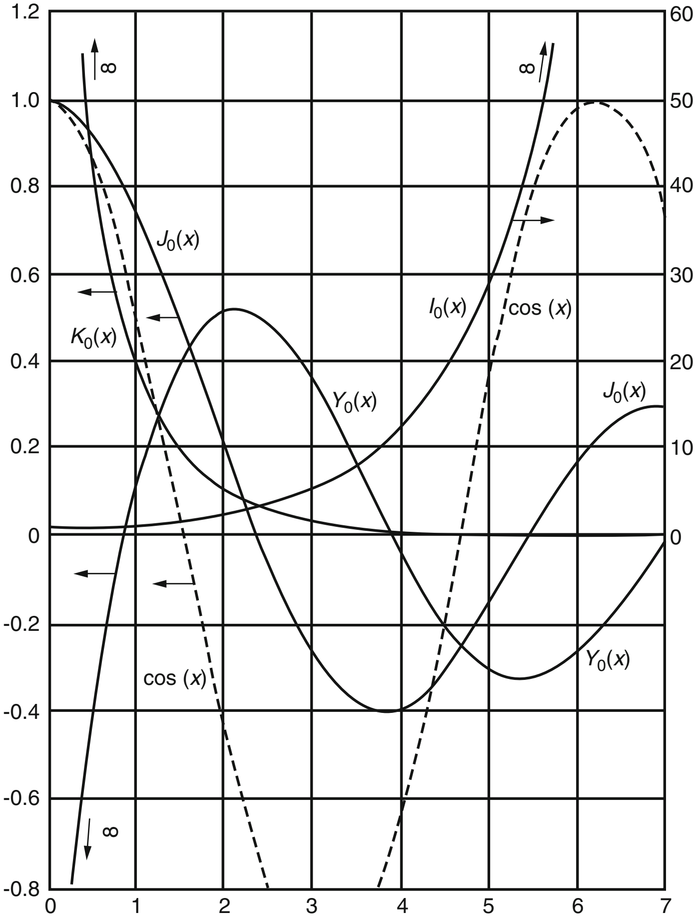

Fig. 3.22 Bessel functions of zero order compared with the cosine function

For the flux to remain positive, we only take $p = 1$ and, $j_{0,p} = 2.405$. Thus, we can write the following conclusion:

$$\gamma = \frac{2.405}{\alpha'} \tag{3.259}$$

and

$$R(r) = EJ_0\left(\frac{2.405}{a'}r\right) \tag{3.260}$$

Choosing also $n = 1$ in Eq. 3.250

$$\phi(r,z)=\phi_{\max}J_0\left(\frac{2.405}{a'}r\right)\cos\left(\frac{\pi z}{h'}\right) \tag{3.261}$$

where $\phi_{\max}$ is the flux at the origin.

However, the criticality conditions will be

$$B^2=\delta_1^2+\gamma_1^2=\left(\frac{\pi}{h'}\right)^2+\left(\frac{2.405}{a'}\right)^2 \tag{3.262}$$

The average flux is then given by

$$\begin{aligned}\overline{\phi}&=\frac{\phi_{\max}}{\pi a^2 h}\int_0^a\int_{-h/2}^{+h/2}\cos\left(\frac{\pi z}{h'}\right)J_0\left(\frac{2.405r}{a'}\right)\cdot(2\pi r dr dz)\\&=\frac{\phi_{\max}}{\pi a^2 h}\left[\frac{h'}{\pi}2\sin\left(\frac{\pi h}{2h'}\right)\right]\cdot\left[2\pi\left(\frac{a'}{2.405}\right)^2\left(\frac{2.405a}{a'}\right)J_1\left(\frac{2.405a}{a'}\right)\right]\end{aligned} \tag{3.263}$$

where $\int rJ_0(r)dr=rJ_1(r)$; thus, we can write the following equation:

$$\frac{\phi_{\max}}{\phi}=\sqrt{\left[\left(\frac{4}{2.405\pi}\right)\left(\frac{a'}{a}\right)\left(\frac{h'}{\pi}\right)J_1\left(\frac{2.405a}{a'}\right)\right]} \tag{3.264}$$

and for $a'\approx a$, $h'\approx h$, it becomes

$$\frac{\phi_{\max}}{\overline{\phi}}=\frac{2.405\pi}{4J_1(2.405)}\approx 1.15\pi \tag{3.265}$$

Table 3.1 shows all the geometric bucking and flux distribution in different nuclear reactor core geometries.

Table 3.1 Geometric bucking and flux distribution in different nuclear reactor core geometries

Reactor core shape	Geometric bucking	Flux distribution
Sphere radius *R*	$B_g^2=\left(\frac{\pi}{R}\right)^2$	$\phi(r)=A\left\{\frac{\sin\left(\frac{\pi r}{R}\right)}{\left(\frac{\pi r}{R}\right)}\right\}$
Rectangular parallelepiped with side lengths of *a*, *b*, and *c*	$B_g^2=\left(\frac{\pi}{a}\right)^2+\left(\frac{\pi}{b}\right)^2+\left(\frac{\pi}{c}\right)^2$	$\phi(x,y,z)=A\cos\left(\frac{\pi x}{a}\right)\cos\left(\frac{\pi y}{b}\right)\cos\left(\frac{\pi z}{c}\right)$
Cube side length of *a*	$B_g^2=3\left(\frac{\pi}{a}\right)^2$	$\phi(x,y,z)=A\cos\left(\frac{\pi x}{a}\right)\cos\left(\frac{\pi y}{a}\right)\cos\left(\frac{\pi z}{a}\right)$
Finite height cylinder radius *R* and height *H*	$B_g^2=\left(\frac{2.405}{R}\right)^2+\left(\frac{\pi}{H}\right)^2$	$\phi(x)=AJ_0\left(\frac{2.405r}{R}\right)\cos\left(\frac{\pi z}{H}\right)$
Semi-infinite cylinder radius *R*	$B_g^2=\left(\frac{2.405}{R}\right)^2$	$\phi(x)=AJ_0\left(\frac{2.405r}{R}\right)$
Semi-infinite slab thickness *a*	$B_g^2=\left(\frac{\pi}{a}\right)^2$	$\phi(x)=A\cos\left(\frac{\pi x}{a}\right)$

3.13 Relating *k* to the Criticality Condition

We have $-DB^2 - \Sigma_a + \nu\Sigma_f = 0$. Since there is uncertainty in the material parameters and since $\nu\Sigma_f$ is the dominant source of error, we introduce a fudge factor to ensure criticality:

$$-DB^2 - \Sigma_a + \frac{\nu\Sigma_f}{k_{\text{fudge}}} = 0 \tag{3.266}$$

Rearranging, we obtain

$$\frac{\nu\Sigma_f}{k_{\text{fudge}}} = DB^2 + \Sigma_a \Rightarrow k_{\text{fudge}} = \frac{\nu\Sigma_f}{\Sigma_a + DB^2} = \frac{\nu\Sigma_f/\Sigma_a}{1 + L^2B^2} \tag{3.267}$$

where $L^2 = D/\Sigma_a$ and Eq. 3.267 has the look of the four-factor formula with a leakage term after we manipulate the above equation a bit.

We can now write

$$k = k_\infty P_{\text{NL}} = p\eta f P_{\text{NL}} \tag{3.268}$$

Now,

$$1, p \sim 1 \quad \text{and} \quad \eta f = \frac{\nu\Sigma_f^{\text{final}}}{\Sigma_a^{\text{final}}} \frac{\Sigma_a^{\text{final}}}{\nu\Sigma_f^{\text{final}}} = \nu\Sigma_f/\Sigma_a \tag{3.269}$$

and

$$\begin{aligned} P_{\text{NL}} &= \frac{\int \Sigma_a \phi dV}{\int \Sigma_a \phi dV + \int \nabla \cdot \vec{J} dV} = \frac{\int \Sigma_a \phi dV}{\int \Sigma_a \phi dV - \int D\nabla^2 \phi dV} \\ &= \frac{\int \Sigma_a \phi dV}{\int \Sigma_a \phi dV - \int DB^2 \phi dV} \approx \frac{1}{1 + L^2B^2} \end{aligned} \tag{3.270}$$

So in Eq. 3.267, if we find that for a given size (i.e., B^2) and material properties $(D, \Sigma_a, \nu\Sigma_f)$ that k_{fudge} must be, say, 1.1 to make the model critical, this is equivalent that the multiplication factor $k = 1.1$, i.e., the arrangement is supercritical as specified and the $\nu\Sigma_f$ term must be reduced or downgraded to bring the reactor model to the critical state.

[Note that in the above equation, we used the relationship $D\nabla^2\phi(x) + DB^2\phi(x) = D\nabla^2\phi + DB^2\phi = 0$.]

3.14 Analytical Solution for the Transient Case for Reactor

We had the general one-speed neutron balance equation as

$$\frac{1}{v}\frac{\partial}{\partial t}\phi(\vec{\boldsymbol{r}},t) = \nabla\cdot D(\vec{\boldsymbol{r}})\nabla\phi(\vec{\boldsymbol{r}},t) - \Sigma_{\mathrm{a}}(\vec{\boldsymbol{r}})\phi(\vec{\boldsymbol{r}},t) + v\Sigma_{\mathrm{f}}(\vec{\boldsymbol{r}})\phi(\vec{\boldsymbol{r}},t) \tag{3.271}$$

For the homogeneous case in one-dimensional, we can write the following:

$$\frac{1}{v}\frac{\partial}{\partial t}\phi(x,t) = D\frac{\partial^2\phi(x,t)}{\partial x^2} - \Sigma_{\mathrm{a}}\phi(x,t) + v\Sigma_{\mathrm{f}}\phi(x,t) \tag{3.272}$$

Now, we will try to solve Eq. 3.272 by separation of variables; thus, we define $\phi(x,t)$ as

$$\phi(x,t) = X(x)T(t) \tag{3.273}$$

and substituting Eq. 3.273 with Eq. 3.272 and all the rearrangement as before, we get

$$\frac{1}{v}X\frac{\partial \mathrm{T}}{\partial t} = TD\frac{\partial^2 X}{\partial x^2} - \Sigma_{\mathrm{a}}XT + v\Sigma_{\mathrm{f}}XT \tag{3.274}$$

Or dividing Eq. 3.274 by XT yields

$$\frac{1}{v}\frac{\partial T}{\partial t} = \frac{v}{X}\left[D\frac{\partial^2 X}{\partial x^2} + (\Sigma_{\mathrm{f}} - \Sigma_{\mathrm{a}})X\right] \equiv -\lambda = \text{constant} \tag{3.275}$$

The left-hand side (LHS) of Eq. 3.275 is a function of T only and has a solution

$$T(t) = T(0)e^{-\lambda t} \tag{3.276}$$

while the right-hand side (RHS) of Eq. 3.275 is a function of X only and can be rewritten as

$$D\frac{\partial^2 X}{\partial x^2} + (v\Sigma_{\mathrm{f}} - \Sigma_{\mathrm{a}})X = -\frac{\lambda}{v}X = 0 \quad \text{when reactor is critical} \tag{3.277}$$

i.e.,

$$D\frac{\partial^2 X}{\partial x^2}+\left(\frac{\lambda}{v}+\nu\Sigma_{\mathrm{f}}-\Sigma_{\mathrm{a}}\right)X=0\Rightarrow\frac{\partial^2 X}{\partial x^2}+B^2X=0 \tag{3.278}$$

Thus,

$$\frac{\lambda}{v}+\nu\Sigma_{\mathrm{f}}-\Sigma_{\mathrm{a}}=DB^2\Rightarrow\lambda=v\left(\Sigma_{\mathrm{a}}+DB^2-\nu\Sigma_{\mathrm{f}}\right) \tag{3.279}$$

Now the flux goes to zero at the boundaries of the slab, $x=+\frac{a}{2}$, and we try a cosine solution:

$$X_n(x)=\cos\left(B_nx\right)\Rightarrow B_n^2=\left(\frac{\pi n}{a}\right)^2\quad\text{for all }\ n=1,3,5,\ \ldots \tag{3.280}$$

This is an eigenvalue problem and we see the eigenvalues as

$$\lambda\Rightarrow\lambda_n=v\left(\Sigma_{\mathrm{a}}+DB_n^2-\nu\Sigma_{\mathrm{f}}\right) \tag{3.281}$$

with the following eigenfunction and solution:

$$\phi(x,t)=\sum_{n\,\text{odd}}A_n\mathrm{e}^{-\lambda_nt}\cos\left(\frac{n\pi x}{a}\right) \tag{3.282}$$

where A_n is the amplitude function of the nth term. We use the initial flux and the orthogonal nature of the cosine function to determine A_n. The initial condition for $t=0$ then is presented as

$$\phi(x,0)=\sum_{n\ \text{odd}}A_n\cos\left(\frac{n\pi x}{a}\right) \tag{3.283}$$

We multiply both sides by $\cos\left(\frac{m\pi x}{a}\right)$ and integrate over the slab:

$$\begin{aligned}&\int_{-\frac{a}{2}}^{+\frac{a}{2}}\phi(x,0)\cos\left(\frac{m\pi x}{a}\right)dx\\&\quad=\sum_{n\ \text{odd}}\int_{-\frac{a}{2}}^{+\frac{a}{2}}A_n\mathrm{e}^{-\lambda_nt}\cos\left(\frac{n\pi x}{a}\right)\cos\left(\frac{m\pi x}{a}\right)dx\\&\quad=\frac{a}{2}A_m\end{aligned} \tag{3.284}$$

Therefore, we have

$$A_n = \frac{2}{a}\int_{-\frac{a}{2}}^{+\frac{a}{2}} \phi(x,0)\cos\left(\frac{n\pi x}{a}\right)dx \tag{3.285}$$

For long times of t, we can write the general solution as

$$\phi(x,t) \approx A_1 \mathrm{e}^{-\lambda_1 t}\cos\left(\frac{\pi x}{a}\right) = A_1 \mathrm{e}^{-\lambda_1 t}\cos B_1 x \tag{3.286}$$

Since **the higher-order modes (larger *n*) decay faster than the lower-order modes (low *n*)**, i.e.,

$$\lambda_1 < \lambda_2 < \lambda_3 < \cdots \tag{3.287}$$

Because

$$B_1^2 < B_2^2 < B_3^2 < \cdots \tag{3.288}$$

[Note that we ignore the even terms in the summation simply because they give nonzero terms at the boundaries, $x = \pm\frac{a}{2}$.]

3.15 Criticality

We had found $\lambda \Rightarrow \lambda_n = v\left(\Sigma_\mathrm{a} + DB_n^2 - \nu\Sigma_\mathrm{f}\right)$ for the transient case. We also found that the slowest decaying mode was that associated with the fundamental eigenvalue, λ_1. It follows that in the steady state

$$\lambda_1 = 0 = v\left(\Sigma_\mathrm{a} + DB_1^2 - \nu\Sigma_\mathrm{f}\right) \tag{3.289}$$

For example, only the fundamental cosine mode remains, and all the other higher-order modes have died away. Thus, we can write the following relationship:

$$B_1^2 = \underbrace{B_g^2}_{\text{geometric buckling}} = \underbrace{\frac{\nu\Sigma_\mathrm{f} - \Sigma_\mathrm{a}}{D}}_{\text{material buckling}} \tag{3.290}$$

To summarize the reactor criticality, we can write

$$\begin{array}{ll} B_{\mathrm{m}}^2 > B_{\mathrm{g}}^2 \Rightarrow \lambda_1 < 0 & \text{Supercritical} \\ B_{\mathrm{m}}^2 = B_{\mathrm{g}}^2 \Rightarrow \lambda_1 = 0 & \text{Critical} \\ \underbrace{B_{\mathrm{m}}^2}_{\text{fission source}} < \underbrace{B_{\mathrm{g}}^2}_{\text{leakage}} \Rightarrow \lambda_1 > 0 & \text{Subcritical} \end{array} \tag{3.291}$$

3.16 Bare Critical Reactor One-Group Model

Now consider the implications of the eigensolutions for the reactor design. For the slab reactor, we have

$$\hat{\Phi}_1(z) = \sin(Bz) \quad \text{and} \quad \hat{\Phi}_2(z) = \cos(Bz) \tag{3.292}$$

Note however that the spatial boundary conditions will determine the value of B^2. That is, for a given eigenfunction to solve the differential equation, it must

1. Replicate itself multiplied by a constant
2. Satisfy the boundary conditions imposed by the geometry

The boundary condition that we will use most often is that the flux goes to zero on the outer boundary of the reactor. In the slab case in z-direction, this means that the flux is 0.0 at $z = 0$ and at $z = H$, where H is the thickness of the slab. The natural eigenfunction for this case is the sin(Bz) eigenfunction as the sin function starts at zero, goes to a maximum, and then returns to zero when its argument reaches and the solution is always positive in between. (Frequently, this solution is referred to as a cosine function due to the placement of the origin at the center of the slab. All that is important is to remember that the solution must be symmetric about the center of the slab, and depending on where the origin is placed determines which function is used.) For the origin at the center of the slab, the equations are

$$\begin{gathered} \varphi(z) = A\hat{\Phi}_1(z) + C\hat{\Phi}_2(z) = A\sin(Bz) + C\cos(Bz) \\ \varphi\left(\frac{-H}{2}\right) = \varphi\left(\frac{H}{2}\right) = 0, \quad \text{therefore } A = 0 \text{ and } \quad \varphi(z) = C\cos(Bz) \\ B\cdot\frac{H}{2} = \frac{\pi}{2}, \quad \text{therefore} \quad B = \frac{\pi}{H} \end{gathered} \tag{3.293}$$

Now referring back to the one-group diffusion equation, we have

$$-\nabla^2\varphi(z) = \frac{\frac{1}{k}\upsilon\Sigma_{\mathrm{f}} - \Sigma_{\mathrm{a}}}{D}\varphi(z) = B^2\varphi(z) \tag{3.294}$$

So if

$$B^2 = \frac{\left(\frac{\nu\Sigma_\mathrm{f}}{k} - \Sigma_\mathrm{a}\right)}{D} \tag{3.295}$$

After dividing $\phi(z)$ out of both sides, this can be rewritten as

$$\begin{aligned} DB^2 &= \frac{\nu\Sigma_\mathrm{f}}{k} - \Sigma_\mathrm{a} \\ DB^2 + \Sigma_\mathrm{a} &= \frac{\nu\Sigma_\mathrm{f}}{k} \\ \frac{1}{k} &= \frac{\left(DB^2 + \Sigma_\mathrm{a}\right)}{\nu\Sigma_\mathrm{f}} \end{aligned} \tag{3.296}$$

Finally, mathematical manipulation gives the following:

$$k = \frac{\nu\Sigma_\mathrm{f}}{\left(DB^2 + \Sigma_\mathrm{a}\right)} \tag{3.297}$$

Now for the infinite reactor with one-group model, we have

$$k_\infty = \frac{\nu\Sigma_\mathrm{f}}{\Sigma_\mathrm{a}} \tag{3.298}$$

Therefore, the term DB^2 must represent a leakage effect. We can define

$$L^2 = D/\Sigma_\mathrm{a} = \text{Diffusion Area}, \quad \text{and} \quad L = \text{Diffusion Length} \tag{3.299}$$

and

$$k = \frac{\nu\Sigma_\mathrm{f}}{\Sigma_\mathrm{a}} \cdot \left(\frac{\Sigma_\mathrm{a}}{DB^2 + \Sigma_\mathrm{a}}\right) = \frac{\nu\Sigma_\mathrm{f}}{\Sigma_\mathrm{a}} \cdot \left(\frac{1}{1 + L^2B^2}\right)$$

and finally we can write

$$k = \frac{\nu\Sigma_\mathrm{f}}{\Sigma_\mathrm{a}} \cdot P_\mathrm{NL} \Rightarrow P_\mathrm{NL} = \frac{1}{\left(1 + L^2B^2\right)} \tag{3.300}$$

Therefore, we can express that

$$k_{\mathrm{eff}} = k_{\infty} \cdot P_{\mathrm{NL}} = k \cdot \frac{1}{\left(1 + L^2 B^2\right)}$$

where

$P_{\mathrm{NL}} =$ non-leakage probability

This leads to the traditional two design questions that are asked of most reactor neutronics calculations

1. How close to critical is a given geometry and configuration? (k?)
2. What is the required geometry for criticality? (B^2?)

Consider an example problem. The following one-group constants are appropriate for a fast, liquid metal-cooled core.

$$\begin{aligned}
\Sigma_{\mathrm{a}} &= 0.004154\,\mathrm{cm}^{-1} \\
\nu\Sigma_{\mathrm{f}} &= 0.006007\,\mathrm{cm}^{-1} \\
3\Sigma_{\mathrm{tr}} &= 0.68493\,\mathrm{cm}^{-1}, \quad \text{and} \quad D = 1.4599\,\mathrm{cm} \\
k &= \frac{\nu\Sigma_{\mathrm{f}}}{\Sigma_{\mathrm{a}}} = (0.006007)/(0.004254) = 1.45
\end{aligned}$$

Now consider an infinite slab that is 200 cm thick.

$$\begin{aligned}
B &= \pi/200 = 0.015708 \\
B^2 &= 0.000247 \\
DB^2 &= 0.000360 \\
DB^2 + \Sigma_{\mathrm{a}} &= 0.004514 \\
k_{\mathrm{eff}} &= \frac{\nu\Sigma_{\mathrm{f}}}{\left(DB^2 + \Sigma_{\mathrm{a}}\right)} = (0.006007)/(0.004514) = 1.33
\end{aligned}$$

However, 200 cm is still too thick for criticality. Therefore, let us calculate the exact width required for criticality.

$$\begin{aligned}
k_{\mathrm{eff}} &= 1.0 = \nu\Sigma_{\mathrm{f}}/\left(DB^2 + \Sigma_{\mathrm{a}}\right) \\
\left(DB^2 + \Sigma_{\mathrm{a}}\right) &= \nu\Sigma_{\mathrm{f}}
\end{aligned}$$

Thus, we can write the following result as

$$B^2 = (\nu\Sigma_{\mathrm{f}} - \Sigma_{\mathrm{a}})/D \tag{3.301}$$

$$B^2 = (0.006007 - 0.004154)/(1.4599)$$

$$B^2 = 0.001269$$

$$B = 0.035626$$

$$H = (\pi/B) = 88.18\,\text{cm}$$

For this case with one group and one medium, we can calculate an analytic solution for the thickness required to achieve criticality. When the problem gets more complicated, we will still want to ask the question, "How thick should the reactor be to achieve criticality?" In this case, we will answer the question with an implicit approach. We will choose a set of sizes covering the range required for criticality and interpolate between values on either side of $k_{\text{eff}} = 1.0$. Consider the following table for this problem.

H	B^2	k_{eff}
200	0.000247	1.330
150	0.000439	1.253
100	0.000987	1.0736
75	0.001755	0.8944
50	0.003948	0.6057

Note that the analytic value for $k_{\text{eff}} = 1.0$ falls between 75.0 and 100.0 cm as expected. The advantage of solving the problem implicitly is that only one computational scheme will be required to answer both design questions. It will become apparent why this is important as our study moves along.

3.17 Bare Critical Reactor One-Group Model: Finite Geometries

Of course, most reactors are not built as infinite slabs. The above example was provided just for simplicity. Consider how it would have to be modified if we were dealing with a finite reactor. We would have to write the diffusion equation in three dimensions as

$$-D\frac{\partial^2}{\partial x^2}\phi(x,y,z) - D\frac{\partial^2}{\partial y^2}\phi(x,y,z) - D\frac{\partial^2}{\partial z^2}\phi(x,y,z) + \Sigma_{\text{a}}\phi(x,y,z) = \frac{1}{k}\upsilon\Sigma_{\text{f}}\phi(x,y,z) \tag{3.302}$$

Now, if the x and y dimensions are each 200 cm and we want to find the z thickness that makes the reactor exactly critical as before, we can choose our origin at the geometric center of the reactor and assume a product form for the flux solution in the reactor. The assumed flux shape would be

$$\phi(x, y, z) = C \cos B_x x \cdot \cos B_y y \cdot \cos B_z z \tag{3.303}$$

Since the flux will have to go to zero on all boundaries and the x and y dimensions are 200 cm, we have

$$\begin{aligned} B_x &= \pi/200 \Rightarrow B_x^2 = 0.000247 \\ B_y &= \pi/200 \Rightarrow B_y^2 = 0.000247 \end{aligned} \tag{3.304}$$

Since these two dimensions are known, the values for B_x^2 and B_y^2 can be substituted back into the differential equation to get

$$+DB_x^2\phi(x, y, z) + DB_y^2\phi(x, y, z) - \frac{\partial^2}{\partial z^2}\phi(x, y, z) + \Sigma_\mathrm{a}\phi(x, y, z) = \frac{1}{k}\upsilon\Sigma_\mathrm{f}\phi(x, y, z) \tag{3.305}$$

Rewriting slightly gives

$$-\frac{\partial^2}{\partial z^2}\phi(x, y, z) + \left\{DB_x^2 + DB_y^2 + \Sigma_\mathrm{a}\right\}\phi(x, y, z) = \frac{1}{k}\upsilon\Sigma_\mathrm{f}\phi(x, y, z) \tag{3.306}$$

So that the leakage in the other two finite dimensions looks like an increase in absorption when the diffusion calculation is performed in the z-direction.

Now performing the differentiation with respect to z on the z dimension eigenfunction and then dividing out the flux eigenfunction from each term gives

$$DB_z^2 + \left\{DB_x^2 + DB_y^2 + \Sigma_\mathrm{a}\right\} = \frac{1}{k}\nu\Sigma_\mathrm{f} \tag{3.307}$$

Or

$$B_z^2 = \frac{\frac{1}{k}\nu\Sigma_\mathrm{f} - \Sigma_\mathrm{a} - \left\{DB_x^2 + DB_y^2\right\}}{D} = \frac{\frac{1}{k}\nu\Sigma_\mathrm{f} - \Sigma_\mathrm{a}}{D} - B_x^2 - B_y^2$$

Thus,

$$\begin{aligned} B^2 &= 0.001269 - 0.000494 = 0.000775 \\ H_z &= 112.8\,\mathrm{cm} \end{aligned}$$

The leakage in the two transverse dimensions required a thicker z dimension to compensate, as compared with the infinite slab.

3.18 Reflected Critical Reactors: One-Group Model

Now consider the same core material in a spherical assembly. The fundamental eigenfunction for the flux in a bare core is

$$\varphi(r) = A\frac{\sin Br}{r} \tag{3.308}$$

The cos(Br) eigenfunction does not show up because it is not bounded at the center of the sphere. The boundary condition at the outer surface requires that the flux goes to zero. This gives

$$BR = \pi, \quad \text{and} \quad B = \frac{\pi}{R} \tag{3.309}$$

Using the above value of B gives

$$B^2 = 0.001269\,\text{cm}^{-2} \quad \text{and} \quad R = 88.19\,\text{cm} \tag{3.310}$$

This corresponds to $2.873 \times 10^6\,\text{cm}^3$ of material. If this amount of material provides more than enough volume to transfer the heat produced by the fissile material to a working fluid, it is possible to reduce the size of the core by adding a reflector. The reflector will reduce the number of neutrons lost through leakage and therefore increase k_{eff} for a constant size. We will have the same one-group diffusion equation in the reflector, but the coefficients will be different. In fact for most "reflector" materials, fissile nuclides are not present. This gives the following diffusion equation:

$$\begin{aligned} &-D\nabla^2\phi(z) + \Sigma_a\phi(z) = 0 \\ &-\nabla^2\phi(z) = (\Sigma_a/D)\phi(z) \\ &\Sigma_a/D = 1/L^2 = 3\Sigma_{tr}\Sigma_a \end{aligned} \tag{3.311}$$

For example, consider one-group constants appropriate for a stainless steel reflector.

$$\begin{aligned} \Sigma_a &= 0.002963 \\ 3\Sigma_{tr} &= 1.4364 \quad D = 0.6962 \\ 1/L^2 &= \Sigma_a/D = (0.002963)/(0.6962) = 0.04256 \\ 1/L &= 0.06524 \\ L &= 15.33\,\text{cm} \end{aligned}$$

Now the differential equation is satisfied in both media, the core and the reflector, if the solutions use the constants derived from the cross sections in both media. All that remains is that the solutions satisfy the boundary conditions. We want to treat the interface between the core and reflector as a boundary condition rather than worrying about infinite derivatives as the solution jumps from the core to the reflector. This can be done if we require the physical quantities of interest to behave appropriately. At the interface, we must have continuity of the angular flux density. This means that each of the spatial coefficients in the expansion of the angular flux density in Legendre polynomials must be continuous across the interface. For the P_1 approximation, this means that $\phi_0(z)$ and $\phi_1(z)$ must be continuous across the interface. It is obvious how to apply the continuity equation to $\phi_0(z)$. To apply the continuity condition on $\phi_1(z)$, we have to refer back to the P_1 equation. We have

$$\phi_{1\mathrm{c}}(R_\mathrm{c}) = -D_\mathrm{c}\frac{\partial}{\partial R_\mathrm{c}}\phi(R_\mathrm{c}) = -D_\mathrm{R}\frac{\partial}{\partial R_\mathrm{c}}\phi(R_\mathrm{c}) = \phi_{1\mathrm{R}}(R_\mathrm{c}) \tag{3.312}$$

The general solution in the reflector is given by

$$\varphi_\mathrm{R}(r) = A_\mathrm{R}\frac{\mathrm{e}^{-r/L}}{r} + C_\mathrm{R}\mathrm{e}^{r/\frac{L}{r}} \tag{3.313}$$

3.19 Infinite Reflector Case

Consider first adding an infinite reflector. This will show the largest effect and assumes that the material of the reflector is much cheaper than the core material. For this case the increasing exponential must have zero coefficient ($C_R = 0$) to keep the solution finite. This leaves one function in each material. Applying the interface conditions at the core–reflector interface gives

1. **Continuity of Flux**

$$A_\mathrm{c}\frac{\sin BR_\mathrm{c}}{R_\mathrm{c}} = A_\mathrm{R}\frac{\mathrm{e}^{-R_\mathrm{c}/L}}{R_\mathrm{c}} \tag{3.314}$$

2. **Continuity of Current**

$$-D_\mathrm{c}A_\mathrm{c}\left(B\frac{\cos BR_\mathrm{c}}{R_\mathrm{c}} - \frac{\sin BR_\mathrm{c}}{R_\mathrm{c}^2}\right) = -D_\mathrm{r}A_\mathrm{R}\left(-\frac{1\mathrm{e}^{-R_\mathrm{c}/L}}{L\;R_\mathrm{c}} - \frac{\mathrm{e}^{-R_\mathrm{c}/L}}{R_\mathrm{c}^2}\right) \tag{3.315}$$

Dividing the flux equation into the current equation gives

$$-D_{\mathrm{c}}B\frac{\cos BR_{\mathrm{c}}}{\sin BR_{\mathrm{c}}}+\frac{D_{\mathrm{c}}}{R_{\mathrm{c}}}=\frac{D_{\mathrm{r}}}{L}+\frac{D_{\mathrm{r}}}{R_{\mathrm{c}}} \tag{3.316}$$

or

$$\tan BR_{\mathrm{c}}=\frac{BR_{\mathrm{c}}}{1-\frac{D_{\mathrm{r}}}{D_{\mathrm{c}}}\left(\frac{R_{\mathrm{c}}}{L}+1\right)} \tag{3.317}$$

This equation is a transcendental equation because the unknown R_{c} occurs on both sides of the equation. The easiest way to find an acceptable solution is to compute both sides of the equation for various values of the unknown R_{c} and find the value of R_{c} where both sides attain the same value.

Consider the following table

Core radius (cm)	Left-hand side	Right-hand side
80.0	−0.30006	−1.45005
70.0	−0.75670	−1.50736
60.0	−1.57131	−1.59122
55.0	−2.44225	−1.64962
59.0	−1.70228	−1.60179
59.8	−1.59631	−1.59329

This gives a core radius of about 59.8 cm which is a very significant reduction from the 88.19 cm of the bare core (or the 85.27 cm if the extrapolation distance is subtracted). The active core volume is only 31.2 % (34.5 %) of the bare core active volume.

Now consider the effect of a finite reflector. Choose the reflector thickness to be one diffusion length or about 15.33 cm. We now must solve for the coefficient of the rising exponential in the reflector based on the boundary condition at the outer surface. Setting the flux equal to zero at the outer boundary gives

$$\begin{aligned}\phi(R_{\mathrm{c}}+t_{\mathrm{c}})=0=A_{\mathrm{R}}\frac{\mathrm{e}^{-\frac{R_{\mathrm{c}}+t_{\mathrm{R}}}{L}}}{R_{\mathrm{c}}+t_{\mathrm{R}}}+C_{\mathrm{R}}\frac{\mathrm{e}^{\frac{R_{\mathrm{c}}+t_{\mathrm{R}}}{L}}}{R_{\mathrm{c}}+t_{\mathrm{R}}}\\ C_{\mathrm{R}}=-A_{\mathrm{R}}\mathrm{e}^{-\frac{2(R_{\mathrm{c}}+t_{\mathrm{R}})}{L}}=-\alpha A_{\mathrm{R}}\end{aligned} \tag{3.318}$$

Then at the core–reflector interface, the continuity of the flux gives

$$A_{\mathrm{C}}\frac{\sin BR_{\mathrm{C}}}{R_{\mathrm{C}}}=A_{\mathrm{R}}\left(\frac{\mathrm{e}^{-R_{\mathrm{C}}/L}}{R_{\mathrm{C}}}-\alpha\frac{\mathrm{e}^{R_{\mathrm{C}}/L}}{R_{\mathrm{C}}}\right) \tag{3.319}$$

And the continuity of the current gives

$$\begin{aligned}&-D_{\mathrm{C}}A_{\mathrm{C}}\left(B\frac{\cos BR_{\mathrm{C}}}{R_{\mathrm{C}}}-\frac{\sin BR_{\mathrm{C}}}{R_{\mathrm{C}}^2}\right)\\&=-D_{\mathrm{R}}A_{\mathrm{R}}\left\{-\frac{\mathrm{e}^{-R_{\mathrm{C}}/L}}{LR_{\mathrm{C}}}-\frac{\mathrm{e}^{R_{\mathrm{C}}/L}}{R_{\mathrm{C}}^2}-\alpha\left(\frac{\mathrm{e}^{R_{\mathrm{C}}/L}}{LR_{\mathrm{C}}}-\frac{\mathrm{e}^{R_{\mathrm{C}}/L}}{R_{\mathrm{C}}^2}\right)\right\}\end{aligned} \tag{3.320}$$

Or

$$D_{\mathrm{C}}A_{\mathrm{C}}\sin BR_{\mathrm{C}}(1-BR_{\mathrm{C}}ctnBR_{\mathrm{C}})=D_{\mathrm{R}}A_{\mathrm{R}}d^{-R_{\mathrm{C}}/L}\left\{1+\frac{R_C}{L}-\left(1-\frac{R_{\mathrm{C}}}{L}\right)\mathrm{e}^{-R_{\mathrm{C}}/L}\right\} \tag{3.321}$$

And the flux equation becomes

$$A_{\mathrm{C}}\sin BR_{\mathrm{C}}=A_{\mathrm{R}}\mathrm{e}^{-R_{\mathrm{C}}/L}\left(1-\mathrm{e}^{-2t_{\mathrm{R}}/L}\right) \tag{3.322}$$

Dividing the flux equation into the current equation gives

$$D_{\mathrm{C}}(1-BR_{\mathrm{C}}ctnBR_{\mathrm{C}})=D_{\mathrm{R}}\frac{\left\{1+\frac{R_{\mathrm{C}}}{L}-\left(1-\frac{R_{\mathrm{C}}}{L}\right)\mathrm{e}^{-2t_{\mathrm{R}}/L}\right\}}{\left\{1-\mathrm{e}^{-2t_{\mathrm{R}}/L}\right\}} \tag{3.323}$$

or

$$BR_{\mathrm{C}}ctnBR_{\mathrm{C}}=1-\frac{D_{\mathrm{R}}}{D_{\mathrm{C}}}\left\{\frac{1+\frac{R_{\mathrm{C}}}{L}-\left(1-\frac{R_{\mathrm{C}}}{L}\right)\mathrm{e}^{-2t_{\mathrm{R}}/L}}{1-\mathrm{e}^{-2t_{\mathrm{R}}/L}}\right\} \tag{3.324}$$

When this is solved for the core thickness with a one diffusion length thick reflector, the core radius comes out to be 65.0 cm. This corresponds to a reduction in volume for the core to 40 % of the bare core and is only 28.4 % greater than the infinite reflector core.

3.20 Criticality for General Bare Geometries

Consider the following equation:

$$\frac{1}{v}\frac{\partial}{\partial t}\phi(\vec{r},t)=\nabla\cdot D(\vec{r})\nabla\phi(\vec{r},t)-\Sigma_{\mathrm{a}}(\vec{r})\phi(\vec{r},t)+v\Sigma_{\mathrm{f}}(\vec{r})\phi(\vec{r},t) \tag{3.325}$$

In the steady state with homogeneous properties, we have

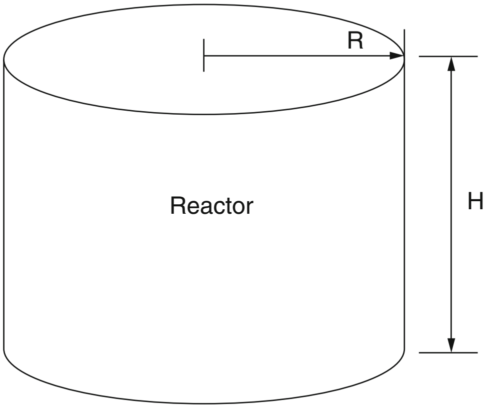

Fig. 3.23 Cylindrical reactor

$$\nabla^2\nabla\phi(\vec{\boldsymbol{r}},t)+\left(\frac{\nu\Sigma_{\mathrm{f}}(\vec{\boldsymbol{r}})-\Sigma_{\mathrm{a}}(\vec{\boldsymbol{r}})}{D(\vec{\boldsymbol{r}})}\right)\phi(\vec{\boldsymbol{r}},t)=0 \tag{3.326}$$

or

$$\nabla^2\nabla\phi(\vec{\boldsymbol{r}},t)+\underbrace{\left(\frac{k_\infty-1}{L^2}\right)}_{\equiv B^2}\phi(\vec{\boldsymbol{r}},t)=0 \quad \text{where} \quad L^2\equiv\frac{D}{\Sigma_{\mathrm{a}}} \quad \text{and} \quad k_\infty\equiv\frac{\nu\Sigma_{\mathrm{f}}}{\Sigma_{\mathrm{a}}} \tag{3.327}$$

The boundary condition is zero flux at the extrapolated boundary (surface):

$$\phi(\widetilde{\boldsymbol{r}}_{\mathrm{s}})=0 \tag{3.328}$$

Consider, for example, a reactor made in the shape of a right cylinder as shown in Fig. 3.23

The one-speed neutron balance equation is then given by

$$\frac{1}{r}\frac{\partial}{\partial r}\left(r\frac{\partial\phi(r,z)}{\partial r}\right)+\frac{\partial^2\phi(r,z)}{\partial z^2}+B^2\phi(r,z)=0 \tag{3.329}$$

with the boundary conditions that are given as

$$\begin{gathered}\phi\left(\widetilde{R},z\right)=0\\ \phi\left(r,\,\pm\widetilde{H}/2\right)\end{gathered} \tag{3.330}$$

We use the separation of variable methods as before and write

$$\phi(r,z)=R(r)Z(z) \tag{3.331}$$

Substituting Eq. 3.230 with Eq. 3.228, we obtain two sets of independent variables for r and z as follows:

$$\begin{aligned}&\frac{d}{dr}\left(r\frac{dR}{dr}\right)+\alpha^2R=0\\&\frac{d^2Z}{dr^2}+\lambda^2Z=0\end{aligned} \tag{3.332}$$

The solution to the radial equation is

$$R(r)=AJ_0(\alpha r)+CY_0(\alpha r) \tag{3.333}$$

The constant C must be 0, because $Y_0(\alpha r)\rightarrow\infty$ as $r\rightarrow 0$. Since the flux must go to zero at the extrapolated boundary, $\alpha=\frac{2.405}{\widetilde{R}}$, the first root of J_0.

The solution to the axial equation is also going to be

$$Z(z)=\cos(\lambda z) \tag{3.334}$$

where $\lambda^2=(\pi/H)^2$ since the flux goes to zero at the extrapolated boundaries. Thus, the full solution to Eq. 3.230 is given by

$$\phi(r,z)=AJ_0\left(\frac{2.405}{\widetilde{R}}r\right)\cos\left(\frac{\pi}{\widetilde{H}}z\right) \tag{3.335}$$

And as a result the criticality condition is

$$\underbrace{\left(\frac{2.405}{R}\right)^2+\left(\frac{\pi}{H}\right)^2}_{B_{\mathrm{g}}^2}=\underbrace{\frac{\nu\Sigma_{\mathrm{f}}-\Sigma_{\mathrm{a}}}{D}}_{B_{\mathrm{m}}^2} \tag{3.336}$$

3.21 Reflected Reactor Geometries

Now let us look at a slab reactor with a reflector on each side. As before, we can write the following as we have seen in Eq. 3.325:

$$\frac{1}{v}\frac{\partial}{\partial t}\phi(\vec{r},t)=\nabla\cdot D(\vec{r})\nabla\phi(\vec{r},t)-\Sigma_{\mathrm{a}}(\vec{r})\phi(\vec{r},t)+\nu\Sigma_{\mathrm{f}}(\vec{r})\phi(\vec{r},t) \tag{3.337}$$

Assuming again the steady-state, homogeneous properties within each region and one-dimensional case, we can write

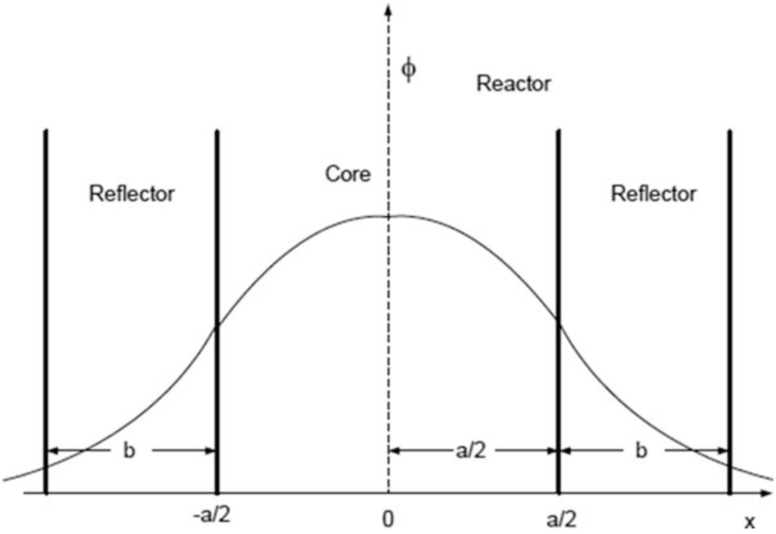

Fig. 3.24 Reflected slab reactor

$$D\frac{\partial^2\phi(x)}{\partial x^2}+(-\Sigma_\mathrm{a}+\nu\Sigma_\mathrm{f})\phi(x)=0 \tag{3.338}$$

This will apply to both the core region and the reflected region, as we can see in Fig. 3.24.

Governing equation of this problem is given by

$$\begin{array}{ll}\text{Core :} & D^\mathrm{C}\dfrac{d^2\phi^\mathrm{C}(x)}{dx^2}+\left(-\Sigma_\mathrm{a}^\mathrm{C}+\nu\Sigma_\mathrm{f}^\mathrm{C}\right)\phi^\mathrm{C}(x)=0\\ \text{Reflector} & D^\mathrm{R}\dfrac{d^2\phi^\mathrm{R}(x)}{dx^2}+-\Sigma_\mathrm{a}^\mathrm{R}\phi^\mathrm{R}(x)=0\end{array} \tag{3.339}$$

with the given boundary condition as

$$\begin{cases}\phi^\mathrm{R}\left(\dfrac{a}{2}+b\right)=0\\ \phi^\mathrm{C}\left(\dfrac{a}{2}\right)=\phi^\mathrm{R}\left(\dfrac{a}{2}\right)\\ J^\mathrm{C}\left(\dfrac{a}{2}\right)=J^\mathrm{R}\left(\dfrac{a}{2}\right)\\ \text{symmetry}\end{cases} \tag{3.340}$$

We will just solve for $x > 0$ since, by symmetry, the solution is the same for $x < 0$. We try

$$\phi^{\mathrm{C}}(x) = A^{\mathrm{C}} \cos\left(B_{\mathrm{m}}^{\mathrm{C}} x\right) \quad \text{where} \quad \left(B_{\mathrm{m}}^{\mathrm{C}}\right)^2 = \frac{\nu \Sigma_{\mathrm{f}}^{\mathrm{C}} - \Sigma_{\mathrm{a}}^{\mathrm{C}}}{D^{\mathrm{C}}} \tag{3.341}$$

and

$$\phi^{\mathrm{C}}(x) = A^{\mathrm{R}} \sinh\left[\frac{\frac{a}{2} + b - x}{L^{\mathrm{R}}}\right] \quad \text{where} \quad \left(L^{\mathrm{R}}\right)^2 = \frac{D^{\mathrm{R}}}{\Sigma_{\mathrm{a}}^{\mathrm{R}}} \tag{3.342}$$

And Eq. 3.342 is equal to 0 at $x = \frac{a}{2} + b$ since $\sinh(t) = \dfrac{\mathrm{e}^{+t} - \mathrm{e}^{+t}}{2}$.

Applying the boundary conditions given in Eq. 3.340 provides the following results:

$$\phi\,\text{equal at interface} \Rightarrow A^{\mathrm{C}} \cos\left(B_{\mathrm{m}}^{\mathrm{C}} x\right) = A^{\mathrm{R}} \sinh\left(\frac{b}{L^{\mathrm{R}}}\right) \tag{3.343}$$

$$J\,\text{equal at interface} \Rightarrow D^{\mathrm{C}} B_{\mathrm{m}}^{\mathrm{C}} A^{\mathrm{C}} \sin\left(\frac{B_{\mathrm{m}}^{\mathrm{C}} a}{2}\right) = \frac{D^{\mathrm{R}}}{L^{\mathrm{R}}} A^{\mathrm{R}} \cosh\left(\frac{b}{L^{\mathrm{R}}}\right) \tag{3.344}$$

We divide Eq. 3.350 by Eq. 3.349 to eliminate the unknown A coefficients to give the **criticality condition**

$$D^{\mathrm{C}} B_{\mathrm{m}}^{\mathrm{C}} \tan\left(\frac{B_{\mathrm{m}}^{\mathrm{C}} a}{2}\right) = \frac{D^{\mathrm{R}}}{L^{\mathrm{R}}} \coth\left(\frac{b}{L^{\mathrm{R}}}\right) \tag{3.345}$$

This relates the geometry of the reactor to the material properties of the reactor. To graphically illustrate this, we plot the LHS and the RHS against $\frac{B_{\mathrm{m}}^{\mathrm{C}} a}{2}$ shown in Fig. 3.25. Where the LHS and the RHS are equal, the reactor is critical. This occurs at multiple values of $\frac{B_{\mathrm{m}}^{\mathrm{C}} a}{2}$, but the lowest value (i.e., smallest core size, a) occurs at just less than $\pi/2$. If you recall, the bare reactor went critical at $B_{\mathrm{m}} = \pi/a$ or equally at $B_{\mathrm{m}} a/2 = \pi/2$. Thus, the core size for a reflected reactor is smaller than a non-reflected reactor, which resulted in a fuel "savings."

3.22 Reactor Criticality Calculations

As you no doubt noticed, any real reactor model would be too complex to be solved analytically. Therefore, we resort to numerical means.

You will recall that we had

$$\frac{1}{v} \frac{\partial}{\partial t} \phi(\vec{r}, t) = \nabla \cdot D(\vec{r}) \nabla \phi(\vec{r}, t) - \Sigma_{\mathrm{a}}(\vec{r}) \phi(\vec{r}, t) + \nu \Sigma_{\mathrm{f}} \phi(\vec{r}, t) \tag{3.346}$$

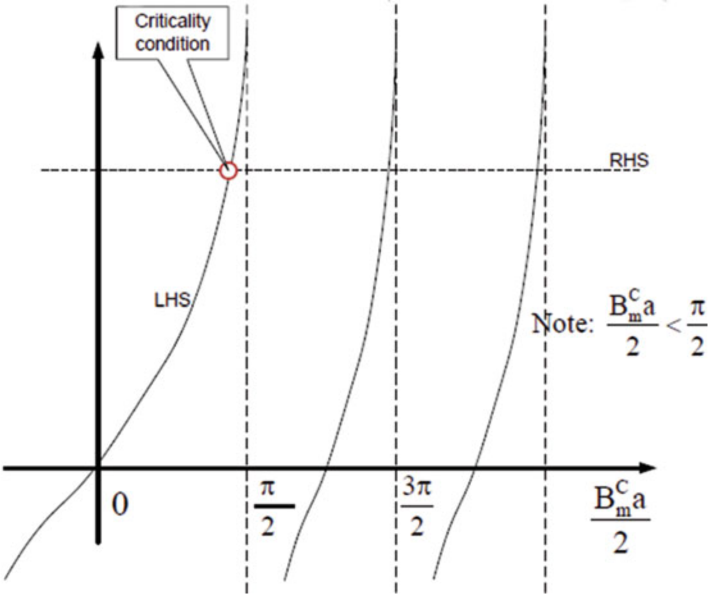

Fig. 3.25 Criticality for a reflected slab reactor

If we postulate that

$$\phi(x,t) = e^{\lambda t}\Psi(x) \tag{3.247}$$

then

$$\frac{\lambda}{v}\Psi(\vec{r},t) = \nabla \cdot D(\vec{r})\nabla\Psi(\vec{r}) - \Sigma_a(\vec{r})\Psi(\vec{r}) + \nu\Sigma_f(\vec{r})\Psi(\vec{r}) \tag{3.348}$$

and we get a steady-state solution when $\lambda = 0$. Therefore, the basic idea is to adjust the equation parameters until $\lambda = 0$. However, which parameters and how to adjust them are the questions.

Generally, you start with a *fixed* geometry and basic design, i.e., the materials are known. Thus, the free variable is the fuel, i.e., reactivity. Therefore, vary ν or, equally, introduce a fudge factor:

$$\begin{gathered} -\nabla \cdot D(\vec{r})\nabla\phi(\vec{r}) + \Sigma_a(\vec{r})\phi(\vec{r}) = \underbrace{\frac{\nu}{k}\Sigma_f(\vec{r})\phi(\vec{r})}_{\text{source term}} \\ \Downarrow \\ M\phi = \frac{1}{k}F\phi \end{gathered} \tag{3.349}$$

where M and F are operators and the fudge factor is k. If you rearrange the equation, solving for k as we did in Sect. 3.14 of this chapter, you will see that k takes on a form like the multiplication factor k that we introduced earlier. The k generated satisfies

$$k_{\text{fudge}} = \frac{\nu\Sigma_{\text{f}}/\Sigma_{\text{a}}}{1 + \underbrace{L^2B^2}_{\text{from the}\nabla\cdot D\nabla\phi\,\text{term}}} \tag{3.350}$$

The numerical algorithm for a fixed design is as follows:

1. Set up a spatial grid as we did for the fixed source case in *Reactor Physics: Numerical Methods*.
2. Guess $k^{(0)}$ and $\phi^{(0)}$ for the initial or zeroth iteration.
3. Calculate the source term $\frac{1}{k}F\phi^{(0)}$.
4. Solve as per the previous numerical methods (G-S, SOR, etc.) with this known source. This involves iteration on ϕ to get a converged spatial distribution of ϕ for this fixed source estimate. This generates $\phi^1(\vec{r})$. This is the **inner loop**. Note that this flux distribution is based on a guess of the source term which is a function of ϕ. Mathematically

$$\begin{aligned} &M\phi^{(1)} = \frac{1}{k^{(0)}}F\phi^{(0)} = \frac{S^{(0)}}{k^{(0)}} \Rightarrow \phi^{(1)} \\ &S^{(1)} = F\phi^{(1)} \end{aligned} \tag{3.351}$$

5. Now we need to update the source and the value of the fudge factor k. The source is easy—just recalculate $F\phi$ as per Eq. 3.349 or Eq. 3.351 using the latest flux values. But what about k? We'll see in a minute that $k^1 = k^0S^1/S^0$.
6. With an updated source term, we now recalculate the flux as above. This is the outer loop. The algorithm can be summarized as

$$\begin{aligned} &\text{Guess } \ \phi^{(0)} \ \text{ and } \ k^{(0)} \\ &[\text{outer loop}] \ \text{ on } \ i \\ &M\phi^{(i+1)} = \frac{1}{k^{(i)}}F\phi^{(i)} = \frac{S^{(i)}}{k^{(i)}} \Rightarrow \text{inner loop} \Rightarrow \phi^{(i+1)} \\ &\text{Update } \ S^{(i+1)} = F\phi^{(i+1)} \\ &\text{Updata } \ k^{(i+1)} = k^{(i)}S^{(i+1)}/S^{(i)} \\ &[\text{outer loop}] \ \text{ until flux converges} \end{aligned} \tag{3.352}$$

If we are clever, we can combine the inner and outer iterations by updating k and S every time we make an inner loop sweep. There is hardly any sense in converging the inner loop to a fine tolerance only to make big changes in the fudge factor and source term and then recompute the flux again to a fine tolerance. It is far better to update k and S as you go.

Now, on to how to update k. we note that

$$k \equiv \frac{\text{Fission sources}}{\text{Sinks}} = \frac{F\phi}{M\phi} \tag{3.353}$$

Thus

$$k \equiv \frac{\int_{\text{volume}} F\phi^{(i+1)} dV}{\int_{\text{volume}} M\phi^{(i+1)} dV} \tag{3.354}$$

However, in our procedure

$$M\phi^{(i+1)} = \frac{1}{k^{(1)}} F\phi^{(i)} = \frac{S^{(i)}}{k^{(i)}} \tag{3.355}$$

Therefore,

$$k^{(i+1)} \equiv \frac{\int_{\text{volume}} S^{(i+1)} dV}{\frac{1}{k^{(i)}} \int_{\text{volume}} S^{(i)} dV} \tag{3.356}$$

We can improve on this by looking ahead based on the past trend (extrapolation).

What does adjusting the k mean physically? Let us say that the converged value of k that you get for a particular case is 1.1. That means that the source term, $\nu\Sigma_{\mathrm{f}}(\vec{r})\phi(\vec{r})$, was too big, causing the reactor to be supercritical. To make the reactor critical, it had to be reduced by 10 %. Then and only then did the source and sink terms balance. Obviously, we could have made the reactor critical in a number of other ways, such as adjusting the absorption term or changing the size of the reactor. But since we typically start with a physical reactor of given (or proposed) dimensions and materials, it is convenient to control the criticality in the way we did. If you run into a case where it makes more sense to adjust another term, by all means, go for it. The overall procedure is similar, and it should work just as well. Just make sure that you are not attempting to find criticality by adjusting a term that is of little influence on the equation set. For instance, a control rod (absorber) at the very edge of a reactor sees few neutrons so it would be ineffective in affecting overall criticality. Use your common sense.

Problems

Problem 3.1 Assuming that the reactivity drop in dollars can be measured by taking the ratio of the neutrons immediately before or after the control rod insertion, given by the relationship

$$\frac{|\rho|}{\beta} = \frac{n_0}{n_1} - 1$$

where n_0 is the initial condition and n_1 is the final one, then consider that a critical reactor operates at a power level of 80 W. Dropping a control rod into the core causes the flux to undergo a sudden decrease to 60 W. How many dollars is the control rod worth?

Problem 3.2 An infinite, bare cylindrical reactor is critical with a cylindrical control rod along its axis.

1. Using one-group theory, derive expressions for the probability that a thermal neutron
   (a) Is absorbed by the rod
   (b) Escapes from the surface of the reactor
   (c) Is absorbed in the reactor core material
2. Show that the increase in the number of neutrons leaking/s from the surface due to the presence of the rod is comparable to the number of neutrons absorbed/s in the rod.

Solution:

I need to write a solution for this problem.

Problem 3.3 Using the integral rod worth curve plotted in following figure, find the reactivity inserted by moving the rod from 12 in. withdrawn out to 18 in. withdrawn.

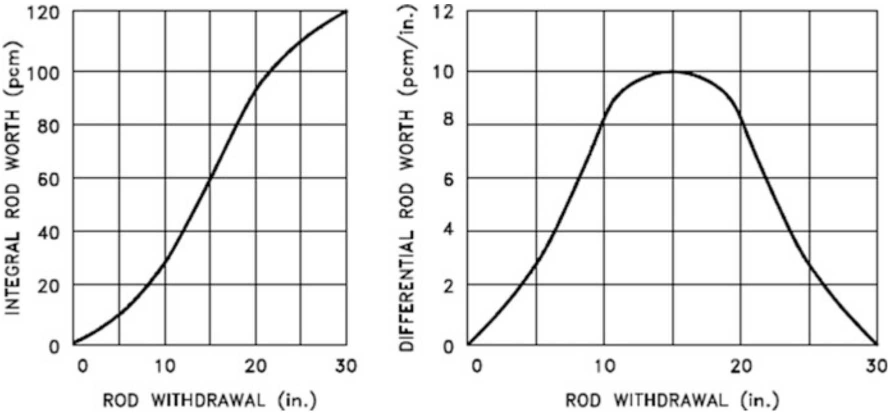

Fig. P3.3 Rod worth curves for Problem 3.3

Problem 3.4 Using the differential rod worth curve provided in the figure of Problem 3.3, calculate the reactivity inserted by moving the rod from 10 in. withdrawn to 6 in. withdrawn.

Problem 3.5 For the differential rod worth data given below, construct differential and integral rod worth curves.

Interval (in.)	Reactivity inserted (pcm)
0–2	10
2–4	20
4–6	40
6–8	60
8–10	60
10–12	40
12–14	20
14–16	10

Problem 3.6 Consider a thermal neutron density of $N = 10^8\ \text{cm}^{-3}$ in a graphite medium using the total cross section of $\Sigma_t = 0.385\ \text{cm}^{-1}$ and a corresponding neutron speed of 2.2×10^5 cm/s, find the reaction rate density.

Problem 3.7 Determine all solutions, if any, to the boundary value problem:

$$y'' + 9y = 0 \quad 0 < x < \pi \quad \text{with boundary conditions} \quad y(0) = 0 \ \text{and} \ y'(\pi) = -6$$

by first finding a general solution to the differential equation.

Problem 3.8 Determine all solutions, if any, to the boundary value problem:

$$y'' + 2y' + y = 0 \quad -1 < x < 1 \quad \text{with boundary conditions} \quad y(-1) = 0 \ \text{and} \ y(1) = 2$$

by first finding a general solution to the differential equation.

Problem 3.9 Find the eigenvalues and the corresponding eigenfunctions for the boundary value problem:

$$y'' + \lambda y = 0 \quad 0 < x < \pi \quad \text{with boundary conditions} \quad y'(0) = 0 \quad y(\pi) = 0.$$

Problem 3.10 Find the eigenvalues and the corresponding eigenfunctions for the boundary value problem:

$$y'' + \lambda y = 0 \quad 0 < x < \pi/2 \quad \text{with boundary conditions} \quad y'(0) = 0 \quad y(\pi/2) = 0$$

Problem 3.11 Find the eigenvalues and the corresponding eigenfunctions for the boundary value problem:

$$y'' - 2y' + \lambda y = 0 \quad 0 < x < \pi \quad \text{with boundary conditions} \quad y(0) = 0 \quad y(\pi) = 0$$

Problem 3.12 Find the eigenvalues and the corresponding eigenfunctions for the boundary value problem:

$$y'' + \lambda y = 0$$

with boundary values $y(0) = 0$ and $y(L) = 0$.

Problem 3.13 Find the eigenvalues and the corresponding eigenfunctions for the boundary value problem:

$$y'' + \lambda y = 0$$

with boundary values $y'(0) = 0$ and $y'(L) = 0$.

Problem 3.14 Find the eigenvalues and the corresponding eigenfunctions for the boundary value problem:

$$y'' + \lambda y = 0$$

with boundary values $y(0) = 0$ and $y'(L) = 0$.

Problem 3.15 Find the eigenvalues and eigenfunctions for the boundary value problem:

$$y'' + \lambda y = 0$$

with boundary values $y(L_1) = 0$ and $y(L_2) = 0$, where $L_2 > L_1 > 0$.

Problem 3.16 Find the eigenvalues and eigenfunctions for the boundary value problem:

$$y'' + \lambda y = 0$$

with boundary values $y(0) = y(L)$ and $y'(0) = y'(L)$.

Problem 3.17 Find the eigenvalues and eigenfunctions for the boundary value problem:

$$y'' + \lambda y = 0$$

with boundary values $y(0) = 0$ and $y(L) + y'(L) = 0$.

Problem 3.18 Find the eigenvalues and eigenfunctions for the boundary value problem:

$$y'' - \frac{2}{x}y' + \left(\lambda + \frac{2}{x^2}\right)y = 0$$

with boundary values $y(1) = 0$ and $y(2) = 0$.

Hint: Let $y = xu(x)$

Problem 3.19 Consider a uniform source as $S(x) = S_0$ in an infinite medium represented by differential equation of the following form:

$$\frac{d^2\phi(x)}{dx^2} - \frac{1}{L^2}\phi(x) = -\frac{S_0}{D}$$

with boundary conditions such that $\phi(x) < \infty$ as $x \rightarrow \pm\infty$. Find the solution for such equation.

Problem 3.20 We will try to determine the neutron flux resulting from an arbitrary distribution source in a finite slab of width a. This results in solving the following nonlinear differential equation:

$$\frac{d^2\phi(x)}{dx^2} - \frac{1}{L^2}\phi(x) = -\frac{S_0}{D} \qquad -\frac{a}{2} \leq x \leq \frac{a}{2}$$

subject to the vacuum boundary conditions as

$$\text{(a)} \quad \phi\left(\frac{\widetilde{a}}{2}\right) = 0$$
$$\text{(b)} \quad \phi\left(-\frac{\widetilde{a}}{2}\right) = 0$$

Hint: Since we have taken the source $S(x)$ to be arbitrary, we cannot assume symmetry to be in the range $0 \leq x \leq \widetilde{a}/2$.

Problem 3.21 Use Green's function to solve the following problem:

$$\frac{d^2y}{dx^2} + y = \operatorname{cosec}(x)$$

subject to the boundary conditions $y(0) = y(\pi/2) = 0$.

Hint: Green's function $G(x, z)$ must satisfy the original ordinary differential equation with the right-hand side (RHS) set equal to a *delta function* such as $£\{G(x, z)\} = \delta(x - z)$. Thus, $G(x, z)$ may be thought of physically as the response of a system to unit impulse at $x = z$.

Problem 3.22 Solve the heat flow problem

$$\begin{aligned} \frac{\partial u}{\partial t}(x, t) &= 3\frac{\partial^2 u}{\partial x^2}(x, t) && 0 < x < \pi \quad t < 0 \\ u(0, t) &= u(\pi, t) = 0 && t < 0 \\ u(x, 0) &= \sin 4x + 3\sin 6x - \sin 10x && 0 < x < \pi \end{aligned}$$

Problem 3.23 Show that if $u(x, t) = X(x)T(t)$ is a solution of the partial differential equation

$$\frac{\partial^2 u(x,t)}{\partial t^2} + \frac{\partial u(x,t)}{\partial t} + u(x,t) = \alpha^2 \frac{\partial^2 u(x,t)}{\partial x^2}$$

then $X(x)$ and $T(t)$ must satisfy the following ordinary differential equations:

$$\begin{aligned} X''(x) - \lambda X(x) &= 0 \\ T''(t) + T'(t) + (1 - \lambda\alpha^2)T(t) &= 0 \end{aligned}$$

where λ is a constant.

Problem 3.24 Show that if $u(r,\theta,z) = R(r)T(\theta)Z(z)$ is a solution of the partial differential equation

$$\frac{\partial^2 u}{\partial r^2} + \frac{1}{r}\frac{\partial u}{\partial r} + \frac{1}{r^2}\frac{\partial^2 u}{\partial \theta^2} + \frac{\partial^2 u}{\partial z^2} = 0$$

then $R(r)$, $T(\theta)$, and $Z(z)$ must satisfy the following ordinary differential equations:

$$\begin{aligned} T''(\theta) + \mu T(\theta) &= 0 \quad (1) \\ Z''(z) + \lambda Z(z) &= 0 \quad (2) \\ r^2 R''(r) + rR'(r) - (r^2\lambda + \mu)R(r) &= 0 \quad (3) \end{aligned}$$

where λ and μ are constants.

Problem 3.25 Problem of steady-state temperature in a rectangular plate (Laplace's equation) with two long sides and the far end at 0 and the base at 1000. See the figure below.

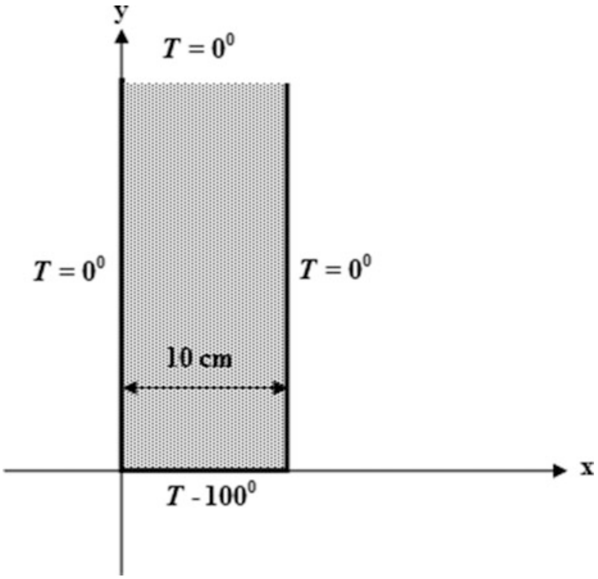

Fig. P3.25

The heat flow equation is given by

$$\begin{cases} \nabla^2 T(x,y) = 0 \\ \dfrac{\partial^2 T(x,y)}{\partial x^2} + \dfrac{\partial^2 T(x,y)}{\partial y^2} = 0 \end{cases}$$

Solve this problem for the boundary conditions associated with this problem as shown in the figure provided by finding the steady-state temperature distribution inside the plate.

Problem 3.26 Solve Problem 3.25 for a finite plate of height 30 cm with top edge at $T = 0^\circ$ and other dimensions and temperatures as given in the figure in Problem 3.25.

Problem 3.27 Problem of diffusion or heat flow equation in a bar or slab
The heat flow equation is given by

$$\nabla^2 u(x,y,z) = \frac{1}{\alpha^2}\frac{\partial u(x,y,z)}{\partial t} \tag{1}$$

where u is the temperature and α^2 is a constant characteristic of material through which the heat is flowing. Using separation methods, argue why the separation constant has to be chosen as $-k^2$?

Problem 3.28 Problem of steady-state temperature in a cylinder

Consider the following problem by finding the steady-state temperature distribution u in a semi-infinite solid cylinder (see the figure in Problem 3.28) of radius $r = 1$ if the base is held at 100° and the curved sides at 0°.

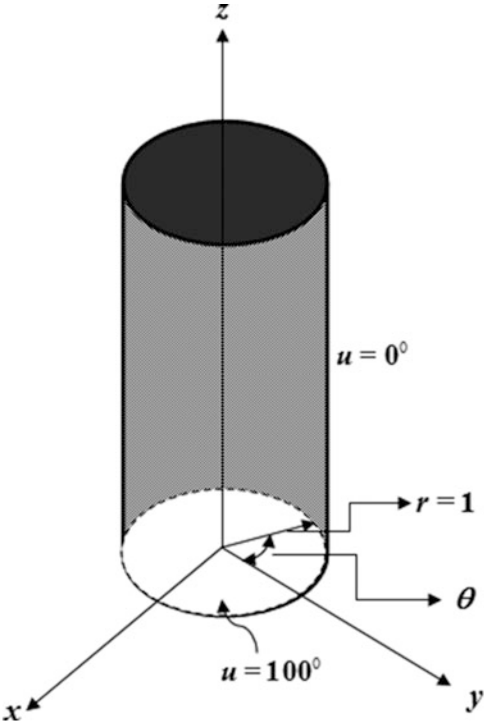

Fig. P3.28

Problem 3.29 Suppose the given temperature of the base of the cylinder in Problem 3.24 is more complicated than just a constant value, say $f(r, \theta)$, some function of r and θ.

Problem 3.30 Steady-state temperature in sphere Bois page 604

Find the steady-state temperature inside a sphere of radius 1 when the surface of the upper half is held at 100° and the surface of the lower half at 0°.

Problem 3.31 Use Laplace's transform to solve the heat conduction problem in an infinitely long circular cylinder of unit radius (i.e., $r = 1$) that has a constant initial temperature T. At the time $t = 0$ a temperature of 0 °C is applied to the surface and is maintained. Find the temperature at any point of the cylinder such as P at any later time t. Use fire below.

Hint: Replace the t by kt.

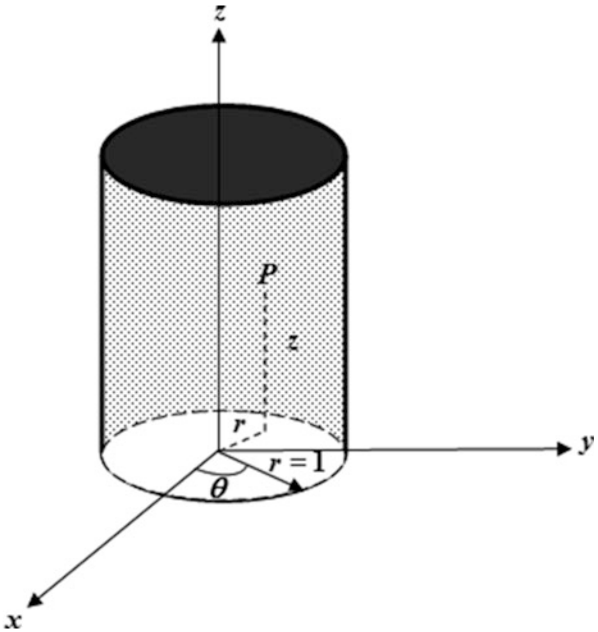

Fig. P3.31

Problem 3.32 Consider a bare homogeneous cylindrical core with material composition typical of modern pressurized water reactor (PWR) operating at full power conditions. The reactor contains a concentration of 2.21 particle per billion (PPB) of natural boron as boric acid is dissolved in the coolant water and is fueled with UO^2 at 2.78 % enrichment in U^{235}.

Based on thermal design considerations, if the core height is fixed at $H = 3.7$ m, then compute the critical core volume and estimate the neutron leakage fraction from the critical core. The macroscopic cross sections for the materials composing this core are given in the table below.

Element/ isotope	Transport cross section [cm^{-1}] Σ_{tr}	Absorption cross section [cm^{-1}] Σ_a	Product of average number of neutrons released in fission and fission cross section [neutron . cm^{-1}] $\nu\Sigma_f$
H	1.79×10^{-2}	8.08×10^{-3}	–
O	7.16×10^{-3}	4.90×10^{-6}	–
Zr	2.91×10^{-3}	7.01×10^{-4}	–
Fe	9.46×10^{-4}	3.99×10^{-3}	–
U^{235}	3.08×10^{-4}	9.24×10^{-2}	1.45×10^{-1}
U^{238}	6.95×10^{-3}	1.39×10^{-2}	1.20×10^{-2}
B^{10}	8.77×10^{-6}	3.41×10^{-2}	–

Problem 3.33 The infinite multiplication factor k_∞ for a heterogeneous lattice of natural uranium fuel is 1.28 for heavy water D_2O moderator. In this particular lattice L^2 for thermal neutron is 175 cm^2 and Fermi age of neutron $\tau = 120$ cm^2. Determine the critical buckling using:

(a) The one-group thermal critical equation
(b) The criticality for a large reactor
(c) The age–diffusion equation
(d) Criticality for the age–diffusion in part c, which is an approximation of the age–diffusion equation for a large reactor and is written as follows:

$$\frac{k_\infty}{\left(1 + \tau B_c^2\right)\left(1 + L^2 B_c^2\right)} = 1$$

Problem 3.34 The system to which Problem 3.33 refers to consists of *i*-in. diameter rods of natural uranium metal arranged in a square lattice with a pitch of 6 in., suspended in a cylindrical vessel containing the heavy water moderator. The ratio of the height to diameter of bare core is 1.2. Estimate the mass of uranium which will make this bare reactor just critical. Assume that the bulking B_c^2 for finite cylinder is given by the following equation:

$$B_c^2 = \left(\frac{2.405}{R_c}\right)^2 + \left(\frac{\pi}{H_c}\right)^2$$

References

1. Y. Oka, T. Kiguchi, *Nuclear Reactor Design (An Advanced Course in Nuclear Engineering)* (Springer, New York, 2014)
2. J.R. Lamarsh, *Introduction to Nuclear Reactor Theory* (Addison-Wesley, Boston, 1966)
3. A.F. Henry, *Nuclear-Reactor Analysis* (MIT Press, Cambridge, 1975)
4. J.J. Duderstadt, L.J. Hamilton, *Nuclear Reactor Analysis* (Wiley, New York, 1976)
5. P.M. Morse, H. Feshbach, *Method of Theoretical Physics* (McGraw-Hill, New York, 1963)
6. K. Okumura, T. Kugo, K. Kaneko, K. Tsuchihashi, *SRAC2006: A Comprehensive Neutronics Calculation Code System, JAEA-Data/Code 2007-004* (Japan Atomic Energy Agency, Tokai-mura, 2007)

Chapter 4
Energy Effects in Modeling Neutron Diffusion: Two-Group Models

In this chapter we derive the multigroup diffusion equation (MGDE), and we illustrate how do we solve them in a way that allows us to calculate an accurate eigenvalue and accurate reaction rates. Since the cross sections vary wildly by multiple orders of magnitude over the energy range in a typical nuclear reactor, the major problem is determining the accurate multigroup cross sections for the design problem under consideration.

4.1 One-Group Diffusion Theory

If we set up the one-group diffusion equation by defining $E_0 = \infty$ and $E_1 = 0$, then we can write the following notation:

$$\int_0^\infty dE\chi(E) = 1 \tag{4.1}$$

$$\text{and 1 group} \begin{cases} -------E_0 = \infty \\ -------E_1 = 0 \end{cases}$$

$$\int_0^\infty dE' \Sigma_\mathrm{s}(E \to E') = \Sigma_\mathrm{s}(E) \tag{4.2}$$

Thus, the multigroup equations yield conversion of the one-speed diffusion equation as

$$\frac{1}{v}\frac{\partial \phi}{\partial t} - \vec{\nabla} \cdot D \vec{\nabla} \phi + \Sigma_\mathrm{a} \phi(\vec{r}, t) = v\Sigma_\mathrm{f} \phi \tag{4.3}$$

B. Zohuri, *Neutronic Analysis For Nuclear Reactor Systems*,
DOI 10.1007/978-3-319-42964-9_4

Note that Eq. 4.3 is important once we provide some means for calculating the group constants of intragroup flux, which is presented as $\phi(\vec{r}, E, t)$. It is also important to know that if we chose the group constant properly, then even one-speed diffusion theory could provide an accurate description of nuclear reactor behavior.

4.2 Two-Group Diffusion Theory

One of the interesting applications of neutronic analysis for reactor system is about application that involves the scenarios of two energy groups, which are characterizing the fast neutrons and associated thermal neutrons respectfully.

For the thermal group that is selected for sufficiently high such that upscattering out of thermal group can be ignored based on the cutoff energy of this thermal group. The corresponding energy in that case is around 0.5–1.0 eV in a water-moderated reactor as an example. However, this may range as high as 3 eV in high-temperature gas-cooled reactors. Figure 4.1 is the presentation of the group structure that one can identify the following relationship as

$$\phi_1(\vec{r}, t) = \int_{E_1}^{E_0} \phi(\vec{r}, E, t)dE \equiv \text{Fast Flux} \tag{4.4}$$

$$\phi_2(\vec{r}, t) = \int_{E_2}^{E_1} \phi(\vec{r}, E, t)dE \equiv \text{Thermal Flux} \tag{4.5}$$

Given Eqs. 4.4 and 4.5, we can simplify the group constants for this model considering first the fission spectrum. Since essentially all fission neutrons are born in the fast group, therefore, we can write the following relationship for the fission spectrum $\chi(E)$ that is also illustrated in Fig. 4.2:

$$\begin{aligned} \chi_1(E) &= \int_{E_1}^{E_0} dE\chi(E) = 1 \\ \chi_2(E) &= \int_{E_2}^{E_1} dE\chi(E) = 0 \end{aligned} \tag{4.6}$$

Hence, the fission source will only appear in the fast group equation:

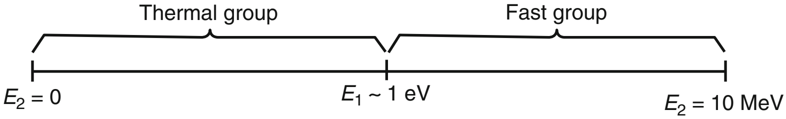

Fig. 4.1 Group structure depiction

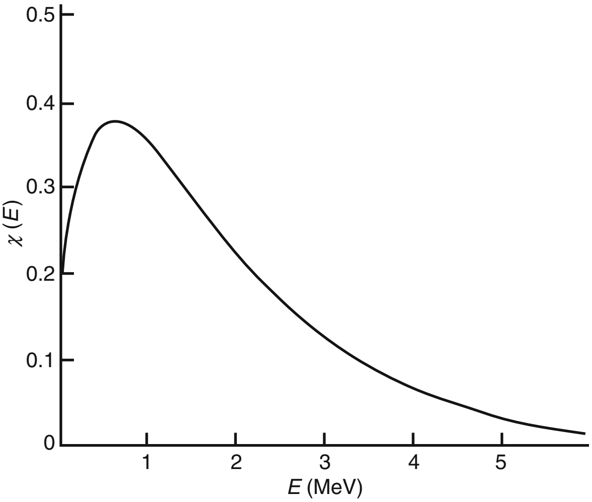

Fig. 4.2 Fission spectrum for thermal neutron-induced fission in ^{235}U (Courtesy of Duderstadt and Hamilton) [1]

$$S_f^1 = \nu_1 \Sigma_f^1 \phi_1 + \nu_2 \Sigma_f^2 \phi_2 \quad (\text{Fast Neutron}) \tag{4.7}$$

$$S_f^2 = 0 \quad (\text{Thermal Neutron}) \tag{4.8}$$

With two sets of equations above, we can go ahead and calculate the scattering and removal cross section. First, since there is no upscattering out of the thermal group,

$$\int_{E_2=0}^{E_1-1\ \text{eV}} dE \Sigma_s(E' \to E) = \Sigma_s(E') \quad E_2 \le E' \le E_1 \tag{4.9}$$

Hence, we can eventually find the following:

$$\begin{aligned} \Sigma_s^{2\to 2} &= \frac{1}{\phi_2}\int_{E_2}^{E_t} dE \int_{E_2}^{E_t} \Sigma_s(E' \to E)\phi(\vec{r}, E') \\ &= \frac{1}{\phi_2}\int_{E_2}^{E_1} dE' \Sigma_s(E')\phi(\vec{r}, E') = \Sigma_s^2 \end{aligned} \tag{4.10}$$

Therefore, the removal cross section for the thermal group is just

$$\Sigma_R^2 = \Sigma_t^2 - \Sigma_s^{2\to 2} = \Sigma_t^2 - \Sigma_s^2 = \Sigma_a^2 \tag{4.11}$$

This is what we are expecting to happen anyway. In practice, first, performing a fine spectrum calculation for the group of interest and then averaging the appropriate cross-sectional data over this spectrum would calculate the remainder of the group constant. This allows us to obtain the group constants, for example, a *fast spectrum calculation* would be performed to calculate the *fast group constant* ν_1, Σ_f^1, Σ_R^1,

$\Sigma_s^{1\to2}$, and D_1, while *thermal group constants* ν_2, Σ_f^2, D_2, and Σ_a^2 handle the situation [1].

If we consider the application of two-group diffusion theory to a reactor criticality analysis as described by Zweifel [2], then we can set both the time derivatives and the external source terms equal to zero to write the two-group diffusion equation as

$$\begin{aligned} &-\vec{\nabla}\cdot D_1\vec{\nabla}\phi_1(\vec{r},t)+\Sigma_R^1\phi_1(\vec{r},t)=\frac{1}{k}\left[\nu_1\Sigma_f^1\phi_1+\nu_2\Sigma_f^2\phi_2\right]\\ &-\vec{\nabla}\cdot D_2\vec{\nabla}\phi_2(\vec{r},t)+\Sigma_a^2\phi_2(\vec{r},t)=\Sigma_s^{1\to2}\phi_1\end{aligned}\tag{4.12}$$

However, in the first equation of Eq. 4.12, we have inserted a multiplication factor $1/k$ in front of the fission source terms since we are eventually analyzing criticality conditions and search. Also, note that while the source terms in the fast group correspond to fission neutrons, the source term in the thermal group is due only to slowing down from the fast group [1].

Now we apply the two-group diffusion equations that are presented as a set in Eq. 4.12, in order to analyze and illustrate the criticality of a bare yet uniform reactor assuming that both fast and thermal fluxes can be characterized by the same spatial shape as $\psi(\vec{r})$:

$$\nabla^2\psi(\vec{r})+B^2\psi(\vec{r})=0\quad \psi(\vec{r}_s)=0\tag{4.13}$$

In the above relationship, we have omitted the subscript g from the geometric bucking $B_g^2=B^2$ so as not to confuse it with the group index g, so we can write:

$$\begin{aligned}\phi_1(\vec{r})=\phi_1\psi(\vec{r})\\ \phi_2(\vec{r})=\phi_2\psi(\vec{r})\end{aligned}\tag{4.14}$$

Then, if we substitute the sets of Eq. 4.14 into Eq. 4.12, we can get the following algebraic equations as

$$\begin{cases}\left(D_1B^2+\Sigma_R^1-\frac{1}{k}\nu_1\Sigma_f^1\right)\phi_1-\frac{1}{k}\nu_2\Sigma_f^2\phi_2=0\\ \Sigma_{s_0}^{1\to2}\phi_1+\left(D_2B^2+\Sigma_a^2\right)\phi_2=0\end{cases}\tag{4.15}$$

However, the solution of Eq. 4.15 can be found as

$$\left(D_1B^2+\Sigma_R^1-\frac{\nu_1\Sigma_f^1}{k}\right)\left(D_2B^2+\Sigma_a^2\right)-\frac{\nu_2\Sigma_f^2\Sigma_{s_0}^{1\to2}}{k}=0\tag{4.16}$$

Now, if we solve for the value of the multiplication factor k, it will yield a nontrivial solution of the two-group equations:

$$k = \frac{\nu_1 \Sigma_{\mathrm{f}}^1}{\left(\Sigma_{\mathrm{R}}^1 + D_1 B^2\right)} + \frac{\Sigma_{\mathrm{s}_0}^{1\to 2}}{\left(\Sigma_{\mathrm{R}}^1 + D_1 B^2\right)} + \frac{\nu_2 \Sigma_{\mathrm{f}}^2}{\left(\Sigma_{\mathrm{a}}^2 + D_2 B^2\right)} \tag{4.17}$$

Equation 4.17 is easily related to our earlier expression for k, notably the six-factor formula. The first term in Eq. 4.17 is representing the neutron multiplication due to fissions occurring in the fast group, and the second term in same equation represents multiplication due to thermal fission.

In case of the thermal fission contribution, we anticipate that to be the dominant factor in these situations in which such a two-group analysis makes sense, let us first examine the following:

$$\begin{aligned} k_2 &= \frac{\Sigma_{\mathrm{s}_0}^{1\to 2}}{\left(\Sigma_{\mathrm{R}_1} + D_1 B^2\right)} \frac{\nu_2 \Sigma_{\mathrm{f}}^2}{\left(\Sigma_{\mathrm{a}_2} + D_2 B^2\right)} \\ &= \frac{\Sigma_{\mathrm{s}_0}^{1\to 2} / \Sigma_{\mathrm{R}}^1}{\left(1 + L_1^2 B^2\right)} \frac{\nu_2 \left(\Sigma_{\mathrm{f}}^2 / \Sigma_{\mathrm{a}}^2\right)}{\left(1 + L_2^2 B^2\right)} \end{aligned} \tag{4.18}$$

Note that the reader should not be deceived into believing that such criticality calculations are always so straightforward and we should take under consideration that for the non-leakage probability $P_{\mathrm{NL}} = \left(1 + L^2 B^2\right)^{-1}$ holds only for uniform, bare reactor geometries (i.e., single-region cores). In addition, one should note that is no longer possible to derive simple expressions for P_{NL} or k in terms of the reactor geometry and composition for multiregional reactors as reflected one.

From our above discussion, it is evident that

$$P_{\mathrm{NL}}^1 = \left(1 + L_1^2 B^2\right)^{-1} \quad \text{and} \quad P_{\mathrm{NL}}^2 = \left(1 + L_1^2 B^2\right)^{-1} \tag{4.19}$$

are just the fast and thermal non-leakage probabilities. Notice that the diffusion length L_1 characterizing the fast group is defined somewhat differently as [1]

$$L_1^2 = \frac{D_1}{\Sigma_{\mathrm{R}}^1} = \frac{D_1}{\Sigma_{\mathrm{a}}^2 + \Sigma_{\mathrm{s}_0}^{1\to 2}} \tag{4.20}$$

As we can see, Eq. 4.20 is inconsistent with our earlier definition of the diffusion length, since both Σ_{a}^2 and $\Sigma_{\mathrm{s}_0}^{1\to 2}$ act to remove neutrons from the fast group. Note that the only common term in Eq. 4.18 is the ratio $\Sigma_{\mathrm{s}_0}^{1\to 2} / \Sigma_{\mathrm{R}}^1$; however, for a homogeneous-type reactor design, we have concluded in previous chapters that this ratio is defined as below:

$$\frac{\begin{array}{c}\text{Rate at which neutrons slow}\\ \text{down to thermal group}\end{array}}{\begin{array}{c}\text{Rate at which neutrons slow}\\ \text{removed from fast group}\end{array}} = \frac{\displaystyle\int \Sigma_{\mathrm{s}_{12}} \phi_1(\vec{r}) d^3 r}{\displaystyle\int \Sigma_{\mathrm{R}}^1 \phi_1(\vec{r}) d^3 r} = \frac{\Sigma_{\mathrm{s}_0}^{1\to 2}}{\Sigma_{\mathrm{R}}^1} = p \tag{4.21}$$

where p is representing the resonance escape probability characterizing slowing down from group 1 to group 2. Hence, we can write the following conclusion based on the above analysis:

$$k_2 = \eta_2 f_2 p P_{\mathrm{NL}}^1 P_{\mathrm{NL}}^2 \tag{4.22}$$

Similarly, we can identify the fast multiplication factor as

$$k_1 = \frac{\nu_2\left(\Sigma_{\mathrm{f}}^1/\Sigma_{\mathrm{R}}^1\right)}{\left(1+L_1^2B^2\right)} = \eta_1 f_1 P_{\mathrm{NL}}^1 \tag{4.23}$$

where $\eta_1 = \nu_1\left(\Sigma_{\mathrm{f}_1}^{\mathrm{F}}/\Sigma_{\mathrm{a}_1}^{\mathrm{F}}\right)$, and we have defined a “fast utilization factor” as $f_1 = \Sigma_{\mathrm{a}_1}^{\mathrm{F}}/\Sigma_{\mathrm{R}}^1$ in analogy to the thermal utilization f_2.

With the above analysis in place, we can easily identify the fast fission factor ε with usual six-factor formula as before and write the following relationship:

$$\varepsilon = \left(1+\frac{k_1}{k_2}\right) = \left\{1+\left(\frac{\nu_1\Sigma_{\mathrm{f}}^1}{\nu_2\Sigma_{\mathrm{f}}^2}\right)\left[\frac{\Sigma_{\mathrm{a}}^2+D_2B^2}{\Sigma_{\mathrm{s}_0}^{1\to 2}}\right]\right\} \tag{4.24}$$

where we can find the six-factor formula as it was shown in Chap. 2 (Eq. 2.77) and it is written here again:

$$k = k_1 + k_2 = \varepsilon k_2 = \eta_2 f_2 p \varepsilon P_{\mathrm{NL}}^1 P_{\mathrm{NL}}^2 \tag{4.25}$$

Going forward, we can conclude similar result as above by using a few-group analysis as presented in the next section.

4.3 Few-Group Analysis

We discussed one-group theory and the typical solutions to the diffusion equation. Then, we talked about the energy dependence of nuclear interaction cross sections. This led to a discussion of the variable energy transport equation, which could be reduced to the multigroup diffusion equations by making three approximations:

1. The P_1 approximation
2. The multigroup approximation
3. The diffusion approximation

In order to make multigroup approximation work in a reasonable fashion, we had to know a little about the actual neutron spectrum in the reactor. Therefore, we used the infinite-medium- or zero-dimensional spectra to collapse a very fine group cross-sectional structure to a few-group structure for spatially dependent calculations. A few-group model constructed in this fashion is the easiest way to deal with the large variation in cross sections as a function of the neutron energy in a nuclear reactor.

In order to demonstrate the difference between a one-energy group model and a few-group energy model, let us consider the simplest of all few-group models—the two-group model. We can write the multigroup diffusion equations in the compact form as

$$\left[-D^g\nabla^2\right]\{\Phi\} + \left[\Sigma_{\mathrm{r}}^g\right]\{\Phi\} = \left[\Sigma_{\mathrm{s0}}^{g'\to g}\right]\{\Phi\} + [\chi^g]\left[\nu\Sigma_{\mathrm{f}}^g\right]\{\Phi\} \tag{4.26}$$

or, in terms of matrix formation, Eq. 4.26 can be written as

$$\begin{aligned}&\begin{bmatrix} -D^1\nabla^2 & \\ & -D^2\nabla^2 \end{bmatrix}\begin{Bmatrix}\phi_1\\ \phi_2\end{Bmatrix} + \begin{bmatrix}\Sigma_{\mathrm{r}}^1 & \\ & \Sigma_{\mathrm{r}}^2\end{bmatrix}\begin{Bmatrix}\phi_1\\ \phi_2\end{Bmatrix}\\ &\quad = \begin{bmatrix} & \Sigma_{\mathrm{s0}}^{2\to 1}\\ \Sigma_{\mathrm{s0}}^{1\to 2} & \end{bmatrix}\begin{Bmatrix}\phi_1\\ \phi_2\end{Bmatrix} + \begin{bmatrix}\chi^1\nu\Sigma_{\mathrm{f}}^1 & \chi^1\nu\Sigma_{\mathrm{f}}^2\\ \chi^2\nu\Sigma_{\mathrm{f}}^1 & \chi^2\nu\Sigma_{\mathrm{f}}^2\end{bmatrix}\begin{Bmatrix}\phi_1\\ \phi_2\end{Bmatrix}\end{aligned} \tag{4.27}$$

Note that both matrices on the left are diagonal, the group scatter matrix can be full with the exception of the diagonal, and the fission source matrix can be full. However and most importantly, the matrices on the left are not symmetric. Using the above analysis, we can easily conclude the two-group thermal reactor equation as we discussed in Sect. 4.1.

4.3.1 Two-Group Thermal Reactor Equations

The most interesting two-group problem is one fast group and one thermal group. Typical energy ranges for these two groups would be

Group 1: 20 MeV – 0.125 eV
Group 2: 0.125 – 10^{-5} eV

These are chosen because thermal cross sections are usually much larger than fast or epithermal cross sections. When these choices are made, we will have

1. $\chi^2 = 0.0, \chi^1 = 1.0$
2. $\Sigma_{\mathrm{s}_0}^{2-1} = 0.0$

Note that epithermal cross section is the result of epithermal neutrons. However, the epithermal neutron is defined as **epithermal neutrons** (0.025 eV; 0.4 eV). These are neutrons of kinetic energy greater than thermal. Some of reactor designs operate with epithermal neutron’s spectrum. This design allows reaching higher fuel breeding ratio than in thermal reactors.

The two-group equations become

$$\begin{bmatrix} -D^1\nabla^2 & \\ & -D^2\nabla^2 \end{bmatrix} \begin{Bmatrix} \varphi^1 \\ \varphi^2 \end{Bmatrix} + \begin{bmatrix} \Sigma_r^1 & \\ & \Sigma_r^2 \end{bmatrix} \begin{Bmatrix} \phi_1 \\ \phi_2 \end{Bmatrix}$$
$$= \begin{bmatrix} & \\ \Sigma_{s0}^{1\to 2} & \end{bmatrix} \begin{Bmatrix} \phi_1 \\ \phi_2 \end{Bmatrix} + \begin{bmatrix} \chi^1 \nu \Sigma_f^1 & \chi^1 \nu \Sigma_f^2 \\ & \end{bmatrix} \begin{Bmatrix} \phi_1 \\ \phi_2 \end{Bmatrix} \tag{4.28}$$

Now since the size of the reactor does not depend on the group structure, if the flux shape is a cosine in an infinite slab reactor, then it must be a cosine shape for each group. If we make the approximate diffusion theory boundary condition assumption that the flux goes to zero on the boundary, we must assume that the flux for each group goes to zero on the boundary and has the same shape within the material of the reactor. Thus, our solution for the flux becomes a product of a spatial function and an energy function. The energy function is a discrete vector with a number for each energy group. We will write it as

$$\{\Phi(E,z)\} = \begin{Bmatrix} \phi_1(z) \\ \phi_2(z) \end{Bmatrix} = \begin{Bmatrix} \phi_1 \cos Bz \\ \phi_2 \cos Bz \end{Bmatrix} = \begin{Bmatrix} \phi^1 \\ \phi^2 \end{Bmatrix} \cos Bz \tag{4.29}$$

where we will use the script $\phi(\vec{r})$ to indicate the energy group constant vector components.

Now in order to obtain a nonzero solution for the flux, we must have a unique relationship between the parameters in the equation. If we substitute the product solution we have identified above into the two-group equation, we can get rid of the del-squared operator. This gives

$$\begin{bmatrix} D^1B^2 & \\ & D^2B^2 \end{bmatrix} \begin{Bmatrix} \phi^1 \\ \phi^2 \end{Bmatrix} + \begin{bmatrix} \Sigma_r^1 & \\ & \Sigma_r^2 \end{bmatrix} \begin{Bmatrix} \phi_1 \\ \phi_2 \end{Bmatrix}$$
$$= \begin{bmatrix} & \\ \Sigma_{s0}^{1\to 2} & \end{bmatrix} \begin{Bmatrix} \phi^1 \\ \phi^2 \end{Bmatrix} + \begin{bmatrix} \chi^1 \nu \Sigma_f^1 & \chi^1 \nu \Sigma_f^2 \\ & \end{bmatrix} \begin{Bmatrix} \phi^1 \\ \phi^2 \end{Bmatrix} \tag{4.30}$$

This can be considered an eigenvalue equation for B^2 as all terms depend on the $\phi(\vec{r})$ vector. With only two groups, the easiest way to set up the problem is to transfer all terms to the left-hand side:

$$\begin{bmatrix} D^1B^2 + \Sigma_r^1 - \chi^1 \nu \Sigma_f^1 & -\chi^1 \nu \Sigma_f^2 \\ -\Sigma_{s_0}^{1\to 2} & D^2B^2 + \Sigma_r^2 \end{bmatrix} \begin{Bmatrix} \phi^1 \\ \phi^2 \end{Bmatrix} = \begin{Bmatrix} 0 \\ 0 \end{Bmatrix} \tag{4.31}$$

In order to obtain a nonzero solution for the $\phi(\vec{r})$ vector, we can set the determinant of the multiplying matrix to zero and solve for the two values of B^2 that will make the determinant equal to zero. This will give

$$\begin{bmatrix} D^1B^2 + \Sigma_\mathrm{r}^1 - \chi^1 v\Sigma_\mathrm{f}^1 & -\chi^1 v\Sigma_\mathrm{f}^2 \\ -\Sigma_{\mathrm{s}_0}^{1\to 2} & D^2B^2 + \Sigma_\mathrm{r}^2 \end{bmatrix} = 0 = \left(D^1B^2 + \Sigma_\mathrm{r}^1 - \chi^1 v\Sigma_\mathrm{f}^1\right)\left(D^2B^2 + \Sigma_\mathrm{r}^2\right) - \left(\chi^1 v\Sigma_\mathrm{f}^2\right)\left(\Sigma_{\mathrm{s}_0}^{1\to 2}\right) \tag{4.32}$$

Then, we can divide the equation by $\Sigma_\mathrm{r}^1\Sigma_\mathrm{r}^2$ and make the following definitions:

$$\begin{aligned} L_1^2 &= \frac{D^1}{\Sigma_\mathrm{r}^1} \\ L_2^2 &= \frac{D^2}{\Sigma_\mathrm{r}^2} \\ \eta f &= \frac{v\Sigma_\mathrm{f}^2}{\Sigma_\mathrm{r}^2} \\ p_{re} &= \frac{\Sigma_{\mathrm{s}_0}^{1\to 2}}{\Sigma_\mathrm{r}^1} \end{aligned} \tag{4.33}$$

This gives

$$\left(L_1^2B^2 + 1 - \frac{v\Sigma_\mathrm{f}^1}{\Sigma_\mathrm{r}^1}\right)\left(L_2^2B^2 + 1\right) - \eta f p_\mathrm{re} = 0 \tag{4.34}$$

Now dividing by both L^2 and collecting terms in powers of B^2 gives

$$B^4 + \left[\frac{1}{L_1^2}\left(1 - \frac{v\Sigma_\mathrm{f}^1}{\Sigma_\mathrm{r}^1}\right) + \frac{1}{L_2^2}\right]B^2 - \frac{1}{L_1^2L_2^2}\left(\eta f p_\mathrm{re} + \frac{v\Sigma_\mathrm{f}^1}{\Sigma_\mathrm{r}^1} - 1\right) = 0 \tag{4.35}$$

This can be written as

$$\begin{aligned} &B^4 + C_1B^2 - C_0 = 0 \\ &C_1 = \left[\frac{1}{L_1^2}\left(1 - \frac{v\Sigma_\mathrm{f}^1}{\Sigma_\mathrm{r}^1}\right)\right] + \frac{1}{L_2^2} \\ &C_0 = \frac{1}{L_1^2L_2^2}\left(\eta f p_\mathrm{re} + \frac{v\Sigma_\mathrm{f}^1}{\Sigma_\mathrm{r}^1} - 1\right) \end{aligned} \tag{4.36}$$

Moreover, it has the solution

$$B^2 = -\frac{C_1}{2} \pm \sqrt{\left(\frac{C_1}{2}\right)^2 + C_0}$$

This will give two solutions for B^2. The largest value must be greater than zero in order to obtain a critical reactor. It is possible for both values to be greater than zero for very highly enriched reactors that have a predominately fast spectrum.

Consider the following parameters for the AGN-201 reactor.

Coefficient	Fast group	Thermal group
Removal cross section	0.05704	0.09583
Diffusion coefficient	0.71514	0.11283
Absorption cross section	0.00193	0.09583
Downscatter cross section	0.05511	–
Nu fission cross section	0.002562	0.15179
L^2	12.5375	1.17740
ηf	–	1.58395
p_{re}	0.96616	–
$\nu\Sigma_{\mathrm{f}}^1/\Sigma_{\mathrm{r}}^1$	0.04492	–

$$\begin{aligned} B_1 &= 0.92551 \\ B_0 &= 0.03897 \\ B^2 &= +0.040347, \quad -0.96586 \\ B_+ &= 0.2008656, \quad B_- = 0.98278i \end{aligned}$$

This gives a bare critical radius of $R_{\mathrm{c}} = 15.64\,\mathrm{cm}$ (diameter equal to 31.28 cm) for the AGN-201 or the equivalent thickness for an infinite slab reactor made of the same material. The radius for an infinite cylinder would be 11.97 cm (diameter equal to 23.94 cm). A right circular cylinder with the height equal to the diameter would be 28.60 cm tall, and a cube would be 27.09 cm on a side.

Consider now the solution for the energy eigenfunction corresponding to this value of the criticality eigenvalue. The thermal equation can be written as

$$\begin{aligned} -\Sigma_{\mathrm{s}_0}^{1\to 2}\phi_1 + \left(D^2B^2 + \Sigma_{\mathrm{r}}^2\right)\phi_2 = 0 \\ \phi_1 = \frac{\left(D^2B^2 + \Sigma_{\mathrm{r}}^2\right)}{\Sigma_{\mathrm{s}_0}^{1\to 2}}\phi_2 \end{aligned} \tag{4.37}$$

So if the group vector is normalized such that $\phi_2 = 1.0$, then ϕ_1 must be equal to 1.822 (i.e., $\phi_1 = 1.822$). For the case of the negative B^2, we would get that $\phi_1 = -0.2386$. Therefore, we have

$$\begin{aligned}&B_{+}^{2}\\&\Phi_{+}=\left\{\begin{matrix}1.822\\1.0\end{matrix}\right\}\cos 0.20086z\\&B_{-}^{2}\\&\Phi_{-}=\left\{\begin{matrix}-0.2386\\1.0\end{matrix}\right\}\cos 0.98278iz\end{aligned}\tag{4.38}$$

Realizing that the imaginary argument can be converted to a real argument by switching the ***cos*** to the cosh function, the general solution can be written as

$$\begin{aligned}\left\{\begin{matrix}\phi_1(z)\\\phi_2(z)\end{matrix}\right\}&=A\left\{\begin{matrix}\phi_{+}^{1}\\\phi_{+}^{2}\end{matrix}\right\}\cos B_{+}z+C\left\{\begin{matrix}\phi_{-}^{1}\\\phi_{-}^{2}\end{matrix}\right\}\cosh B_{-}z\\&=A\left\{\begin{matrix}1.822\\1.0\end{matrix}\right\}\cos 0.20086z+C\left\{\begin{matrix}-0.2386\\1.0\end{matrix}\right\}\cosh 0.98278z\end{aligned}\tag{4.39}$$

Realize that since we are operating in an eigenvalue state and one of the coefficients is either A or C, cannot be determined by this type of calculation. The power level of the reactor will determine the overall magnitude of the flux in the reactor. However, we can eliminate the C coefficient in terms of the A coefficient by applying boundary conditions. C must be zero if we truly stick to the zero flux on the boundary condition. If we are willing to consider extrapolation lengths though, it is possible to evaluate C in terms of A, and we will do that shortly.

k **Eigenvalue Equation**

So far we have answered the criticality question: “Given the material and the requirement for exact criticality, how big is the reactor?” The other criticality question that we are often concerned with is “Given the material and size of the reactor, how far from exactly critical are we?” To answer this question, we must introduce the k eigenvalue. We do this by writing the multigroup diffusion equation (MGDE) in the following fashion:

$$\left[-D^{g}\nabla^{2}\right]\{\Phi\}+\left[\Sigma_{\mathrm{r}}^{g}\right]\{\Phi\}=\left[\Sigma_{\mathrm{s0}}^{g'\to g}\right]\{\Phi\}+\frac{1}{k}\left[\chi^{g}\right]\left[\nu\Sigma_{\mathrm{f}}^{g}\right]\{\Phi\}\tag{4.40}$$

For the two-group, thermal reactor problem, this becomes

$$\begin{bmatrix}D_1B^2&\\&D_2B^2\end{bmatrix}\left\{\begin{matrix}\phi_1\\\phi_2\end{matrix}\right\}+\begin{bmatrix}\Sigma_{\mathrm{r}}^{1}&\\&\Sigma_{\mathrm{r}}^{2}\end{bmatrix}\left\{\begin{matrix}\phi_1\\\phi_2\end{matrix}\right\}=\begin{bmatrix}&\\\Sigma_{\mathrm{s0}}^{1\to 2}&\end{bmatrix}\left\{\begin{matrix}\phi_1\\\phi_2\end{matrix}\right\}+\frac{1}{k}\begin{bmatrix}\nu\Sigma_{\mathrm{f}}^{1}&\nu\Sigma_{\mathrm{f}}^{2}\\&\end{bmatrix}\left\{\begin{matrix}\phi_1\\\phi_2\end{matrix}\right\}\tag{4.41}$$

In addition, the expanded determinant equation becomes

$$\begin{bmatrix} D_1B^2 + \Sigma_r^1 - \frac{1}{k}\nu\Sigma_f^1 & -\frac{1}{k}\nu\Sigma_f^2 \\ -\Sigma_{s_0}^{1\to 2} & D_2B^2 + \Sigma_r^2 \end{bmatrix} = 0 = \left(D_1B^2 + \Sigma_r^1 - \frac{1}{k}\nu\Sigma_f^1\right)\left(D_2B^2 + \Sigma_r^2\right) - \left(\frac{1}{k}\nu\Sigma_f^2\right)\left(\Sigma_{s_0}^{1\to 2}\right) \tag{4.42}$$

We can then solve this equation for k to get

$$\begin{gathered} \left(D_1B^2 + \Sigma_r^1\right)\left(D_2B^2 + \Sigma_r^2\right) = \frac{1}{k}\left\{\nu\Sigma_f^2\Sigma_{s_0}^{1\to 2} + \nu\Sigma_f^1\left(D_2B^2 + \Sigma_r^2\right)\right\} \\ k = \frac{\nu\Sigma_f^2\Sigma_{s_0}^{1\to 2} + \nu\Sigma_f^1\left(D_2B^2 + \Sigma_r^2\right)}{\left(D_1B^2 + \Sigma_r^1\right)\left(D_2B^2 + \Sigma_r^2\right)} \end{gathered} \tag{4.43}$$

This can then be solved iteratively by plugging in values for B^2 and finding a value that gives $k = 1.0$.

It is also useful to divide the numerator and denominator by $\Sigma_r^1\Sigma_r^2$ and inserting the definitions of the diffusion lengths and $\eta f p_{\mathrm{re}}$ to obtain

$$k = \frac{\eta f p_{\mathrm{re}} + \frac{\nu\Sigma_f^1}{\Sigma_r^1}\left(L_2^2B^2 + 1\right)}{\left(1 + L_1^2B^2\right)\left(1 + L_2^2B^2\right)} \tag{4.44}$$

Then, defining the fast fission factor as

$$\varepsilon = \frac{\text{Total Fissions}}{\text{Thermal Fissions}} = \frac{\nu\Sigma_f^1\phi^1 + \nu\Sigma_f^2\phi^2}{\nu\Sigma_f^2\phi^2} = 1 + \frac{\nu\Sigma_f^1\phi^1}{\nu\Sigma_f^2\phi^2} \tag{4.45}$$

and remembering that the thermal equation gives

$$\phi_1 = \frac{\left(D_2B^2 + \Sigma_r^2\right)}{\Sigma_{s_0}^{1\to 2}}\phi_2 \tag{4.46}$$

This becomes

$$\varepsilon = 1 + \frac{\nu\Sigma_f^1\frac{D_2B^2 + \Sigma_r^2}{\Sigma_{s_0}^{1\to 2}}}{\nu\Sigma_f^2} = 1 + \frac{\nu\Sigma_f^1}{\Sigma_r^1}\frac{\left(1 + L_2^2B^2\right)}{\frac{\Sigma_{s_0}^{1\to 2}}{\Sigma_r^1}\frac{\nu\Sigma_f^2}{\Sigma_r^2}} = 1 + \frac{\nu\Sigma_f^1}{\Sigma_r^1}\frac{\left(1 + L_2^2B^2\right)}{\eta f p_{\mathrm{re}}} \tag{4.47}$$

Then,

$$k = \frac{\eta f p_{\mathrm{re}}\varepsilon}{\left(1 + L_1^2B^2\right)\left(1 + L_2^2B^2\right)} \tag{4.48}$$

and defining

$$\begin{aligned} P_{\mathrm{NL}}^1 &= \frac{1}{1+L_1^2B^2} = \text{Fast Non-leakage Probability} \\ P_{\mathrm{NL}}^2 &= \frac{1}{1+L_2^2B^2} = \text{Thermal Non-leakage Probability} \end{aligned} \tag{4.49}$$

This gives the classic six-factor formula:

$$k = \eta f p_{\mathrm{re}} \varepsilon P_{\mathrm{NL}}^1 P_{\mathrm{NL}}^2 \tag{4.50}$$

This is exactly the same equation as it was derived in the previous section as Eq. 4.25.

4.3.2 Two-Group Fast Reactor Equations

Now consider the two-group equations for a fast reactor where fission neutrons show up in both groups:

$$\begin{aligned} &\begin{bmatrix} -D_1B^2 & \\ & -D_2B^2 \end{bmatrix} \begin{Bmatrix} \phi_1 \\ \phi_2 \end{Bmatrix} + \begin{bmatrix} \Sigma_{\mathrm{r}}^1 & \\ & \Sigma_{\mathrm{r}}^2 \end{bmatrix} \begin{Bmatrix} \phi_1 \\ \phi_2 \end{Bmatrix} \\ &\quad = \begin{bmatrix} & \\ \Sigma_{\mathrm{s0}}^{1\to 2} & \end{bmatrix} \begin{Bmatrix} \phi_1 \\ \phi_2 \end{Bmatrix} + \begin{bmatrix} \chi_1 \nu \Sigma_{\mathrm{f}}^1 & \chi_1 \nu \Sigma_{\mathrm{f}}^2 \\ \chi_2 \nu \Sigma_{\mathrm{f}}^1 & \chi_2 \nu \Sigma_{\mathrm{f}}^2 \end{bmatrix} \begin{Bmatrix} \phi_1 \\ \phi_2 \end{Bmatrix} \end{aligned} \tag{4.51}$$

or

$$\begin{bmatrix} D_1B^2 + \Sigma_{\mathrm{r}}^1 - \chi_1 \nu \Sigma_{\mathrm{f}}^1 & -\chi_1 \nu \Sigma_{\mathrm{f}}^2 \\ -\Sigma_{\mathrm{s_0}}^{1\to 2} - \chi_2 \nu \Sigma_{\mathrm{f}}^1 & D_2B^2 + \Sigma_{\mathrm{r}}^2 - \chi_2 \nu \Sigma_{\mathrm{f}}^2 \end{bmatrix} \begin{Bmatrix} \phi_1 \\ \phi_2 \end{Bmatrix} = \begin{Bmatrix} 0 \\ 0 \end{Bmatrix} \tag{4.52}$$

Three- and Four-group Equations

The equations for three groups without upscatter are

$$\begin{aligned} &\begin{bmatrix} D_1B^2 + \Sigma_{\mathrm{r}}^1 & & \\ -\Sigma_{\mathrm{s_0}}^{1\to 2} & D_2B^2 + \Sigma_{\mathrm{r}}^2 & \\ -\Sigma_{\mathrm{s_0}}^{1\to 3} & -\Sigma_{\mathrm{s_0}}^{2\to 3} & D_3B^2 + \Sigma_{\mathrm{r}}^3 \end{bmatrix} \begin{Bmatrix} \phi_1 \\ \phi_2 \\ \phi_3 \end{Bmatrix} \\ &\quad = \frac{1}{k} \begin{bmatrix} \chi_1 \nu \Sigma_{\mathrm{f}}^1 & \chi_1 \nu \Sigma_{\mathrm{f}}^2 & \chi_1 \nu \Sigma_{\mathrm{f}}^3 \\ \chi_2 \nu \Sigma_{\mathrm{f}}^1 & \chi_2 \nu \Sigma_{\mathrm{f}}^2 & \chi_2 \nu \Sigma_{\mathrm{f}}^3 \\ \chi_3 \nu \Sigma_{\mathrm{f}}^1 & \chi_3 \nu \Sigma_{\mathrm{f}}^2 & \chi_3 \nu \Sigma_{\mathrm{f}}^3 \end{bmatrix} \begin{Bmatrix} \phi_1 \\ \phi_2 \\ \phi_3 \end{Bmatrix} \end{aligned} \tag{4.53}$$

The equations for four groups without upscatter are

$$\begin{bmatrix} D_1B^2+\Sigma_{\mathrm{r}}^1 & & & \\ -\Sigma_{\mathrm{s0}}^{1\to 2} & D_2B^2+\Sigma_r^2 & & \\ -\Sigma_{\mathrm{s0}}^{1\to 3} & -\Sigma_{\mathrm{s0}}^{2\to 3} & D_3B^2+\Sigma_{\mathrm{r}}^3 & \\ -\Sigma_{\mathrm{s0}}^{1\to 4} & -\Sigma_{\mathrm{s0}}^{2\to 4} & -\Sigma_{\mathrm{s0}}^{3\to 4} & D_4B^2+\Sigma_{\mathrm{r}}^4 \end{bmatrix} \begin{Bmatrix} \phi_1 \\ \phi_2 \\ \phi_3 \\ \phi_4 \end{Bmatrix}$$

$$= \frac{1}{k} \begin{bmatrix} \chi_1\nu\Sigma_{\mathrm{f}}^1 & \chi_1\nu\Sigma_{\mathrm{f}}^2 & \chi_1\nu\Sigma_{\mathrm{f}}^3 & \chi_1\nu\Sigma_{\mathrm{f}}^4 \\ \chi_2\nu\Sigma_{\mathrm{f}}^1 & \chi_2\nu\Sigma_{\mathrm{f}}^2 & \chi_2\nu\Sigma_{\mathrm{f}}^3 & \chi_2\nu\Sigma_{\mathrm{f}}^4 \\ \chi_3\nu\Sigma_{\mathrm{f}}^1 & \chi_3\nu\Sigma_{\mathrm{f}}^2 & \chi_3\nu\Sigma_{\mathrm{f}}^3 & \chi_3\nu\Sigma_{\mathrm{f}}^4 \\ \chi_4\nu\Sigma_{\mathrm{f}}^1 & \chi_4\nu\Sigma_{\mathrm{f}}^2 & \chi_4\nu\Sigma_{\mathrm{f}}^3 & \chi_4\nu\Sigma_{\mathrm{f}}^4 \end{bmatrix} \begin{Bmatrix} \phi_1 \\ \phi_2 \\ \phi_3 \\ \phi_4 \end{Bmatrix} \tag{4.54}$$

In general, we will write the MGDE in shorthand notation for an arbitrary number of groups as

$$[\boldsymbol{M}]\{\Phi\}=\frac{1}{k}[\boldsymbol{F}]\{\Phi\} \tag{4.55}$$

where $[\boldsymbol{M}]$ is called the migration operator or matrix and $[\boldsymbol{F}]$ is called the fission operator or matrix.

4.4 Transverse Buckling Approximation

Note that in the migration matrix, the $\boldsymbol{D}^g\boldsymbol{B}^2$ terms play the same role and show up in the same places as the Σ_{r}^g terms do. Typically, in multidimensional problems, we will get a buckling term that corresponds to each of the dimensions. For instance, in $R-Z$ geometry for a homogeneous media, the $\boldsymbol{DB}^2$ term can be written as the sum of a $\boldsymbol{B}^2$ for the r direction and a B^2 term for the z direction:

$$\boldsymbol{DB}^2=\boldsymbol{D}\left(\boldsymbol{B}_r^2+\boldsymbol{B}_z^2\right) \tag{4.56}$$

Also for $X-Y-Z$ geometry, we have

$$\boldsymbol{DB}^2=\boldsymbol{D}\left(\boldsymbol{B}_x^2+\boldsymbol{B}_x^2+\boldsymbol{B}_z^2\right) \tag{4.57}$$

Now, in a real reactor design problem, fuel assemblies are changing material properties in the radial direction, but do not change significantly in the z direction due to the requirement for fuel pins and coolant channels. This configuration can easily be manufactured, and it is often possible to reduce the two-dimensional calculation in the r and z directions to a one-dimensional calculation in the r direction by assuming the flux in the z direction to be cosine shaped and correcting for leakage in this direction with a $\boldsymbol{DB}_{\mathrm{z}}^2$ term. This term is then added to the Σ_{r}^g term and the calculation conducted in the radial direction, with an increased removal due to the transverse leakage in the z direction.

4.5 Consistent Diffusion Theory Boundary Conditions

Now let us return to the issue of applying the consistent diffusion theory boundary conditions. Consider the slab case, and realize that the extrapolation distance is given by $2D_g$ or $2/3(\lambda_g)$. For the AGN-201, this gives the following two distances:

$$\begin{aligned}\text{Fast group}:\quad & z_{\text{ex}} = 2^* D_1 = 2^*0.71514 = 1.43028\,\text{cm}\\ \text{Thermal group}:\quad & z_{\text{ex}} = 2^* D_2 = 2^*0.11283 = 0.22566\ \ \text{cm}\end{aligned}$$

We can then write the general solution as

$$\begin{aligned}& A\left\{\begin{array}{c}1.822\cos\left[0.20086(H/2+1.43028)\right]\\ 1.0\cos\left[0.20086(H/2+0.22566)\right]\end{array}\right\}\\ & \quad + C\left\{\begin{array}{c}-0.2386\cosh[0.9278(H/2+1.43028)]\\ 1.0\cosh[0.9278(H/2+0.22566)]\end{array}\right\} = \left\{\begin{array}{c}0\\0\end{array}\right\}\end{aligned}$$

We have two equations in three unknowns, so we cannot completely solve for all of the unknowns. However, if we divide the second equation into the first, we can eliminate both *A* and *C* and come up with one equation in one unknown, *H*/2. So we get

$$\frac{1.822\cos\left[0.20086(H/2+1.43028)\right]}{\cos\left[0.20086(H/2+0.22566)\right]} = -\frac{0.2386\cosh[0.9278(H/2+1.43028)]}{\cosh[0.9278(H/2+0.22566)]} \tag{4.58}$$

We can solve for the critical *H*/2 by plugging in values for the right-hand side and the left-hand side as a function of *H*. When they are equal, we have the critical *H*.

H	RHS	LHS
15.64	11.4091	−0.7296
15.60	12.3494	−0.7296
15.50	15.7590	−0.7296
15.00	−21.1808	−0.7296
14.50	−4.5265	−0.7296
14.00	−1.8684	−0.7296
13.50	−0.7794	−0.7296
13.40	−0.6343	−0.7296
13.46	−0.7193	−0.7296
13.48	−0.7490	−0.7296
13.467	−0.7296	−0.7296

So the $2^*z_{\text{ex}} = 15.64 - 13.467 = 2.173\,\text{cm}$. $z_{\text{ex}} = 1.0865\,\text{cm}$. This value of z_{ex} is in between the value for the fast and thermal groups. Now that we have an *H*, we can go back and evaluate C in terms of A from either of the equations. From the thermal equation, we have

$$C = A\frac{1.822\cos[0.20086*7.82]}{0.2386\cosh[0.9728*7.82]} = -5.4\times 10^{-7}A$$

Therefore, our final solution is

$$\begin{Bmatrix} \phi_1(z) \\ \phi_2(z) \end{Bmatrix} = A\begin{Bmatrix} 1.822 \\ 1.0 \end{Bmatrix}\cos(0.20086z) - 5.4\times 10^{-7}A\begin{Bmatrix} -0.2386 \\ 1.0 \end{Bmatrix}\cosh(0.9278z)$$

The A coefficient must be determined by the power level.

4.6 Derivation of the One-Dimensional Multigroup P_N Equations

The most accurate description of the behavior of neutrons in a nuclear reactor is obtained by solving the three-dimensional, energy-dependent, time-dependent Boltzmann transport equation. However, solutions to this equation are time consuming and expensive for simple reactors and impossible for very complicated ones. Therefore, approximations are necessary and very useful. For many problems of interest in reactor design and safety, the general time-dependent equation can be simplified to a time-independent eigenvalue problem. A critical reactor maintains the flux level at which it becomes critical indefinitely, and therefore the time-dependent part of the Boltzmann equation can be neglected. This time-independent equation is still too complicated to solve in all of its generality, so further approximations are usually made. For preliminary design analysis and scoping studies, one-dimensional approximations are often very useful. With this in mind, it is very instructive to derive the one-dimensional, multigroup P_N equations from the one-dimensional Boltzmann equation. This derivation will cover all of the main points required to perform the same reduction for the two- or three-dimensional problem and save on a great deal of extraneous and confusing notation. The one-dimensional P_1 equations can be reduced to the multigroup diffusion equations, which by analogy can easily be extended to two or three dimensions. The multigroup diffusion equations are by far the most extensively used description of neutron behavior in nuclear reactors, though they suffer in accuracy for small reactors and near strong absorbers.

Therefore, let us begin with the three-dimensional, time-dependent, energy-dependent Boltzmann transport equation, and it is given by

$$\begin{aligned}\frac{1}{v(E)}\frac{d\phi\left(\vec{\boldsymbol{r}},E,\vec{\boldsymbol{\Omega}}\right)}{dt} = {} & S\left(\vec{\boldsymbol{r}},E,\vec{\boldsymbol{\Omega}}\right)+\int\limits_{E'}\int\limits_{\vec{\boldsymbol{\Omega}}'}\Sigma_{\mathrm{s}}\left(\vec{\boldsymbol{r}},E',\vec{\boldsymbol{\Omega}}'\rightarrow E,\vec{\boldsymbol{\Omega}}'\right)\phi\left(\vec{\boldsymbol{r}},E,\vec{\boldsymbol{\Omega}}'\right)dEd\vec{\boldsymbol{\Omega}}' \\ & +\int\limits_{E'}\int\limits_{\vec{\boldsymbol{\Omega}}'}\frac{\chi(E)}{4\pi}v\Sigma_{\mathrm{f}}(\vec{\boldsymbol{r}},E')\phi\left(\vec{\boldsymbol{r}},E,\vec{\boldsymbol{\Omega}}'\right)dE'd\vec{\boldsymbol{\Omega}}'-\nabla\cdot\vec{\boldsymbol{\Omega}}\phi\left(\vec{\boldsymbol{r}},E,\vec{\boldsymbol{\Omega}}\right) \\ & -\Sigma_{\mathrm{T}}(\vec{\boldsymbol{r}},E)\phi\left(\vec{\boldsymbol{r}},E,\vec{\boldsymbol{\Omega}}\right)\end{aligned} \tag{4.59}$$

where

$\phi\left(\vec{\boldsymbol{r}},E,\vec{\boldsymbol{\Omega}}\right)$ = neutron angular flux density

$\Sigma_{\mathrm{T}}(\vec{\boldsymbol{r}},E)$ = total interaction cross section

$\Sigma_{\mathrm{s}}\left(\vec{\boldsymbol{r}},E',\vec{\boldsymbol{\Omega}}'\rightarrow E,\vec{\boldsymbol{\Omega}}\right)$ = scattering cross section for transfer from energy E' and angle $\vec{\boldsymbol{\Omega}}'$ to energy E and angle $\vec{\boldsymbol{\Omega}}$

$\chi(E)v\Sigma_{\mathrm{f}}(\vec{\boldsymbol{r}},E)$ = number of neutrons produced per fission at energy E times the fission cross section for a neutron of energy E' (i.e., fission is generally considered to be isotropic in the laboratory reference frame, and it will be treated that way here)

$S\left(\vec{\boldsymbol{r}},E,\vec{\boldsymbol{\Omega}}\right)$ = the time-independent source of neutrons at position $\vec{\boldsymbol{r}}$, with energy E, and moving in direction $\vec{\boldsymbol{\Omega}}$

Note that this is simply a balance equation that says the rate of change of the neutron density at a point, with energy and direction specified, is the difference between the sources and the sinks. It is essentially a linear equation, as none of the cross sections depends on the neutron angular flux density. This is an excellent approximation for the most reactor analysis questions; moreover, since criticality questions are the first priority, the time-derivative term can be neglected by setting the sum of sources equal to the sum of sinks. This gives the time-independent equation.

Also, $S\left(\vec{\boldsymbol{r}},E,\vec{\boldsymbol{\Omega}}\right)$ is generally insignificant and changes dramatically the type of problem to be solved if it is significant. To show how it could be treated, it will be carried along for a while. If this term is present, the equation is called an inhomogeneous equation. If it is not present, the equation is called homogeneous or an eigenvalue equation. In this case, all terms depend on the neutron angular flux density and for only certain values of the cross-sectional parameters can a nonzero flux density solution be found.

The general three-dimensional transport equation is a function of six independent variables. These are the three position coordinates, two angular directions, and the neutron energy. In order to conserve effort and still reflect the essence of the reduction from this general equation to a coupled set of multigroup P_N equations, it

Fig. 4.3 Slab reactor

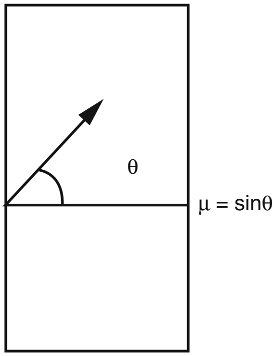

is useful to simplify to a one-dimensional problem. For the one-dimensional problem, consider a slab of thickness L in the z dimension, an infinite in the x and y dimensions. This simplification allows us to get rid of the spatial dependence on x and y, and only the angular dependence relative to the z-axis need be considered. Consider Fig. 4.3:

Then, the transport equation immediately simplifies to

$$\begin{aligned}\mu\frac{\partial\phi(z,E,\mu)}{\partial z}&+\Sigma_{\mathrm{t}}(z,E)\phi(z,E,\mu)=q(z,E,\mu)\\&+\int_{E'}\int_{\vec{\Omega}'}\Sigma_{\mathrm{s}}(z,E',\mu'\to E,\mu)\phi\left(z,E',\vec{\Omega}'\right)dE'd\vec{\Omega}'\\&+\frac{\chi(E)}{4\pi}\int_{E'}\int_{\vec{\Omega}'}\nu(E')\Sigma_{\mathrm{f}}(z,E')\phi\left(z,E',\vec{\Omega}'\right)dE'd\vec{\Omega}'\end{aligned}\tag{4.60}$$

This equation is still exact for the problem we are considering.

At this point, it is useful to digress slightly and introduce the Legendre polynomials and the associated Legendre functions. These are defined as follows:

Legendre Polynomials: Definition

$$P_n(\mu)=\frac{1}{2^n n!}\frac{d^n}{d\mu^n}\left(\mu^2-1\right)^n\tag{4.61}$$

Associated Legendre Functions: Definition

$$P_n^k(\mu)=(-1)^k\left(1-\mu^2\right)^{k/2}\frac{d^k}{d\mu^k}P_n(\mu)\tag{4.62}$$

These functions are introduced because they have some very useful properties for expanding solutions to the transport equation. They possess recursion relationships that allow easy calculation on the computer and allow one order to be related to another.

Legendre Polynomials: Recursion Relation

$$nP_n(\mu) = (2n-1)\mu P_{n-1}(\mu) - (n-1)P_{n-2}(\mu), \quad P_0(\mu) = 1.0, \quad P_1(\mu) = \mu \tag{4.63}$$

Associated Legendre Functions: Recursion Relations

$$P_n^{k+2}(\mu) + 2(k+2)\frac{\mu}{\sqrt{\mu^2-1}}P_n^{k+1}(\mu) = (n-k)(n+k+1)P_n^k(\mu) \tag{4.64}$$

$$(2n+1)\mu P_n^k(\mu) = (n-k+1)P_{n+1}^k(\mu) + (n+k)P_{n-1}^k(\mu) \tag{4.65}$$

The Legendre polynomials and associated Legendre functions are orthogonal on the interval $(-1,1)$. The normalization relationships are given by:

Legendre Polynomials: Orthogonality and Normalization

$$\begin{aligned}\int_{-1}^{1} P_n(\mu)P_m(\mu)d\mu &= \frac{2}{2n+1} \qquad n = m \\ &= 0 \qquad\qquad n \neq m\end{aligned} \tag{4.66}$$

Associated Legendre Functions: Orthogonality and Normalization

$$\begin{aligned}\int_{-1}^{1}\int_{0}^{2\pi} P_n^k(\mu)\cos(k\omega)P_m^p(\mu)\cos(p\omega)d\mu d\omega &= \frac{2\pi}{2n+1}\frac{(n+k)!}{(n-k)!}, \qquad n = m, \ k = p \\ &= 0, n \neq m, \ \text{or} \ k \neq p\end{aligned} \tag{4.67}$$

Finally, for the problem that is being considered here, they possess a very useful property called the expansion theorem, which is given by:

Legendre Polynomials: Expansion Theorem

$$P_n(\mu_{\text{LAB}}) = P_n(\mu)P_n(\mu) + 2\sum_{k=1}^{k=l} P_n^k(\mu)P_n^k(\mu')\cos\{k(\omega-\omega')\} \tag{4.68}$$

where μ_{LAB} is the cosine of the angle in the laboratory system between the neutron's velocity vector prior to scattering and its velocity vector after scattering and μ' and μ are the polar angles before and after scattering.

For the slab problem considered here, the angular flux density can be expanded in terms of the Legendre polynomials as

$$\psi(z,E,\mu) = \sum_{l=0}^{\infty} \frac{2l+1}{2}\phi_l(z,E)P_l(\mu)$$

and it is possible to expand the scattering cross section in terms of the angle of scattering in the lab system as

$$\Sigma_{\mathrm{s}}\left(z, E', \overline{\Omega}' \to E, \overline{\Omega}\right) = \sum_{m=0}^{M} \Sigma_{\mathrm{s}m}(z, E' \to E)\frac{2m+1}{4\pi}P_m(\mu_{\mathrm{LAB}}) \tag{4.69}$$

Then, the inhomogeneous source can also be expanded as

$$S(z, E, \mu) = \sum_{l=0}^{L}\frac{2l+1}{2}S_l(z, E)P_l(\mu) \tag{4.70}$$

Substituting all of this into the transport equation and noting $d\vec{\Omega}' = d\mu' d\omega'$

$$\begin{aligned}
&\mu\sum_{l=0}^{\infty}\frac{2l+1}{2}\frac{\phi_l(z,E)}{dz}P_l(\mu) + \Sigma_{\mathrm{T}}(z,E)\sum_{l=0}^{\infty}\frac{2l+1}{2}\phi_l(z,E)P_l(\mu) = \sum_{l=0}^{L}\frac{2l+1}{2}s_l(z,E)P_l(\mu)\\
&\quad + \int_{E'}\int_{\mu'}\int_{\omega'}\frac{\chi(E)}{4\pi}\nu\Sigma_{\mathrm{f}}(z,E')\sum_{k=0}^{\infty}\frac{2k+1}{2}P_k(\mu')dE'd\mu d\omega'\\
&\quad + \int_{E'}\int_{\mu'}\int_{\omega'}\sum_{m=0}^{M}\Sigma_{sm}(z,E')\frac{2m+1}{4\pi}P_m(\mu_{\mathrm{LAB}})\sum_{k=0}^{\infty}\frac{2k+1}{2}\phi_k(z,E')P_k(\mu)dE'd\mu'd\omega'
\end{aligned} \tag{4.71}$$

We can immediately perform the integrals over μ' and ω' for the fission term on the right-hand side of the equation to obtain, making use of the orthogonality relation,

$$\int_{E'}\int_{\mu'}\int_{\omega'}\frac{\chi(E)}{4\pi}\nu\Sigma_{\mathrm{f}}(z,E')\sum_{k=0}^{\infty}\frac{2k+1}{2}\phi_k(z,E')P_k(\mu')dE'd\mu'd\omega' = \frac{\chi(E)}{2}\int_{E'}\nu\Sigma_{\mathrm{f}}(z,E')\phi_0(z,E')dE' \tag{4.72}$$

The scattering integral can be reduced substituting in the expansion for $P_m(\mu_{\mathrm{LAB}})$ and integrating over ω' to obtain, noting that a cosine function integrated over a full period or multiple full periods is always zero,

$$\begin{aligned}
&\int_{E'}\int_{\mu'}\int_{\omega'}\sum_{m=0}^{M}\Sigma_{sm}(z,E')\frac{2m+1}{2}\left\{\{P_m(\mu))P_m(\mu') + 2\sum_{j=1}^{j=m}P_m^j(\mu)P_m^j(\mu')\cos\{j(\omega-\omega')\}\right\}\\
&\cdot\sum_{k=0}^{\infty}\frac{2k+1}{2}\varphi_k(z,E')P_k(\mu')dE'd\mu'd\omega'\\
&= \int_{E'}\int_{\mu'}\sum_{m=0}^{M}\Sigma_{sm}(z,E')\frac{2m+1}{2}P_m(\mu)P_m(\mu')\sum_{k=0}^{\infty}\frac{2k+1}{2}\varphi_k(z,E')P_k(\mu')dE'd\mu'
\end{aligned} \tag{4.73}$$

Then, integrating over $d\mu'$ and applying the orthogonality relation, we obtain

$$= \sum_{m=0}^{M} P_m(\mu) \frac{2m+1}{2} \int_{E'} \Sigma_{sm}(z,E')\phi_m(z,E')dE' \tag{4.74}$$

The divergence term can be manipulated to remove the $\mu P_1(\mu)$ term using the recursion relation:

$$\begin{aligned} \sum_{l=0}^{\infty} \frac{d\phi_l(z,E)}{dz} \frac{2l+1}{2} \mu P_l(\mu) &= \sum_{l=0}^{\infty} \frac{d\phi_l(z,E)}{dz} \frac{2l+1}{2} \left\{ \frac{l+1}{2l+1} P_{l+1}(\mu) + \frac{l}{2l+1} P_{l-1}(\mu) \right\} \\ &= \sum_{l=1}^{\infty} \frac{l}{2} \frac{d\phi_{l-1}(z,E)}{dz} P_l(\mu) + \sum_{l=0}^{\infty} \frac{l+1}{2} \frac{d\phi_{l+1}}{dz} P_l(\mu) \end{aligned} \tag{4.75}$$

After multiplying by 2, the transport equation for the one-dimensional slab becomes

$$\begin{aligned} &\sum_{l=1}^{\infty} l \frac{d\phi_{l-1}(z,E)}{dz} P_l(\mu) + \sum_{l=1}^{\infty} (l+1) \frac{d\phi_{l=1}(z,E)}{dz} P_l(\mu) + \Sigma_{\mathrm{T}}(z,E) \sum_{l=0}^{\infty} (2l+1)\phi_l(z,E) \times P_l(\mu) \\ &\quad = \sum_{l=0}^{L} (2l+1) s_l(z,E) P_l(\mu) + \chi(E) \int_{E'} \nu\Sigma_{\mathrm{f}}(z,E)\phi_0(z,E')dE' \\ &\quad + \sum_{m=0}^{M} (2m+1) P_m(\mu) \int_{E'} \Sigma_{sm}(z,E' \to E)\phi_m(z,E')dE' \end{aligned} \tag{4.76}$$

At this point, there is still only one equation, but it is exact for the problem under consideration. However, it contains an infinite number of terms. In order to proceed, it is useful to multiply this equation by each of the Legendre polynomials in turn and integrate from -1 to +1. This will produce an infinite set of coupled equations with potentially an infinite number of terms in each equation. Luckily, this turns out not to be the case, and after the multiplication and integration, only a few terms are left in any one equation. All of the terms but one in each of the summations are orthogonal to the polynomial used for the multiplication, and therefore, they disappear from the resulting equation. The general equation obtained when this is done becomes

$$\begin{aligned} &(n+1)\frac{d\phi_{n+1}(z,E)}{dz} + n\frac{d\phi_{n-1}(z,E)}{dz} + (2n+1)\Sigma_{\mathrm{T}}(z,E)\phi_n(z,E) = (2n+1)s_n(z,E) \\ &\quad + (2n+1)\int_{E'} \Sigma_{sn}(z,E' \to E)\phi_n(z,E')dE' + \delta_{n0}\chi(E)\int_{E'} \nu\Sigma_{\mathrm{f}}(z,E')\phi_0(z,E')dE' \end{aligned} \tag{4.77}$$

As an aside, if the same steps had been followed in cylindrical or spherical geometry, the following two general equations would have been obtained:

P_N Equation in Cylindrical Coordinates

$$
\begin{aligned}
&\frac{1}{2}\left[\frac{d}{dr}+\frac{k+1}{r}\right]\left\{(n+k+2)(n+k+1)\phi_{n+1,k+1}(r,E)-(n-k-1)(n-k)\phi_{n-1,k+1}(r,E)\right\}\\
&\quad+\frac{1}{2}\left[\frac{d}{dr}+\frac{k-1}{r}\right]\left\{\phi_{n-1,k-1}(r,E)-\phi_{n+1,k-1}(r,E)\right\}+(2n+1)\Sigma_{\mathrm{T}}(r,E)\phi_n(r,E)\\
&\quad=(2n+1)s_n(r,E)+(2n+1)\int_{E'}\Sigma_{sn}(r,E'\to E)\phi_n(r,E')dE'\\
&\quad+\delta_{0n}\chi(E)\int_{E'}\nu\Sigma_{\mathrm{f}}(r,E')\phi_0(r,E')dE')
\end{aligned}
\tag{4.78}
$$

P_N Equation in Spherical Coordinates

$$
\begin{aligned}
&(n+1)\left[\frac{d}{dr}+\frac{n+2}{r}\right]\phi_{n+1}(r,E)+n\left[\frac{d}{dr}+\frac{n-1}{r}\right]\phi_{n-1}(r,E)+(2n+1)\Sigma_{\mathrm{T}}(r,E)\phi_n(r,E)\\
&=(2n+1)s_n(r,E)+(2n+1)\int_{E'}\Sigma_{snn}(r,E'\to E)\phi_n(r,E')dE'\\
&\quad+\delta_{0n}\chi(E)\int_{E'}\nu\Sigma_{\mathrm{f}}(r,E')\phi_n(r,E')dE'
\end{aligned}
\tag{4.79}
$$

Returning to the slab case, the first two equations are the P_0 and P_1 equations. They are:

For P_0,

$$
\begin{aligned}
&\frac{d\phi_1(z,E)}{dz}+\Sigma_{\mathrm{T}}(z,E)\phi_0(z,E)=s_0(z,E)+\int_{E'}\Sigma_{\mathrm{s}_0}(z,E'\to E)\phi_0(z,E')dE'\\
&\quad+\chi(E)\int_{E'}\nu\Sigma_{\mathrm{f}}(z,E')\phi_0(z,E')dE'
\end{aligned}
\tag{4.80a}
$$

For P_1,

$$
\begin{aligned}
&2\frac{d\phi_2(z,E)}{dz}+\frac{d\phi_0(z,E)}{dz}+3\Sigma_{\mathrm{T}}(z,E)\phi_1(z,E)=3s_1(z,E)\\
&\quad+3\int_{E'}\Sigma_{\mathrm{s}_1}(z,E'\to E)\phi_1(z,E')dE'
\end{aligned}
\tag{4.80b}
$$

Note that these two equations contain three unknowns, ϕ_0, ϕ_1, and ϕ_2. In order to solve them, an additional equation must be obtained or one of the unknowns neglected. The standard procedure is to neglect ϕ_2. This approximation is known as the P_1 approximation. If the first six equations are considered and ϕ_6 is neglected, the resulting approximation is known as the P_5 approximation. This is the first approximation that has been made for the slab problem and is known as:

1. "***P_N* Approximation**"

Roughly, this approximation says that the magnitude of the expansion coefficients is decreasing with increasing N, and above some highest N, they will have negligible effect on the solution for the low-order coefficients, in particular, which are generally the quantities of most interest.

At this point the inhomogeneous source terms will be dropped. If they are important, then the equations will require different solution techniques that will be used for reactor criticality analyses. Their inclusion is obvious in what follows and the approach is straightforward, if they are required.

Next, the energy dependence must be considered. This is accomplished by breaking the energy region of interest (usually 0.00001 eV–20 MeV) up into intervals called energy groups. As most neutron transport problems start with high-energy neutrons, born because of fission or fusion reactions that slow down to lower energies, these intervals are generally numbered from the highest energy to the lowest energy. The lowest group number corresponds to the highest-energy neutrons. If the energy dependence of the angular flux density is mild over large energy ranges, then only a small number of groups are required for an accurate solution to the transport problem. However, if the energy dependence of the angular flux density is significant over many short energy intervals, then a large number of groups must be used. No matter how many groups are used, some estimate of the energy dependence within the group interval must be made, and this dependence is considered to remain constant throughout any given reactor material. That is, for the gth energy group extending from energy E_{g+1} to E_g, the following holds

$$\phi_n(z,E) = f(E)\phi_n^g(z), \quad E_{g+1} \le E < E_g \tag{4.81}$$

$$\phi_n^g(z) = \frac{\displaystyle\int_{E_{g+1}}^{E_g} \phi_n(z,E)dE}{\displaystyle\int_{E_{g+1}}^{E_g} f(E)dE} \tag{4.82}$$

for all z and E of interest within any one material. This is known as:

2. "**Multigroup Approximation**"

Essentially, the energy and spatial dependence of the angular flux density expansion coefficients are assumed to be "separable" within the energy group width. This is the second major approximation that is made, and in the limit of an infinite number of groups, it is not really an approximation at all. However, few computers have an infinite amount of storage, and therefore, the assumed separability does become an approximation.

Group-averaged parameters are then defined in the following manner:

$$\Sigma_{\mathrm{T}}^g(z) = \frac{\displaystyle\int_{E_{g+1}}^{E_g} f(E)\Sigma_{\mathrm{T}}(z,E)dE}{\displaystyle\int_{E_{g+1}}^{E_g} f(E)dE} \tag{4.83}$$

and

$$\chi^g = \int_{E_{g+1}}^{E_g} \chi(E)dE \tag{4.84}$$

with

$$\Sigma_{sn}^{g'>g}(z) = \frac{\displaystyle\int_{E_{g11}}^{E_g}\int_{E_{g'+1}}^{E_{g'}} f(E')\Sigma_{sn}(z, E' \to E)dE'dE}{\displaystyle\int_{E_{g'+1}}^{E_g} f(E')dE'} \tag{4.85}$$

Having made this approximation and dropping the inhomogeneous terms, the multigroup P_1 equations can be written as

$$\begin{aligned}
&\frac{d\phi_1^g(z)}{dz} + \Sigma_{\mathrm{T}}^g(z)\phi_0^g(z) = \sum_{g'=1}^{\mathrm{NOG}} \Sigma_{\mathrm{s0}}^{g'>g}(z)\phi_0^{g'}(z) + \chi^g \sum_{g'=1}^{\mathrm{NOG}} \nu\Sigma_{\mathrm{f}}^{g'}(z)\phi_0^{g'}(z), 1 \le g \le \mathrm{NOG}\\
&\frac{d\phi_0^g(z)}{dz} + 3\Sigma_{\mathrm{T}}^g(z)\phi_1^g(z) = 3\sum_{g'=1}^{\mathrm{NOG}} \Sigma_{\mathrm{s1}}^{g'>g}(z)\phi_1^{g'}(z), 1 \le g \le \mathrm{NOG}
\end{aligned} \tag{4.86}$$

For most reactor problems, the summation over scattering is really only a summation over groups with higher energy than the group of interest (upscatter is impossible). If the term expressing scattering within the group is then pulled over to the left-hand side and combined with the total cross-sectional term, this can be written as

$$\begin{aligned}
&\frac{d\phi_1^g(z)}{dz} + \left\{\Sigma_{\mathrm{T}}^g(z) - \Sigma_{\mathrm{s0}}^{g>g}(z)\right\}\phi_0^g(z) = \sum_{g'>g} \Sigma_{\mathrm{s0}}^{g'>g}(z)\phi_0^{g'}(z) + \chi^g \sum_{g'=1}^{\mathrm{NOG}} \nu\Sigma_{\mathrm{f}}^{g'}(z)\phi_0^{g'}(z)\\
&\frac{d\phi_0^g(z)}{dz} + 3\left\{\Sigma_{\mathrm{T}}^g(z) - \Sigma_{\mathrm{s1}}^{g>g}(z)\right\}\phi_1^g(z) = 3\sum_{g'>g} \Sigma_{\mathrm{s1}}^{g'>g}(z)\phi_0^{g'}(z)
\end{aligned} \tag{4.87}$$

Two of the within-group cross sections have special names. They are

1. **Removal Cross Section**

$$\Sigma_{\mathrm{R}}^g(z) = \Sigma_{\mathrm{T}}^g(z) - \Sigma_{\mathrm{s0}}^{g>g}(z) \tag{4.88}$$

2. **Transport Cross Section**

$$\Sigma_{\mathrm{TR}}^g(z) = \Sigma_{\mathrm{T}}^g(z) - \Sigma_{\mathrm{s1}}^{g>g}(z) \tag{4.89}$$

This coupled set of equations then becomes the multigroup P_1 equations. The slab case considered here is by far the simplest, but the steps and approximations are the same in reducing other one-dimensional geometries and two-/three-dimensional geometries. As a more concise notation, the multigroup P_1 equations can be written in matrix form by treating the expansion coefficients for all groups as a vector quantity of length equal to the number of groups, and the cross sections can be written as a square matrix in the following form:

$$\begin{aligned}&\frac{d}{dz}\{\phi_1(z)\} + [\Sigma_{\mathrm{R}}(z)]\{\phi_0(z)\} = [\Sigma_{\mathrm{s}0d}(z)]\{\phi_0(z)\} + [\chi\nu\Sigma_{\mathrm{f}}(z)]\{\phi_0(z)\}\\ &\frac{d}{dz}\{\phi_0(z)\} + [3\Sigma_{\mathrm{TR}}(z)]\{\phi_1(z)\} = [3\Sigma_{\mathrm{s}1d}]\{\phi_1(z)\}\end{aligned} \tag{4.90}$$

This notation is a little obscure, but it makes it easier to emphasize the important parts for the following remarks.

The multigroup diffusion equations (MGDE) can be easily derived from the multigroup P_N equations. First, the P_1 approximation is made and then the P_1 equation is solved for the coefficient vector.

$$\{\phi_1(z)\} = -[3\Sigma_{\mathrm{TR}}(z) - 3\Sigma_{\mathrm{s}1d}(z)]^{-1}\frac{d}{dz}\{\phi_0(z)\} \tag{4.91}$$

If anisotropic downscatter is neglected and only the transport cross-sectional term retained, then the transport minus the anisotropic-downscatter matrix becomes a diagonal matrix, and its inverse can be instantly computed by finding the inverse of each diagonal term. This is called the

1. "**Diffusion Approximation**"

and is the only difference between the multigroup P_1 equations and the multigroup diffusion equations. The P_1 group vector can be eliminated from the P_0 group equations to obtain

$$\frac{d}{dz}[3\Sigma_{\mathrm{TR}}(z)]^{-1}\frac{d}{dz}\{\phi_0(z)\} + [\Sigma_{\mathrm{R}}(z)]\{\phi_0(z)\} = [\Sigma_{\mathrm{s}0d}(z)]\{\phi_0(z)\} + [\chi\nu\Sigma_{\mathrm{f}}(z)]\{\phi_0(z)\} \tag{4.92}$$

These then are the multigroup diffusion equations for the slab problem. Conveniently, and it will not be shown here, the two-dimensional and three-dimensional multigroup diffusion equations can be obtained from the one-dimensional equations by replacing the partial derivatives with respect to z, in the slab case, with the gradient operator in the general case. This gives for the general dimensional multigroup diffusion equations:

$$-\nabla[3\Sigma_{\mathrm{TR}}(\vec{r})]^{-1}\nabla\{\phi_0(\vec{r})\} + [\Sigma_{\mathrm{R}}(\vec{r})]\{\phi_0(\vec{r})\} = [\Sigma_{\mathrm{s}0d}(\vec{r})]\{\phi_0(\vec{r})\} + [\nu\Sigma_{\mathrm{f}}(\vec{r})]\{\phi_0(\vec{r})\} \tag{4.93}$$

In addition, a group diffusion coefficient can be defined by

$$D^g(\bar{r}) = \frac{1}{3\Sigma_{\mathrm{TR}}^g(\bar{r})} \tag{4.94}$$

In summary the three major approximations made to derive the multigroup diffusion equations from the Boltzmann transport equation were

1. **$\mathbf{P_1}$ approximation**
2. **Multigroup approximation**
3. **Diffusion approximation**

Two further simplifications can be considered. The first is simply the neglect of upscatter except for within the thermal group, and the second is the case of group structures wide enough such that the equations become direct coupled.

1. **Downscatter-Only Case**
   The multigroup diffusion equations become

$$-\frac{d}{dz}\left\{3\Sigma_{\mathrm{TR}}^g(z)\right\}^{-1}\frac{d}{dz}\phi_0^g(z) + \Sigma_{\mathrm{R}}^g(z)\phi_0(z) = \sum_{g'=1}^{g-1}\Sigma_{\mathrm{s}_0(z)}^{g'>g}(z)\phi_0^{g'} + \chi^g\sum_{g'=1}^{\mathrm{NOG}}\nu\Sigma_{\mathrm{f}}^{g'}(z)\phi_0^{g'}(z) \tag{4.95}$$

2. **Direct-Coupled Case**

$$-\frac{d}{dz}\left\{3\Sigma_{\mathrm{TR}}^g(z)\right\}^{-1}\frac{d}{dz}\phi_0^g(z) + \Sigma_{\mathrm{R}}^g(z)\phi_0(z) = \Sigma_{\mathrm{s}_0}^{g-1>g}(z)\phi_0^{g-1} + \chi^g\sum_{g'=1}^{\mathrm{NOG}}\nu\Sigma_{\mathrm{f}}(z)\phi_0^{g'}(z) \tag{4.96}$$

   Now that we are here, we can pay our attention to the solution of multigroup diffusion equation in the next section.

4.7 Multigroup Diffusion Equations: Solution Approach

Now that we have derived the MGDE, how do we solve them in a way that allows us to calculate an accurate eigenvalue and accurate reaction rates? This is the subject we are going to pay further attention. Since the cross sections vary wildly by multiple orders of magnitude over the energy range in a typical nuclear reactor, the major problem is determining the accurate multigroup cross sections for the design problem under consideration.

The data for the cross sections for each individual nuclide are stored in the ENDF/B files as data points with interpolation schemes defined for representing the cross sections between the data points. Each nuclide has its unique basic set of energy values for representing its cross sections. Some cross sections are very smooth and don't require many basic points in the energy grid required to represent a nuclide cross section. The smoothly varying scattering cross section of hydrogen would be an example. Others have many data points to represent the multiple changes in cross-sectional values in both a positive and negative direction as the energy varies only in slight amounts. An example of this type would be iron. Others vary so rapidly that a simple grid is inadequate, and specific functions must be chosen to represent the "resonance" structure of the nuclide. An example of this type of cross section would be U-238. We will ignore resonances for the present and come back to them later.

However, any reactor of interest involves multiple isotopes or nuclides, and it is impossible to perform a calculation on multiple energy grids. So initially a very fine group grid is established that can involve thousands of groups, but they are the same groups for each nuclide. The nuclide cross sections are processed into multigroup form for this very fine grid. The first approximation is simply to use constant weighting or flux spectrum within these very fine groups. However, it is also possible to use a spectral shape that is the characteristic of the likely flux shape in the energy region of interest. Usually this breaks down too three different flux shapes. Above about 100 keV, a fission spectrum is usually adequate. Below about 1 eV, a Maxwellian flux shape works, and in between a 1/E spectrum is the norm. Of course we are now talking about the within-group spectrum for very narrow groups within which we do not expect the flux to vary much.

Once we have all of the cross sections for every nuclide converted to this several thousand-group grid, we can now start on generating an approximate energy spectrum for the reactor under consideration. We set up the MGDE in matrix form and introduce the k eigenvalue. We have

$$-[D]\nabla^2\{\phi\} + [\Sigma_\mathrm{r}]\{\phi\} = [\Sigma_\mathrm{d}]\{\phi\} + \frac{1}{k}[\nu\Sigma_\mathrm{f}]\{\phi\} \tag{4.97}$$

The simplest approximation is to choose an infinite-medium spectrum by neglecting the first term.

4.7.1 Infinite Medium for Group Collapse

For the infinite-medium case, the MGDE becomes

$$[\Sigma_\mathrm{r}]\{\phi\} = [\Sigma_\mathrm{d}]\{\phi\} + \frac{1}{k}[\nu\Sigma_\mathrm{f}]\{\phi\} \tag{4.98}$$

This can simply be solved by guessing a spectrum for the individual group fluxes and plugging that in on the left-hand side. Then, we can calculate the fission source, setting $k = 1$, and the downscatter source. The Σ_r matrix is easy to invert because it is diagonal. So we can solve for a new flux vector on the left-hand side. If we call the flux guess we used on the right-hand side ϕ_0 and the solution we obtained on the left-hand side ϕ_1, then the multiplication constant k-infinity can be written as

$$k_\infty = \frac{\sum_{g=1}^{\mathrm{NOG}} \nu\Sigma_{\mathrm{f}}^{g}\phi_1^{g}}{\sum_{g=1}^{\mathrm{NOG}} \nu\Sigma_{\mathrm{f}}^{g}\phi_0^{g}} \tag{4.99}$$

This is really a fairly, straightforward process and essentially converges in one iteration. That means that as long as we choose a guessed spectrum ϕ_0 that contains a value in each group, the calculated spectrum will give us an estimate of the multiplication constant when substituted into the above formula. Of course the easiest guess is to simply choose all of the ϕ_0^g to be equal to 1.0.

However, since we get a k infinity that is not equal to 1.0, the infinite-medium spectrum is not the best approximation that we can obtain. (If k is less than 1.0, we need to reconsider what is going on because that says an infinite reactor will not be critical.) A better approximation can be obtained by using what is called the zero-dimensional approximation.

4.7.2 Zero-Dimensional Spectrum for Group Collapse

Remember when we considered an infinite slab reactor, we chose as a boundary condition that the flux would go to zero on the boundary of the reactor. If that is the case, then the flux is cosine shaped, and we have the following equation for the diffusion operator:

$$-D\nabla^2\phi(z) = B^2\phi(z) \tag{4.100}$$

converting the differential operator to multiplication by a constant. Of course when we did the same problem for the infinite cylinder or the homogeneous sphere, we were able to do the same thing. In fact when we considered any of the forms of the ∇^2 operator, we were able to find eigenfunctions whose value went to zero on the surface and allowed us to replace the differential operator by a constant which we always called B^2. Now if we do the same thing for the MGDE and require each group flux to go to zero on the boundary, we can replace the differential operator in each equation by the same constant. This allows us to take into account the effects of leakage on our very fine group calculation. The MGDE then becomes

$$\begin{aligned}\left[DB^2\right]\{\phi\} + [\Sigma_{\mathrm{r}}]\{\phi\} &= [\Sigma_{\mathrm{d}}]\{\phi\} + \frac{1}{k}[\nu\Sigma_{\mathrm{f}}]\{\phi\} \\ \left[DB^2 + \Sigma_{\mathrm{r}}\right]\{\phi\} &= [\Sigma_{\mathrm{d}}]\{\phi\} + \frac{1}{k}[\nu\Sigma_{\mathrm{f}}]\{\phi\}\end{aligned} \tag{4.101}$$

The solution to this set of equations proceeds exactly the way the solution to the infinite-medium equations proceeds. But this time we have to guess a value for B^2 and a flux vector for the right-hand side. Substitute the flux vector and calculate the fission source term $(k = 1)$ and the scattering source term. This gives a total source for each group. This source is then divided by the $\left[D^g B^2 + \Sigma_{\mathrm{r}}^g\right]$ term to give the new flux. If the new flux is substituted into the k equation, it gives the multiplication constant k_{eff} in this case:

$$k_{\mathrm{eff}} = \frac{\sum_{g=1}^{\mathrm{NOG}} \nu\Sigma_{\mathrm{f}}^g \phi_1^g}{\sum_{g=1}^{\mathrm{NOG}} \nu\Sigma_{\mathrm{f}}^g \phi_0^g} \tag{4.102}$$

Of course k_{eff} will not be exactly 1.0 unless we chose very accurately for B^2. Since B ^{2} represents a leakage term, if k_{eff} is greater than 1.0, we need to increase B^2 and solve the equations again. If k_{eff} is less than 1.0, we need to decrease B^2 and solve the equations again. We can iterate on B^2 until we get k_{eff} exactly equal to 1.0. This then will give us our zero-dimensional spectrum, which takes into account the first-order effects of leakage appropriate to the reactor under consideration. Note that the iteration proceeds very quickly, and even for thousands of groups, it will never amount to more than a few seconds of computer time.

4.7.3 Group Collapsing

Once we have obtained a reasonable very fine group spectrum, we can now collapse this group structure to a more manageable form. The more manageable form will be a small number of broad groups. Typically, this number varies from two, to say twenty or so, depending on how large of a problem is to be solved. The basic formula for group collapsing of cross sections is

$$\Sigma^G = \frac{\int_{E^{G+1}}^{E^G} \Sigma(E)\phi(E)dE}{\int_{E^{G+1}}^{E^G} \phi(E)dE} = \frac{\sum_{g \in G} \Sigma^g \phi^g}{\sum_{g \in G} \phi^g} \tag{4.103}$$

where g represents a very fine group and G represents a broad group.

This works well for the total, absorption, removal, and nu*fission cross sections.

$$\Sigma^G = \frac{\int\limits_{E^{G+1}}^{E^G} \Sigma(E)\phi(E)dE}{\int\limits_{E^{G+1}}^{E^G} \phi(E)dE} = \frac{\sum\limits_{g\in G} \Sigma^g \phi^g}{\sum\limits_{g\in G} \phi^g} \tag{4.104a}$$

$$\Sigma_{\mathrm{a}}^G = \frac{\int\limits_{E^{G+1}}^{E^G} \Sigma_{\mathrm{a}}(E)\phi(E)dE}{\int\limits_{E^{G+1}}^{E^G} \phi(E)dE} = \frac{\sum\limits_{g\in G} \Sigma_{\mathrm{a}}^g \phi^g}{\sum\limits_{g\in G} \phi^g} \tag{4.104b}$$

$$\Sigma_{\mathrm{r}}^G = \frac{\int\limits_{E^{G+1}}^{E^G} \Sigma_{\mathrm{r}}(E)\phi(E)dE}{\int\limits_{E^{G+1}}^{E^G} \phi(E)dE} = \frac{\sum\limits_{g\in G} \Sigma_{\mathrm{r}}^g \phi^g}{\sum\limits_{g\in G} \phi^g} \tag{4.104c}$$

$$v\Sigma_{\mathrm{f}}^G = \frac{\int\limits_{E^{G+1}}^{E^G} v\Sigma_{\mathrm{f}}(E)\phi(E)dE}{\int\limits_{E^{G+1}}^{E^G} \phi(E)dE} = \frac{\sum\limits_{g\in G} v\Sigma_{\mathrm{f}}^g \varphi^g}{\sum\limits_{g\in G} \phi^g} \tag{4.104d}$$

The downscatter cross sections are a little more subtle, they are given by

$$\Sigma_{\mathrm{s}}^{G'\to G} = \frac{\int\limits_{E^{G+1}}^{E^G} dE \int\limits_{E^{G'+1}}^{E^{G'}} \Sigma_{\mathrm{s}}(E' \to E)\, \phi\, (E')dE'}{\int\limits_{E^{G'+1}}^{E^{G'}} \phi(E')dE'} = \frac{\sum\limits_{g\in G} \sum\limits_{g'\in G'} \Sigma_{\mathrm{s}}^{g'\to g} \phi^{g'}}{\sum\limits_{g'\in G'} \phi^{g'}} \tag{4.105}$$

Note that in this case, g' must be a group in G' and g must be a group in G. In many cases, the very fine group that is being scattered out of and the very fine group that is being scattered into will belong to the same broad group. In this case the scattering is not counted and the cross section is neglected. Only those very fine groups that scatter from one broad group to another broad group are counted. Thus, as the group structure gets broader and broader, the downscatter cross sections decrease in magnitude.

Though χ is not really a cross section, a system needs to be defined for collapsing it from very fine groups to broad groups. This is really very simple, the solution is

$$\chi^G = \sum_{g \in G} \chi^g \tag{4.106}$$

χ for a broad group is simply the sum of the χ's for the very fine groups that make it up.

Finally, the most difficult to understand is the diffusion coefficient. Many organizations and individuals have tried to collapse the very fine group D's based on some sort of current model. This runs into difficulties because the current can in some cases be negative and that complicates the problem severely. The simplest and a suitably accurate approach is to collapse D by finding a broad group transport cross section and taking the inverse of that. The weighting spectrum that will be used in the P_0 flux spectrum is ϕ.This gives

$$\Sigma_{\mathrm{tr}}^G = \frac{\int_{E^{G+1}}^{E^G} \Sigma_{\mathrm{tr}}(E)\phi(E)dE}{\int_{E^{G+1}}^{E^G} \phi(E)dE} = \frac{\sum_{g \in G} \Sigma_{\mathrm{tr}}^g \phi^g}{\sum_{g \in G} \phi^g} \qquad D^G = \frac{1}{3\Sigma_{\mathrm{tr}}^G} \tag{4.107}$$

Example 4.1 As an example problem, let us consider a BWR core with 2 % enriched fuel. We will assume that we can simply mix the cross sections together based on their smeared volume fractions. This is not very accurate in many cases because heterogeneous effects can be important. However, for the sake of this example problem, let us simply mix the fuel and moderator and clad together based on volume fractions. For our very fine group calculation, we will use four groups to demonstrate the solution methods. For our broad group set of constants, we will choose two groups. Therefore, we are going to calculate an infinite-medium spectrum and a zero-dimensional (ZD) spectrum with four groups and collapse based on the ZD spectrum to two broad groups.

The group constants for the four fine groups are

	Group 1	Group 2	Group 3	Group 4
Chi	0.5503	0.4348	0.0149	0.0
Removal	0.10297	0.14361	0.09292	0.02569
3 * Transport	0.46484	0.99536	1.82077	7.00474

(continued)

	Group 1	Group 2	Group 3	Group 4
Diffusion coefficient	2.15128	1.00466	0.54922	0.14276
Absorption	0.00169	0.00031	0.00220	0.02569
Nu*fission	0.00288	0.00017	0.00122	0.04114
$\Sigma_{g\to g+1}$	0.09490	0.14330	0.09083	–
$\Sigma_{g\to g+2}$	0.00646	–	–	–

The fission sources by group can then be given by
$\mathrm{FS}^1 = 0.5503 * (0.00288 * \phi_1 + 0.00017 * \phi_2 + 0.00122 * \phi_3 + 0.04114 * \phi^4)$
$\mathrm{FS}^2 = 0.4348 * (0.00288 * \phi_1 + 0.00017 * \phi_2 + 0.00122 * \phi_3 + 0.04114 * \phi^4)$
$\mathrm{FS}^3 = 0.0149 * (0.00288 * \phi_1 + 0.00017 * \phi_2 + 0.00122 * \phi_3 + 0.04114 * \phi^4)$
$\mathrm{FS}^4 = 0.0 * (0.00288 * \phi_1 + 0.00017 * \phi_2 + 0.00122 * \phi_3 + 0.04114 * \phi^4)$

Notice that the term in parentheses is constant which is essentially the total number of neutrons produced by the fluxes. We can now write the MGDE for the infinite-medium case as

$$0.10297{*}\phi_1 = +\mathrm{FS}^1 0.14361{*}\phi_2 = 0.09490{*}\phi_1 + \mathrm{FS}^2 0.09292{*}\phi_3 = 0.00646{*}\phi_1 \\ +0.14330{*}\phi_2 + \mathrm{FS}^3 0.02569{*}\phi_4 = 0.09083{*}\phi_2 \\ +\mathrm{FS}^4$$

Choose the initial guess for the fluxes to be all equal to 1.0. This gives for the total fission source = 0.00288 + 0.00017 + 0.00122 + 0.04114 = 0.04541. This then gives for the group fission sources:
$\mathrm{FS}^1 = 0.5503 * 0.04541 = 0.024989$
$\mathrm{FS}^2 = 0.4348 * 0.04541 = 0.019744$
$\mathrm{FS}^3 = 0.0149 * 0.04541 = 0.000677$
$\mathrm{FS}^4 = 0.0$

Then,
$\phi_1 = 0.024989/0.10297 = 0.24268$
$\phi_2 = (0.019744 + 0.0949 * 0.24268)/0.14361 = 0.29785$
$\phi_3 = (0.000677 + 0.00646 * 0.24268 + 0.14330 * 0.29785)/0.09292 = 0.48350$
$\phi_4 = 0.09083 * 0.48350/0.02569 = 1.70948$

The new total fission source

$$= 0.00288{*}0.24268 + 0.00017{*}0.29785 + 0.00122{*}0.48350 + 0.04114{*}1.70948 \\ = 0.07167$$

Therefore, the multiplication constant is

$$k\text{-infinity} = 0.07167/0.04541 = 1.57823$$

We will normally normalize the spectrum for a thermal reactor such that the thermal flux has a value of 1.0. When we do this, we get

$\phi_1 = 0.142$
$\phi_2 = 0.174$
$\phi_3 = 0.283$
$\phi_4 = 1.0$

For the ZD case, the solution procedure proceeds in the same manner except in each case we add a DB^2 term to the Σ_r term before we divide it into the total source to that group on the right-hand side. A summary of the iteration is provided below, with a plot to follow giving k_eff as a function of B^2.

B^2	FS^1	ϕ_1	ϕ_2	ϕ_3	ϕ_4	FS^2	k
0	0.04541	0.24269	0.29787	0.48353	1.70959	0.07167	1.57823
0.002	0.04541	0.23295	0.28741	0.46128	1.61299	0.06764	1.48946
0.004	0.04541	0.22397	0.27773	0.44074	1.52444	0.06394	1.40808
0.006	0.04541	0.21565	0.26872	0.42174	1.44303	0.06054	1.33326
0.008	0.04541	0.20793	0.26033	0.40411	1.36799	0.05741	1.26429
0.01	0.04541	0.20075	0.25249	0.38771	1.29864	0.05452	1.20054
0.012	0.04541	0.19404	0.24514	0.37241	1.23441	0.05184	1.14149
0.014	0.04541	0.18777	0.23824	0.35812	1.17478	0.04935	1.08666
0.016	0.04541	0.18189	0.23175	0.34473	1.11932	0.04703	1.03566
0.017	0.04541	0.17908	0.22864	0.33835	1.09302	0.04593	1.01148
0.0174	0.04541	0.17798	0.22742	0.33585	1.08276	0.0455	1.00204
0.01742	0.04541	0.17793	0.22736	0.33573	1.08225	0.04548	1.00157
0.01744	0.04541	0.17788	0.2273	0.3356	1.08174	0.04546	1.00111
0.01746	0.04541	0.17782	0.22724	0.33548	1.08123	0.04544	1.00064
0.01748	0.04541	0.17777	0.22718	0.33536	1.08072	0.04542	1.00017
0.017486	0.04541	0.17775	0.22717	0.33532	1.08057	0.04541	1.00003
0.017487	0.04541	0.17775	0.22716	0.33531	1.08055	0.04541	1.00001
0.017488	0.04541	0.17774	0.22716	0.33531	1.08052	0.04541	0.99998
0.01749	0.04541	0.17774	0.22715	0.33529	1.08047	0.04541	0.99994
0.0175	0.04541	0.17771	0.22712	0.33523	1.08022	0.0454	0.9997
0.018	0.04541	0.17636	0.22563	0.33216	1.06763	0.04487	0.98813
0.02	0.04541	0.17117	0.21984	0.32035	1.01937	0.04286	0.94374
0.022	0.04541	0.16627	0.21437	0.30923	0.97424	0.04097	0.90223
0.024	0.04541	0.16164	0.20918	0.29875	0.93197	0.0392	0.86334

The normalized flux spectrum is
$\phi_1 = 0.164$
$\phi_2 = 0.210$
$\phi_3 = 0.310$
$\phi_4 = 1.0$

It is a little bit harder than the infinite-medium spectrum. More high-energy neutrons are required to make up for leakage (Fig. 4.4).

Fig. 4.4 k_{eff} versus buckling

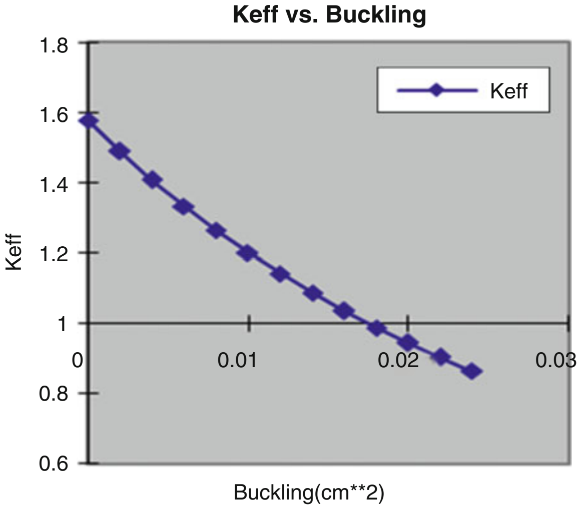

4.7.4 Group Collapse

Now collapse the upper three groups to a fast group and leave the thermal group alone. Then, we have for the nu*fission cross section:

$$\begin{aligned} \nu\Sigma_{\mathrm{f}}^{1} &= (0.164{*}0.00288 + 0.210{*}0.00017 + 0.310{*}0.00122) \\ &\quad /(0.164 + 0.210 + 0.310) = 0.0008862/0.684 = \mathbf{0.00130} \end{aligned}$$

$$\begin{aligned} 3\Sigma_{\mathrm{tr}}^{1} &= (0.164{*}0.46484 + 0.210{*}0.99536 + 0.310{*}1.82077)/0.684 \\ &= 0.8497/0.684 = \mathbf{1.2422} \end{aligned}$$

$$D_1 = 1/1.2422 = \mathbf{0.805}$$

$$\chi_1 = 0.5503 + 0.4348 + 0.0149 = \mathbf{1.0}$$

$$\begin{aligned} \Sigma_{\mathrm{r}}^{1} &= (0.164{*}0.10297 + 0.210{*}0.14361 + 0.310{*}0.09292)/0.684 \\ &= 0.07585/0.684 = \mathbf{0.1109} \end{aligned}$$

$$\Sigma_{\mathrm{s}}^{1\to 2} = 0.310{*}0.09083/0.684 = \mathbf{0.04117}$$

Problems

Problem 4.1: List and describe the three approximations made in deriving the multigroup diffusion equations from the neutron transport equation.

Problem 4.2: Listed below are a set of typical group constants for a BWR. Calculate the multiplication factor for this reactor if it can be treated as a right circular cylinder of height of 370 cm and a diameter of 340 cm.

Group constant	Group 1	Group 2
$\nu\Sigma^{g}_{\text{fission}}$	0.001348	0.040783
$\Sigma^{g}_{\text{absorption}}$	0.001469	0.040249
D_g	0.859599	0.142481
$\Sigma^{g}_{\text{removal}}$	0.044587	0.040249
χ_g	1.0	0.0

Problem 4.3: Using the group constants from the previous Problem 4.1, calculate k_∞, the resonance escape probability, the fast fission factor, and the fast and thermal non-leakage probabilities for this reactor.

Problem 4.4: Calculate the critical radius for an unreflected right circular cylinder reactor characterized by the following group constants.

Group constant	Group 1	Group 2
$\nu\Sigma^{g}_{\text{fission}}$	0.002562	0.15180
$\Sigma^{g}_{\text{absorption}}$	0.001930	0.09509
$\Sigma^{g}_{\text{transport}}$	0.466100	2.95420
$\Sigma^{g}_{\text{downstream}}$	0.055140	–
χ_g	1.0	0.0

Reactor height = 25 cm

Problem 4.5: Calculate the multiplication factor for an unreflected fast reactor with the following cross-sectional data and core size

Group constant	Group 1	Group 2
$\nu\Sigma^{g}_{\text{fission}}$	0.011040	0.005486
$\Sigma^{g}_{\text{absorption}}$	0.004598	0.004108
$\Sigma^{g}_{\text{downstream}}$	0.023420	–
$\Sigma^{g}_{\text{transport}}$	0.028020	0.242200
χ_g	0.55	0.45

Core radius = 111 cm Core height = 91.44 cm

Problem 4.6 Derive an equation for k_{eff} in case of the three-group problem described by the following equations:

$$\begin{bmatrix} D_1B^2+\Sigma^1_{\text{r}} & 0 & 0 \\ -\Sigma^{1\to 2}_{\text{s}_0} & D_2B^2+\Sigma^2_{\text{r}} & 0 \\ -\Sigma^{1\to 3}_{\text{s}_0} & -\Sigma^{2\to 3}_{\text{s}_0} & D_3B^2+\Sigma^3_{\text{r}} \end{bmatrix} \begin{Bmatrix} \phi_1 \\ \phi_2 \\ \phi_3 \end{Bmatrix} = \begin{bmatrix} \nu\Sigma^1_{\text{f}} & \nu\Sigma^2_{\text{f}} & \nu\Sigma^3_{\text{f}} \\ 0 & 0 & 0 \\ 0 & 0 & 0 \end{bmatrix} \begin{Bmatrix} \phi_1 \\ \phi_2 \\ \phi_3 \end{Bmatrix}$$

Problem 4.7 Compute an infinite-medium spectrum for the following six-group fast reactor problem that is directly coupled.

	Group 1	Group 2	Group 3	Group 4	Group 5	Group 6
D	3.1348	2.5292	1.8095	0.7256	0.30601	0.1350
Σ_r	0.08175	0.05189	0.00813	0.03373	0.51380	0.37846
$\Sigma^{sg \to g+1}$	0.07066	0.041489	0.002214	0.015413	0.00192	–
$\nu\Sigma_f$	0.037445	0.023684	0.010181	0.020241	0.42601	4.1648
χ	0.052579	0.52040	0.41085	0.016081	0.0008	0.0

Problem 4.8 Use the spectrum calculated as solution for Problem 4.7 to collapse the upper three groups to one group and the lower three groups to a second group for broad group cross sections. Calculate all five cross sections.

Problem 4.9 Estimate the minimum group spacing that will yield directly coupled multigroup equations for C^{12}, D^2, Be^9, and Na^{22}.

Problem 4.10 What percentage of the neutrons slowing down in hydrogen will tend to skip groups if the group structure is chosen that $\left(E_{g-1}/E_g\right) = 100$?

Problem 4.11 Write out the detailed of the multigroup diffusion equations, $\boldsymbol{M}\phi = k^{-1}\boldsymbol{F}\phi$, for a four-group model in which:

(a) There is direct coupling.
(b) The fission source exists only in the upper two groups.
(c) Only the lowest group contains thermal neutrons.

Problem 4.12 Solve the collision rate equation for hydrogen as

$$F(E) = \int_E^{E_0} dE' \frac{f(E')}{E'} + S_0\delta(E - E_0)$$

by restricting our attention to $E < E_0$ and using the source as boundary condition as $E \to E_0$

Problem 4.13 Determine the neutron flux $\phi(E)$ resulting from an arbitrary source in an infinite hydrogenous medium by solving the infinite-medium slowing down equation with a general source term $S(E)$.

Problem 4.14 Show that for a mixture of N nuclides, the collision rate density $F(E)$ can be written in asymptotic region as

$$F(E) = \frac{S_0}{E\xi} \quad \text{and} \quad \bar{\xi} = \frac{\sum_{i=1}^{N} \Sigma_{si}\xi_i}{\Sigma_s}$$

Problem 4.15 Show that for $A > 1$ and a monoenergetic source S_0 at E_0, we have the following relation:

$$F(E) = \frac{S_0 E_0^{(\alpha/(1-\alpha))}}{E\bar{\xi}} \frac{1}{E^{(\alpha/(1-\alpha))}}, \qquad \alpha E_0 < E < E_0$$

Problem 4.16 Show that for $A > 1$, compute and plot the collision density function $F_3(E)$ for neutrons that have had three collisions. Discuss the continuity of $F_3(E)$ and its derivatives at $E - E_0$, αE_0, $\alpha^2 E_0$, and $\alpha^3 E_0$:

Problem 4.17 By means of the one-group treatment, estimate the critical radius of a spherical core of uranium-235 surrounded by a thick reflector of uranium-238. The cross sections may be taken as the average values for neutrons in the energy range of 0.4 to 1.35 MeV; then

Uranium-235:	$\sigma_f = 1.27$ (barn)	$\sigma_a = 1.40$ (barn)	$\sigma_{tr} = 5.7$ (barn)	$v = 2.52$
Uranium-238:	$\sigma_f = 1.27$ (barn)	$\sigma_a = 1.40$ (barn)	$\sigma_{tr} = 5.7$ (barn)	$v = 2.52$

Solution The solution to this problem is as follows:

The density of uranium is approximately 19 g/cm^3, so that atoms N for both uranium-235 and uranium-238 are close to 0.048×10^{24} nuclei per cm^3.

For the *core*,

$$\Sigma_a = 0.048 \times 1.40 = 0.067\,\text{cm}^{-1} \quad \text{and} \quad \Sigma_{tr} = 0.048 \times 5.7 = 0.27\,\text{cm}^{-1}$$

Thus,

$$L^2 = \frac{1}{3\Sigma_{tr}\Sigma_a} = \frac{1}{(3)(0.27)(0.067)} = 18\,\text{cm}^2$$
$$L = 4.24\,\text{cm}$$

For the *reflector*,

$$\Sigma_a = 0.048 \times 0.13 = 0.0062\,\text{cm}^{-1} \quad \text{and} \quad \Sigma_{tr} = 0.048 \times 5.8 = 0.28\,\text{cm}^{-1}$$

Thus,

$$L^2_{\text{refl.}} = \frac{1}{3\Sigma_{tr}\Sigma_a} = \frac{1}{(3)(0.28)(0.0062)} = 190\,\text{cm}^2$$
$$L_{\text{reff.}} = 13.78\,\text{cm}$$

In uranium-235 core, k_∞ is equal to η, i.e., to $v\sigma_f/\sigma_a$, so that

$$k_\infty = (2.52)(1.27)/(1.40) = 2.3$$

Hence, by the one-group critical equation, we can write

$$B_c^2 = \frac{k_\infty - 1}{L^2} = \frac{2.3 - 1}{18} = \frac{1.3}{18} = 0.072\,\text{cm}^{-2}$$

or

$$B_{\mathrm{c}} = 0.27\,\mathrm{cm}^{-1}$$

It is found that $R_{\mathrm{c}}/L_{\mathrm{refl.}}$ is not large in this case, so that for one-group critical equation for a spherical core with an infinitely thick reflector written as below must be used:

$$B_{\mathrm{c}}R_{\mathrm{c}}\coth(B_{\mathrm{c}}R_{\mathrm{c}}) = -\frac{D_{\mathrm{r}}}{D}\left(1 + \frac{R_{\mathrm{c}}}{L_{\mathrm{refl.}}}\right) + 1$$

However, since D and D_{r} are approximately equal, it reduces to

$$\tan\left(B_{\mathrm{c}}R_{\mathrm{c}}\right) = -B_{\mathrm{c}}L_{\mathrm{refl.}}$$

Hence, $\tan(0.27R_{\mathrm{c}}) = -(0.27)(14) = -3.8$ and R_{c} is 6.8 cm. Note that the experimental value is close to 6.0 cm.

References

1. J.J. Duderstadt, L.J. Hamilton, *Nuclear Reactor Analysis* (Wiley, New York, 1976)
2. P.F. Zweifel, *Reactor Physics* (McGraw-Hill, New York, 1973)

Chapter 5
Numerical Methods in Modeling Neutron Diffusion

The constructive techniques of functional analysis, using a computer code, allow us to build up directly, in their original domain of definition, solutions to linear transport equation. FEMP code is a computer code written in FORTRAN 77, to approximate the Boltzmann transport equation in one-dimensional form using a spherical harmonic for the angular variable and a linear finite element for the spatial variable.

5.1 Introduction

FEMP1D stands for **f**inite **e**lement, **m**ultigroup, $\mathbf{P_N}$, **one-d**imensional code. The code approximates the Boltzmann transport equation in one dimension using a spherical harmonic basis for the angular variable and a linear finite element (hat function) basis for the spatial variable. The energy variable is dealt with by the fairly standard multigroup approximation. In rectangular and spherical coordinates, the spherical harmonic basis reduces to the Legendre polynomials. The code was developed partly as a tutorial for a nuclear reactor analysis class, where this book is going to be used as a text. The code partly is providing a flexible code that could take its input to a number of forms, particularly cross-sectional data, and partly to provide a testing ground for algorithms to be implemented in the multidimensional versions of this code series. It has proven to be fairly, efficient and fairly, robust. It has been run on a number of mainframes, minis, workstations, and micros. FEMP1D is written in FORTRAN 77 and should be reasonably transportable.

B. Zohuri, *Neutronic Analysis For Nuclear Reactor Systems*,
DOI 10.1007/978-3-319-42964-9_5

5.2 Problem(s) Solved

FEMP1D solves a number of steady-state neutral particle radiation transport problems based on the Boltzmann model for the energy-dependent, angular flux density conservation equation. It approximates the energy-dependent, angular flux density with a spherical harmonic basis in the angle variables, with finite element hat functions in the spatial variable, and with the standard multigroup coefficients for the energy variable. It will provide four types of strategies for iterating over the group structure to obtain solutions. The four outer iteration options are:

1. Inhomogeneous source only (no fission)
2. Inhomogeneous source with fission
3. Fission eigenvalue calculation
4. Fission eigenvalue searches

It will accept volume and surface sources. It will efficiently solve problems with a significant number of upscatter groups. It will accept cross-sectional input from ANISN style libraries, AMPX style libraries, and input stream data, as long as they have the same group structure. It will collapse ANISN and AMPX cross sections to generate problem-dependent libraries. FEMP will accept response functions as part of the input stream that can be multiplied against the isotropic flux solution. It integrated over energy and possibly volume, to obtain macroscopic reaction rates. It also allocates core storage dynamically to make the most efficient use of high-speed memory no matter how much or how little is available.

5.2.1 Transport Equation

The steady-state Boltzmann transport equation for the multidimensional energy and angular-dependent angular flux density is given by

$$\begin{aligned}\vec{\nabla}\cdot\vec{\boldsymbol{\Omega}}\,\phi\left(\vec{r},E,\,\vec{\boldsymbol{\Omega}}\right)+\Sigma_T\left(\vec{r},E,\,\vec{\boldsymbol{\Omega}}\right)\phi\left(\vec{r},E,\,\vec{\boldsymbol{\Omega}}\right)&=S\left(\vec{r},E,\,\vec{\boldsymbol{\Omega}}\right)\\&+\int_{E'}\int_{\Omega'}\Sigma_s\left(\vec{r},E',\,\vec{\boldsymbol{\Omega}}'>,\,\vec{\boldsymbol{\Omega}}\right)\phi\left(\vec{r},E',\,\vec{\boldsymbol{\Omega}}'\right)dE'\,d\vec{\boldsymbol{\Omega}}'\\&+\int_{E'}\int_{\Omega'}\frac{\chi(E')}{4\pi}\nu\Sigma_f(\vec{r},\,E)\phi\left(\vec{r},E',\,\vec{\boldsymbol{\Omega}}'\right)dE'\,d\vec{\boldsymbol{\Omega}}'\end{aligned}\tag{5.1}$$

where

$\phi\left(\vec{r},E,\,\vec{\boldsymbol{\Omega}}\right)$ = neutron angular flux density

$\Sigma_T\left(\vec{r},E,\,\vec{\boldsymbol{\Omega}}\right)$ = scattering cross section for transfer from energy. E' and solid angle $\vec{\boldsymbol{\Omega}}'$ to energy E and solid angle $\vec{\boldsymbol{\Omega}}$

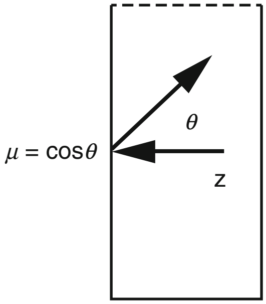

Fig. 5.1 Simple slab reactor

$\Sigma_S\left(\vec{r}, E,\ \vec{\Omega}' > E,\ \vec{\Omega}\right)$ = scattering cross section for transfer from energy

$\chi(E')\ v\Sigma_f(\vec{r}, E)$ = number of neutrons produced per fission at energy E times the fission cross section for a neutron of energy E' (fission is generally considered to be isotropic in the laboratory reference frame, and this was explained in Chap. 3 of the book

$S\left(\vec{r}, E,\ \vec{\Omega}\right)$ = the time-independent source of neutrons at position $\vec{r}$, with energy E and moving in direction of $\vec{\Omega}'$, and for simplicity, it will be called inhomogeneous source

5.2.2 *Angle Discretization*

Rather than deriving the general spherical harmonic approximation to the above equation, consider the case of a one-dimensional infinite slab.

Taking the Fig. 5.1 under consideration, the transport Eq. 5.1 immediately simplifies to

$$\begin{aligned}\mu\phi(z, E, \mu) + \Sigma_T(z, E, \mu)\phi(z, E, \mu) &= S(z, E, \mu)\\ &+ \int\limits_{E'}\int\limits_{\Omega'} \Sigma_S(z, E',\ \Omega' > E,\ \Omega)\phi(z, E',\ \Omega')dE'\,d\Omega'\\ &+ \int\limits_{E'}\int\limits_{\Omega'} \frac{\chi(E')}{4\pi} v\Sigma_f(z, E)\phi(z, E,\ \Omega')dE'\,d\Omega'\end{aligned} \tag{5.2}$$

The angular flux density can be expanded in Legendre polynomials.

$$\phi(z, E, \mu) = \sum_{\ell=1}^{\infty} \phi_\ell(z, E)\frac{2\ell}{2}P_\ell(\mu) \tag{5.3}$$

The scattering cross section can be expanded in terms of the angle of scattering in the lab system as

$$\Sigma_S(z, E', \Omega' > E, \Omega) = \sum_{m=0}^{M} \Sigma_{sm}(z, E) \frac{2m+1}{4\pi} P_m(\mu_{\mathrm{LAB}}) \tag{5.4}$$

In addition, the inhomogeneous source can be expanded as

$$S(z, E, \mu) = \sum_{\ell=0}^{L} S_\ell(z, E) \frac{2\ell+1}{4\pi} P_\ell(\mu) \tag{5.5}$$

When these expansions are substituted into the transport equation and the addition theorem used to express the angle of scattering in the lab reference frame in terms of the incoming and outgoing cosines of the angle the scattered neutron makes with the fixed problem axis, a fairly, complicated equation with an infinite number of terms is obtained. In order to reduce this equation for solution on the computer, it is multiplied in term by each of the Legendre polynomials and integrated from $a - 1\mathrm{to}a + 1$. By making use of the orthogonality relationship for the Legendre polynomials, this reduces to a coupled set of equations infinite in extent. The general equation obtained when this is done becomes

1. **P_N equation in rectangular coordinate**

$$\begin{aligned}(n+1)\frac{d\phi_{n+1}(z,E)}{dz} + n\frac{d\phi_{n-1}(z,E)}{dz} + (2n+1)\Sigma_T(z,E)\phi_n(z,E) \\ = (2n+1)\int\limits_{E'} \Sigma_{sn}(z,E' > E)\phi(z,E)dE' + \delta_{on}\chi(E)\int\limits_{E} \mathrm{v}\Sigma_f(z,E')\phi_0(z,E') \\ + (2n+1)s_n(z,E)\end{aligned} \tag{5.6}$$

2. **P_N equation in cylindrical coordinate**

$$\begin{aligned}\frac{1}{2}\left(\frac{d}{dr} + \frac{k+2}{r}\right) \times \left\{(n+k+2)(n+k+1)\phi_{n+1,k+1}(r,E) - (n-k-1)(n-k)\phi_{n+1,k+1}(r,E)\right\} \\ + \frac{1}{2}\left(\frac{d}{dr} + \frac{k+2}{r}\right)\left\{\phi_{n+1,k+1}(r,E) - \phi_{n+1,k+1}(r,E)\right\} + (2n+1)\Sigma_T(,E)\phi_n(r,E) \\ = (2n+1)\int\limits_{E'} \Sigma_{sn}(z,E' > E)\phi_n(z,E')dE' + \delta_{on}\chi(E) \times \int\limits_{E} \mathrm{v}\Sigma_f(z,E')\phi_0(z,E')dE' + (2n+1)s_n(z,E)\end{aligned} \tag{5.7}$$

3. **P_N equation in spherical coordinate**

$$\begin{aligned}(n+1)\left(\frac{d}{dr} + \frac{n+2}{r}\right)\phi_{n+1}(r,E) + n\left(\frac{d}{dr} + \frac{n-2}{r}\right)\phi_{n-1}(r,E)(2n+1)\Sigma_T(r,E)\phi_n(r,E) \\ = (2n+1)\int\limits_{E'} \Sigma_{sn}(z,E' > E)\phi_n(z,E')dE' + \delta_{on}\chi(E)\int\limits_{E} \mathrm{v}\Sigma_f(z,E')\phi_0(z,E')dE' + (2n+1) \\ \times s_n(z,E)\end{aligned} \tag{5.8}$$

Since each of the above equations contains terms from the previous order and the next highest order, there will always be more unknowns than there are equations. In order to obtain a finite set of equations, the highest order coefficients are neglected and a solvable system is achieved. The only way to determine if this produces an acceptable solution is to obtain the same answer from at least two consecutive orders of solution. Normally the spherical harmonic expansion used here converges very rapidly and with a little experience; an appropriate order can be chosen quickly. The highest order for the flux expansion must be chosen as an odd number. This is required by the code, as choosing an even order produces no better solution than the next lower odd order, and allowing both even and odd highest orders would complicate the programming slightly.

5.2.3 Energy Discretization

The energy discretization is carried out using the standard multigroup approximation. That is, for the g$^{\text{th}}$ energy group extending from energy E_{g+1} to E_g, the following holds:

$$\phi_n(z,E) = f(E)\phi_n^g \quad E_{g+1} \le E \le E_g \tag{5.9}$$

$$\phi_n^g(z) = \frac{\int_{E_{g+1}}^{E_g} \phi_n(z,E)\,dE}{\int_{E_{g+1}}^{E_g} f(E)\,dE} \tag{5.10}$$

$$\sum\nolimits_T^g(z) = \frac{\int_{E_{g+1}}^{E_g} f(E)\Sigma_T(z,E)\,dE}{\int_{E_{g+1}}^{E_g} f(E)\,dE} \tag{5.11}$$

and

$$\chi_g \int_{E_{g+1}}^{E_g} \chi(E)\,dE \tag{5.12}$$

with

$$\sum\nolimits_{sn}^{g'>g}(z) = \frac{\int\limits_{E_{g+1}}^{E_g}\int\limits_{E_{g'+1}}^{E_{g'}} f(E')\Sigma_{sn}(z,E')dE'\,dE}{\int\limits_{E_{g'+1}}^{E_{g'}} f(E)\,dE} \tag{5.13}$$

Having made this approximation, the multigroup P_N equation (slab) can be written as

$$\begin{aligned}&(n+1)\frac{d\phi_{n+1}^{g}(z)}{dz} + n\frac{d\phi_{n-1}^{g}(z)}{dz} + (2n+1)\Sigma_T^g(z)\phi_n^g(z)\\ &= (2n+1)\sum_{g'=1}^{g'=NOG}\sum\nolimits_{sn}^{g'>g}(z)\phi_n^{g'>g}(z)\phi_n^{g'} + \delta_{on}\chi_g\sum_{g'=1}^{g'=NOG} v\sum\nolimits_{f}^{g'}(z)\,\phi_0^g(z)\\ &\quad + (2n+1)s_g^n(z)\end{aligned} \tag{5.14}$$

where

$$1 \le g \le \mathrm{NOG} \tag{5.15}$$

This will give a set of NOG*$(N+1)$ equations in the spatially dependent group flux expansion coefficients. This set could be solved directly by finite differencing these equations. However, further mathematical manipulation will reduce computer storage and run times by at least a factor of two.

Once the energy constants have been defined and calculated, the multigroup P_N equations can be reduced further by solving each of the odd-order equations for the highest odd-order flux coefficients and substituting each odd-order coefficient solution into the next lower even-order equation. This reduces the total number of equations to be solved by a factor of two. The gth order equation then becomes coupled to the $1-2$ order and $1+2$ order equations. This substitution also introduces second derivatives that can be integrated out by parts in the spatial discretization process.

5.2.4 Spatial Discretization

The spatial discretization is accomplished by expanding flux coefficients in a sum of linear splines or "hat" functions. Each "hat" function is defined as being equal to 1.0 at one mesh point and zero at all others. A picture of the i$^{\text{th}}$ "hat" function is given in Fig. 5.2.

The flux coefficient expansion can then be written as

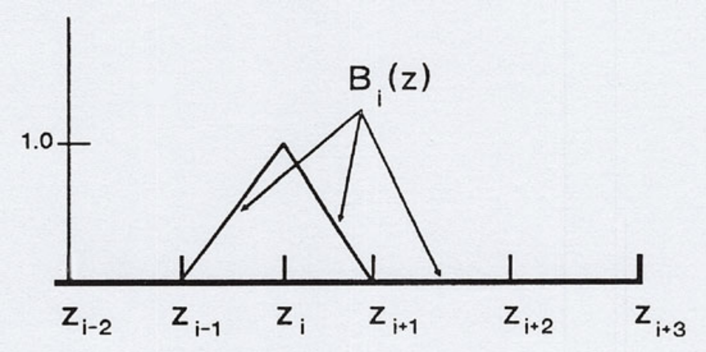

Fig. 5.2 *i*th "hat" function

$$\phi_n^g(z) = \sum_{i=1}^{NZ} \phi_{li}^g B_i(z) \tag{5.16}$$

where each of the $B_i(z)$ is given by

$$\begin{aligned} B_i(z) = 0 \qquad & z \le z_{i-1}, \quad z \ge z_{i+1} \\ = \frac{z - z_{i-1}}{z - z_{i-1}}, \quad & z_{\mathrm{i}-1} \le z \le z_i \\ = \frac{z_{i+1} - z}{z_{i+1} - z}, \quad & z_{\mathrm{i}} \le z \le z_{i+1} \end{aligned} \tag{5.17}$$

This expansion is inserted into each of the P_N equations, and a system of NOG*(N + 1)/2 equations is obtained with NZ*NOG*(N + 1)/2 unknowns. In order to obtain a solution, each of the P_N equations is multiplied by one of the $B_i(z)$ and an integration performed over all z as per the standard Galerkin procedure of finite element analysis. This will lead to a set of NZ*NOG*(N + 1)/2 equations for the NZ*NOG*(N + 1)/2 unknowns. That can then be solved by matrix methods.

5.2.5 Matrix Formulation

Finally, the spatial, energy and angle discretized equations can be written in the following symbolic matrix equation:

$$|\boldsymbol{M}|\{\boldsymbol{\phi}\} = \{\boldsymbol{S}\} + \left(\boldsymbol{k}^{-1}\right)[\boldsymbol{F}]\{\boldsymbol{\phi}\} \tag{5.18}$$

where ***M*** is the migration matrix that considers the effects *of* transfers between groups and transport in the spatial dimension. The ***S*** vector is the inhomogeneous source. The ***F*** matrix is the fission source matrix and corresponds to the generation *of* neutrons because of fission. The eigenvalue k must be introduced if a solution is desired for the pure eigenvalue problem ($\boldsymbol{S} = 0$). It should be kept in mind that though the set *of* equations solved by FEMP1D only considers one spatial dimension, the equations are actually the solution to a three-dimensional problem in space, angle, and energy.

Each of the matrices is NZ*{(N+1)/2}*NOG by NZ*{(N+ 1)/2}*NOG with the majority *of* the elements identically equal to zero. In order to take advantage of this zero structure, the flux vector is ordered in a special way. Mesh point, Legendre order, and energy group index the flux vector. Thus the locations in the flux vector would start with the first energy group, lowest Legendre order, and run from the first to the last spatial index. Then the Legendre order would be incremented and the spatial mesh covered again. After the highest Legendre order is complete, the second-group coefficients would be included. In order to make this ordering scheme a little clearer, consider an example problem that uses four groups, six Legendre orders, and five mesh points. This will be a matrix that is 60 by 60 (5*{6/2}*4).

The matrix ordering scheme can be clarified by considering the overall matrices to be made up of sub-matrices. At the first level, the problem matrices will be made up of the group sub-matrices. The above equation can be written as

$$\begin{bmatrix} M_{11} & 0 & 0 & 0 \\ M_{21} & M_{22} & 0 & 0 \\ M_{31} & M_{32} & 0 & 0 \\ M_{41} & M_{42} & M_{43} & M_{44} \end{bmatrix} \begin{bmatrix} \phi_1 \\ \phi_2 \\ \phi_3 \\ \phi_4 \end{bmatrix} = \begin{bmatrix} S_1 \\ S_2 \\ S_3 \\ S_4 \end{bmatrix} + 1/k \begin{bmatrix} F_{11} & F_{12} & F_{13} & F_{14} \\ F_{21} & F_{22} & F_{23} & F_{24} \\ F_{31} & F_{32} & F_{33} & F_{34} \\ F^{41} & F^{42} & F^{43} & F^{44} \end{bmatrix} \begin{bmatrix} \phi_1 \\ \phi_2 \\ \phi_3 \\ \phi_4 \end{bmatrix} \tag{5.19}$$

where the $M_{g.g'}$ matrix is now 15 by 15 (5*{6/2}) square and the ϕ_g vectors are 15 elements long. The equation for ϕ_2 vector can be written as

$$[M_{22}][\phi_2] = [S_2] + 1/k[FS_2] - [M_{21}][\phi_1] \tag{5.20}$$

where

$$[FS_2] = [F_{21}][\phi_1] + [F_{22}][\phi_2] + [F_{24}][\phi_3] + [F_{24}][\phi_4] \tag{5.21}$$

And the M_{22} and F_{22} matrices can be written as

$$[M_{22}] = \begin{bmatrix} \mu_{00} & \mu_{02} & 0 \\ \mu_{20} & \mu_{22} & \mu_{24} \\ 0 & \mu_{42} & \mu_{44} \end{bmatrix}_{22} \quad [F_{22}] = \begin{bmatrix} f_{00} & 0 & 0 \\ 0 & 0 & 0 \\ 0 & 0 & 0 \end{bmatrix}_{22} \tag{5.22}$$

where each of the μ_k matrices is 5 by 5 square and the sub-vector that they multiply in the vector is five elements long. Finally, we obtain

$$[FS_2] = [F_{21}][\phi_1] + [F_{22}][\phi_2] + [\mu_{00}]_{21}[\phi_0]_1 - [\mu_{02}]_{21}[\phi_2]_1 \tag{5.23}$$

And the μ_{00} matrix, for example, is given by

$$[\mu_{00}]_{22} = \begin{bmatrix} m_{11} & m_{12} & 0 & 0 & 0 \\ m_{21} & m_{22} & m_{23} & 0 & 0 \\ 0 & m_{32} & m_{33} & m_{34} & 0 \\ 0 & 0 & m_{43} & m_{44} & m_{45} \\ 0 & 0 & 0 & m_{54} & m_{55} \end{bmatrix}_{22} \tag{5.24}$$

Not all options are complete for every case at this time. In a rectangular coordinate system, it is capable of dealing with angular approximations of (r, θ, z) cylindrical coordinate system; it is only capable of dealing with a P_1 spherical (r, θ, φ) of the angular flux density.

5.3 Solution Strategy

In order to efficiently solve all of the coefficients of the energy-dependent angular flux density, a strategy must be implemented that takes advantage of the sparsity of the overall system matrices. This strategy can best be implemented by using a series of iterative sweeps through the spatial, angular, and energy meshes. The outermost iterative solution process is implemented with a sweep over the energy groups. The middle iterative process involves a sweep over the Legendre orders. And finally the inner solution over the spatial mesh can be implemented iteratively, but a direct solution is very rapid in one-dimensional and is used by FEMPID. (FEMP2D and FEMP3D use iterative techniques to solve the spatial mesh.)

The entire iterative process begins by assuming a fission source distribution is available and can be combined with any inhomogeneous sources that are to be considered. Then the outer iteration process starts with the highest energy group and solves for the angular flux coefficients based on the "known" source. In most problems, these sources will be largely isotropic, so the isotropic flux coefficients are calculated assuming that the higher-order coefficients are zero. The isotropic flux then provides a within-group scatter source to the next higher Legendre order coefficients. The P_2 coefficients are found based on the P_0 isotropic flux components previously calculated and assuming that the P_4 components are zero. This process is then repeated for the P_4 components and on up until the highest order coefficients have been found. Then the iteration (middle) is started over for the Po components using the calculated P, components from the previous sweep. This process is repeated until a convergence criterion is satisfied on the isotropic flux. At each Legendre order, the spatially dependent flux coefficients are found using a direct tri-diagonal solver. After a given group is converged, the process moves on to the next lower group. The recently completed group then provides an update in scatter source to this group below it. Since most neutral particle radiation transport problems are dominated by downscatter, sweeping from high-energy to low-energy groups speeds the convergence of this type of outer iteration.

Once a sweep through the groups is completed, a new fission source is computed. This source is then rationed to the previous source for fission eigenvalue problems in order to obtain an estimate of K_{e1C} for the assembly. Once the fission source is calculated, the process can be repeated. The process continues until the fission source is converged. Then, one more outer iteration is performed in order to obtain the flux coefficients for the converged fission source.

5.3.1 Types of Outer Iterations

FEM11D performs, basically, four types of outer iterations depending upon the type of problem data available and desired. It will perform a transport calculation for an inhomogeneous source without any fission present. It will perform a transport calculation for an inhomogeneous source with fission present. It will perform a fission eigenvalue calculation for a given geometry. Moreover, it will perform a fission eigenvalue calculation to achieve a desired k_{eff} by varying the problem data. Each of these calculations will now be discussed in more details.

5.3.2 Inhomogeneous Source (No Fission)

The inhomogeneous source calculation corresponds to calculating the transport of particles throughout an assembly that are emitted independent of the flux of those particles in the assembly. A typical example of this type of calculation is the calculation of the gamma fluxes produced by a radioactive gamma source in a shielded cavity.

For the inhomogeneous source case, the source of particles is specified for all energies and angles, so one outer iteration will generally be all that is required to completely solve the problem. However, since the middle iteration process is an iterative one, if the middle iterations do not converge for a given group, FEMPID will attempt to perform a second outer if the middle iterations do not converge for every group. If there is upscatter in the problem, a separate mini-outer iteration is performed over the upscatter groups. The most likely place that this will occur is if an adjoint problem is being run, and the adjoint source is a thermal neutron detector that perturbs the flux. If the mini-outers over the upscatter groups converge during the first outer iteration, only one outer iteration will be performed.

Generally, there is no full upscatter involving all groups, and so a mini- or sub-outer iteration to converge only the upscatter groups is efficient.

FEMP1D accepts both volumetric and surface sources. Both types of sources must be represented by their Legendre component expansions. A fist scatter source is planned, but has not been implemented yet.

5.3.3 Inhomogeneous Source (With Fission)

The second type of outer that FEMPID performs is an inhomogeneous source with fission calculation for a subcritical assembly driven by an external source. If the assembly is critical, or supercritical, the FEMP1D calculation will not converge. For this case, FEMP1D starts out with a zero fission source for the first iteration and allows the fission source to build up over a series of outers. This is not very efficient if the assembly is only slightly subcritical and some acceleration is attempted. For this type of problem, a large number of outer iterations (200–500) should be planned. FEMP1D has a very flexible restart capability, and periodic restart tapes may be useful in observing the solution progression for this type of problem.

No attempt is made to obtain rebalance factors to accelerate the fission source by treating this problem as if it were an upscatter one. This probably could be done, but source-driven fissionable assemblies near critical do not appear to be that common at this time.

5.3.4 Fission Eigenvalue Calculation

The third type of problem that FEMP1D solves is the fission eigenvalue problem. This entails solving for a multiplication constant, k_{eff}, for a defined assembly of interest. This is the classic fission reactor problem and is the major reason for structuring the FEMP1D solution strategy as it is.

The solution proceeds by guessing a flux and computing a fission source. It is essential that a nonzero flux be chosen so that a nonzero first fission source is obtained. It is not too critical how this flux is chosen and a constant flux guess over space and energy is about as good as on processing a nearly correct spatial shape with a poor energy shape. A flux guess can be obtained automatically from a previous FEMP1D run if the results of the previous run have been saved to a file. In fact it is possible to obtain an approximate flux shape with a very coarse mesh, save the calculation, restart with a fine mesh, and converge in less CPU time than using the fine mesh from the start in one long calculation. The question really comes down to how expensive the CPU time is relative to storage space and analyst effort.

FEMP1D attempts to estimate the condition number for the solution process so as to achieve a relative error in the calculated eigenvalue that represents its deviation from the “true” eigenvalue of the assembly, rather than simply the difference between two calculated eigenvalue in a converging sequence.

5.3.5 Eigenvalue Search Calculation

FEMP1D performs three types of searches to determine the appropriate assembly configuration to give a desired fission eigenvalue. These are a transverse buckling search, an overall dimension search, and a fissile material concentration search.

The transverse buckling search allows an assembly to be modeled quite accurately in one dimension, the dimension of the calculation, and approximates the transport in the opposite dimension by a buckling height. This often is a very useful technique to get an assembly close to critical and obtain a representative spectral shape in each of the materials in the calculation. This can often produce very accurate relative reaction rates. It also can be used to estimate the height that will be required for a critical assembly. However, since materials often change in the transverse direction as well as the calculation direction, this tends not to be a very accurate estimate.

The material outer dimension search is really an order of magnitude estimate for the amount of fissile material required for a critical assembly. It is simply an expansion of all boundaries by a constant factor to obtain a desired k_{eff}.

The fissile material search assumes the material of interest to be composed of three components represented by their respective volume fractions. The reactant material is the fissile material whose concentration per unit volume is required. The diluent material is the material that must be removed to make room for more reactant material. The volume fraction of diluents is decreased by the same volume as the reactant material is increased. The background material is always present and does not change as the search progresses.

This type of search can be used to determine the approximate fissile loading required to achieve a desired k_{eff}. All material thicknesses and the appropriate transverse buckling must be reasonably correct for this type of search to be useful in one dimension.

Obviously, the fission eigenvalue search is merely a loop over the standard fission eigenvalue calculation. However, it is broken out as a separate calculation so that efficient convergence parameters can be chosen easily.

5.4 Middle Iterations

Middle iterations are sweeps through the Legendre order coefficient matrices starting with the isotropic fluxes and increasing to the highest Legendre order required. Each set of Legendre order equations is coupled over three orders except for the lowest and highest which are only coupled over two. On the first sweep, all but the isotropic flux axe assumed to be zero. Then as the sweep moves up in order, subsequent Legendre orders are filled in. When the highest order is solved, the next higher order is truly assumed to be zero, and it remains that way. Each sweep starts over with the isotropic flux and moves up in order. Convergence is achieved when two iterations of the isotropic flux match within the tolerance EPSK. Two options are available for this tolerance. The tolerance check can be applied to the L_{inf} norm of the flux, or it can be applied to the L_{inf} norm of the relative deviation. The L norm is appropriate for fission eigenvalue problems, and the LL norm is appropriate for deep penetration problems where accuracy at flow flux levels is important.

5.5 Inner Iterations

FEMP1D does not perform inner iterations, but rather solves the diffusion matrix equation exactly because it has been reduced to a tri-diagonal matrix that can be solved very efficiently using vector methods.

5.6 Upscatter Iterations

Upscatter problems are handled by performing a mini-outer iteration over the upscatter groups. A rebalance matrix is developed by integrating the upscatter groups over all space and attempting to balance the flow in energy exactly. This accelerates convergence very significantly. The number of mini-outers per real outer is controlled by the parameter NUPS. It usually does not make much sense to perform more than about five mini-upscatter outers per real outer if the fission source has not been spatially converged. However, for a source-only problem, NUPS can be set as high as desired to get convergence in one true outer.

5.7 Inhomogeneous Sources

Inhomogeneous sources can be entered as incident on either the left or the right surface. These sources are represented by their Legendre expansions. Of course, for plane wave sources incident on a slab, a very high-order Legendre expansion will be required.

Volume sources are input as a tensor product in energy and space. Each source is assumed to have its own energy spectrum. The energy spectra should be normalized to 1.0 particle released; however, FEMP1D will attempt to normalize over the assembly to the total number of particles emitted equal to the variable SNORM particles/sec. Once the spectra have been input, the location of the sources by spatial interval is entered in the 46$$ array. Then the relative magnitude of the sources is entered by spatial interval in the 47** array. Thus to obtain the number of source particles emitted in a specific energy group and spatial interval, the value entered in the source spectrum group assigned to that interval is multiplied by the source strength for that spatial interval. This is a fairly flexible scheme but can be complicated if a number of multigroup source spectra are involved.

5.8 Background Concepts

In order to efficiently use a transport code, there are a number of algorithms and simplifications that are important to understand but have never been worthy of a separate publication. This section is an attempt to provide some documentation of these concepts that will make FEMP1D easier to use and understand.

5.8.1 *Mixing Tables*

Mixing tables are required to specify the correct material compositions for the macroscopic materials that make up the transport problem. In order to describe the composition of a given material to the code, three data pieces are required. The material that contains a particular nuclide, or cross-sectional set, must be identified; the nuclide, or cross-sectional set, must be identified; and the quantity of the nuclide, or cross section, set that will go into the material must be determined. Quantities are most easily specified in terms of atoms or molecules per cubic centimeter. However, since cross sections are specified in barns (cm^{-4}), it is usually easier to specify number densities (atoms/volume) in terms of atoms/barn/cm. This convention saves a lot of notation to carry along powers of 10 and makes the magnitude of typical number densities vary from 0.1 atom/barn/cm to 0.01 atom/barn/cm.

Returning to the problem of mixing materials together, the mixing table generally consists of three sets of numbers, two of which are integers and one that is a floating point in the range 0.2–0.0. These numbers can most easily be specified by setting up three arrays or columns and letting the same position in each array identify an operation that is to be performed on a specific nuclide. In FEMPID these three arrays are the 10$, 11$, and the 12* arrays. The 10$ array entry at a specific position identifies the macroscopic material that is under consideration. The 11$ array entry at that position identifies the nuclide or cross-sectional array that will be mixed into that macroscopic material, and the 12* array quantifies how much of that nuclide will be entered. Thus, we might have the following three arrays:

10S$	1	1	1	2	2
11S$	1261	1262	1276	1269	1276
12**	0.00223	0.0201	0.0446	0.0670	0.0335

These arrays correspond to a problem with two materials—UO_2 and H_2O. The first material identified by the first three entries contains three cross-sectional sets. It contains U-235, U-238, and oxygen. The second material contains two cross-sectional sets—hydrogen and oxygen. The first set of three entries tells the code to take 0.00223 atoms/barn/cm of U-235 and place it in material 1. The number 1261 is a common identifier for U-235 in many cross-sectional libraries. The second set of three numbers tells the code to take 0.0201 atoms/barn/cm of U-238 and place it in material 1. The third set of three numbers tells the code to take 0.0446 atoms/bam/cm of oxygen and place it in material 1. Note that oxygen is an element composed of at least three nuclides. Oxygen is not treated in as much detail as uranium because the properties of the minor isotopes do not affect the transport properties significantly and seldom would there be an economic advantage to changing the isotopic composition of natural oxygen. This completes material 1, but additional numbers could be added to each of the three arrays to add (or subtract) more nuclides to (or from) material 1 if that was desirable at a later date. The fourth set of entries adds 0.067 atoms/bam/cm of hydrogen to material 2, and the last set of entries adds 0.0335 atoms/barn/cm of oxygen to material 2. Note that an individual cross-sectional set can occur as many times as necessary to complete the materials.

The mixing table length for this problem is 5 and it bears no relationship to the number of materials in the problem. The mixing table length is determined simply by the number of instructions that the analyst wishes to give the code.

FEMP1D will accept cross-sectional sets from three sources. It can read an ANISN binary library tape. It can read an AMPX working library binary tape, and it can accept cross-sectional input as part of the input stream. It can mix if they have the same group structure. This makes inputting cross-sectional sets by hand an easy way of correcting cross-sectional sets stored on electronic media. The set ID numbers for the 11$ array must match the numbers on the ANISN or AMPX library tapes in order to retrieve these data sets. The input nuclide ID numbers are chosen for the cross-sectional sets coming in through the input stream in the 13S array. The number in the first position in the 13$ array corresponds to the first cross-sectional set read in the 20*, 21*, and 22* arrays. The number in the second position corresponds to the second set of these arrays. It is important to realize that each nuclide in a problem must have a unique nuclide ID number, and therefore, some care must be exercised in assigning nuclide ID numbers for the cross-sectional sets in the input stream.

In order to activate the reading of the ANISN library or the AMPX library, the variables MANSN and MAMPX must be nonzero. In order to mix the input stream cross sections, the variable MCRD must be nonzero.

Premixed cross-sectional sets can be used by entering the cross-sectional sets in the 20*, 21*, and 22* arrays. Then the entries corresponding to these cross sections in the 12* array should be set to 1.0.

5.8.2 Cross-Sectional Collapsing

This will be provided at future data for the FEMP computer code series.

5.9 Input Description

The following annotated input description is an attempted explanation of the input variables and data required by FEMP1D as of the writing of this manual. The current input requirements are always maintained in the first lines of the code listing. If the information in the code conflicts with what is printed here, believe the code listing. If an individual array is not needed for a particular problem, it should be skipped. If an individual variable is not needed for a particular problem, a default value of zero should be entered.

```
PROGRAM FEMP1D
C
C  INPUT DATA
C
C  TITLE CARD(18A4)
C
```

A title card is required to start each problem. More than one problem can be stacked, and the way the code knows to continue with a new problem is when it reads the new title card. If it hits the end of the file, it quits.

```
C
C  1$ ARRAY (32)
C
C  MGEOM=1,   SLAB GEOMETRY
C     =2,     CYLINDRICAL GEOMETRY
C     =3,     SPHERICAL GEOMETRY
C
```

This variable describes the shape of the assembly modeled.

```
C  NOUTR=1,   INHOMOGENEOUS SOURCE
C       =2,   INHOMOGENEOUS SOURCE WITH FISSION
C       =3,   FISSION EIGENVALUE
C       =4,   EIGENVALUE SEARCH PROBLEM
C
```

NOUTR controls the type of problem solved.

```
C  MADJ=0,   FORWARD PROBLEM
C      =1,   ADJOINT PROBLEM
C
```

MADJ decides whether the code will try to solve an adjoint problem or not.

```
C  LPN=SPHERICAL HARMONIC ORDER
C
```

LPN tells the code how many Legendre orders to retain in the approximation to the angular flux density. It should always be an odd number, as even numbers give no better answer than the previous odd-order approximation. In slab and spherical geometries, this can be set to any value. In cylindrical geometry, it can be set to any value, but the code will only perform a P_1 equivalent calculation.

```
C  NMAT=NUMBER OF MATERIAL MIXTURE
C
```

This variable sets the number of mixtures to be generated in the mixing table. Note that all mixtures generated do not have to be used in any given calculation. For instance, one mixing table may be generated for a series of problems, and the materials that are mixed and not chosen in the 33$ array are mixed and ignored. This wastes core storage, but that is not usually a critical parameter.

```
C  MNG=NUMBER OF NEUTRON GROUPS
C
```

The number of neutron groups is used in the calculation. This must match the number of neutron groups on any AMPX libraries used for cross sections. The sum of NNG and NPG must equal the number of groups on an ANISN library or those read in through the input stream.

```
C  MPN=PN ORDER OF CROSS SECTIONS RETAINED
C
```

The Legendre order of the cross-sectional expansion is used for the calculation. This must be equal to or less than the data available on any of the cross-sectional files used in the calculation.

```
C   IHT=TOTAL CROSS SECTION POSITION(ANISM TAPE)
C
```

The location in the ANISN is the cross-sectional table of the total cross section. Normally the default position is location 3. In this case it is preceded by the absorption and fission yield for the particular group. If additional one-dimensional cross sections are used, they are normally stored before the total cross section in the group vectors.

```
C   IHT=WITHIN GROUP SCATTER CROSS SECTION POSITION(ANISM TAPE)
C
```

The location in the ANISN is the cross-sectional table of the within-group scattering cross section. If there is no upscatter, then the within group directly follows the total cross section and IHS is normally 4. If there is upscatter, then a place between the total and the within-group cross sections must be saved for the maximum number of upscatter transfers required.

```
C   LTBL=CROSS SECTION TABLE LENGTH (ANISM TAPE)
C
```

LTBL specifies the total length of the group vector for each group in an ANISN cross-sectional array. It is the sum of the number of one-dimensional cross sections (IHT) plus the upscatter and within-group cross sections (IHS-IHT) plus the number of downscatters. If a complete downscatter problem including hydrogen is modeled, this works out to NOG-1 + IHS. Many truncated tables exist, and the correct value of LTBL must usually be obtained by listing the data titles on an ANISN library file with DIAL.

```
C   MTL=MIXING TABLE LENGTH
C
```

MTL specifies the number of entries anticipated and required in the 10$, 11$, and 12* arrays. It is the total number of mixing instructions and bears no relationship to the number of materials used in the problem.

```
C   MCRD=NUMBER OF MATERIL CROSS SECTIONS FROM CARDS
C
```

MCRD identifies the number of cross-sectional descriptions to be in the 20*, 21*, and 22* arrays. Data Block 2 containing these arrays must be read MCRD times.

```
C  MAMPX=NUMBER OF MATERIL CROSS SECTIONS TO BE READ IN AMPX
C  WORKING LIBRARY FORMAT FROM TAPE16
C
```

If MAMPX is greater than zero, FEMP1D will search for a file on LUN16 with cross sections in the AMPX working library format. The actual value greater than zero is not relevant.

```
C  NX=NUMBER OF MESH POINTS
C
```

NX is the total number of mesh points in the direction of the calculation. This must be 1 more than the number of intervals.

```
C  NZONE=NUMBER OF MATERIAL ZONE IN PROBLEM
C
```

NZONE is the total number of homogeneous material zones in the problem.

```
C  IBL=0, LEFT BOUNDARY IS VACUM
C     =1, LEFT BOUNDARY IS REFLECTING
C     =2, LEFT BOUNDARY HAS SOURCE INCIDENT
C
```

IBL specifies how the left or inner boundary is to be treated with regard to an incident flux. IBL = 0 is not allowed in cylindrical of spherical geometry.

```
C  IBL=0, RIGHT BOUNDARY IS VACUM
C     =1,  RIGHT BOUNDARY IS REFLECTING
C     =2,  RIGHT BOUNDARY HAS SOURCE INCIDENT
C
```

IBR specifies how the right or outer boundary is to be treated with regard to an incident flux.

```
C  ISTRT=0, SET FLUX EQUAL TO ZERO EVERYWHERE
C       =1,  SET FLUX EQUAL TO 1.0 EVERYWHERE
C       =2,  SET FLUX EQUAL TO INPUT FROM TAPES
C
```

ISTRT controls the initial flux estimate. It must be 2 or 3 for a fission eigenvalue or eigenvalue search problem. TAPE3 is the restart tape, and its group structure must match, but its spatial mesh structure does not have to match the actual calculation, as FEMP1D will perform an interpolation onto the selected calculation mesh.

```
C  MCT=0, USE INTEGRAL CONVERGENCE TEST FOR NIDDLE ITERATIONS
C      =1, USE POINTWISE CONVERGENCE TEST FOR MIDDLE ITERATIONS
C
```

The integral test computes the L_2, norm of the error vector for the P_0 component of the angular flux density. It compares this relative error with the input value for EPSK. The pointwise test computes the L_{inf}, norm of the error vector for the P_0 component of the angular flux density. This process is not vectorizable, and therefore it takes a bit longer than the integral test. The integral test is more appropriate for fission problems, and the pointwise test is more appropriate for shielding or deep penetration problems.

```
C  ITMX2=MAXIMUM NUMBER OF OUTER INTERATIONS FOR FISSION PROBLEMS
C
```

ITMX3 should be set large enough to get convergence. For inhomogeneous source problems, a value of 1 should be adequate; however, setting it higher will not mean that the code will use more than what is required. For inhomogeneous source with fission problems, a fairly high value will be required, particularly if the assembly is nearly critical. Writing a restart file is highly recommended for this type of problem if a reasonable estimate of ITMX3 cannot be obtained “a priori.” For fission eigenvalue problems, a reasonably high value is also required. Several hundred is reasonable if the problem has been debugged to the extent that the input is correct. Upscatter will increase the number of outers required for convergence even if upscatter acceleration is elected. For eigenvalue search problems, approximately ten times the number that would be required for similar fission eigenvalue problems is reasonable. This may seem like a very large number, but two things should always be kept in mind. First, the code will not iterate more than what is required for convergence, and, second, the restart file can always be used to cover the case of ITMX3 set too low. If the code does not converge, and a restart file has not been written, the effort put into the calculation must be restarted from scratch.

```
C  IACC=0, NO FISSION SOURCE ACCELERATION
C      =1, SINGLE STEP CHEBYCHEV ACCELERATION
C      =2, MULTIPLE STEP CHEBYCHEV ACCELERATION
C
```

FEMP1D will accelerate the fission source with either one-step or two-step Chebyshev acceleration. This process is covered in *Applied Iterative Methods* by Hageman and Young.

```
C  NPOW=NUMBER OF POWER ITERATIONS PERFORMED BEFORE STARTING
C     THE CHEBYCHEV ACCELERATION
C
```

In order to obtain estimates of the parameters to be used for fission source acceleration, a number of unaccelerated outer (power) iterations must be performed first. It is recommended that approximately ten outers be performed before attempting to accelerate the fission source.

```
C  NUPS=0, NO UPSCATTER SCALING
C        =N, NUMBER OF SUB-OUTERS PER OUTER TO SACLE UPSCATTER
C
```

Upscatter scaling is very efficient slid highly recommended if the cross sections include upscatter. For inhomogeneous source-only problems, NUPS should be set quite high, 30 or greater. For fission problems, a value of 3–8 has been found to work quite well.

```
C  NS=NIUMBER OF SOURCE SPECTRA
C
```

NS is the number of different source spectra to be input in the 47* array.

```
C  IPX=-2, DO NOT PRINT CROSS SECTIIMS
C   =-1,    PRINT 10 CROSS SECTIONS
C   = N,    PRINT 20 CROSS SECTIONS THRU PM
C
```

IPX controls the printing of the mixed cross sections. Note that large group structures and numerous materials can produce very large output files, and the printing of every mixed cross section is not recommended.

```
C  NPPUT=NUMBER OF POINTS FOR FLUX PRINT
C
```

After FEMP1D achieves a converged solution, it will print the flux at selected points if desired. NPOUT specifies the number of these points to be input in the 36* array.

```
C  MRF=NUMBER OF CARD INPUT RESPONSE FUNCTIONS
C
```

NRF specifies the number of response functions that will be read in the 39* array. These response functions will be integrated over the flux at the desired flux output points, and they will be multiplied by the zone fluxes and integrated over energy to obtain the zone and energy-integrated response.

```
C  IPFLX=0, DO NOT PRINT FLUX OUTPUT
C       =1, PRINT FLUX AT REQUESTED OUTPUT POINTS
C       =2, PRINT FLUX AT CALCULATION MESH POINTS
C
```

IPFLX determines if and where the final isotropic flux will be printed.

```
C  IWFIL=0, DO NOT WRITE SAVE FILE
C       =1, WRITE SAVE FILE TO FORT 4
C       =2, WRITE SAVE FILE TO (4TH) FILE NAMED AFTER BLOCK 0
C
```

IWFIL determines if a SAVE file will be written. The easiest way to write a SAVE file is to set IWFIL = −1. The SAVE file will be written to FORT.4. However, if the SAVE file is to be used later, it can be identified as the fourth file name in the input file after the Block 0 data. If the three previous files are not required, then it will move up in position depending on how many are not required.

```
C  2* ARRAY(3)
C
C  EPK=CONVERGENCE TOLERANCE ON EIGENVALUE
C
```

EPSK is the relative error convergence test to be used on the fission eigenvalue, the isotropic flux during middle iterations, and the eigenvalue search parameter during searches.

```
C  XK=EIGENVALUE ESTIMATE
C
```

XK is the initial estimate for K_{eff}. A nonzero value must be specified for all eigenvalue calculations.

```
C  SNORM=SOURCE NORMALIZATION
C
```

SNORM specifies the total number of source particles to be produced per centimeter of transverse length for the problem specified. At the end of the calculation, FEMP1D renormalizes all output values based on this value.

```
C  3$ ARRAY(5)
C
C  KSRCH=1,  BUCLING SEARCH
C         =2, DIMENSION SEARCH
C         =3, MIXTURE SEARCH
C
```

KSRCH specifies the type of search performed. A buckling search changes the input transverse bucklings to achieve the desired k_{eff}. All material bucklings are multiplied by the same factor. A dimension search scales all of the mesh points by the same factor to achieve the desired k_{eff}. A mixture search scales the volume fraction for the reactant to achieve the desired $_{\mathrm{Kerr}}$.The diluent volume fraction is reduced appropriately and the background volume fraction remains constant.

```
C  MSRCH=MATERIAL TO BE MIXED FOR SEARCH
C
```

MRS is the material in the mixing table whose volume fraction in MSRCH will be adjusted to increase fissile content.

```
C  MDS=MATERIAL TO BE USED FOR DILUENT IN SEARCH
C
```

MDS is the material in the mixing table whose volume fraction in MSRCH will be adjusted downward to account increased for fissile content in MRS.

```
C  MBS=MATERIAL TO BE USED FOR BACKGROUND IN SEARCH
C
```

MBS is a background material that retains the same volume fraction in MSRCH throughout the mixing process. A search example might involve determining the enrichment of $\mathbf{^{335}U}$required in a $\mathbf{UO_2}$ fuel to achieve criticality. For this case, $\mathbf{^{235}U}$would be the reactant, $\mathbf{^{235}U}$ would be the diluent, and **O** would be the background material.

```
C  4* ARRAY(4)
C
C  DKEFF=DESIRED KEFF FOR SEARCH
C
```

DKEFF is the desired eigenvalue for the search. Often this will be greater than 1.0 in order to provide a control margin and a burnup lifetime.

```
C   VFR=INITIAL VOLUME FRACTION FOR REACTION MATERIAL
C
```

VFR is the initial volume fraction of material MRS in MSRCH. The factor found during the search to achieve the desired k_{eff} multiplies this volume fraction for the final volume fraction for this material.

```
C   VFD=INITIAL VOLUME FRACTION FOR DILUENT MATERIAL
C
```

VFD is the initial volume fraction of MDS in MSRCH. It is adjusted during the search such that $VFR + VFD = Constant = 1.0 - VFB$.

```
C   VFB=INITIAL VOLUME FRACTION FOR BACKGROUND MATERIAL
C
```

VFB is the volume fraction in MSRCH for material MBS used during the search. It is not adjusted by the search.

```
C   5$ ARRAY(4)
C
C   NAN=NUMBER OF COLLAPSED ANISN CROSS SECTION SETS
C
```

NAN is the number of cross-sectional sets from LUN15 that will be collapsed and written to LUN25. It is the number of input cross sections, not the number of output sets.

```
C   NAW=NUMBER OF COLLAPSED WORKING LIBRARY CROSS SECTION SETS
C
```

NAW is the number of cross-sectional sets from LUN16 that will be collapsed and ten to LUN26. It is the number of input cross sections, not the number of output sets.

```
C   NBNG=NUMBER OF BROAD NEUTRON GROUPS
C
```

NBNG is the number of broad, or few, neutron groups that the collapsing process will reduce to in the output library.

```
C  NBPG=NUMBER OF BROAD PHOTON GROUPS
C
```

NBPG is the number of broad or few photon groups that the collapsing process will reduce to in the output library.

```
C  LTBLB=ANISN TABLE LENGTH FOR COLLAPSED LIBRARY
C
```

LTBLB is the length of the broad group library table for the collapsed ANISN library if one is produced. This is the end of Data Block 0 specifying the major parameters of the desired calculation.

```
C  DATA BLOCK NO.1 (MIXING TABLE)
C
C  10$ ARRAY(MTL)
C
C  MATERIAL NUMBERS
C
```

The 10$ array is made up of the material numbers to which cross-sectional sets will be assigned during the mixing process. The values at the same relative position in the 10$, 11$, and 12* arrays determine a specific mixing action.

```
C  11$ ARRAY(MTL)
C
C  NUCLIDE NUMBERS
C
```

The 11$ array lists cross-sectional sets that are to be used in the mixing operation. ANISN, AMPX, and input stream numbers can be mixed so long as no two sets have the same number.

```
C  12$ ARRAY(MTL)
C
C  NUMBER DENSITIES (ATOMS/BARN/CM)
C
```

The 12* array contains the number densities for the cross-sectional sets identified in the 11$ array that are to be mixed into the materials specified in the 10$ array. The units to be used are atoms/barn/cm.

```
C  13$ ARRAY(MCRD)
C
```

```
C  NUCLIDE IDS FOR CROSS SECTIONS INPUT ON CARDS
C
```

These are the ID numbers to be assigned to the input stream cross-sectional sets. The first number entered corresponds to the cross sections read in the first Data Block 2. The second number entered corresponds to the second Data Block 2 read in the input stream. These numbers should not be the same as any of the numbers on the ANISN or AMPX data files.

```
C  14* ARRAY(NOG)
C
C  CHI SPECTRUM
C
```

These are the fractional neutron yields for fission by group.

```
C  15* ARRAY(NNG+1)
C
C  NEUTRON GROUP BOUNDARIES
C
```

These are the energy bounds for the neutron group boundaries. They are used to compute the average neutron group velocity. They can also be used to compute a chi spectrum if one is not input.

```
C  16* ARRAY(NPG+1)
C
C  NEUTRON GROUP BOUNDARIES
C
```

These are the energy bounds for the gamma group boundaries.

```
C  17* ARRAY(NOG)
C
C  GROUP AVERAGE VELOCITIES
C
C  T
```

The group *average* velocities can be input and the 17* array will override the code calculation. This is the last array in Data Block 1.

```
C  DATA BLOCK NO.2 (CROSS SECTIONS-ONE BLOCK FOR NUCLIDE/MATERIAL)
C
C  20* ARRAY(NOG*4)
C
```

```
C  NOTE THE 1D CROSS SECTIONS ARE STORED IN THE FOLLOWING ORDER
C  1. TOTAL
C  2. TOTAL FISSION YIELD(NU*SIGF)
C  3. ABSORPTION
C  4. GROUP FRACTIONAL YIELD(CHI)
C
C  1D CROSS SECTIONS FOR THIS MATERIAL
```

Data Block 2 is optional, but it must be entered MCRD times if cross sections are to be read in from the input stream. The 20* array is the input for the one-dimensional cross sections. Based on the way numbers are processed in FORTRAN, the TOTAL cross section for all groups is read first and then the NU*SIGF cross section for all groups, etc.

```
C  21* ARRAY(NOG*NOG)
C
C  P0 SCATTERING ARRAY FOR THIS NUCLIDE
C
```

The P_0 scattering cross-sectional array is read in the 20* array. The first set of NOG numbers is the cross sections for scattering within and out of the first or highest energy group. The second set of NOG numbers is the within and outscatter cross sections for the second group. This process repeats itself until all groups have been read. Due to the way numbers are stored and used, the look of the 20* array data stream can be confusing. When printed out by FEMP1D, the two-dimensional cross-sectional sets should look like a standard matrix to be multiplied by a flux vector ordered from high to low energy.

```
C  22* ARRAY(NOG*NOG)
C
C  P1 SCATTERING ARRAY FOR THIS NUCLIDE
C
C  T
C
```

The P_1 scattering array is read in the 22* array exactly analogous to the way the 21* array is read. No provision is made to read higher than P_1 expansions, as it is not likely that the large number of numbers required will often be manipulated in hand input.

Note: A Data Block 2 must be entered for each data set to be entered from the input stream.

```
C  DATA BLOCK NO.3 (MESH POINTS AND MATERIAL ZONES)
C
C  30• ARRAY(NK)
```

```
C
C  X MESH POINTS
C
```

This array contains the mesh point values in centimeters. Values should be entered in increasing numerical order. The 31* and 32* arrays are skipped in FEMP1D in an attempt to keep array numbering consistent between FEMP1D, FEMF2D, and FEMP3D.

```
C  33$ ARRAY(NZONE)
C
C  NACROSCOPIC MATERIALS BY ZONE
C
```

The 33$ array identifies the macroscopic materials mixed in the 10S array to be assigned to each zone. The number entered in the first position in the 33S array will be the material assigned to the first zone, the number entered in the second position in the 33$ array will be the material entered in the second zone, and so on.

```
C  34$ ARRAY(NX-1)
C
C  ZONE NUMBERS BY MESH INTERVAL
C
```

Since a given material zone will often be more than one mean free path thick, it is usually required to have more than one mesh interval per zone. The 34$ array assigns mesh intervals to zones. The first value in the 34$ array is the zone to which the first interval is assigned, the second value in the 34S array is the zone to which the second interval is assigned, and so on.

```
C  35* ARRAY(NMAT)
C
C  TRANSVERSE DIMENSIONS FOR BUCKLING CORRECTION BY MATERIAL
C
```

The values entered in the 35* array are the dimensions for the assembly transverse to the direction of calculation. These are entered by material. This gives some flexibility in allowing an assembly without a constant transverse dimension and an assembly with a very low-density material to be modeled. For the low-density materials, an attempt should be made to have the same transverse leakage per material across the assembly. Obviously this is an approximate technique, and the one-dimensional results computed should be evaluated with that in mind. The transverse dimension in the slab calculation case is assumed to represent a radius for a cylindrical assembly. The transverse dimension in the cylindrical calculation case is assumed to represent a height for a cylindrical assembly. The transverse dimension in a spherical calculation is ignored by the code.

```
C  36* ARRAY(NPOUT)
C
C  OUTPUT X MESH POINTS FOR FLUX PRINT OUT
C
```

The 36* array contains values for the spatial points at which a flux print out or a response function evaluation is desired.

```
C  39* ARRAY(NOG*NRF)
C
C  RESPONSE FUNCTIONS
C
C  T
C
```

The 39* array contains the energy group-dependent response functions that can be multiplied times the group fluxes to obtain a measured response at a point in the assembly. They are also multiplied times the zone integrated fluxes to give an integral reaction rate over each zone. Note that the code does not know which response applies to which zone, so it evaluates all responses for all zones.

```
C  DATA BLOCK NO. 4 (INHOMOGENEOUS SOURCES)
C
C  40* ARRAY((LPNt1)*NOG)
C
C  LEFT MMDARY Sa)RCE SPECTRUM
C
```

The 40* array is the Legendre expansion for the source incident on the left side of the assembly, ordered by Legendre order and group number.

```
C  41*ARRAY((LPN+1)*NOG)
C
C  RIGHT BOUNDARY SOURCE SPECTRUM
C
```

The 41* array is the Legendre expansion for the source incident on the left side of the assembly, ordered by Legendre order and group number.

```
C  46*ARRAY(NOG*NS)
C
```

```
C  FIXED SOURCE SPECTRA
C
```

The 46* array contains the energy-dependent information for inhomogeneous sources. It is ordered by group and then spectrum. The spectra can be unnormalized or normalized, but if more than one spectrum is input, the relative normalization must be correct. The volume sources are assumed to be isotropic. The 42* through 45* arrays are reserved for input to FEMP2D and FEMP3D.

```
C  47*ARRAY(NX-1)
C
C  INHOMOGENEOUS SOURCES BY MESH INTERVAL
C
C  T
C
```

The 47$ array assigns the spectra input in the 46* array to mesh intervals. This completes Data Block 4.

```
C  DATA BLOCK NO.5 (COLLAPSING INSTRUCTIIXIS)
C
C  50$ ARRAY(NNG)
C
C  BROAD NEUTRON GROUP NUMBERS BY FINE GROUP
C
```

These are essentially the instructions that assign the neutron fine group identified by position within the array to the neutron broad group identified by the numerical value entered. For instance, if the fifth entry in this array is a 2, that would direct that the fifth fine group be included in the second broad group.

```
C  51$ ARRAY(MPG)
C
C  BROAD GAMMA GROUP NUMBERS BY FINE GROUP
C
```

These are essentially the instructions that assign the photon fine group identified by position within the array to the photon broad group identified by the numerical value entered. For instance, if the fifth entry in this array is a 2, that would direct that the fifth fine group be included in the second broad group.

```
C  52$ ARRAY(NAN)
C
C  ANISN FINE GROUP LIBRARY IDS FM COLLAPSE
C
```

The 52$ array identifies the ANISN sets on LUN15 that will be collapsed.

```
C   53$ ARRAY(NAN)
C
C   ANISN BROAD GROUP LIBRARY IDS
C
```

The 53$ array gives the new ID numbers that are to be assigned to the ANISN broad group sets.

```
C   54$ ARRAY(NAN)
C
C   ZONES FOR COLLAPSING ANISN CROSS SECTION SETS
C
```

The 54$ array identifies the zone fluxes to be used to collapse the ANISN sets.

```
C   55' ARRAY(18*NAN)
C
C   TITLES OF COLLAPSED AMISS CROSS SECTION SETS
C
```

The 55* array identifies the titles to be used for the ANISN broad group sets to be created.

```
C   56$ ARRAY(NAW)
C
C   WORKING LIBRARY FINE GROUP LIBRARY IDS
C
```

The 56$ array identifies the AMPX sets on LUN16 that will be collapsed.

```
C   57$ ARRAY(NAW)
C
C   WORKING LIBRARY BROAD GROUP LIBRARY IDS
C
```

The 57$ array gives the new ID numbers that are to be assigned to the AMPX broad group sets.

```
C   58$ ARRAY(NAW)
C
C   ZONES FOR COLLAPSING WORKING LIBRARY CROSS SECTION SETS
C
```

The 58$ array identifies the zone fluxes to be used to collapse the AMPX sets.

```
C   59* ARRAY(18*NAM)
C
C   TITLES FOR COLLAPSED LURKING LIBRARY SETS
C
C   T
C
```

The titles for the AMPX collapsed data sets are read as character data and cannot be free form. This completes the input data stream for one problem.

```
C   FEMP1D QTTPUT TAPE FORMAT - (LUN4)
C
C   RECORD 1: TITLE
C   FORMAT - (1BA4)
C   DATA - (CODE(I), I=1,6),(TITLE(I), I=1,18)
```

The output tape is a convenient way of electronically saving the output of a calculation for additional processing or to restart a calculation. It is written in ASCII format to facilitate reading by a number of processors including the eyeball if required. The first record is the problem title.

Note that provisions are made for a three-dimension format. This allows some passing of information between different dimension-level calculations.

```
C   RECORD 2: INTEGER PARAMETERS
C   FORMAT - (1216)
C   DATA - MADJ,NGEOM,NZOIE,NX,NZ,NOG1 YNG,NPG,LPN,ITER,IDU(
C   MADJ=FORWARD/ADJOINT INDICATOR (0/1-FORWARD/ADJOINT)
C   NGEOM=GEOMETRY INWICATWR (1/2/3-XZ/RZT/RTZ)
C   NZOME=NUMBER Of DISTINCT MATERIAL ZONES
C   NX=NUMBER OF FIRST DIMENSION MESH POINTS
C   NY=NUBER OF SECOND DIMENSION MESH POINTS
C   NZ=MONGER Of THIRD DIMENSION MESH POINTS
C   NOGI=NUMBER OF ENERGY GR JP BOUNDS
C   NNG=NUBER OF NEUTRON ENERGY GROUPS
C   MPG=NUBER OF GANIA ENERGY GRQIPS
C   LPN=SPHERICAL HARMONIC ORDER(0/1-P0/P1)
C   ITER=WINGER OF COMPLETED OUTER ITERATIONS
C   IDLAM=SPARE
```

The second record is a listing of the integer problem control parameters.

```
C   RECORD 3: REAL PARAIEIERS
C   FORMAT - (1P6EI2.4)
```

```
C   DATA - XKEFF,DMRTO,OMEGA,SNORM,DUM1, DUM2
C   XKEFF=CRITICALITY EIGENVALUE
C   DMRT6LOIINANCE RATIO
C   OMEGA=UPSCATTER OVER-RELAMTION FACTOR
C   SNORM=SOURCE NORMALIZATION FACTO
C   DUM1=SPARE
C   DUM2=SPARE
```

The third record is a listing of the floating point problem control parameters.

```
C   RECORD 4: (NEUTRON,GAMA) ENERGY GROUP BONNDS
C   FORMAT - (1P6E12.4)
C   DATA - (EN(IG),IG=1,NNG+1),(EN(IG),I=1,NPG+1)
```

The fourth record gives the group energy bounds.

```
C   RECORD 5: MESH BOUNDRIES
C   FORMAT - (1P6E12.4)
C   DATA - (X(I),I=1,NX),(Y(J),J=1,NY),(Z(K),K=1,NZ)
```

The fifth record gives the calculation mesh boundaries.

```
C   RECORD 6: ZONE MAP, MATERIAL BY ZONE ARRAY
C   FORMAT - (2413)
C    DATA – (((NZ(I,J,K), I=1,NX-1), J=1,NY), K=1,NZ-1), (NZ(L), L=1,
NZONE)
```

The sixth record specifies the material map.

```
C   RECORD 7-NOG+6: GROW FLUX MOMENTS
C   FOMAT - (1P6E12.4)
C   DATA - (((FLXM (I,J,K),I=1,NX),J=1,NY),K=1,NZ)
C   CODING - DO 10 IG=1,NOG
C      DO 10 L=1,LPN
C      READ(NTFLX,FORMAT) (((ELXM(I, J,K),1=1,NX), J=1, NY),K=1,NZ)
C      10 CONTINUE
C
```

The seventh and subsequent records are the Legendre flux expansions generated during the calculation.

5.10 Output Description

The best description of the output to be expected from a typical problem can be obtained by perusing the sample problems contained in the code package. Please contact this author for further information. Further information is provided in the user's manual of FEMP computer code [1].

Problems

This chapter has no problem developed for it except you need to obtain FEMB computer code. Please contact the author of the book at bahmanz@aol.com

Reference

1. P. McDaniel, Finite Element Multi-Group PN 1-Dimensional Computer Code, User's Manual, University of New Mexico, Albuquerque, New Mexico (March 8, 2007)

Chapter 6
Slowing Down Theory

In neutronic analysis for nuclear reactor systems, we look at three types of reactors depending upon the average energy of neutrons, which cause the bulk of the fission in the system. *Thermal reactors*, in which most fission are, are induced by neutrons, and these neutrons more or less are in thermal equilibrium with the atoms in the reactor and maintain energy below approximately 0.3 eV. *Intermediate reactor* or resonance reactors, in which neutrons have energy above thermal up to 10 keV and most of these neutrons are responsible for fission, lie in the resonance region of the heavy elements. This type of reactor is also largely responsible for producing fissions. Finally, the third one is the *fast reactor*, in which fissions are induced primarily by neutrons with energy of the order of 100 keV and above. Finally, yet importantly, one should be aware of the fact that in a thermal reactor, the fission neutrons are slowed down by the use of a *moderator*, and that is a mass of material, such as carbon, beryllium, or water, which is distributed throughout the fueled region or *core* of the reactor [1].

6.1 Neutron Elastic and Inelastic Scattering for Slowing Down

Over a broad range of energies from about 1.0 MeV down to just above thermal energies, the energy spectrum in a thermal reactor is dominated by elastic scattering interactions. This single fact allows a number of approximations to be made that are generally very accurate and of great use in analyzing the behavior of this type of reactor. In fact, the process of slowing down that goes on in most reactors, and large light-water power reactors in particular, can be approximated by considering the slowing down medium to be infinite in extent. This allows the consideration of neutron energy changes to separate from spatial density changes and decouples the isotropic neutron flux equation from higher-order terms. Therefore, a solution can

B. Zohuri, *Neutronic Analysis For Nuclear Reactor Systems*,
DOI 10.1007/978-3-319-42964-9_6

be obtained for the isotropic flux for an infinite medium that should be a good approximation to the actual spectrum in the slowing down range of an actual reactor.

6.2 Derivation of the Energy and Transfer Cross Section

Derivation of the energy and transfer cross section will be discussed in this section, and they are approached from two points of view as:

1. Elastic scattering
2. Inelastic scattering

Both topics are discussed in the following subsections.

6.2.1 Elastic Scattering

In order to derive the fundamental spectrum that is produced by elastic scattering in the slowing down region, the following diagram relating the angle of scattering in the laboratory and the center of mass reference frames is of great use.

The laboratory and center of mass reference frames are defined as follows:

Laboratory frame of reference (L): This is a fixed frame of reference with a neutron moving with velocity u and a stationary nucleus. Thermal motions of the nucleus can be neglected when the neutron's energy is in the slowing down range.

Center of mass frame of reference (C): The moving frame of reference is a frame in which the sum of the momentum of both particles is equal to zero. This frame of reference is moving toward the nucleus prior to the collision, and since no external forces act on the particles during the collision, it continues moving at the same velocity after the collision. The neutron and nucleus themselves also have the same velocity magnitudes after the collision as they did before the collision in order to satisfy the conservation of momentum. The only thing that the collision change has is their relative direction of motion.

Velocities before collision will be identified by u and U and after collision by v and V. A subscript ***C*** will identify velocities measured in the center of mass frame, and a subscript ***L*** will identify velocities measured in the lab frame.

Consider now the total momentum in the ***C*** frame, then we can write

$$mu_{\mathrm{C}} + MU_{\mathrm{C}} = 0 \tag{6.1}$$

$$U_{\mathrm{C}} = -\frac{m}{M}u_{\mathrm{C}} \tag{6.2}$$

$$u_{\mathrm{L}} = u_{\mathrm{C}} - U_{\mathrm{C}} = \left(1 + \frac{m}{M}\right) u_{\mathrm{C}} \tag{6.3}$$

Or the velocity of the nucleus in the ***C*** frame can be related to its ***L*** frame velocity by

$$u_{\mathrm{C}} = \frac{1}{1 + \frac{m}{M}} u_{\mathrm{L}} \tag{6.4}$$

Now since a neutron is approximately 1 amu and a nucleus with atomic number A is approximately A amu,

$$\frac{M}{m} = A \tag{6.5}$$

$$u_{\mathrm{C}} = \frac{A}{A+1} u_{\mathrm{L}} = v_{\mathrm{C}} \tag{6.6}$$

$$U_{\mathrm{C}} = \frac{1}{A} u_{\mathrm{C}} \tag{6.7}$$

The velocity of the ***C*** frame relative to the ***L*** frame can be found by

$$u_{\mathrm{CM}} = -U_{\mathrm{C}} = \frac{1}{A} u_{\mathrm{C}} = \frac{1}{A+1} u_{\mathrm{L}} \tag{6.8}$$

The reduced mass, μ, is defined by

$$\mu = \frac{mM}{m+M} = \frac{A}{A+1} m \tag{6.9}$$

Then from the angle relationships of Fig. 6.1,

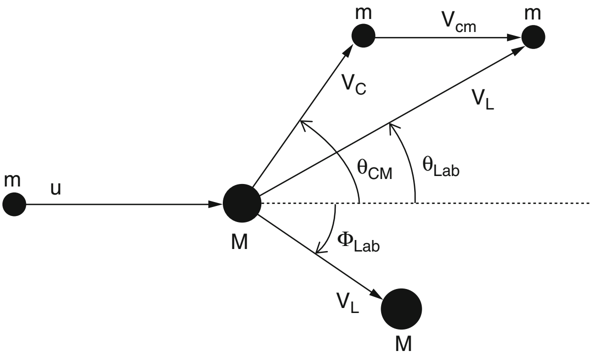

Fig. 6.1 Laboratory and center of mass reference frames

$$v_{\mathrm{L}} \sin \theta_{\mathrm{L}} = v_{\mathrm{C}} \sin \theta_{\mathrm{C}} \tag{6.10}$$

$$v_{\mathrm{L}} \cos \theta_{\mathrm{L}} = v_{\mathrm{CM}} + v_{\mathrm{C}} \cos \theta_{\mathrm{C}} \tag{6.11}$$

Dividing the second into the first gives

$$\frac{\sin \theta_{\mathrm{L}}}{\cos \theta_{\mathrm{L}}} = \frac{\sin \theta_{\mathrm{C}}}{\frac{v_{\mathrm{CM}}}{v_{\mathrm{C}}} + \cos \theta_{\mathrm{C}}} \tag{6.12}$$

or

$$\tan \theta_{\mathrm{L}} = \frac{\sin \theta_{\mathrm{C}}}{\frac{1}{A} + \cos \theta_{\mathrm{C}}} \tag{6.13}$$

This gives a method for obtaining the angle of scattering in the ***L*** frame, given an angle of scattering in the ***C*** frame. However, a more useful relationship for neutron-scattering purposes can be obtained by squaring both equations and adding

$$v_{\mathrm{L}}^2 \left(\cos^2 \theta_{\mathrm{L}} + \sin^2 \theta_{\mathrm{L}} \right) = v_{\mathrm{C}}^2 \sin^2 \theta_{\mathrm{C}} + (v_{\mathrm{CM}} + v_{\mathrm{C}} \cos \theta_{\mathrm{C}})^2 \tag{6.14}$$

$$v_{\mathrm{L}}^2 = v_{\mathrm{C}}^2 + v_{\mathrm{CM}}^2 + 2 v_{\mathrm{C}} v_{\mathrm{CM}} \cos \theta_{\mathrm{C}} \tag{6.15}$$

$$\frac{1}{2} m v_{\mathrm{L}}^2 = \frac{1}{2} m v_{\mathrm{C}}^2 + \frac{1}{2} m v_{\mathrm{CM}}^2 + 2 \frac{1}{2} m v_{\mathrm{C}} v_{\mathrm{CM}} \cos \theta_{\mathrm{C}} \tag{6.16}$$

$$E = \left[\frac{A}{A+1} \right]^2 E' + \left[\frac{1}{A+1} \right]^2 E' + 2 \left[\frac{1}{A+1} \frac{A}{A+1} \right] E' \cos \theta_{\mathrm{C}} \tag{6.17}$$

where the usual notation of E2232 E' as the neutron energy before the collision and E as the neutron energy after collision (both measured in the lab frame) has been introduced. This can be written as

$$\frac{E}{E'} = \frac{A^2 + 2A \cos \theta_{\mathrm{C}} + 1}{(A+1)^2} \tag{6.18}$$

Considering the two extremes for θ_c gives

(a)

$$\theta_c = 0$$

$$\frac{E}{E'} = \frac{A^2 + 2A + 1}{(A+1)^2} = 1.0 \tag{6.19}$$

(b)

$$\theta_c = \pi$$

$$\frac{E}{E'} = \frac{A^2 - 2A + 1}{(A+1)^2} = \frac{(A-1)^2}{(A+1)^2} \tag{6.20}$$

This then leads to the definition of a convenient new variable, α,

$$\alpha = \frac{(A-1)^2}{(A+1)^2} \tag{6.21}$$

The energy change equation can then be written as

$$E = \frac{(1+\alpha) + (1-\alpha)\cos\theta_{\mathrm{C}}}{2} E' \tag{6.22}$$

Differentiating this equation gives

$$dE = -\frac{(1-\alpha)}{2} E' \sin\theta_{\mathrm{C}}\, d\theta_{\mathrm{C}} \tag{6.23}$$

This can be written as

$$dE = \frac{(1-\alpha)}{2} E'\, d\mu_{\mathrm{C}} \quad \mu_{\mathrm{C}} = \cos\theta_{\mathrm{C}} \tag{6.24}$$

Now defining a cross section for scattering through a given μ_{CM} as $\sigma_s(\mu_{\mathrm{CM}})$ and realizing that it can be related to the total scattering cross section by

$$\sigma_s = 2\pi \int_{-1}^{1} \sigma_s(\mu_{\mathrm{C}}) d\mu_{\mathrm{C}} \tag{6.25}$$

The probability of scattering through a given μ_{CM} into an incremental $d\mu_{\mathrm{CM}}$ is given by

$$P(\mu_{\mathrm{C}}) d\mu_{\mathrm{C}} = 2\pi \frac{\sigma_s(\mu_{\mathrm{C}})}{\sigma_s} d\mu_{\mathrm{C}} \tag{6.26}$$

And the probability of going from energy E' to a differential energy dE about energy E is the same as scattering through a CM angle corresponding to μ_{C}

$$P(E' \to E) dE' = P(\mu_C) d\mu_C \tag{6.27}$$

or

$$P(E' \to E) dE' = 2\pi \frac{\sigma_s(\mu_{\mathrm{C}})}{\sigma_s} d\mu_{\mathrm{C}} \tag{6.28}$$

Then the differential relationship between dE and $d\mu_C$ can be used.

$$dE = \frac{(1-\alpha)}{2} E' d\mu_C \tag{6.29}$$

This gives

$$P(E' \to E)\,\frac{(1-\alpha)}{2} E'\, d\mu_C = 2\pi \frac{\sigma_s(\mu_C)}{\sigma_C} d\mu_C \tag{6.30}$$

which reduces to

$$P(E' \to E) = \frac{\sigma_s(\mu_C)}{\sigma_s} \frac{4\pi}{(1-\alpha)E'} \tag{6.31}$$

This can be used for an arbitrary scattering distribution in the ***C*** frame. However, for isotropic scattering in the ***C*** frame (by far the most common case for realistic moderators),

$$\sigma_s(\mu_C) = \frac{\sigma_s}{4\pi} \tag{6.32}$$

Then the energy transfer probability reduces to

$$P(E' \to E) = \frac{1}{(1-\alpha)E'} \tag{6.33}$$

In addition, the isotropic transfer cross section from energy E' to energy E is given by

$$\sigma_{s0}(E' \to E) = \sigma_{s0} P(E' \to E) = \frac{\sigma_{s0}}{(1-\alpha)E'} \tag{6.34}$$

6.2.2 Inelastic Scattering

For the case of inelastic scattering, everything remains the same except that the excitation energy must be introduced into the conservation of energy equation. The excitation energy will be identified by the symbol Q. For inelastic scattering, Q will be negative as the energy of excitation is removed from the kinetic energy of the system. The energy balance equation in the center of mass frame is then

$$\frac{1}{2} m u_C^2 + \frac{1}{2} M U_C^2 + Q = \frac{1}{2} m v_C^2 + \frac{1}{2} M V_C^2 \tag{6.35}$$

This can be simplified by multiplying by 2 and dividing by m. Then

$$u_{\mathrm{C}}^2 + \frac{M}{m} U_{\mathrm{C}}^2 + \frac{2Q}{m} = v_{\mathrm{C}}^2 + \frac{M}{m} V_{\mathrm{C}}^2 \tag{6.36}$$

and remembering that

$$m u_{\mathrm{C}} = -M U_{\mathrm{C}} \quad \text{and} \quad m v_{\mathrm{C}} = -M V_{\mathrm{C}} \tag{6.37}$$

$$u_{\mathrm{C}}^2 + \frac{2QA}{m(1+A)} = v_{\mathrm{C}}^2 = \left(\frac{A}{A+1}\right)^2 u_{\mathrm{L}}^2 + \frac{2QA}{m(A+1)} \tag{6.38}$$

$$v_{\mathrm{C}}^2 = \left(\frac{A}{A+1}\right)^2 u_l^2 \left(1 + \frac{Q}{\frac{1}{2} m u_{\mathrm{L}}^2} \frac{A+1}{A}\right) \tag{6.39}$$

In addition, from Eq. 6.15, we have

$$v_{\mathrm{L}}^2 = v_{\mathrm{C}}^2 + 2 v_{\mathrm{C}} v_{\mathrm{CM}} \cos \theta_{\mathrm{C}} + v_{\mathrm{CM}}^2 \tag{6.40}$$

$$v_{\mathrm{L}}^2 = u_{\mathrm{L}}^2 \left\{ \left(\tfrac{A}{A+1}\right)^2 \left(1 + \frac{Q}{\frac{1}{2} m u_{\mathrm{L}}^2} \frac{A+1}{A}\right) + \frac{2A}{(A+1)^2} \sqrt{1 + \frac{Q}{\frac{1}{2} m u_{\mathrm{L}}^2} \frac{A+1}{A}} \cos \theta_{\mathrm{C}} + \left(\frac{1}{A+1}\right)^2 \right\} \tag{6.41}$$

or

$$E = E' \left\{ \left(\frac{A}{A+1}\right)^2 \left(1 + \frac{Q}{E'} \frac{A+1}{A}\right) + \frac{2A}{(A+1)^2} \sqrt{1 + \frac{Q}{E'} \frac{A+1}{A}} \cos \theta_{\mathrm{C}} + \left(\frac{1}{A+1}\right)^2 \right\} \tag{6.42}$$

Note that the lowest energy that can excite a level with an excitation energy of Q is

$$E' = \frac{A+1}{A} Q \tag{6.43}$$

When this happens, we will have

$$E = \frac{E'}{(A+1)^2} \tag{6.44}$$

Note that this is a significantly greater energy loss than elastic scattering.

6.3 Derivation of the Isotropic Flux in an Infinite Hydrogen Moderator

Now in order to obtain the energy-dependent flux in an infinite reactor, begin by considering the balance equation for an infinite medium where the only scattering element is hydrogen. Hydrogen is chosen first because it will be assumed that a neutron and a proton are of equal mass, and a collision between a neutron and a hydrogen atom will allow the neutron to lose all of its energy. The balance equation can be written as:

$$\Sigma_T(E)\phi(E) = \int_E^\infty \Sigma_s(E' \to E)\phi(E')dE' + S(E) \tag{6.45}$$

For the sake of simplicity, assume that all neutrons are introduced at a single energy, E_0, by a delta function source, $S(E) = S^*\delta(E - E_0)$. This approximates the fission spectrum and can be handled analytically as well as produce reasonable results. It will also allow treatment of the high-energy source as a boundary condition. Then, for isotropic scattering in the center of mass reference frame for hydrogen, the energy transfer cross section is

$$\Sigma_s(E' \to E) = \frac{\Sigma_s(E')}{(1-\alpha)E'} = \frac{\Sigma_s^H(E')}{E'} \tag{6.46}$$

Inserting this into the balance equation, and considering a source and absorption-free region below the delta function source, gives

$$\Sigma_s^H(E)\phi(E) = \int_E^{E_0} \frac{\Sigma_s^H(E')\phi(E')}{E'}dE' \tag{6.47}$$

It will prove useful to define a new quantity, $F(E)$, called the collision density as

$$F(E) = \Sigma_s(E)\phi(E) \tag{6.48}$$

Inserting this quantity into the P_0 equation and differentiating with respect to E gives

$$F'(E) = -\frac{F(E)}{E} \tag{6.49}$$

This can be written as

$$EF'(E) + F(E) = 0 \tag{6.50}$$

and is of the form

$$\frac{d}{dE}[EF(E)] = 0 \tag{6.51}$$

This can be integrated directly to obtain

$$EF(E) = \text{Constant} = Q_0 \tag{6.52}$$

Therefore, in pure hydrogen the collision density varies as $1/E$.

$$F(E) = \frac{Q_0}{E} \tag{6.53}$$

The flux varies as

$$\phi(E) = \frac{Q_0}{\Sigma_s(E)E} = \frac{\text{Constant}}{\Sigma_s E} \tag{6.54}$$

If the total scattering cross section is constant, then the flux varies as $1/E$ also.

At this point, it is useful to introduce a new variable called lethargy, defined by

$$u = \ln\frac{E_0}{E} \tag{6.55}$$

The lethargy will vary from near zero to some maximum value as a neutron slows down; thus, it is a conceptually useful concept in terms of following the life of a neutron. Because it is a logarithmic variable, it condenses the 8 or 9 orders of magnitude change in energy into a number less than 30.

In addition, since a neutron tends to lose a fraction of its energy in any given collision, scattering phenomena will be more constant when expressed on a lethargy scale. In order to relate the flux as a function of energy to the flux as a function of lethargy, the following mathematical relationship for the two collision densities can be used:

$$|F(E)dE| = |F(u)du| \tag{6.56}$$

or

$$F(E)\left|\frac{dE}{du}\right| = F(u) \tag{6.57}$$

And noting

$$\left|\frac{dE}{du}\right| = E \tag{6.58}$$

gives

$$F(u) = EF(E) \tag{6.59}$$

Thus, $F(u)$ is a constant. Moreover, since over broad expanses of the slowing down range, the total cross section of hydrogen is only elastic scattering and relatively constant, this gives

$$\phi(u) = \frac{Q_0}{\Sigma_s^H(u)} \tag{6.60}$$

This result means that for multigroup cross sections used in typical light-water reactors, the weighting spectrum within a group can be very adequately represented as a constant in the lethargy variable.

In order to evaluate the constant Q_0, a new quantity, $q(E)$, called the "slowing down density" must be defined. This is basically the number of neutrons per unit volume that slow past a given energy on a continuous basis. It is defined by the integral equation

$$q(E) = \int_0^E dE'' \int_E^{E_0} \Sigma_s\left(E' \to E''\right)\phi(E')dE' + \int_0^E dE'' \int_E^{E_0} \Sigma_s\left(E' \to E''\right)S(E')dE' \tag{6.61}$$

For isotropic scattering in hydrogen, this can be written as

$$q(E) = E\int_E^{E_0} \frac{F(E')}{E'}dE' + E\int_E^{E_0} \frac{\Sigma_s^H(E')S(E')}{E'}dE' \tag{6.62}$$

As indicated above, consider the source at energy E_0 to be a delta function. This allows integration over the source energy

$$q(E) = E\int_0^{E_0} \frac{F(E')}{E'}dE' + \frac{E}{E_0}\Sigma_s^H(E_0)S_0 \tag{6.63}$$

Moreover, performing the in-scatter integration between the source energy and the energy of interest, E, gives

$$q(E) = E\left[\frac{1}{E} - \frac{1}{E_0}\right]Q_0 + \frac{E}{E_0}\Sigma_s^H(E_0)S_0 \tag{6.64}$$

At the source energy, E_0, this will give

$$q(E_0) = \frac{E_0}{E_0}\Sigma_s^H(E_0)S_0 = \Sigma_s^H(E_0)S_0 \tag{6.65}$$

For an infinite medium with no absorption, the same number of neutrons must slow past the energy E as start out at energy E_0, and $q(E) = q(E_0)$. The general slowing down density becomes

$$q(E) = \Sigma_s^H(E_0)S(E_0) = \left[1 - \frac{E}{E_0}\right]Q_0 + \frac{E}{E_0}\Sigma_s^H(E_0)S_0 \tag{6.66}$$

$$\left[1 - \frac{E}{E_0}\right]\Sigma_s^H(E_0)S_0 = \left[1 - \frac{E}{E_0}\right]Q_0 \tag{6.67}$$

$$Q_0 = \Sigma_s^H(E_0)S_0 \tag{6.68}$$

So for slowing down in an infinite medium,

$$\phi(E) = \frac{Q_0}{E\Sigma_s^H(E)} = \frac{S_0\Sigma_s^H(E_0)}{E\Sigma_s^H(E)} \tag{6.69}$$

6.4 Derivation of the Isotropic Flux in a Moderator Other than Hydrogen A > 1

Consider now the case of a single moderator with A > 1. The balance equation becomes

$$\Sigma_s(E)\phi(E) = \int_E^{E/\alpha} \frac{\Sigma_s(E')}{(1-\alpha)E'}\phi(E')dE' + S(E). \tag{6.70}$$

Where the isotropic, in the center of mass, scattering transfer function has been used. This is a good approximation for most light moderators. For fast reactors, and all-metal assemblies, this is not a good approximation, a priori. However, experience has shown that even for these cases, the results obtained by making this approximation are quite good, when a large enough number of groups are used.

Once again, the high-energy source of neutrons can be assumed to be a delta function and the homogeneous problem solved first. Defining the collision density, $F(E)$, as before, the balance equation becomes

$$F(E) = \int_{E}^{E/\alpha} \frac{F(E')dE'}{(1-\alpha)E'} \tag{6.71}$$

Differentiating this equation gives

$$F'(E) = \frac{1}{(1-\alpha)}\left[\frac{F(E/\alpha)}{E/\alpha}\frac{1}{\alpha}\frac{F(E)}{E}\right] \tag{6.72}$$

Now due to the presence of the $F(E/\alpha)$ term in this equation, it is difficult to easily proceed beyond this point. This equation cannot be solved in a direct manner. It has been solved in the literature for the case of a true delta function source at energy, E_0. The solution in terms of so-called Placzek functions is discontinuous at the end of the first scattering interval below the source. At the boundary to each subsequent scattering interval, a higher-order derivative is discontinuous. Though the Placzek functions produce the correct mathematical solution to the approximate problem, the introduction of the delta function source causes too much of a simplification in this case and produces the unphysical result of a discontinuous flux at the energy αE_0. The actual fission source, spread over a range of energies, will smooth this effect out, and the discontinuity will not be seen. Therefore, the approach taken here will be to assume a form for the asymptotic spectrum at a number of scattering intervals below the source and show that the assumed spectrum is a solution to the differential difference equation. This solution is also the Placzek solution for energies removed by more than three scattering intervals from a delta function source.

The solution assumed will be

$$F(E) = \frac{\text{Constant}}{E} = \frac{C_0}{E} \tag{6.73}$$

Then differentiating,

$$\frac{dF(E)}{dE} = -\frac{C_0}{E^2} \tag{6.74}$$

And evaluating

$$F\left[\frac{E}{\alpha}\right] = \frac{\alpha C_0}{E} \quad F(E) = \frac{C_0}{E} \tag{6.75}$$

$$-\frac{C_0}{E^2} = \frac{1}{(1-\alpha)}\left[\frac{\frac{\alpha C_0}{E}\frac{1}{\alpha}}{\frac{E}{\alpha}} - \frac{\frac{C_0}{E}}{E}\right] \tag{6.76}$$

$$-\frac{C_0}{E^2}=\frac{1}{(1-\alpha)}\left[\frac{(\alpha-1)C_0}{E^2}\right] \tag{6.77}$$

$$-\frac{C_0}{E^2}=-\frac{C_0}{E^2} \quad \text{QED} \tag{6.78}$$

Therefore, the solution $EF\ (E)=C_0$ is clearly an acceptable solution.

Now consider the slowing down density.

$$q(E)=\int_{\alpha E'}^{E} dE'' \int_{E}^{E/\alpha} \Sigma_s(E'\to E)\phi(E')\,dE' \tag{6.79}$$

Note that only one scattering interval above and below the energy of interest is all that must be considered for this case. This means that a neutron cannot scatter from the source energy, E_0, to an energy below αE_0 without first scattering in the interval above αE_0.

Transforming to the lethargy variable and continuing to assume isotropic scattering in the center of mass reference frame give the following equation for $q(E)$:

$$q(u)=\int_{u'-\ln\alpha}^{u} du'' \int_{u}^{u+\ln\alpha} \frac{\Sigma_s(u')}{(1-\alpha)}\phi(u')e^{-\left(u''-u'\right)}du' \tag{6.80}$$

Pulling out the constant cross section flux product and reversing the order of integration gives

$$q(u)=\frac{\Sigma_s(u)\phi(u)}{(1-\alpha)}\int_{u+\ln\alpha}^{u} e^{u'}du' \int_{u}^{u'-\ln\alpha} e^{-u''}\,du'' \tag{6.81}$$

$$q(u)=\frac{\Sigma_s(u)\phi(u)}{(1-\alpha)}\int_{u+\ln\alpha}^{u} e^{u'}\left[e^{-u}-\alpha e^{u}\right]du' \tag{6.82}$$

$$q(u)=\Sigma_s(u)\phi(u)\left[1+\frac{\alpha}{1-\alpha}\right]\ln\alpha \tag{6.83}$$

And then defining

$$\xi=1+\frac{\alpha}{1-\alpha}\ln\alpha \tag{6.84}$$

finally gives

$$q(u)=\xi\Sigma_s(u)\phi(u)=\xi F(u) \tag{6.85}$$

6.5 Summary of Slowing Down Equations

Summarizing the above analysis, the following relationships apply to the slowing down fluxes in an infinite medium dominated by moderators that scatter isotropically in the center of mass reference frame:

(1) $A = 1$

$$\phi(E) = \frac{Q_0}{E\Sigma_s^H(E)} \tag{6.86}$$

$$\phi(u) = E\phi(E) = \frac{Q_0}{\Sigma_s^H} \approx \text{constant} \tag{6.87}$$

$$q(u) = \Sigma_s^H(u)\phi(u) \tag{6.88}$$

(2) $A > 1$

$$\phi(E) = \frac{Q_0}{\xi E\Sigma_s(E)} \tag{6.89}$$

$$\varphi(u) = \frac{Q_0}{\xi\Sigma_s(u)} \approx \text{constant} \tag{6.90}$$

$$q(E) = \xi\Sigma_s(u)\phi(u) \tag{6.91}$$

Problems

Problem 6.1 An atom of uranium (U) with a mass of 3.9529×10^{-25} kg (i.e., $m = 3.9529 \times 10^{-25}$ kg) at rest decays spontaneously into an atom of helium (He) with a mass of 3.8864×10^{-27} kg (i.e., $m = 3.8864 \times 10^{-27}$ kg). The helium atom is observed to move in the positive x-direction with a velocity of 1.423×10^7 m/s (Fig. P6.1). Do the following analyses:

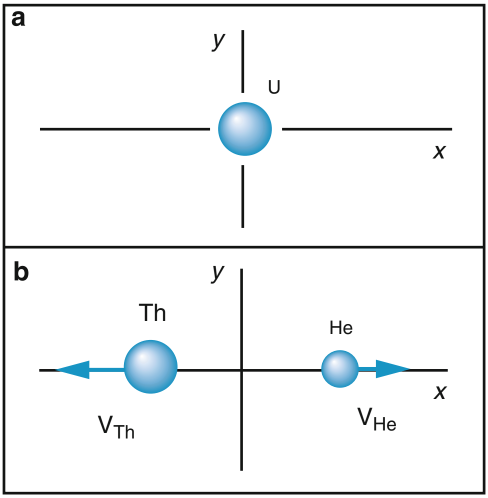

Fig. P6.1 (**a**) Before decay and (**b**) after decay

(a) Find the velocity (i.e., magnitude and direction) of the thorium atom.
(b) Find the total kinetic energy of the two atoms after the decay.

Problem 6.2 A helium atom ($m = 6.6465 \times 10^{-27}$ kg) moving at a speed of $v_{He} = 1.518 \times 10^6$ m/s collides with an atom of nitrogen ($m = 2.3253 \times 10^{-26}$ kg) at rest. After the collision, the helium atom is found to be moving with a velocity of $v_{He} = 1.199 \times 10^6$ m/s at an angle of $\theta_{He} = 78.75°$ relative to the direction of the original motion of the helium atom.

(a) Find the velocity (magnitude and direction) of the nitrogen atom after the collision.
(b) Compare the kinetic energy before the collision with the total kinetic energy of the atoms after the collision. Use Fig. P6.2 to solve this problem.

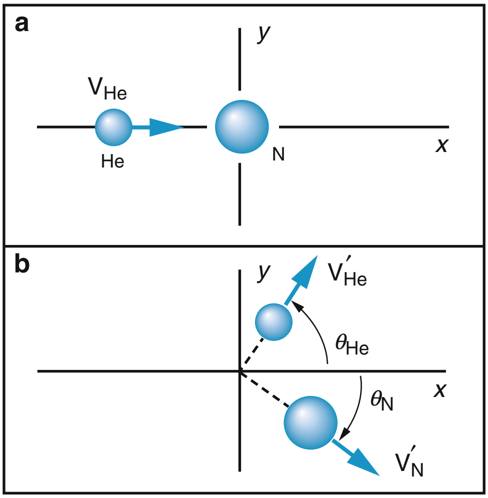

Fig. P6.2 (**a**) Before collision and (**b**) after collision

Problem 6.3 A particle of mass M is elastically scattered from a stationary proton of mass m. The proton is projected at an angle of $\varphi = 22.1°$, while the incident particle is scattered through an angle of $\theta = 5.6°$ with the incident direction. Calculate M in atomic mass units. (This event was recorded in photographic emulsions in the Wills Lab, Bristol).

Problem 6.4 A particle of mass M is elastically scattered through an angle θ from a target particle of mass m initially at rest ($M > m$).

(a) Show that the largest possible scattering angle $\theta_{\max}$ in the laboratory system is given by $\sin\theta_{\max} = m/M$, the corresponding angle in the center of mass system (CMS) being $\cos\theta^*_{\max} = -m/M$.
(b) Further show that the maximum recoil angle for m is given by $\sin\varphi_{\max} = [(M-m)/2M]^{1/2}$.
(c) Calculate the angle $\theta_{\max} + \varphi_{\max}$ for elastic collisions between the incident deuterons and target protons.

Problem 6.5 A deuteron of velocity u collides with another deuteron initially at rest. The collision results in the production of a proton and a triton (^{3} H), the former moving at an angle of 45° with the direction of incidence. Assuming that this rearrangement collision may be approximated to an elastic collision (quasi-scattering), calculate the speed and direction of triton in the lab and center of mass (CM) system.

Problem 6.6 An α-particle from a radioactive source collides with a stationary proton and continues with a deflection of 10°. Find the direction in which the proton moves (α-mass = 4.004 amu; proton mass = 1.008 amu).

Problem 6.7 An α-particle of kinetic energy of 20 MeV pass through a gas; it is found to be elastically scattered at angles up to 30° but not beyond. Explain this, and identify the gas. In what way, if any, does the limiting angle vary with energy?

Problem 6.8 A perfectly smooth sphere of mass m_1 moving with velocity v collides elastically with a similar but initially stationary sphere of mass m_2 ($m_1 > m_2$) and is deflected through an angle θ_L. Describe how this collision would appear in the center of mass frame of reference and show that the relation between θ_L and the angle of deflection θ_M, in the center of mass frame, is $\tan \theta_L = \sin \theta_M / [m_1/m_2 + \cos \theta_M]$. Show also that θ_L cannot be greater than about 15° if $(m_1/m_2) = 4$.

Problem 6.9 Show that the maximum velocity that can be imparted to a proton at rest by nonrelativistic alpha particle is 1.6 times the velocity of the incident alpha particle.

Problem 6.10 Show that the differential cross section $\sigma(\theta)$ for the scattering of protons by protons in the lab system is related to $\sigma(\theta^*)$ corresponding to the center of mass system (CMS) by the formula $\sigma(\theta) = 4\cos(\theta^*/2)\, \sigma(\theta^*)$.

Problem 6.11 If E_0 is the neutron energy and σ the total cross section for low-energy n–p scattering assumed to be isotropic in the center of mass system (CMS), then show that in the laboratory system (LS), the proton energy distribution is given by $(d\sigma_\mathrm{p}/dE_\mathrm{p}) = (\sigma/E_0) =$ constant.

Problem 6.12 Particles of mass m are elastically scattered off target nuclei of mass M initially at rest. Assuming that the scattering in the center of mass system (CMS) is isotropic, show that the angular distribution of M in the laboratory system (LS) has $\cos \varphi$ dependence.

Problem 6.13 A beam of particles of negligible size is elastically scattered from an infinitely heavy hard sphere of radius R. Assuming that the angle of reflection is equal to the angle of incidence in any encounter, show that $\sigma(\theta)$ is constant, that is, scattering is isotropic, and that the total cross section is equal to the geometric cross section, πR^2.

Problem 6.14 Calculate the maximum wavelength of γ-rays which in passing through matter can lead to the creation of electrons.

Problem 6.15 A positron and an electron with negligible kinetic energy meet and annihilate one another, producing two γ-rays of equal energy. What is the wavelength of these γ-rays?

Problem 6.16 Show that electron–positron pair cannot be created by an isolated photon.

Problem 6.17 In dealing with the diffusion of monoenergetic neutrons from a point source, the source diffusion equation for the flux distribution for a spherical symmetry is given in the following form:

$$\frac{d^2\phi}{dr^2} + \frac{2}{r}\frac{d\phi}{dr} - k^2\phi = 0 \tag{6.92a}$$

Solve the differential equation (6.92a) and show that the general solution is in the form of the following type:

$$\phi(r) = A\left(\frac{e^{-kr}}{r}\right) \tag{6.92b}$$

where in Eq. (6.92b), the parameter A can be evaluated based on what is so-called source condition. Hint: Assume $\phi\,(r) \equiv y/r$.

Problem 6.18 Determine the value of parameter A, in Problem 6.17, if $\vec{J}$ is the neutron current density at the surface of a sphere of radius r, with the source at the center. Utilize Fick's law that you have learned in Chap. 3 in r-direction due to symmetrical condition. Assume the source strength is Q neutrons per second, i.e., to the number of neutrons emitted by the point source in all directions per second.

Problem 6.19 A hypothetical source of thermal neutrons emits 10^6 neutrons per second into a surrounding "infinite" graphite block. Determine the neutron flux at distances of 27, 54, and 108 cm from this source. For graphite $k = 1/L$ is 0.0185 cm^{-1}, and the appropriate diffusion coefficient D is 0.94 cm. **Hint:** Use the result of the solution that you found in Problem 6.18.

Reference

1. J.R. Lamarsh, *Introduction to Nuclear Reactor Theory* (Addison-Wesley, Reading, 1966)

Chapter 7
Resonance Processing

In this chapter, we will study the Doppler broadening of resonances. The Doppler effect improves reactor stability. Broadened resonance or heating of a fuel results in a higher probability of absorption, thus causes negative reactivity insertion or reduction of reactor power. One of the most important virtues of the optical model is that it takes into account the existence of *giant* or *broad resonances* in the total cross section as part of neutronic analysis for nuclear reactor systems. For resonances of energy levels, which are spaced widely apart, we can describe the energy dependency of the absorption cross section via the *Breit–Wigner single-level resonance formula*.

7.1 Difficulties Presented by Resonance Cross Sections

Interactions between neutrons and nuclei in nuclear reactors can be classified broadly into scattering and absorption reactions as shown in Table 7.1 and were described in Chap. 1.

Scattering is further classified into elastic scattering in which the kinetic energy is conserved before and after the reaction and inelastic scattering in which a part of the kinetic energy is used in exciting a target nucleus. In absorption, the main reactions are capture, fission, charged particle emission, and neutron emission. Thus, the microscopic cross sections of the total, scattering, and absorption reactions are given by

B. Zohuri, *Neutronic Analysis For Nuclear Reactor Systems*,
DOI 10.1007/978-3-319-42964-9_7

Table 7.1 Classification of key nuclear reactions in a nuclear reactor [1]

Classification	Reaction	Transcription	Cross section symbol	Reaction example
Scattering (σ_s)	Elastic scattering	(n, n)	σ_e	$\mathrm{H}^1(n, n)$
Absorption (σ_a)	Inelastic scattering	(n, n')	σ_{in}	$\mathrm{U}^{238}(n, n')$
	Radiative capture Fission	(n, γ)	σ_γ	$\mathrm{U}^{238}(n, \gamma)$
	Charged particle emission	(n,f)	σ_f	$\mathrm{U}^{235}(n,f)$
	Neutron emission	(n, p)	σ_p	$\mathrm{N}^{14}(n, p)$
		(n, α)	σ_α	$\mathrm{B}^{10}(n, \alpha)$
		$(n, 2n)$[a]	$\sigma_{(n,2n)}$	$\mathrm{Be}^9(n, 2n)$

[a] The $(n, 2n)$ reaction can be treated as a special scattering reaction. Here this reaction, which transmits the nuclide, is classified as an absorption reaction

$$\text{Total cross section :} \qquad \sigma_t(E) = \sigma_s(E) + \sigma_a(E) \tag{7.1}$$

$$\text{Scattering cross section :} \qquad \sigma_s(E) = \sigma_e(E) + \sigma_{\text{in}}(E) \tag{7.2}$$

$$\text{Absorption cross section :} \quad \sigma_a(E) = \sigma_\gamma(E) + \sigma_f(E) + \sigma_p(E) + \sigma_\alpha(E) \; + \sigma_{(n,2n)}(E) \tag{7.3}$$

To further have, a general discussion of energy dependency of these microscopic cross sections and neutron energy range for design of nuclear reactors. The neutron energy range to be considered in the design of nuclear reactors is from the Maxwellian distribution of the thermal neutrons at room temperature to the fission spectrum of the prompt neutrons. As we have learned in reactor design, most nuclear design codes handle the range of 10^{-5} eV to 10 MeV. In this energy range, the microscopic cross sections introduced in Eqs. 7.1–7.3 and they behave as shown in Fig. 7.1 [1].

In Chap. 6, we learned that the elastic scattering cross section is mostly constant in all the energies except for the MeV region. Meanwhile, in inelastic scattering, the incident neutron should have sufficient kinetic energy to place the target nucleus in its excited state. Hence, the inelastic scattering cross section is zero up to some threshold energy of several MeV. Fast neutrons can be moderated by inelastic scattering with heavy nuclides, but by elastic scattering with light nuclides below threshold energies of the heavy nuclides [1].

Most absorption cross sections including the fission cross section appear as a straight line with a slope of $-1/2$ on a log–log scale. This means that the absorption cross sections are inversely proportional to the neutron speed ($1/v$ law) and therefore increase as the neutron energy decreases. Using such large fission cross sections at low neutron energies and thermal neutrons in the Maxwellian distribution makes it possible that natural or low-enrichment uranium-fueled reactors reach a critical state. The current thermal reactors, represented by LWRs, use the characteristics of the cross section.

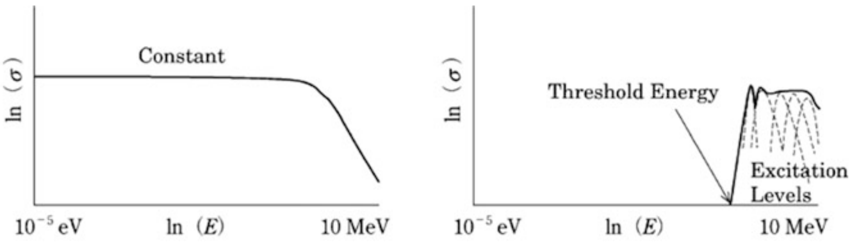

(a) Elastic Scattering

(b) Inelastic Scattering

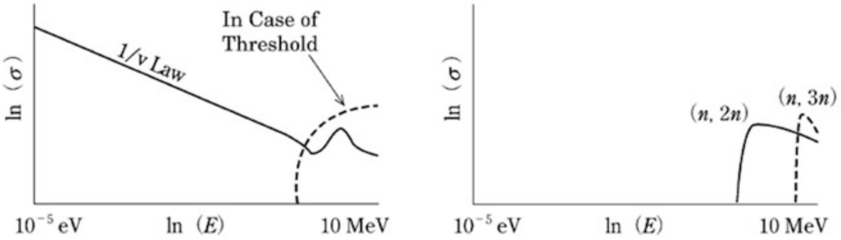

(c) Absorption
(Capture, Fission, and Charged-Particle Emission)

(d) Neutron Emission

Fig. 7.1 Energy dependence of cross sections [1]

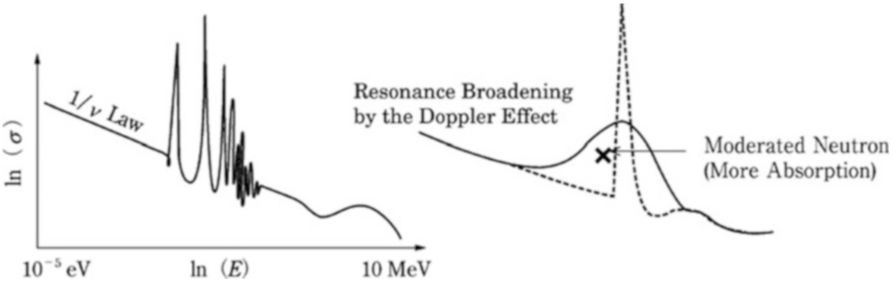

Fig. 7.2 Resonance absorption cross section and Doppler effect [1]

For heavy nuclides such as fuel materials, many resonances are observed in elastic scattering and absorption cross section as shown in Fig. 7.2. The widths of the resonances broaden as fuel temperature increases. This is called the Doppler effect, which is the subject of our next section (i.e., Secs. 7.1 and 7.2) in this chapter. The width broadening facilitates resonance absorption of neutrons under moderation. Most low-enrichment uranium fuel is composed of fertile U^{238}, and thermal neutrons escaping from the resonance of capture reaction induce fissions for the next generation.

Hence, a rise in fuel temperature leads to a decrease in the resonance escape probability of moderated neutrons and then fission events in the reactor decrease with thermal neutrons. Such a mechanism is called negative temperature feedback. The temperature dependence is not described in the Boltzmann equation of Eq. 3.1; however, it is reflected in the cross sections of the equation.

The Doppler effect arises from the dependence of neutron cross sections on the relative velocity between a neutron and a nucleus. The probability of the radiative capture depends on the center of mass energy; therefore, it depends on the kinetic energy of the incident neutron and the velocity of the target nucleus. Target nuclei are themselves in continual motion owing to their thermal energy. Because of these thermal motions, neutrons' impinging on a target appears to the nuclei in the target to have a continuous spread in energy. This, in turn, has an effect on the observed shape of resonance. Raising the temperature causes the nuclei to vibrate more rapidly within their lattice structures, effectively broadening the energy range of neutrons that may be resonantly absorbed in the fuel. The resonance becomes shorter and wider than when the nuclei are at rest.

7.2 What Is Nuclear Resonance: Compound Nucleus

For us to be able to write about this topic, we start our discussion with the subject of *radiative capture*, which its reactions are playing significant roles in reactor analysis because they remove neutrons from the chain reaction, and we briefly did expand upon it in both Chaps. 1 and 2.

"Further we can see that such reactions proceed via compound nucleolus formation in which the incident neutron is first absorbed to form the compound nucleolus of atomic mass number $A + 1$, and this nucleolus subsequently decays by eliminating a cascade of high-energy gammas" [2].

For the reason stated above, the capture cross section is a function of the neutron kinetic energy E and illustrates a resonance behavior at those energies at which the center of mass (CM) energy E_c plus the neutron binding energy E_b does match an energy level of the compound nuclease. Such definition can be demonstrated for neutron capture in U^{238} and schematically can be depicted in Fig. 7.3.

Figure 7.3, in particular, is demonstrating the energy level diagram for the U^{239} for one of the low-lying resonances at $E = 6.67$ eV. Since the excited energy levels are typically in the MeV range, the total energy of the emitted gammas will be quite large.

For resonance, energy levels are presented by Fig. 7.3 and are spaced widely apart. It is possible to describe the absorption cross section dependency by a very simple mathematical formula, which is known as the Breit–Wigner single-level resonance formula as it was expressed in the form of Eq. 1.30, which is again shown here as follows:

$$\sigma_\gamma(E_c) = \sigma_0 \frac{\Gamma_\gamma}{\Gamma}\left(\frac{E_0}{E_c}\right)^{1/2} \frac{1}{1+\gamma^2} \quad \text{and} \quad y = \frac{2}{\Gamma}(E_c - E_b) \tag{7.4}$$

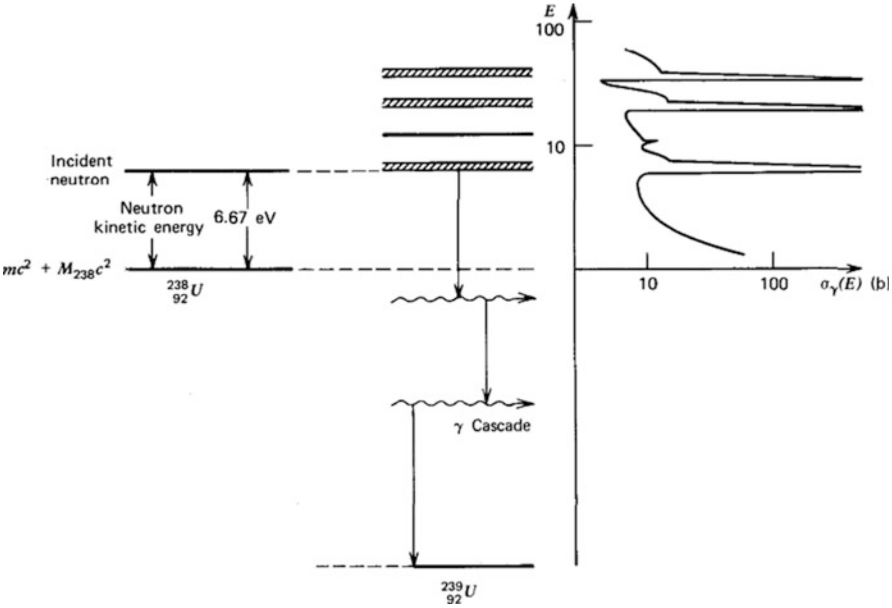

Fig. 7.3 Energy level diagram of the capture resonance in U^{238} at $E = 6.67$ eV (Courtesy of Duderstadt and Hamilton) [2]

In Eq. 7.4, E_0 is the energy at the level where the resonance takes place, namely, the energy E_c at which $E_c + E_b$ matches the energy level of the compound nucleus. The symbol Γ which is the so-called total line width of resonance is characterizing the width of the energy level and the full width at half maximum (FWHM) of the resonance, while Γ_γ is the *radiative line width* and is characterizing the probability that the compound nucleus will decay via gamma emission.

In Eq. 7.4, the symbol of σ_0 is the value of the *total cross section* $\sigma_{\text{tot}}(E)$ at the resonance energy E_0 and can be expressed in terms of the reduced neutron wavelength $\lambda\!\!\!^{-}_0$ at E_0 and atomic mass A as

$$\sigma_0 = 4\pi\lambda\!\!\!^{-}{}_0^2\frac{\Gamma_n}{\Gamma}g - 2.608 \times 10^6\frac{(A+1)^2}{A^2E_0(\text{eV})}\frac{\Gamma_n}{\Gamma}g \tag{7.5}$$

In Eq. 7.5, $g = (2J+1)/(2I+1)$ is a statistical spin factor that is given in terms of the nuclear spin I and total spin J, while Γ_n is the *neutron line width* and varies in energy as presented in following equation:

$$\Gamma_n \sim E^{1/2} \tag{7.6}$$

The Breit–Wigner resonance shape versus the center of mass (CM) kinetic energy E_c is depicted in Fig. 7.4, and note that the resonance absorption is in the order of importance in heavy nuclei, and we can approximate $E_c \sim E$.

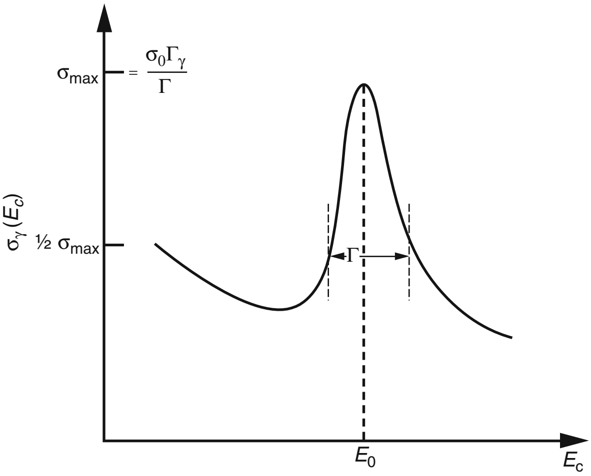

Fig. 7.4 Single-level capture resonance (Courtesy of Duderstadt and Hamilton) [2]

Note as well that for low energies, i.e., $E \ll E_0$, the cross section behaves as essentially $1/E^{1/2} = E^{-1/2}$ or $1/v$ velocity of neutron and for large energies, i.e., $E \gg E_0$, the cross section drops off quite rapidly as $1/E^{5/2} = E^{-5/2}$, and it is also important to know that such absorption cross sections are largest at low energies.

In summary, if we ask "What is a compound nucleus and what is resonance?," we can answer that by saying, there is really no difference between the compound nucleus and nuclear resonance.

The compound nucleus is the intermediate state formed in a compound nucleus reaction. It is normally one of the excited states of the nucleus formed by the combination of the incident particle and target nucleus. If a target nucleus with atomic mass number A is bombarded with particles x, it is sometimes observed that the ensuing nuclear reaction takes place with appreciable probability only if the energy of the particle x is in the neighborhood of certain definite energy values. These energy values are referred to as resonance energies. The compound nuclei of these certain energies are referred to as nuclear resonances. Resonances are usually found only at relatively low energies of the projectile. The widths of the resonances increase in general with increasing energies. At higher energies, the widths may reach the order of the distances between resonances and then no resonances can be observed. The narrowest resonances are usually the compound states of heavy nuclei (such as fissionable nuclei) and thermal neutrons (usually in (n, γ) capture reactions; see Table 7.1 as well). The observation of resonances is by no means restricted to neutron nuclear reactions, and both illustrations (a) and (b) in Fig. 7.5, in general, are illustrating the energy levels of a compound state. For the neutron absorption reaction of U^{238}, the first resonance E_1 corresponds to the excitation energy of 6.67 eV as we said, and E_0 is a base state of U^{239} [3].

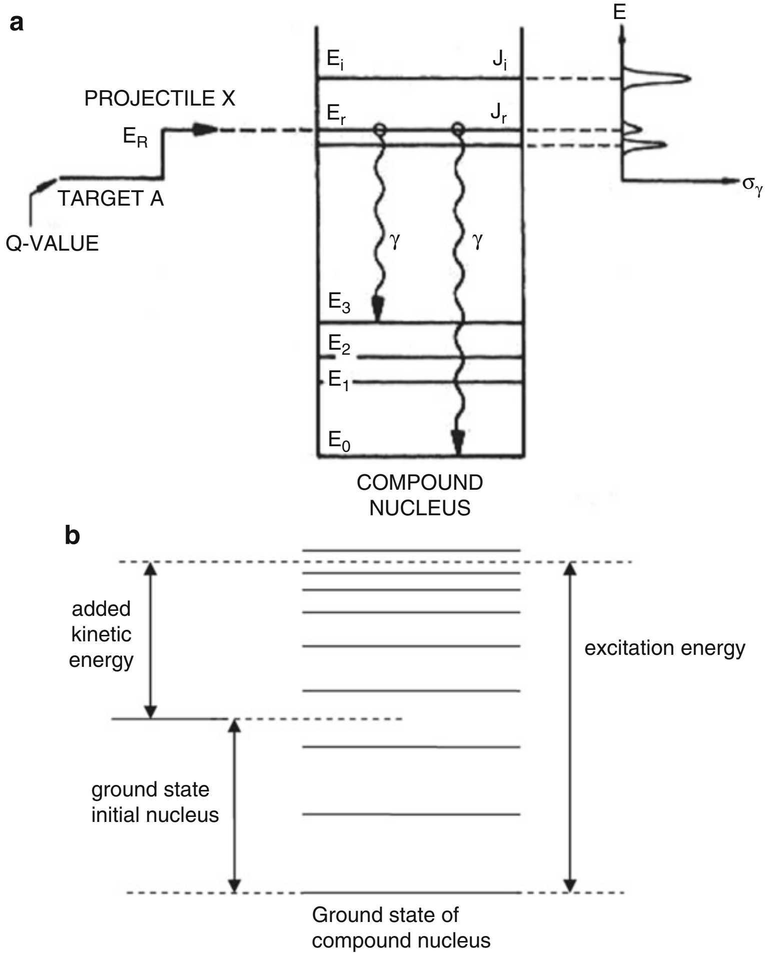

Fig. 7.5 Energy levels of a compound state

7.2.1 Breit–Wigner Resonance Reaction Cross Sections

We have the formula that the total cross section is given by

$$\sigma_t = 4\pi ƛ^2 \sin^2\delta_0 \tag{7.7}$$

For the orbital angular momentum quantum number, $l = 0$ total cross section. Now if we assume a Lorentzian shape for the $\sin^2\delta_0$ term at an interaction resonance at energy E_r and a full width at half maximum Γ, such that

$$\sin^2\delta_0 = \frac{\left(\frac{\Gamma}{2}\right)^2}{(E - E_r)^2 + \left(\frac{\Gamma}{2}\right)^2} \tag{7.8}$$

and realizing that for an absorption, the fraction of time the compound nucleus can be formed is Γ_n/Γ and the fraction of time it can decay by an absorption (gamma decay) is given by Γ_r/Γ, we get that the cross section for neutron absorption is given by

$$\sigma_a = \sigma_\gamma = 4\pi ƛ^2 \frac{\frac{\Gamma_n}{\Gamma}\frac{\Gamma_\gamma}{\Gamma}\left(\frac{\Gamma}{2}\right)^2}{(E - E_r)^2 + \left(\frac{\Gamma}{2}\right)^2} = \pi ƛ^2 \frac{\Gamma_n\Gamma_\gamma}{(E - E_r)^2 + \left(\frac{\Gamma}{2}\right)^2} \tag{7.9}$$

This is the correct equation but it does not include the effects of neutron or nucleus spin. The effects of spin are included by multiplying by the g factor, where g is given by

$$\begin{aligned} g &= \frac{J + 1}{(2s + 1)(2l + 1)} \\ J &= s + l + I \end{aligned} \tag{7.10}$$

where

$s =$ spin quantum number of the neutron
$l =$ orbital angular momentum quantum number
$J =$ total angular momentum quantum number
$I =$ ground state spin quantum number of the nucleus

Therefore, we have the absorption cross section written as

$$\begin{aligned} \sigma_\gamma &= \pi ƛ^2 g \frac{\Gamma_n\Gamma_\gamma}{(E - E_r)^2 + \left(\frac{\Gamma}{2}\right)^2} = \frac{\Gamma_\gamma}{\Gamma}\frac{\sigma_o}{1 + y^2} \\ \sigma_o &= 4\pi ƛ^2 g\left(\frac{\Gamma_n}{\Gamma}\right) \\ y &= \frac{2}{\Gamma}(E - E_r) \end{aligned} \tag{7.11}$$

Note that the neutron width varies with the square root of energy such that $\Gamma_n = \Gamma_n^0 E^{1/2}$, and $ƛ \sim 1/E^{1/2}$. Thus as the energy goes to zero, the cross section behaves as $E^{1/2}$, which is the classic $1/v$ behavior that is observed in many nuclides.

The resonance scattering cross section is slightly different as the potential scattering cross section interferes with the compound nucleus resonance scattering cross section. The complete scattering cross section is given by

$$\begin{aligned}
\sigma_n(E) &= 4\pi R^2 + 4\pi \lambdabar^2 g\left[\left|\tfrac{\Gamma_n/2}{E-E_r+i\Gamma/2}+\tfrac{R}{\lambdabar}\right|^2-\left(\tfrac{R}{\lambdabar}\right)^2\right] \\
\sigma_n(E) &= \sigma_p + \frac{\Gamma_n}{\Gamma}\frac{\sigma_o}{1+y^2} + \left(\sigma_{on}\sigma_p\frac{\Gamma_n}{\Gamma}\right)^{1/2}\frac{2y}{1+y^2} \\
\sigma_o &= 4\pi\lambdabar^2 g\left(\frac{\Gamma_n}{\Gamma}\right) \\
\sigma_p &= 4\pi R^2
\end{aligned} \tag{7.12}$$

This gives the total resonance cross section as

$$\begin{aligned}
\sigma_t(E) &= \sigma_p + \frac{\Gamma_n}{\Gamma}\frac{\sigma_o}{1+y^2} + \left(\sigma_{on}\sigma_p g\frac{\Gamma_n}{\Gamma}\right)^{1/2}\frac{2y}{1+y^2} + \frac{\Gamma_\gamma}{\Gamma}\frac{\sigma_o}{1+y^2} \\
\sigma_t(E) &= \frac{\sigma_o}{1+y^2} + \left(\sigma_o\sigma_p\frac{\Gamma_n}{\Gamma}\right)^{1/2}\frac{2y}{1+y^2} + \sigma_p
\end{aligned} \tag{7.13}$$

7.2.2 *Resonance and Neutron Cross Section*

For the compound nucleus, peaks in the cross section are typical. Each peak is manifesting a particular compound state of the nucleus. These peaks and the associated compound nuclei are usually called resonances. The behavior of the cross section between two resonances is usually strongly affected by the effect of nearby resonances.

Resonances (particular compound states) are mostly created in neutron nuclear reactions, but it is by no means restricted to neutron nuclear reactions. The formation of resonances is caused by the quantum nature of nuclear forces. Each nuclear reaction is a transition between different quantum discrete states or energy levels. The discrete nature of energy transitions plays a key role. If the energy of the projectile (the sum of the Q value and the kinetic energy of the projectile) and the energy of target nucleus are equal to a compound nucleus at one of the excitation states, a resonance can be created, and peak occurs in the cross section. For light nucleus, the allowable state density in this energy region is much lower, and the "distance" between states is higher. For heavy nuclei, such as U^{238}, we can observe a large resonance region in the neutron absorption cross section.

As illustrated in Fig. 7.6, this figure shows region of resonance of U^{238} nuclei, while Fig. 7.7 is a presentation of uranium-235 comparison of total fission cross section and cross section for radiative capture, which was described in the previous section.

It is obvious the compound states (resonances) are observed at low excitation energies. This is due to the fact that the energy gap between the states is large. At high excitation energy, the gap between two compound states is very small, and the

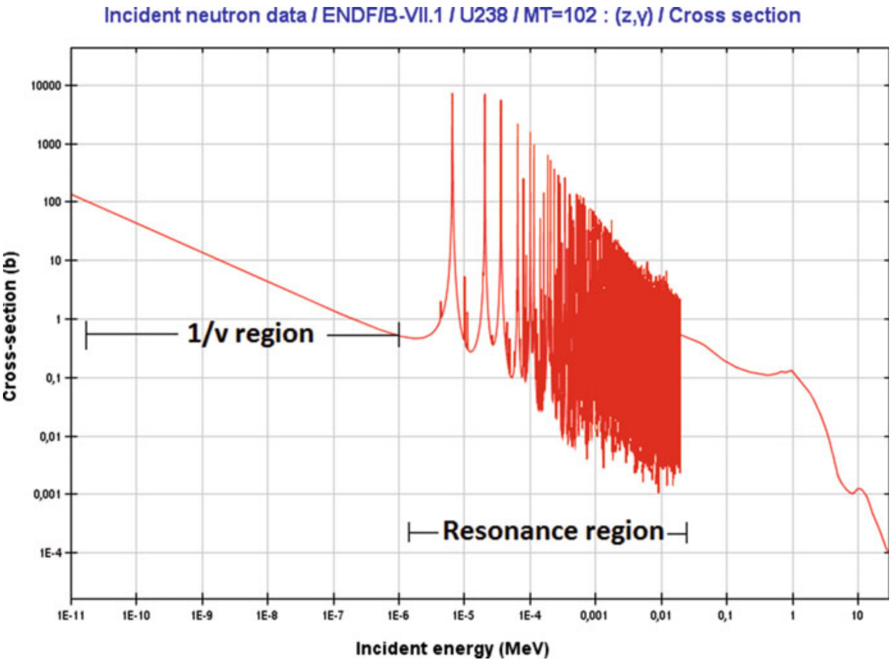

Fig. 7.6 Region of resonance of U238 nuclei. *Source*: JANIS (Java-Based Nuclear Data Information Software); The ENDF/B-VII.1 Nuclear Data Library

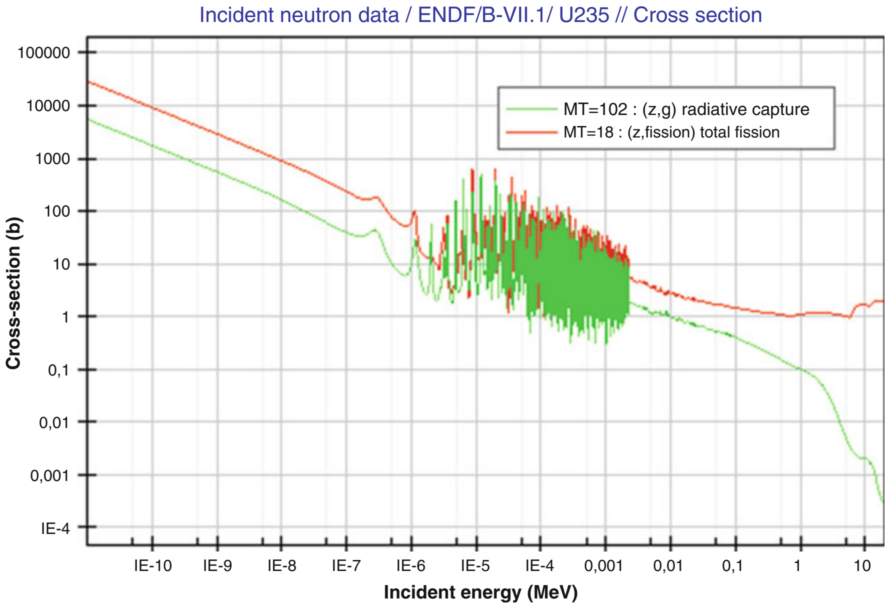

Fig. 7.7 Comparison of total fission cross section and cross section for radiative capture for U^{238}. *Source*: JANIS (Java-Based Nuclear Data Information Software); The ENDF/B-VII.1 Nuclear Data Library

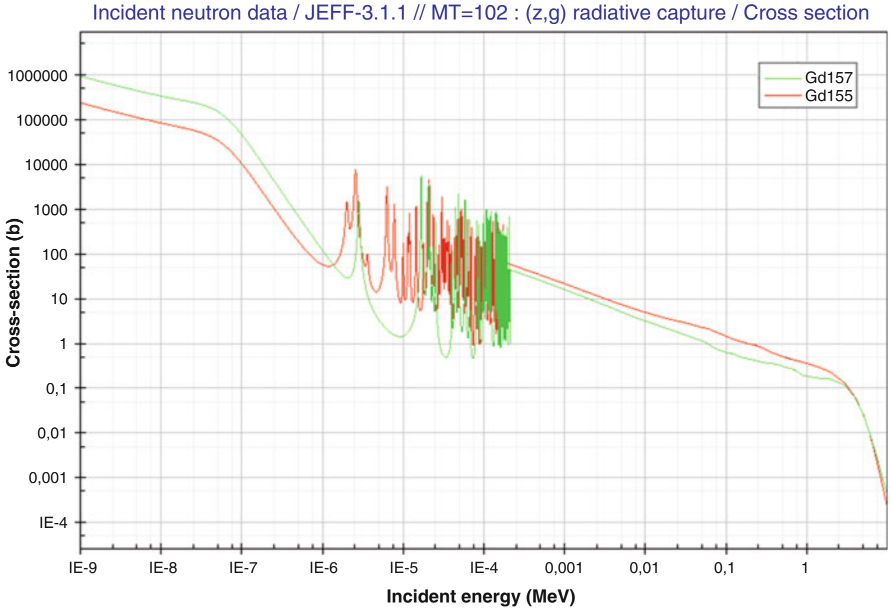

Fig. 7.8 Gadolinium-155 and gadolinium-157 incident neutron data. *Source*: JANIS (Java-Based Nuclear Data Information Software); The JEFF-3.1.1 Nuclear Data Library

widths of resonances may reach the order of the distances between resonances. Therefore, at high energies, no resonances can be observed, and the cross section in this energy region is continuous and smooth.

Here, both Figs. 7.8 and 7.9 are illustrating the comparison of radiative capture cross sections, both for gadolinium-155 and gadolinium-157 nuclei that have region of resonance, and comparison of the total cross section of boron-10 and cross section for (n, α), respectively. B^{10} does not have any region of resonance.

Now, we are in position to go forward, with the description of the Doppler effect and Doppler broadening of resonances in the next section.

7.3 Doppler Effect and Doppler Broadening of Resonance

The Doppler-broadened Breit–Wigner resonance cross section, first derived many years ago by Bethe and Placzek [4], is more commonly found in textbooks. In general, Doppler broadening is the broadening of spectral lines due to the Doppler effect caused by a distribution of kinetic energies of molecules or atoms. In reactor physics, a particular case of this phenomenon is the thermal Doppler broadening of the resonance capture cross sections of the fertile material (e.g., U^{238} or Pu^{240}) caused by thermal motion of target nuclei in the nuclear fuel.

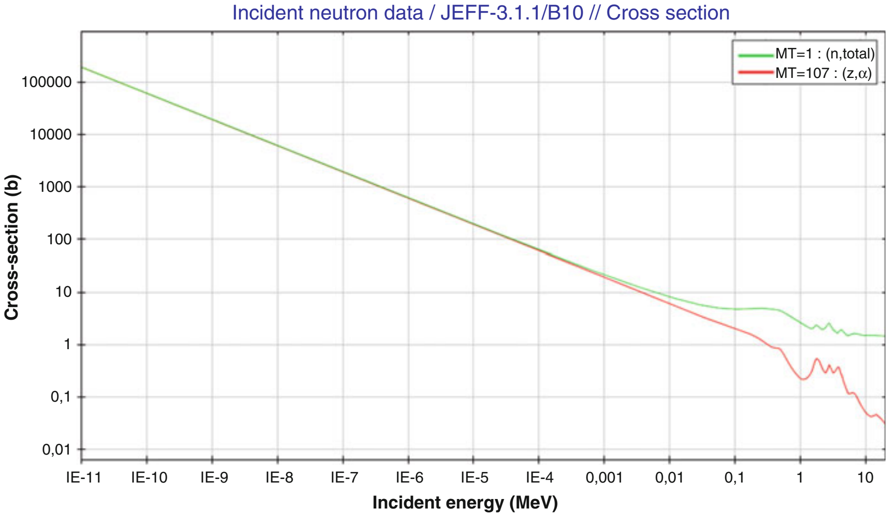

Fig. 7.9 Boron-10 incident neutron data. *Source*: JANIS (Java-Based Nuclear Data Information Software); The JEFF-3.1.1 Nuclear Data Library

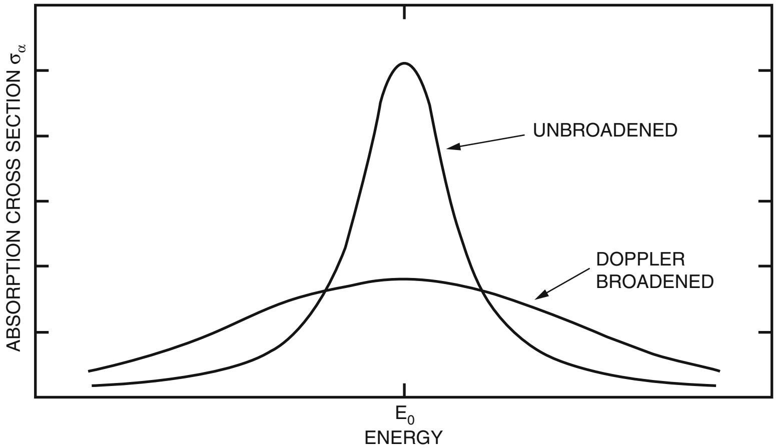

Fig. 7.10 Doppler effect improves reactor stability [5]

The Doppler effect improves reactor stability. Broadened resonance (heating of a fuel) results in a higher probability of absorption and, thus, causes negative reactivity insertion (reduction of reactor power), and this can be seen as an illustration in Fig. 7.10 schematically.

For heavy nuclides such as fuel materials, many resonances are observed in elastic scattering and absorption cross section as shown in Fig. 7.2. The widths of the resonances broaden as fuel temperature increases. This is called the Doppler effect, and the width broadening facilitates resonance absorption of neutrons under moderation. As we have mentioned previously, most low-enrichment uranium fuel is composed of fertile U^{238}, and thermal neutrons escaping from the resonance of capture reaction induce fissions for the next generation.

Hence, a rise in fuel temperature leads to a decrease in the resonance escape probability of moderated neutrons, and then fission events in the reactor decrease with thermal neutrons. Such a mechanism is called negative temperature feedback. Note that temperature dependence is not described in the Boltzmann equation of Eq. 3.1; however, it is reflected in the cross sections of the equation.

The Doppler broadening of resonances is a very important phenomenon, which improves reactor stability, because it accounts for the dominant part of the fuel temperature coefficient (the change in reactivity per degree change in fuel temperature) in thermal reactors and makes a substantial contribution in fast reactors as well. This coefficient is also called the prompt temperature coefficient because it causes an immediate response on changes in fuel temperature. The prompt temperature coefficient of most thermal reactors is negative.

A negative fuel temperature coefficient is generally considered to be even more important than a negative moderator temperature coefficient. Especially in the case of reactivity-initiated accidents (RIA), the Doppler coefficient of reactivity would be the first and most important effect in the compensation of the inserted positive reactivity. The time for heat to be transferred to the moderator is usually measured in seconds, while the Doppler coefficient is effective almost instantaneously. Therefore, the moderator temperature cannot turn the power up for several seconds, whereas the fuel temperature coefficient starts adding negative reactivity immediately. The fuel temperature coefficient α_f may be defined as

$$\alpha_f = \frac{1}{k}\frac{\partial k}{\partial \overline{T}_f} \tag{7.14}$$

The Doppler effect arises from the dependence of neutron cross sections on the relative velocity between neutron and nucleus. The probability of the radiative capture depends on the center of mass energy; therefore, it depends on the kinetic energy of the incident neutron and the velocity of the target nucleus. Target nuclei are themselves in continual motion owing to their thermal energy. Because of these thermal motions, neutrons impinging on a target appear to the nuclei in the target to have a continuous spread in energy. This, in turn, has an effect on the observed shape of resonance. Raising the temperature causes the nuclei to vibrate more rapidly within their lattice structures, effectively broadening the energy range of neutrons that may be resonantly absorbed in the fuel. The resonance becomes shorter and wider than when the nuclei are at rest.

Although the shape of a resonance changes with temperature, the total area under the resonance remains essentially constant. Nevertheless, this does not imply constant neutron absorption. Despite the constant area under resonance, the resonance integral, which determines the absorption, increases with increasing target temperature. The broadened resonances result in a larger percentage of neutrons

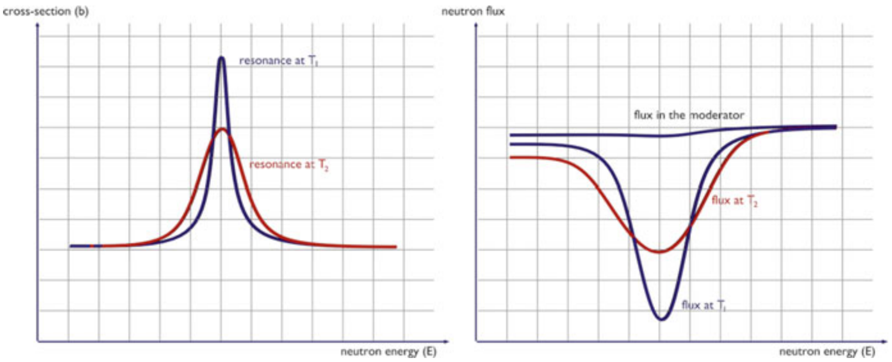

Fig. 7.11 Cross section and neutron flux versus neutron energy E [5]

having energies that are susceptible to capture in the fuel pellets. On the other hand, with colder fuel, only neutrons very close to the resonance energy are absorbed.

Moreover, there is a further phenomenon closely connected with “Doppler broadening”. The vicinity of the resonance causes an increase in the neutron absorption probability, when a neutron has energy near a resonance. This results in a reduction of the effective absorption per nucleus due to the depression of the energy-dependent flux $\phi(E)$ near the resonance in comparison to a flat flux. At energies just below the resonance, where $\Sigma_a(E)$ becomes small again, the neutron flux reaches almost the same value just above the resonance. This reduction in the energy-dependent neutron flux near the resonance energy is known as energy self-shielding. These two phenomena provide negative reactivity feedback against fuel temperature increase. See Fig. 7.11 for the thermally averaged capture cross section as determined by Doppler broadening of a resonance with increasing temperature.

This effect can be mathematically derived by utilizing the Maxwell–Boltzmann distribution of target nuclei, if we perform the integration over nuclear velocity V of the nucleus with mass of M in the following equation and the relationship for thermally averaged cross section as [2]

$$\overline{\sigma}(v,T)=\frac{1}{v}\int d^3V|v-V|\sigma(|v-V|)M(V,T) \tag{7.15}$$

In Eq. 7.15, the element v is the neutron velocity, while $\sigma(|v-V|)=\gamma/|v-V|$, which is relationship based on nuclear cross section behavior below a capture resonance as $1/v$, if nuclear motion behaves as such and $\gamma\equiv 2(E_C-E_0)/\Gamma$ [2].

Note that it is sufficient for most purposes to represent the nuclear velocity distribution by the Maxwell–Boltzmann distribution that was discussed in Chaps. 1 and 2, characterizing an ideal gas in thermal equilibrium at a temperature T.

Now if we integrate Eq. 7.15 over nuclear velocity of V and apply the Maxwell–Boltzmann distribution of target nuclei, we can write

$$\overline{\sigma}_\gamma(v,T)=\frac{1}{\sqrt{\pi}v_{\text{th}}^2 v}\int_0^\infty v_r^2\sigma_\gamma(v_r)dv_r\left[\exp\left(-\frac{(v-v_r)^2}{2v_{\text{th}}^2}\right)-\exp\left(-\frac{(v+v_r)^2}{2v_{\text{th}}^2}\right)\right] \tag{7.16}$$

where $v_r=|v-V|$, while $v_{\text{th}}=(kT/m)^{1/2}$, and if we substitute the Breit–Wigner formula defined in Eq. 7.4 into Eq. 7.16 for $\sigma_r(v_r)$, we find an exact expression for the averaged cross section as below:

$$\overline{\sigma}_\gamma(v,T)=\sigma_0\frac{\Gamma_\gamma}{\Gamma}\frac{1}{\sqrt{\pi}v_{\text{th}}^2 v}\int_0^\infty \frac{v_r dv_r}{1+y^2}\left[\exp\left(-\frac{(v-v_r)^2}{2v_{\text{th}}^2}\right)-\exp\left(-\frac{(v+v_r)^2}{2v_{\text{th}}^2}\right)\right] \tag{7.17}$$

Note that in relation v_{th} and k in the form of $v_{\text{th}}=(kT/m)^{1/2}$, constant k is known as the Boltzmann constant and is $k = 0.8617\text{E-}4$ eV/K = 1/11,600 eV/K.

We already have defined γ, where we recall that the ***CM*** energy is $E_C=\frac{1}{2}\mu v_r^2$; now if we define the following variables such as

$$x\equiv 2(E-E_0)/\Gamma \quad \text{and} \quad \xi\equiv\Gamma/\Gamma_D \tag{7.18}$$

where Γ_D is the so-called Doppler width of the resonance as we have described as before as

$$\Gamma_D\equiv\left(\frac{4E_0kT}{A}\right)^{1/2} \tag{7.19}$$

with Eq. 7.19 on hand, one can write the following result:

$$\overline{\sigma}_\gamma(E,T)=\sigma_0\frac{\Gamma_\gamma}{\Gamma}\left(\frac{E_0}{E}\right)^{1/2}\Psi(\xi,x) \tag{7.20}$$

where

$$\Psi(\xi,x)=\int_{-2E/\Gamma}^\infty\frac{dy}{1+y^2}\left[\exp\left(-\frac{(v-v_r)^2}{2v_{\text{th}}^2}\right)-\exp\left(-\frac{(v+v_r)^2}{2v_{\text{th}}^2}\right)\right] \tag{7.21}$$

Using any numerical integration technique, one is able to calculate the value of ξ and x in the real world of a reactor design.

The sketch of thermally averaged capture cross section as determined by Eq. 7.20, which is presented in Fig. 7.12, provides the better understanding of the matter.

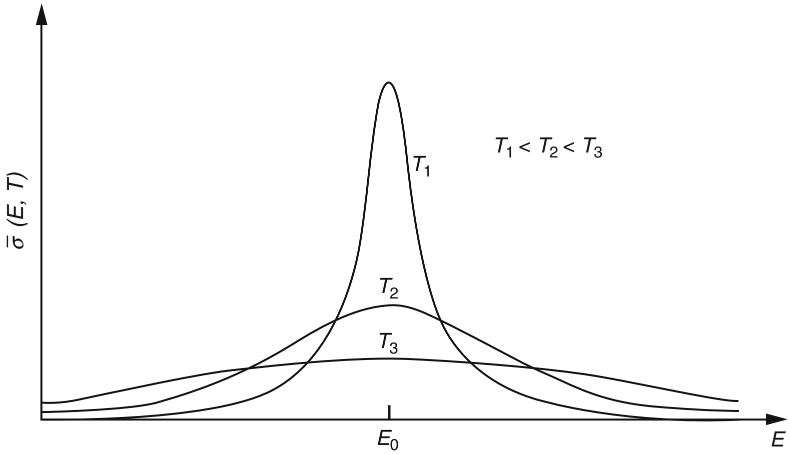

Fig. 7.12 Doppler broadening of a resonance with increasing temperature (Courtesy of Duderstadt and Hamilton) [2]

Figure 7.12, in particular, shows the dependence of a cross section on energy for several different temperatures T.

Further analysis of Fig. 7.12 reveals that as the temperature T increases, the resonance broadens, while its peak magnitude decreases. For this reason, one frequently refers to resonance cross sections that have been averaged over the distribution of nuclear velocities as "Doppler-broadened" cross sections.

Duderstadt and Hamilton [2] show that the high temperature limit $T \rightarrow \infty$ implies that $\xi \rightarrow 0$ and in this case Eq. 7.21 reduces to the following form, which is a Gaussian shape characterized by the Doppler width Γ_D rather than the "natural" line width Γ. Hence, as the temperature increases, the resonance broadens out from its natural width to eventually approach a width that depends on the temperature as $T^{1/2}$ [2].

7.4 Doppler Coefficient in Power Reactors

In power reactors, the Doppler coefficient is always negative. It is ensured by the fuel composition. In PWRs, the Doppler coefficient can range, for example, from -5 pcm/K to -2 pcm/K. The value of the Doppler coefficient α_f in Eq. 7.14 depends on the temperature of the fuel and depends on the fuel burnup as well, and the following points do apply. See Fig. 7.13.

- *Fuel temperature*: The dependency on the fuel temperature is determined by the fact that the rate of broadening diminishes at higher temperatures. Therefore, the Doppler coefficient becomes less negative (but always remains negative) as the reactor core heats up.

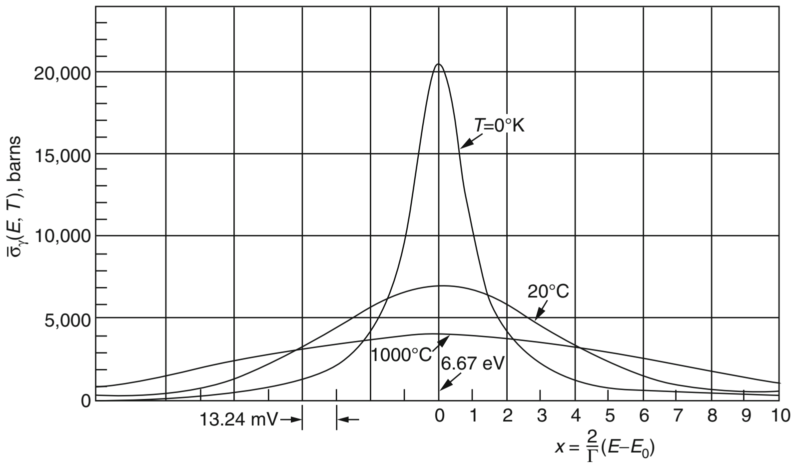

Fig. 7.13 Doppler broadening of the capture cross section of U^{238} at the 6.67 eV (Courtesy of Lamarsh) [6]

- *Fuel–cladding gap*: There is also one very important phenomenon which influences the fuel temperature. As the fuel burnup increases, the fuel–cladding gap reduces. This reduction is caused by the swelling of the fuel pellets and cladding creep. Fuel pellet swelling occurs because fission gases cause the pellet to swell resulting in a larger volume of the pellet. At the same time, the cladding is distorted by outside pressure (known as the cladding creep). These two effects result in direct fuel–cladding contact (e.g., at burnup of 25 GWd/tU). The direct fuel–cladding contact causes a significant reduction in the fuel temperature profile, because the overall thermal conductivity increases due to conductive heat transfer.
- *Fuel burnup*: During fuel burnup, the fertile materials (conversion of U^{238} to fissile Pu^{239} known as fuel breeding) partially replace fissile U^{235}. The plutonium content rises with the fuel burnup. For example, at a burnup of 30 GWd/tU (gigawatt-days per metric ton of uranium), about 30 % of the total energy released comes from bred plutonium. However, with the Pu^{239} rises also the content of Pu^{240}, which has significantly higher resonance cross sections than U ^{238}. Therefore, the Doppler coefficient becomes more negative as the Pu^{240} content rises. See Fig. 7.14.

In fast neutron reactors, the Doppler effect becomes less dominant (due to the minimization of the neutron moderation), but strongly depends on the neutron spectrum (e.g., gas-cooled reactors have harder spectra than other fast reactors) and the type of the fuel matrix (metal fuel, ceramic fuel, etc.). In fast reactors, other effects, such the axial thermal expansion of fuel pellets or the radial thermal expansion of reactor core, may also contribute to the fuel temperature coefficient. In thermal reactors, these effects tend to be small relative to that of "Doppler broadening."

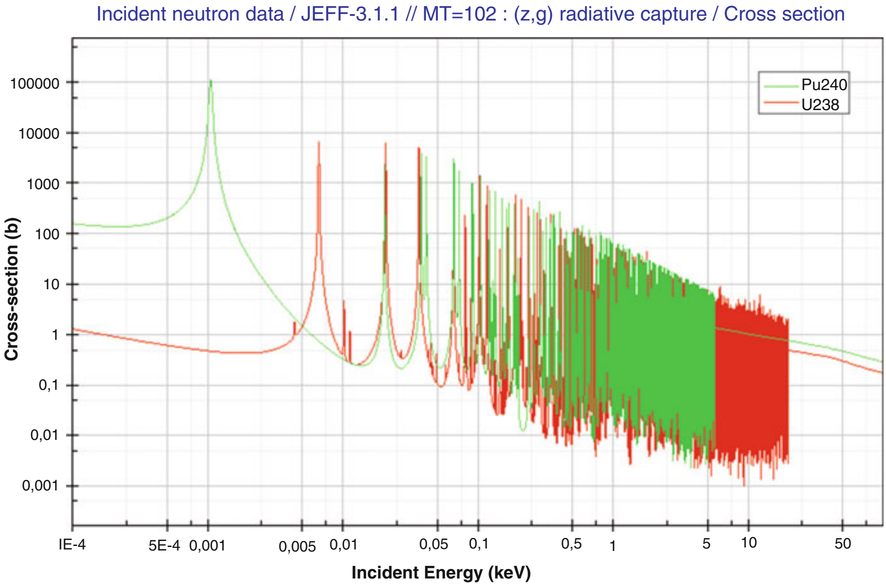

Fig. 7.14 Doppler broadening of Pu^{240} and U^{238}

Figure 7.14 here is presenting a schematic of comparison of the resonance capture cross section of U^{238} and Pu^{240}.

Note that in summary, it is difficult to define the dependency, because these effects have opposite directions.

7.5 Infinite Resonance Integrals and Group Cross Section

Here we can study the resonance absorption due to an infinity massive absorber distributed uniformly through an infinite medium of hydrogen that is mixed with U^{238}. The infinite absorber mass implies that all neutrons slowing down due to elastic scattering will be due to hydrogen, while we are ignoring any inelastic scattering circumstances. However, we want to include an absorption term in an infinite medium slowing down equation, which was described previously, knowing that in real situation, the absorption cross section of hydrogen will be assumed negligible, but the physical situation we want to describe is that of a strongly absorbing isotope mixed in hydrogen such as U^{238}.

However, for the simplicity of our analysis here, we assume the absorber to be “infinitely massive” so it does not slow down neutron, yet it only absorbs them. This assumption comes from the fact that the mentioned isotope can also scatter, and since its atomic mass number is not in unity, it will be difficult to validate our analysis for resonance integral and group cross section, so that is why the assumption of an infinite mass will be a reasonable approach.

Then, the appropriate slowing down equation with a monoenergetic source at energy E_0 is written as

$$[\Sigma_a(E)+\Sigma_s(E)]\phi(E)=\int_E^{E_0}dE'\frac{\Sigma_s(E')\phi(E')}{E'}+S_0(E_0)\delta(E-E_0) \tag{7.22}$$

where, in Eq. 7.22, the factor $S_0(E_0)$ is the rate at which source neutrons are emitted at energy level E_0.

To seek a solution for Eq. 7.22, Duderstadt and Hamilton [2] show more details of the analysis for the total collision density as the sum of collided and uncollided contribution, and we refer our readers to their book.

Furthermore, in open literature and available computer codes such as NJOY, which is dealing with group self-shielding for studying the neutron slow down in a medium with resonance absorption presence, for calculating the flux spectrum. The code NJOY looks at methods known as self-shielding to analyze the flux calculator method in an infinite medium spectrum or another one that is known as the Bondarenko method.

There is another method which is used by the NJOY computer code and that is known as the **CENTRM** (continuous energy transport module) method, where the code solves the Boltzmann transport equation using both pointwise and multigroup cross sections in a defined energy range to compute a pointwise flux spectrum [7].

7.5.1 The Flux Calculator Method

The method of the flux calculator expresses Eq. 7.15 in a general form as follows, by assuming that $\Sigma_t(E)=\Sigma_a(E)+\Sigma_s(E)$, so we can write

$$\Sigma_t(E)\phi(E)=\int_0^{\infty}dE'\,\Sigma_s(E'\to E)\phi(E')+S(E) \tag{7.23}$$

where the term on the left-hand side (LHS) of Eq. 7.16 represents the collision, the integral on the right-hand side (RHS) is the scattering source, and finally $S(E)$ is the external source.

Next, we can write Eq. 7.23 by considering a homogeneous medium consisting of two materials, an absorber and a moderator, represented by a and m, respectively, and write it in the form of Eq. 7.24. Elastic scattering cross sections that are isotropic in the center of mass are used. A neutron slowing down in a single resonance of the absorber material is assumed.

$$\Sigma_t(E)\phi(E) = \int_E^{E/\alpha_m} dE' \frac{\Sigma_{sm}(E')}{(1-\alpha_m)E'}\phi(E') + \int_E^{E/\alpha_a} dE' \frac{\Sigma_{sa}(E')}{(1-\alpha_a)E'}\phi(E') \tag{7.24}$$

where α_a and α_m are the absorber and the moderator collision parameter, respectively, and in terms of atomic mass number A are defined as

$$\alpha = \left(\frac{A-1}{A+1}\right)^2 \tag{7.25}$$

Note that for us to be able to establish and write down Eq. 7.24, the following approximations are introduced:

- The moderator scattering cross section is assumed to be constant and equal to the potential scattering cross section, i.e., $\Sigma_s^M(E') = \Sigma_p^M$.
- The moderator absorption cross section is assumed to be negligible, i.e., $\Sigma_t^M(E') = \Sigma_p^M$.
- The narrow resonance approximation is used for the moderator. This states that the resonance width is very small, compared to the energy loss from scattering with the moderator nucleus. Therefore, the flux distribution in the moderator integral is assumed to have an asymptotic form. In general, the moderator integral is assumed to be a smooth function of energy represented as $C(E)$.
- The moderator is assumed to represent all nuclides other than the absorber. This enables the inclusion of the dilution microscopic cross section of the absorber σ_d in Eq. 7.24. The dilution (or background) cross section of an isotope i is defined to be all cross sections representing isotopes other than the isotope i. The dilution cross section is a measure of energy self-shielding. It determines the significance of a resonance compared to other cross sections. If the dilution cross section (σ_d) is small, it indicates that the resonance has a significant impact on the flux and a large self-shielding effect exists. If σ_d is very large (infinite dilution), the cross sections of the absorber do not affect the flux spectrum, and the flux may be represented as a smooth function of energy.

Taking all the above approximations under consideration, Eq. 7.24 becomes

$$[\sigma_d + \sigma_{ta}]\phi(E) = C(E)\sigma_d + \int_E^{E/\alpha_a} dE' \frac{\sigma_{sa}(E')}{(1-\alpha_a)E'}\phi(E') \tag{7.26}$$

The dilution cross section for an isotope i is then given as

$$\sigma_d = \frac{1}{\rho_i}\sum_{j\neq i}\rho_j\sigma_{tj} \tag{7.27}$$

where i and j represent isotope indexes and ρ is the atomic density. Equations such as the one written as Eq. 7.26 are used in codes such as NJOY for computing the flux with the flux calculator option. In NJOY, several dilution cross sections are provided as input. Depending on a system of interest, the cross sections corresponding to the appropriate dilution cross section are used [7].

7.5.2 The Bondarenko Method: The Bondarenko Factor

Prof. Bondarenko of the USSR came up with a very efficient method for calculating fast reactor cross sections for a specific reactor design from pre-calculated tables of what have come to be called self-shielding factors. Bondarenko's insight for fast reactor cross sections got the technique started, and it has been widely applied to many problems.

The Bondarenko method is obtained by using the narrow resonance approximation in the absorber integral of Eq. 7.26. The practical width of a resonance of the absorber is considered to be much smaller than the energy loss due to a collision with the absorber. This enables the absorber integral to be represented as a smooth function of energy. Therefore, the flux is represented by

$$\phi(E) = \frac{C(E)}{(\sigma_{ta}(E) + \sigma_d)} \tag{7.28}$$

Consider the general form for resonance absorption cross sections.

$$\begin{aligned}
\Sigma_a^g &= N_a \sigma_a^g = \frac{N_a}{\Delta u} \sum_i \frac{\sigma_{di}\Gamma_{\gamma i}}{E_{ri}} \beta_i J(\theta_i, \beta_i) \\
\sigma_a^g &= \frac{1}{\Delta u} \sum_i \frac{\sigma_{di}\Gamma_{\gamma i}}{E_{ri}} \beta_i J(\theta_i, \beta_i) \\
\beta_i^{NR} &= \frac{\Sigma_{sm} + \Sigma_{pA}}{\Sigma_{di}} \quad \text{or} \quad \frac{\Sigma_{sm} + \Sigma_{pa} + \Sigma_e}{\Sigma_{di}} \\
\beta_i^{WR} &= \frac{\Sigma_{sm}}{\Sigma_{di} \dfrac{\Gamma_{\gamma i}}{\Gamma_i}} \quad \text{or} \quad \frac{\Sigma_{sm} + \Sigma_e}{\Sigma_{di} \dfrac{\Gamma_{\gamma i}}{\Gamma_i}}
\end{aligned} \tag{7.29}$$

The β_i can be written as

$$\begin{aligned}
\beta_i^{NR} &= \frac{\sigma_b}{\sigma_{di}} \\
\sigma_b &= \frac{N_m \sigma_{sm} + N_a \sigma_{pa}}{N_A} \\
\beta_i^{WR} &= \frac{\sigma_b}{\sigma_{di}} \\
\sigma_b &= \frac{N_m \sigma_{sm}}{N_a}
\end{aligned} \tag{7.30}$$

Then we can write the cross section as

$$\begin{aligned}\sigma_a^g &= \frac{1}{\Delta u}\sum_i \frac{\sigma_{oi}\Gamma_{\gamma i}}{E_{ri}}\frac{\sigma_b}{\sigma_{oi}}J\left(\theta_i,\frac{\sigma_b}{\sigma_{oi}}\right)\\ &= \frac{1}{\Delta u}\sum_i \frac{\sigma_{oi}\Gamma_{\gamma i}}{E_{ri}}\frac{\pi}{2}f(\theta_i,\sigma_b)\\ &= \sigma_{a,\infty}^g f(T,\sigma_b)\end{aligned} \tag{7.31}$$

Or the absorption cross section can be expressed in terms of the infinite dilution cross section times some sort of self-shielding or Bondarenko factor that is only a function of the background scatterer and the temperature. This will allow the calculation of the infinite dilution cross section and a table of *f* factors as accurately as desired. The narrow resonance and wide resonance approximations are no longer required. This will allow the interpolation of the resonance effects for any mixture of nuclides that is physically possible. There are two advantages of this approach. First, the infinite dilution cross section and *f* factor cross section table can be computed for a single nuclide without specifically considering other nuclides present. Second, when it comes to setting up cross sections for a design mixture, the *f* factor table can be easily interpolated to get the appropriate cross sections for that specific mixture. This approach requires a large amount of computation to be performed one time and the results of that calculation used many times in short design-specific calculations.

A typical *f* factor table for an absorption cross section might look like

Σ_b(b)	10^0	10^1	10^2	10^3	10^4	10^5	10^6
T(K)							
300	0.75	0.85	0.89	0.93	0.96	0.98	1.0
600	0.78	0.87	0.90	0.94	0.96	0.98	1.0
900	0.81	0.89	0.91	0.95	0.97	0.99	1.0
1200	0.84	0.90	0.93	0.96	0.97	0.99	1.0
1500	0.87	0.91	0.94	0.97	0.98	0.99	1.0
1800	0.90	0.92	0.96	0.98	0.99	1.0	1.0
2100	0.93	0.94	0.96	0.98	0.99	1.0	1.0

Bondarenko extended the concept to fission and scattering cross sections. Since that time, the concept has been extended to almost all cross sections. The concept of a background scattering cross section has been extended to a background total cross section. Since the total cross section in the resonance range is dominated by scattering except in the resonances, basing everything on a total background cross section is a logical extension.

By basing everything on a total cross section, this simplified a number of things.

In particular, if a given mixture requires two or more resonance absorbers, then the calculation to solve for the appropriate background total cross section will require iteration. Consider the case of a mixture containing both U^{235} and U^{238} in the compound UO_2. We have

$$\begin{aligned}
\sigma_t^{g,235} &= \sigma_t^{g,235,\infty} f\left(T, \sigma_{t,b}^{g,235}\right) \\
\sigma_{t,b}^{g,235} &= \frac{N_O \sigma_{sO}^g + N_{238}\sigma_{t,238}^g}{N_{235}} \\
\sigma_t^{g,238} &= \sigma_t^{g,238,\infty} f\left(T, \sigma_{t,b}^{g,238}\right) \\
\sigma_{t,b}^{g,238} &= \frac{N_O \sigma_{sO}^g + N_{235}\sigma_{t,235}^g}{N_{238}}
\end{aligned} \tag{7.32}$$

Note that the total cross section for U^{238} appears in the background cross section used to calculate the total cross section for U^{235}. The total cross section for U^{235} appears in the background cross section used to calculate the total cross section for U^{238}. Therefore, iteration will be necessary to get both total cross sections. The iteration proceeds as follows:

1. Use the infinite dilution total cross sections to calculate a background cross section for each absorber.
2. Estimate new total cross sections for all absorbers based on these background cross sections.
3. Calculate new background cross sections based on these updated total cross sections.
4. Repeat the process until the total cross sections converge.
5. When the total cross sections have converged, and it has used the estimated background cross sections to calculate scattering, absorption, and fission cross sections.

This process is fairly efficient and converges in less than three or four iterations in most cases. Note that all subordinate cross sections must be calculated based on the same background cross section to ensure that they add up to the correct total.

The iterative process when two or more resonance species are present does correct slightly for resonance overlap, but a strong theoretical justification for its accuracy is lacking.

7.5.3 The CENTRM Method

The CENTRM code in NJOY divides the energy range into three intervals: upper multigroup range, pointwise range, and lower multigroup range. The user can control the energy boundaries of these ranges. However, it is desirable to set the boundaries of the pointwise energy range such that it includes the resonance structure of an important isotope. This way, a detailed flux calculation in the resonance range can be obtained. Calculations can be performed for an infinite homogeneous medium or for one-dimensional problems having a slab, cylindrical, or spherical geometry. Several methods are available for solving the transport equation in the multigroup and pointwise energy ranges. The methods for multigroup calculations are: discrete ordinates (SN), diffusion, homogenized infinite medium, zone-wise infinite medium, and BN. For the pointwise calculations, the SN, collision probability, homogenized infinite medium, and zone-wise infinite medium methods exist [7].

7.6 Infinite Resonance Integrals and Group Cross Sections

In this section, we introduce infinite resonance integrals (RI) very briefly as flux weighted, and that is weighted with $1/E$ spectrum when $\phi(E) \sim 1/E$ considering microscopic cross section $\sigma(E)$:

$$\begin{aligned}
\mathrm{RI} &= -\int_{E_1}^{E_2} \sigma(E)dE \\
E &= \ln\left(\frac{E_2}{E_1}\right) = \ln(E_2) - \ln(E_1) \\
dE &= -\frac{1}{E}dE \\
\mathrm{RI} &= \int \sigma(E)dE
\end{aligned} \tag{7.33}$$

Notice that

- RI is defined directly from cross section data; no flux calculation is required because $1/E$ spectrum is assumed.
- RI depends on the normalization of the $1/E$ flux spectrum; it is also implicitly assumed that flux equals 1 when $E = 1$ through normalization.
- RI is independent of energy bounds for isolated resonances.
- RI is independent of temperature. This is because if the energy bound is larger enough, then as temperature increases, the spectrum would broaden, but because the area under the curve remains the same, assuming the cross section is constant, then RI is essentially integrating the spectrum, which would not change upon temperature change.
- RI is useful for intercomparing libraries or cross-sectional models. It is a classic way to evaluate new resonance data typically from 0.5 eV to 10 keV. We use RI to check our resonance data, in particularly the three big resonances at 6.67, 20.9, 36.7, and 66 eV. A numerical test of the SLBW RIs shows that the RI comes out to be within 1 % of the ENDF/B-VII Reich–Moore data.

Group cross section is a similar but much more useful quantity. From its definition, we see g does not depend on the flux normalization:

$$\sigma_g = \frac{\displaystyle\int_{E_1}^{E_2} \sigma(E)\phi(E)dE}{\displaystyle\int_{E_1}^{E_2} \phi(E)dE} \tag{7.34}$$

If we make an assumption on the flux spectrum, then we can relate the group cross section σ_g to the effective resonance integral $\mathrm{RI}_{\mathrm{eff}}$ as

$$\begin{aligned}
&\phi(E) \sim \frac{1}{E}\\
&\sigma_g = \frac{\displaystyle\int_{E_1}^{E_2} \sigma(E)\frac{1}{E}dE}{\displaystyle\int_{E_1}^{E_2} \frac{1}{E}dE} = \frac{\mathrm{RI}_{\mathrm{eff}}}{\ln(E_2) - \ln(E_1)} = \frac{\mathrm{RI}_{\mathrm{eff}}}{\ln(E_2/E_1)}\\
&\mathrm{RI}_{\mathrm{eff}} = \sigma_g \ln(E_2/E_1)
\end{aligned} \tag{7.35}$$

Notice that:

- Group cross section by definition depends on both cross section and flux spectrum.
- Group cross section depends on the flux, but not on the normalization of flux (i.e., only the shape matters, not the magnitude).
- Group cross section depends explicitly on energy bounds (widths) of the groups.
- Effective RI can be computed from group cross sections and group energy bounds as in Eq. 7.31; as spectrum approaches $1/E$, the effective resonance integrals (RI) computed from group cross sections will approach infinite RI.

7.7 Dilution Cross Section: Dilution Factor

In an infinite homogeneous medium with one resonance absorber and one moderator, we write removal rates equal scattering rates very similar to Eq. 7.15 as before

$$\begin{aligned}
[N_r\sigma_r(E) + N_m\sigma_m(E)]\phi(E) &= \int_{-\infty}^{E} N_m\sigma_m(E')\phi(E')P(E' \to E)dE'\\
&= N_m\sigma_m(E)\int_{-\infty}^{E} \phi(E')P(E' \to E)dE'\\
&= N_m\sigma_m(E)C
\end{aligned} \tag{7.36a}$$

where

$$\phi(E) \propto \frac{N_m\sigma_m(E)}{N_r\sigma_r(E) + N_m\sigma_m(E)}$$
$$\phi(E) \propto \frac{\frac{N_m}{N_r}\sigma_m(E)}{\sigma_r(E) + \frac{N_m}{N_r}\sigma_m(E)} \tag{7.36b}$$

In the above derivation, we made two assumptions as

- The moderator's cross section is independent of energy near resonances. For almost any moderator, we can pick the assumption that the elastic scattering cross section is constant and is valid in the thermal range as in Fig. 7.15.
- $\int_{-\infty}^{E} \phi(E')P(E' \to E)dE'$ is constant (i.e., C). We know that the flux above the resonance is $1/E$ and hence constant in lethargy. If we assume scattering into the resonance comes from this constant lethargy region, then the resonance lethargy is constant as well.

Equation 7.36b suggests that *in infinite medium the flux shape near resonance depends only on the ratio of the number density of the moderator to the resonance absorber and the moderator cross section*. However, once we move into a finite medium or we take into account leakage, the absolute number densities are needed.

To capture the ratio of number densities and the moderator cross section, we define **dilution cross section** as

$$\sigma_d = \frac{N_m\sigma_m}{N_r} \tag{7.37}$$

Then, the flux shape near resonance is

$$\phi(E) \propto \frac{\sigma_d}{\sigma_r + \sigma_d} \tag{7.38}$$

The flux shapes in Eq. 7.38 let us compare approximated effective resonance integrals (RI). Recall resonance integral (RI) is defined in Eq. 7.33 as $\mathrm{RI} = \int \sigma(E)dE$, then the approximated effective resonance integrals $\mathrm{RI}_{\mathrm{eff}}$ is given as

$$\mathrm{RI}_{\mathrm{eff}} = \int \sigma_r(E)\frac{\sigma_d}{\sigma_r + \sigma_d}dE \tag{7.39}$$

Based on what we have derived so far, the two extremes of $\mathrm{RI}_{\mathrm{eff}}$ and σ_d are

- As $\sigma_d \to \infty$, the entire media is a moderator, we reach the limit of infinite dilution, and $\mathrm{RI}_{\mathrm{eff}} \to \mathrm{RI}$; we should get within 1 % of the ENDF/B-VII cross-sectional data.

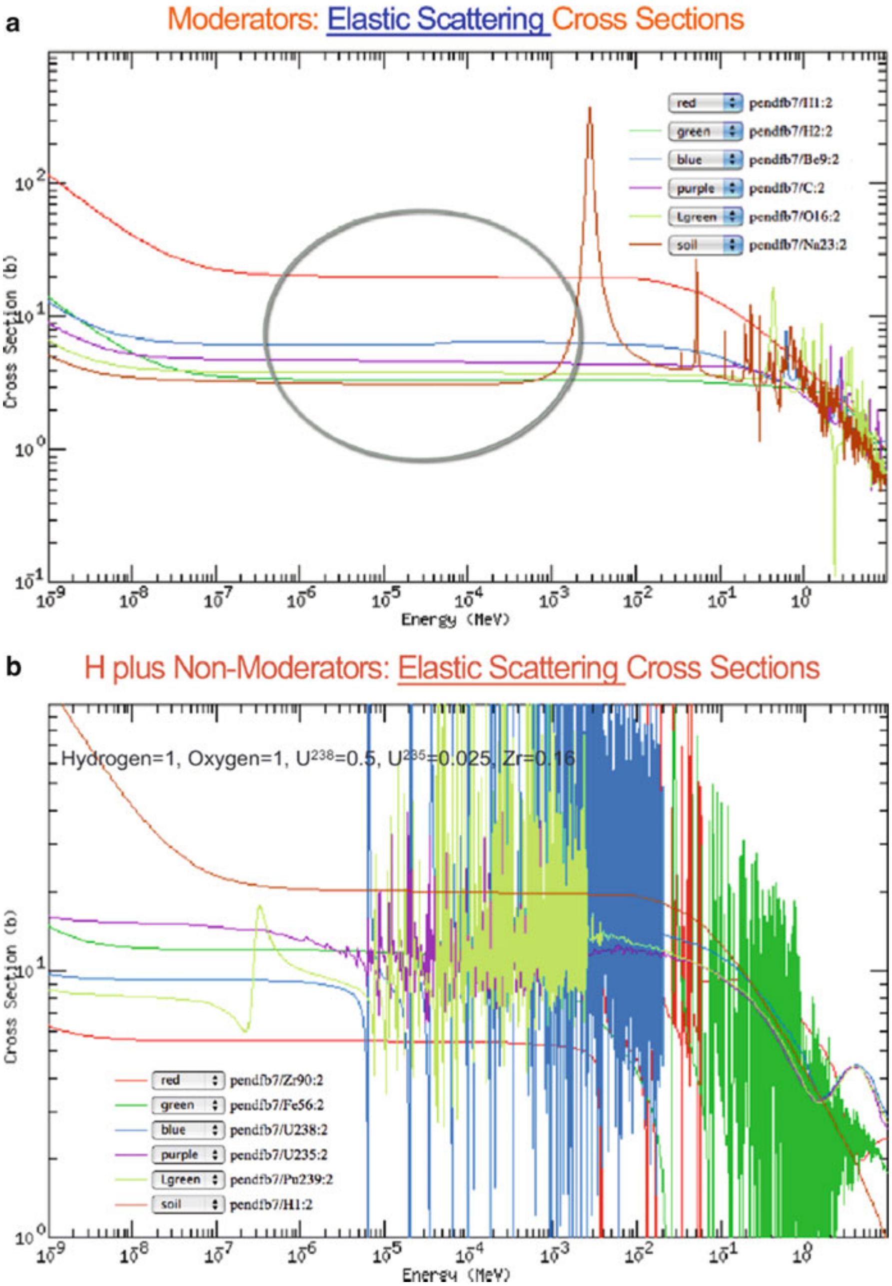

Fig. 7.15 Elastic scattering cross sections

- As $\sigma_d \rightarrow 0$, analytically our assumptions do not hold true anymore, but the MC is true, that is, $\mathrm{RI}_{\mathrm{eff}} \rightarrow 0$ and $\phi(E) \rightarrow 0$ as seen in Fig. 7.16. Interpretation: as we have no moderator, every atom is essentially self-shielding because they are all resonant isotopes and, hence, infinite flux depression.

The scattering down to resonance is independent of the resonance. In other words, if the spectrum above a resonance returns to $1/E$ as in Fig. 7.17, the group cross sections will be independent of higher energy absorptions. This may be related to what we talked about before.

7.8 Resonance Effects

Cross sections, much like spectra, can be broken down into three major regions. Absorption cross sections tend to vary as $1/v$ in the thermal energy range below about 0.5 eV. In the slowing down region from 0.5 eV to about 0.1 MeV, absorption is dominated by resonance effects with very large peaks at the resonance energies and zero absorption between resonances. Above 0.1 MeV, absorption cross sections tend to be smoothly varying and close to the constant. There are still resonances in this range, but they tend to be so close together that they cannot be resolved and their effects are simply averaged out. The thermal range and fast range are fairly easily handled in the multigroup approach, but the resonance region presents some difficulties. Scattering cross sections are dominated by a fairly constant potential scattering cross section over most of the region of interest for nuclear reactors and do not show a significant variation with energy.

The resonance range is normally split into two regions identified as resolved resonances and unresolved resonances. The energy span of the resolved resonance range varies with the nuclide and tends to be a function of both the atomic number and the spacing of the resonances. For instance, in a low mass number A nuclide like aluminum, the entire range is essentially resolved. In a high mass number A nucleus like U^{238} with fairly, widely separated resonances, the resolved resonance range extends up to about ~10 keV. In U^{235}, however, the resolved resonance range only goes up to about 500 eV as its resonances are much closely spaced.

The sharpness of the resonance cross sections causes problems in producing multigroup data sets. The absorption cross section can vary by several orders of magnitude over a range of less than 0.025 eV. The standard procedure of choosing very narrow groups and calculating an infinite medium or zero-dimensional spectrum becomes very difficult if a range of 0.5 eV to 1.0 MeV must be spanned with say 0.005 eV wide groups. This would require ~2E + 8 groups. This is still too large of a number even for today's computers. So a fundamental spectrum must be calculated analytically within fairly broad groups. The techniques for accomplishing this are fairly well developed.

However, like any infinite medium or zero-dimensional spectrum, the actual spectrum will depend on all of the nuclides present in the material zone of interest.

Numerical	U/H = .00001	U/H = .001	U/H = .01	U/H = .1	U/H = 1.0
5.09	4.39	4.39	4.39	4.38	4.32
1.70	1.71	1.71	1.71	1.71	1.69
1.45	1.48	1.48	1.48	1.47	1.41
126.84	124.8	101.0	47.1	14.0	3.96
65.88	67.3	54.4	21.2	6.8	2.15
41.58	40.0	31.1	11.5	5.2	1.60
12.2	11.7	10.7	6.4	2.8	0.73
271.61	264	216	99.4	38.0	12.2

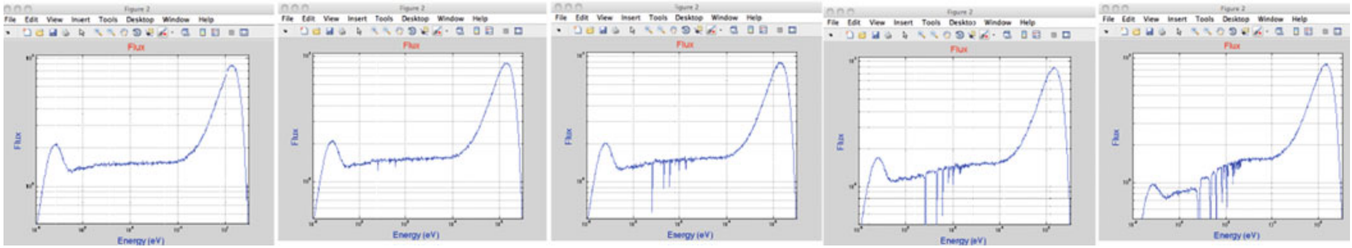

Fig. 7.16 Impact of energy self-shielding on effective resonance integrals

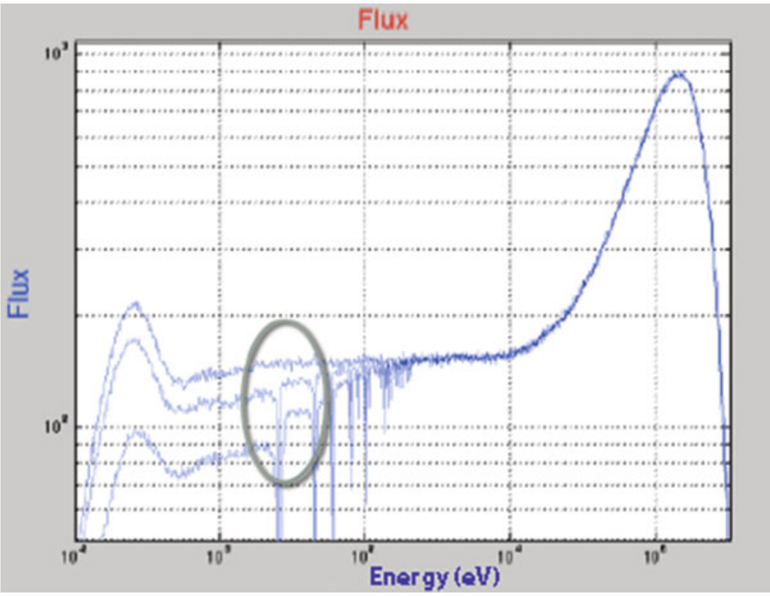

Fig. 7.17 1/E spectrum above a resonance suggests group cross section independent of higher energy absorption

Consider what happens to the total cross section and the neutron flux near the 6.67 eV resonances in U^{238} as a function of the materials present in the material region.

Start by considering that the material is a one-to-one mixture of U^{238} to hydrogen with a scattering cross section of 20 barns per atom. The total cross section and flux in the resonance region is given in Fig. 7.18. The cross section varies by approximately a factor of one million over an energy range of a few eV. The flux takes a very strong dip at the resonance energy, going down by a factor of several hundred thousand. Since the absorption is the product of the flux and the cross section, it is important to get a good estimate for the flux in the resonance range to accurately calculate the absorption reaction rate. Also, note that the total cross section exceeds the background scattering cross section over a range from about 1–15 eV.

Now consider when the U^{238} is diluted relative to the hydrogen concentration and we have 104 hydrogen atoms for every U^{238} atom. This case is plotted in Fig. 7.19. In this case, the cross section goes up by a factor of a little over 1000, and the flux drops in the resonance range by about the same amount.

It is still important to get a good approximation for the flux in the resonance region. It is also worth noting that the resonance cross section exceeds the asymptotic scattering cross section only over a range from 5 to 8 eV. The range over which the resonance cross section is important is about 1/5 of what it was in Fig. 7.18.

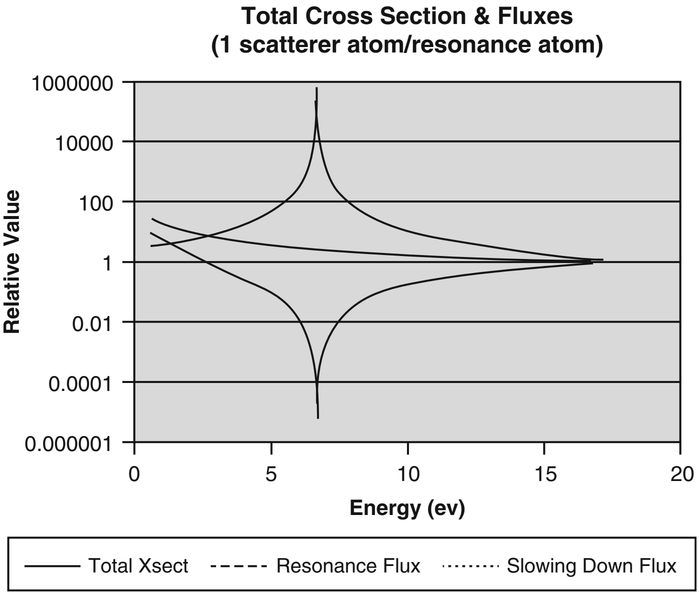

Fig. 7.18 One scatterer atom per absorber atom

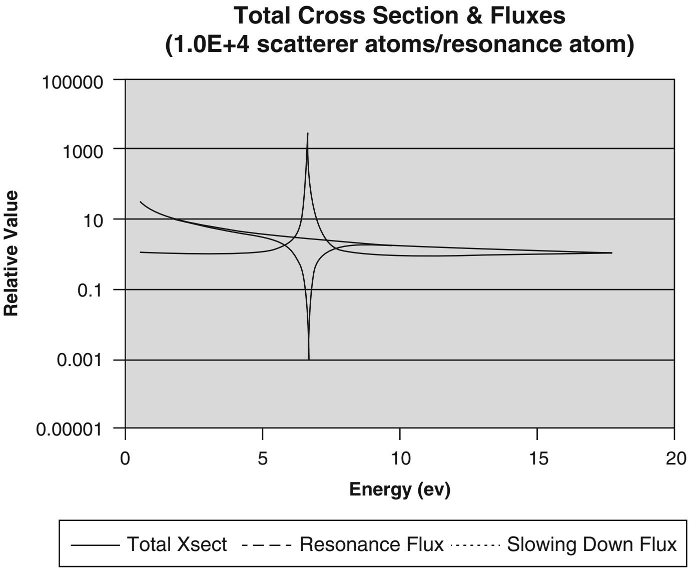

Fig. 7.19 10^4 scatterer atoms per absorber atom

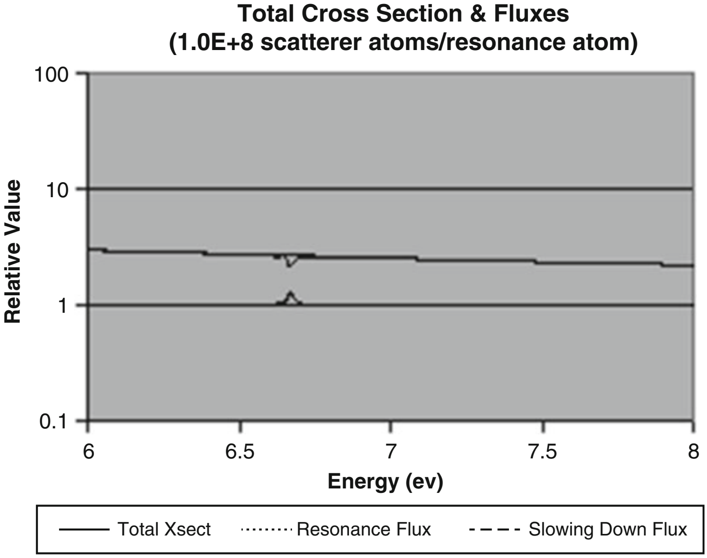

Fig. 7.20 10^8 scatterer atoms per absorber atom

Now consider when there are 10^8 scatterer atoms per absorber atom. This case is described in Fig. 7.20.

Note that in this case, the absorber is a small perturbation on the total cross section, and the change in the flux is a small fraction of the total flux. For this case, an average flux is probably adequate to evaluate the absorption in this resonance. This case is generally referred to as the infinite dilution limit. The cross section is referred to as the infinite dilution cross section.

Therefore, the absorption cross section for a resonance absorber will depend on the amount of background absorber mixed into the material mixture that the absorber is in. Obviously, this complicates the production of multigroup cross sections for resonance absorbers a significant amount.

There is another effect which also affects resonance cross sections. Since the typical width of a resonance in high atomic mass *A* nucleus is on the order of 0.025 eV, the relative velocity between the neutrons and the nuclei in a material will be greatly affected by the thermal velocity of the nuclei. Increases in temperature of the material containing the resonance absorber will greatly affect the absorption in the resonance.

Multigroup cross sections will depend on the amount of background scatterer present and the temperature of the medium.

In order to develop these dependencies, the temperature effects will be treated first. Start with the conservation of reactions equation given by

$$
\begin{aligned}
\phi(E)\sigma_\gamma(E) = nv(E)\sigma_\gamma(E) &= \int_0^\infty v_{\text{rel}}\sigma_\gamma(E_{\text{rel}})np\left(\overline{V}\right)_{\text{MB}}d\overline{V} \\
\sigma_\gamma(E) &= \frac{1}{v(E)}\int_0^\infty v_{\text{rel}}\sigma_\gamma(E_{\text{rel}})p\left(\overline{V}\right)_{\text{MB}}d\overline{V}
\end{aligned}
\tag{7.40}
$$

where the nuclei of the absorber are assumed to have a Maxwell–Boltzmann distribution and the bar over the V represents a vector velocity. The Maxwell–Boltzmann energy distribution is given by

$$
\begin{aligned}
&p\left(\overline{V}\right)_{\text{MB}}d\overline{V} = \left(\frac{M}{2\pi kT}\right)^{3/2} e^{-\frac{MV^2}{2kT}}dV_x dV_y dV_z \\
&\int_0^\infty p\left(\overline{V}\right)_{\text{MB}}d\overline{V} = 1.0
\end{aligned}
\tag{7.41}
$$

Since only the relative velocity is important in evaluating the reaction cross section, it is convenient to define the axis system for evaluating the velocities of the nuclei relative to the direction the neutron is traveling. If the direction of neutron travel is chosen as the z-axis, then the relative energy can be written as

$$
E_{\text{rel}} = \frac{1}{2}m\left(v_n - \left|\overline{V}\right|\right)^2 = \frac{1}{2}m\left([v_n - V_z]^2 + V_x^2 + V_y^2\right) \tag{7.42}
$$

In addition, the resonance absorption cross section is given by

$$
\begin{aligned}
\sigma_\gamma &= \frac{\Gamma_\gamma}{\Gamma}\frac{\sigma_o}{1+y^2} \\
y &= \frac{2}{\Gamma}(E - E_r)
\end{aligned}
\tag{7.43}
$$

Then

$$
\begin{aligned}
\sigma_\gamma(E) &= \sigma_o\frac{\Gamma_\gamma}{\Gamma}\int_0^\infty \frac{v_{\text{rel}}}{v(E)}\left(\frac{M}{2\pi kT}\right)^{3/2}\frac{e^{-\frac{M\left(V_x^2+V_y^2+V_z^2\right)}{ekT}}}{1+\left(\frac{2}{\Gamma}[E_{\text{rel}} - E_r]\right)^2}dV_x dV_y dV_z \\
\frac{\sigma_\gamma(E)}{\sigma_o\frac{\Gamma_\gamma}{\Gamma}} &= \int_0^\infty e^{-\frac{MV_x^2}{2kT}}dV_x\int_0^\infty e^{-\frac{MV_y^2}{2kT}}dV_y\int_0^\infty\left(\frac{M}{2\pi kT}\right)^{3/2}\frac{v_{\text{rel}}}{v(E)}\frac{e^{-\frac{MV_z^2}{2kT}}}{1+y^2}dV_z
\end{aligned}
\tag{7.44}
$$

The integrals over the velocity distributions in the x and y directions can be performed immediately as the relative energy or velocity does not matter. The ratio of v_{rel} to $v(E)$ can be set to one as it will not vary significantly over the range that the rests of the integrand varies. The equation then becomes

$$\frac{\sigma_\gamma(E)}{\sigma_o \frac{\Gamma_\gamma}{\Gamma}} = \int_0^\infty \left(\frac{M}{2\pi kT}\right)^{3/2} \frac{e^{-\frac{MV_z^2}{2kT}}}{1+y^2} dV_z \tag{7.45}$$

Now E_{rel} can be expanded to give

$$\begin{aligned} E_{\text{rel}} &= \frac{1}{2}m(v_n - V_z)^2 = \frac{1}{2}mv_n^2 - mv_nV_z + \frac{1}{2}mV_z^2 \\ &\approx \frac{1}{2}mv_n^2 + mv_nV_z = E - mv_nV_z = E - V_z\sqrt{2mE} \\ V_z &= \frac{E - E_{\text{rel}}}{\sqrt{2mE}} \\ dV_z &= \frac{dE_{\text{rel}}}{\sqrt{2mE}} \end{aligned} \tag{7.46}$$

Substituting all of this into the cross section integral and changing the limits from 0 to ∞ to $-\infty$ to +∞, as the peak in the integrand is far above the lower limit, gives

$$\begin{aligned} \frac{\sigma_\gamma(E)}{\sigma_o \frac{\Gamma_\gamma}{\Gamma}} &= \left(\frac{M}{2\pi kT}\right)^{1/2} \Gamma^2 \int_{-\infty}^{\infty} \frac{e^{-\frac{M}{2kT}\frac{(E-E_{\text{rel}})^2}{2mE}}}{4(E_{\text{rel}} - E_r) + \Gamma^2} \frac{dE_{\text{rel}}}{\sqrt{2mE}} \\ \frac{\sigma_\gamma(E)}{\sigma_o \frac{\Gamma_\gamma}{\Gamma}} &= \left(\frac{A}{4kTE}\right)^{1/2} \frac{\Gamma^2}{\sqrt{\pi}} \int_{-\infty}^{\infty} \frac{e^{-\frac{A}{4kTE}}[(E - E_r) - (E_{\text{rel}} - E_r)]^2}{4(E_{\text{rel}} - E_r)^2 + \Gamma^2} dE_{\text{rel}} \end{aligned} \tag{7.47}$$

Now define

$$\begin{aligned} x &= \frac{2}{\Gamma}(E_{\text{rel}} - E_r) \\ y &= \frac{2}{\Gamma}(E - E_r) \end{aligned} \tag{7.48}$$

and

$$\begin{aligned} \Delta &= \sqrt{\frac{4kTE}{A}} \approx \sqrt{\frac{4kTE_r}{A}} \\ \theta &= \frac{\Gamma}{\Delta} \end{aligned} \tag{7.49}$$

The integral then becomes

$$\begin{aligned} \frac{\sigma_\gamma(E)}{\sigma_o \frac{\Gamma_\gamma}{\Gamma}} &= \frac{\theta}{2\sqrt{\pi}} \int_{-\infty}^{\infty} \frac{e^{-\frac{\theta^2}{4}(y-x)^2}}{1+x^2} dx = \psi(\theta, y) \\ \sigma_\gamma(E) &= \sigma_o \frac{\Gamma_\gamma}{\Gamma} \psi(\theta, y) \end{aligned} \tag{7.50}$$

Moreover, $\psi(\theta, y)$ is a tabulated function known as the symmetric Voigt profile.

If we were to consider the total cross section including the scattering cross section, we would get an asymmetric term due to the interference part of the scattering cross section, and this would give us the asymmetric Voigt profile. The total cross section could be written as

$$\sigma_t(E) = \sigma_o \psi(\theta, y) + \left(\sigma_o \sigma_p \frac{\Gamma_n}{\Gamma}\right)^{1/2} \chi(\theta, y) + \sigma_p \tag{7.51}$$

Now remembering that $y = 2(E - E_r)/T$ and $dy = 2\,dE/\mathit{\Gamma}$, we can integrate the absorption cross section over all energy:

$$\int_0^\infty \sigma_\gamma(E)dE = \frac{\sigma_o \Gamma_\gamma}{2} \int_0^\infty \psi(\theta, y)dy \approx \frac{\sigma_o \Gamma_\gamma}{2} \int_{-\infty}^\infty \psi(\theta, y)dy = \frac{\sigma_o \Gamma_\gamma}{2} \pi \tag{7.52}$$

The most interesting aspect of this result is that it is independent of temperature. That is, if we do simply integrate the cross section over all energy, the final result does not depend on the temperature that the nuclei are at. It would seem that all of this effort has been for naught. However, in the end we must remember that we are trying to conserve reaction rates, and we must consider the product of the flux times the cross section. The result we have just obtained is for a constant flux across the energy range of the resonance. This is seldom the case and only occurs when the resonance does not perturb the flux. For this to be the case, the absorber must not make a significant contribution to the total cross section. Only if the absorber is distributed in the media in very small amounts can this be the case. This condition is called the "infinitely dilute" case.

For the infinitely dilute case, the contribution of the i^{th} resonance to a group absorption cross section can be written as

$$\sigma_{\gamma i}^g = \frac{\displaystyle\int_{E_{g+1}}^{E_g} \sigma_{\gamma i}(E, T)\phi(E)dE}{\displaystyle\int_{E_{g+1}}^{E_g} \phi(E)dE} \tag{7.53}$$

Assuming that $\phi(E) = \phi_o/E$, the denominator becomes

$$\int_{E_{g+1}}^{E_g} \frac{\phi_o}{E} dE = \phi_o \int_{E_{g+1}}^{E_g} \frac{dE}{E} = \phi_o \Delta u_g \tag{7.54}$$

Moreover, the contribution from the i^{th} resonance can then be written as

$$\sigma_{\gamma i}^g = \frac{1}{\Delta u_g} \int_{E_{g+1}}^{E_g} \sigma_{\gamma i}(E, T) \frac{dE}{E} = \frac{1}{\Delta u_g E_{ri}} \int_{E_{g+1}}^{E_g} \sigma_{\lambda i}(E, T)dE = \frac{1}{\Delta u_g E_{ri}} \frac{\sigma_{oi} \Gamma_{\gamma i} \pi}{2} \tag{7.55}$$

where it has been assumed that E_{ri} can be taken out of the integral because it does not vary significantly over the contribution interval. Therefore, this gives for the group absorption cross section

$$\begin{aligned}\sigma_a^g &= \frac{1}{\Delta u_g}\sum_{i\in g}\frac{\sigma_{oi}\Gamma_{\gamma i}}{E_{ri}}\frac{\pi}{2} = \frac{1}{\Delta u_g}\sum_{i\in g} I_i^\infty \\ I_i^\infty &= \frac{\sigma_{oi}\Gamma_{\gamma i}}{E_{ri}}\frac{\pi}{2} = \text{Infinite Dilute Resonance Integral}\end{aligned}\tag{7.56}$$

7.9 Homogeneous Narrow Resonance Approximation

In order to estimate the flux in the resonance, we must solve the neutron transport equation in the energy range of the resonance. Fortunately, we can obtain a good approximation by solving the infinite media equation. We will start by considering a homogeneous medium as it is simpler. The infinite medium equation in a homogeneous material is

$$\Sigma_t\phi(E) = \int_E^{E/\alpha_A}\frac{\Sigma_{sA}(E')}{(1-\alpha_A)E'}\phi(E')dE' + \int_E^{E/\alpha_m}\frac{\Sigma_{sm}(E')}{(1-\alpha_m)E'}\phi(E')dE' \tag{7.57}$$

where we have lumped all scatterers into one. We will only treat one absorber at a time. This means that other absorbers in the material are treated as scatterers. We are assuming that the resonances of one absorber do not overlap those of another absorber in energy. It will be obvious why this can be done as we solve for the flux. Since we are interested in approximating the flux in the resonance, we will be interested in the energy range over which the resonance perturbs the cross section by a significant amount. To quantify this choose the range of interest as that energy range over which the resonance part of the cross section doubles the scattering cross section outside of the resonance.

We have

$$\begin{aligned}\frac{\Sigma_o}{1+y^2} &= \Sigma_{sm} \\ \frac{\Sigma_o}{\Sigma_{sm}} &= 1+y^2 = 1+\left(\tfrac{2}{\Gamma}[E-E_r]\right)^2 \\ E-E_r &= \frac{\Gamma}{2}\sqrt{\frac{\Sigma_o}{\Sigma_{sm}}-1} \\ \Delta E = 2(E-E_r) &= \Gamma_p = \Gamma\sqrt{\frac{\Sigma_o}{\Sigma_{sm}}-1} \approx \Gamma\sqrt{\frac{\Sigma_o}{\Sigma_{sm}}}\end{aligned}\tag{7.58}$$

where Γ_p is called the practical width. Now the practical width is the region over which the total cross section is perturbed by the resonance. To determine how much this effects the flux in the resonance, we must compare this range with the range over which neutrons can scatter into the resonance. If the range over which neutrons can scatter into the resonance is large compared to the range over which the resonance perturbs the cross section, then we can neglect the effects of the resonance. For the moderator, the range over which neutrons can be scattered by moderator atoms into the resonance is always large compared to the practical width of all resonances. The scatter-in range for the moderator is $(1/\alpha_m - 1)E_r$. Therefore, we will in general have

$$\Gamma_p \ll (1/\alpha_m - 1)E_r \tag{7.59}$$

for all moderators.

For typical absorbers like the fissile isotopes, whether the in-scatter range is large or small compared to the practical width for the resonance, will depend on the mixture parameters. In general, as the resonance energy increases, the in-scatter range increases, so it is likely that the effects of the resonance can be neglected as a perturbation on the in-scatter flux. The narrow resonance approximation refers to the way the in-scatter integral is treated for the absorber. If

$$\mathit{\Gamma}_p \ll (1/\alpha_A - 1)E_r \tag{7.60}$$

We will evaluate the flux in the resonance with the narrow resonance approximation. This means that we can use the asymptotic form for the flux in the in-scatter integrals. This gives

$$\begin{aligned}
\Sigma_t(E)\phi(E) &= \int_E^{E/\alpha_A} \frac{\Sigma_{pA}}{(1-\alpha_A)E'}\frac{\phi_o}{E'}dE' + \int_E^{E/\alpha_m} \frac{\Sigma_{sm}}{(1-\alpha_m)E'}\frac{\phi_o}{E'}dE' \\
\Sigma_t(E)\phi(E) &= \frac{\Sigma_{pA}}{E}\phi_o + \frac{\Sigma_{sm}}{E}\phi_o = \frac{\Sigma_{pA}+\Sigma_{sm}}{E}\phi_o \\
\phi(E) &= \frac{\Sigma_{pA}+\Sigma_{sm}}{E\Sigma_t(E)}\phi_o
\end{aligned} \tag{7.61}$$

Then we can use this approximation for the flux in the resonance integral. This becomes

$$\sigma_\gamma^g = \frac{\displaystyle\int_{E_{g+1}}^{E_g} \frac{\sigma_{oA}\frac{\Gamma_\gamma}{\Gamma}\psi(\theta,y)\left(\Sigma_{pA}+\Sigma_{sm}\right)}{\Sigma_{oA}\psi(\theta,y)+N_A\left(\sigma_{pA}\sigma_o\frac{\Gamma_n}{\Gamma}\right)^{1/2}\chi(\theta,y)+\Sigma_{pA}+\Sigma_{sm}}\frac{\phi_o}{E}dE}{\displaystyle\int_{E_{g+1}}^{E_g}\frac{\phi_o}{E}dE} \tag{7.62}$$

Now that the denominator can be integrated to get $\phi_o\Delta u$, the ϕ_0 will cancel with the one in the numerator. In order to integrate the numerator, we have to neglect the asymmetric term, $\chi(\theta, y)$. The rationale for this is that it is asymmetric, so it adds and subtracts across the resonance, so its effect can be neglected. We will also extend the upper limit to infinity as most groups are a great deal larger than the resonance width. Since the integral is symmetric, we will set the lower limit to zero and double it. We will also pull the E out of the integral and set it equal to E_r. This gives

$$\begin{aligned}
\sigma_\gamma^g &= \frac{\sigma_o\Gamma_\gamma}{E_r}\frac{1}{\Delta u_g}\int_0^\infty \frac{(\Sigma_{pA}+\Sigma_{sm})\psi(\theta,y)}{\Sigma_{oA}\psi(\theta,y)+\Sigma_{pA}+\Sigma_{sm}}\frac{2dE}{\Gamma} \\
\sigma_\gamma^g &= \frac{1}{\Delta u_g}\frac{\sigma_o\Gamma_\gamma}{E_r}\beta\int_0^\infty \frac{\psi(\theta,y)}{\psi(\theta,y)+\beta}dy \\
\beta &= \frac{\Sigma_{pA}+\Sigma_{sm}}{\Sigma_o} \\
\sigma_\gamma^g &= \frac{1}{\Delta u_g}\frac{\sigma_o\Gamma_\gamma}{E_r}\beta^* J(\theta,\beta)
\end{aligned} \tag{7.63}$$

$J(\theta, \beta)$ is a tabulated function called Dresner's integral. Note that the product $\beta * J(\theta, \beta)$ must lie between 0 and $\pi/2$.

Then the group absorption cross section with multiple resonances in an energy group is

$$\sigma_a^g = \frac{1}{\Delta u_g}\sum_{i\in g}\frac{\sigma_{oi}\Gamma_{\gamma i}}{E_{ri}}\beta_i{}^* J(\theta,\beta_i) \tag{7.64}$$

7.10 Homogeneous Wide Resonance Approximation

Now consider the case when the in-scatter interval for the absorber is smaller than the practical width for the resonance. In this case, we will make the wide resonance approximation or the infinite mass approximation. We have

$$\Gamma_p \gg (1/\alpha_A - 1)E_r \tag{7.65}$$

In this case, we will assume that when the absorber scatters, it remains at the energy of interest. So our infinite medium equation becomes

$$\begin{aligned}
\Sigma_t(E)\phi(E) &= \Sigma_{sA}(E)\phi(E) + \Sigma_{sm}\frac{\phi_o}{E} \\
[\Sigma_t(E) - \Sigma_{sA}(E)]\phi(E) &= \Sigma_{sm}\frac{\phi_o}{E} \\
\phi(E) &= \frac{\Sigma_{sm}}{\Sigma_t(E)-\Sigma_{sA}(E)}\frac{\phi_o}{E}
\end{aligned} \tag{7.66}$$

Then the absorption cross section for this resonance becomes

$$\sigma_\gamma^g = \frac{\displaystyle\int_{E_{g+1}}^{E_g} \frac{\sigma_{oA}\frac{\Gamma_\gamma}{\Gamma}\psi(\theta,y)\Sigma_{sm}}{\Sigma_{oA}\frac{\Gamma_\gamma}{\Gamma}\psi(\theta,y)+\Sigma_{sm}}\frac{\phi_o}{E}dE}{\displaystyle\int_{E_{g+1}}^{E_g}\frac{\phi_o}{E}dE} \tag{7.67}$$

Once again, the denominator can be integrated to get $\phi_0\Delta u$, and the ϕ_0 will cancel with the one in the numerator. This time we do not have to neglect anything because the asymmetric term has been subtracted out. We will extend the upper limit to infinity, as most groups are a great deal larger than the resonance width. Since the integral is symmetric, we will set the lower limit to zero and double it. We will also pull the E out of the integral and set it equal to E_r. This gives

$$\sigma_\gamma^g = \frac{\sigma_o\Gamma_\gamma}{E_r}\frac{1}{\Delta u_g}\int_0^\infty \frac{\Sigma_{sm}\psi(\theta,y)}{\Sigma_{oA}\frac{\Gamma_\gamma}{\Gamma}\psi(\theta,y)+\Sigma_{sm}}\frac{2dE}{\Gamma} \tag{7.68}$$

$$\sigma_\gamma^g = \frac{1}{\Delta u_g}\frac{\sigma_o\Gamma_\gamma}{E_r}\beta'\int_0^\infty \frac{\psi(\theta,y)}{\psi(\theta,y)+\beta'}dy \tag{7.69}$$

and

$$\begin{aligned}\beta' &= \frac{\Sigma_{sm}\Gamma}{\Sigma_o\Gamma_\gamma}\\ \sigma_\gamma^g &= \frac{1}{\Delta u_g}\frac{\sigma_o\Gamma_\gamma}{E_r}\beta' * J(\theta,\beta')\end{aligned} \tag{7.70}$$

Therefore, we have a result that is of the same form as for the narrow resonance approximation, and it can be evaluated with Dresner's J function once again. In the end, the difference is only in how we calculate the two β's. Since Γ/Γ_γ is always greater than 1.0 and $\Sigma_{sm} < \Sigma_{sm} + \Sigma_{pA}$, no general statement can be made about the ratio of the two evaluations.

So what happens if we don't have either $\Gamma_p \gg (1/\alpha_A - 1)E_r$ or $\Gamma_p \ll (1/\alpha_A - 1)E_r$. There have been methods developed to interpolate between these limits and they work quite well. However, that is beyond the level of this course and they are not widely used. The approximate treatment of resonances has been rendered a thing of the past by the ultrafast computers that can numerically solve the equations to create tables that can be easily interpolated.

Before we get to that, however, let us consider the much more useful case of heterogeneous resonances.

7.11 Heterogeneous Narrow Resonance Approximation

So far, we have only considered resonance absorption when the fuel or absorber nuclei are intimately mixed with the scattering or moderator nuclei. This is really only the case in a few reactors like the AGN-201 or Sandia's SPR reactors. In most commercial reactors, the fuel is consolidated into fuel elements and surrounded by moderator. This condition greatly affects the average resonance absorption in the fuel nuclei because the nuclei in the center of the fuel see very few neutrons at resonance energies as most of the neutrons are stopped on the surface of the fuel element.

Start the analysis by considering one fuel element lump in a sea of moderator. At energies far above the resonance, the neutron flux is flat across both media, and a given neutron does not know whether it is in the fuel or the moderator. We will assume that in each of the regions, as we approach the resonance energy, the flux in both media can be represented by its average value. (This is probably a weak assumption as we get close to the resonance.) In the resonance energy range, the average flux in the fuel will be depressed relative to its value in the moderator.

Now the total interaction rate in the fuel can be written as

$$\text{Collision Rate in Fuel} = V_F \Sigma_t^F(E)\phi_{\text{avg}}^F(E) \tag{7.71}$$

where V_F is the volume of the fuel and $\Sigma_t^F(E)$ is the total cross section for the fuel material which may include one or more moderators mixed in with the resonance absorber. Neutrons that collide in the fuel at energy E must have either come from the fuel via a downscatter process and not leak out before interacting or have come from the moderator and leaked into the fuel before interacting. So an approximate infinite medium equation can be written as

$$\begin{aligned} V_F \Sigma_t^F(E)\phi^F(E) = {} & [1 - P_{FO}(E)]V_F \int_E^{E/\alpha_A} \frac{\Sigma_{sA}^F(E')\phi^F(E')dE'}{(1-\alpha_A)E'} \\ & + [1 - P_{FO}(E)]V_F \int_E^{E/\alpha_{mf}} \frac{\Sigma_{smf}^F(E')\phi^F(E')dE'}{(1-\alpha_{mf})E'} \\ & + P_{MO}(E)V_m \int_E^{E/\alpha_m} \frac{\Sigma_{sm}^M(E')\phi^M(E')dE'}{(1-\alpha_M)E'} \end{aligned} \tag{7.72}$$

where

α_A, Σ_{sA}^F are the properties of the absorber in the fuel region.

$\alpha_{mf}, \Sigma_{smf}^F$ are the properties of the moderator in the fuel region (admixed moderator).

α_M, Σ_{sm}^M are the properties of the moderator in the moderator region (outside moderator).

$P_{FO}(E)$ is the probability of traveling from a collision in the fuel lump to a collision in the moderator in one flight.

$P_{MO}(E)$ is the probability of traveling from a collision in the moderator to a collision in the fuel in one flight.

Note that $P_{FO}(E)$ and $P_{FO}(E)$ are averages over both the volume of the fuel and the volume of the moderator in both cases. Then $[1 - P_{FO}(E)]$ is the probability of not escaping the fuel in one flight.

Now by a general theorem known as the reciprocity theorem, the collision rate in the fuel times the fuel escape probability from the fuel to the moderator must be equal to the collision rate in the outside moderator times the escape probability from the outside moderator to the fuel. We have

$$P_{FO}(E)V_F\Sigma_t^F(E)\phi^F(E) = P_{MO}(E)V_M\Sigma_t^M\phi^M(E) \tag{7.73}$$

at energies above the resonance. This must hold that, as if it did not, the flux would build up in one material or the other. Making use of this relationship and making the narrow resonance approximation for both moderators, the equation for the collision rate in the fuel becomes

$$\begin{aligned} V_F\Sigma_t^F(E)\phi^F(E) = [1 - P_{FO}(E)]V_F\int_E^{E/\alpha_A} \frac{\Sigma_{sA}^F(E')\phi^F(E')dE'}{(1-\alpha_A)E'} \\ + [1 - P_{FO}(E)]V_F\frac{\Sigma_{smf}\phi_o}{E} + P_{FO}(E)V_F\frac{\Sigma_t^F(E)\phi_o}{E} \end{aligned} \tag{7.74}$$

Dividing out V_F gives

$$\Sigma_t^F(E)\phi^F(E) = [1 - P_{FO}(E)]\int_E^{E/\alpha_A} \frac{\Sigma_{sA}^F(E')\phi^F(E')dE'}{(1-\alpha_A)E'} + [1 - P_{FO}(E)]\frac{\Sigma_{smf}\phi_o}{E} + P_{FO}(E)\frac{\Sigma_t^F(\phi_o}{E} \tag{7.75}$$

Note that we have eliminated any dependence on the outside moderator at this point. Now it is time to make the narrow resonance approximation for the absorber as we have done before.

$$\begin{aligned} \Sigma_t^F(E)\phi^F(E) &= [1 - P_{FO}(E)]\frac{\Sigma_{pA}^F\phi_o}{E} + [1 - P_{FO}(E)]\frac{\Sigma_{smf}\phi_o}{E} + P_{FO}(E)\frac{\Sigma_t^F(E)\phi_o}{E} \\ \Sigma_{FP}^F &= \Sigma_{pA}^F + \Sigma_{smf}^F \\ \Sigma_t^F(E)\phi^F(E) &= [1 - P_{FO}(E)]\frac{\Sigma_{PF}^F\phi_o}{E} + P_{FO}(E)\frac{\Sigma_t^F(E)\phi_o}{E} \end{aligned} \tag{7.76}$$

Now define a pseudo-cross section called the "escape" cross section such that

$$\begin{aligned}\Sigma_{\text{esc}}(E) &= \frac{P_{FO}(E)}{1 - P_{FO}(E)}\Sigma_t^F(E)\\ \text{or}&\\ P_{FO}(E) &= \frac{\Sigma_{\text{esc}}(E)}{\Sigma_{\text{esc}}(E) + \Sigma_t^F(E)}\end{aligned} \tag{7.77}$$

Inserting this into the infinite media equation gives

$$\begin{aligned}\Sigma_t^F(E)\phi^F(E) &= \frac{\Sigma_{\text{esc}}(E) + \Sigma_t^F(E) - \Sigma_{\text{esc}}(E)}{\Sigma_{\text{esc}}(E) + \Sigma_t^F(E)}\frac{\Sigma_{PF}^F\phi_o}{E} + \frac{\Sigma_{\text{esc}}(E)}{\Sigma_{\text{esc}}(E) + \Sigma_t^F(E)}\frac{\Sigma_t^F(E)\phi_o}{E}\\ \phi_F(E) &= \frac{\Sigma_{pF}^F + \Sigma_{\text{esc}}(E)}{\Sigma_{\text{esc}}(E) + \Sigma_t^F(E)}\frac{\phi_o}{E}\end{aligned} \tag{7.78}$$

after the total cross section in the fuel has been divided out of both sides.

7.12 Heterogeneous Wide Resonance Approximation

If we make the wide resonance approximation for the absorber, we will obtain

$$\Sigma_t^F(E)\phi^F(E) = [1 - P_{FO}(E)]\Sigma_{sA}^R\phi^F(E) + [1 - P_{FO}(E)]\frac{\Sigma_{smf}^F\phi_o}{E} + P_{FO}(E)\frac{\Sigma_t^F\phi_o}{E} \tag{7.79}$$

Now substituting for $P_{FO}(E)$, dividing out $\Sigma_t^F(E)$, and multiplying by $\Sigma_{\text{esc}} + \Sigma_t^F(E)$, this becomes

$$\left[\Sigma_{\text{esc}}(E) + \Sigma_t^F(E)\right]\phi^F(E) = \Sigma_{sA}^R(E)\phi^F(E) + \frac{\Sigma_{smf}^F\phi_o}{E} + \frac{\Sigma_{\text{esc}}(E)\phi_o}{E} \tag{7.80}$$

Subtracting $\Sigma_{sA}^F(E)\phi^F(E)$ from both sides and solving for $\phi^F(E)$ give

$$\phi^F(E) = \frac{\Sigma_{smf}^F + \Sigma_{\text{esc}}(E)}{\Sigma_{smf}^F + \Sigma_{\text{esc}}(E) + \Sigma_{aA}^F(E)}\frac{\phi_o}{E} \tag{7.81}$$

Now remembering that we had for the homogeneous cases

Narrow resonance	Wide resonance
$\phi(E) = \frac{\Sigma_{sm}+\Sigma_{pA}}{\Sigma_t(e)}\frac{\phi_o}{E}$	$\phi(E) = \frac{\Sigma_{sm}}{\Sigma_{sm}+\Sigma_{aA}(E)}\frac{\phi_o}{E}$

We make the following substitutions in going from the homogeneous to the heterogeneous case:

	Homogeneous		Heterogeneous
Narrow resonance	$\Sigma_{sm} + \Sigma_{pA}$	→	$\Sigma_{\text{esc}} + \Sigma_{smf}^{F} + \Sigma_{pA}^{F}$
Wide resonance	Σ_{sm}	→	$\Sigma_{\text{esc}} + \Sigma_{smf}^{F}$

and simply use the formulas for the homogeneous approximations. These are known as the ***equivalence relations***.

All that remains is to determine a value for Σ_{esc}. The most useful relationship for determining the "escape cross section" is due to Wigner and is called the Wigner rational approximation. Wigner proposed that we approximate $P_{FO}(E)$ by

$$P_{FO}(E) = \frac{\frac{S_F}{4V_F\Sigma_t^F}}{1 + \frac{S_F}{4V_F\Sigma_t^F(E)}} \tag{7.82}$$

S_F = fuel element surface area
V_F = fuel element volume
He noted that this gives the correct limits as the ratio V_F/S_F goes to 0 and infinity.

$$\begin{array}{llllll} V_F/S_F & \rightarrow & 1, & P_{Fo}(E) & \rightarrow & 1.0 \\ V_F/S_F & \rightarrow & \text{Infinity}, & P_{Fo}(E) & \rightarrow & S_F/4V_F\Sigma_t^F(E) \end{array}$$

The maximum error in this approximation is about 10 % over portions of the range between the limits. Then $4V_F/S_F$ can be defined as the average chord length $<R>$ in the fuel material. Then we have

$$P_{FO}(E) = \frac{\frac{1}{\langle R\rangle\Sigma_t^F(E)}}{1 + \frac{1}{\langle R\rangle\Sigma_t^F(E)}} = \frac{\Sigma_{\text{esc}}(E)}{\Sigma_{\text{esc}}(E) + \Sigma_t^F(E)} = \frac{1}{1 + \langle R\rangle\Sigma_t^F(E)} = \frac{\frac{1}{\langle R\rangle}}{\frac{1}{\langle R\rangle} + \Sigma_t^F(E)}$$
$$\Sigma_{\text{esc}} = \frac{1}{\langle R\rangle} \tag{7.83}$$

Note that Σ_{esc} in the rational approximation is not a function of energy. This is particularly convenient computationally and is what makes the rational approximation so useful. It gives quite good answers.

Remember that what we have developed is for a single fuel lump in a sea of moderator. Also, remember that we completely eliminated the dependence of the resonance integral on the outside moderator. When we consider a fuel pin array, these simplifying assumptions are no longer valid. Specifically we have to take into account the fact that a neutron can escape from one fuel element, escape from the outside moderator, and collide in a second fuel element. The correction for this effect is accomplished with the Dancoff factor. We modify our escape cross section to become

$$\Sigma_{\text{esc}} = \frac{1-c}{\langle R\rangle} \tag{7.84}$$

where c is called the Dancoff factor. There are a number of useful correlations for calculating the Dancoff factor, but the one most widely used appears to be attributed to Sauer. Sauer's approximation is given by

$$c = \frac{e^{-\tau\Sigma_{sm}\langle l_M\rangle}}{1+(1-\tau)\Sigma_{sm}\langle l_m\rangle} \tag{7.85}$$

$\langle l_m\rangle = \langle R\rangle{*}(V_M/V_F) = \langle R\rangle VR$
Σ_{sm} = outside moderator total cross section
$\langle R\rangle$ = average chord length in the fuel
V_M = moderator volume fraction
V_F = fuel volume fraction
VR = Moderator to fuel volume ration

τ is for a square lattice of fuel pins similar to those in light-water reactors.

$$\tau_{\text{sq}} = \sqrt{\frac{\frac{\pi}{4}(1+VR)-1.0}{VR}} - 0.08 \tag{7.86}$$

In addition, for a hex lattice like fast reactors

$$\tau_{\text{hex}} = \sqrt{\frac{\frac{\pi}{\sqrt{12}}(1+VR)-1.0}{VR}} - 0.12 \tag{7.87}$$

Therefore, we can use the homogeneous formulas for the heterogeneous integrals if we calculate the β's as

$$\text{Narrow Resonance} \quad \beta = \frac{\frac{1-c}{\langle R\rangle} + \Sigma_{smf} + \Sigma_{pA}}{\Sigma_o} \tag{7.88}$$

$$\text{Wide Resonance} \quad \beta = \frac{\frac{1-c}{\langle R\rangle} + \Sigma_{smf}}{\Sigma_o}\frac{\Gamma}{\Gamma_\gamma} \tag{7.89}$$

Problems

Problem 7.1 Explain how the temperature coefficient of reactivity is largely determined by the resonances in U^{238}.

Problem 7.2 Why does a PWR need to be refueled well before all the U^{235} in the fuel rod is used up?

Problem 7.3 The 129 keV gamma ray transitioning in Ir^{191} was used in a Mösbauer experiment in which a line shift equivalent to the full width at half maximum (Γ) was observed for a source speed of 1 cm/s. Estimate the value of Γ and the mean lifetime of the excited state in Ir^{191}.

Problem 7.4 An excited atom of total mass M at rest with respect to a certain inertial system emits a photon, thus going over into a lower state with an energy smaller by Δw. Calculate the frequency of the photon emitted.

Problem 7.5 Calculate the spread in energy of the 661 keV internal conversion line of Cs^{137} due to the thermal motion of the source. Assume that all atoms move with the root mean square velocity for a temperature of 15 °C.

Problem 7.6 Pound and Rebka at Harvard performed an experiment to verify the red shift predicted by the general theory of relativity. The experiment consisted of the use of 14 keV γ-ray of ^{57}Fe source placed on the top of a tower 22.6 m high and the absorber at the bottom. The red shift was detected by the Mösbauer technique. What velocity of the absorber foil was required to compensate the red shift and in which direction?

Problem 7.7 Obtain an expression for the Doppler line width for a spectral line of wavelength λ emitted by an atom of mass m at a temperature T.

Problem 7.8 For the $2P_{3/2} \rightarrow 2S_{1/2}$ transition of an alkali atom, sketch the splitting of the energy levels and the resulting Zeeman spectrum for atoms in a weak external magnetic field (express your results in terms of the frequency v_0 of the transition in the absence of an applied magnetic field).

$$\left\{\text{The Lande g-factor is given by } g = 1 + \frac{j(j+1) + s(s+1) - l(l+1)}{2j(j+1)}\right\}$$

Problem 7.9 The spacings of adjacent energy levels of increasing energy in a calcium triplet are 30×10^{-4} and 60×10^{-4} eV. What are the quantum numbers of the three levels? Write down the levels using the appropriate spectroscopic notation.

Problem 7.10 An atomic transition line with a wavelength of 350 nm is observed to be split into three components in a spectrum of light from a sunspot. Adjacent components are separated by 1.7 pm. Determine the strength of the magnetic field in the sunspot. $\mu_B = 9.17 \times 10^{-24}\ \mathrm{JT}^{-1}$.

Problem 7.11 Calculate the energy spacing between the components of the ground state energy level of hydrogen when split by a magnetic field of 1.0 T. What frequency of electromagnetic radiation could cause a transition between these levels? What is the specific name given to this effect?

Problem 7.12 Consider the transition $2P_{1/2} \rightarrow 2S_{1/2}$ for sodium in the magnetic field of 1.0 T, given that the energy splitting $\Delta E = g\mu_B B m_j$, where μ_B is the Bohr magneton. Draw the sketch.

Problem 7.13 Find the Doppler shift in wavelength of H line at 6563 Å emitted by a star receding with a relative velocity of $3 \times 10^6\ \mathrm{ms}^{-1}$.

Problem 7.14 Show that for slow speeds, the Doppler shift can be approximated as $(\Delta\lambda/\lambda) = (v/c)$ where $\Delta\lambda$ is the change in wavelength.

Problem 7.15 A physicist was arrested for going over the railway level crossing on a motorcycle when the lights were red. When he was presented before the magistrate, the physicist declared that he was not guilty as the red lights ($\lambda = 670$ nm) appeared green ($\lambda = 525$ nm) due to the Doppler effect. At what speed was he travelling for the explanation to be valid? Do you think such a speed is feasible?

Problem 7.16 Find the wavelength shift in the Doppler effect for the sodium line 589 nm emitted by a source moving in a circle with a constant speed of 0.05 c observed by a person fixed at the center of the circle.

Problem 7.17 A π-meson with a kinetic energy of 140 MeV decays in flight into a μ-meson and a neutrino. Calculate the maximum energy, which

(a) The μ-meson has
(b) The neutrino may have in the laboratory system

(Mass of π-meson = 140 MeV/c2, mass of μ-meson = 106 MeV/c, mass of neutrino = 0)

Problem 7.18 A linear accelerator produces a beam of excited carbon atoms of a kinetic energy of 120 MeV. Light emitted on de-excitation is viewed at right angles to the beam and has a wavelength of λ'. If λ is the wavelength emitted by a stationary atom, what is the value of $(\lambda' - \lambda)/\lambda$? (Take the rest energies of both protons and neutrons to be 109 eV.)

Problem 7.19 A certain spectral line of a star has a natural frequency of 5×10^{17} c/s. If the star is approaching the earth at 300 km/s, what would be the fractional change of frequency?

Problem 7.20 Show that deuteron energy E has twice the range of proton of energy $E/2$.

Problem 7.21 If the mean range of 10 MeV protons in lead is 0.316 mm, calculate the mean range of 20 MeV deuterons and 40 MeV α-particles.

Problem 7.22 Show that the range of α-particles and protons of energy 1–10 MeV in aluminum is 1/1600 of the range in air at 15 °C, 760 mm of Hg.

Problem 7.23 Show that except for small ranges, the straggling of a beam of ^{3}He particles is greater than that of a beam of ^{4}He particles of equal range.

Problem 7.24 The range of a 15 MeV proton is 1100 ìm in nuclear emulsions. A second particle whose initial ionization is the same as the initial ionization of proton has a range of 165 μm. What is the mass of the particle? (The rate at which a singly ionized particle loses energy, E, by ionization along its range is given by $dE/dR = K/(\beta c)^2$ MeV μm where βc is the velocity of the particle and K is a constant depending only on emulsion; the mass of proton is 1837 mass of electron.)

Problem 7.25 (a) Show that the specific ionization of 480 MeV á-particle is approximately equal to that of 30 MeV proton.

(b) Show that the rate of change of ionization with distance is different for the two particles, and indicate how this might be used to identify one particle, assuming the identity of the other is known.

Problem 7.26 Calculate the 6.67 eV resonance integral for U^{238} in a typical PWR. Compare the actual resonance integral with its infinite dilution value.

Fuel	Moderator	Resonance
UO_2 −3 % enriched	Water	$E_R = 6.67\,\text{eV}$
$N^{UO}{}_2 = 0.0223$ mol/barn/cm	$N^{H}{}_2{}^{O} = 0.0335$ mol/barn/cm	$\sigma_0 = 216{,}000\,\text{barns}$
$\sigma_s^O = 4.2\,\text{barns/atom}$	$\sigma_s^H = 20.2\,\text{barns/atom}$	$\Gamma_t = 0.0275\,\text{eV}$
$\sigma_p^U = 8.3\,\text{barns/atom}$	Volume fraction = 0.55	$\Gamma_\gamma = 0.026$ eV
$\langle R \rangle = 0.94\,\text{cm}$	Square lattice	$\Gamma_n = 0.0015$ eV
Volume fraction = 0.45	$T_{\text{fuel}} = 600\,\text{K}$	

References

1. Y. Oka, T. Kiguchi, *Nuclear Reactor Design (An Advanced Course in Nuclear Engineering)* (Springer, New York, 2014)
2. J. Duderstadt, L. Hamilton, *Nuclear Reactor Analysis* (Wiley, New York, 1976)
3. http://www.nuclear-power.net/nuclear-power/reactor-physics/nuclear-engineering-fundamentals/neutron-nuclear-reactions/compound-nucleus-reactions/what-is-nuclear-resonance-compound-nucleus/
4. H.A. Bethe, G. Placzek, Resonance effects in nuclear processes. Phys. Rev. **51**, 450 (1937)
5. http://www.nuclear-power.net/glossary/doppler-broadening/#prettyPhoto
6. J.R. Lamarsh, *Introduction to Nuclear Reactor Theory* (Addison Wesley, Reading, 1966)
7. A. Alpan, L.C. Leal, A. Courcelle, *Effect of Energy Self-Shielding Methods on U^{238} for Criticality Safety, PHYSOR 2004*. The Physics of Fuel Cycles and Advanced Nuclear Systems: Global Developments. Chicago, April 25–29, 2004, on CD-ROM, American Nuclear Society, Lagrange Park, IL. (2004)

Chapter 8
Heterogeneous Reactors and Wigner–Seitz Cells

When deterministic neutron transport methods are applied to lattice or whole-core problems, the multigroup approximation is usually applied to the cross-sectional treatment for the energy domain. Due to the complicated energy behavior of resonance cross sections, the weighting spectrum for collapsing multigroup cross sections is very dependent on energy and space, which becomes a crucial challenge when analyzing a lattice or full-core configuration.

8.1 Homogeneous and Heterogeneous Reactors

So far, all of our analyses are assumed based on homogeneous-type reactors, where a mixture of fuel and moderator is combined in their design and consequently their structure, yet in the real world of commercial reactors, very few reactors are of this type. However, in most reactors, the fuel is speared out in some kind of structural material to form *solid fuel elements*, which are usually in a uniform lattice configuration. At this stage, it is important for us to recognize and distinguish these two types of reactors and understand the difference between them.

If a reactor core consists of fuel, moderator, coolant, and structural were assumed to be combined and homogeneously mixed, where the neutron mean free path at *all* energies is large compared with thickness of the fuel element; the reactor is called *quasi-homogeneous* or ultimately *homogeneous reactor*.

On the other hand, if the reactor is structurally constructed to facilitate thermal design such as:

1. Coolant channel, heat transfer surfaces (i.e., thermal hydraulic analysis of reactor design) [1]
2. Integrity of core structure such as fuel fabrication
3. Reactivity control such as control rods, burnable poisons, etc.

B. Zohuri, *Neutronic Analysis For Nuclear Reactor Systems*,
DOI 10.1007/978-3-319-42964-9_8

where, also, the mean free path of neutrons at *any* energy is comparable to, or less than, the thickness of a fuel element, then the reactor is said to be *heterogeneous* type. The analysis of this type of reactor is not easy as what have been dealt with so far and rather is a very complicated problem from neutronic analysis point of view.

A typical commercial heterogeneous reactor is the pressurized water reactor (PWR) as it is shown in Fig. 8.1 with its fuel assembly depicted in Fig. 8.2. As it can be seen in these pictures, heterogeneities in the reactor fuel array or *lattice* must be taken into consideration in the design of nuclear fission reactor, because they will cause a local spatial variation in the neutron flux, which may have strong influence

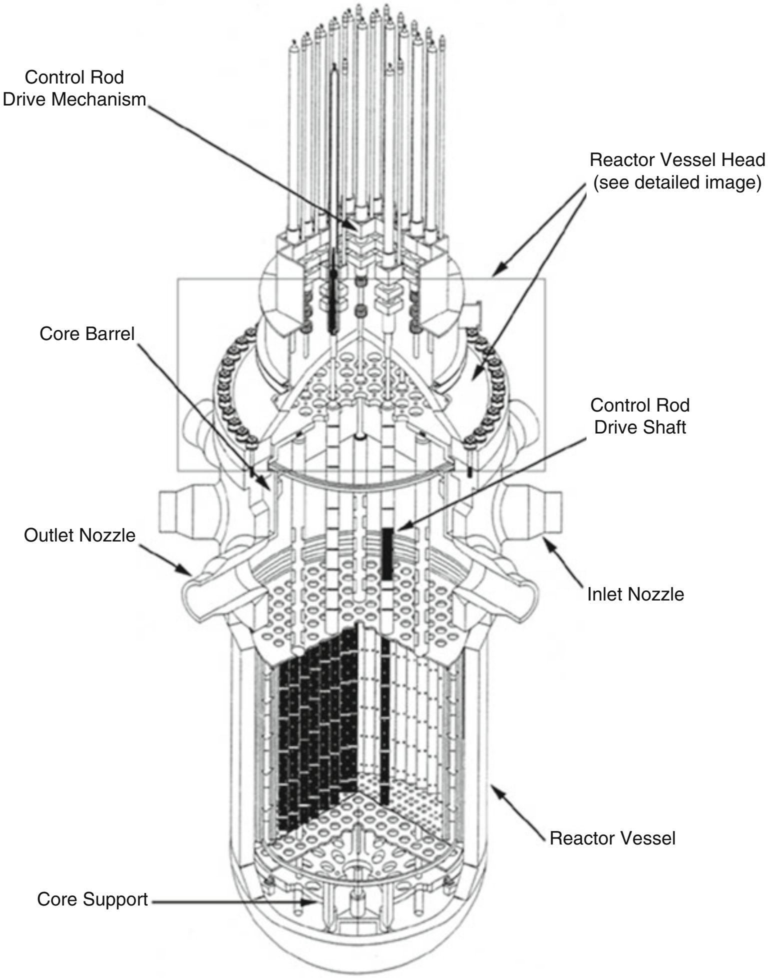

Fig. 8.1 A typical pressurized water reactor (Courtesy of the US Nuclear Regulatory Commission, NRC)

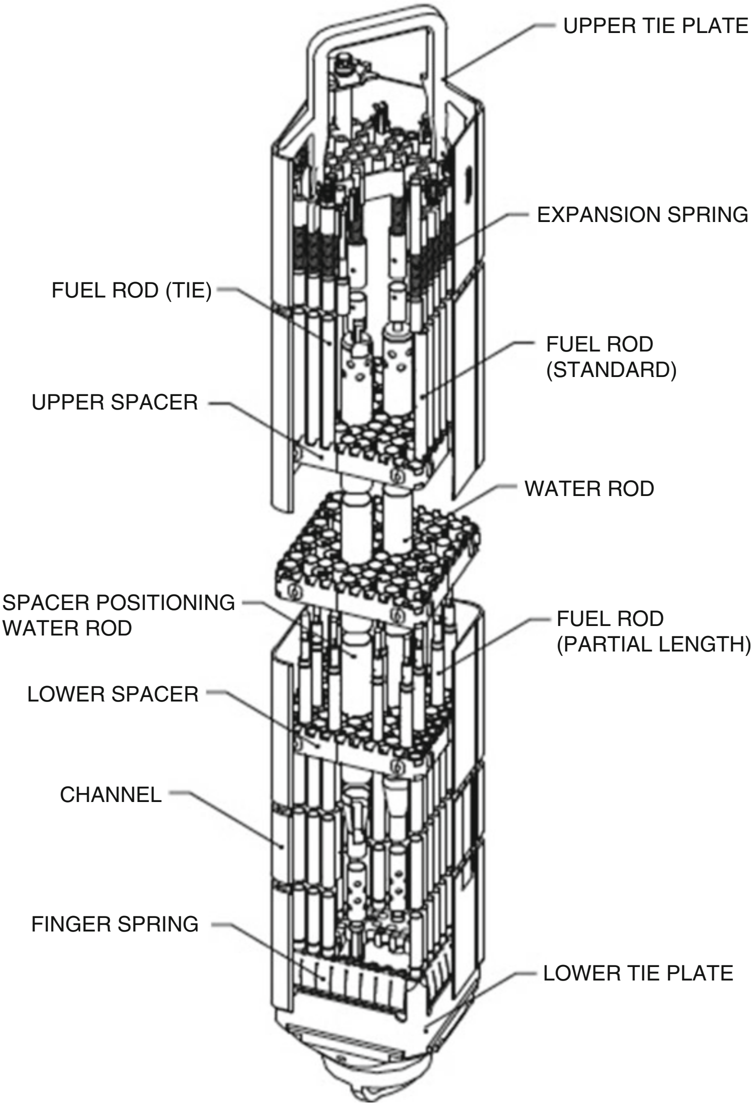

Fig. 8.2 Fuel element and fuel assembly (Courtesy of the US Nuclear Regulatory Commission, NRC)

for core multiplication. The degree of consideration for core lattice effect in reactor design depends on the characteristic dimension of lattice structure, such as fuel pin diameter or the spacing between fuel elements, which may be compared to the mean free path of neutron in the core that is typically in the order of centimeter.

Typically, light-water reactor (LWR) designs can be used as an example, where the core lattice dependency of thermal neutrons has centimeter order of mean free path within the core of reactor, compared to the fuel pin diameter. Therefore, the flux distribution in the fuel might be expected to be different from that on the moderator or coolant channel. Hence, the details of heterogeneity analysis may apply, and it is necessary to find the number of the fuel elements or the concentration of fuel configuration of them for the purpose of criticality versus the fuel concentration in the moderator, as it is for the case of homogeneous reactor design. In books by Duderstadt and Hamilton [2] as well as Lamarsh [3], one can find more details for mathematical analysis approach of such conditions, where we encourage the readers to refer to them.

Now that we have covered the basic differences between these two fission reactors, i.e., homogeneous versus heterogeneous, we can continue with our subject of spectrum calculation in heterogeneous-type reactor and move on to the cross-sectional self-shielding as well as Wigner–Seitz cells in the next few sections of this chapter.

8.2 Spectrum Calculation in Heterogeneous Reactors

Before we launch into this subject, “it is convenient to divide the fuel-moderator lattice into *unit cells*, each containing one fuel lump at its center” [3] where two most commonly used lattice and the unit cells are depicted in Fig. 8.3. Note that since all the cells are identical in an infinite uniform lattice, there is no net flow of neutrons from one cell to the next one, and due to this argument, *the current density is zero along the boundary of each cell*. Thus, for the purpose of the flux calculation within the cell, we need to replace the actual lattice cell by a cell having a more simple geometry, such as fuel lump sum in shape of cylinder. The actual cell then is replaced by a cylindrical cell of the *same volume* as in Fig. 8.3. Since there is no flow of thermal neutrons from one cell to another, the thermal neutron current density may consider being zero on the surface of the equivalent cell from our knowledge of electromagnetic science. This consideration, where we used an

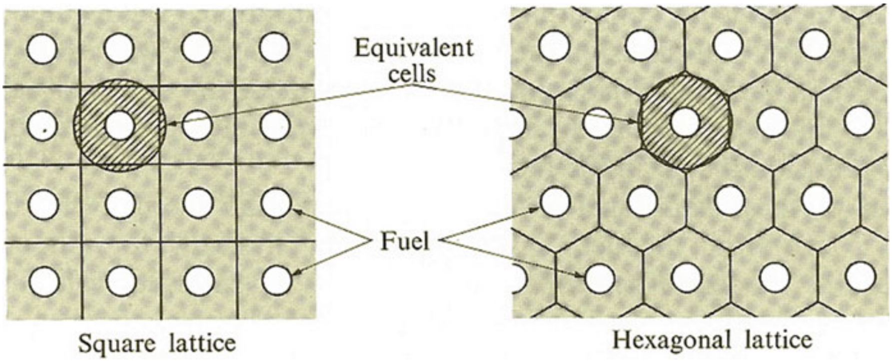

Fig. 8.3 Two typical heterogeneous lattices and equivalent cells for each [2]

equivalent cell with a zero-current boundary condition, is known as the *Wigner–Seitz method*, which is the discussion in the following sections of this chapter.

So far, for any treatment of spectrum analysis, we have only paid attention on homogeneous-type fission reactors, and for all practical purposes; we are encountering fission reactor systems that are containing various levels of heterogeneity. The entire commercial nuclear power fission reactors consist of at least two regions, namely, *core* and *reflector*. For design purposes in terms of power shaping, the core is normally configured either radially or axially, and they are subdivided in different composition regions. Usually a spectrum calculation needs to be done independent of these regions for each reactor. In order to achieve such calculation, we couple these regions using energy-dependent bucklings, obtained from a few-group two- or three-dimensional calculations over the complete reactor shape, and require iteration analysis as necessary. For the purpose of this iteration approach, one needs to guess the buckling for the first-round spectrum calculations, and it can be performed by producing condensed few-group constants for two- or three-dimensional calculations, out of which new energy-dependent buckling is yielding for each region. This process of iteration continues until the desired accuracy is achieved, and then the second level of heterogeneity analysis will take place by the fine structure of the reactor cells [4].

Note that heterogeneity effect in fuel structure cannot be neglected, even for high-temperature reactors (HTRs) that are homogeneous-type fission reactor compared with many other reactors. As we have mentioned above, all reactors consist of regular lattices of cells containing fuel pins, coolant channels, moderators, and absorbers as schematically shown in Figs. 8.1 and 8.2.

For the purpose of spectrum calculations, we need to choose either a multigroup space-dependent transport treatment or an analysis over a homogenized cell. In today's computer code that is commercially available to us, we have examined so far to follow the second procedure.

Once the fine structure of the flux within the cell is becoming obvious, then the homogenization can be performed multiplying the cross sections by energy-dependent self-shielding, which is also called disadvantage factors. We can represent this self-shielding as $S_k(E)$ that is defined for each material k in such a way as to yield the same reaction rate in the homogenized calculation as in the real cell. However, as we have learned in neutronic analysis of reactor so far, the homogenized calculation deals only with a reference flux $\phi_{\mathrm{R}}(E)$, yet in real analysis the reference flux depends on the position within cell, thus can be symbolized as $\phi_{\mathrm{R}}(\vec{r}, E)$.

If we take the reference flux $\phi_{\mathrm{R}}(E)$ at any point of the cell, let us say at its center, or at the boundary of interest, or an average vale, then we can write the following relation as

$$\phi_{\mathrm{R}}(E) = \frac{\int \phi_{\mathrm{R}}(\vec{r}, E) d\vec{r}}{V} \tag{8.1}$$

where V is the cell volume and the integral is taken over the whole cell. The spectrum, which resulted from the flux calculation, depends, of course, on the reference, which has been chosen, although reaction rates and reactivity are independent of this reference.

Now, if we define the average concentration of isotope k using symbol of $\overline{N}_k(\vec{r})$, which is space dependent and written as

$$\overline{N}_k(\vec{r}) = \frac{\int N_k(\vec{r}) d\vec{r}}{V} \tag{8.2}$$

then, to obtain the proper reaction rates, the self-shielding $S_k(E)$, which must satisfy the following equation, is

$$\sigma_k \overline{N}_k(\vec{r}) \phi_{\mathrm{R}}(E) = \frac{1}{V} \int \sigma_k N_k(\vec{r}) \phi_{\mathrm{R}}(\vec{r}, E) d\vec{r} \tag{8.3}$$

where σ_k is the cross section of isotope k.

The self-shielding then has to be defined as follows:

$$S_k = \frac{\int N_k(\vec{r}) \phi_{\mathrm{R}}(\vec{r}, E) d\vec{r}}{V \overline{N}_k(\vec{r}) \phi_{\mathrm{R}}(E)} = \frac{\int N_k(\vec{r}) \phi_{\mathrm{R}}(\vec{r}, E) d\vec{r}}{\phi_{\mathrm{R}}(E) \int N_k(\vec{r}) d\vec{r}} \tag{8.4}$$

The cross section of each material must be multiplied by its self-shielding. In most cases, the average cell flux is used as ϕ_{R}, which may give rise to some difficulty in imposing boundary conditions, so that sometimes the flux at the outer cell boundary is used as reference. A homogenization by means of self-shielding as in the case of cell calculation is very possible. In the case of resonance absorption, this gain structure can become very important [4].

8.3 Cross-Sectional Self-Shielding and Wigner–Seitz Cells

The Wigner–Seitz cell, named after Eugene Wigner and Frederick Seitz, is a type of Voronoi cell used in the study of crystalline material in solid-state physics. A Wigner–Seitz cell is an example of another kind of primitive cell. The primitive unit cell (or simply primitive cell) is a special case of unit cell, which has only one lattice point combined and shared by eight other primitive cells. It is the most

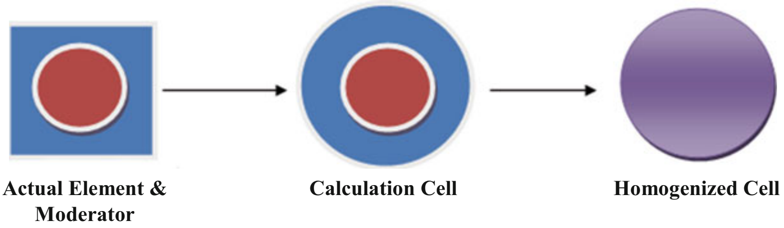

Fig. 8.4 Typical cell sequence

"primitive" cell one can construct, and it is a parallelepiped. The general unit cell has an integral number of lattice points. The simple cubic lattice is the only primitive unit cell conventionally. The body-centered cubic (BCC) and face-centered cubic (FCC) lattices are simply unit cells, not primitive cells.

Consider a typical PWR core that contains between 51,000 and 57,000 fuel elements or a boiling water reactor (BWR) core that contains around 46,000 fuel elements. In order to calculate critical size, control rod positions, poison concentration, and fuel burnup, it is important to get the reaction rates correct in each fuel element. It is virtually impossible to run a three-dimensional calculation that places enough mesh points in each fuel element to get the detailed neutron flux very accurate. So some form of homogenization of fuel elements is required to get average cross sections for fuel assemblies (typical 17 × 17 elements in a PWR and 8 × 8 in a BWR). Since most fuel assemblies are repeating arrays, the standard approach is to consider one fuel element and its associated moderator as a cell and calculate average cross sections for the cell. A typical sequence is described in Fig. 8.4.

The square cell (or hexagonal cell) is converted to a cylindrical cell for a one-dimensional calculation conserving the volumes of the fuel and moderator regions. It is possible to do a two-dimensional calculation for the square cell, but the utility of this is negligible for most reactors that have been designed to date. A k-effective (k_∞) calculation is performed for the cylindrical cell with enough leakage to get a near-critical system. Then the cross sections are homogenized to get values as if all of the materials in the fuel element and moderator were smeared out across the cell. The obvious thing that must be accomplished here is that in the smeared cell, we must have the same number of atoms of each nuclide as we have in the actual element and moderator. The conservation of atoms relationship gives us

$$\int_{\text{cell}} N_{\text{cell}}\sigma_x^{\text{cell}}dV_{\text{cell}} = \int_{\text{FE}} N_{\text{FE}}\sigma_x^{\text{FE}}dV_{\text{FE}} \tag{8.5}$$

In addition, assuming a constant cross section as always, this gives

$$N_{\mathrm{cell}} = (V_{\mathrm{FE}}/V_{\mathrm{cell}})^{*}N_{\mathrm{FE}} \tag{8.6}$$

However, we not only want to conserve atoms, but we want to conserve reaction rates. If we were only conserving atoms, we would not need to do a cell calculation to get the relative fluxes in the cell. So in order to conserve reaction rates, we have

$$\int\limits_{\mathrm{cell}} N_{\mathrm{cell}}\sigma_x^{\mathrm{cell}}\phi_{\mathrm{cell}}(V)dV_{\mathrm{cell}} = \int\limits_{\mathrm{FE}} N_{\mathrm{FE}}\sigma_x^{\mathrm{FE}}\phi_{\mathrm{FE}}(V)dV_{\mathrm{FE}} \tag{8.7}$$

Now assuming the number density and cross sections are constant as always, this gives

$$N_{\mathrm{cell}}\sigma_x^{\mathrm{cell}}\int\limits_{\mathrm{cell}} \phi_{\mathrm{cell}}(V)dV_{\mathrm{cell}} = N_{\mathrm{FE}}\sigma_x^{\mathrm{FE}}\int\limits_{\mathrm{FE}} \phi_{\mathrm{FE}}(V)dV_{\mathrm{FE}} \tag{8.8}$$

which can be written as

$$N_{\mathrm{cell}}\sigma_x^{\mathrm{cell}}\overline{\phi}_{\mathrm{cell}}V_{\mathrm{cell}} = N_{\mathrm{FE}}\sigma_x^{\mathrm{FE}}\overline{\phi}_{\mathrm{FE}}V_{\mathrm{FE}} \tag{8.9}$$

Then to conserve atoms, we have

$$N_{\mathrm{cell}} = (V_{\mathrm{FE}}/V_{\mathrm{cell}})^{*}N_{\mathrm{FE}} \tag{8.10}$$

So we must have

$$\sigma_x^{\mathrm{cell}} = \left(\overline{\phi}_{\mathrm{FE}}/\overline{\phi}_{\mathrm{cell}}\right)\sigma_x^{\mathrm{FE}} \tag{8.11}$$

in order to conserve reaction rates. Thus, when we homogenize the cell, we have to modify the cross sections which are called *flux disadvantage factors* or *self-shielding factors*. They are the ratio of the average flux in the region the material of interest is in to the average flux for the whole cell.

The term *self-shielding factor* is more appropriate because it is the average flux in the region under consideration divided by the cell average flux. This ratio could be greater or less than 1.0 depending on many things. The term *disadvantage factor* came from the fact that it is usually less than 1.0 for the thermal flux in a thermal reactor. The concept was first applied only to the thermal flux in the fuel element, but as time went on, it became obvious that all cross sections no matter what material they are in could merit from this approach. So typically the moderator cross sections in the thermal region are weighted with a *flux disadvantage factor* that is greater than 1.0. This tends not to be a very big deal because scattering reactions in the moderator do not affect criticality or burnup very significantly. Of course, when a burnable poison is added to the coolant, the situation changes, and *self-shielding factors* must be applied to all materials in all energy ranges. Typically, cell codes used to homogenize cells do this automatically.

It is important to realize that a Wigner–Seitz cell, as they are called, does not have to consist of just fuel and moderator. Any other material that is in the repeating array can be put in the cell and self-shielding factors calculated for its cross sections. However, there are other problems. Some fuel element positions have the fuel element replaced with an instrumentation thimble or a control rod. There are also fuel assembly cans and coolant channels between fuel assemblies that have nuclides in the core, but not in our repeating array cell. We could do a separate cell calculation for these positions, except they do not contain fissile materials so we could not find a k effective (k_∞). Normally, what is done is that instrumentation materials, control materials, assembly structures, and inter-assembly materials are added as an outer layer on our cylindrical cell calculation, and we calculate self-shielding factors for them in that position. It is also possible that we could take the homogenized cross sections from the fuel element calculation and build another larger cell, nominally two-dimensional, which had the additional materials in their correct positions, and do a second homogenization calculation. This is normally not worth the effort.

Problems

Problem 8.1 Cadmium has a resonance for neutrons of energy 0.178 eV, and the peak value of the total cross section is about 7000 b. Estimate the contribution of scattering to this resonance.

Problem 8.2 A nucleus has a neutron resonance at 65 eV and no other resonances nearby. For this resonance, $\Gamma_n = 4.2\,\text{eV}$, $\Gamma_\gamma = 1.3\,\text{eV}$ and $\Gamma_\alpha = 2.7\,\text{eV}$, and all other partial widths are negligible. Find the cross section for (n, γ) and (n, α) reactions at 70 eV.

Problem 8.3 Neutron incidents on a heavy nucleus with spin JN = 0 show a resonance at an incident energy $E_R = 250$ eV in the total cross section with a peak magnitude of 1300 barns, the observed width of the peak being $\Gamma = 20$ eV. Find the elastic partial width of the resonance.

Problem 8.4 The diffusion length of beryllium metal is determined by measuring the flux distribution in an assembly 100 cm × 100 cm x 65 cm high, at the base of which is a plane source of thermal neutrons. The corrected saturation activities in counts per minute of foils located at various vertical distances above the base are given in the table below. Similar measurements in a horizontal direction gave a value of 2.5 cm as the extrapolation distance, i.e., the distance from the assembly at which the neutron flux extrapolated to zero. Using the figure below, what would be the diffusion length of thermal neutron in beryllium?

Vertical distance (*z* cm)	Saturation activity (c/m)
10	310
20	170
30	90
40	48
50	24
60	12

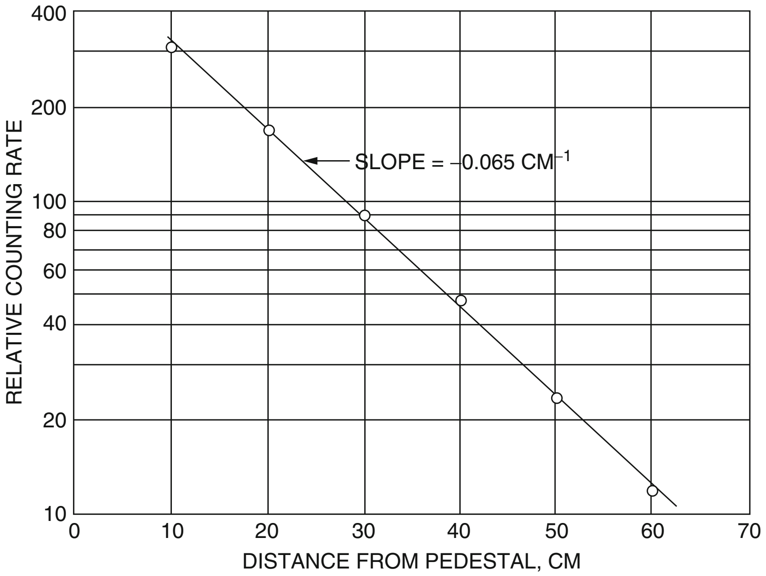

Fig. P8.4 Data for evaluation of diffusion length of beryllium

Problem 8.5 A reactor core contains enriched uranium as fuel and beryllium oxide as moderator ($\Sigma_s = 0.64\,\text{cm}^{-1}$ and $\xi = 0.17$ at a neutron energy of 7 eV). The thermal neutron flux is 2×10^{12} neutrons/(cm^2) (s), and Σ_a for these neutrons, the fuel is 0.005 cm^{-1}; for each thermal neutron absorbed, 1.7 fission neutrons are produced. Neglecting all absorption during slowing down, estimate the epithermal neutron flux at 7 eV per unit *lethargy* interval. **Hint**: use Eq. 3.75 that is given in Chap. 3 for *lethargy* or the so-called *logarithmic energy decrement* as well.

Problem 8.6 An experiment was performed to measure the Fermi age of fission neutron slowing down to indium resonance in an assembly of beryllium oxide blocks, using a fission plate as the neutron source. The corrected indium foil saturation activities, normalized to 1000 at the source plate, are given in the table below. Using the equation

(a) below for the age of neutron of specified energy in a given medium, determine the neutron age at the indium resonance energy.

Distance from fission plate (r cm)	Relative activity (A_0)	($A_0 r$)	($A_0 r^4$)
0	1000	–	–
4.0	954	1.53×10^4	2.44×10^5
7.9	828	5.16×10^4	5.16×10^5
11.7	660	9.04×10^4	1.24×10^7
19.35	303	1.13×10^5	5.59×10^7
27.15	103	7.59×10^4	4.24×10^7
34.5	29.3	3.55×10^4	4.3×10^7
42.7	7.2	1.31×10^4	2.4×10^7
50.5	1.6	4.08×10^3	1.04×10^7
62.2	0.45	1.74×10^3	6.7×10^6
77.8	0.15	9.08×10^2	5.5×10^6

Problem 8.7 A reactor consists of natural uranium rods of 1-in. diameter, arranged in a square lattice with a pitch of 6 in. in heavy water. If the thermal utilization f is given, the following equation is

$$\frac{1}{f} = 1 + \left(\frac{V_1 \Sigma_{a1}}{V_0 \Sigma_{a0}}\right) F + (E - 1)$$

where F and E for a cylindrical fuel rod are given as follows:

$$F = \frac{\kappa_0 r_0}{2} \cdot \frac{I_0(\kappa_0 r_0)}{I_1(\kappa_0 r_0)}$$

and

$$E = \frac{\kappa_1 \left(r_1^2 - r_0^2\right)}{2 r_0} \left[\frac{I_0(\kappa_1 r_0) K_1(\kappa_1 r_1) + K_0(\kappa_1 r_0) I_1(\kappa_1 r_1)}{I_1(\kappa_1 r_1) K_1(\kappa_1 r_0) - K_1(\kappa_1 r_1) I_1(\kappa_1 r_0)}\right]$$

I_0 and K_0 are being zero-order modified Bessel functions of first and second kinds, respectively, and I_1 and K_1 are the corresponding first-order function.

Note that the modified Bessel functions may be expanded in a series form for cases where the ratio of moderator to fuel is fairly high and absorption in the fuel is weak. When $\kappa_0 r_0$ is less than 1 and $\kappa_1 r_1$ is less than 0.75, the results may be approximated to give the following results [5]:

$$F \approx 1 + \frac{(\kappa_0 r_0)^2}{8} - \frac{(\kappa_0 r_0)^4}{192}$$

and

$$E \approx 1 + \frac{(\kappa_1 r_1)^2}{2}\left[\frac{r_1^2}{r_1^2 - r_0^2}\ln\frac{r_1}{r_0} + \frac{1}{4}\left(\frac{r_0}{r_1}\right)^2 - \frac{3}{4}\right]$$

Then calculate the thermal utilization for this lattice. The diffusion length of thermal neutron in natural uranium metal is 1.55 cm; the effective macroscopic absorption cross section is 0.314 cm^{-1}.

Problem 8.8 Calculate the resonance escape probability for the natural uranium heavy-water lattice in Problem 8.7. Use the following table of data as well.

Table P8.8 Resonance neutron data for moderators

Moderator	κ_1 (cm^{-1})
Water	0.885
Heavy	0.22
Beryllium	0.325
Beryllium Oxide	0.19
Graphite	0.145

References

1. B. Zohuri, N. Fathi, *Thermal-Hydraulic Analysis of Nuclear Reactors*, 1st edn. (Springer, New York, 2015)
2. J.J. Duderstadt, L.J. Hamilton, *Nuclear Reactor Analysis* (Wiley, New York, 1976)
3. J.R. Lamarsh, *Introduction to Nuclear Reactor Theory* (Addison-Wesley, Reading, 1966)
4. L. Massimo, *Physics of High-Temperature Reactors*, 1st edn. (Pergamon, New York, 2013)
5. A.M. Weinberg, E.P. Wigner, *The Physical Theory of Neutron Chain Reactors* (University of Chicago, Chicago, 1958), p. 635

Chapter 9
Thermal Spectra and Thermal Cross Sections

Although accurate determination of the thermal spectrum also requires advanced computational methods, average oversimplified spectra often serve as a reasonable first approximation in performing rudimentary reactor calculations. The main aspect of nuclear reactor analysis, as we have learned so far, is multigroup diffusion theory. In previous chapters, we developed the general form of multigroup diffusion equations and recommended a strategy for their solution. However, these set of equations contained various parameters known as group constants formally defined as the average over the energy-dependent intergroup flux which must be determined before these equations play formal important roles. In this chapter, we introduce the calculation of neutron energy spectrum characterizing fast neutrons, and as a result, the calculation of *fast neutron spectra* as well as generation of *fast group constants* will be of concern. At the conclusion, we will deal with the development of the theory of neutron slowing down and resonance absorption.

9.1 Coupling to Higher Energy Sources

In order to generate group constants for the thermal neutron groups, it is necessary to calculate detailed thermal neutron spectra. However, due to the fact that thermal neutron mean free paths are small, the heterogeneities that are present in typical thermal reactor cores are very significant and must be included in any reactor design calculation. Since we have not talked about heterogeneities yet, we will only treat thermal spectra in a very simplified form. Later in the section on generating cell cross sections, we will deal with the problem directly and calculate thermal group constants. The treatment we will apply here only applies to homogeneous thermal reactors like the AGN-201 reactor. Let us begin with the equation in an infinite medium. The P_0 equation for an energy E in the thermal range can be written as

B. Zohuri, *Neutronic Analysis For Nuclear Reactor Systems*,
DOI 10.1007/978-3-319-42964-9_9

$$\Sigma_t(E)\phi_0(E)=\int_0^{E_{\text{th}}}\Sigma_{s0}(E'\rightarrow E)\phi_0(E')dE'+S(E) \tag{9.1}$$

Equation 9.1 is a significantly reduced version of transport equation that is written in the form of an *integral equation* in the single variable E, which will refer to as the *infinite medium spectrum equation*. Note that the abbreviation of th stands for thermal in all equations below.

Note that both downscattering and upscattering must be included. Now if we write

$$\Sigma_a(E)\phi_0(E)+\Sigma_s(E)\phi_0(E)=\int_0^{E_{\text{th}}}\Sigma_{s0}(E'\rightarrow E)\phi_0(E')dE'+S(E) \tag{9.2}$$

and integrate the P_0 equation over the thermal energy range, we will have

$$\begin{aligned}&\int_0^{E_{\text{th}}}\Sigma_a(E)\phi_0(E)dE+\int_0^{E_{\text{th}}}\Sigma_a(E)\phi_0(E)dE\\&=\int_0^{E_{\text{th}}}\int_0^{E_{\text{th}}}\Sigma_{s0}(E'\rightarrow E)\phi_0(E')dEdE'+\int_0^{E_{\text{th}}}S(E)dE\end{aligned} \tag{9.3}$$

But noting that for thermal neutrons, the order of integral can be interchanged, therefore, we can write the following result:

$$\Sigma_s(E')=\int_0^{E_{\text{th}}}\Sigma_{s0}(E'\rightarrow E)dE \tag{9.4}$$

The two scattering terms will cancel and we obtain

$$\int_0^{E_{\text{th}}}\Sigma_a(E)\phi(E)dE=\int_0^{E_{\text{th}}}S(E)dE \tag{9.5}$$

or we arrive at the balance equation that

Thermal absorptions = thermal sources

If we now consider a finite homogeneous medium and make the diffusion approximation for the fundamental mode, we have

$$\begin{aligned}&D(E)B^2\phi(E)+\Sigma_a(E)\phi(E)+\Sigma_s(E)\phi(E)\\&=\int_0^{E_{\text{th}}}\Sigma_s(E'\rightarrow E)\phi_0(E')dE'+S(E)\end{aligned} \tag{9.6}$$

Integrating this equation over all energy and making the same order of integration change for the scattering integral on the right-hand side, we will have

$$B^2\int_0^{E_{\rm th}} D(E)\phi(E)dE + \int_0^{E_{\rm th}} \Sigma_a(E)\phi(E)dE = \int_0^{E_{\rm th}} S(E)dE \tag{9.7}$$

or we can state that

Thermal leakage + thermal absorptions = thermal sources

Now let us consider how one would determine the source for an infinite medium calculation. We begin by noting that the flux in the slowing down region above thermal has its asymptotic shape:

$$\phi(E) = \frac{Q_0}{E\xi\Sigma_s(E)} \tag{9.8}$$

where we can take the source, Q_0, equaled to 1.0 without loss of generality. Then, we can treat the slowing down flux as producing our source by writing the P_0 equation as

$$\begin{aligned}\{\Sigma_a(E) + \Sigma_s(E)\}\phi(E) = &\int_0^{E_{\rm th}} \Sigma_s(E' \to E)\phi_0(E')dE' \\ &+ \int_{E_{\rm th}}^{E/\alpha} \frac{\Sigma_s(E')}{(1-\alpha)E'}\frac{1}{E\xi\Sigma_s(E)}dE'\end{aligned} \tag{9.9}$$

or we have

$$\begin{aligned}S(E) &= \int_{E_{\rm th}}^{E/\alpha} \frac{\Sigma_s(E')}{(1-\alpha)E'}\frac{1}{E\xi\Sigma_s(E)}dE' \\ &= \frac{1}{\xi}\int_{E_{\rm th}}^{E/\alpha} \frac{dE'}{(1-\alpha)E'2}\end{aligned} \tag{9.10}$$

This gives

$$\begin{aligned} S(E) &= \frac{1}{\xi(1-\alpha)}\left\{\frac{1}{E_{\rm th}}\frac{\alpha}{E}\right\} \quad &&\text{for} \quad E \geq \alpha E_{\rm th} \\ S(E) &= 0 &&\text{for} \quad E < \alpha E_{\rm th}\end{aligned} \tag{9.11}$$

The total source to the thermal range is given by

$$\int_0^{E_{\rm th}} S(E)dE = \frac{1}{\xi(1-\alpha)}\int_0^{E_{\rm th}}\left(\frac{1}{E_{\rm th}} - \frac{\alpha}{E}\right)dE = \frac{1}{\xi(1-\alpha)}[1-\alpha+\alpha\ln\alpha] \tag{9.12}$$

or we have

$$\int_0^{E_{\text{th}}} S(E)dE = \frac{1}{\xi}\left(1 + \frac{\alpha}{1-\alpha}\ln\alpha\right) = 1.0 \tag{9.13}$$

as required to meet the normalization we established when we let $Q_0 = 1.0$.

Note that so far we have not been able to say anything about the energy dependence of the flux in the thermal range. To do this we will begin with a very simplified model and assume the following:

1. Infinite medium—no leakage
2. No absorption
3. No sources or slowing down

Under these assumptions, the principle of detailed balance must hold. This principle states that

$$\Sigma_s(E' \to E)\phi(E')dE' = \Sigma_s(E \to E')\phi(E)dE \tag{9.14}$$

Basically, it states that at equilibrium, the number of neutrons scattering from energy E') to energy E must exactly equal the number scattering from energy E to energy E'. If this were not true, neutrons would continue to build up at one energy, which must be impossible. Under this restriction, we essentially have two nuclear species in equilibrium with each other. If we treat the neutrons as a high-temperature monatomic gas, the distribution of neutron energies assumes the form of a Maxwell–Boltzmann distribution. This is in the form of

$$\phi(E) = \phi_{\text{MB}}(E) = vm_0M(E) = \frac{2\pi n_0}{(\pi KT)^{3/2}}\left(\frac{2}{m}\right)^{1/2} E\mathrm{e}^{-E/KT} \tag{9.15}$$

where

$n_0 =$ the number of thermal neutrons per cm^3
$T =$ the media temperature in degrees Kelvin
$K =$ the Maxwell–Boltzmann constant
$m =$ the mass of the neutron
$E =$ the neutron energy

Thus, as our thermal spectrum, we can use the Maxwell–Boltzmann distribution, and temperature T is Kelvin:

$$\phi_{\text{MB}}(E) = \frac{2\pi n_0}{(\pi KT)^{3/2}}\left(\frac{2}{m}\right)^{1/2} E\mathrm{e}^{-E/KT} \tag{9.16}$$

This distribution is characterized by a:

Most probable energy

$$\phi_{\mathrm{MB}}(E) = KT = \frac{T}{11600}\,\mathrm{eV} \tag{9.17}$$

Most probable speed

$$V_0 = \sqrt{\frac{2KT}{m}} = 1.28 \times 10^4 \sqrt{T}\,\mathrm{cm/s} \tag{9.18}$$

Note also that at $T = 293\ \mathrm{K} = 20\ ^\circ\mathrm{C}$, $E_{\mathrm{T}} = 0.0253$ eV, and $V_{\mathrm{T}} = 2200$ m/s. As this temperature is fairly easily obtainable around the world, typical parameters are evaluated at it or referenced to it. In particular, consider the common 1/v thermal absorption cross section. It can be expressed in the form of

$$\sigma_a(E) = \frac{\sigma_a(E_0)v_0}{v} \quad \begin{cases} E_0 = 0.0253\,\mathrm{eV} \\ v_0 = 2200\,\mathrm{cm/s} \end{cases} \tag{9.19}$$

Most tabulation of thermal data list the value of

$$\sigma_a(E_0) = \sigma_a(0.0253\,\mathrm{eV}) = \sigma_a(2200\,\mathrm{cm/s}) \tag{9.20}$$

Now that we have obtained a spectrum for the thermal range, let us evaluate some group constants. In particular, consider the thermal absorption cross section:

$$\sigma_a^{\mathrm{th}} = \frac{\displaystyle\int_0^{E_{\mathrm{th}}} \sigma_a(E)\phi_{\mathrm{MB}}(E)dE}{\displaystyle\int_0^{E_{\mathrm{th}}} \phi_{\mathrm{MB}}(E)dE} \tag{9.21}$$

For all practical purposes, we can let E_{th} be infinite and obtain for the denominator:

$$\int_0^{\infty} \phi_{\mathrm{MB}}(E)dE = \frac{2}{\sqrt{\pi}} v_0 n_0 = 2\sqrt{\frac{2KT}{\pi m}} v_0 \tag{9.22}$$

where T is the moderator temperature. This can be written as

$$\phi^{\mathrm{th}} = \frac{2}{\sqrt{\pi}} \left(\frac{T}{T_0}\right)^{1/2} \phi_0 \tag{9.23}$$

and $T_0 = 20\ ^\circ\mathrm{C}$, $v_0 = 2200$ m/s.

The numerator is equal to

$$\int_0^\infty \frac{\sigma_a(E_0)v_0}{v}\phi_{\mathrm{MB}}(E)dE = \int_0^\infty \frac{\sigma_a(E_0)v_0}{v}vM(E)dE = \sigma_a(E_0)\phi^0 \tag{9.24}$$

Therefore, the thermal absorption cross section becomes

$$\begin{cases} \sigma_a^{\mathrm{th}} = \dfrac{\sigma_a(E_0)\phi_0}{\dfrac{2}{\sqrt{\pi}}\left(\dfrac{T}{T_0}\right)^{1/2}\phi_0} = \sqrt{\dfrac{\pi}{4}}\left(\dfrac{T_0}{T}\right)^{1/2}\sigma_a(E_0) \\ \sigma_a^{\mathrm{th}} = 0.886\sqrt{\dfrac{T_0}{T}}\sigma_a(E_0) \end{cases} \tag{9.25}$$

Note that not all nuclides are strictly absorbers, and therefore this simple relationship does not always hold. However, a relationship of this form can be developed by introducing the so-called g factor to give

$$\sigma_a^{\mathrm{th}} = \sqrt{\frac{\pi}{4}g(T)g(T)\left(\frac{T_0}{T}\right)^{1/2}\sigma_a(E_0)} \tag{9.26}$$

Normally, scattering cross sections do not vary significantly in the thermal range if crystal or binding effects are not considered; therefore:

$$\sigma_s^{\mathrm{th}} = \sigma_s(E_0) \tag{9.27}$$

We will deal with binding effects later. Thus, we can define group constants for an infinite medium considering no absorption or sources. When we consider real media, we must consider the effects of these phenomena. In general, the following changes take place. As absorption is introduced, the fundamental spectrum tends to harden as more of the lower energy neutrons are absorbed by the typical 1/v absorbers. As leakage takes place, more of the higher energy neutrons leak out due to the longer mean free paths at these energies. This effect tends to soften the spectrum and is known as "diffusion cooling." As sources are introduced (slowing down sources), the spectrum tends to harden due to the increased number of neutrons at the higher energies.

All three effects can be included by defining an effective temperature neutron and temperature model. We have

$$T_{\mathrm{n}} = T(1 + A\Gamma) \quad \Gamma = \frac{\sigma_a(E_0)}{\xi\Sigma_s} \tag{9.28}$$

Typical values for atomic number A lie in the range 1.2–1.8. T_{n} is called the neutron temperature and is typically higher than the actual moderator temperature T. It should also be pointed out that the Maxwell–Boltzmann distribution will be in

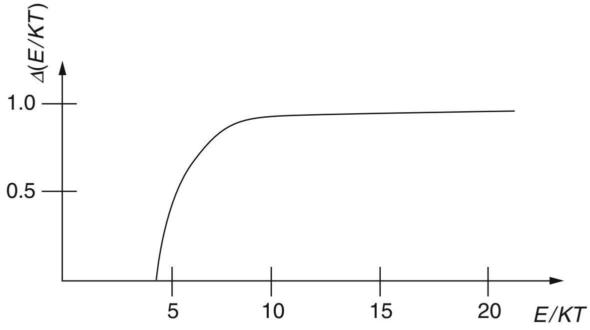

Fig. 9.1 Depiction of joining function

error at higher-neutron energies as it fails to yield the $1/E$ slowing down flux behavior at epithermal energies. This has traditionally been corrected by defining the flux as

$$\phi(E) = \phi_{\mathrm{MB}}(E, T_{\mathrm{n}}) + \lambda \frac{\Delta(E/KT)}{E} \tag{9.29}$$

where

$$\lambda = \phi_{\mathrm{th}} \sqrt{\frac{\pi}{4} \left\{ \frac{\Gamma}{1 - \Gamma} \right\}} \tag{9.30}$$

where $\Delta(E/KT)$ is called a joining function and is given by Fig. 9.1.

The joining function $\Delta(E/KT)$ is obtained by using one of the numerical techniques described in the text to calculate an actual thermal–epithermal spectrum and then subtracting a Maxwell–Boltzmann distribution at T_{n} from it. The residual is the joining function. Luckily $\Delta(E/KT)$ does not vary much as a function of the absorption cross section so it is a very nearly universal function.

9.2 Chemical Binding and Scattering Kernels

Now let us consider the effects of chemical binding on the scattering nucleus. When the scattering nucleus is bound in a crystal or large moderator, this binding affects the size of the thermal neutron cross section. When the energy of the neutron is large relative to the binding energy of the crystal, the atom scatters as an essentially unbound nucleus. When the energy of the neutron is significantly less than the binding energy of the atom in the crystal, the neutron effectively interacts with the whole crystal (or molecule).

In order to calculate this effect, a detailed quantum mechanical analysis must be performed. The results of this analysis simply state that the scattering cross section is given by

$$\sigma_0 = 4\pi a^2 \tag{9.31}$$

where a is known as the scattering length and is given by

$$a = \frac{m}{4\pi\hbar^2}\int_{\text{All Space}} V(\vec{\boldsymbol{r}})d\boldsymbol{r} \tag{9.32}$$

$V(\vec{\boldsymbol{r}})$ is the nucleus potential for the interaction and m is the reduced mass of the system. We can then write

$$\sigma_s^{\text{Bound}} = \sigma_s^{\text{Free}}\left(\frac{m_{\text{Bound}}}{m_{\text{Free}}}\right)^2 \tag{9.33}$$

Now for a free atom, we have for the reduced mass

$$m_{\text{Free}} = \frac{mM}{m+M} = \frac{A}{1+A} \tag{9.34}$$

And for a bound atom, we have

$$m_{\text{Bound}} = \frac{mM_{\text{eff}}}{m+M_{\text{eff}}} = \frac{A_{\text{eff}}}{1+A_{\text{eff}}} \tag{9.35}$$

Plugging this into the equation for the cross section and comparing bound cross sections with unbound ones, we have

$$\begin{aligned} \sigma_s^{\text{Bound}} &= \sigma_s^{\text{Free}}\left(\frac{\frac{A_{\text{eff}}}{1+A_{\text{eff}}}}{\frac{A}{1+A}}\right)^2 \\ &= \sigma_s^{\text{Free}}\frac{\left(1+\frac{1}{A}\right)^2}{\left(1+\frac{1}{A_{\text{eff}}}\right)^2} \end{aligned} \tag{9.36}$$

If we let A_{eff} becomes very large, this reduces to

$$\sigma_s^{\text{Bound}} = \sigma_s^{\text{Free}}\left(1+\frac{1}{A}\right)^2 \tag{9.37}$$

Thus, the cross section of a bound nucleus will increase in effective size as the neutron slows down to energies of the order of the chemical binding energy.

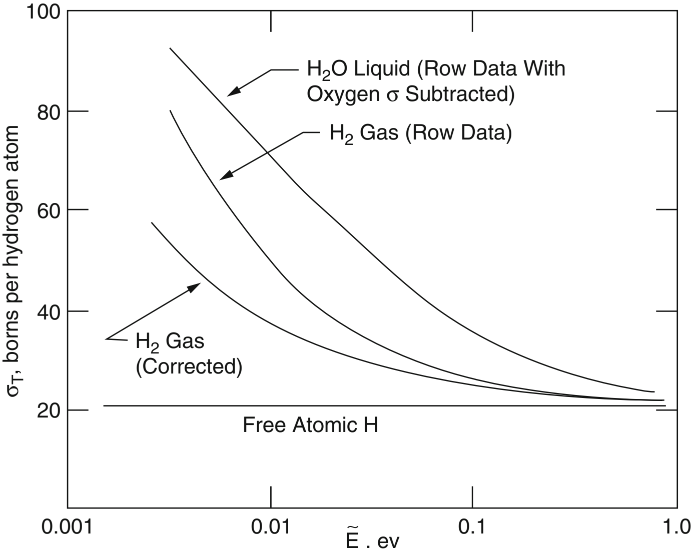

Fig. 9.2 The total slow down cross section per proton bound in H_2 and in water (Courtesy after K.-H. Beckurts and K. Wirtz) [1]

Hydrogen will show the most significant increase as its atomic mass is approximately 1.0. We have

$$\begin{aligned} \sigma_s^{\text{Bound}} &= \sigma_s^{\text{Free}} \quad E_M > 1.0\,\text{eV} \\ \sigma_s^{\text{Bound}} &= 4\sigma_s^{\text{Free}} \quad E_M \approx 0.0\,\text{eV} \end{aligned} \tag{9.38}$$

The total slow-neutron cross section per proton bound in H_2 gas and in water is depicted, and plots are shown in Fig. 9.2. Analyzing this figure indicates that the water curve has been corrected by subtracting the oxygen cross section 3.73 b atom, but has not been corrected for thermal motion. Both the raw data and the corrected H_2 curves are shown. The scattering cross section of atom hydrogen is 20.4 b. The absorption cross section is 0.33 at 0.025 eV and varies as 1 $\tilde{E}$.

In addition, it is worth noting that the actual increase is dependent on the binding energy of the crystal or molecule and its molecular mass. Consider some examples for hydrogen in terms of $\sigma_s^{\text{Bound}}/\sigma_s^{\text{Free}}$:

$$\mathbf{H{=}1.0} \quad H_2{=}1.78 \quad \mathbf{H_2O{=}3.31} \quad \mathbf{C_{22}H_{46}(Poly){=}3.98}$$

9.2.1 Scattering Materials

Polyethylene has a low energy limit for the hydrogen scattering cross section that is about 80 b as opposed to the 20 b recorded for hydrogen in the epithermal region. Typically, the 2200 m/s cross section for hydrogen is given as 38 b. This corresponds to hydrogen gas. The 2200 m/s cross section in water is about 49.4 b.

Now let us consider the other significant effects of scattering of thermal neutrons that are of inelastic scattering of thermal neutrons by a crystal. Basically, we have considered the atoms of the moderator as a monatomic gas. When we do this, we obtained the monatomic gas scattering transfer function as

$$\sigma_s(E')f(E' \to E) = \left\{ \begin{array}{l} \mathrm{e}^{\varepsilon'-\varepsilon}\left[\operatorname{erf}(\eta\sqrt{\varepsilon} - \rho\sqrt{\varepsilon}) \pm \operatorname{erf}\left(\eta\sqrt{\varepsilon'} - \rho\sqrt{\varepsilon}\right)\right] \\ +\operatorname{erf}(\eta\sqrt{\varepsilon} - \rho\sqrt{\varepsilon}) \mp \operatorname{erf}\left(\eta\sqrt{\varepsilon} - \rho\sqrt{\varepsilon'}\right) \end{array} \right\} \tag{9.39a}$$

where

$$\eta = \frac{A+1}{2\sqrt{A}} \quad \rho = \frac{A-1}{2\sqrt{A}} \quad \varepsilon = E/KT \quad \varepsilon' = E'/KT \tag{9.39b}$$

The upper signs are used for $E > E'$ and the lower signs for $E < E'$.

We considered this scattering function to be totally elastic. That is, energy went from the neutron's translational motion to the translational motion of the nuclei with which it interacted. Both energies were capable of varying continuously over their allowed range. However, when the scattering atoms are bound in a crystal, it is possible to raise an atom to a higher vibrational state in the crystal. This process is considered "inelastic" and is known as creating a phonon of vibrational energy. Note that there are discrete levels of vibrational excitation, and therefore energies can only be interchanged in discrete packets. In order to calculate the scattering cross section and transfer probabilities for this type of analysis, the interaction of the neutron with the whole crystal or molecule must be considered. See Figs. 9.3 and 9.4 for energy transfer function in a monatomic gas with $A = 1$ and $A = 16$, respectively.

The wavelength of neutrons at low energies is given by

$$\lambdabar = \frac{\lambda}{2\pi} = \frac{0.445 \times 10^2(\mathrm{cm})}{\sqrt{\frac{A}{A+1}E}(\mathrm{MeV})} = \frac{2.86 \times 10^2(\mathrm{cm})}{\sqrt{E}(\mathrm{eV})} \tag{9.40}$$

And for neutrons of energies like 0.01 eV, their wavelength is on the order of 3×10^{-8} cm, which is comparable to the atomic spacing in crystals. Therefore, it is possible for a neutron to scatter coherently off of the crystal itself. An additional complication is introduced by the fact that scattering depends on the neutron spin and the nucleus spin and the manner in which they combine. If we write

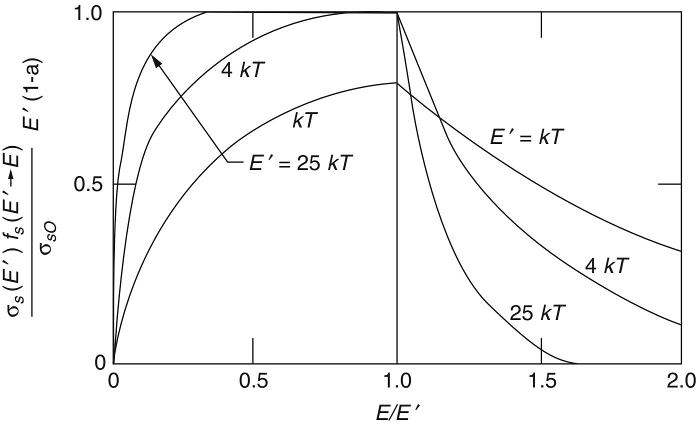

Fig. 9.3 Energy transfer function in a monatomic gas with $A = 1$ (Courtesy after K.-H. Beckurts and K. Wirtz) [1]

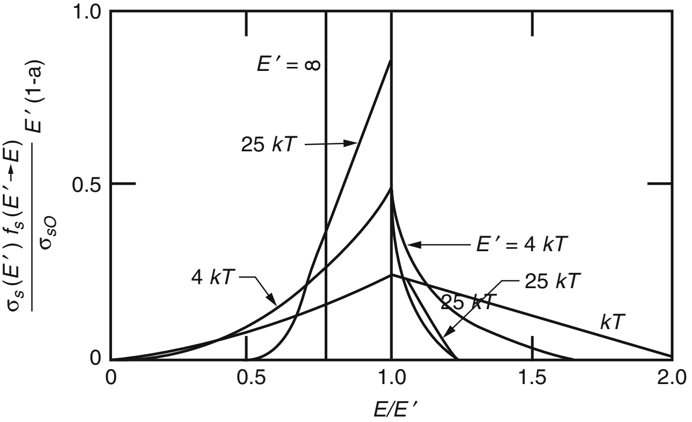

Fig. 9.4 Energy transfer function in a monatomic gas with $A = 16$ (Courtesy after K.-H. Beckurts and K. Wirtz) [1]

$$\sigma_{\text{Coh}} = 4\pi a_{\text{Coh}}^2 \tag{9.41}$$

then, a_{Coh} is given by

$$a_{\text{Coh}} = \frac{I+1}{2I+1}a_{+} + \frac{I}{2I+1}a_{-} \tag{9.42}$$

where

$I =$ the spin of the nucleus (the neutron spin $= 1/2$)

$a_{\mathrm{Coh}} =$ the coherent scattering length
$a_+ =$ the scattering amplitude for the $I + 1/2$ state
$a_- =$ the scattering amplitude for the $I - 1/2$ state

The average scattering cross section is given by

$$\sigma_{\mathrm{Ave}} = 4\pi \left\{ \frac{I+1}{2I+1} a_+^2 + \frac{I}{2I+1} a_-^2 \right\} \tag{9.43}$$

and the incoherent cross section is given by

$$\sigma_{\mathrm{Incoh}} = \sigma_{\mathrm{Ave}} - \sigma_{\mathrm{Coh}} = 4\pi \left[\frac{I(I+1)}{(2I+1)^2} \right] (a_+ - a_-)^2 \tag{9.44}$$

The following table gives the interesting result of all of these definitions when applied to the common moderators.

Moderator	Type scattering	Comments	
Hydrogen	Incoherent	$a_{\mathrm{Coh}} = 1.8$ b	$\sigma_{\mathrm{Ave}} = 81.5$ b
Deuterium	Mixed	$a_{\mathrm{Coh}} = 5.4$ b	$\sigma_{\mathrm{Ave}} = 7.6$ b
Beryllium	Coherent		
Carbon	Coherent		
Oxygen	Coherent		

The common assumption that hydrogen scatters incoherently is probably a very good approximation based on the above data.

So far, above, we have covered the subject of thermal spectrum calculations and thermal group constants to generate multigroup constant characterization for low energy neutron. Once again the general approach was to develop methods for determining the details on energy dependence or spectrum of such neutrons in those situations in which spatial dependence was ignored. Now we can briefly pay our attention to thermal cross-sectional averages, and for further information, we encourage our readers to refer to a book by Lewis [2].

9.2.2 *Thermal Cross-Sectional Average*

For the purpose of neutron energy spectra, we have learned that the distribution of neutrons in energy is determined largely by the competition between absorption and scattering reactions, and this distribution may be expressed in terms of density distribution [2].

A more quantitative understanding of neutron energy distributions results from writing a balance equation in terms of the neutron flux $\phi(E)$ and total *macroscopic cross section* $\Sigma_t(E)$; thus, we can write the balance equation in the following form as

$$\Sigma_t(E)\phi(E) = \int p(E \to E')\Sigma_s(E')\phi(E')dE' + \chi(E)S_f \tag{9.45}$$

where the specific form of the probability $p(E \to E')$ for elastic scattering by a single nuclide where the neutron energy following collision will be between E' and $E' + dE'$E will be given by the following equation at energy E:

$$p(E \to E')dE' = \begin{cases} \frac{1}{(1-\alpha)E}dE' & \alpha E \leq E' \leq E \\ 0 & \text{othrwise} \end{cases} \tag{9.46}$$

where α is proven in the following as it was shown in the past section:

$$\alpha = (A-1)^2/(A-1)^2 \tag{9.47}$$

Note that the probability of $p(E \to E')dE'$ is that of a neutron elastic scattering with initial E which will emerge with a new energy E' in the interval E' to $E' + dE'$.

Now, if we let $\Sigma_s(E' \to E) = p(E \to E')\Sigma_s(E')$, then Eq. 9.45 shapes to the following form as

$$\Sigma_t(E)\phi(E) = \int \Sigma_s(E' \to E)\phi(E')dE' + \chi(E)S_\mathrm{f} \tag{9.48}$$

The balance equation is normalized by the fission term, which indicates a rate of S_f fission neutrons produced/s/cm^3.

Using Eq. 3.15 to examine idealized situations over three different energy ranges provides some insight into the nature of neutron spectra, particularly of thermal reactors, and these three situations are listed below as [2].

1. The fast neutrons, whose energies are sufficient that are significant
2. The slowing down region of the energy spectra, which is an intermediate energy range and is often referred to as the resonance
3. Thermal neutrons with energies less than 1.0 eV, where at the lower energies thermal motions of the surrounding nuclei play a predominant role in determining the form of the spectrum

In each of the three energy ranges, general restrictions apply to Eq. 9.48. In the thermal and intermediate ranges, no fission neutrons are born, and thus, $\chi(E) = 0$. In the intermediate and fast ranges, there is no upscatter, and therefore, $\Sigma_s(E' \to E)$ for $E' < E$.

However, about thermal neutron, which is the third case above, at lower energies, within thermal neutron range, we utilize Eq. 9.48 as our departing point. The fission term on the right vanishes, and the source of neutrons then comes from those scattering down from higher energies. We may represent this as a scattering source, and we divide the integral in Eq. 9.48 according to whether energy E is less or greater than the cutoff energy for the thermal neutron range. Typically, this range is taken as $E_0 = 1.0$ eV. We then partition Eq. 9.48 as follows and write

$$\begin{aligned} \Sigma_t(E)\phi(E) \quad = \quad & \int_0^{E_0} \Sigma_s(E' \to E)\phi(E')dE' \\ & + \int_{E_0}^{\infty} \Sigma_s(E' \to E)\phi(E')dE' \end{aligned} \quad \text{for} \quad E < E_0 \tag{9.49}$$

or we can reduce Eq. 9.49 to the following form as

$$\Sigma_t(E)\phi(E) = \int_0^{E_0} \Sigma_s(E' \to E)\phi(E')dE' + S(E)q_0 \quad \text{for} \quad E < E_0 \tag{9.50}$$

where we have assumed that

$$S(E)q_0 = \int_{E_0}^{\infty} \Sigma_s(E' \to E)\phi(E')dE' \quad \text{for} \quad E < E_0 \tag{9.51}$$

which is nothing more than just being the source of thermal neutrons that arise from neutron making a collision at energies $E' > E_0$, but having an energy of $E < E_0$ after the collision. This was explained at the previous section that the source might be shown to be proportional to the slowing down density at E_0, and if pure scattering and a $1/E$ flux are assumed at energies $E' > E_0$, then a simple expression results for $S(E)$, the energy distribution of the source neutrons. In the thermal range, the scattering distribution is difficult to represent in a straightforward manner, for not only thermal motion but also binding of the target nuclei to molecules or within a crystal lattice must be factored into the analysis [2].

Now with all these said, the solution to Eq. 9.49 or for that matter Eq. 9.50 is time dependent, considering an idealized case of pure scattering materials for a situation of no neutron absorption in an infinite medium. In this case the neutron population will grow continuously with time, because each slowed down neutron would go on through scattering process forever. However, if after sometime it collapses, the slowing down density was equal to zero, and using Maxwell–Boltzmann distribution criteria, an equilibrium distribution will reach out to satisfy the following equation in terms of neutron flux as

$$S(E)q_0 = \int_{E_0}^{\infty} \Sigma_s(E' \to E)\phi_{\mathrm{MB}}(E')dE' \tag{9.52}$$

which is the first term on the right-hand side (RHS) of integral Eq. 9.49 or 9.50.

One of the beauties of kinetic theory in any nuclear-related analysis is to prove that for this to be satisfied, the principle of detained balance should be enforced, and putting this detailed balance states in perspective, the following equation is given as Eq. 9.53, no matter what law of scattering applies.

$$\Sigma_s(E \to E')\phi_{\mathrm{MB}}(E) = \Sigma_s(E' \to E)\phi_{\mathrm{MB}}(E) \tag{9.53}$$

Now, recall the Maxwell–Boltzmann distribution of Eq. 9.16 and reform it as the following equation:

$$M(E) = \frac{2\pi}{(\pi KT)^{3/2}} E^{1/2} \exp(-E/KT) \tag{9.54}$$

where E is the energy in electron volt (eV) range and again Boltzmann's constant is $K = 8.617 \times 10^{-5}$ eV/K and $M(E)$ over the energy range is normalized to one as

$$\int_0^\infty M(E)dE) = 1 \tag{9.55}$$

Figure 9.5 shows $M(E)$ along with $\chi(E)$ for fission and thermal neutron energy spectra to indicate the energy range over which neutrons may exist in a nuclear reactor.

Now, taking the new form of Maxwell–Boltzmann distribution in Eq. 9.54 under consideration, we can do further analysis if we find the following result. We notice that, for Eq. 9.53 to be satisfied, it is important that the principle states where these circumstances exist, the flux that satisfies the condition stated in that Eq. 9.53 is the form found by multiplying the Maxwell–Boltzmann distribution in Eq. 9.54, by the neutron speed, to obtain similar form of mathematical equation analogous to Eq. 9.16 as follows:

$$\phi_{\mathrm{MB}}(E) = \frac{1}{(KT)^2} E \exp(-E/KT) \tag{9.56}$$

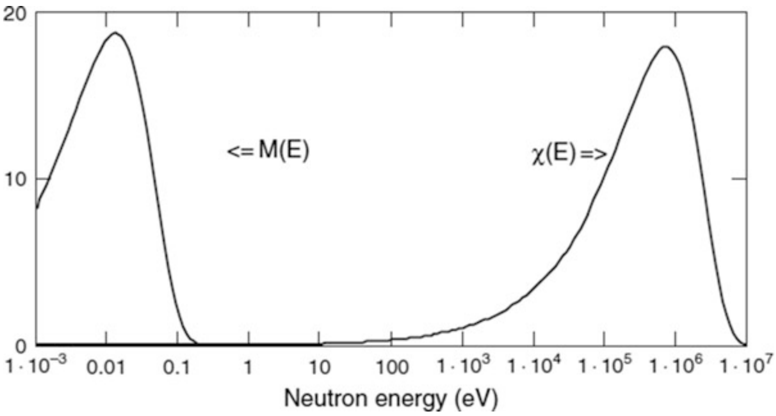

Fig. 9.5 Fission and thermal neutron energy spectra [2]

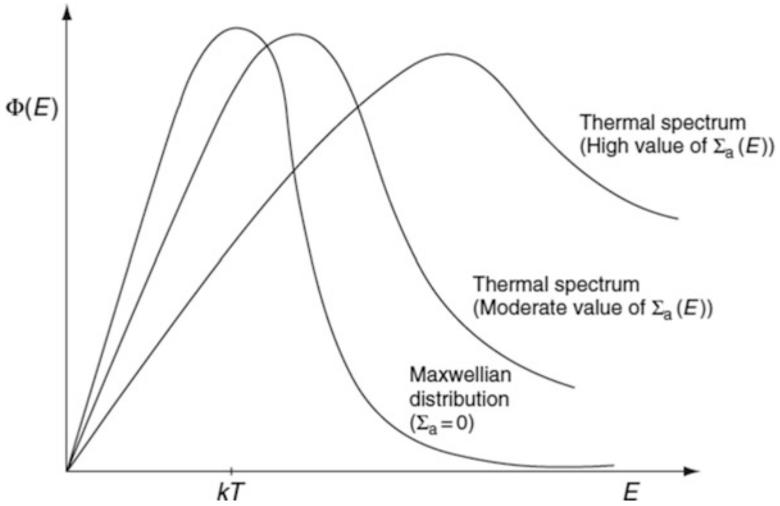

Fig. 9.6 Thermal spectra compared to a Maxwell–Boltzmann distribution (Courtesy of A. F. Henry) [3]

Following the normalization similar to Eq. 9.55 as a new form of the following relation over all the neutron energy exists in nuclear reactor as

$$\int_0^\infty \phi_{\mathrm{MB}}(E)dE\Big) = 1 \tag{9.57}$$

In reality, some absorption is always present. Absorption shifts the thermal neutron spectrum upward in energy from the Maxwell–Boltzmann distribution, since complete equilibrium is never reached before neutron absorption takes place.

Figure 9.6 illustrates the upward shift, called spectral hardening, which increases with the size of the absorption cross section. Nevertheless, Eq. 9.56 provides a rough approximation to a reactor's thermal neutron distribution. A somewhat better fit to hardened spectra, such as those in Fig. 9.6, may be obtained by artificially increasing the temperature T by an amount that is proportional to $\Sigma_a/\xi\Sigma_a$ [2].

9.3 Derivation of the Maxwell–Boltzmann Spectrum

Consider now a closed system of particles consisting of two different types. These particles can be identified as the nuclei in a material and the neutrons that diffuse through the material. The system will be restricted to a fixed number of nuclei and a fixed number of neutrons. Both of these fixed numbers are very large for any real system. The system will also be restricted to a fixed quantity of energy that can be shared between the two types of particles. There are a set number of energy levels to which a particle can be assigned. The neutron energy levels will be identified by E_s and the nuclei levels will be identified by E_r. The width of these energy levels will be identified by dE_s and dE_r. The levels are fixed and do not depend on the relative location of the particles to each other. They could depend on the location of the particles within an external field, but that will not be considered here. Energy can be exchanged between any two particles but the total energy is conserved.

The total number of neutrons will be N_n and the total number of nuclei is N_N. We will want to determine the location of the neutrons and nuclei in the allowed energy levels. Now each level can also be degenerated, that is, each level can have different states with the same energy, but the states are identified as different. An example would be several particles with the energy E_s, but having different momentum by virtue of traveling in different directions. The number of different states at a particular level will be identified by m_s and m_r.

Now consider the arrangement of the N_n particles among the energy levels available to the neutrons and the arrangement of the N_N particles among the energy levels available to the nuclei. We will attempt to determine the most likely arrangement of the two sets of particles into the allowed energy levels. If n_{n1} particles are selected at energy level E_1 from the N_n total neutrons, the number of ways they can be chosen is given by

$$P_1 = \frac{N_n!}{(N_n - n_{n1})!n_{n1}!} \tag{9.58}$$

For the second set of energy levels at energy E_2, the number of ways that n_{n2} particles can be arranged is

$$P_2 = \frac{(N_n - n_{n1})!}{(N_n - n_{n1} - n_{n2})!n_{n2}!} \tag{9.59}$$

Or the number of ways that $n_{\mathrm{n}1}$ particles can be arranged in energy level E_1 and the number of ways that particles can be arranged in energy level E_2 are given by

$$P_{12} = \frac{N_n!}{n_{n1}!n_{n2}!(N_n - n_{n1} - n_{n2})!} \tag{9.60}$$

For k total energy levels, we have

$$P_k = \frac{N_n!}{n_{n1}!n_{n2}!n_{n3}!\cdots n_{nk}!} \tag{9.61}$$

or as k becomes very large or approaches infinity

$$P_\infty = N_n! \prod_{s=1}^{\infty} \frac{1}{n_{ns}!} \tag{9.62}$$

Now let us assume that there are m_s degenerate levels in each level s and then there are $m_s^{n_{ns}}$ ways that the n_{ns} particles may be arranged in the m_s degenerate levels. Then the number of distinct microscopic distributions is

$$P = N_n! \prod \frac{m_s^{n_{ns}}}{n_{ns}!} \tag{9.63}$$

The same analysis would hold for the nuclei. The number of distinct microscopic distributions for the nuclei is

$$Q = N_N! \prod \frac{m_r^{n_{Nr}}}{n_{Nr}!} \tag{9.64}$$

Therefore, the total number of microscopic arrangements is

$$PQ = N_n! N_N! \prod_{s=1}^{\infty} \frac{m_s^{n_{ns}}}{n_{ns}!} \prod_{r=1}^{\infty} \frac{m_r^{n_{Nr}}}{n_{Nr}!} \tag{9.65}$$

Now in order to maximize the number of distinct distributions which is the most likely state to find the system in, with the largest entropy as postulated by Boltzmann, consider the log of PQ. The log of PQ will be maximized when PQ is maximized, but it is easier to perform the analysis with the log of PQ. The following auxiliary conditions must also be met to conserve particles and the system total energy:

$$\sum_{s=1}^{\infty} n_{ns} = N_n \tag{9.66}$$

$$\sum_{r=1}^{\infty} n_{Nr} = N_N \tag{9.67}$$

$$\sum_{s=1}^{\infty} E_s n_{ns} + \sum_{r=1}^{\infty} E_r n_{Nr} = E_{\text{total}} \tag{9.68}$$

The natural log of PQ can be maximized subject to these three constraints by introducing three Lagrange multipliers into the equation for $\ln(PQ)$ and forming the variational equation:

$$\delta \ln PQ - \alpha \delta N_n - \beta \delta N_N - \gamma \delta E_{\text{total}} = 0 \tag{9.69}$$

Expanding $\delta \ln(PQ)$ gives

$$\delta \ln PQ = \delta \ln P + \delta \ln Q \tag{9.70}$$

$$\ln P = \ln N_n! + \sum_{s=1}^{\infty} [n_{ns} \ln m_s - \ln(n_{ns}!)] \tag{9.71}$$

$$\ln Q = \ln N_N! + \sum_{r=1}^{\infty} [n_{Nr} \ln m_r - \ln(n_{Nr}!)] \tag{9.72}$$

$$\delta \ln P = \sum_{s=1}^{\infty} [\delta n_{ns} \ln m_s - \delta(\ln n_{ns}!)] \tag{9.73}$$

$$\delta \ln Q = \sum_{r=1}^{\infty} [\delta n_{Nr} \ln m_r - \delta(\ln n_{Nr}!)] \tag{9.74}$$

Then using Stirling's approximation for the ln function for a factorial of a very large number

$$\ln n! \approx \ln n - n \approx n \ln n \tag{9.75}$$

$$\delta \ln P + \delta \ln Q = \sum_{s=1}^{\infty} (\ln m_s - \ln n_{ns}) \delta n_{ns} + \sum_{r=1}^{\infty} (\ln m_r - \ln n_{Nr}) \delta n_{Nr} \tag{9.76}$$

Then the whole balance equation becomes

$$\begin{aligned} &\sum_{s=1}^{\infty} (\ln m_s - \ln n_{ns}) \delta n_{ns} + \sum_{s=1}^{\infty} (\ln m_r - \ln n_{Nr}) \delta n_{Nr} - \alpha \sum_{s=1}^{\infty} \delta n_{ns} - \beta \sum_{r=1}^{\infty} \delta n_{Nr} - \gamma \sum_{s=1}^{\infty} E_s \delta n_{ns} \\ &\quad - \gamma \sum_{r=0}^{\infty} E_r \delta n_{Nr} = 0 \end{aligned} \tag{9.77}$$

Combining sums for δn_{ns} and δn_{Nr} gives

$$\begin{aligned} &\sum_{s=1}^{\infty} (\ln m_s - \ln n_{ns} - \alpha - \gamma E_s) \delta n_{ns} \\ &\quad + \sum_{r=1}^{\infty} (\ln m_r - \ln n_{Nr} - \beta - \gamma E_r) \delta n_{Nr} = 0 \end{aligned} \tag{9.78}$$

Now if the changes in n_{ns} and n_{Nr} are chosen as arbitrary, their coefficients in the above equation must be identically zero. This gives the following equation for the neutrons:

$$\ln m_s - \ln n_{ns} - \alpha - \gamma E_s = 0 \tag{9.79}$$

or

$$n_{ns} = m_s \mathrm{e}^{-(\alpha+\gamma E_s)} \tag{9.80}$$

For the nuclei, a similar equation can be derived:

$$n_{Nr} = m_r \mathrm{e}^{-(\beta+\gamma E_r)} \tag{9.81}$$

Up to this point, the number of degenerate states at each energy level has not been specified and the above equations are very general. If only kinetic energy of the neutrons is considered, then the degeneracy at energy E is due to different velocity vectors. Or

$$m_s = dv_x dv_y dv_z \tag{9.82}$$

If the velocity components are expressed in spherical coordinates, this can be written as

$$m_s = dv_x dv_y dv_z = v^2 \sin\theta d\theta d\varphi dv \tag{9.83}$$

This can be integrated over θ and ϕ to get

$$m_s = 4\pi v^2 dv$$

Now noting that n_{ns} is equal to $n(E)dE$, we have

$$n(E)dE = 4\pi v^2 \mathrm{e}^{-(\alpha+\gamma E)} dv \tag{9.84}$$

and if γ is set to $1/kT$ and E is substituted for $\frac{1}{2}mv^2$ and $dE = md$v, this becomes

$$n(E)dE = \frac{4\pi}{m^{3/2}} 2^{1/2} E^{1/2} \mathrm{e}^{-\alpha} \mathrm{e}^{-E/kT} dE \tag{9.85}$$

Note that this does not depend on the distribution of energy levels for the nuclei and is a quite general result. The Lagrange multiplier turns α out to be normalization constant. The equation can be normalized for one neutron to give

$$M(E,T) = \frac{2}{\pi^{1/2}(kT)^{3/2}} E^{1/2} \mathrm{e}^{-E/KT} \tag{9.86}$$

which is known as a Maxwell–Boltzmann distribution. If this distribution is multiplied by the neutron velocity to get the flux at energy E, the resulting distribution is

$$\phi_{\mathrm{MB}}(E,T) = v(E)M(E,T) = \frac{2^{3/2}}{(m\pi)^{1/2}(kT)^{3/2}}E\mathrm{e}^{-E/kT} \tag{9.87}$$

This represents the energy distribution of the thermal range neutron flux in an infinite medium without absorption, leakage, or sources.

Note that this distribution is unsymmetrical about its peak and skewed to the high-energy side. The peak of the neutron number distribution is given by

$$E_{M(E,T)}^{\max} = \frac{kT}{2} \tag{9.88}$$

and the average value of the neutron number distribution is given by

$$E_{M(E,T)}^{ave} = \frac{3kT}{2} \tag{9.89}$$

The peak of the neutron flux distribution is given by

$$E_{\phi(E,T)}^{\max} = kT \tag{9.90}$$

and the average value for the neutron flux distribution is given by

$$E_{\phi(E,T)}^{\max} = 2kT \tag{9.91}$$

The above derivation strictly only applies when the nuclei are the constituents of an ideal gas. However, if the nuclei are bound in the solid matrix such that their motion can be described by a particle trapped in a potential, this will given by

$$V(r) = \frac{1}{2}Kr^2 \quad \text{or Hooke's law in three dimensions} \tag{9.92}$$

Then, at high temperatures, the nuclei behave exactly as an ideal gas, and all of the above formulas apply directly.

At low temperatures, two models are used to describe an equivalent temperature, T^*, so that the Maxwellian distributions can be used. For the Einstein model of a solid, the atoms are assumed to vibrate independently with frequencies that are integral multiple of the fundamental frequency v_E.

For example, the hydrogen atoms in zirconium hydride, the moderator used in a TRIGA reactor, and the solid nuclei can be represented by this model:

$$T^* = \frac{1}{2}\theta_E \coth\left(\frac{\theta_E}{2T}\right) \quad k\theta_E = hv_E = E_{\mathrm{vib}} \tag{9.93}$$

where $E_{\mathrm{vib}} = 0.137$ eV. This gives a θ_E of 1589 K and a T^* of 795 K for a moderator temperature of 300 K.

Table 9.1 T^*/T as a function of T/θ_D

T/θ_D	T^*/T
0.10	3.77
0.25	1.68
0.50	1.19
0.75	1.09
1.0	1.05
2.0	1.01
3.0	1.00

Table 9.2 Debye temperatures for several solids

Solid	θ_D (K)
Graphite	1000
Aluminum	375
Beryllium	1160
Cadmium	165
Iron	355
Hafnium	213
Indium	109
Manganese	410
Molybdenum	360
Sodium	160
Nickel	413
Lead	96
Tin	195
Tantalum	230
Uranium	200
Tungsten	270
Zirconium	265
Uranium dioxide	160

An alternative model for calculating T^* is given by the Debye model for a solid. In this case the following Table 9.1 gives an estimate of T^* as a function of θ_D, the Debye temperature, and the true temperature.

The following Table 9.2 gives some typical Debye temperatures for various solids.

Problems

Problem 9.1 **Fission Spectra**

Calculate the most probable energy and the average energy of a neutron emitted in fission, if the fission spectrum is given by one of the following two formulas: (E in MeV)

$$N(E) = 0.453\left(e^{-1.036E}\right)\sinh\left\{(2.29{*}E)^{0.5}\right\} \quad \text{Watt-Cranberg Spectrum}$$
$$N(E) = 0.77{*}E^{0.5}{*}e^{-E/1.29} \quad \text{Maxwellian Spectrum}$$

For the one of the above two spectra, what is the probability that a neutron will have an energy in the range 1–2 eV? What is the probability that it will have an energy of 1 eV?

Problem 9.2: **Decay from Fission**

There are two popular equations available for predicting the decay heat from fission after a nuclear reactor is shut down. The oldest and least accurate is given by the power law point kernel:

$$E(t) = 2.66t^{-1/2}\,\text{MeV/s/fission}, \ \{t\,\text{in second}\}$$

A more current and more accurate kernel is given by the sum of exponential kernel, as shown below:

$$E(t) = \sum \alpha_\gamma \exp\left(-{}^{t}/_{\tau_\gamma}\right) + \sum \alpha_\beta \exp\left(-t/\tau_\beta\right)\ \text{MeV/s/fission}, \ \{t\ \text{in second}\}$$

Where the α_γ and τ_γ constants apply to gamma decay energy and the α_β and τ_β apply to beta decay energy. A consistent set of constants for U^{235} is given below:

α_γ	τ_γ	α_β	τ_β
2.808×10^{-11}	1.364×10^{9}	6.169×10^{-11}	1.257×10^{9}
6.038×10^{-10}	2.307×10^{7}	2.249×10^{-9}	3.626×10^{7}
3.227×10^{-8}	5.176×10^{6}	2.365×10^{-8}	4.803×10^{6}
4.055×10^{-7}	6.031×10^{5}	2.194×10^{-7}	5.417×10^{5}
8.439×10^{-6}	4.658×10^{4}	1.140×10^{-5}	4.160×10^{4}
2.421×10^{-4}	4.699×10^{3}	1.549×10^{-4}	4.279×10^{3}
1.792×10^{-3}	522.2	1.991×10^{-3}	527.1
2.810×10^{-2}	56.53	3.256×10^{-2}	51.92
0.1516	6.053	0.2227	6.357
0.4162	0.7899	0.5381	0.7911
0.1053	0.1915	0.1282	0.1925

Use one of the above kernels and answer the following questions. Suppose a reactor operates at 2400 MW for 1 year and is then shut down. What would be the decay power in megawatts 1 year after shutdown? (**Hint:** Use a Simpson's rule integration for integrating over the 1 year of operation. Use only onetime interval with three data evaluations, beginning of interval, middle of interval, and end of interval). Suppose, instead, that all the energy released during the 1 year of power operation had been released at the beginning of that period, what would the decay power of the debris be 2 years after the burst?

Problem 9.3: **Macroscopic Cross Sections**
What is the probability per centimeter of travel that a neutron having energy 0.025 eV and moving in pure Pu239, with a density of 19.6 g/cm^3, will be captured? The thermal absorption cross section for Pu239 is 1029 b.

Problem 9.4: Estimate the minimum group spacing that will yield directly coupled equations for the following moderators.

Carbon	($A = 12$)
Deuterium	($A = 2$)
Beryllium	($A = 9$)
Sodium	($A = 22$)
Uranium	($A = 238$)

Express your answer as the ratio of the upper energy bound to the lower energy bound and as the group width in lethargy units.

Problem 9.5: What fraction of neutron scattering in hydrogen at 1.0 MeV, the lower bound of energy group 1, will jump to group 3, if the groups are set up with a constant lethargy spacing such that the ratio of the upper to lower energy group bounds is 100?

Problem 9.6: For the four-group cross-sectional data given below, calculate an infinite medium spectrum. Assume the groups are directly coupled.

Cross section	Group 1	Group 2	Group 3	Group 4
$\Sigma g_{\text{Absorption}}$	0.001394	0.000315	0.001881	0.03552
$\text{v}\Sigma g_{\text{Fission}}$	0.00287	0.000196	0.001480	0.04970
$\Sigma g_{\text{Downscatter}}$	0.04148	0.06503	0.04106	0.0
$\Sigma g_{\text{Transport}}$	0.0789	0.16704	0.3095	1.09223
χ_g	0.5503	0.4348	0.0149	0.0

Problem 9.7: Given the infinite medium spectrum that you calculated for problem 6, collapse the four-group set to two groups. Collapse groups 1 and 2 to group 1 of the two-group set, and collapse groups 3 and 4 to group 2 of the two-group set.

Problem 9.8: As a reactor heats up, thermal cross sections change due to a shift toward higher energies of the thermal neutron population. The following relationship holds for thermal fission and absorption cross sections:

$$\Sigma_{\text{th}} = (\pi/4)^{/12}(T_0/T_{\text{m}})^{1/2}\Sigma_{2200}$$

Note: Σ_{th} is the multigroup cross section (i.e., absorption or fission) for the thermal group. The only thing that changes when reactor heats up is T_{m}, the moderator temperature. Evaluate the derivative at 300 K.

Using the following data for Sandia's ACRR reactor, calculate an isothermal (core all at same temperature) feedback coefficient for this reactor based on zero-dimensional perturbation theory.

Parameter	Fast group	Thermal group
$\Sigma g_{\mathrm{Absorption}}$	0.00364	0.2062
$v\Sigma g_{\mathrm{Fission}}$	0.00595	0.3959
$\Sigma g_{\mathrm{Downscatter}}$	0.02935	–
Dg	2.0043	0.2055
ϕg_{Vector}	7.124	1.0000
$\phi g^{*}_{\mathrm{Vector}}$	0.528	1.0000
	Temperature = 300 K	Core $B^2 = 0.01405$

References

1. K.-H. Beckurts and K. Wirtz, Neutron physics by Karl-Heinrich Beckurts (2013-03-25) Paperback 1656, Springer
2. E. Elmer, *Lewis, fundamentals of nuclear reactor physics* (Academic, New York, 2008)
3. A.F. Henry, *Nuclear reactor analysis* (MIT Press, Cambridge, 1975)

Chapter 10
Perturbation Theory for Reactor Neutronics

Perturbation theory in neutronic analysis for nuclear reactor system is often necessary, when we analyze and compute the effect of small changes on the behavior of a reactor. On the other hand, if there is a uniform occurrence of perturbation throughout the entire reactor or a region, then, we use methods that we have so far discussed and presented in previous chapters, although we never encounter uniform perturbation in practice of reactor operations. However, most of the changes, which occur in the operation mode of a reactor, are nonuniform, and there are numerous examples of such nonuniform perturbations.

10.1 Perturbation Theory

From reactor analysis point of view, the effect of nonuniform perturbations on the performance of a reactor could be observed by performing a multigroup calculation in which perturbations are represented by appropriate space-dependent group constants. However, if we take under consideration any small, yet localized perturbation, this procedure is not usually practical.

By the very nature, a localized perturbation requires that a multigroup calculation be performed in at least two dimensions and more probably in three dimensions as it was mentioned in previous chapters.

Now let us consider a mathematical technique that has quite general applicability and is particularly useful for calculating the deviations from criticality produced by small changes in a critical system. There are many uses for perturbation theory, and it can be used to calculate changes in the fundamental eigenvalue of a reactor due to changes in any of the parameters that describe that reactor or the numerical approximations that go into modeling it. Consider the eigenvalue equation that shows up in multigroup diffusion theory:

B. Zohuri, *Neutronic Analysis For Nuclear Reactor Systems*,
DOI 10.1007/978-3-319-42964-9_10

$$[\boldsymbol{M}]\{\boldsymbol{\phi}\} = \mathbf{1}/\boldsymbol{k}[\boldsymbol{F}]\{\boldsymbol{\phi}\} \tag{10.1}$$

Let $\lambda = \mathbf{1}/\boldsymbol{k}$ and then Eq. 4.108 will reduce to the following form as

$$\{[\boldsymbol{M}] - \lambda[\boldsymbol{F}]\}\{\boldsymbol{\phi}\} = \{\mathbf{0}\} \tag{10.2}$$

as the reactor criticality equation. The $\boldsymbol{M}$ and $\boldsymbol{F}$ matrices can represent infinite-medium multigroup parameters, zero-dimensional multigroup parameters, and one-group spatially dependent numerical approximations to differential operators, or they can represent multigroup, multidimensional numerical approximations to partial differential operators. Any reactor criticality problem can be written in this form. In general, for a critical reactor, we have $\boldsymbol{k}=\mathbf{1.0}$ and $\lambda=\mathbf{1.0}$. We can solve this equation for the fundamental eigenfunction.

Frequently, we want to know what happens to $\boldsymbol{k}$ as we change $\boldsymbol{M}$ and/or $\boldsymbol{F}$ slightly. We do not necessarily want to recalculate the new flux vector in order to determine the change in $\boldsymbol{k}$.

10.2 Zero-Dimensional Methods

As perhaps the most straightforward example of this type of problem that exhibits all of the important features of the general problem, consider a zero-dimensional, two-group problem described by the following set of equations:

$$\left\{\begin{bmatrix} M_{11}^0 & M_{12}^0 \\ M_{21}^0 & M_{22}^0 \end{bmatrix} - \lambda_o \begin{bmatrix} F_{11}^0 & F_{12}^0 \\ F_{21}^0 & F_{22}^0 \end{bmatrix}\right\}\begin{Bmatrix} \phi_0^1 \\ \phi_0^2 \end{Bmatrix} = \begin{Bmatrix} 0 \\ 0 \end{Bmatrix} \tag{10.3}$$

where

$$\begin{array}{ll} M_{11}^0 = D^1B^2 + \Sigma_R^1 & M_{12}^0 = 0 \\ M_{21}^0 = -\Sigma_S^{12} & M_{22}^0 = D^2B^2 + \Sigma_a^2 \\ F_{11}^0 = \chi_1 \mathrm{v}\Sigma_f^1 & F_{12}^0 = \chi_1 \mathrm{v}\Sigma_f^2 \\ F_{21}^0 = \chi_2 \mathrm{v}\Sigma_f^1 & F_{22}^0 = \chi_2 \mathrm{v}\Sigma_f^2 \end{array} \tag{10.4}$$

Now we will represent a perturbation in the system as

$$\begin{array}{ll} M_{11} = M_{11}^0 + m_{11} & F_{11} = F_{11}^0 + f_{11} \\ \lambda = \lambda_0 + d\lambda & \phi = \phi_0 + d\phi \end{array} \tag{10.5}$$

If we substitute the perturbed quantities into our equations, we will obtain the following set of equations:

$$\begin{aligned}&\left\{\begin{bmatrix} M_{11}^0+m_{11} & M_{12}^0+m_{12} \\ M_{21}^0+m_{21} & M_{22}^0+m_{22}\end{bmatrix} - (\lambda_0+\delta\lambda)\begin{bmatrix} F_{11}^0+f_{11} & F_{12}^0+f_{12} \\ F_{21}^0+f_{21} & F_{22}^0+f_{22}\end{bmatrix}\right\}\left\{\begin{matrix}\phi_0^1+\delta\phi^1 \\ \phi_0^2+\delta\phi^2\end{matrix}\right\} \\ &= \left\{\begin{matrix}0\\0\end{matrix}\right\}\end{aligned} \tag{10.6}$$

Note that from notation point of view and convenient, we are moving all the subscripts for ϕ to superscript position.

We would like to calculate the change in k for the above set of equations without completely resolving them. As we have two equations and three unknowns, the change in k and the perturbations in both fluxes, we must in general combine them in some way to obtain one equation that expresses the change in k as a function of the change in M and F. The easiest way to accomplish this is to multiply each of the equations by a weighting function and then add them. The resulting equation can be solved for the change in k. Of course, we would like to choose the weighting function in some optimal way. Since we do not wish to recalculate ϕ, we would prefer a weighting function that is insensitive to changes in the perturbed flux eigenfunction. We can derive a set of equations for this weighting function by expanding our perturbed equations:

$$\begin{aligned}&\{W_1,W_2\}\left\{\begin{bmatrix} M_{11}^0+m_{11} & M_{12}^0+m_{12} \\ M_{21}^0+m_{21} & M_{22}^0+m_{22}\end{bmatrix} - (\lambda_0+\delta\lambda)\begin{bmatrix} F_{11}^0+f_{11} & F_{12}^0+f_{12} \\ F_{21}^0+f_{21} & F_{22}^0+f_{22}\end{bmatrix}\right\}\left\{\begin{matrix}\phi_0^1+\delta\phi^1 \\ \phi_0^2+\delta\phi^2\end{matrix}\right\} \\ &= \left\{\begin{matrix}0\\0\end{matrix}\right\}\end{aligned} \tag{10.7}$$

We have

$$\begin{aligned}
&\{W_1,W_2\}\left\{\begin{bmatrix} M_{11}^0 & M_{12}^0 \\ M_{21}^0 & M_{22}^0\end{bmatrix} - \lambda_0\begin{bmatrix} F_{11}^0 & F_{12}^0 \\ F_{21}^0 & F_{22}^0\end{bmatrix}\right\}\left\{\begin{matrix}\phi_0^1 \\ \phi_0^2\end{matrix}\right\} && (1)\\
&+\{W_1,W_2\}\left\{\begin{bmatrix} M_{11}^0 & M_{12}^0 \\ M_{21}^0 & M_{22}^0\end{bmatrix} - \lambda_0\begin{bmatrix} F_{11}^0 & F_{12}^0 \\ F_{21}^0 & F_{22}^0\end{bmatrix}\right\}\left\{\begin{matrix}\delta\phi^1 \\ \delta\phi^2\end{matrix}\right\} && (2)\\
&+\{W_1,W_2\}\left\{\begin{bmatrix} m_{11} & m_{12} \\ m_{21} & m_{22}\end{bmatrix} - \lambda_0\begin{bmatrix} f_{11} & f_{12} \\ f_{21} & f_{22}\end{bmatrix} - \delta\lambda\begin{bmatrix} F_{11}^0 & F_{12}^0 \\ F_{21}^0 & F_{22}^0\end{bmatrix}\right\}\left\{\begin{matrix}\phi_0^1 \\ \phi_0^2\end{matrix}\right\} && (3)\\
&+\{W_1,W_2\}\left\{\begin{bmatrix} m_{11} & m_{12} \\ m_{21} & m_{22}\end{bmatrix} - \lambda_0\begin{bmatrix} f_{11} & f_{12} \\ f_{21} & f_{22}\end{bmatrix} - \delta\lambda\begin{bmatrix} F_{11}^0 & F_{12}^0 \\ F_{21}^0 & F_{22}^0\end{bmatrix}\right\}\left\{\begin{matrix}\delta\phi^1 \\ \delta\phi^2\end{matrix}\right\} && (4)\\
&+\{W_1,W_2\}\left\{-\delta\lambda\begin{bmatrix} f_{11} & f_{12} \\ f_{21} & f_{22}\end{bmatrix}\right\}\left\{\begin{matrix}\delta\phi^1 \\ \delta\phi^2\end{matrix}\right\} = \left\{\begin{matrix}0\\0\end{matrix}\right\} && (5)
\end{aligned} \tag{10.8}$$

Examining this series of inner products on a term-by-term basis, we find that the first (1) set of terms is identically zero as it represents the solution of the unperturbed problem. The second (2) and third (3) inner products contain terms of the first order in the changes in $\boldsymbol{M}, \boldsymbol{F}, \boldsymbol{k}$, and the fluxes, and the fourth (4) and fifth (5) inner products contain terms of that are either second or third order in the system changes. If the system changes are small, then we should be able to neglect the fourth and fifth terms relative to the second and third terms. If we do this, the equations become

$$\{W_1, W_2\}\left\{\begin{bmatrix} M_{11}^0 & M_{12}^0 \\ M_{21}^0 & M_{22}^0 \end{bmatrix} - \lambda_0 \begin{bmatrix} F_{11}^0 & F_{12}^0 \\ F_{21}^0 & F_{22}^0 \end{bmatrix}\right\}\left\{\begin{matrix} \delta\phi^1 \\ \delta\phi^2 \end{matrix}\right\}+$$
$$\{W_1, W_2\}\left\{\begin{bmatrix} m_{11} & m_{12} \\ m_{21} & m_{22} \end{bmatrix} - \lambda_0 \begin{bmatrix} f_{11} & f_{12} \\ f_{21} & f_{22} \end{bmatrix} - \delta\lambda \begin{bmatrix} F_{11}^0 & F_{12}^0 \\ F_{21}^0 & F_{22}^0 \end{bmatrix}\right\}\left\{\begin{matrix} \phi_0^1 \\ \phi_0^2 \end{matrix}\right\} = \left\{\begin{matrix} 0 \\ 0 \end{matrix}\right\} \tag{10.9}$$

The changes in the flux eigenfunction only show up in the first set of terms above. Therefore, if we choose our weighting function such that this set of terms exactly cancels to zero, irrespective of changes in the eigenfunction, we will be able to neglect first-order changes in the flux. For this to be the case, we must have the coefficient of the flux change exactly equal to 0.0 in each equation. Thus, we must have

$$\begin{aligned} W_1\left(M_{11}^0 - \lambda_0 F_{11}^0\right) + W_2\left(M_{21}^0 - \lambda_0 F_{21}^0\right) &= 0 \\ W_1\left(M_{12}^0 - \lambda_0 F_{12}^0\right) + W_2\left(M_{22}^0 - \lambda_0 F_{22}^0\right) &= 0 \end{aligned} \tag{10.10}$$

This can be written in matrix form as

$$\left\{\begin{bmatrix} M_{11}^0 & M_{12}^0 \\ M_{21}^0 & M_{22}^0 \end{bmatrix} - \lambda_o \begin{bmatrix} F_{11}^0 & F_{12}^0 \\ F_{21}^0 & F_{22}^0 \end{bmatrix}\right\}\left\{\begin{matrix} W^1 \\ W^2 \end{matrix}\right\} = \left\{\begin{matrix} 0 \\ 0 \end{matrix}\right\} \tag{10.11}$$

Note that the two matrices above that multiply the weighting function vector are simply the transposes of the original two-group diffusion equations. It is a well-known theorem of linear algebra that the eigenvalues of the original problem are also the eigenvalues of the transposed problem, and the solution of the transposed problem is called the adjoint function. Therefore, if we choose our weighting function as the adjoint function, we will not have to compute a new flux eigenfunction to obtain changes in $\boldsymbol{k}$ due to changes in $\boldsymbol{M}$ or $\boldsymbol{F}$ to first order. (Though this demonstration has only dealt with the two-group zero-dimensional equations, this property holds quite generally for an arbitrary number of groups and spatial dimensions.) Then if we choose our weighting function to be the zero-dimensional adjoint function, we will have

$$\left(\phi^{1^*},\phi^{2^*}\right)\left\{\begin{bmatrix} m_{11} & m_{12} \\ m_{21} & m_{22}\end{bmatrix} - \lambda_0\begin{bmatrix} f_{11} & f_{12} \\ f_{21} & f_{22}\end{bmatrix} - \delta\lambda\begin{bmatrix} F_{11}^0 & F_{12}^0 \\ F_{21}^0 & F_{22}^0\end{bmatrix}\right\}\begin{Bmatrix}\phi_0^1 \\ \phi_0^2\end{Bmatrix} = \begin{Bmatrix} 0 \\ 0\end{Bmatrix} \tag{10.12}$$

where the asterisk will be used to denote the adjoint and the equation can be rewritten as

$$\begin{aligned}&\left[\phi^{1^*}(m_{11}-\lambda_0 f_{11})+\phi^{2^*}(m_{21}-\lambda_0 f_{21})\right]\phi_0^1+\left[\phi^{1^*}(m_{21}-\lambda_0 f_{21})+\phi^{2^*}(m_{22}-\lambda_0 f_{22})\right]\phi_0^2\\ &\quad=\delta\lambda\left[\left(\phi^{1^*}F_{11}^0+\phi^{2^*}F_{21}^0\right)\phi_0^1+\left(\phi^{1^*}F_{12}^0+\phi^{2^*}F_{22}^0\right)\phi_0^2\right]\end{aligned} \tag{10.13}$$

Rearranging terms and solving for the change in the eigenvalue give

$$\delta\lambda=\frac{\left[\phi^{1^*}(m_{11}-\lambda_0 f_{11})+\phi^{2^*}(m_{21}-\lambda_0 f_{21})\right]\phi_0^1+\left[\phi^{1^*}(m_{21}-\lambda_0 f_{21})+\phi^{2^*}(m_{22}-\lambda_0 f_{22})\right]\phi_0^2}{\left(\phi^{1^*}F_{11}^0+\phi^{2^*}F_{21}^0\right)\phi_0^1+\left(\phi^{1^*}F_{12}^0+\phi^{2^*}F_{22}^0\right)\phi_0^2} \tag{10.14}$$

Now since $\boldsymbol{\lambda = 1/k}$, we have $\boldsymbol{d\lambda = dk/k}$. And since for criticality we have $\boldsymbol{k=1}$, we then obtain for $\boldsymbol{dk=\rho}$ the following expression:

$$\delta k\ =\rho=-\frac{\left[\phi^{1^*}(m_{11}-\lambda_0 f_{11})+\phi^{2^*}(m_{21}-\lambda_0 f_{21})\right]\phi_0^1+\left[\phi^{1^*}(m_{12}-\lambda_0 f_{12})+\phi^{2^*}(m_{22}-\lambda_0 f_{22})\right]\phi_0^2}{\left(\phi^{1^*}F_{11}^0+\phi^{2^*}F_{21}^0\right)\phi_0^1+\left(\phi^{1^*}F_{21}^0+\phi^{2^*}F_{22}^0\right)\phi_0^2} \tag{10.15}$$

In order to demonstrate the utility of this last expression, consider a rather straightforward example. Let us assume that our slab (or zero-dimensional) reactor is critical, and a small amount of boron is added to the core material of the reactor. The effect of adding the boron can be represented as a perturbation in the thermal absorption cross section of the reactor core. To calculate the change in reactivity of the reactor, we can simply evaluate our perturbation formula. We have

$$\begin{aligned}&m_{11}=f_{11}=m_{21}=f_{21}=m_{12}=f_{12}=f_{22}=0\\ &m_{22}=\delta\Sigma_a^2\end{aligned} \tag{10.16}$$

As a result

$$\rho=-\frac{\phi^{2^*}\delta\Sigma_a^2\phi_0^2}{\left(\phi^{1^*}F_{11}^0+\phi^{2^*}F_{21}^0\right)\phi_0^1+\left(\phi^{1^*}F_{21}^0+\phi^{2^*}F_{22}^0\right)\phi_0^2} \tag{10.17a}$$

and

$$\rho=-\frac{\phi^{2^*}\delta\Sigma_a^2\phi_0^2}{\phi^{1^*}F_{11}^0\phi_0^1+\phi^{2^*}F_{21}^0\phi_0^1+\phi^{1^*}F_{21}^0\phi_0^2+\phi^{2^*}F_{22}^0\phi_0^2} \tag{10.17b}$$

If we choose $\phi^{2^*}=\phi_0^2=1.0,\chi_2=0.0$

then,

$$\rho = -\frac{\delta\Sigma_a^2}{\phi^{1^*}\left(v\Sigma_f^1\phi_0^1 + v\Sigma_f^2\right)} \tag{10.18}$$

Note that the adjoint equations for the general two-group zero-dimensional model are

$$\begin{bmatrix} D^1B^2 + \Sigma_F^1 - \chi^1 v\Sigma_f^1 & -\Sigma_s^{12} - \chi^2 v\Sigma_f^1 \\ -\chi^1 v\Sigma_f^2 & D^2B^2 + \Sigma_a^2 - \chi^2 v\Sigma_f^2 \end{bmatrix} \begin{Bmatrix} \phi^{1^*} \\ \phi^{2^*} \end{Bmatrix} = \begin{Bmatrix} 0 \\ 0 \end{Bmatrix} \tag{10.19}$$

Moreover, the determinant equation for criticality is

$$\left(D_1B^2 + \Sigma_R^1 - \chi_1 v\Sigma_f^1\right)\left(DB^2 + \Sigma_a^2 - \chi_2 v\Sigma_f^2\right) - \chi_2 v\Sigma_f^2\left(\Sigma_s^{12} + \chi_2 v\Sigma_f^1\right) = 0 \tag{10.20}$$

which has the same solutions for B^2 as the forward (flux) determinant equation. However, the eigenfunctions are different. We have

$$\begin{array}{ll} \underline{\textbf{Flux Eigenvector}} & \underline{\textbf{Adjoint Eigenvector}} \\ \left(D_2B^2 + \Sigma_a^2 - \chi_2 v\Sigma_f^2\right)\phi_0^2 = \left(\Sigma_s^{12} + \chi_2 v\Sigma_f^1\right)\phi_0^1 & \left(D^2B^2 + \Sigma_a^2 - \chi^2 v\Sigma_f^2\right)\phi^{2^*} = \chi^1 v\Sigma_f^2\phi^{1^*} \\ \varphi_0^1 = \left[\dfrac{D_2B^2 + \Sigma_a^2 - \chi_2 v\Sigma_f^2}{\Sigma_s^{12} + \chi_2 v\Sigma_f^1}\right] & \varphi^{1^*} = \left[\dfrac{D_2B^2 + \Sigma_a^2 - \chi_2 v\Sigma_f^2}{\chi_1 v\Sigma_f^2}\right] \\ \phi_0^2 = 1.0 & \phi^{2^*} = 1.0 \end{array} \tag{10.21}$$

Thus, we can evaluate the reactivity change caused by a small homogeneous change in the core composition.

10.3 Spatial Method (1 Group)

It is also possible to treat changes in the spatial makeup of the reactor. In order to keep the analysis as simple as possible, consider a one-group model for the homogeneous slab and introduce a small perturbation that is a function of z in the slab. We have

$$\begin{aligned}
&-D\frac{d^2\phi(z)}{dz^2}+\left(\Sigma_{aa}-\frac{1}{k}\nu\Sigma_f\right)\phi(z)=0\\
&D(z)=D_0+\delta D(z)\\
&\Sigma_a(z)=\Sigma_{a0}+\delta\Sigma_a(z)\\
&\nu\Sigma_f(z)=\nu\Sigma_{f0}+\delta\nu\Sigma_f(z)
\end{aligned}\tag{10.22}$$

Now we want to find the change in $\boldsymbol{k}$ caused by this spatial perturbation. Note that $\boldsymbol{k}$ is an integral parameter for the reactor and not a function of z within the reactor. The differential equation with $\boldsymbol{\lambda}=\mathbf{1}/\boldsymbol{k}$ becomes

$$\begin{aligned}
&-[D_0+\delta D(z)]\frac{d^2}{dz^2}[\phi_0(z)+\delta\phi(z)]+\left[\Sigma_{a0}+\delta\Sigma_a(z)-\{\lambda_0+\delta\lambda\}\left\{\nu\Sigma_{f0}\delta\nu\Sigma_f(z)\right\}\right]\\
&\quad[\phi_0(z)+\delta\phi(z)]=0
\end{aligned}\tag{10.23}$$

Or

$$\begin{aligned}
&-D_0\frac{d^2}{dz^2}\phi_0(z)+\left[\Sigma_{a0}-\lambda_0\nu\Sigma_{f0}\right]\phi_0(z) && (1)\\
&-D_0\frac{d^2}{dz^2}\delta\phi(z)+\left[\Sigma_{a0}-\lambda_0\nu\Sigma_{f0}\right]\delta\phi(z) && (2)\\
&-\delta D(z)\frac{d^2}{dz^2}\phi_0(z)+\left[\delta\Sigma_a(z)-\lambda_0\delta\nu\Sigma_f(z)-\delta\lambda\nu\Sigma_{f0}\right]\phi_0(z) && (3)\\
&-\delta D(z)\frac{d^2}{dz^2}\delta\phi(z)+\left[\delta\Sigma_a(z)-\delta\lambda\nu\Sigma_{f0}-\lambda_0\delta\nu\Sigma_f(z)\right]\phi_0(z) && (4)\\
&-\delta\lambda\delta\nu\Sigma_f(z)[\delta\phi(z)]=0 && (5)
\end{aligned}\tag{10.24}$$

Note that line (1) is the original equation and lines (4) and (5) are second order or higher in the small perturbations. Thus, making the small perturbation assumption, we can reduce the equation down to lines (2) and (3). We have

$$\begin{aligned}
&-D_0\frac{d^2}{dz^2}\delta\phi(z)+\left[\Sigma_{a0}-\lambda_0\nu\Sigma_{f0}\right]\delta\phi(z)-\delta D(z)\frac{d^2}{dz^2}\phi_0(z)\\
&\quad+\left[\delta\Sigma_a-\lambda_0\delta\nu\Sigma_f(z)-\delta\lambda\nu\Sigma_f\right]\phi_0(z)=0
\end{aligned}\tag{10.25}$$

If we want to calculate one $\delta\lambda$ for this differential equation, we must convert it to an algebraic expression of some form. The simplest way to do this is to multiply the equation by some weighting function, $W(z)$, and integrate from 0 to L. When we do this, we have

$$\begin{aligned}&\int_0^L W(z)\left\{-D_0\frac{d^2}{dz^2}\delta\phi(z)+\left[\Sigma_{a0}-\lambda_0\nu\Sigma_{f0}\right]\delta\phi(z)\right\}dz\\&+\int_0^L W(z)\left\{-\delta D(z)\frac{d^2}{dz^2}\phi_0(z)+\left[\delta\Sigma_a-\lambda_0\delta\nu\Sigma_f(z)\right]\phi_0(z)\right\}dz\\&-\int_0^L W(z)\delta\lambda\nu\Sigma_f\phi_0(z)dz=0\end{aligned}\tag{10.26}$$

Solving for $\delta\lambda$ gives

$$\delta\lambda=\frac{\int_0^L W(z)\left[-D_0\frac{d^2}{dz^2}+\Sigma_{a0}-\nu\Sigma_{f0}\right]\delta\phi_0(z)\}dz+\int_0^L W(z)\left[-\delta D(z)\frac{d^2}{dz^2}+\delta\Sigma_a-\nu\Sigma_f\right]\phi_0(z)dz}{\int_0^L W(z)\nu\Sigma_{f0}\phi_0(z)dz}\tag{10.27}$$

In order for the solution not to depend on the flux perturbation, we must perform some manipulations. Consider the first term above:

$$\int_0^L W(z)\left[-D_0\frac{d^2}{dz^2}+\Sigma_{a0}-\nu\Sigma_{f0}\right]\delta\phi_0(z)dz=0\tag{10.28}$$

The second derivative term can be integrated by parts as follows:

$$\begin{aligned}&\int_0^L W(z)\left[-D_0\frac{d^2}{dz^2}\delta\phi(z)\right]dz=-W(z)D_0\frac{d\delta\phi_0(z)}{dz}\Big|_0^L+\int_0^L\frac{dW(z)}{dz}D_0\frac{d\delta\phi(z)}{dz}dz\\&=-W(z)D_0\frac{d\delta\phi(z)}{dz}\Big|_0^L+\frac{dW(z)}{dz}D_0\delta\phi(z)\Big|_0^L-\int_0^L\delta\phi(z)D_0\frac{d^2W(z)}{dz^2}dz\end{aligned}\tag{10.29}$$

Since the boundary condition on the flux at zero and L has not changed, the flux perturbation must be zero on the boundary. Therefore,

$$\delta\phi(0)=\delta\phi(L)=0\tag{10.30}$$

This will eliminate the first set of boundary terms. The second set of boundary terms can be eliminated by requiring $W(z)$ to be zero at $z = 0$ and $z = L$. This corresponds to applying the "approximate diffusion theory" boundary conditions. If the "consistent diffusion theory" boundary conditions are applied, similar results will be obtained, with the necessary boundary conditions on $W(z)$ involving a derivative term in the same manner that the flux equations do.

Therefore, we have the following equation and boundary conditions on **W(z)**:

$$-D_0\frac{d^2W(z)}{dz^2} + \left[\Sigma_{a0} - \nu\Sigma_{f0}\right]W(z) = 0, \quad W(0) = 0, \quad W(L) = 0 \tag{10.31}$$

We can completely eliminate any dependence of $\delta\lambda$ on changes in the flux to first order by this choice of weighting function. This equation and boundary conditions define the spatially dependent adjoint function. Note that for the one-group problem, the adjoint equation is identical with the flux equation. We can say that the one-group problem is self-adjoint. In fact, all multigroup diffusion problems are spatially self-adjoint. The adjoint flux is

$$\phi^*(z) = \phi_0^* \sin(Bz) \tag{10.32}$$

Using this in our perturbation equation, we have

$$\delta\lambda = \frac{\int\limits_0^L \varphi^*(z)\left[-\delta D(z)\frac{d^2}{dz^2} + \delta\Sigma_a(z) - \delta\nu\Sigma_f(z)\right]\phi_0(z)dz}{\int\limits_0^L \varphi^*(z)\nu\Sigma_{f0}\phi_0(z)dz} \tag{10.33}$$

This equation is the equivalent of the reactivity change equation for the zero-dimensional case that was considered earlier. For real perturbations in real reactors, the two forms have to be combined to treat real perturbations as energy and spatially dependent. Once again, the problem of writing the equations down becomes massive. However, the form and process should be fairly easy to combine and it should be obvious how to do it.

Now consider two spatial perturbations. In one case a control poison will be inserted into the slab from the left to a distance z_1. This could simulate a uniform change in core or moderator absorption. It would be a reasonable approximation to a thermal reactor with banked control rods moving down from the top of the core or up from the bottom of the core. It also is similar to a first approximation for the effects of the change in the boiling level in a boiling water reactor (BWR).

A schematic picture is included in Fig. 10.1.

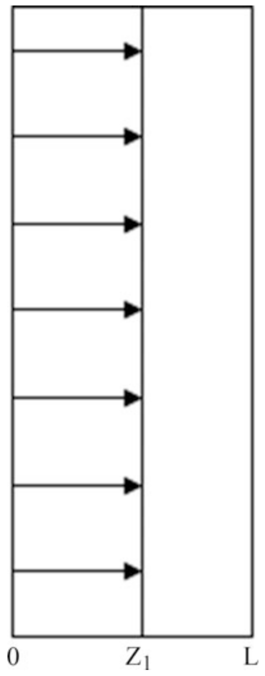

Fig. 10.1 Homogeneous perturbation scenario

We have

$$\delta\lambda = \frac{\int_0^{z_1} \varphi^*(z)\delta\Sigma_a(z)\phi_0(z)dz}{\int_0^L \varphi^*(z)v\Sigma_{f0}\phi_0(z)dz} \tag{10.34}$$

$$\delta\lambda = \frac{\delta\Sigma_a}{v\Sigma_{f0}} \frac{\int_0^{z_1} \phi^*(z)\varphi_{0(z)}dz}{\int_0^L \phi^*(z)\varphi_0(z)dz} \tag{10.35}$$

$$\phi^*(z) = \phi_0^* \sin(Bz), \qquad \phi_0(z) = \phi_0 \sin(Bz) \tag{10.36}$$

$$\delta\lambda = \frac{\delta\Sigma_a}{\nu\Sigma_{f0}}\frac{2}{\pi}\int_0^{z_1}\sin^2(Bz)dz \tag{10.37}$$

$$\delta k = \rho = -\frac{\delta\Sigma_a}{\nu\Sigma_{f0}}\left[\frac{z_1}{L} - \frac{1}{2\pi}\sin\left(\frac{2\pi z_1}{L}\right)\right] \tag{10.38}$$

Now consider the perturbation introduced by running a plane absorber down through the reactor at a position z_1 in the reactor. We have

$$\delta\lambda = \frac{\int_0^{z_1}\phi^*(z)\delta\Sigma_a\delta(z - z_1)\phi_0(z)dz}{\int_0^{L}\phi^*(z)\nu\Sigma_{f0}\phi_0(z)dz} \tag{10.39a}$$

or

$$\delta\lambda = \frac{\delta\Sigma_a\phi^*(z_1)\phi_0(z_1)}{\nu\Sigma_{f0}\int_0^{L}\phi^*(z)\phi_0(z)dz} \tag{10.39b}$$

$$\delta k = \rho = -\frac{\delta\Sigma_a}{\nu\Sigma_{f0}}\frac{2}{\pi}\sin^2(Bz_1) \tag{10.40}$$

This can be seen as Fig. 10.2, which is a representation of a delta function perturbation.

Problems

Problem 10.1: Listed below are a set of typical group constants for a BWR. Calculate the multiplication factor for this reactor if it can be treated as a right circular cylinder of a height of 370 cm and a diameter of 340 cm.

Group constant	Group 1	Group 2
$\nu\Sigma_{g_{\text{Fission}}}$	0.001348	0.040783
$\Sigma_{g_{\text{Absorption}}}$	0.001469	0.040249
Σ_g	0.859599	0.142481
$\Sigma_{g_{\text{Removal}}}$	0.044587	0.040249
χ_g	1.0	0.0

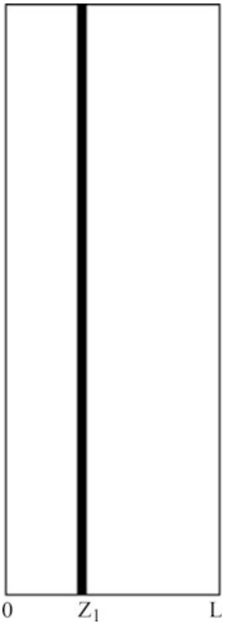

Fig. 10.2 Delta function perturbation

Problem 10.2: Using the group constants from the previous problem, calculate the following for this reactor:

(a) The k_∞
(b) The resonance escape probability
(c) The fast fission factor
(d) The fast and thermal non-leakage probabilities

Problem 10.3: Calculate the critical radius for an unreflected right circular cylinder reactor characterized by the following group constants. Assume the reactor height = 25 cm.

Group constant	Group 1	Group 2
$v\Sigma_{g_{\text{Fission}}}$	0.002562	0.15180
$\Sigma_{g_{\text{Absorption}}}$	0.001930	0.09509
$\Sigma_{g_{\text{Transport}}}$	0.466100	2.95420
$\Sigma_{g_{\text{Downstream}}}$	0.055140	–
χ_g	1.0	0.0

Problem 10.4: Calculate the multiplication factor for an unreflected fast reactor with the following cross-sectional data and core size. Assume that

$$\text{Core radius} = 111\ \text{cm} \quad \text{and} \quad \text{Core height} = 91.44\ \text{cm}$$

Group constant	Group 1	Group 2
$v\Sigma g_{\text{Fission}}$	0.011040	0.005486
$\Sigma g_{\text{Absorption}}$	0.004598	0.004108
$\Sigma g_{\text{Downstream}}$	0.023420	–
$\Sigma g_{\text{Transport}}$	0.028020	0.242200
χ_g	0.55	0.45

Problem 10.5: Calculate the critical height for a fast reactor core that is reflected on top and bottom by a blanket with the cross sections given below. Assume that

$$\text{Core radius} = 100 \text{ cm}$$

1 Group cross sections	Core	Blanket
$v\Sigma_{\text{Fission}}$	0.006017	0.000594
$\Sigma_{\text{Absorption}}$	0.004159	0.001471
$\Sigma_{\text{Transport}}$	0.22836	0.31325

Problem 10.6: Given the flux solutions below for a two-group calculation in a sphere for a pebble-bed reactor, calculate the self-shielding factors for both the fast and thermal groups. The fuel extends from 0.0 to 0.8 cm and the moderator extends from 0.8 to 1.2 cm. Assume linear variation across each of the regions. The plot below gives a picture even though it is not labeled very well.

Flux radius	Thermal	Flux fast
0.0	0.1	1.0
0.8	0.5	0.95
1.2	1.0	0.30

Chapter 11
Reactor Kinetics and Point Kinetics

The point kinetics model can be obtained directly from the space- and time-dependent transport equations. However, these equations are too complicated to be of any practical application. The diffusion approximation, obtained by keeping only the PI terms of the spherical harmonics expansion in the angular variable of the directional flux, is frequently used in neutronic analysis. This chapter discusses reactor characteristics that change because of changing reactivity. A basic approach using a minimum of mathematics has been followed. Emphasis has been placed on distinguishing between prompt and delayed neutrons and showing relationships among reactor variables, k_{eff}, period, neutron density, and power level.

11.1 Time-Dependent Diffusion Equation

For the analysis of point reactor kinetics, the situation arises where one needs to consider the transient changes resulting from the departure of the reactor condition from the critical state. This results under the following conditions as:

1. Startup
2. Shutdown
3. Accidental disturbances in the course of what is intended to be steady-state operation

The power produced during a reactor transient is one of the most significant factors, which is determining the degree of damage that can happen from an accident, within reactor.

The time-dependent power production is related to the effective multiplication factor k_{eff} and the prompt and delayed neutron properties through the reactor kinetic equations. The spatial distribution of the reactor neutron flux can be ignored in lieu of an emphasis on its time behavior. The reactor is viewed as a point; hence, the

B. Zohuri, *Neutronic Analysis For Nuclear Reactor Systems*,
DOI 10.1007/978-3-319-42964-9_11

terminology of point reactor kinetics arises. In this regard, a distinction must be made between the behaviors of the prompt and delayed neutrons.

Point kinetics is very interesting because of the apparent simplicity of the resulting differential equations. The method is very frequently used, but the underlying difficulties in obtaining the parameters are hidden. In spite of all this, many inherent characteristics of the dynamics of nuclear cores can be deduced from these equations. In addition, these same equations provide a tool for the analysis, the comparison, and the practical implementation of various numerical schemes that may eventually be used in more complex situations. An integration technique that does not pass the test of point kinetics will certainly not be used in space–time kinetics. Point kinetics can thus play the role of an experimental bench before expensive problems are attempted with more advanced methods [1].

The driving factor behind point kinetics is to separate the flux into two factors, the first one being a shape function depending both on space and time and, in addition, a second factor depending only on time, in the following fashion:

$$\phi(\vec{\boldsymbol{r}},t) = S(\vec{\boldsymbol{r}},t)T(t). \tag{11.1}$$

Note that this equation for the flux does not involve any approximation and that the equality is maintained. However, the shape function $S(\vec{\boldsymbol{r}},t)$ depends both on space and on time in this approach. We now introduce a column vector of weight functions as

$$W(\vec{\boldsymbol{r}}) = \begin{bmatrix} W_1(\vec{\boldsymbol{r}}) \\ W_1(\vec{\boldsymbol{r}}) \\ \vdots \\ W_G(\vec{\boldsymbol{r}}) \end{bmatrix}, \tag{11.2}$$

whose function will be to give *rise* to general equations. In effect, Eq. 11.1 presents a degree of arbitrariness in the choice of $S(\vec{\boldsymbol{r}},t)$ and of $T(t)$; only the product of the two variables needs to be specified. We will use $W(\vec{\boldsymbol{r}})$ to introduce normalization constraints, which it will obey at all times during a transient condition. Specifically, we define

$$T(t) = \left\langle [W]^{\mathrm{T}}[v]^{-1}[\phi] \right\rangle \tag{11.3}$$

and it follows that Eq. 11.1 and the shape function $S(\vec{\boldsymbol{r}},t)$ must obey the following constraint as follows, by substituting Eq. 11.1 into Eq. 11.3:

$$\left\langle [W]^{\mathrm{T}}[v]^{-1}[S(\vec{\boldsymbol{r}},t)] \right\rangle = 1, \tag{11.4}$$

where the symbol $\langle\ \rangle$ means spatial integration over the whole domain of the nuclear core.

Note that the factor $T(t)$ in Eq. 11.3 is called the amplitude function and the shape function $S(\vec{\boldsymbol{r}}, t)$ represents in some sense the total number of neutrons in the reactor but that this number depends on the weight function. As the constraint on $S(\vec{\boldsymbol{r}}, t)$ does not depend on time, the shape function may change in time, but its integral is time independent. Thus, $T(t)$ itself represents the neutron population change in the reactor.

We can now seek for a differential equation for the time-dependent variable $T(t)$ by replacing $\phi(\vec{\boldsymbol{r}}, t)$ by the product of $S(\vec{\boldsymbol{r}}, t)T(t)$ in the *space–time kinetics* equations, by *pre-multiplying the resulting equations* by $W(\vec{\boldsymbol{r}})]^{\mathrm{T}}$, and by integrating over the whole core volume. Thus, using Eq. 11.4, we obtain the following results as

$$\begin{aligned}
&\left\langle [W(\vec{\boldsymbol{r}})]^{\mathrm{T}} \left\{ \begin{array}{c} \left\langle [W]^{\mathrm{T}} [v]^{-1} [S] \right\rangle \dfrac{\partial T}{\partial t} \\ \nabla \cdot [D] \vec{\nabla} [S] - [\Sigma][S] \\ + \left((1-\beta)[\chi^{p}] + \displaystyle\sum_{i=1}^{D} \beta_i \left[\chi_i^{d}\right] \right) \left[v\Sigma_f\right]^{\mathrm{T}} [S] \end{array} \right\} \right\rangle T(t) \\
&- \left\langle [W(\vec{\boldsymbol{r}})]^{\mathrm{T}} \sum_{i=1}^{D} \beta_i \left[\chi_i^{d}\right] \left[v\Sigma_f\right]^{\mathrm{T}} [S] \right\rangle T(t) + \sum_{i=1}^{D} \lambda_i \left\langle [W]^{\mathrm{T}} \left[\chi_i^{d}\right] C_i \right\rangle,
\end{aligned} \tag{11.5}$$

where, in order to conform to certain conventions, we have added and subtracted the term in

$$\sum_{i=1}^{D} \beta_i \left[\chi_i^{d}\right] \left[v\Sigma_f\right]^{\mathrm{T}} [S]. \tag{11.6}$$

Very similar operations are performed on the precursor equations that we pre-multiply by $[W]^{\mathrm{T}}[\chi_i^{d}]$ before integrating over space to get the following relationship as

$$\frac{\partial}{\partial t} \left\langle [W]^{\mathrm{T}} \left[\chi_i^{d}\right] C_i \right\rangle = \left\langle [W]^{\mathrm{T}} \beta_i \left[\chi_i^{d}\right] [S] \right\rangle T - \lambda_i \left\langle [W]^{\mathrm{T}} \left[\chi_i^{d}\right] C_i \right\rangle. \tag{11.7}$$

We now *define* the following quantities as

$$C_i(t) = \frac{\left\langle [W]^{\mathrm{T}} \left[\chi_i^{d}\right] C_i \right\rangle}{\left\langle [W]^{\mathrm{T}} [v]^{-1} [S] \right\rangle}. \tag{11.8}$$

Now, we first define another quantity that is known as the *mean neutron generation time* as $\Lambda(t)$ so we can write

$$\Lambda(t) = \frac{\left\langle [W]^{\mathrm{T}}[v]^{-1}[S]\right\rangle}{\left\langle [W]^{\mathrm{T}}\left\{(1-\beta)[\chi^{P}] + \sum_{i=1}^{D}\beta_i\left[\chi_i^d\right]\right\}\left[v\Sigma_f\right]^{\mathrm{T}}[S]\right\rangle}, \tag{11.9}$$

where again $\Lambda(t)$ is defined as

$\Lambda(t) \times \equiv \frac{1}{k} \equiv$ *mean generation time* between birth of neuron and subject absorption inducing fission.

Note that if $k \sim 1$, then $\Lambda(t)$ is essentially just the prompt neutron lifetime ℓ.

Now, if, we introduce the quantity of $\beta_i(t)$, as the following form:

$$\beta_i(t) = \beta_i \frac{\left\langle [W]^{\mathrm{T}}\left[\chi_i^d\right]\left[v\Sigma_f\right]^{\mathrm{T}}[S]\right\rangle}{\left\langle [W]^{\mathrm{T}}\left\{(1-\beta)[\chi^{P}] + \sum_{i=1}^{D}\beta_i\left[\chi_i^d\right]\right\}\left[v\Sigma_f\right]^{\mathrm{T}}[S]\right\rangle}. \tag{11.10}$$

Then, we can write

$$\beta(t) \approx \sum_{i=1}^{D}\beta_i(t). \tag{11.11}$$

Now if we define a very important quantity known as the *reactivity* and represented by $\rho(t)$, which essentially measures the deviation of core multiplication from its critical value, where $k = 1$, then we can write the following equation by utilizing what we have shown in Eq. 11.5 as

$$\rho(t) = \frac{[W(\vec{\boldsymbol{r}})]^{\mathrm{T}}\left\{\nabla\cdot[D]\vec{\nabla}[S] - [\Sigma][S] + \left((1-\beta)[\chi^{p}] + \sum_{i=1}^{D}\beta_i\left[\chi_i^d\right]\right)\left[v\Sigma_f\right]^{\mathrm{T}}[S]\right\}}{\left\langle [W]^{\mathrm{T}}\left\{(1-\beta)[\chi^{P}] + \sum_{i=1}^{D}\beta_i\left[\chi_i^d\right]\right\}\left[v\Sigma_f\right]^{\mathrm{T}}[S]\right\rangle}. \tag{11.12}$$

Another form of reactivity factor $\rho(t)$ is presented by Duderstadt and Hamilton [2] in the following as well:

$$\rho(t) = \frac{k(t)-1}{k(t)} \equiv \textit{reactivity}. \tag{11.13}$$

Note that in Eq. 11.13, explicitly indicates criticality factor, k as a function of time t; hence, reactivity factor ρ may be a function of time as well.

Now that we have definitions in Eqs. 11.10 and 11.12, the *space–time kinetics equation* becomes

$$\begin{cases} \dfrac{dT}{dt} = \dfrac{[\rho(t) - \beta]}{\Lambda(t)} T + \displaystyle\sum_{i=1}^{D} \lambda_i C_i \\ \dfrac{dC_i}{dt} = \dfrac{\beta_i(t)}{\Lambda(t)} - \lambda_i C_i \quad i = 1, \cdots, 6 \end{cases} . \tag{11.14}$$

Note that the Eq. 11.14 presents a set of seven coupled ordinary differential equations, in time, which describe both the time dependence of the neutron population in the reactor and the decay of the delayed neutron precursor [2].

11.2 Derivation of Exact Point Kinetics Equations (EPKE)

The most accurate description of the neutron behavior in a near critical nuclear reactor is given by the three-dimensional, energy, angle, and time-dependent form of the Boltzmann transport equation given by

$$\begin{aligned} \frac{1}{v(E)} \frac{d\phi\left(\vec{r}, E, \vec{\Omega}, t\right)}{dt} &+ \vec{\Omega} \cdot \nabla \phi\left(\vec{r}, E, \vec{\Omega}, t\right) + \Sigma_t(\vec{r}, E, t)\phi\left(\vec{r}, E, \vec{\Omega}, t\right) = q\left(\vec{r}, E, \vec{\Omega}, t\right) \\ &+ \int_{E'} \int_{\vec{\Omega}'} \Sigma_s\left(\vec{r}, E', \vec{\Omega}' \to E, \vec{\Omega}, t\right) \phi\left(\vec{r}, E', \vec{\Omega}', t\right) dE' d\vec{\Omega}' \\ &+ \chi(E, t) \int_{E'} \int_{\vec{\Omega}'} \frac{v(E')}{4\pi} \Sigma_f\left(\vec{r}, E', \vec{\Omega}', t\right) \phi\left(\vec{r}, E', \vec{\Omega}', t\right) dE' d\vec{\Omega}'. \end{aligned} \tag{11.15}$$

where fission has been assumed to be isotropic in the laboratory reference frame. In addition, the following quantities are defined:

$\phi\left(\vec{r}, E, \vec{\Omega}, t\right)$ = The time-dependent angular flux density (the number of neutrons at position $\vec{r}$, moving in direction $\vec{\Omega}$ with energy E, at time t)

$v(E)$ = The velocity of neutrons with energy E

$\sum_t(\boldsymbol{r}, E, t)$ = The macroscopic material total cross section for neutrons of energy E, at position $\vec{r}$ and time t

$q\left(\vec{r}, E, \vec{\Omega}, t\right)$ = The source of neutrons at position $\vec{r}$, energy E, and moving in direction $\vec{\Omega}$ at time t

$\Sigma_s\left(\vec{\boldsymbol{r}}, E', \vec{\boldsymbol{\Omega}}' \to E, \vec{\boldsymbol{\Omega}}, t\right)$ = The macroscopic material cross section for scattering from direction $\vec{\boldsymbol{\Omega}}'$ and energy E' to direction $\vec{\boldsymbol{\Omega}}$ and energy E, at position $\vec{\boldsymbol{r}}$ and time t

$\chi(E, t)$ = The time-dependent yield of fission neutrons at energy E

$\upsilon(E')$ = The total yield of neutrons because of fission caused by a neutron of energy E'

$\Sigma_f\left(\vec{\boldsymbol{r}}, E', \vec{\boldsymbol{\Omega}}', t\right)$ = The macroscopic fission cross section for neutrons of energy E', at position $\vec{\boldsymbol{r}}$ and time t

Fission has been assumed isotropic in the laboratory reference frame.

Since not all neutrons are produced at the moment of fission, the source term must be broken up into an independent source term and a delayed neutron source term. This can be accomplished as follows. Let

$$\begin{aligned}
&\chi(E,t)\int_{E'}\int_{\vec{\boldsymbol{\Omega}}'}\frac{\nu}{4\pi}\Sigma_f\left(\vec{\boldsymbol{r}}, E', \vec{\boldsymbol{\Omega}}', t\right)\phi\left(\vec{\boldsymbol{r}}, E', \vec{\boldsymbol{\Omega}}', t\right)dE'd\vec{\boldsymbol{\Omega}}' \\
&= \chi_p(E)(1-\beta)\int_{E'}\int_{\vec{\boldsymbol{\Omega}}'}\frac{\nu}{4\pi}\Sigma_f\left(\vec{\boldsymbol{r}}, E', \vec{\boldsymbol{\Omega}}', t\right)\phi\left(\vec{\boldsymbol{r}}, E', \vec{\boldsymbol{\Omega}}', t\right)dE'd\vec{\boldsymbol{\Omega}}' + \sum_{i=1}^{M}\chi_{id}(E)\lambda_i C_i(\vec{\boldsymbol{r}}, t),
\end{aligned} \tag{11.16}$$

where a separate energy spectrum has been prescribed for prompt and delayed neutrons and the precursor concentrations have been introduced as $C_i(\vec{\boldsymbol{r}}, t)$.

This equation can theoretically be solved by applying straightforward finite difference methods in all variables (seven for the most general case). However, this is a very, very large computational task and has never really been accomplished for the most general case. Usually the number of dimensions has been reduced, by taking advantage of symmetry in the spatial dimensions and the lack of a strong angular dependence in the energy-dependent flux. Even so, the energy-dependent diffusion equations in more than one spatial dimension present a formidable computation task. It has been found that this level of effort is not required for a significant number of reactor kinetics problems, and a heuristic point kinetics equation approach is very accurate. The objective of the following derivation is to make explicit the approximations inherent in the point kinetics equations and therefore in some way provide an indication of their adequacy in untried circumstances.

With this goal in mind, it is useful to factor the time-dependent angular flux density into two parts:

$$\phi\left(\vec{\boldsymbol{r}}, E', \vec{\boldsymbol{\Omega}}', t\right) = \varphi\left(\vec{\boldsymbol{r}}, E', \vec{\boldsymbol{\Omega}}', t\right)\cdot P(t), \tag{11.17}$$

where $P(t)$ will hopefully contain the major time dependence and ϕ will not be a strong function of time. In order to unambiguously perform this splitting or factorization, a rule for sorting out $P(t)$ is required. The most useful rule is

$$\int\limits_{\vec{\boldsymbol{r}},E,\,\vec{\boldsymbol{\Omega}}} W\left(\vec{\boldsymbol{r}},E,\,\vec{\boldsymbol{\Omega}}\right)\frac{1}{v(E)}\varphi\left(\vec{\boldsymbol{r}},E,\,\vec{\boldsymbol{\Omega}},t\right) = 1.0, \tag{11.18}$$

where $W\left(\vec{\boldsymbol{r}},E,\,\vec{\boldsymbol{\Omega}}\right)$ is some arbitrary weighting function yet to be selected. Multiplying the transport equation by $W\left(\vec{\boldsymbol{r}},E,\,\vec{\boldsymbol{\Omega}}\right)$ and integrating over all space, energies, and angles, the following equation can be obtained:

$$\frac{d}{dt}\int\limits_{\vec{\boldsymbol{r}},E,\,\vec{\boldsymbol{\Omega}}} W\left(\vec{\boldsymbol{r}},E,\,\vec{\boldsymbol{\Omega}}\right)\frac{1}{v(E)}\varphi\left(\vec{\boldsymbol{r}},E,\,\vec{\boldsymbol{\Omega}},t\right)P(t)d\vec{\boldsymbol{r}}dEd\vec{\boldsymbol{\Omega}} \tag{11.19a}$$

$$+\int\limits_{\vec{\boldsymbol{r}},E,\,\vec{\boldsymbol{\Omega}}} W\left(\vec{\boldsymbol{r}},E,\,\vec{\boldsymbol{\Omega}}\right)\vec{\boldsymbol{\Omega}}\cdot\nabla\varphi\left(\vec{\boldsymbol{r}},E,\,\vec{\boldsymbol{\Omega}},t\right)P(t)d\vec{\boldsymbol{r}}dEd\vec{\boldsymbol{\Omega}} \tag{11.19b}$$

$$+\int\limits_{\vec{\boldsymbol{r}},E,\,\vec{\boldsymbol{\Omega}}} W\left(\vec{\boldsymbol{r}},E,\,\vec{\boldsymbol{\Omega}}\right)\Sigma_t(\vec{\boldsymbol{r}},E,t)\varphi\left(\vec{\boldsymbol{r}},E,\,\vec{\boldsymbol{\Omega}},t\right)P(t)d\vec{\boldsymbol{r}}dEd\vec{\boldsymbol{\Omega}} \tag{11.19c}$$

$$=\int\limits_{\vec{\boldsymbol{r}},E,\,\vec{\boldsymbol{\Omega}}} W\left(\vec{\boldsymbol{r}},E,\,\vec{\boldsymbol{\Omega}}\right)q\left(\vec{\boldsymbol{r}},E,\,\vec{\boldsymbol{\Omega}},t\right)d\vec{\boldsymbol{r}}dEd\vec{\boldsymbol{\Omega}} \tag{11.19d}$$

$$+\int\limits_{\vec{\boldsymbol{r}},E,\,\vec{\boldsymbol{\Omega}}} W\left(\vec{\boldsymbol{r}},E,\,\vec{\boldsymbol{\Omega}}\right)\int\limits_{E',\,\vec{\boldsymbol{\Omega}}}\Sigma_s\left(\vec{\boldsymbol{r}},E',\,\vec{\boldsymbol{\Omega}}'\to E,\,\vec{\boldsymbol{\Omega}},t\right)\varphi\left(\vec{\boldsymbol{r}},E',\,\vec{\boldsymbol{\Omega}}',t\right)P(t)dE'd\vec{\boldsymbol{\Omega}}'d\vec{\boldsymbol{r}}dEd\vec{\boldsymbol{\Omega}} \tag{11.19e}$$

$$+\int\limits_{\vec{\boldsymbol{r}},E,\,\vec{\boldsymbol{\Omega}}} W\left(\vec{\boldsymbol{r}},E,\,\vec{\boldsymbol{\Omega}}\right)\chi_p(E)(1-\beta)\int\limits_{E',\,\vec{\boldsymbol{\Omega}}'}\frac{v(E')}{4\pi}\Sigma_f\left(\vec{\boldsymbol{r}},E',\,\vec{\boldsymbol{\Omega}}',t\right)\varphi\left(\vec{\boldsymbol{r}},E',\,\vec{\boldsymbol{\Omega}}',t\right)P(t)$$
$$\times dE'd\vec{\boldsymbol{\Omega}}'d\vec{\boldsymbol{r}}dEd\vec{\boldsymbol{\Omega}} \tag{11.19f}$$

$$+\int\limits_{\vec{\boldsymbol{r}},E,\,\vec{\boldsymbol{\Omega}}} W\left(\vec{\boldsymbol{r}},E,\,\vec{\boldsymbol{\Omega}}\right)\sum_{i=1}^{M}\chi_{id}(E)\lambda_i C_i(\vec{\boldsymbol{r}},t)d\vec{\boldsymbol{r}}dEd\vec{\boldsymbol{\Omega}}. \tag{11.19g}$$

The individual terms in this equation are identified because it will be convenient to reduce them one at a time.

Consider first Eq. 11.19a. Removing $P(t)$ from the phase space integrals gives

$$\text{Eq. 11.19a} = \begin{cases} \dfrac{d}{dt}P(t) \displaystyle\int\limits_{\vec{r}, E, \vec{\boldsymbol{\Omega}}} W\left(\vec{\boldsymbol{r}}, E, \vec{\boldsymbol{\Omega}}\right)\frac{1}{v(E)}\varphi\left(\vec{\boldsymbol{r}}, E, \vec{\boldsymbol{\Omega}}, t\right)d\vec{\boldsymbol{r}}dEd\vec{\boldsymbol{\Omega}} + \\ P(t)\dfrac{d}{dt} \displaystyle\int\limits_{\vec{r}, E, \vec{\boldsymbol{\Omega}}} W\left(\vec{\boldsymbol{r}}, E, \vec{\boldsymbol{\Omega}}\right)\frac{1}{v(E)}\varphi\left(\vec{\boldsymbol{r}}, E, \vec{\boldsymbol{\Omega}}, t\right)d\vec{\boldsymbol{r}}dEd\vec{\boldsymbol{\Omega}} \end{cases}.$$

Applying the normalization condition reduces this term to

$$\text{Eq. 11.19a} = \frac{d}{dt}P(t)\cdot 1.0 + P(t)\cdot\frac{d}{dt}1.0 = \frac{d}{dt}P(t).$$

This is the major motivation for choosing the normalization condition in the form it was specified.

The next step is to define the equilibrium, fission source term. The equilibrium fission source is composed of the prompt and delayed components. At equilibrium, or the critical condition, the spatial dependence of the delayed spectrum is the same as the prompt spectrum spatial dependence. The difference between the equilibrium spectrum and the conventional spectrum is that the delayed part of the neutron emission has a different energy spectrum. We have, for the equilibrium or critical condition, fission source

$$\begin{aligned} &\chi(E)\int\limits_{E', \vec{\boldsymbol{\Omega}}'} \frac{\mathrm{v}(E')}{4\pi}\Sigma_f\left(\vec{\boldsymbol{r}}, E', \vec{\boldsymbol{\Omega}}'\right)\phi\left(\vec{\boldsymbol{r}}, E', \vec{\boldsymbol{\Omega}}'\right)dE'd\vec{\boldsymbol{\Omega}}' = \\ &\chi_p(E)(1-\beta)\int\limits_{E, \vec{\boldsymbol{\Omega}}'} \frac{\mathrm{v}(E')}{4\pi}\Sigma_f\left(\vec{\boldsymbol{r}}, E', \vec{\boldsymbol{\Omega}}'\right)\phi\left(\vec{\boldsymbol{r}}, E', \vec{\boldsymbol{\Omega}}'\right)dE'd\vec{\boldsymbol{\Omega}}' \\ &+\sum_{i=1}^{M}\chi_{id}(E)\beta_i\int\limits_{E', \vec{\boldsymbol{\Omega}}'} \frac{\mathrm{v}(E')}{4\pi}\Sigma_f\left(\vec{\boldsymbol{r}}, E', \vec{\boldsymbol{\Omega}}'\right)\phi\left(\vec{\boldsymbol{r}}, E', \vec{\boldsymbol{\Omega}}'\right)dE'd\vec{\boldsymbol{\Omega}}. \end{aligned} \tag{11.20}$$

Therefore, to incorporate the equilibrium fission source, we must add and subtract the delayed fission source components from the transport equation. When this is done, and the terms are added to *T6*, it becomes

$$\text{Eq. 11.19f} = \left\{ \begin{array}{l} \displaystyle\int\limits_{\vec{r},E,\vec{\boldsymbol{\Omega}}} W\left(\vec{r},E,\vec{\boldsymbol{\Omega}}\right)\{\chi_p(E)(1-\beta) \int\limits_{E',\vec{\boldsymbol{\Omega}}'} \frac{\nu(E')}{4\pi}\Sigma_f\left(\vec{r},E',\vec{\boldsymbol{\Omega}}',t\right)\varphi\left(\vec{r},E',\vec{\boldsymbol{\Omega}}',t\right)P(t)dE'd\vec{\boldsymbol{\Omega}}' \\ \displaystyle +\sum_{i=1}^{M}\chi_{id}(E)\beta_i \int\limits_{E',\vec{\boldsymbol{\Omega}}'} \frac{\nu(E')}{4\pi}\Sigma_f\left(\vec{r},E',\vec{\boldsymbol{\Omega}}',t\right)\varphi\left(\vec{r},E',\vec{\boldsymbol{\Omega}}',t\right)P(t) \\ \displaystyle -\sum_{i=1}^{M}\chi_{id}(E)\beta_i \int\limits_{E',\vec{\boldsymbol{\Omega}}'} \frac{\nu(E')}{4\pi}\Sigma_f\left(\vec{r},E',\vec{\boldsymbol{\Omega}}',t\right)\varphi\left(\vec{r},E',\vec{\boldsymbol{\Omega}}',t\right)P(t)\}d\vec{r}dEd\vec{\boldsymbol{\Omega}} \end{array} \right. . \tag{11.21}$$

Now define an equilibrium-reduced fission source, FS, as

$$\begin{aligned} &\int\limits_{\vec{r},E,\vec{\boldsymbol{\Omega}}} W\left(\vec{r},E,\vec{\boldsymbol{\Omega}}\right) \\ &\times\left\{\chi_p(E)(1-\beta)+\sum_{i=1}^{M}\chi_{id}(E)\beta_i\right\}\int\limits_{E',\overline{\Omega}'} \frac{\nu(E')}{4\pi}\Sigma_f\left(\vec{r},E',\vec{\boldsymbol{\Omega}}',t\right)\varphi\left(\vec{r},E',\vec{\boldsymbol{\Omega}}',t\right) \\ &\times dE'd\vec{\boldsymbol{\Omega}}'d\vec{r}dEd\vec{\boldsymbol{\Omega}}. \end{aligned} \tag{11.22}$$

And dividing every term by FS will give the following equation:

$$\{\text{Eq. 11.19a} + \text{Eq. 11.19b} + \text{Eq. 11.19c}\}/\text{FS} = \{\text{Eq. 11.19d} + \text{Eq. 11.19e} \\ + \text{Eq. 11.19f} + \text{Eq. 11.19g}\}/\text{FS}.$$

Identify 1/FS as Λ and rearranging terms give

$$\Lambda\text{Eq. 11.19a} = \Lambda\{\text{Eq. 11.19e} + \text{Eq. 11.19f} - \text{Eq. 11.19b}\} - \text{Eq. 11.19c} \\ + \Lambda\text{Eq. 11.19d} + \Lambda\text{Eq. 11.19g}.$$

Now consider Eq. 11.19d and define a reduced independent source as

$$Q(t) = \int\limits_{\vec{r},E,\vec{\boldsymbol{\Omega}}'} W\left(\vec{r},E,\vec{\boldsymbol{\Omega}}\right)q\left(\vec{r},E,\vec{\boldsymbol{\Omega}},t\right)d\vec{r},\ dE,\ d\vec{\boldsymbol{\Omega}}. \tag{11.23}$$

Define $Z_i(t)$ as

$$Z_i(t) = \int\limits_{\overline{r},E,\overline{\Omega}} W\left(\vec{r},E,\vec{\boldsymbol{\Omega}}\right)C_i(\vec{r},t)\chi_{id}(E)d\vec{r}dEd\vec{\boldsymbol{\Omega}}. \tag{11.24}$$

The transport equation can now be written as

$$\Lambda \frac{dP(t)}{dt} = \Lambda \{\text{Eq. 11.19f} + \text{Eq. 11.19e} - \text{Eq. 11.19b} - \text{Eq. 11.19c}\}. \tag{11.25}$$

Consider Eq. 11.19f again and write it as

$$\text{Eq. 11.19f} = \text{FS*}P(t) + \text{Eq. 11.19f}, \tag{11.26}$$

where

$$\text{Eq. 11.19f} = -\sum_{i=1}^{M} \beta_i \chi_{id}(E) \int\limits_{E', \vec{\boldsymbol{\Omega}}'} \frac{\nu(E')}{4\pi} \Sigma_f\left(\vec{\boldsymbol{r}}, E', \vec{\boldsymbol{\Omega}}', t\right) \varphi\left(\vec{\boldsymbol{r}}, E', \vec{\boldsymbol{\Omega}}', t\right) P(t) dE' d\vec{\boldsymbol{\Omega}}'. \tag{11.27}$$

Then, defining

$$\beta = -\frac{\text{Eq. 11.19f}'\Lambda}{P(t)} \tag{11.28}$$

and

$$\rho = \frac{\{\text{Eq. 11.19e} + \text{FS*}P(t) - \text{Eq. 11.19b} - \text{Eq. 11.19c}\}\Lambda}{P(t)} \tag{11.29}$$

gives

$$\Lambda \frac{dP(t)}{dt} = (\rho - \beta)P(t) + \Lambda Q(t) + \Lambda \sum_{i=1}^{M} \lambda_i Z_i(t) \tag{11.30}$$

or

$$\frac{dP(t)}{dt} = \frac{\rho - \beta}{\Lambda} P(t) + Q(t) + \sum_{i=1}^{M} \lambda_i Z_i(t). \tag{11.31}$$

This is essentially the power equation for the point kinetics description of reactor behavior.

Now consider the precursor equations given by

$$\frac{dC_i(\vec{\boldsymbol{r}},t)}{dt}=\beta_i\int\limits_{E,\,\vec{\boldsymbol{\Omega}}}\frac{\nu(E)}{4\pi}\Sigma_f\left(\vec{\boldsymbol{r}},E,\,\vec{\boldsymbol{\Omega}},t\right)\varphi\left(\vec{\boldsymbol{r}},E,\,\vec{\boldsymbol{\Omega}},t\right)P(t)dEd\vec{\boldsymbol{\Omega}}-\lambda_iC_i(\vec{\boldsymbol{r}},t) \tag{11.32}$$

Multiplying these equations by

$$\int\limits_{\vec{\boldsymbol{r}},E,\,\vec{\boldsymbol{\Omega}}}W\left(\vec{\boldsymbol{r}},E,\,\vec{\boldsymbol{\Omega}}\right)\chi_{id}(E)d\vec{\boldsymbol{r}}dEd\vec{\boldsymbol{\Omega}} \tag{11.33}$$

will give

$$\begin{aligned}\frac{dZ_i(\vec{\boldsymbol{r}},t)}{dt}= \; &\beta_i\int\limits_{\vec{\boldsymbol{r}},E,\,\vec{\boldsymbol{\Omega}}}\chi_{id}(E)\times W\left(\vec{\boldsymbol{r}},E,\,\vec{\boldsymbol{\Omega}}\right)\int\limits_{E',\,\vec{\boldsymbol{\Omega}}'}\frac{\nu(E)}{4\pi}\Sigma_f\left(\vec{\boldsymbol{r}},E,\,\vec{\boldsymbol{\Omega}},t\right)\varphi\left(\vec{\boldsymbol{r}},E,\,\vec{\boldsymbol{\Omega}},t\right)\\ &\times P(t)dE'd\vec{\boldsymbol{\Omega}}'d\vec{\boldsymbol{r}}dEd\vec{\boldsymbol{\Omega}}-\lambda_iC_i(\vec{\boldsymbol{r}},t).\end{aligned} \tag{11.34}$$

Remember that

$$\begin{aligned}\beta&=\frac{-\text{Eq. 11.19f}'\Lambda}{P(t)}\\ &=\frac{\sum\limits_{i=1}^{M}\beta_i\int\limits_{\bar{r},E,\bar{\Omega}}\chi_{id}W\int\limits_{E',\bar{\Omega}'}\frac{\nu(E')}{4\pi}\Sigma_f\varphi P(t)dE'd\bar{\Omega}'d\vec{\boldsymbol{r}}dEd\bar{\Omega}}{P(t)\int\limits_{\vec{\boldsymbol{r}},E,\,\vec{\boldsymbol{\Omega}}}W\left\{\chi_p(1-\beta)+\sum\limits_{i=1}^{M}\chi_{id}\beta_i\right\}\int\limits_{E',\bar{\Omega}'}\frac{\nu(E')}{4\pi}\Sigma_f\varphi dE'd\vec{\boldsymbol{\Omega}}'d\vec{\boldsymbol{r}}dEd\vec{\boldsymbol{\Omega}}}.\end{aligned} \tag{11.35}$$

The precursor equations become

$$\frac{dZ_i(t)}{dt}=\frac{\beta_i}{\Lambda}P(t)-\lambda_iZ_i(t). \tag{11.36}$$

The "exact" point kinetics equations are then

$$\frac{dP(t)}{dt}=\frac{\rho-\beta}{\Lambda}P(t)+\sum_{i=1}^{M}\lambda_iZ_i(t), \tag{11.37}$$

$$\frac{dP(t)}{dt} = \frac{\rho - \beta}{\Lambda} P(t) + \sum_{i=1}^{M} \lambda_i Z_i(t). \tag{11.38}$$

These equations are exact if all of the parameters in them are computed according to the formulas given above. However, to apply the formulas given above exactly would be as difficult a task as integrating the original transport equation directly. The real advantage of deriving the "exact" equations in this manner is to rigorously prescribe how to compute the quantities used to predict kinetic behavior. When approximations are introduced in computing these quantities, at least there is a standard to compare against in order to understand the impact of the approximations.

Consider the definition of ρ. The complete expression for ρ is given by

$$\rho = \frac{\{\text{Eq. 11.19e} + \text{FS}^{*}P(t) - \text{Eq. 11.19b} - \text{Eq. 11.19c}\}\Lambda}{P(t)} \tag{11.39}$$

or

$$\left\{ \begin{array}{l} \displaystyle\int_{\vec{\boldsymbol{r}}, E, \vec{\boldsymbol{\Omega}}} W \int_{E', \vec{\boldsymbol{\Omega}}'} \Sigma_s\left(E', \vec{\boldsymbol{\Omega}}' \to E, \vec{\boldsymbol{\Omega}}'\right) \varphi dE' d\vec{\boldsymbol{\Omega}}' d\vec{\boldsymbol{r}} dE d\vec{\boldsymbol{\Omega}} + \\ \displaystyle\int_{\vec{\boldsymbol{r}}, E, \vec{\boldsymbol{\Omega}}} W\left\{\chi_p(1-\beta) + \sum_{i=1}^{M} \chi_{id}\beta_i\right\} \int_{E', \vec{\boldsymbol{\Omega}}'} \frac{v}{4\pi} \Sigma_f \phi dE' d\overline{\Omega}' d\vec{\boldsymbol{r}} dE d\overline{\Omega} \end{array} \right. \tag{11.40a}$$

or we find ρ to be as follows:

$$\rho = \frac{- \displaystyle\int_{\vec{\boldsymbol{r}}, E, \vec{\boldsymbol{\Omega}}} W \vec{\boldsymbol{\Omega}} \cdot \nabla \varphi d\vec{\boldsymbol{r}} dE d\vec{\boldsymbol{\Omega}} - \int_{\vec{r}, E, \overline{\Omega}} W \Sigma_t \varphi d\vec{\boldsymbol{r}} dE d\vec{\boldsymbol{\Omega}}}{\displaystyle\int_{\vec{\boldsymbol{r}}, E, \vec{\boldsymbol{\Omega}}} W\left\{\chi_p(1-\beta) + \sum_{i=1}^{M} \chi_{id}\beta_i\right\} \int_{E', \vec{\boldsymbol{\Omega}}'} \frac{v}{4\pi} \Sigma_f \phi dE' d\vec{\boldsymbol{\Omega}}' d\vec{\boldsymbol{r}} dE d\vec{\boldsymbol{\Omega}},} \tag{11.40b}$$

where the functional dependence of the major variables has been suppressed. The notation can be further simplified by defining

$$F\varphi = \int_{E, \vec{\boldsymbol{\Omega}}'} \frac{v(E')}{4\pi} \Sigma_f\left(\vec{\boldsymbol{r}}, E', \vec{\boldsymbol{\Omega}}', t\right) \varphi\left(\vec{\boldsymbol{r}}, E', \vec{\boldsymbol{\Omega}}', t\right) dE' d\vec{\boldsymbol{\Omega}}' \tag{11.41}$$

$$\chi = \chi_p(1-\beta) + \sum_{i=1}^{M} \chi_{id}\beta_i \tag{11.42}$$

and suppressing most of the variable dependence. Then,

$$\rho = \frac{-\int\limits_{\vec{r},E,\vec{\boldsymbol{\Omega}}} W\left(\vec{\boldsymbol{\Omega}}\cdot\nabla\varphi + \Sigma_t\varphi - \chi F\varphi - \Sigma_s\varphi\right)}{\int\limits_{\vec{r},E,\vec{\boldsymbol{\Omega}}} W\chi F\varphi} \qquad \beta = \frac{\sum_{i=1}^{M}\beta_i\int W\chi_{id}F\varphi}{\int\limits_{\vec{r},E,\vec{\boldsymbol{\Omega}}} W\chi F\varphi} \tag{11.43}$$

$$\Lambda = \frac{1}{\int\limits_{\vec{r},E,\vec{\boldsymbol{\Omega}}} W\chi F\varphi} \qquad Q(t) = \int\limits_{\vec{r},E,\vec{\boldsymbol{\Omega}}} Wq \qquad Z_i(t) = \int\limits_{\vec{r},E,\vec{\boldsymbol{\Omega}}} W\chi_{id}C_i. \tag{11.44}$$

Note that for a critical reactor, the static eigenvalue equation is given by

$$\vec{\boldsymbol{\Omega}}\cdot\nabla\varphi + \Sigma_i\varphi = \chi F\varphi + \Sigma_s\varphi. \tag{11.45}$$

It is also worth noting at this time that ϕ is not the diffusion flux, but is actually a reduced transport flux and definitely can contain anisotropic components that may be necessary to evaluate in order to correctly calculate the reactivity. However, the analysis that we have gone through will apply to both transport models and diffusion theory models.

11.3 The Point Kinetics Equations

Now that we have derived the point kinetics equations (PKE), we should investigate what they say about nuclear reactor behavior. We begin by noting that form a homogeneous set of ordinary differential equations. As we know the solution to a homogeneous set of equations only exists for certain parameters called eigenvalues. We can write the equations as

$$\begin{aligned}
\frac{dP}{dt} &= \frac{\rho-\beta}{\Lambda}P && +\lambda_1 z_1 && +\lambda_2 z_2 && +\lambda_3 z_3 && +\lambda_4 z_4 && +\lambda_5 z_5 && +\lambda_6 z_6 \\
\frac{dz_1}{dt} &= \frac{\beta_1}{\Lambda}P && -\lambda_1 z_1 \\
\frac{dz_2}{dt} &= \frac{\beta_2}{\Lambda}P && && -\lambda_2 z_2 \\
\frac{dz_3}{dt} &= \frac{\beta_3}{\Lambda}P && && && -\lambda_3 z_3 \\
\frac{dz_4}{dt} &= \frac{\beta_4}{\Lambda}P && && && && -\lambda_4 z_4 \\
\frac{dz_5}{dt} &= \frac{\beta_5}{\Lambda}P && && && && && -\lambda_5 z_5 \\
\frac{dz_6}{dt} &= \frac{\beta_6}{\Lambda}P && && && && && && -\lambda_6 z_6
\end{aligned} \quad . \tag{11.46}$$

And if we assume a form for P and each z_i that incorporates an eigenvalue ω such that

$$P(t) = P_0 e^{\omega t} \quad \frac{dP(t)}{dt} = \omega P(t) \quad Z_i(t) = Z_{i0} e^{\omega t} \quad \frac{dZ_i(t)}{dt} = \omega Z_i(t) \tag{11.47}$$

then each of the $Z_i(t)$ equations can be solved for Z_i to get

$$(\omega + \lambda_i) z_i(t) = \frac{\beta_i}{\Lambda} P(t) \qquad z_i(t) = \frac{\beta_i}{\Lambda(\omega+\lambda_i)} P(t). \tag{11.48}$$

Then

$$\omega P(t) = \frac{\rho-\beta}{\Lambda} P(t) + P(t) \sum_{i=1}^{6} \frac{\lambda_i \beta_i}{\Lambda(\omega+\lambda_i)}. \tag{11.49}$$

And dividing out $P(t)$ gives

$$\begin{cases} \sum_{i=1}^{6} \frac{\lambda_i \beta_i}{\omega+\lambda_i} = \rho - \sum_{i=1}^{6} \beta_i \frac{\omega+\lambda_i}{\omega+\lambda_i} + \sum_{i=1}^{6} \beta_i \frac{\lambda_i}{\omega+\lambda_i} = \rho - \omega \sum_{i=1}^{6} \frac{\beta_i}{\omega+\lambda_i} \\ \rho = \omega \left(\Lambda + \sum_{i=1}^{6} \frac{\beta_i}{\omega+\lambda_i} \right) \end{cases} . \tag{11.50}$$

There are seven roots for w in this inhour equation.

Inhour Equation

The relationship between a step change in reactivity (ρ) and the resulting reactor period (T) allowing for the delayed neutrons can be derived in the form of an equation such as

$$\rho = \frac{\ell}{kT} + \sum_{i=1}^{6} \frac{\beta_i}{1 + \lambda_i T},$$

where

β_i = Delayed neutron fraction for group i
λ_i = Decay constant of delayed neutron group $i(s^{-1}) = \ln 2/t_{1/2}$
ℓ = Prompt neutron lifetime (s)
T = Reactor period

This equation is often called the reactivity equation or the inhour equation, although strictly speaking this is not the inhour equation proper. (The term inhour comes from expressing reactivity in the units of inverse hours. The inhour unit is then that reactivity which will make the stable reactor period equal to 1 h.) These are numerous different formulations of the reactivity equation, but this one will suffice for the purposes of this book.

Now consider the One Delay Family model. The inhour equation in this case becomes

$$\left[\begin{array}{l} \rho = \omega\left(\Lambda + \dfrac{\beta}{\omega + \lambda}\right) \\ (\omega + \lambda)\rho = \omega\Lambda(\omega + \lambda) + \omega\beta \\ \omega\dfrac{\rho - \beta}{\Lambda} + \dfrac{\lambda\rho}{\Lambda} = \omega^2 + \lambda\omega \\ \omega^2 + \left(\lambda - \dfrac{\rho - \beta}{\Lambda}\right)\omega - \dfrac{\lambda\rho}{\Lambda} = 0 \end{array}\right. . \tag{11.51}$$

Note that for most cases if $\rho < \beta$, $\lambda \ll (\rho - \beta)/\Lambda$, so λ can be neglected. Then,

$$\omega = \frac{\rho - \beta}{2\Lambda} \pm \sqrt{\left(\frac{\rho - \beta}{2\Lambda}\right)^2 + \frac{\lambda\rho}{\Lambda}} = \frac{\rho - \beta}{2\Lambda} \pm \frac{\rho - \beta}{2\Lambda}\sqrt{1 + \frac{4\lambda\rho}{\Lambda\left(\frac{\rho - \beta}{\Lambda}\right)^2}}. \tag{11.52}$$

And noting that $\sqrt{1 + x} = 1 + \frac{x}{2} + \ldots$. for small x,

$$\begin{cases} \omega_1 = \dfrac{\rho-\beta}{\Lambda} + \dfrac{\rho-\beta}{\Lambda}\dfrac{\lambda\rho}{\Lambda\left(\frac{\rho-\beta}{\Lambda}\right)^2} = \dfrac{\rho-\beta}{\Lambda} + \dfrac{\lambda\rho}{\rho-\beta} \approx \dfrac{\rho-\beta}{\Lambda} \\ \omega_2 = -\dfrac{\lambda\rho}{\rho-\beta} = \dfrac{\lambda\rho}{\beta-\rho} \end{cases}. \tag{11.53}$$

Therefore, the general solution for a step reactivity change is

$$P(t) = P_{01}e^{\frac{\rho-\beta}{\Lambda}t} + P_{02}e^{\frac{\lambda\rho}{\beta-\rho}t}. \tag{11.54}$$

We will find the unknown coefficients P_{01} and P_{02} from the initial conditions. Continuity of the power and the derivative of the power gives

$$P_0 = P_{01} + P_{02}, \tag{11.55a}$$

$$\begin{aligned} \frac{dP}{dt}(0) &= \frac{\rho-\beta}{\Lambda}P_0 + \lambda z_0 \\ &= \frac{\rho-\beta}{\Lambda}P_0 + \lambda\frac{\beta}{\lambda\Lambda}P_0 \\ &= P_0\left(\frac{\rho}{\Lambda}\right) \\ &= \omega_1 P_{01} + \omega_2 P_{02}, \end{aligned} \tag{11.55b}$$

$$\begin{aligned} P_0\left(\frac{\rho}{\Lambda}\right) &= \frac{\rho-\beta}{\Lambda}(P_0 - P_{02}) + \frac{\lambda\rho}{\beta-\rho}P_{02} \\ P_0\frac{\beta}{\Lambda} &= \left(\frac{\lambda\rho}{\beta-\rho} - \frac{\rho-\beta}{\Lambda}\right)P_{02} \\ P_{02} &\approx \frac{\beta}{\beta-\rho}P_0 \\ P_{01} &= \frac{-\rho}{\beta-\rho}P_0. \end{aligned} \tag{11.55c}$$

This gives the complete solution for a step insertion of reactivity as

$$P(t) = P_0\left\{\frac{\beta}{\beta-\rho}e^{\frac{\lambda\rho}{\beta-\rho}t} - \frac{\rho}{\beta-\rho}e^{\frac{\rho-\beta}{\Lambda}t}\right\}. \tag{11.56}$$

Now that we are here, next we have dynamic and static reactivity, which is the subject of the next section here.

11.4 Dynamic Versus Static Reactivity

An often-discussed concept is the difference between dynamic and static reactivity. There are a large number of ways of computing reactivity that are being used in the field today. The simplest, most straight forward, and least accurate is the eigenvalue difference method. That is, two reactor configurations are mocked up as critical systems. An eigenvalue, K, is found that makes each of them critical, and the difference between these two eigenvalues is assumed to be the same as the reactivity defined above. In the limit of small reactivity, this will be approximately correct; however, as the time-dependent flux shape changes in a reactor, it becomes more and more difficult to evaluate reactivity based on a hypothetical eigenvalue.

A more accurate method would be to use the formalism defined above for the time-dependent case, but use a time-independent shape function. This static function usually corresponds to the shape function for an exactly critical reactor, $k = 1.0$. In this case, the weighting function, W, can be chosen to make this approximate reactivity as accurate as possible by letting it equal the *ADJOINT* function for the exactly critical reactor. If the critical *ADJOINT* function is used, then the reactivity will be insensitive to first-order changes in the shape function; thus, the static reactivity will be as accurate an approximation to the actual reactivity as possible.

The most accurate method of computing the reactivity is to use the actual time-dependent shape function in the integral. Of course, this is much more difficult to do, as somehow the time dependence has to be calculated. It is also important to note that for this case, the choice of W is somewhat arbitrary. A constant value of 1.0 could be chosen, but the *ADJOINT* function for an exactly critical reactor is normally used in hopes of mitigating some of the errors introduced in calculating the time-dependent shape function.

The three definitions are:

1. **Eigenvalue difference reactivity**

$$\rho = \frac{k_1 - k_0}{k_1 k_0} \tag{11.57}$$

2. **Static reactivity**

$$\rho = \frac{\displaystyle\int\limits_{\vec{r},E,\vec{\Omega}} \varphi^* \left(\vec{\Omega} \cdot \nabla\varphi + \Sigma_t\varphi - \chi F\varphi - \Sigma_s\varphi\right) d\vec{r}\,dE\,d\vec{\Omega}}{\displaystyle\int\limits_{\vec{r},E,\vec{\Omega}} \varphi^* \chi F\varphi\, d\vec{r}\,dE\,d\vec{\Omega}} \tag{11.58}$$

where the *ADJOINT* function for the critical configuration is used as the weighting function and the fluxes are obtained from a static criticality calculation for the current configuration of the reactor assembly.

3. **Dynamic reactivity**

$$\rho = \frac{\int\limits_{\vec{r},E,\vec{\Omega}} \varphi^*\left(\overline{\Omega}\cdot\nabla\varphi + \Sigma_t\varphi - \chi F\varphi - \Sigma_s\varphi\right)d\vec{r}dEd\vec{\boldsymbol{\Omega}}}{\int\limits_{\vec{r},E,\vec{\Omega}} \varphi^*\chi F\varphi d\vec{r}dEd\vec{\boldsymbol{\Omega}}} \tag{11.59}$$

where the *ADJOINT* function for the critical configuration is used as the weighting function and the fluxes are obtained from a time-dependent calculation for the shape function. The difference between the most accurate approach for static reactivity, *ADJOINT* weighting, and the true dynamic reactivity is the use of the time-dependent shape function in the dynamic reactivity case. So now, consider how to calculate this shape function.

11.5 Calculating the Time-Dependent Shape Function

Given that the dynamic reactivity is the actual quantity required in the point kinetics equations, an integrodifferential equation can be derived for its calculation. This equation can then be approximated in many ways in order to obtain solutions that are useful for particular problems. Substituting the factored flux into the transport equation and dividing by $P(t)$ give

$$\begin{aligned}
&\frac{1}{v(E)}\left\{\frac{d\varphi\left(\vec{r},E,\vec{\boldsymbol{\Omega}},t\right)}{dt} + \varphi\left(\vec{r},E,\vec{\boldsymbol{\Omega}},t\right)\frac{dP(t)}{dt}/P(t)\right\} \\
&\quad + \overline{\Omega}\cdot\nabla\varphi\left(\vec{r},E,\vec{\boldsymbol{\Omega}},t\right) + \Sigma_t(\vec{r},E,t)\varphi\left(\vec{r},E,\vec{\boldsymbol{\Omega}},t\right) = \\
&\int\limits_{E',\overline{\Omega}'} \Sigma_s\left(\vec{r},E',\vec{\boldsymbol{\Omega}}'\to E,\vec{\boldsymbol{\Omega}},t\right)\varphi\left(\vec{r},E',\vec{\boldsymbol{\Omega}}',t\right)dE'd\vec{\boldsymbol{\Omega}}' \\
&\quad + \chi_p(1-\beta)\int\limits_{E',\overline{\Omega}'} \frac{v(E')}{4\pi}\Sigma_f\left(\vec{r},E',\vec{\boldsymbol{\Omega}}',t\right)\varphi\left(\vec{r},E',\vec{\boldsymbol{\Omega}}',t\right)dE'd\vec{\boldsymbol{\Omega}}' \\
&\quad + \frac{1}{P(t)}\left\{q\left(\vec{r},E,\vec{\boldsymbol{\Omega}},t\right) + \sum_{i=1}^{M}\chi_{id}(E)\beta_i\lambda_i Z_i(\vec{r},t)\right\}.
\end{aligned} \tag{11.60}$$

Of course, this equation is more complicated than the original transport equation. It would be much harder to integrate it directly for any particular problem. However, by performing the factorization and writing the equation in this manner, simplifications are possible depending on the problem.

In short-hand notation, this equation can be written as

$$\frac{1}{v(E)}\frac{d\varphi}{dt}+\frac{1}{v(E)}\varphi\frac{dP}{dt}/P+\vec{\boldsymbol{\Omega}}\cdot\nabla\varphi+\Sigma_t\varphi=\Sigma_s\varphi+\chi_pF\varphi+\frac{1}{P}\left\{q+\sum_{i=1}^{M}\chi_{id}\beta_i\lambda_iZ_i\right\}. \tag{11.61}$$

Rearranging terms gives

$$\frac{1}{v(E)}\frac{d\varphi}{dt}+\vec{\boldsymbol{\Omega}}\cdot\nabla\varphi+\Sigma_t\varphi=\Sigma_s\varphi+\chi_pF\varphi+S/P, \tag{11.62}$$

where

$$S=q+\sum_{i=1}^{M}\chi_{id}\beta_i\lambda_iZ_i-\frac{1}{v}\varphi\frac{dP}{dt}.$$

This looks almost identical to the complete transport equation except for the S/P term. If P is large and S (fast transients), this term can be neglected and the shape function equation is essentially the same as the original transport equation. Thus, it would appear that no simplification has been achieved, and for the most general case, this is indeed true. However, in many cases, the time dependence of the shape function is considerably smaller than the time dependence of the angular flux density, and significantly larger time steps can be taken in its integration.

11.6 Point Kinetics Approximations

If the time dependence of the shape function is completely neglected, all quantities can be evaluated for the critical reactor. This is often considered the least accurate of the methods for dealing with the shape function. However, it will be accurate enough for many applications.

11.6.1 Level of Approximation to the Point Kinetics Equations

As we have seen, the point kinetics equations (PKE) are an approximation to the full spatial and time-dependent behavior of a nuclear reactor. For very many cases of reactor behavior, they are a quite accurate approximation and are a more than adequate approximation to allow complete control of the reactor and characterization of its behavior.

However, the PKE are still too complicated to easily explain some behavior and derive physical data about the reactor from observed measurements. Therefore, we are going to look at several levels of approximation the PKE mainly based on how accurately or detailed we treat the delayed neutron phenomena. The following levels of approximation have applications as noted and are frequently used to describe reactor transients:

No Delayed Neutron Approximation (**NDN**)
Prompt Kinetics (**PK**)
Constant Delayed Source (**CDS**)
Precursor Accumulation (**PA**)
One Delay Family (**ODF**)
Prompt Jump Approximation [Zero Lifetime] (**PJA** or **ZL**)

11.7 Adiabatic Approximation

If the reactor configuration at any point in time is considered to be static, the problem becomes a homogenous one. This is exactly the problem most design codes are set up to calculate. (However, the eigenvalue K must now be introduced in order to obtain a solution. Note this eigenvalue will also compensate for the fact that the reduced equation is based on $\chi_p(E)$ rather than $\chi(E)$.) Note that the eigenfunction obtained may not in this case correspond to any real reactor flux shape. And even if the critical *ADJOINT* solution is used, the accuracy of this technique can be questioned. In addition, since this method requires the computation of an eigenvalue–eigenfunction solution every time it is desired to update the shape function, it can be computationally expensive.

11.8 Adiabatic Approximation with Precomputed Shape Functions

One method that has been proposed for overcoming this computation obstacle is the use of precomputed shape functions and their mixing as time goes on to approximate the actual shape function. This is one of those tricks which will usually work if you know the answer to your problem before you try to solve it, but for "extrapolation" cases, "let the analyst beware." In general, it is not recommended, and accuracy limits cannot be specified.

11.9 Quasi-Static Approximation

In this approximation the shape function is integrated on a much longer time interval than the power function, $P(t)$. The "inhomogeneous" source term S/P can be included or not included. The form used will depend on which terms are relevant for a particular problem, and the part of the transient is being evaluated. Normally a less than second-order implicit scheme will be used for this integration.

That means either Euler's backward method or trapezoidal rule integration method. The Euler's backward method is much faster to compute and therefore has generally been the method of choice.

For the no-source (S/P) case, this would be written as

$$\left\{\frac{1}{v(E)\Delta t}+\vec{\boldsymbol{\Omega}}\cdot\nabla+\Sigma_t-\Sigma_s-\chi_p F\right\}\varphi_2=\frac{1}{v(E)\Delta t}\varphi_1 \tag{11.63}$$

and the flux shape at the start of the time interval becomes the source for the shape at the end of the time interval. If parts of the S/P source are to be included, they are time differenced and added to the equation on the right- and left-hand sides as appropriate.

11.10 Zero-Dimensional Reactors

Now consider a diffusion theory model of a zero-dimensional reactor. We will base this on an infinite slab, but the analysis is the same for any zero-dimensional model. The flux and adjoint solutions are

$$\begin{aligned}\phi(E,z)&=\sum_{g=1}^{\mathrm{NOG}}\varphi^g\cos Bz\\ \phi^*(E,z)&=\sum_{g=1}^{\mathrm{NOG}}\varphi^{*g}\cos Bz.\end{aligned} \tag{11.64}$$

Now consider evaluating some of the terms in the point kinetics equations. Start with the generation time:

$$\Lambda=\frac{1}{\displaystyle\int_{-H/2}^{H/2}\left[\sum_{g=1}^{\mathrm{NOG}}\varphi^{*g}\cos Bz\left\{\chi_p^g(1-\beta)+\sum_{i=1}^{M}\beta_i\chi_{id}^g\right\}\sum_{g=1}^{\mathrm{NOG}}\nu\Sigma_f^g\varphi^g\cos Bz\right]dz}. \tag{11.65}$$

There are a couple of items to note about this definition. First of all, this is the only term where the absolute normalization of φ^{*g} is important. In all other terms, there will be a φ^{*g} on the bottom and on the top of the parameter definition so only the relative values will be important. In order to get the absolute normalization, we must go back to the definition of the factorization:

$$\int\limits_{\vec{r},E,\vec{\Omega}} W\left(\vec{\boldsymbol{r}},E,\vec{\boldsymbol{\Omega}}\right)\frac{1}{v(E)}\varphi\left(\vec{\boldsymbol{r}},E,\vec{\boldsymbol{\Omega}},t\right)=1.0=\sum_{g=1}^{\mathrm{NOG}}\frac{\varphi^{*g}\varphi^{g}}{v^{g}}\int\limits_{-H/2}^{H/2}\cos^{2}Bzdz\frac{\pi}{2}\sum_{g=1}^{\mathrm{NOG}}\frac{\varphi^{*g}\varphi^{g}}{v^{g}}=1.0. \tag{11.66}$$

This will give us the absolute normalization of the weighting function or adjoint function. The weighting function can be written as some constant W_0 times the normalized adjoint function. The inner product of the normalized adjoint and flux divided by the group velocity can then be computed and the normalizing constant becomes one over the inner product:

$$\begin{aligned} W(E,z)&=W_0\sum_{g=1}^{\mathrm{NOG}}\varphi^{*g}\cos Bz\\ W_0&=\frac{1}{\frac{\pi}{2}\sum_{g=1}^{\mathrm{NOG}}\frac{\varphi^{*g}\varphi^{g}}{v^{g}}}. \end{aligned} \tag{11.67}$$

Then we can define a χ^g as

$$\chi^{g}=\chi_{p}^{g}(1-\beta)+\sum_{i=1}^{M}\beta_{i}\chi_{id}^{g}. \tag{11.68}$$

Also note that the second summation in the denominator is completed before it is multiplied by the first two terms, so we can sum the fission source once and for all and use it in evaluating all of the other integrals.

Thus, we can write a simplified generation time computation as

$$\begin{aligned} \Lambda&=\frac{1}{W_0\frac{\pi}{2}\left(\sum_{g=1}^{\mathrm{NOG}}\varphi^{*g}\chi^{g}\right)(\mathrm{FS})}\\ &=\frac{1}{W_0\frac{\pi}{2}\left(\sum_{g=1}^{\mathrm{NOG}}\varphi^{*g}\chi^{g}\right)\left(\sum_{g=1}^{\mathrm{NOG}}\nu\Sigma_{f}^{g}\varphi^{g}\right)}. \end{aligned} \tag{11.69}$$

Now we can calculate $\beta_{\text{effective}}$ as

$$\beta = \frac{\sum_{i=1}^{M} \beta_i \int_{-H/2}^{H/2} \sum_{g=1}^{\mathrm{NOG}} W_0 \varphi^{*g} \cos Bz \chi_{id}^{g} \sum_{g=1}^{\mathrm{NOG}} \nu \Sigma_f^g \varphi^g \cos Bz dz}{W_0 \frac{\pi}{2} \left(\sum_{g=1}^{\mathrm{NOG}} \varphi^{*g} \chi^g \right) \left(\sum_{g=1}^{\mathrm{NOG}} \nu \Sigma_f^g \varphi^g \right).} \tag{11.70}$$

Note that in this case, the W_0 divides out on the top and bottom as does the $\pi/2$ factor and the total fission source. The formula becomes

$$\beta = \frac{\sum_{i=1}^{M} \beta_i \sum_{g=1}^{\mathrm{NOG}} \varphi^{*g} \chi_{id}^{g}}{\sum_{g=1}^{\mathrm{NOG}} \varphi^{*g} \chi^g}. \tag{11.71}$$

Finally, it is worth making some comments about the reactivity term. We have for the diffusion model

$$\begin{cases} \rho = -\dfrac{\displaystyle\int_{\vec{r}, E, \vec{\boldsymbol{\Omega}}} W \left(\vec{\boldsymbol{\Omega}} \cdot \nabla \varphi + \Sigma_t \varphi - \chi F \varphi - \Sigma_s \varphi \right)}{\displaystyle\int_{\vec{r}, E, \vec{\boldsymbol{\Omega}}} W \chi F \varphi} \\ \rho = -\dfrac{\displaystyle\int_{-H/2}^{H/2} \sum_{g'=1}^{\mathrm{NOG}} W_0 \varphi^{*g} \left(D^g B^2 \varphi^g + \Sigma_r^g \varphi^g - \chi^g \sum_{g'=1}^{\mathrm{NOG}} \nu \Sigma_f^{g'} \varphi^{g'} - \sum_{g'=g-1}^{1} \Sigma_s^{g' \to g} \varphi^{g'} \right) \cos^2 Bz dz}{\displaystyle W_0 \frac{\pi}{2} \left(\sum_{g=1}^{\mathrm{NOG}} \varphi^{*g} \chi^g \right) \left(\sum_{g=1}^{\mathrm{NOG}} \nu \Sigma_f^g \varphi^g \right)}. \\ \rho = -\dfrac{\displaystyle\sum_{g'=1}^{\mathrm{NOG}} \varphi^{*g} \left(D^g B^2 \varphi^g + \Sigma_r^g \varphi^g - \chi^g \sum_{g'=1}^{\mathrm{NOG}} \nu \Sigma_f^{g'} \phi^{g'} - \sum_{g'=g-1}^{1} \Sigma_s^{g' \to g} \varphi^{g'} \right)}{\displaystyle\left(\sum_{g=1}^{\mathrm{NOG}} \varphi^{*g} \chi^g \right) \left(\sum_{g=1}^{\mathrm{NOG}} \nu \Sigma_f^g \varphi^g \right)} \end{cases} \tag{11.72}$$

Note that the numerator contains the exact material properties and flux shape functions. If we make the linear perturbation approximation, this can be rewritten as

$$\rho = -\frac{\sum_{g'=1}^{\mathrm{NOG}} \varphi_0^{*g} \left(\delta D^g B^2 \varphi_0^g + \delta \Sigma_r^g \varphi_0^g - \chi^g \sum_{g'=1}^{\mathrm{NOG}} \delta v \Sigma_f^{g'} \varphi_0^{g'} - \sum_{g'=g-1}^{1} \delta \Sigma_s^{g' \to g} \varphi_0^{g'} \right)}{\left(\sum_{g=1}^{\mathrm{NOG}} \varphi^{*g} \chi^g \right) \left(\sum_{g=1}^{\mathrm{NOG}} v \Sigma_f^g \varphi^g \right)}, \tag{11.73}$$

where basically we have subtracted off the critical equation and said that the product of two small changes is negligible compared to a single small change.

Problems

Problem 11.1: Thermal Reactor Example

Consider a thermal reactor example. The following results were obtained for a six-group model of the Advanced Reactivity Measurement Facility reactor: a small 93 % enriched aluminum, slab core reactor. The model is based on a bare core version of this reactor shaped into a cube with a 51.09 cm side dimension. This gave a buckling of $B^2 = 0.011344/\text{cm}^2$. Note that this is a fairly small reactor.

Consider the following results.

Group	Upper energy	Velocity (cm/s)	$v\Sigma_f$	Flux	Adjoint	χ_p	χ_d	χ
1	17.33 MeV	4.24(+9)	0.000643	0.03691	0.122862	0.05258	1.27(−6)	0.05221
2	4.97.MeV	2.24(+9)	0.000492	1.00383	0.531294	0.52040	0.050525	0.51711
3	1.35 MeV	8.66(+8)	0.000433	2.03885	0.695888	0.41086	0.803196	0.41361
4	111.0 keV	1.93(+8)	0.000854	0.59341	0.849079	0.01608	0.145344	0.01699
5	3.35 keV	5.95(+6)	0.01863	1.89784	0.875391	8.0(−5)	0.000933	8.6(−5)
6	0.100 eV	2.20(+5)	0.18219	1.00000	1.000000	0.0	0.0	0.0

Calculate the normalization factor.

Calculate $\beta_{\text{effective}}$ and β_{physica} for this problem.

Problem 11.2: The thermal absorption cross section for Xe-135 at 2200 m is 2.7E + 6 barns. Based on the bounds developed in class, what is the maximum absorption cross section that could be expected at 0.0253 eV for this nuclide? Estimate the total cross section at 2.0 MeV also.

Problem 11.3: Determine the thermal lifetime or diffusion time of neutron in the bare critical reactor where $L^2 = 57.3$ and $B^2 = 0.0051\ \text{cm}^{-2}$ and consisting of beryllium and uranium-235 in the atomic ratio of 10^4 to 1.

Problem 11.4: The reactivity in a steady-state reactor, in which the neutron generation time is 10^{-3} s, is suddenly made 0.0022 positive; assuming one group of delayed neutrons, determine the subsequent change of neutron flux with time. Compare the stable period with that which would result no delayed neutrons. Use the following equation for the variation of the neutron density with time as

$$n \approx n_0 \left[\frac{\beta}{\beta - \rho} \mathrm{e}^{\frac{\lambda \rho t}{\mathrm{e}\beta - \rho}} - \frac{\rho}{\beta - \rho} \mathrm{e}^{-\frac{(\beta - \rho)t}{l^*}} \right] \tag{11.74}$$

In addition, for the stable reactor period, assuming one (average) group of delayed neutron is given by

$$T_{\mathrm{p}} \approx \frac{\beta - \rho}{\lambda \rho} \tag{11.75}$$

Assume, on average, for one group of delayed neutron, λ is 0.08 s^{-1}; ρ is given as 0.0022 and neutron generation time l^* as 10^{-3} s; β for uranium-235 is 0.0065.

Problem 11.5: The prompt neutron lifetime in a reactor moderated by heavy water is 5.7×10^{-4} s. For a reactivity of 0.00065, express the reactor period in (a) second, (b) inhours (Ih), using the relationship between reactor period T_{p} and inhours (Ih) as $T_{\mathrm{p}} \approx 3600/\mathrm{Ih}$. What is the reactivity in dollar units? Assume for very long periods and very small reactivity following equation applies and $(\beta/\lambda) = 0.084$

$$T_{\mathrm{p}} \approx \frac{\beta}{\lambda \rho} \tag{11.76}$$

where:

T_{p} = Reactor period
β = Total fraction of delayed neutrons = 0.0065
λ = Radioactive decay constant
ρ = Reactivity

In addition, the unit that is called “the dollar” is defined by

$$\text{Reactivity in dollars} \equiv \frac{\rho}{\beta}$$

Problem 11.6: As part of one-group point kinetics equation, if we assume a case for when only one group of delayed neutron is assumed, the results of solution provide a polynomial in the denominator as part of general solution, when we assume source term is constant and equal to S_0 with two roots of s_1 and s_2 of the following mathematical notation:

$$s_{1,2} = \frac{-\left(\frac{\beta}{\Lambda} - \frac{\rho_0}{\Lambda} + \lambda\right) \pm \sqrt{\left(\frac{\beta}{\Lambda} - \frac{\rho_0}{\Lambda} + \lambda\right)^2 + 4\frac{\lambda\rho_0}{\Lambda}}}{2} \tag{11.77}$$

where:

β = Fractional yield of the delayed neutrons
Λ = Average neutron generation time
ρ_0 = Reactivity for constant source S_0
λ = Decay constant

Then, the neutron flux can be obtained as

$$\begin{aligned} n(t) &= n_e x(t) + n_e \\ &= n_e\left\{1 + \left(\frac{\rho_0}{\Lambda} + \frac{S_0}{n_e}\right)\left[\frac{\lambda}{s_1 s_2} + \frac{s_1 + \lambda}{s_1(s_1 + s_2)}e^{s_1 t} + \frac{s_2 + \lambda}{s_2(s_2 - s_1)}e^{s_2 t}\right]\right\} \end{aligned} \tag{11.78}$$

where:

$n(t)$ = Neutron density as function of time t
n_e = Neutron density at equilibrium

Assuming one group of delayed neutrons, determine the subsequent change of neutron flux with time. Additionally, the reactivity is taking place in a steady-state thermal reactor with no external neutron source, in which the neutron generation time $\Lambda = 10^{-3} s$ is suddenly made 0.0022 positive and following data applies. $\lambda = 0.08 s^{-1}$ and $\beta = 6.5 \times 10^{-3}$.

Problem 11.7: A critical reactor operated during a long period of time; the mean weighted number of neutrons was equal to $n_e = 10^6$. Suddenly a source of neutrons with mean weighted yield equal to $S_0 = 10^6 \mathrm{s}^{-1}$ was introduced into the reactor. Find the number of neutrons as a function of time, $n(t)$. In calculations assume one group of delayed neutrons with $\lambda = 0.1\, s^{-1}$ and $\beta = 6.4 \times 10^{-3}$ and the mean generation time $\Lambda = 10^{-3}$ s.

Problem 11.8: An under-critical reactor operated during a long period of time with the reactivity equal to $\rho_0 = -9\beta$. A source of neutrons with a mean weighted yield equal to $S_0 = 10^6 \mathrm{s}^{-1}$ was present in the reactor. Suddenly the source of neutrons was removed from the reactor. Find the number of neutrons as a function of time, $n(t)$. In calculations assume one group of delayed neutrons with $\lambda = 0.1\, s^{-1}$ and $\beta = 6.5 \times 10^{-3}$ and the mean generation time $\Lambda = 10^{-3}$ s. Note that the equilibrium number of neutrons before the removal of the source is given by $n_e = -S_0\Lambda/\rho_0$.

References

1. J. Koclas, Neutronic Analysis of Reactor, Nuclear Engineering Department at Ecole Polytechnique de Montreal (1998)
2. J. Duderstadt, L. Hamilton, *Nuclear Reactor Analysis* (Wiley, New York, 1976)

Chapter 12
Reactor Dynamics

In order for nuclear fission power to operate at a constant power level, the rate of neutron production via fission reactions must be exactly balanced by neutron loss via absorption and leakage. If we deviate from this simple balancing role, it would cause in a time dependence of neutron population and therefore the power level of the reactor. Such situation may take place, for a number reasons, such as reactor operator may have a requirement to change the reactor power level by temporarily altering the control fuel rod so it will change the core or source multiplication, or there may be long-term changes in core multiplication due to fuel depletion and isotopic buildup. Other examples may also be encountered that requires attention and adjustment to the day-to-day operation of the reactor, such as unforeseen accident or failure of primary coolant pump system, etc. The topic of *nuclear kinetic reactor* as we have learned in the previous chapter is handling this situation by allowing us to be able to predict the time behavior of the neutron population in a reactor core driven by changes in reactor multiplication, which is not a circumstance that is totally controlled by the operator of power plant and reactor core. Furthermore, variables such as indirect accessibility to control such fuel temperature or coolant density distribution throughout the reactor do have impact to the situation. However, these variables depend on the reactor power level and hence the neutron fluxes itself. Additionally, the study of the time dependence of the related process, which is involved with determining the core multiplication as a function of power level of the reactor multiplication, is the subject of our study in this chapter, and it is called *nuclear reactor dynamics*. This usually involves with detailed modeling of the entire nuclear steam supply system, which is part of *feedback* system as well.

B. Zohuri, *Neutronic Analysis For Nuclear Reactor Systems*,
DOI 10.1007/978-3-319-42964-9_12

12.1 Background on Nuclear Reactor

As we know from our basic knowledge of nuclear reactor, their main task is to produce and control the release of energy from splitting the atoms of certain elements, via carrying out the chain reaction in a controlled way and then using the resultant heat to produce steam that turns a generator to produce electricity for our day-to-day consumption. See Fig. 12.1, which shows a typical modern pressurized water reactor (PWR) with its primary and secondary loops.

For a nuclear power plant to achieve the task of producing electricity driven by split of atom of certain elements in a controlled chain reaction way, there exist three fundamental ways, and they are listed below as:

1. Thermal MWt, which depends on the design of the actual nuclear reactor itself and relates to the quantity and quality of the steam it produces.
2. Gross electrical MWe indicates the power produced by the attached steam turbine and generator and takes into account the ambient temperature for the condenser circuit (cooler means more electric power, warmer means less) as well. Rated gross power assumes certain conditions with both.
3. Net electrical MWe, which is the power available to be sent out from the plant to the grid, after deducting the electrical power needed to run the reactor (cooling and feed-water pumps, etc.) and the rest of the plant [1].

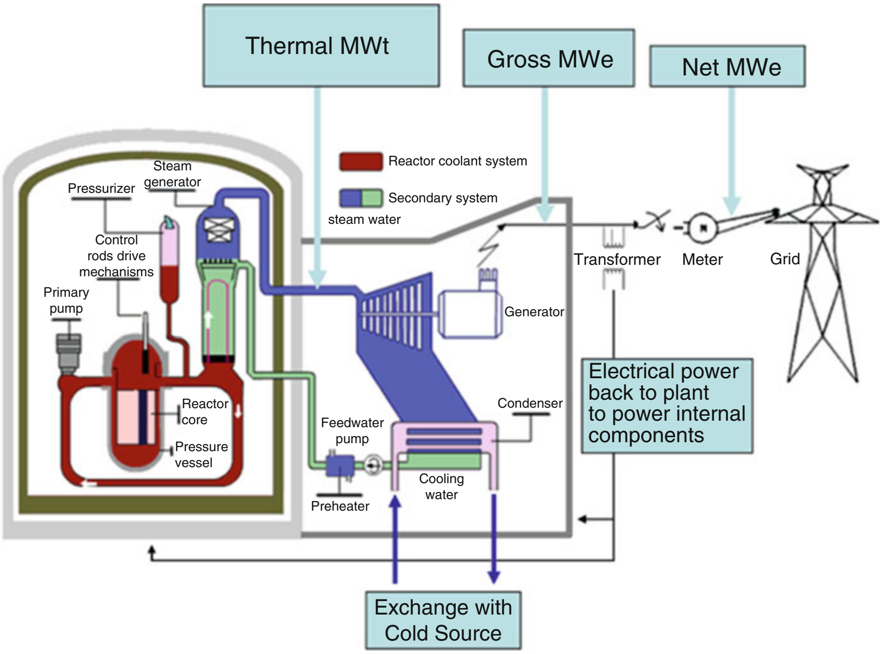

Fig. 12.1 Typical schematic of pressurized water reactor producing electricity (Courtesy of US National Nuclear Regulatory Commission)

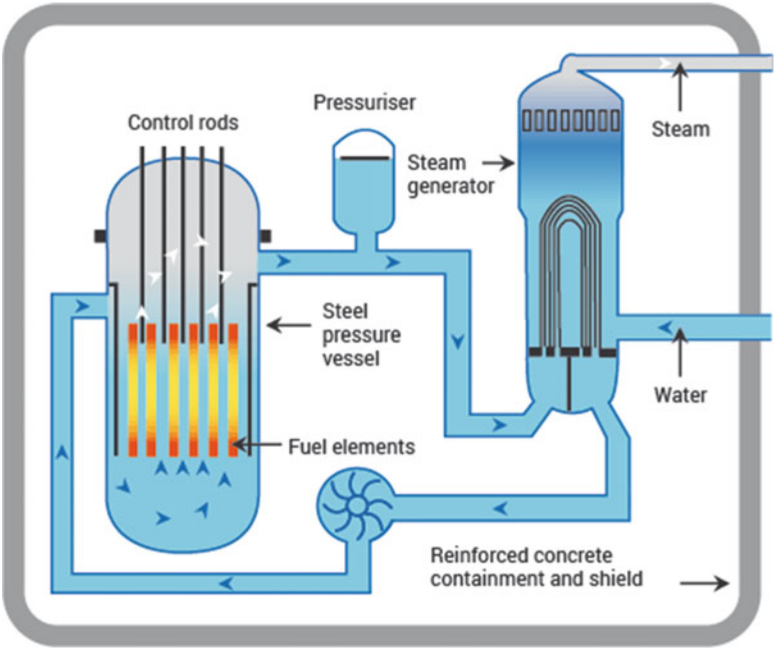

Fig. 12.2 Core of a pressurized water reactor (PWR) (Courtesy of US National Nuclear Regulatory Commission)

The relationship between those three fundamental ways is expressed in two ways as below:

- Thermal efficiency %, the ratio of gross MWe to thermal MW. This relates to the difference in temperature between the steam from the reactor and the cooling water. It is often 33–37 %.
- Net efficiency %, the ratio of net MWe achieved to thermal MW. This is a little lower and allows for plant usage.

Pressurized water reactor (PWR), as it is shown in Fig. 12.2, is the most common type, with estimated over 230 in use for power generation and several hundred more employed for naval propulsion. The design of PWRs originated as a submarine power plant. PWRs use ordinary water as both coolant and moderator. The design is distinguished by having a primary cooling circuit, which flows through the core of the reactor under very high pressure and a secondary circuit in which steam is generated to drive the turbine. In Russia, these are known as VVER types—water moderated and cooled.

A PWR has fuel assemblies of 200–300 rods each, arranged vertically in the core, and a large reactor would have about 150–250 fuel assemblies with 80–100 tons of uranium.

Water in the reactor core reaches about 325 °C; hence, it must be kept under about 150 times atmospheric pressure to prevent it boiling. Pressure is maintained by steam in a pressurizer (see diagram). In the primary cooling circuit, the water is also the moderator, and if any of it turned to steam, the fission reaction would slow down. This negative feedback effect is one of the safety features of the type. The secondary shutdown system involves adding boron to the primary circuit.

The secondary circuit is under less pressure, and the water here boils in the heat exchangers, which are thus steam generators. The steam drives the turbine to produce electricity and is then condensed and will be returned to the heat exchangers in contact with the primary circuit.

12.2 Neutron Multiplication

It is important for a reactor operator to know how to handle starting of a reactor for the first time. For instance, either first-time start-up of a new reactor coming on line, after refueling the critical level of the control fuel rods, is not known; therefore, the control rod withdrawal must be done cautiously in order to avoid supercriticality and an unexpected power. The level of control rod criticality could be determined by monitoring the neutron flux in the core, while withdrawing the control rods, which is a common practice as part of safety procedure and always should be performed at first start-up of any nuclear fission-powered reactors.

Having the basic consideration in the above, we introduce a source of neutrons, represented by symbol of S into a subcritical reactor with multiplication factor k. In that case, there will be $S.\ k$ neutrons after the first fission generation, $S.\ k^2$ neutrons after the second generation, and so on, so that the total number of neutrons per source neutrons after many generations approaches a geometrical series as

$$M = \frac{\left(1 + k + k^2 + \cdots\right)S}{S} = \frac{1}{1 - k} \tag{12.1}$$

In Eq. 12.1, M is called the *core or source multiplication*, describing the ratio of the fission source to the external source, and gives consequently the total number of neutrons appearing in the fissionable materials per source neutron.

The multiplication factor k is defined as before:

$$k \equiv \text{Multiplication factor} \equiv \frac{\text{Number of neutrons in one generation}}{\text{Number of neutrons in preceding generation}}$$

However, since the number of fission neutrons v in any generation is proportional to the number of fission events spawning that generation, by knowing the fact that each fission reaction releases, on the average, v fission neutrons, then we could justify to easily defining multiplication factor k using the number of fission events in each generation as well.

Additionally, note that since the expression is valid for a subcritical system, where multiplication factor $k < 1$. It can also be seen that both reciprocal source multiplication factors, $1/M$ and $1 - k$, decrease when approaching criticality, so we can write

$$\frac{1}{M} = 1 - k \tag{12.2}$$

This relationship is often employed in bringing a reactor system to criticality, by extrapolating to the critical condition. If, for example, the operator starts withdrawing control rods, the multiplication constant, and thus the source multiplication factor M, increases with increasing rod withdrawal. When the reactor reaches critical condition, the source multiplication factor becomes infinite. This "approach to criticality" is monitored by placing a neutron source in the reactor and measuring the neutron flux for various rod positions. The neutron count rate is proportional to M. A plot of the inverse counting rate or $1/M$ as a function of rod position becomes equal to zero at the critical condition. If we extrapolate a curve to the zero value, then we can predetermine the control rod position at which the critical condition will be reached.

This discussion is valid under the assumptions that the reactor is reasonably close to critical and that the neutron population is in equilibrium. If the reactor is far below critical, then Eq. 12.2 is not valid. Equation 12.2 only applies to the multiplication of neutrons in the *eigenstate*. Eigenstate in this sense refers to neutrons such that their energy spectrum and spatial distribution are characteristic of the reactor, i.e., asymptotic spectrum, so-called fundamental mode distribution, and with an effective multiplication factor k_{eff}. Source neutrons, in general, do not have these properties and multiply differently compared to eigenstate neutrons. In that case, we cannot formulate a simple geometric series, based on a single k-value. In close-to-critical conditions, this effect has negligible influence since source neutrons are small in number in comparison to the total neutron population. The neutron flux is characterized by the eigenstate at criticality.

Although the measurement of source multiplication is a static technique, there are time-dependent effects that can be important in the interpretation of results. The multiplication following a reactivity change (e.g., change in control rod position) in a subcritical system is observed only after all delayed neutrons have attained equilibrium concentration. During a sequence of stepwise addition of reactivity, as in following "$1/M$" approach to criticality, the total asymptotic multiplication will clearly be observed at each step if one waits sufficiently long after each reactivity addition. Nevertheless, if reactivity is added too rapidly—either stepwise or continuously—the observed multiplication will lag the asymptotic multiplication thus giving an underestimate of the instantaneous multiplication of the system. The physical reason for this transient effect is clear. The equilibrium condition is identified by a self-sustained constant power level only when all delayed neutron precursors are in equilibrium, meaning that the formation rate of delayed neutron precursors equals the decay rate.

Under very weak source conditions, the neutron level during the early stages of start-up is so low that statistical fluctuations tend to dominate and the kinetics equations are not applicable. At later stages, the power level becomes sufficiently high and statistical fluctuations are no longer important. In general, distorting effects become relatively small near criticality, and extrapolated critical points become progressively more reliable as the critical condition is approached.

12.3 Simple Feedbacks

The feedback system plays an important role in the study of nuclear reactor dynamics, where the detailed modeling of steam supply system is involved. The feedback mechanisms is consist of determining core multiplication and mainly concentrates in the prediction of the time behavior of the neutron flux in the reactor for a given change in multiplication, basically, transient analysis that we need to study and model.

The main task of such application is an analysis not only dealing with the study of operating transients in the reactor but also to the predication of the consequences of accidents involving changes in core multiplication and to the interpretation of experimental techniques measuring reactor parameters by inducing time-dependent changes in neutron flux [2].

As we started our discussion about nuclear reactor dynamics, which it concerns with the analysis of the time-dependent behavior of the nuclear reactor both under normal operation status and during accidents encountering. In addition, this concern deals with the interpretation of most reactor physics, experiments that are involving with reactivity $\rho(t)$ changes required by the analysis of core dynamics, which is a time-dependent and transient form.

Again talking about nuclear reactor kinetics, which is generally an indication of time dependency of the neutron population. On the contrary, the dynamics of nuclear reactor also includes all the aspect of reactor kinetics and additionally is involved in the temperature T and feedback of control system. Kinetics of nuclear reactor could be described as a set of equations connecting the variables describing the state of the system, and variables involve in this are the neutron flux $\phi(\vec{r}, t)$ and the temperatures of the various reactor components. This together with the parameters, which can drive quantities such as poison concentrations, cross sections, coolant mass flow, etc., of the system as well as data describing the causes of the transients, is part of nuclear reactor kinetics studies [3].

The part of the task assigned to the study of nuclear reactor kinetics involves with a parameter known as *kinetics equation*, which is the equation connecting the neutron flux to the other system variables such as temperatures at each component level. Further analysis of kinetics equation indicates that its coefficients are usually temperature dependent, and the equation cannot be solved without taking the reactor heat transfer equations, under consideration. This includes the point reactor kinetics modeling and the involvement of delayed neutron β in reactor kinetics analysis. Therefore, understanding time-dependent behaviors of nuclear reactors and the methods of their control is essential to the operation and safety of nuclear power plants.

As we did learn from previous chapters for a simple bare slab reactor analysis, we found the neutron flux $\phi(\vec{r}, t)$ in such a system as a superposition of spatial modes in terms of eigenfunctions which represents the characteristic of the reactor geometry and each weighing with an exponentially varying time dependence presented in the following equation as [2]

$$\phi(\vec{r}, t) = \sum_n A_n \exp(-\lambda_n t)\psi_n(\vec{r}) \tag{12.3}$$

Equation 12.3 is the solution of the eigenvalue problem of the following:

$$\nabla^2\psi_n(\vec{r}) + B_n^2\psi_n(\vec{r}) = 0 \qquad \psi_n(\widetilde{r}_s) = 0 \tag{12.4}$$

The time eigenvalues λ_n were given by

$$\lambda_n = vDB_n^2 + v\Sigma_a + \nu v\Sigma_f \tag{12.5}$$

where v is neutron velocity corresponding to energy E, and it is the distance traveled by the neutron in unit time, with that velocity, while ν is the average number of fission neutron emitted per fission at the energy E as well.

Note that Eq. 12.3 is a form of Helmholtz equation, where $\psi_1(\vec{r})$ is the fundamental mode or eigenfunction of this equation.

These eigenvalues are ordered as $-\lambda_1 > -\lambda_2 > \cdots$. Hence, for long times the flux approaches an asymptotic form as

$$\phi(\vec{r}, t) \approx A_1 \exp(-\lambda_1 t)\psi_1(\vec{r}) = A_1 \exp\left[\left(\frac{k-1}{l}\right)\right]$$

$$\equiv \text{Mean lifetime of neutron in reactor} \tag{12.6}$$

$$k \equiv \frac{\nu\Sigma_f/\Sigma_a}{1 + L^2B_g^2} \equiv \text{Multiplication factor} \tag{12.7}$$

However, the concern is how long it takes for this asymptotic behavior to settle. This matter can be answered simply by assuming that the reactor is operating in a critical state such that $\lambda_1 = 0$ and then estimate λ_n. The estimation of λ_n also can be done by recalling that for a slab $B_n^2 = n^2(\pi/\widetilde{a})^2$ and for a typical reactor, where $\widetilde{a} \sim 300\,\text{cm}$, $v \sim 3 \times 10^{15}\,\text{cm/s}$, and $D \sim 1$, we have

$$\begin{cases} \lambda_n = -vD\left(B_n^2 + B_m^2\right) \\ \quad = -vD\left(B_n^2 + B_g^2\right) \\ \quad = -vD(n^2 - 1)\left(\dfrac{\pi}{\widetilde{a}}\right) \end{cases} \tag{12.8}$$

Alternatively, plugging the give values for thermal reactor, we obtain

$$\begin{cases} \lambda_n = -3 \times 10^5 (\mathrm{cm/s}) \cdot (1) \cdot (n^2 - 1) \cdot \left(\dfrac{3.14}{300\ \mathrm{cm}} \right)^2 \\ \lambda_n \approx 3.28(n^2 - 1) \end{cases} \tag{12.9}$$

Hence, it shows that the higher order of λ_n is of the order of 100–1000 s^{-1}, which implies that the higher-order spatial modes die out very rapidly indeed [2].

Now that we briefly have discussed a nuclear power reactor and we have better understanding of reactor kinetics, we pay our attention to the subject in hand and that is reactor dynamics. Reactor dynamics starts with handling a simple reactivity feedback for the reactivity $\rho(t)$ that was appearing in the study of point kinetics equation in Chap. 11 of the book, and it is given as function of time t. In reality, the reactivity $\rho(t)$ depends on the neutron flux which is the presentation power level in any nuclear reactors. This dependency is due to the fact that reactivity depends on macroscopic cross sections, which themselves depend on the atomic number density $N(\vec{\boldsymbol{r}}, t)$ of materials in the core as it is shown mathematically here:

$$\Sigma(\vec{\boldsymbol{r}}, t) = N(\vec{\boldsymbol{r}}, t)\sigma(\vec{\boldsymbol{r}}, t) \tag{12.10}$$

Further, analysis of Eq. 12.10 reveals why the atomic number density $N(\vec{\boldsymbol{r}}, t)$ can depend on the nuclear reactor power level, and the reasons are summarized here as: [2]

(a) Material densities have dependency on the temperature T, which itself depends on the power distribution and hence the flux.
(b) The concentrations of certain nuclei that are constantly changing due to neutron interactions such as buildup of poison or burnup of fuel.

However, we should note that so far we have treated the microscopic cross section as explicit function of spatial position $\vec{\boldsymbol{r}}$ and time t. This can be achieved, because the cross sections that appear in one-speed diffusion model of neutronic analysis are actually averages of the true energy-dependent microscopic cross sections over an energy $\chi(E)$ spectrum characterizing the neutrons in the nuclear reactor core. Additionally, this neutron energy spectrum will itself depend on the temperature distribution T in the core and hence the reactor power level.

As we talked and learned from Chap. 7 so far, the elastic scattering cross section is mostly constant in all the energies except for the MeV region. Meanwhile, in inelastic scattering, the incident neutron should have sufficient kinetic energy to place the target nucleus in its excited state. Hence, the inelastic scattering cross section is zero up to some threshold energy of several MeV. Fast neutrons can be moderated by inelastic scattering with heavy nuclides, but by elastic scattering with light nuclides below threshold energies of the heavy nuclides [4].

In Chap. 7, we discussed that most absorption cross sections including the fission cross section appear as a straight line with a slope of $-1/2$ on a log–log scale.

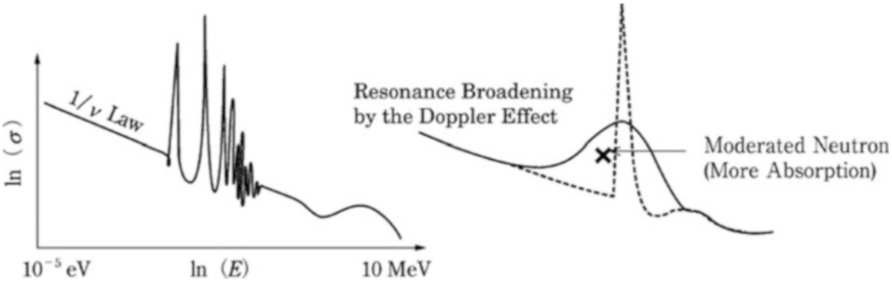

Fig. 12.3 Resonance absorption cross section and Doppler effect [4]

This means that the absorption cross sections are inversely proportional to the neutron speed ($1/v$) law as we discussed before and therefore increase as the neutron energy decreases. Using such large fission cross sections at low neutron energies and thermal neutrons in the Maxwellian distribution makes it possible that natural or low-enrichment uranium-fueled reactors reach a critical state. The current thermal reactors, represented by LWRs, use the characteristics of the cross section [4].

For heavy nuclides such as fuel materials, many resonances are observed in elastic scattering and absorption cross section as shown in Fig. 12.3. The widths of the resonances broaden as fuel temperature increases. And also, as what we have learned from Chap. 7, this was called Doppler effect, and the width broadening facilitates resonance absorption of neutrons under moderation [4].

Most low-enrichment uranium fuel is composed of fertile U^{238}, and thermal neutrons escaping from the resonance of capture reaction induce fissions for the next generation.

Hence, a rise in fuel temperature leads to a decrease in resonance escape probability of moderated neutrons, and then fission events in the reactor decrease with thermal neutrons. Such a mechanism is called *negative temperature feedback*. The temperature dependence, T, is not described in the Boltzmann Eq. 3.1; however, it is reflected in the cross sections of the equation [4].

One more phenomenon is worth to mention in the analysis of nuclear reactor dynamics, and characterizing its behavior is the presence of the delayed neutrons. The β-decay of a fission product leads in some cases to a highly excited similar product, which can then emit a neutron. These fission products as we have said are commonly called delayed neutrons precursors.

Note that in nuclear reactor dynamics, for reactivity ρ much larger than neutron decay β, i.e., $\rho \gg \beta$, we can ignore the delayed neutron, and as a result, the precursor equation in point kinetics equation (PKE) goes away. In that case, we are left with the power distribution $P(t)$ with no precursor term as below, which is same equation as what it was mentioned in Chap. 11, and it was written in the form of Eqs. 11.31, 11.37, and 11.38:

$$\frac{d}{dt}P(t) = \frac{\rho(t) - \beta}{\Lambda}P(t) + \sum_i \lambda_i C_i(t) \approx \frac{\rho(t) - \beta}{\Lambda}P(t) \tag{12.11}$$

The historical reason behind ignorance of the delayed neutron for $\rho \gg \beta$ assumption goes to the nuclear weapon design, where the model was developed and used, hence $\rho \gg \beta$ and rapid transient. We also use $P(t)$ instead of $T(t)$ that was used in Chap. 11 to represent the amplitude function, to avoid the confusion with temperature T that we are using repeatedly in this section. The ignorance assumption can be explained by Fuchs–Nordheim for no precursors in Eq. 12.8, which is the subject of the next section of this chapter and can be observed in Fig. 12.4:

The analysis of Fig. 12.4 reveals that we can see that the power with precursor is small enough that the Fuchs–Nordheim (F–N) model provides a good approximation; the bottom row images are plotted on a log–log scale to show the small difference made by the precursors.

Back to the mainstream of our subject of feedback phenomena and nuclear reactor dynamics analysis, we mention that the neutron emission follows, almost immediately within roughly 10^{-14} s, the β radiation, and the delay of the neutron is

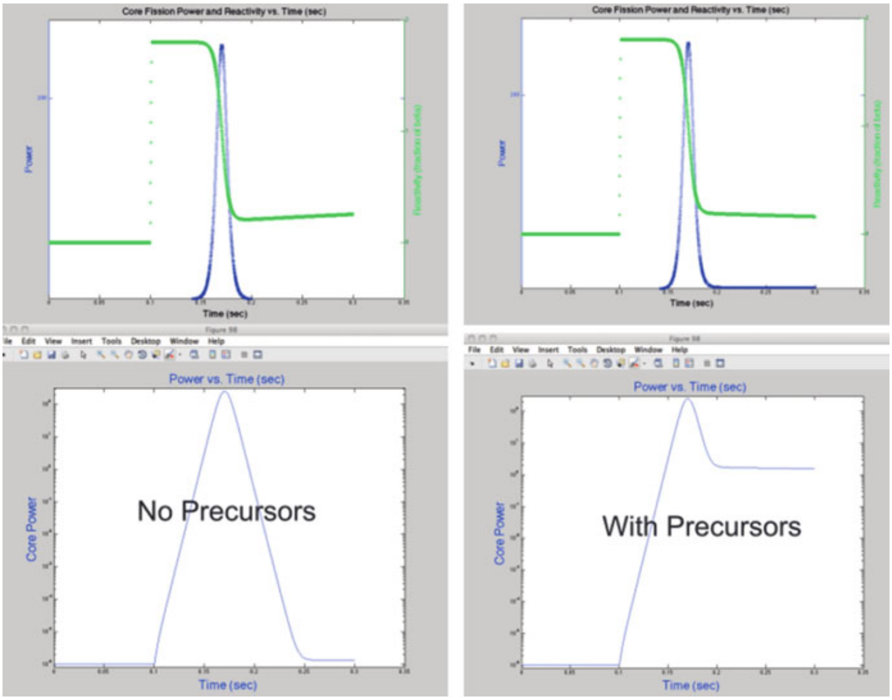

Fig. 12.4 Assumption in Fuchs–Nordheim, no precursors

Table 12.1 Delayed neutron data for thermal fission U^{235}

Group	Half-life[a], $t_{1/2}$ [s]	Decay constant, λ_i [s^{-1}]	Mean energy [keY]	Yield, v_i [n/ fissions × 100]	Fraction, β_i [pcm]
1	54.6 ± 0.9	0.0127 ± 0.0002	250 ± 20	$0.060 \pm 0.0\ 05$	21.5
2	21.9 ± 0.6	0.0317 ± 0.0008	460 ± 10	0.364 ± 0.0013	142.4
3	6.0 ± 0.2	0.115 ± 0.003	405 ± 20	$0.349 \pm 0.0\ 24$	127.4
4	2.23 ± 0.06	0.311 ± 0.003	450 ± 20	0.628 ± 0.015	256.8
5	0.50 ± 0.03	1.40 ± 0.081	–	0.179 ± 0.014	74.8
6	0.18 ± 0.02	3.87 ± 0.37	–	0.070 ± 0.005	27.3

[a] The values are calculated from the decay constants, which are true experimental values, through the relation $t_{1/2} = \ln(2)/\lambda$

determined by the β-decay constants of the parent nuclide, which ranges from milliseconds to minutes. The delayed neutrons are usually grouped to more or less six groups according to the β-decay of the parent nuclides. Table 12.1 shows the six groups as an example of experimental data collected for delayed neutron β_i data for thermal fission in U^{235} along with decay constant λ_i and other related parameters. Here, β-decay is related to β_i by the following relationship:

$$\sum_{i=1}^{m} \beta_i = \beta \qquad i = 1, 2, \ldots, m \tag{12.12}$$

Equation 12.12 defines β_i as the yield of group i of delayed neutrons and β_i and β are for various fissionable isotopes. These are given in Tables 12.1 and 12.2, together with the decay constant of the delayed neutron precursors.

G. R. Keepin [5] provides more complicated version of Table 12.1, and we are presenting a partial version of it here in Table 12.2.

The time variation of the reactor state is the result of various phenomena, which includes:

- Fuel burnup
- Fission product buildup and decay
- Temperature variations
- Reactivity changes due to movement of absorber rod or other geometrical and material changes within the reactor

Each of these phenomena is characterized by a different time constant. The result of reactivity changes $\rho(t)$ is usually rapid transients, which as we mentioned in above has historical weapon design applications. However, in our case the time constant is determined by the lifetime of the prompt and delayed neutrons.

Table 12.2 Delayed neutron, half-lives, decay constants, and yield [5]

Group index, *i*	Half-life, s	Decay constant λ_i s^{-1}	Relative abundance $\alpha_i \equiv \beta_i/\beta$
^{235}U (99.9 % 235)			
1	54.51 ± 0.94	0.0127 ± 0.0002	0.038 ± 0.003
2	21.84 ± 0.54	0.0317 ± 0.0008	0.213 ± 0.005
3	6.00 ± 0.17	0.115 ± 0.003	0.188 ± 0.016
4	2.23 ± 0.06	0.311 ± 0.008	0.407 ± 0.007
5	0.496 ± 0.029	1.40 ± 0.081	0.128 ± 0.008
6	0.179 ± 0.017	3.87 ± 0.369	0.026 ± 0.003
^{238}U (99.98 % 238)			
1	52.38 ± 1.29	0.0132 ± 0.0003	0.013 ± 0.001
2	21.58 ± 0.39	0.0321 ± 0.0006	0.137 ± 0.002
3	5.00 ± 0.19	0.139 ± 0.005	0.162 ± 0.020
4	1.93 ± 0.07	0.358 ± 0.014	0.388 ± 0.012
5	0.490 ± 0.023	1.41 ± 0.067	0.225 ± 0.013
6	0.172 ± 0.009	4.02 ± 0.214	0.075 ± 0.005
^{238}U (100 % 233)			
1	55.11 ± 1.86	0.0126 ± 0.0004	0.086 ± 0.003
2	20.74 ± 0.86	0.0334 ± 0.0014	0.274 ± 0.005
3	5.30 ± 0.19	0.131 ± 0.005	0.227 ± 0.035
4	2.29 ± 0.18	0.302 ± 0.024	0.317 ± 0.011
5	0.546 ± 0.108	1.27 ± 0.266	0.073 ± 0.014
6	0.221 ± 0.042	3.13 ± 0.675	0.023 ± 0.007
^{239}Pu (99.8 % 239)			
1	53.75 ± 0.95	0.0129 ± 0.0002	0.086 ± 0.003
	22.29 ± 0.36	0.0311 ± 0.0005	0.274 ± 0.005
3	5.19 ± 0.12	0.134 ± 0.003	0.216 ± 0.018
4	2.09 ± 0.08	0.331 ± 0.012	0.328 ± 0.010
5	0.549 ± 0.049	1.26 ± 0.115	0.103 ± 0.009
6	0.216 ± 0.017	3.21 ± 0.255	0.035 ± 0.005
^{240}Pu (81.5 % 240)			
i	53.56 ± 1.21	0.0129 ± 0.0004	0.028 ± 0.003
	22.14 ± 0.38	0.0313 ± 0.0005	0.273 ± 0.004
3	5.14 ± 0.42	0.135 ± 0.011	0.192 ± 0.053
4	2.08 ± 0.19	0.333 ± 0.031	0.350 ± 0.020
s	0.511 ± 0.077	1.36 ± 0.205	0.128 ± 0.018
6	0.172 ± 0.033	4.04 ± 0.782	0.029 ± 0.006
^{232}Th (100 % 232)			
1	56.03 ± 0.95	0.0124 ± 0.0002	0.034 ± 0.002
i	20.75 ± 0.66	0.0334 ± 0.00 11	0.150 ± 0.005
3	5.74 ± 0.24	0.121 ± 0.005	0.155 ± 0.021
4	2.16 ± 0.08	0.321 ± 0.011	0.446 ± 0.015
5	0.571 ± 0.042	1.21 ± 0.090	0.172 ± 0.013
6	0.211 ± 0.019	3.29 ± 0.297	0.043 ± 0.006

12.4 Multiple Time Constant Feedbacks

We also need to know that temperature feedbacks have time constants determined by the heat capacity and conductivity of the fuel as well as moderator. Fission product build, decay, and fuel burnup are usually characterized by very long-time constants. Most short-lived fission products do not have a need to be treated explicitly, with exception of element Xe^{135}, because of its huge high thermal absorption cross section [3].

The stable nuclide Sm^{149} element gives rise to transients with short time constant because it has a high cross section and a short-lived parent element. For Xe^{135} and Sm^{149} transients, the time constants vary between 9 and 48 h.

Each of these phenomena could mathematically be expressed in terms of sets of differential equations, and as a general rule, it is possible to treat independently transients with widely differing time constants. Readers should refer themselves to the book by Massimo [3] to seek solution procedures for these differential equations.

As we have already mentioned, the feedback of the control system on the reactor acts through two quantities and they are as follows:

1. The control of fuel rod position
2. The coolant mass flow

For reactor accident analysis, where we deal with short-time dynamics, it is not usually necessary to involve the complicated system of equations describing the core dynamics behavior in order to describe the control system. However, it is sufficient to assume that when given quantities such as neutron flux, coolant outlet temperature, etc., exceed a previously determined designed threshold value, a scram will take place. This induced that a negative reactivity Δk_c given by the control fuel rods and a reduction of the coolant mass flow are introduced as given functions of time [3].

The analysis of long-time dynamics, in the nuclear reactor operation and stability studies for the control system, has to be simulated in the dynamics equations. It is also usually required in this case that power $P_r(t)$ released by the reactor follows a given power diagram $P(t)$, while a given gas outlet temperature T must be maintained. Various methods of regulation and a general regulation of the thermal power through the coolant mass flow $\dot{m}\cdot$ in the reactor can be implemented, and it is presented by [3]

$$\dot{m} = K_P[P(t) - P_r(t)] + K_I \int [P(t) - P_r(t)]dt + K_D \frac{d}{dt}[P(t) - P_r(t)] \tag{12.14}$$

where K_P, K_I, and K_D are the coefficients of the proportional, integral, and differential member, respectively, and

$$P_r(t) = c_p \dot{m} (T_{c2} - T_{c1}) \tag{12.15}$$

where

T_{c1} = coolant inlet temperature
T_{c2} = coolant outlet temperature
C_P = specific heat at constant pressure

A regulation of the gas outlet temperature through the control rod reactivity Δk_c would be given by the following equation as

$$\Delta k_c = K_P(T_{c2} - T_{c1}) + K_I \int [P(t) - P_r(t)]dt + K_D \frac{d}{dt}(T_{c2} - T_{c1}) \tag{12.16}$$

12.5 Fuchs–Nordheim Model

Before we jump on this subject, we remind the readers again about the effect of temperature on reactivity ρ, and as a general consideration, we look as if the power of a nuclear reactor stays constant during the multiplication factor $k_{\text{eff}} = 1$.

At constant power, the cooling system of the reactor removes all the heat that is generated. If the multiplication factor is increased by $\Delta k_{\text{eff}} = k_{\text{eff}} - 1 > 0$, the power of the reactor starts to grow at a rate determined by the magnitude of Δk_{eff}. The cooling system cannot at least immediately absorb all the thermal energy released in fission. However, part of it will raise the temperature of the reactor core. In the absence of any limiting factors, the temperature would rise indefinitely, and finally the core would melt. In cases like this, the temperature dependence of the reactivity $\rho = \Delta k_{\text{eff}}/k_{\text{eff}}$ and the feedback caused by it usually constitute a limiting factor.

The dependence of the reactivity on temperature is described by the temperature coefficient of the reactivity. For that matter, we have to assume that the whole reactor core can be characterized by one single temperature T. The temperature coefficient α is defined as a derivative:

$$\alpha = \frac{d\rho}{dT} \tag{12.17}$$

If we assume that reactivity ρ is expanded into a series of $(T - T_0)$, then the series can be truncated after the first-degree term for a linear relationship. Here T_0 is some suitable reference temperature and α has unit of 1/°C.

If the temperature coefficient α is negative, i.e., the reactivity ρ decreases as the temperature T increases, the reactor will behave stably. When the multiplication factor k for some reason or other undergoes a positive change, the neutron flux and thus the power start to rise. Since all the heat generated is not removed from the reactor, the core temperature will rise. This reduces the reactivity and slows down the increase in power. Finally, the temperature reaches a level where it is sufficient to compensate the completely original reactivity insertion. The power will stop increasing and still rising temperature will start decreasing [6].

Finally, the system will stabilize at a new power level between the original level and the power peak. Such a behavior is, of course, highly desirable for safety reasons. It is easy to accomplish reactor designs, which lead to increased reactivity with rising temperature and, consequently, are inherently unstable. Chernobyl accident is an example of such situation [6].

However, merely a negative temperature coefficient is not a sufficient guarantee for safe operation. Often there is a delay in the feedback between power increase and reduced reactivity. This delay is usually caused by the time needed for heat transfer or, e.g., for expelling the excess water volume created by thermal expansion from the core. If a reactor achieves strong prompt criticality, the power increase will be extremely fast. The heat transfer from the fuel elements to the coolant and moderator is then far too slow to have an influence on phenomena whose time behavior is determined by the neutron lifetime in the core [6].

The phenomena associated with the expulsion of matter from the core also require a time, which is of the same order as the reactor dimensions divided by the speed of sound. For a reactor to be safe even in a prompt critical state, one must therefore require that the temperature coefficient of reactivity be not only negative but also be fast. By fast, we here mean a time, which is short compared to the neutron lifetime [6].

Now that we have established our simple ground rules, we can continue to study the kinetic behavior of the reactor, by stating that the time-dependent neutron flux in a reactor can be described by the point kinetics equation (PKE), which was defined in Chap. 11 as follows without source $S(t)$:

$$\begin{cases} \dfrac{dP(t)}{dt} = \dfrac{k_{\text{eff}}(1-\beta_{\text{eff}})^{-1}}{l}P(t) + \displaystyle\sum_{i=1}^{6}\lambda_i C_i(t) \\ \dfrac{dC_i(t)}{dt} = -\lambda_i C_i(t) + \dfrac{\beta_i k_{\text{eff}}}{l}P(t) \text{ for } i = 1, 2, \ldots, 6 \end{cases} \tag{12.18}$$

Equation 12.18 has been reduced to the form that is shown, based on utilizing the following parameters as

$$\begin{cases} \rho \dfrac{k_{\text{eff}}-1}{k_{\text{eff}}} \\ k_{\text{eff}} = \dfrac{l}{\Lambda} \end{cases} \tag{12.19}$$

where

$P(t)$ = is the reactor power
l = is the prompt neutron lifetime
Λ = is the neutron generation or reproduction time
k_{eff} = is the effective multiplication factor

$C_i(t) =$ is the concentration of delayed neutron precursor of group i

$\lambda_i =$ is the decay constant for delayed neutron precursors of group i

$\beta_i =$ is the fraction of the total number of fission neutrons emitted as delayed neutrons of Group i

Equation 12.18 along with parameters in Eq. 12.19 is considered as one-group space-independent kinetics equation analysis and most frequently used form of point kinetics equation (PKE). Equation 12.18 can be derived easily via the kinetics equation, the neutron energy, and the space dependence to be eliminated by averaging over all energies that is known as one-group approximation. This also requires assumptions that the neutron flux $\phi(\vec{r}, t)$, neutron source $S(\vec{r}, t)$, and delayed neutron precursor concentration $C_i(\vec{r}, t)$ of group i are separable in space and time. See Problem 12.1.

For Eq. 12.19, the effective multiplication factor k_{eff} could be written in the following form:

$$k_{\text{eff}} = 1 + \Delta k_{\text{eff}} + \alpha(T - T_0) \simeq 1 + \rho + \alpha \Delta T \tag{12.20}$$

where $\Delta T = (T - T_0)$ is the value of the temperature T with the reactor running at constant power P_0. The temperature coefficient α has been assumed negative in Eq. 12.20.

In addition, the cooling system of the reactor must be modeled in some way. In the following treatment, the reactor core is assumed to consist only of fuel. It is assumed that during the time interval under consideration, the cooling system removes heat from the fuel elements with a power $\gamma(T - T_c)$ proportional to the difference between the core temperature and an external temperature T_{c}, which is assumed to remain constant. T_{c} mainly describes the temperature of the cooling system, and the proportionality factor γ, which is assumed constant, is then the heat transfer coefficient between the core and the cooling system. Since at constant power the cooling system removes all the heat generated in the core, we have

$$\gamma = \frac{P_0}{T_0 - T_c} \tag{12.21}$$

Here, we have also assumed the heat capacity of the core C also sometimes designated as the heat capacity of the reactor fuel elements is also assumed constant.

Under the above assumptions, we obtain the following equation for the temperature change:

$$\frac{d\Delta T}{dt} = \frac{P - \gamma(T - T_c)}{C} = \frac{(P - P_0) - \gamma \Delta T}{C} \tag{12.22}$$

When the reactivity injection is large enough to make the reactor prompt critical, the so-called Fuchs–Nordheim model can be applied.

However, in all practical purpose of importance, for many cases, the heat capacity, C, of the reactor fuel elements may be assumed to vary linearly with temperature, T, and is written as

$$C = C_0 + \gamma T \tag{12.23}$$

where C_0 and γ are constants. Equation 12.23 is again the definition of Fuchs–Nordheim model, which yields for the equations of motion of the reactor as

$$\frac{dP(t)}{dt} = \frac{\delta k_p - \alpha T(t)}{l} P(t) \tag{12.24a}$$

and

$$C \frac{dT(t)}{dt} = P(t) \tag{12.24b}$$

In both Eqs. 12.24a and 12.24b, the power reactor at time t is designated as $P(t)$, and δk_{p} is the prompt reactivity insert, α is the magnitude of the prompt reactivity temperature that is assumed constant, and, finally, l is the prompt neutron lifetime.

For reactors with narrow pluses, such as TRIGA reactor, delayed neutron and heat transfer effects in Eq. 12.24a and 12.24b could be neglected.

12.6 Fuchs–Hansen Model

Large power excursions in the reactor and neutronic analysis for nuclear reactor, where this large power excursions are a matter of interest, bring to a treatment that is known as the Fuchs–Hansen model.

This model comes to play when a system is brought rapidly to a state above prompt critical, so that the neutron population then begins to multiply at rapid rate. The normal cooling cannot remove the heat that is being generated, and so the temperature rises until some compensation sets in that reduces the reactivity to zero, thereby terminating the excursion [7].

In practice, the manner in which the reactivity is reduced may depend in detail on the reactor design and on the rate at which the neutron population (and power) increases. Hence, for computing the reactivity reduction, a point reactor model may not be adequate. Nevertheless, some useful conclusions can be drawn from such a model of the excursion in which the reactivity reduction is included as a simple feedback parameter. This treatment then is called Fuchs–Hansen model and it is the subject of this section.

Let us assume that, all of sudden, the reactivity is increased, i.e., step function-type scenario; thus, it is bringing the value of reactivity $\rho'(t)$ as function of time t to above the prompt critical, which is shown as $\rho'(t) = \rho(t) - \beta$ where $\rho(t)$ is the actual reactivity as function of time t. The assumption is now made that the feedback reactivity is proportional to the energy generated.

Now, assume in general that the power reactor that consists of the source and precursor terms is described as

$$\frac{dP(t)}{dt}=\frac{\rho(t)-\beta(t)}{\Lambda(t)}P(t)+\sum_j \lambda_j C_j(t)+Q(t)\; j=1,2,\cdots,6 \tag{12.25}$$

where

$P(t)$ = Reactor power density as function of time t
$\rho(t)$ = Actual reactivity as function of time t
$\beta(t)$ = Total fraction of delayed neutron as function of time t
$\Lambda(t)$ = Average neutron generation time as function of time t
λ_j = Decay constant
$C_j(t)$ = Precursor nuclei of ith kind as function of time t
$Q(t)$ = Volumetric heat source strength (rate of heat release per unit volume) as function of time t

However, under the Fuchs–Hansen model treatment, since the response to the sudden increase in reactivity is fast, it is justifiable to neglect the delayed neutrons while the transient is under way; hence, Eq. 12.25 will reduce to the following form as

$$\frac{dP(t)}{dt}=\frac{\rho(t)-\beta(t)}{\Lambda(t)}P(t) \tag{12.26}$$

The reactivity at time t is given by

$$\rho(t)-\beta(t)=\rho'(t)-\gamma E(t)=\rho'(t)-\gamma\int_0^t P(t')dt' \tag{12.27}$$

where γ represents the energy feedback coefficient and $E(t)$ is the total energy generated between time zero and time t. Upon combining Eqs. 12.26 and 12.27, the result is

$$\frac{dP(t)}{dt}=P(t)\left[\frac{\rho'(t)}{\Lambda(t)}-\frac{\gamma}{\Lambda(t)}\int_0^t P(t')dt'\right] \tag{12.28}$$

Now if we define constant α_0 as the initial multiplication rate and set it to be as $\alpha_0=\rho'/\Lambda$ and constant b as $b=\gamma/\Lambda$ at time $t=0$ and $(dP(t)/dt)=\alpha_0\,P(t)$, then we can write compact version of Eq. 12.28 as

$$\frac{dP(t)}{dt}=P(t)\left[\alpha_0-b\int_0^t P(t')dt'\right] \tag{12.29}$$

Equation 12.29 can be solved in closed form (see homework Problem 12.8 for the solution); it is found that

$$E(t) = \frac{\alpha_0 + c}{b}\left[\frac{1 - \mathrm{e}^{-ct}}{A\mathrm{e}^{-ct} + 1}\right] \tag{12.30}$$

and

$$P(t) = \frac{2c^2 A\mathrm{e}^{-ct}}{b(A\mathrm{e}^{-ct} + 1)^2} \tag{12.31}$$

where

$$c \equiv \sqrt{\alpha_0^2 + 2bP_0} \tag{12.32}$$

and

$$A \equiv \frac{c + \alpha_0}{c - \alpha_0} \tag{12.33}$$

A number of interesting results can be derived from these solutions and we refer the readers to the classical textbook by Bell and Glasstone [7].

Problems

Problem 12.1: The AGN-201 is operating at 5 W. It is then placed on a positive transient by inserting a reactivity of 0.00375. After 30 s, the reactor scrams automatically. At what power level is the scram point set? Use a One Delay Family model for the reactor's behavior. The following data apply.

$$\beta_{\text{effective}} = 0.0075 \quad \Lambda = 0.00015\ \text{s} \quad \lambda\text{-bar-inv} = 0.07675\,\text{s}^{-1}$$

Problem 12.2: Given the following solution for half of a cell in slab geometry, then calculate the fast and thermal self-shielding factors for the cross sections in this cell.

Z dimension	0.0	Fuel	0.2	Moderator	0.3
Fast flux	1.0		0.85		0.85
Thermal flux	0.15		0.9		1.0

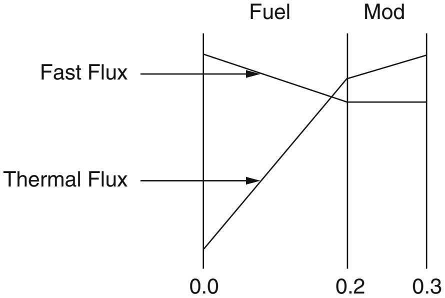

Figure Problem 12.2

Problem 12.3: Consider a hypothetical reactor in which all of the materials have the same volumetric coefficient of thermal expansion. Thus, all of the nuclide densities decrease according to the same ratio: $N'/N = \text{constant} < 1$. Additionally, consider that relationship between leakage effects and infinite medium is given by the following equation as

$$\frac{dk}{k} = \frac{dk_\infty}{k_\infty} - \frac{M^2B^2}{k_\infty}\left(\frac{dM^2}{M^2} + \frac{dB^2}{B^2}\right) \tag{12.34}$$

Moreover, since the leakage probability P_L for large power reactors usually is quite small, so we can write

$$P_L = \frac{M^2B^2}{1 + M^2B^2} \ll 1 \tag{12.35}$$

In addition, the effective multiplication k_∞ can be expressed as Eq. 12.35 below, using energy-averaged cross section. This is based on examination of neutron spectra assuming that all the constituents of a reactor core are exposed to the same energy-dependent flux $\phi(E)$

$$k_\infty = \frac{\int_0^\infty \nu\Sigma_f(E)\phi(E)dE}{\int_0^\infty \Sigma_a(E)\phi(E)dE} \tag{12.36}$$

(a) Show that the expansion with increased temperature has no effect on k_∞.

(b) Use the facts that the core mass, NV, remains constant and that $M \propto N^{-1}$ shows from Eq. 9.4 that the reactivity change from expansion is negative, with a value of $\frac{dk}{k} = -\frac{4}{3}P_L\frac{dV}{V}$.

Problem 12.4: Heat Transmission in System with Internal Sources

If the heat transfer balance for steady state is defined as below for a thin slab of thickness dx at x,

$$\text{Heat conducted out of } Adx\text{-Heat conducted into } Adx = \text{Heat generated in } Adx$$

where A is the heat conduction area and Adx is the volume of the section A normal to the direction of x, then (a) define the flow of heat by conduction and describe your parameters in the equation defining the heat flow. This is what we know as Fourier law. (b) Expand the Fourier law to a volumetric thermal source that is expressed by $Q(x)$, which is heat generated per unit time per unit volume at x with dimension of Btu/(h)(ft^2) in the British system.

Problem 12.5: Using the part (b) of solution for Problem 12.4:

Part (a): Provide the appropriate differential equation for a situation, where we have heat transmission in shields and pressure vessels, i.e., slab with exponential heat source $Q(x) = Q_0 e^{-\mu x}$, where again $Q(x)$ is volumetric heat source strength rate of heat release per unit volume, Q_0 is constant for heat source, and μ is the linear attenuation coefficient or macroscopic cross section of the radiations.

Part (b): Solve the differential equation of Part (a), by first finding the general solution and secondly giving the boundary condition as $T(x)|_{x=0} = T_1$ and $T(x)|_{x=L} = T_2$; find the particular solution of the general solution in the first part. Thirdly, draw the depiction of heat transmission in slab with exponential source and the given boundary conditions.

Part (c): Under certain condition, one can find the maximum for the particular solution in the second step of part (b) and then find that maximum expression.

Problem 12.6: A water-cooled and water-moderated power reactor is contained within a thick-walled pressure vessel. This vessel is protected from excessive irradiation and, thus, excessive thermal stress by a series of steel thermal shields between the reactor core and the pressure vessel. One of these shields, 2 in. thick, whose surfaces are both maintained at 500 °F, receives a gamma-ray energy flux of 10^{14} MeV/(cm^2)(s). Calculate the location and magnitude of the maximum temperature in this shield. The linear attenuation coefficient of the radiation in the steel may be taken to be 0.27 cm^{-1}, and the thermal conductivity as 23 Btu/(h)(ft^2)(°F/ft). Hint: use the results of solution that you found in Part (c) of Problem 15.5 and figure in Part (b). Additionally, assume that for steel $Q_0 = \phi E \mu_e$, where μ_e is energy absorption coefficient, which is 0.164 for steel and ϕE is gamma-ray energy flux of gamma-ray energy E.

Problem 12.7: The Fuchs–Nordheim model predicts the shape and magnitude of the transient. We do not really solve analytical solution of the model, but instead some characteristic from it. If we write the first part of Eq. 12.18 as the following form for point kinetics equation (PKE), you have to:

(a) Argue under what assumption Eq. 12.18 (i.e., first part) reduces to Eq. 12.25 and why historically this assumption was made by Manhattan Project weapon designers.
(b) Assume that if transient is so rapid that no heat is transferred from the fuel (i.e., the time constant for heat to be removed from UO_2 fuel is about 5 min) with heat capacity, C_P is given by the following relation:

$$T_{\text{fuel}}(t) = T_{\text{fuel}}^0 + \frac{1}{C_p}\int P(t)dt \tag{12.37}$$

In addition, assume a Doppler feedback coefficient independent of temperature (recall that we calculate that PWRs have a Doppler coefficient of about −3 pcm/K), and we can write

$$\rho(t) = \rho_{\text{rod}} - \alpha\left(T_{\text{fuel}} - T_{\text{fuel}}^0\right) \tag{12.38}$$

Then calculate the peak temperature characteristics for power distribution $P(t)$.

(a) Calculate asymptotic characteristics for power distribution $P(t)$.
(b) Finally yet importantly, show that asymptotic temperature is independent on the reactivity insertion rate.

Problem 12.8: Solve Eq. 12.29.

References

1. Net electrical MWe and gross MWe vary slightly from summer to winter, so normally the lower summer figure, or an average figure, is used. If the summer figure is quoted plants may show a capacity factor greater than 100% in cooler times. Watts Bar PWR in Tennessee is, reported to run at about 1125 MWe in summer and about 1165 MWe net in winter, due to different condenser cooling water temperatures. Some design options, such as powering the main large feed-water pumps with electric motors (as in Evolutionary Power Reactor (EPR)) rather than steam turbines (taking steam before it gets to the main turbine-generator), explains some gross to net differences between different reactor types. The EPR has a relatively large drop from gross to net MWe for this reason.
2. J. Duderstadt, L. Hamilton, *Nuclear reactor analysis* (Wiley, New York, 1976)
3. L. Massimo, *Physics of the high temperature reactors* (Pergamon Press, Oxford, 1976)
4. Y. Oka, T. Kiguchi, *Nuclear reactor design (an advanced course in nuclear engineering)* (Springer, New York, 2014)

5. G.R. Keepin, *Physics of nuclear kinetic* (Addison-Wesley, Boston, 1965)
6. J. Ala-Heikkila, T. Seren, and C. Persson, Student reactor exercises at VTT, KTH Engineering Science, Center of Finland and Royal Institute of Technology (KTH) (2008)
7. G.I. Bell and S. Glasstone, Nuclear reactor theory, Published Under Auspices of the Davison of Technical Information, United Sates Atomic Energy Commission (Van Nostrand Reinhold Company, 1970)

Chapter 13
Reactor Stability

Understanding time-dependent behaviors of nuclear reactors and the methods of their control is essential to the operation and safety of nuclear power plants. This chapter provides researchers and engineers in nuclear engineering very general yet comprehensive information on the fundamental theory of nuclear reactor kinetics and control and the state-of-the-art practice in actual plants, as well as the idea of how to bridge the two. The dynamics and stability of engineering equipment that affects their economical and operation from safety and reliable operation point of view. In this chapter, we will talk about the existing knowledge that is today's practice for design of reactor power plants and their stabilities as well as available techniques to designers. Although, stable power processes are never guaranteed. An assortment of unstable behaviors wrecks power apparatus, including mechanical vibration, malfunctioning control apparatus, unstable fluid flow, unstable boiling of liquids, or combinations thereof. Failures and weaknesses of safety management systems are the underlying causes of most accidents.

13.1 Frequency Response

The engineers and designers of today's nuclear power reactors are doing their best to provide us commercially safe reactors, using inherent reactor kinetics and dynamics characteristic to limit undesirable/unwanted rise in reactor power. A necessary condition for stable reactor power is that the reactor perturbation or distortion, accompanying a temperature rise, decreases the reactivity, thus slowing any further rise in power. For instance, the reactor distortion caused by a temperature rise could allow more neutrons to be wasted by leakage, thus decreasing the reactivity. Overly simple equations for reactor power dynamics indicate that this idea should work, and sometimes it does.

The supposition that satisfying the above condition guarantees power stability is based on a false assumption that the reactor distortion occurs simultaneously with

B. Zohuri, *Neutronic Analysis For Nuclear Reactor Systems*,
DOI 10.1007/978-3-319-42964-9_13

the temperature rise, which caused it. The distortion lags behind the temperature change by a time determined by the mechanical dynamics of the reactor system. Therefore, the change in reactivity also lags behind the temperature change, raising the possibility of unstable power oscillations. This conclusion is supported by the actual experience with seriously unstable reactors such as the inoperable Ft. St. Vrain power reactor [1].

As part of failure analysis, the utilization of *frequency response* allows to take a quantitative measure of the output spectrum of a system such as overall nuclear power plant or device at the component level, in response to a stimulus of the design process. This process uses to characterize the dynamics of the system, and it measures the magnitude and *phase* of the output as a function of *frequency*, in comparison to the input.

As an example of such circumstances, we look at a sine wave condition. If a sine wave is injected into a system at a given frequency, a linear system will respond at that same frequency with a certain magnitude and a certain phase angle relative to the input. However, if a linear time-invariant (LTI) theory applies for a linear system, doubling the amplitude of the input will double the amplitude of the output. In addition, if the system is time invariant or LTI, then the frequency response also will not vary with time. Thus, for LTI systems, the frequency response can be seen as applying the system's transfer function to a purely imaginary number argument representing the frequency of the sinusoidal excitation.

Note that linear time-invariant theory, commonly known as LTI system theory, comes from applied mathematics and has direct applications in nuclear magnetic resonance (NMR) spectroscopy, seismology, circuits, signal processing, control theory, and other technical areas. It investigates the response of a linear and time-invariant system to an arbitrary input signal. Trajectories of these systems are commonly measured and tracked as they move through time (e.g., an acoustic waveform), but in applications like image processing and field theory, the LTI systems also have trajectories in spatial dimensions. Thus, these systems are also called linear translation invariant to give the theory the most general reach. In the case of generic discrete-time (i.e., sampled) systems, linear shift invariant is the corresponding term. A good example of LTI systems is electrical circuits that can be made up of resistors, capacitors, and inductors.

In addition, *nuclear magnetic resonance* (NMR) spectroscopy, commonly known as NMR spectroscopy, is a research technique that exploits the magnetic properties of certain atomic nuclei. It determines the physical and chemical properties of atoms or the molecules in which they are contained.

Figure 13.1 is the presentation of H^1 NMR spectrum, one dimensional of ethanol, which is plotted as signal intensity versus chemical shift. As it can be seen in this figure, the hydrogen H on the —OH group is not coupling with the other H atoms and appears as a singlet, but the CH^3 and the $—CH^2$ hydrogens are coupling with each other, resulting in a triplet and quartet, respectively.

Overall view of property definitions of LTI system, are *linearity* and *time invariance*, and they fall into the two following categories as:

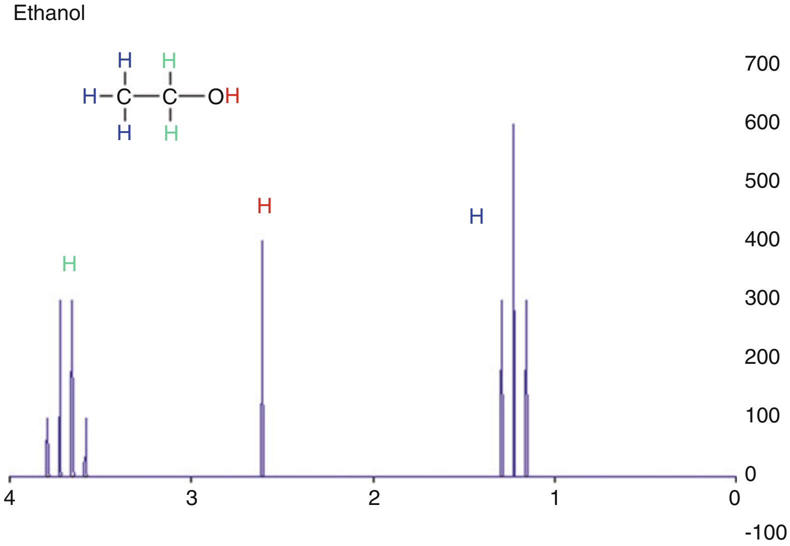

Fig. 13.1 H^1 nuclear magnetic resonance spectrum

1. *Linearity*
This means that the relationship between the input and the output of the system is a linear map and mathematically could be presented as a linear input process, and in responses, it produces a linear output. If input $x_1(t)$ produces response $y_1(t)$ and input $x_2(t)$ produces response $y_2(t)$, then the *scaled* and *summed* input $a_1x_1(t) + a_2x_2(t)$ produces the scaled and summed response $a_1y_1(t) + a_2y_2(t)$, where a_1 and a_2 are real scalars. It follows that this can be extended to an arbitrary number of terms and, thus, for real numbers $c_1, c_2, \ldots, c_k$, and we can write the following relations in mathematical notation as

$$\text{Input } \sum_k c_k x_k(t) \quad \text{produces output as } \sum_k c_k y_k(t) \tag{13.1}$$

In particular, we can write

$$\text{Input } \int_{-\infty}^{+\infty} c_\omega x_\omega(t)\,d\omega \qquad \text{produces output as } \int_{-\infty}^{+\infty} c_\omega y_\omega(t)\,d\omega \tag{13.2}$$

where c_ω and x_ω are scalars and inputs that vary over a continuum index by ω. Thus, if an input function can be represented by a continuum of input functions, combined "linearly" as shown, then the corresponding output function can be represented by the corresponding continuum of output functions, *scaled* and *summed* in the same way.

2. *Time Invariance*
   This means that whether we apply an input to the system now or T seconds from now, the output will be identical except for a time delay of T seconds. That is, if the output due to input $x(t)$ is $y(t)$, then the output due to input $x(t-T)$ is $y(t-T)$. Hence, the system is time invariant because the output does not depend on the particular time the input is applied.

A single function known as system's impulse response can characterize the fundamental result in linear time-invariant (LTI) system theory. The output of the system is simply the convolution of the input to the system with the system's impulse response. This method of analysis is often called the time domain point of view. The same result is true of discrete-time linear shift-invariant systems in which signals are discrete-time samples and convolution is defined on sequences.

Equivalently, any LTI system can be characterized in the frequency domain by the system's transfer function, which is the Laplace transform of the system's impulse response (or Z transform in the case of discrete-time systems). Because of the properties of these transforms, the output of the system in the frequency domain is the product of the transfer function and the transform of the input. In other words, convolution in the time domain is equivalent to multiplication in the frequency domain. Figure 13.2 is depicting such situation, where relationship between the time domain and the frequency domain is shown.

For all LTI systems, the eigenfunctions, and the basic functions of the transforms, are complex exponentials, that is, if the input to a system is the complex waveform Ae^{st} for some complex amplitude A and complex frequency s, then the output will be some complex constant times the input, let us say Be^{st} for some new complex amplitude B. However, the ratio B/A is the transfer function at frequency s.

Since sinusoids are a sum of complex exponentials with complex-conjugate frequencies, if the input to the system is a sinusoid, then the output of the system will also be a sinusoid, perhaps with a different amplitude and a different phase, but always with the same frequency upon reaching steady state. Linear time-variant (LTI) systems cannot produce frequency components that are not in the input.

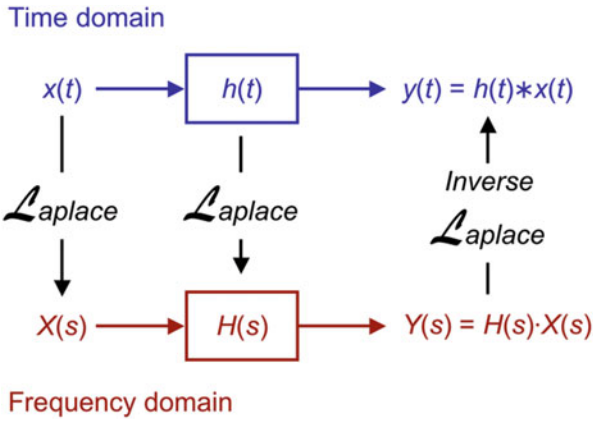

Fig. 13.2 Relationship between the time domain and the frequency domain

LTI system theory is good at describing many important systems. Most LTI systems are considered "easy" to analyze, at least compared to the time-varying and/or nonlinear case. Any system that can be modeled as a linear homogeneous differential equation with constant coefficients is an LTI system. Examples of such systems are electrical circuits made up of resistors, inductors, and capacitors (RIC circuits). Ideal spring–mass–damper systems are also LTI systems and are mathematically equivalent to RIC circuits [2].

Most LTI system concepts are similar between the continuous-time and discrete-time (linear shift-invariant) cases. In image processing, the time variable is replaced with two space variables, and the notion of time invariance is replaced by two-dimensional shift invariance. When analyzing filter banks and multiple-input and multiple-output (MIMO) systems, it is often useful to consider vectors of signals.

A linear system that is not time invariant can be solved using other approaches such as the Green function method. The same method must be used when the initial conditions of the problem are not null. Estimating the frequency response for a physical system generally involves exciting the system with an input signal, measuring both input and output time histories, and comparing the two through a process such as the fast Fourier transform (FFT). One thing to keep in mind for the analysis is that the frequency content of the input signal must cover the frequency range of interest or the results will not be valid for the portion of the frequency range not covered. Figure 13.3 is presenting frequency response of a low-pass filter with 6 dB (decibel) per octave or 20 dB per decade.

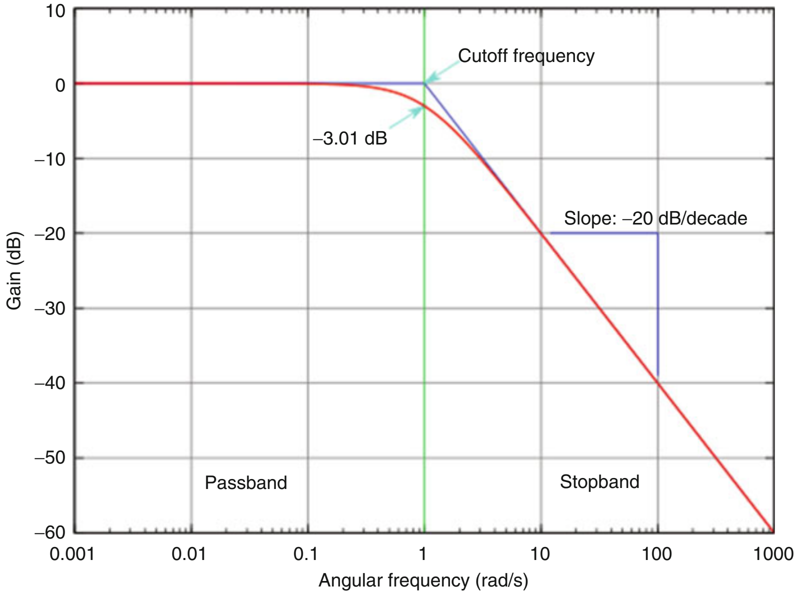

Fig. 13.3 Frequency response of a low-pass filter with 6 dB per octave or 20 dB per decade

In summary, the two applications of frequency response, namely, phase and frequency analyses, are related but have different objectives. For an audio system, the objective may be to reproduce the input signal with no distortion that would require a uniform (flat) magnitude of response up to the bandwidth limitation of the system, with the signal delayed by precisely the same amount of time at all frequencies. That amount of time could be seconds, or weeks, or months in the case of recorded media. In contrast, for a feedback apparatus used to control a dynamic system, the objective is to give the closed-loop system improved response as compared to the uncompensated system. The feedback generally needs to respond to system dynamics within a very small number of cycles of oscillation (usually less than one full cycle) and with a definite phase angle relative to the commanded control input. For feedback of sufficient amplification, getting the phase angle wrong can lead to instability for an open-loop stable system or failure to stabilize a system that is open loop unstable. Digital filters may be used for both audio systems and feedback control systems, but since the objectives are different, generally the phase characteristics of the filters will be significantly different for the two applications [3].

13.2 Nyquist Plots

The Nyquist stability criterion is used to investigate stability of any open or closed system using its frequency characteristics. Usually the criterion is used for closed systems, though. A useful, but not the most general formulation of the Nyquist criterion is as follows: if the mapping of the transfer function of an open system $G(s)*H(s)$ on the plane *GH* encircles point $(-1, 0)$, then the system is unstable if it is closed. The criterion is illustrated in Fig. 13.4, with Nyquist plots of a stable and unstable closed system. Curve *A* does not encircle point $(-1, 0)$ and then, the system is stable. On the other hand, Curve *B* encircle point $(-1, 0)$ and the system therefore is called to be unstable.

Fig. 13.4 Nyquist plots

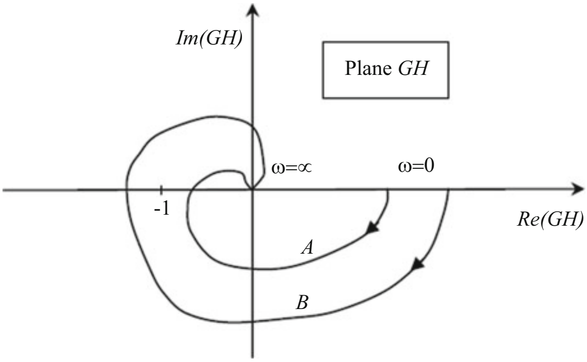

The Nyquist criterion can be easily proved, which requires basic knowledge of mathematics of complex variables, and we assume the readers have such background. With the assumption of such knowledge, we let $f(s)$ to be meromorphic throughout the bounded region inside and continuous on a closed contour C on which $f(s) \neq 0$. Let Z be the number of zeros and P be the number of poles of $f(s)$ inside C, respectively, where a zero or pole of order m is counted m times. Then, using knowledge of our complex variables, we can write the following relation as

$$\frac{1}{2\pi i}\oint_C \frac{f'(\xi)}{f(\xi)} d\xi = Z - P \tag{13.3}$$

For $P = 0$, we can obtain the principle of the argument as

$$N = \frac{\Delta_C \vartheta}{2\pi} \tag{13.4}$$

where $\Delta_C \vartheta$ is the variation of the argument ϑ of $f(s)$ around the contour C. This equation means that $f(s)$ maps a moving point s describing the contour C once into a moving point $f(s)$ which encircles the f plane origin $N = 1,2,\ldots$ times, if $f(s)$ has, respectively, 0,1,2,... zeros inside the contour C in the s plane. The above criterion is used for locating zeros and poles of $f(s)$ and is known as the Nyquist criterion.

As an example, consider a function $f(s)$ that has two zeros as $s = z_1$ and $s = z_2$ as well as one pole $s = p_1$. The function can be given as [4]

$$f(s) = \frac{(s - z_1)(s - z_2)}{(s - p_1)} \tag{13.5}$$

The locations of the zeros and the pole are depicted in Fig. 13.5.

Assume that point s is moving along the contour and encircles it. The argument of the number $(s - z_1)$ will increase by 2π. It means that with a single encirclement of the contour C by point s, the argument of function $f(s)$ will increase by 2π for each zero, which is inside of the contour. In a similar way, it is obtained that the argument of function $f(s)$ decreases with 2π for each pole located inside of the contour C. As a consequence, the mapping of $f(s)$ on the plane f will encircle the plane origin in the corresponding number of times. In the considered case, $f(s)$ will encircle the origin only once, since its argument will increase with $(2, -1)$ multiplied by 2π.

The Nyquist criterion is very useful in the theory of stability. To evaluate the stability of any system, it is necessary to find the locations of zeros of the characteristic function of the system. If any of the zeros is located on the right-hand side of the s plane, then the system is unstable. The contour on the s plane is shown in Fig. 13.6.

An example of the corresponding mapping of function $f(s)$ on the f plane is shown in Fig. 13.7, where it shows the mapping function $f(s)$ for encircling the right half plane as shown in Fig. 13.6.

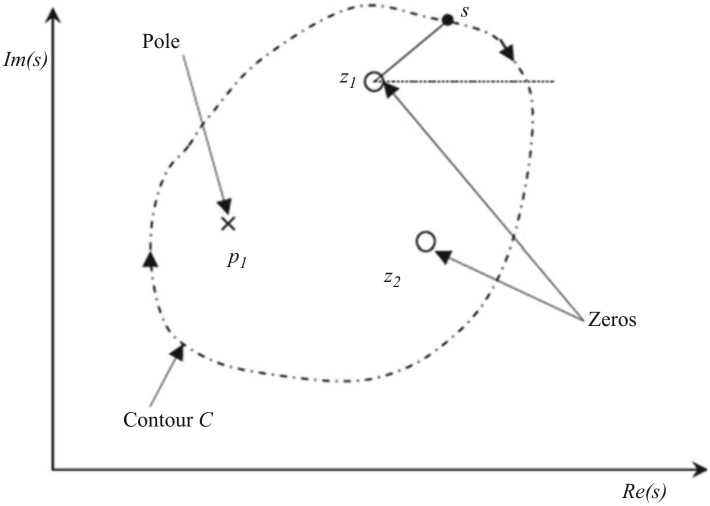

Fig. 13.5 Location of zeros and poles on *s* plane

Fig. 13.6 Contour in the *s* plane that covers the whole right-hand side half plane when $\boldsymbol{R} \rightarrow \infty$

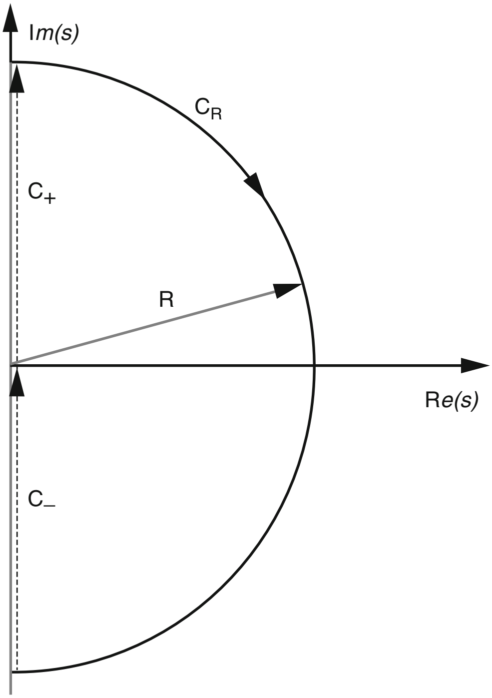

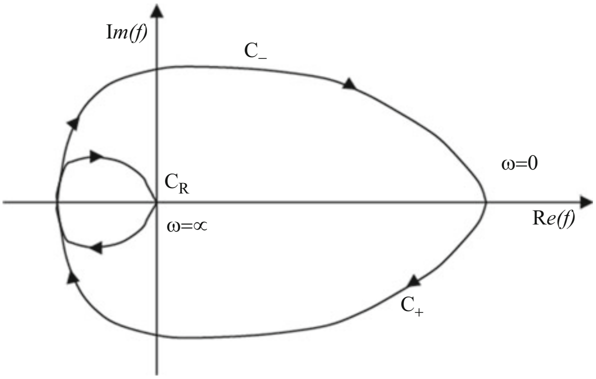

Fig. 13.7 Mapping of function *f(s)* for *s* encircling the right half plane

As we have stated, the frequency-domain method can be used for linear systems only and is an approach similar to the Laplace transformation. If the system under consideration is nonlinear, then it should be first linearized around a certain operational point for the frequency-domain approach to work. A frequency response of any system is the behavior of the system that should be subjected to a sinusoidal-type forcing function or input signal, and such forcing function is described here as

$$u(t) = u_0 \sin(\omega t) \tag{13.5}$$

where u_0 is the amplitude of the input signal and ω is the signal frequency expressed in radiance per second.

When a linear system is subject to a sinusoidal signal at input, the system response will also be a signal of the same shape and frequency. However, the output signal will have different amplitude and phase. Thus, the output signal can be written as

$$x(t) = x_0 \sin(\omega t + \theta) \tag{13.6}$$

Graphically, the input or forcing function and its output signal for a linear system can be depicted as Fig. 13.8 [4].

However, the system amplification can be expressed in terms of the transfer function $G(s)$, and the amplification is as follows [4]:

$$L = 20\lg\frac{|G(j\omega)|}{|G(0)|}\ \text{dB (decibels)} \tag{13.7}$$

while the phase shift θ is given as

$$\theta = \arg G(j\omega) \tag{13.8}$$

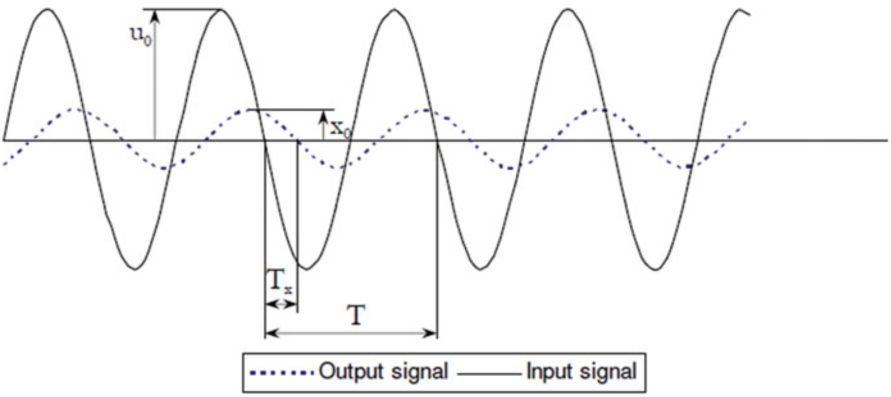

Fig. 13.8 A linear system response to a sinusoidal forcing function at steady state. The system introducing a lag to the signal and reducing its amplitude [4]

The frequency approach can give an answer whether the system is stable or not without specifically finding the poles of the transfer function. For that purpose the Nyquist plot is used, in which the imaginary part of $G(j\omega)$ is plotted against the real part of $G(j\omega)$.

For the first-order system expressed by the following differential equation along its initial condition as

$$u(t) = \frac{dx(t)}{dt} + \omega_0 x(t) \qquad \text{Initial condition} \quad x(0) = 0 \tag{13.9}$$

The transfer function could be obtained by utilizing the Laplace transformation of Eq. 13.9 over variable t on both sides of equation, as it is shown below:

$$\begin{aligned} £\{u(t)\} &= £\left\{\frac{dx(t)}{dt}\right\} + \omega_0 £\{x(t)\} \\ u(s) &= sx(s) + x(0) + \omega_0 x(s) \end{aligned} \tag{13.10}$$

Here, we have assumed $£\{u(t)\} = x(s)$ and Eq. 13.10 will be reduced to the following form as

$$G(s) = \frac{x(s)}{u(s)} = \frac{1}{s + \omega_0} \tag{13.11}$$

The real and the imaginary parts of $G(j\omega)$ are readily obtained as

$$G(j\omega) = \frac{1}{j\omega + \omega_0} = \frac{(-j\omega + \omega_0)}{(j\omega + \omega_0)(-j\omega + \omega_0)} = \frac{\omega_0}{\omega^2 + \omega_0^2} - j\frac{\omega}{\omega^2 + \omega_0^2} \tag{13.12}$$

Thus,

$$\begin{aligned}\mathrm{Re}[G(j\omega)] &= \frac{\omega}{\omega^2+\omega_0^2}\\ \mathrm{Im}[G(j\omega)] &= -\frac{\omega}{\omega^2+\omega_0^2}\end{aligned} \tag{13.13}$$

The module and argument of $G(j\omega)$ are now found as

$$\begin{aligned}\left|G(j\omega)\right| &= \sqrt{\mathrm{Re}^2[G(j\omega)]+\mathrm{Im}^2[G(j\omega)]}\\ &= \sqrt{\left(\tfrac{\omega_0}{\omega^2+\omega_0^2}\right)^2+\left(\tfrac{\omega_0}{\omega^2+\omega_0^2}\right)^2}\\ &= \frac{1}{\sqrt{\omega^2+\omega_0^2}}\end{aligned} \tag{13.14}$$

Now, from Eq. 13.7, the system amplification is found as

$$L = 20\lg\frac{|G(j\omega)|}{|G(0)|} = 20\log\left\{\frac{\left|\frac{1}{j\omega+\omega_0}\right|}{\left|\frac{1}{\omega_0}\right|}\right\} = 20\lg\left(\frac{1}{\sqrt{1+\beta^2}}\right) \tag{13.13}$$

where $\beta = \omega/\omega_0$. Similarly, from Eq. 13.8, the phase shift is found to be

$$\theta = \arg\ G(j\omega) = \arctan\left(\frac{\mathrm{Im}G(j\omega)}{\mathrm{Re}G(j\omega)}\right) = \arctan(-\beta) \tag{13.14}$$

As it can be seen, identical expressions have been obtained for L and θ as previously derived in the time domain analysis.

The Bode plots for the first-order system have been already shown in Fig. 13.8. The Nyquist plot can be obtained in an analytical form by expressing the imaginary part of $G(j\omega)$ with its real part. This can be achieved as follows:

$$\mathrm{Im}[G(j\omega)] = \frac{\omega}{\omega^2+\omega_0^2} = -\frac{\omega}{\omega^2+\omega_0^2}\frac{\omega}{\omega_0} = -\mathrm{Re}[G(j\omega)]\frac{\omega}{\omega_0} \tag{13.15}$$

Thus,

$$\omega = -\frac{\mathrm{Im}[G(j\omega)]}{\mathrm{Re}[G(j\omega)]}\omega_0 \tag{13.16}$$

The imaginary part can be now expressed as

Fig. 13.9 Nyquist plot for the first-order system

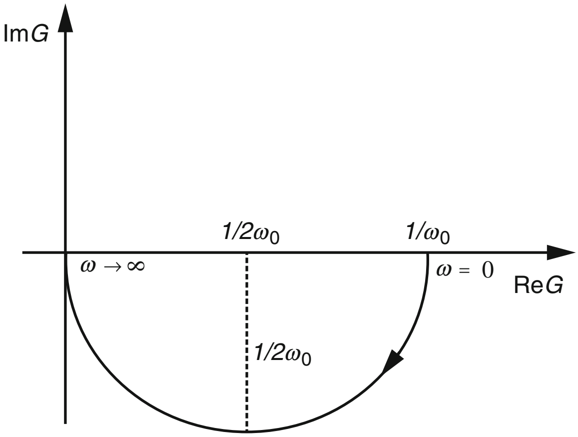

$$\mathrm{Im}[G(j\omega)] = -\frac{\frac{\mathrm{Im}[G(j\omega)]}{\mathrm{Re}[G(j\omega)]}\omega_0}{\omega_0^2 + \left(\frac{\mathrm{Im}[G(j\omega)]}{\mathrm{Re}[G(j\omega)]}\omega_0\right)^2} = -\frac{-\frac{\mathrm{Im}[G(j\omega)]}{\mathrm{Re}[G(j\omega)]}}{1 + \left(\frac{\mathrm{Im}[G(j\omega)]}{\mathrm{Re}[G(j\omega)]}\right)^2 \omega_0} \tag{13.17}$$

or

$$\mathrm{Re}^2[G(j\omega)] + \mathrm{Im}^2[G(j\omega)] = \frac{\mathrm{Re}[G(j\omega)]}{\omega_0} \tag{13.18}$$

This equation represents a half circle on the $G(j\omega)$ plane, which can be readily seen from the following form of the equation:

$$\left(\mathrm{Re}[G(j\omega)] - \frac{1}{2\omega_0}\right) + \mathrm{Im}^2[G(j\omega)] = \left(\frac{1}{2\omega_0}\right)^2 \tag{13.19}$$

The Nyquist plot for the first-order system is shown in Fig. 13.9.

The Bode and Nyquist characteristics can be plotted with dedicated Scilab functions.

Nyquist and Bode. See Problem 13.1.

13.3 Nonlinear Stability

In the design, construction, and operation of nuclear reactors, an attempt is made to maintain a steady operation at any desired power level from fission of the nuclear fuels, uranium or plutonium. This attempt can fail, sometimes catastrophically. A nuclear power plant is a nuclear system and a mechanical system. It is also a heat transfer system, tied in with controls, boilers, turbines, human operators, and a multiplicity of other complicating factors. The possibilities for instability are myriad. This fiercely complicated set of systems is such as to preclude any possibility of the formation of adequate analytical equations and their solution to guarantee the stability of power. An experimental program sufficient to eliminate the possibilities of power instability in reactors would be expected to be ruinous of both the economy and the environment. Our program covers only a small part of the complicated possibilities and demonstrates only one type of power instability.

Changes in reactor temperature also affect the density. A decrease in the density of reactor parts tends to increase the leakage of neutrons, which in turn decreases the reactivity. This adds the complications of mechanical dynamics to the analysis of reactor stability. Fast density changes in a reactor structure may cause it to vibrate, and reactor power may oscillate as a result. Accounting for this effect requires adding to the temperature coefficient described above a “density coefficient of reactivity.” The density coefficient couples mechanical and nuclear power oscillations. As previously mentioned, the inclusion of mechanical effects requires a solution of a fourth-order differential equation of reactor kinetics, as opposed to the second-order nuclear equation. Prediction of power stability becomes more precarious [1].

Nonlinearity or perturbation to reactor power can be studied by calculating the power dynamics of a reactor, based on Thompson and Thompson [5, 6] paper, where they present some necessary conditions for power stability provided by nuclear physics, as analyzed by Weinberg and Wigner [7].

Their analysis generated a second-order differential equation whose solution is always stable if the coefficients in the equation are all positive. Then, we consider mechanical characteristics of reactors, which render the nuclear analysis insufficient to assure stability. This results in a fourth-order differential equation whose stability requires not only that all coefficients be positive but also that a relationship among the coefficients be satisfied (Routh’s criterion). It turns out that, for power stability, motion of any reactor parts, which affect reactivity, must be sufficiently damped by mechanical friction in the moving parts.

Routh’s Criterion

In control system theory, the Routh–Hurwitz stability criterion is a mathematical test that is a necessary and sufficient condition for the stability of a linear time-invariant (LTI) control system. The Routh test is an efficient recursive algorithm that English mathematician Edward John Routh proposed in 1876 to determine whether all the roots of the characteristic polynomial of a linear system have negative real parts.

German mathematician Adolf Hurwitz independently proposed in 1895 to arrange the coefficients of the polynomial into a square matrix. This is called the Hurwitz matrix and showed that the polynomial is stable if and only if the

(continued)

sequence of determinants of its principal submatrices is all positive. The two procedures are equivalent, with the Routh test providing a more efficient way to compute the Hurwitz determinants than computing them directly. A polynomial satisfying the Routh–Hurwitz criterion is called a Hurwitz polynomial.

Reactivity and stability are unavoidably affected by depletion of reactor fuels and the accumulation of "poisons" during operation. Other destabilizing effects not considered here, or anywhere else, are so numerous and so complicated in their interrelationships as to thwart human efforts to guarantee reactor stability.

Thompson and Thompson [5] in their paper are demonstrating that mechanical friction in a reactor core structure, like the shock absorber in an automobile, is necessary to limit oscillations of reactor power. Without adequate internal friction, a nuclear power driven by mechanical oscillation increases toward destruction of the reactor core. Design engineers in many fields have found to their sorrow that any given level of mechanical friction is difficult to guarantee. Some of the computer-generated examples later in this section show the changing core temperature and reactor power for a reactor without adequate friction to provide stability. A small perturbation in power causes an initially small oscillation, which either builds rapidly to destruction, blows up, or melts down. Their approach is based on a computer program, which they had developed together. Their program solves by finite-difference mathematics a nonlinear, fourth-order differential equation involving nuclear, mechanical, and thermal characteristics of reactors. Our paper, "A Model of Reactor Kinetics," and it is demonstrating a mechanism for catastrophic instability [1].

In the design, construction, and operation of nuclear reactors, an attempt is made to maintain a steady operation at any desired power level from fission of the nuclear fuels, uranium or plutonium. This attempt can fail, sometimes catastrophically. A nuclear power plant is a nuclear system and a mechanical system. It is also a heat transfer system, tied in with controls, boilers, turbines, human operators, and a multiplicity of other complicating factors. The possibilities for instability are myriad. This fiercely complicated set of systems is such as to preclude any possibility of the formation of adequate analytical equations and their solution to guarantee the stability of power. An experimental program sufficient to eliminate the possibilities of power instability in reactors would be expected to be ruinous of both the economy and the environment. Their program covers only a small part of the complicated possibilities and demonstrates only one type of power instability [1].

Problems

Problem 13.1: Perform the Nyquist and Bode plots for first-order system using Scilab functions.

Problem 13.2: *The Stability of Dynamic System*

The equations which describe the dynamic behavior of a reactor are complicated and, in particular, are essentially nonlinear for the diffusion equation:

$$l\frac{\partial P(\vec{\boldsymbol{r}},t)}{\partial t} = M^2\nabla^2 P(\vec{\boldsymbol{r}},t) + (k_\infty - 1)P(\vec{\boldsymbol{r}},t) \tag{13.20}$$

where

$l =$ prompt neutron life time (sec)
$P =$ reactor power density (W/cm^2)
$M =$ migration length (cm)
$k =$ multiplication factor

Equation 13.20 necessarily involves the product $k_\infty P(\vec{\boldsymbol{r}},t)$. Since k_∞ is itself a function of the reactor temperature, xenon concentration, and so on, this term is essentially nonlinear as well. Consequently, it is not in general possible to solve the dynamic equation (13.20) in analytic terms, and extensive numerical integrations are normally necessary. Such calculations are carried out, for example, in the investigation of fault conditions. In stability studies, however, a number of simplifications are possible.[1] Assume that Eq. 13.20 reduces to form Eq. 13.21, by setting up a mesh of points in three dimensions covering the reactor, and to define each variable–power density, fuel temperature, xenon concentration, and so on—at each point of mesh. Terms in the equations like $\partial^2 p(x)/\partial x^2$ can now be represented approximately as

$$\frac{\partial^2 p(x)}{\partial x^2} = \frac{1}{h^2}\{p(x-h,y,z) - 2p(x,y,z) + p(x+h,y,z)\} \tag{13.21}$$

and so on. This can be made as accurate as one wishes by taking a fine enough mesh, the provided one is not concerned with quantities that vary arbitrarily steeply in space. For physical considerations, however, such variations are of no interest in a stability study, for the stabilizing effect of neutron leakage must dominate all other

---

[1] See for details the book by A Hitchcock, *Nuclear Reactor Stability*, published by Temple Press, 1960.

effects in a highly localized disturbance. Thus, such a representation is legitimate. Then, Eq. 13.21 now takes the following form as

$$\frac{dx_i}{dt} = \sum_{j=1}^{n} a_{ij} x_j \; i = 1, 2 \cdots, n \tag{13.22}$$

where x_i is the various representations of reactor temperature, power densities, and so on, at the different mesh points. The a_{ij} is independent of t. Equation 13.22 is a very simple set of differential equations, and they can, in principle, be solved easily. Find the general solution of this equation.

References

1. A.S. Thompson, *Unstable nuclear power*. http://www.ratical.org/radiation/CoNP/3instability.html
2. https://en.wikipedia.org/wiki/LTI_system_theory
3. https://en.wikipedia.org/wiki/Frequency_response
4. Henryk Anglart, *Nuclear reactor dynamics and stability*, (KTH Engineering Science, Center of Finland and Royal Institute of Technology (KTH), 2011)
5. A.S. Thompson, B.R. Thompson, A model of reactor kinetics. Nucl. Sci. Eng. **100**(1), 83–88 (1988)
6. A.S. Thompson, O.E. Rodgers, *Thermal power from nuclear reactors* (Wiley, New York, 1956)
7. A.M. Weinberg, E.P. Wigner, *The physical theory of neutron chain reactors*, (The University of Chicago Press, 1958), pp. 603–609

Chapter 14
Numerical Modeling for Time-Dependent Problems

The possibility of a plutonium-fueled nuclear-powered reactor, such as a fast breeder reactor that could produce more fuel than it consumed, was first raised during World War II, in the United States by scientists involved in Manhattan Project and the US Atomic Bomb Program. In the past two decades, the Soviet Union, the United Kingdom, France, Germany, Japan, and India followed the United States in developing a nationalized plutonium breeder reactor programs, while Belgium, Italy, and the Netherlands collaborated with the French and German programs. In all of these programs, the main driver of this effort was the hope of solving the long-term energy supply problem using the large-scale deployment of fissional nuclear energy for electric power. Breeder reactors, such as plutonium-fueled breeder reactors, appeared to offer a way to avoid a potential shortage of the low-cost uranium required to support such an ambitious vision using other kinds of reactors, including today's new generation of power reactors known as GEN IV.

14.1 Fast Breeder Reactor History and Status

The International Panel on Fissile Materials (IPFM) was founded in January 2006. It is an independent group of arm-control and nonproliferation experts from 17 countries, including both nuclear weapon and nonnuclear weapon states [1].

The mission of the IPFM is to analyze the technical basis for practical and achievable policy initiatives to secure, consolidate, and reduce stockpiles of highly enriched uranium and plutonium. These fissile materials are the key ingredients in nuclear weapons, and their control is critical to nuclear disarmament, halting the proliferation of nuclear weapons, and ensuring that terrorists do not acquire nuclear weapons [1].

Both military and civilian stocks of fissile materials have to be addressed. The nuclear weapon states still have enough fissile materials in their weapon stockpiles for tens of thousands of nuclear weapons. On the civilian side, enough plutonium

B. Zohuri, *Neutronic Analysis For Nuclear Reactor Systems*,
DOI 10.1007/978-3-319-42964-9_14

has been separated to make a similarly large number of weapons. Highly enriched uranium is used in civilian reactor fuel in more than 100 locations. The total amount used for this purpose is sufficient to make about 1000 Hiroshima-type bombs, a design potentially within the capabilities of terrorist groups [1].

Uranium is proved to be much more abundant than originally imagined, and, after a fast start, nuclear power growth slowed dramatically in the late 1980s, and global nuclear capacity is today about one-tenth the level that had been projected in the early 1970s. The urgency of deploying fast neutron reactors for plutonium breeding therefore has abated—at least in the western Organization for Economic Co-operation and Development (OECD) countries. In India and Russia, however, concerns about potential near-term uranium shortages persist, and new demonstration breeder reactors are being built. China, which currently is building up its nuclear capacity at an enormous rate, is considering the possibility of building two Russian-designed breeder reactors. Because of the high costs and reliability and safety issues, no commercial breeder reactors have been deployed, at least not in the United States [1].

Interest in fast neutron (energetic neutron) reactors persists in the OECD countries for a new reason, political difficulties with storing or disposing of spent fuel. "Reprocessing" spent fuel does not eliminate the problem of sitting a geological repository, but a reprocessing plant does provide an interim destination that has proved a path forward with regard to the spent fuel problem in a number of nations.

Spent fuel reprocessing was originally launched in countries that planned to deploy breeder reactors. They wanted separated plutonium for manufacturing start-up fuel for their first breeder reactors. The standard light-water reactor spent fuel contains about 1 % plutonium. In the absence of breeder reactors, the separated plutonium has become a disposal problem, and some countries have decided to recycle it into fuel for the same reactors that produced it. Slow-neutron reactors are relatively ineffective, however, in fissioning some of the plutonium isotopes, which therefore build up in recycled fuel.

Fast neutron reactor advocates argue that, if the plutonium and other long-lived transuranics in spent fuel could be fissioned almost entirely, the political problem of finding a geological disposal site for radioactive waste consisting of mostly shorter-lived fission products would become much easier. Fast neutron reactors would be more effective in fissioning all the transuranic isotopes. Fast neutron breeder reactors could be converted into transuranic "burner" reactors by removing the plutonium-breeding uranium blankets around their cores and flattening the cores into more of a "pancake" shape so that more neutrons would leak out of them.

Cochran et al. [1] look at the experience and status of breeder reactor programs in France, India, Japan, the Soviet Union/Russia, the United Kingdom, and the United States. The major breeder reactors built in these countries are listed in Table 14.1. Germany also built two breeder reactors. All were sodium cooled.

In the United States and around the world, countries that are capable of having technology of fission reactor power plant are looking for energy production by fast breeding reactors, especially the main goal of the liquid metal fast breeder reactor (LMFBR) remains in order to ensure a sustainable long-term fissile fuel supply.

Table 14.1 Major experimental, pilot, and demonstration fast breeder reactors [29]

	MWe	MWt	Operation		MWe	MWt	Operation
France				*USSR/Russia (cont.)*			
Rapsodie		40	1967–1983	BN-350 (Kazakhstan)	350		1972–1999
Phénix	250		1973–2009	BN-600	600		1980–
Superphénix	1240		1985–1998	BN-800	800		2014?
India				*United Kingdom*			
FBTR		40	1985–	DFR	15		1959–1977
PFBR	500		2010?	PFR	250		1974–1994
Japan				*United States*			
Joyo		140	1977–	EBR-I	0.2		1951–1963
Monju	280		1994–1995, 2010?	EBR-II	20		1963–1994
USSR/Russia				Fermi 1	66		1963–1972
BR-5		5	1959–2004	SEFOR		20	1969–72
B0R-60	12		1969–	Fast Flux Test Facility		400	1980–1993

In addition, the use of LMFBRs allows the recycling of the minor actinide content of nuclear waste by burning them to produce energy and reduce the amounts of disposed waste. Another advantage of the LMFBR is its higher efficiency compared with water-cooled reactors, which makes it a good candidate among other commercial reactors for the purpose of thermal efficiency output driven by a combined cycle [2–11].

The basic operational concept, behind the fast neutron breeder reactors, lies behind the nature of fissile isotopes which are the essential nuclear materials in both nuclear reactors and nuclear weapons. They undergo fission when they absorb neutrons and, on average, release more neutrons than they absorb. This makes a sustained chain reaction possible in a “supercritical mass.” This supercritical mass must contain a significant concentration of fissile isotopes and must be large enough so that only a small fraction of the neutrons escape without interacting.

The most important fissile materials are uranium-235 and plutonium-239. Uranium-235 is found in nature, constituting 0.7 % of natural uranium. Plutonium-239 is created when uranium-238 (99.3 % of natural uranium) absorbs a neutron as depicted in Fig. 14.1. Observation in Fig. 14.1 shows that a plutonium breeder reactor produces more plutonium than it consumes by using its extra fission neutrons to convert uranium-238 to uranium-239, which changes by radioactive decays involving electron and neutrino emission into neptunium-239 and then plutonium-239.

The sustainable, environmentally clean long-term use of nuclear power can be achieved with fast reactors, since thermal reactors are capable of burning less than 1 % of the uranium fuel.

The plutonium-239 breeder reactor is commonly called a fast breeder reactor, and the cooling of a liquid metal does heat transfer. The metals, which can

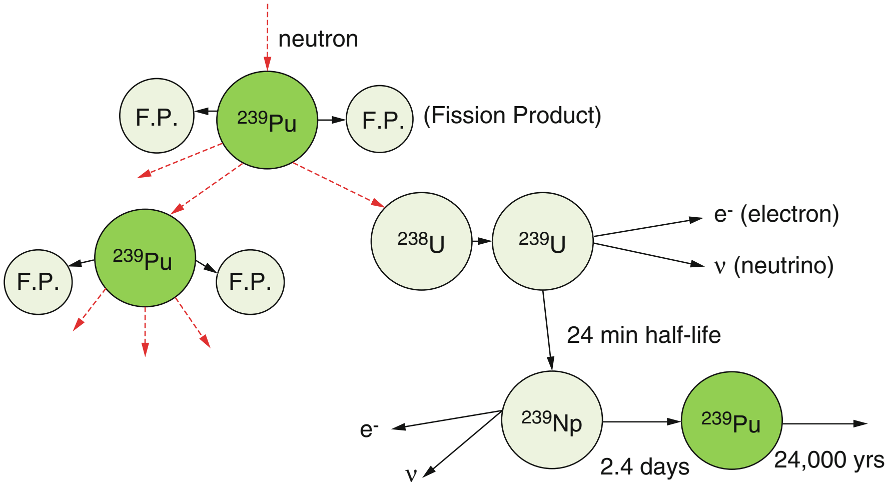

Fig. 14.1 Plutonium breeding process [1]

accomplish this, are sodium and lithium, with sodium being the most abundant and most commonly used. The construction of the fast breeder requires a higher enrichment of U-235 than a light-water reactor, typically 15–30 %. The reactor fuel is surrounded by a "blanket" of nonfissionable U-238. No moderator is used in the breeder reactor since fast neutrons are more efficient in transmuting U-238 to Pu-239. At this concentration of U-235, the cross section for fission with fast neutrons is sufficient to sustain the chain reaction. Using water as coolant would slow down the neutrons, but the use of liquid sodium avoids that moderation and provides a very efficient heat transfer medium. Figure 14.2 is a typical schematic and layout of a liquid metal fast reactor.

The Superphenix was the first large-scale breeder reactor. It was put into service in France in 1984. It ceased operation as a commercial power plant in 1997. Such a reactor can produce about 20 % more fuel than it consumes by the breeding reaction. Enough excess fuel is produced over about 20 years to fuel another such reactor. Optimum breeding allows about 75 % of the energy of the natural uranium to be used compared to 1 % in the standard light-water reactor. The commercialized LMFBR, namely, Superphenix, in France, is depicted in Fig. 14.3.

The reactor core, the primary coolant pump, and the intermediate heat exchanger are contained in the main reactor tank in the pool design. The liquid sodium metal is contained in a simple double-walled tank as shown in Fig. 14.4, without penetrations below the sodium surface level and operating at atmospheric pressure. The loss of primary coolant becomes as unlikely as to be incredible.

The primary sodium has such a large thermal heat capacity that it can survive the loss of decay heat cooling after the reactor has been shut down for about 10 h. There exist a substantial margin between normal operating temperatures and the coolant boiling temperature.

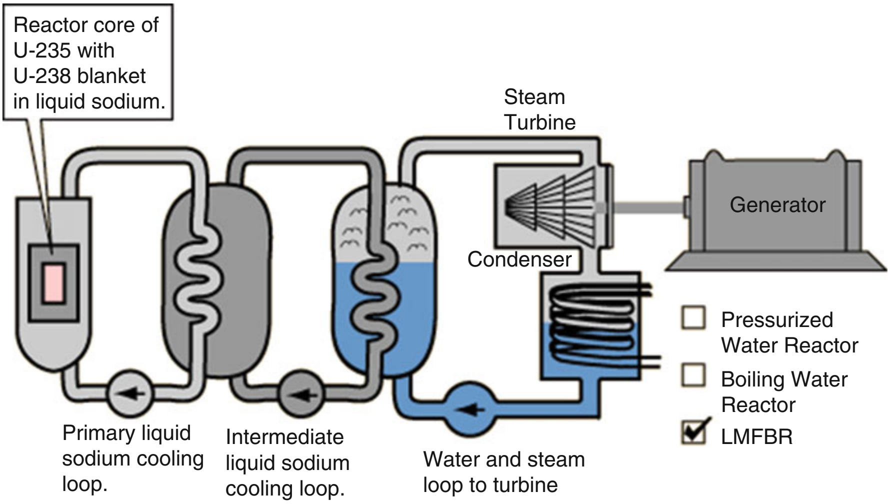

Fig. 14.2 A typical layout of liquid metal fast breeder reactor

Fig. 14.3 Superphenix fast reactor in France

Under appropriate operating conditions, the neutrons given off by fission reactions can "breed" more fuel from otherwise nonfissionable isotopes. The most common *breeding reaction* is that of plutonium-239 from non-fissile uranium-238. The term "fast breeder" refers to the types of configurations, which can actually produce more fissionable fuel than they use, such as the LMFBR. This

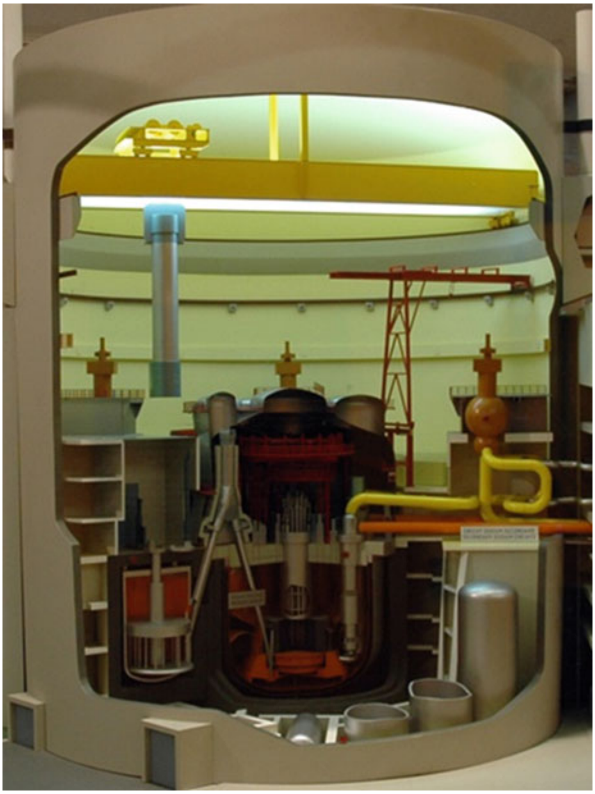

Fig. 14.4 This is a photo of a model of the containment vessel of the Superphenix. It is displayed at the National Museum of Nuclear Science and Technology in Albuquerque, NM

scenario is possible because the non-fissile uranium-238 is 140 times more abundant than the fissionable U-235 and can be efficiently converted into Pu-239 by the neutrons from a fission chain reaction.

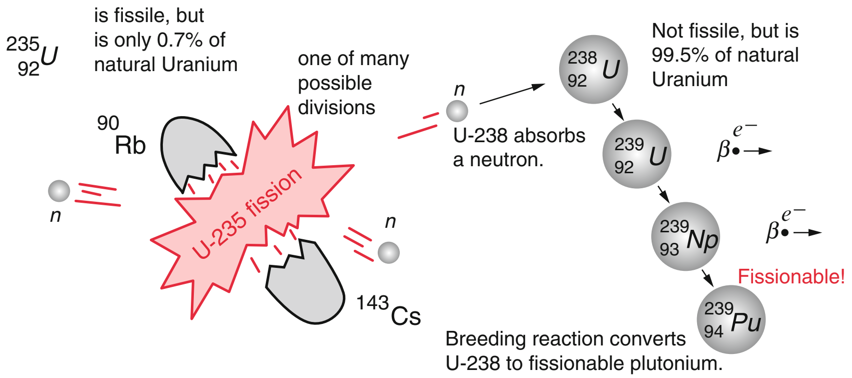

France has made the largest implementation of breeder reactors with its large Superphenix reactor (today is not in production line) and an intermediate Russian scale reactor (BN-600) on the Caspian Sea for electric power and desalinization [12].

Breeding plutonium-239 can be accomplished from non-fissile uranium-238 by the reaction as illustrated.

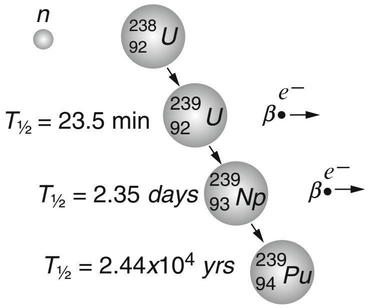

The bombardment of Uranium-238 with neutrons triggers two successive *beta decays* with the production of plutonium. The amount of plutonium produced depends on the *breeding ratio.*

The concept of breeding ratio of plutonium-239 can be defined in following. In the breeding of plutonium fuel in breeder reactors, an important concept is the breeding ratio, the amount of fissile plutonium-239 produced compared to the amount of fissile fuel (like U-235) used to produce it. In the liquid metal fast breeder reactor (LMFBR), the target breeding ratio is 1.4, but the results achieved have been about 1.2. This is based on 2.4 neutrons produced per U-235 fission, with one neutron used to sustain the reaction.

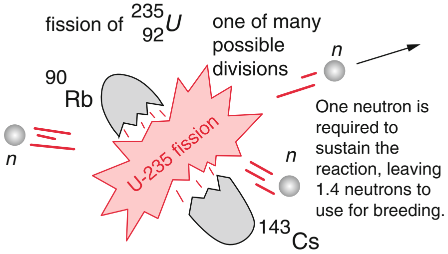

One neutron is required to sustain the reaction, leaving 1.4 neutrons to use for breeding.

This particular fission path yields three neutrons, but the average neutron yield is 2.4 neutrons.

The time required for a breeder reactor to produce enough material to fuel a second reactor is, called its doubling time, and present design plans target about ten years as a doubling time. A reactor could use the heat of the reaction to produce energy for 10 years, and at the end of that time have enough fuel to fuel another reactor for 10 years.

Liquid sodium is used as the coolant and heat transfer medium in the LMFBR reactor. This immediately raised the question of safety since sodium metal is an extremely reactive chemical and burns on contact with air or water (sometimes explosively on contact with water). It is true that the liquid sodium must be protected from contact with air or water at all times and kept in a sealed system. However, it has been found that the safety issues are not significantly greater than those with high-pressure water and steam in the light-water reactors.

Sodium is a solid at room temperature but liquefies at 98 °C. It has a wide working temperature since it does not boil until 892 °C. That brackets the range of operating temperatures for the reactor so that it does not need to be pressurized, as does a water-steam coolant system. It has a large *specific heat* so that it is an efficient heat transfer fluid.

In practice, those reactors, which have used liquid metal coolants, have been fast neutron reactors. The liquid metal coolant has a major advantage there because water as a coolant also moderates or slows down the neutrons. Such fast neutron reactors require a higher degree of enrichment of the uranium fuel than do the water-moderated reactors.

14.2 The Concept of Stiffness

Scientists and engineers often are in need of solving mathematical models that are defined by means of partial differential equations (PDEs). The solution of such PDEs using the concept of stiffness method is achieved by integrating the equations in the time domain, with special regard for the constraints prescribed by the fact that the time-dependent ordinary differential equations (ODEs) in space and time. Aiken [13] in his published paper under title of "Stiff Computation" shows cases that are studied in solving these PDEs through this concept via time-dependent ODEs. As part of his case studies in particular, we can mention:

1. When a partial differential equation (PDE) is discretized in the spatial domain by using a finite-difference, finite element, or global collection method, where the resulting equations in time are stiff and the degree of stiffness can more often be estimated.
2. When integration schemes that work well for large error tolerance are valuable.
3. Schemes and packages must be applicable to combined ODEs and algebraic equation, since these often occur in practice.
4. For large time-dependent problems in two and three spatial dimensions, extensive codes have already been developed using schemes that may not be the best for stiff problems.

Case studies can be applied to chemical reactors in the form of packed beds for kinetic behavior that traditionally are stiff, and the reactor of this type can become stiffer due to sharp changes in temperature. These type reactors provide a useful and require more testing ground for stiff integrators. The other studies are observed for flow within porous media, where the problem is extremely stiff and good numerical solutions are not easy to find given the conditions of the problem in hand. In this particular case, the spatial variation of the solution plays a role both in defining the stiffness and in limiting certain advantages of stiff integration codes. The other examples of stiffness concept are in the convective diffusion equations, where these equations have similar difficulties to the equation for flow through porous media, but they are linear-type PDEs or ODEs. However, in two-dimensional time-dependent simulations, the most sophisticated techniques are in demand [13].

For a chemical reactor with packed-bed model, the following partial differential equations including the appropriate boundary and initial conditions do apply:

$$\frac{\partial c}{\partial r} = \frac{\alpha}{r}\frac{\partial}{\partial r}\left(r\frac{\partial c}{\partial r}\right) + \beta R(c,T) \tag{14.1}$$

$$\frac{\partial T}{\partial t} = \frac{\alpha'}{r}\frac{\partial}{\partial r}\left(r\frac{\partial T}{\partial r}\right) + \beta' R(c,T) \tag{14.2}$$

$$\frac{\partial c}{\partial r} = \frac{\partial T}{\partial r} = 0 \;\; \rightarrow \text{at } r = 0 \tag{14.3}$$

$$c = c_0 \; T = T_0 \rightarrow \text{at } t = 0 \tag{14.4}$$

$$\frac{\partial c}{\partial r} = 0 \qquad -\frac{\partial T}{\partial r} = Bi_{\mathrm{w}}(T - T_{\mathrm{w}}) \;\; \rightarrow \;\; \text{at } r = 1 \tag{14.5}$$

One method to solve these equations numerically is the utilization of a finite-difference method in order to illustrate the spatial variation of the solution and then use some other methods such as the Runge–Kutta method for the solution in time, giving the Crank–Nicolson strategy [13].

Other method worth mentioning here, in order to solve these types of PDEs above, is to illustrate the spatial variation of the solution with a polynomial defined over the entire domain, $0 \le r \le 1$, where the collocation is applied at the Gaussian quadrature points, giving the orthogonal collocation method.

In case of neutronic analysis for nuclear reactor systems, one can use an original methodology based on the Padé and Chebyshev rational approximations for the solution of the nonlinear point kinetics equations with temperature reactivity feedback. In this type approach, one can make an assumption of piecewise constant approximations of the reactivity and source function, where the applied technique is enhancing the case by explicitly accounting for the feedback and the reactivity variations within a time step through an iterative cycle [14].

In approach like the above, Chebyshev rational method can be employed, and an important feature of such rational method is that good numerical approximations to the solutions of the stiff coupled kinetics differential equation can be obtained, using a single time step, as opposed to several time steps required for the conventional methods. As part of Chebyshev rational method, we can point out the following as:

- The stiffness of the kinetic systems are resolved by piecewise approximation.
- The Chebyshev rational approximations are one-step approach and not alpha stable.
- The results confirm the theoretical analysis and indicate the range of applicability.
- The Chebyshev exhibits a significant computational advantage by reducing the CPU time.

- The great advantage is that the method remains valid for full space–time kinetics.

The Aboanber [14] study indicates that the cases of approximations, which combined with its alpha (α) stability, lead to a better reduction of the errors when intermediate and large times are reached after series of small time steps if the inserted reactivity is positive and sufficiently large. Numerical studies are presented for different benchmark problems of various reactivity insertions, time-varying reactivity, and temperature feedback reactivity. The results confirm the theoretical analysis and indicate the range of applicability of the methods presented. The computational results indicate that the method is efficient and accurate.

14.3 The Quasi-Static Method

The study of the dynamic behavior of the present-generation, namely, Generation III (GEN III), and next-generation (GEN IV) nuclear reactors is a fundamental aspect for safety and reliability assessments. Despite the growing performances of modern computers, the full solution of the neutron Boltzmann equation in the time domain is still an impracticable task; thus, several approximate dynamic models have been proposed for the simulation of nuclear reactor transients; the quasi-static method represents the standard tool currently adopted for the space–time solution of neutron transport problems. All the practical applications of this method that have been proposed contain a major limit, consisting in the use of isotropic quantities, such as scalar fluxes and isotropic external neutron sources, being the only data structures available in most deterministic transport codes. The loss of the angular information produces both inaccuracies in the solution of the kinetics model and the inconsistency of the quasi-static method itself [15].

The innovative features introduced by next-generation nuclear reactors require as much innovation in the analysis of their performances and safety aspects. The safety assessment of such reactors, in particular, requires the accurate simulation of the behavior of the reactor core during typical operational and accidental conditions, with the need for the solution of the neutron transport equation. Being the full-time inversion of the neutron Boltzmann equation, an impracticable task, the study of the dynamics of a reactor, has to rely on the definition of approximate mathematical models. Hence, several approaches have been proposed during the years; as a result of such efforts, the quasi-static method has become a reference procedure to address reactor dynamics, and several implementations of the method can be found in the literature, both in diffusion and in transport [12, 15–22].

Generally speaking, the quasi-static method is a standard tool for the space–time solution of neutron transport problems in multiplying media. Its basic principle lies in a factorization of the angular flux into the product of two functions, "amplitude" and "shape," where the amplitude depends only on time (and contains the major part of the time dependence) while the shape function depends on all variables, with time included. The shape equation is solved on a long time scale, while the amplitude is determined on a short time scale. The factorization is made unique by proper normalization conditions for the shape function. Most implementations replace the basic equation (transport or diffusion) by a set of coupled amplitude and shape equations derived from the factorization, the so-called improved quasi-static method (IQM). An alternate approach already known for some time is called "predictor–corrector quasi-static method" (PCQM). We discuss its efficiency for both solid and liquid fuel system dynamics [19].

14.4 Bethe–Tait Models

It has been calculated that the core of a fast breeder reactor could explode with an explosion intensity equivalent to that up to 3000 t of TNT. This greatly exceeds the explosive energy needed to destroy the containment and release the vaporized plutonium fuel and fission products into the atmosphere.

In an accident in which no significant explosion occurred, the molten fuel may collect at the bottom of the reactor vessel and melt through it. Sodium fires may become fierce enough to breach the containment, releasing radioactivity into the atmosphere, even way beyond safety level. The interaction of sodium with some materials produces hydrogen, which is also inflammable or can accumulate to a concentration, which is explosive. In most safety analyses that are done, for fast breeder reactors (FBRs), even the basic information needed to make a rough judgment is not within the public domain.

The amount of energy release (i.e., the size of the explosion), which would challenge the containment for most of these breeder reactors around the world, is not publicly known.

Due to the nature of FBRs and the fuel that they use, there is a very real risk that an explosion at some breeder reactor is equivalent to a 3-kt nuclear weapon. In fact, in terms of radiation hazard, an FBR nuclear explosion would lead to greater contamination.

The amount of the radioactive fission products in the core of an FBR reactor will eventually build up to possibly about 300 million curies. This is equivalent to the amount of radioactivity initially released by the explosion of a nuclear weapon with the explosive power equivalent to that of the explosion of about 3000 t of TNT (3 Kt). The explosive power of the nuclear weapon, which destroyed Hiroshima, was about 12.5 Kt.

Although the radioactivity produced in a reactor is of the same origin as that produced by a nuclear weapon (i.e., nuclear fission), its composition is very different. The main difference is that in a nuclear weapon only the primary fission fragments are present at the moment of explosion. These are mostly short-lived radioisotopes, which subsequently decay into longer-lived ones. In a reactor, these longer-lived radioisotopes are continuously produced by the decay of the shorter-lived ones. The longer-lived radioisotopes, therefore, steadily accumulate.

This means that in a nuclear reactor the proportion of longer-lived radioisotopes is much greater than in a nuclear weapon. The decay of the radioactivity from a reactor is, therefore, much slower than that from a nuclear weapon. Thus, after 1 week, the radioactivity of the fission products from a nuclear weapon will have decayed to only 0.5 % of the initial amount, whereas the radioactivity from the fission products of a nuclear reactor will have decayed to one-third of the initial amount.

It takes nearly 3 months before the radioactivity from the fission products of a nuclear reactor to decay to a tenth of the initial amount. Therefore, the radiation doses resulting from a release of fission products from a nuclear reactor would remain at unacceptably high levels for a great deal longer than those from a nuclear weapon, which initially produced the same amount of radioactivity.

The nuclear accident at the Chernobyl reactor released about 50 million curies of radioactivity, some 5 % of the total in the core. If a very serious accident at any FBR were releasing about 17 % of the maximum amount of radioactivity in the core, it would release about the same amount as did the Chernobyl accident. In addition, a large amount of plutonium could be released into the environment.

Dealing with situation like the described above, from nuclear power accidental point of view, is called core disruptive accidents (CDAs), and that is the event resulting in significant damage to a reactor core. In an FBR, a CDA could be the melting of part of the reactor core, a meltdown of the core, or an energetic explosion.

CDAs are sometimes called hypothetical (or unthinkable) core disruptive accidents. This is usually done by those not wishing to acknowledge that such accidents are credible and could happen.

An energetic CDA is sometimes called a Bethe–Tait event [23].

Beth and Tait [23] devised a method of providing a rough estimate of the energy released in an energetic CDA, founding an approach widely used to find an upper limit for the containment of an FBR [23].

Events that can lead to a core disruptive accident (CDA) in a fast breeder reactor (FBR) are:

1. A loss of flow of the sodium together with a failure to automatically insert the control or safety rods to shut down the fission chain reaction (i.e., a failure to scram)
2. The introduction of too much reactivity into the core of the reactor, which in this scenario will cause a rapid increase in power (called an over-power transient) together with a failure to scram

In short, a serious accident can occur with an FBR either from losing cooling capacity without reducing the power level or from increasing the power without increasing the cooling capacity [2].

A scram has to be automated because a human being cannot generally react quickly enough to control a reactor in an emergency. For example, there is less than a millisecond to control a reactor, which has gone prompt critical, whereas the reaction of a human is typically about 200 milliseconds.

The Fermi 1 reactor accident was an example of a loss of flow of sodium, caused by a blockage of the coolant, causing the fuel to melt. The melting point of the fuel is about 2800 °C.

There may also be a major fracture in a pipe carrying coolant. A loss of power to the main pumps circulating the coolant and a failure of the diesel emergency generators to restart these pumps, or any standby pumps, in time, could lead to a CDA.

Because of the large mass of sodium in a pool-type FBR, it takes a few hours for the temperature to fall to the temperatures at which the cladding fails if the emergency cooling system does not work and no decay heat can be removed from the primary circuit. If there is a total loss of power to the pumps, the sodium will circulate naturally and cool the reactor core sufficiently to maintain its integrity. This will make few hours available to provide emergency cooling. An accident will, of course, be avoided only if the reactor is scrammed immediately after the power to the pumps is lost.

An earthquake could destroy the pumps and the control and safety rods and result to inevitable damage to the core of the reactor. An earthquake could also produce an over-power transient (a rapid increase in power due to the addition of reactivity), which could also be produced from the misuse or malfunction of the control and safety systems. As described earlier, unexplained positive reactivity fluctuations occurred in the Phenix FBR, which is still shut down.

Note that Westinghouse Corporation, which was known as the Clinch River Project around the 1980s, originally designed a prototype of Phenix reactor, a liquid metal fast breeder reactor (LMFBR). This author was involved with the analysis of fully inherent shutdown heat removal system for fast breeder reactors [24] as well as designing the mercury heat pipe [25, 26] for cooling systems as part of secondary loop.

A serious loss of flow of the sodium coolant or a fluctuation in positive reactivity could cause the fuel elements to melt. This may cause an explosion in the core of the reactor. Cochran describes how such an explosion could be produced after a loss of flow of the coolant.

The accident begins when power is lost to the pumps and the redundant safety and control systems fail to shut down (scram) the reactor. Sodium begins to boil near the center of the core of the reactor (the hottest part of the core). Bubbles are formed in the coolant when the sodium boils, reducing the moderating effect on the neutrons and causing the average energy of the neutrons to increase. The fission cross section for plutonium increases with increasing neutron energies. The rate of fission, therefore, increases. In other words, the loss of coolant leads to a positive reactivity coefficient in the reactor core and an increase in the power level.

The increase in power causes the sodium to boil more vigorously, which adds more reactivity, and so on. Webb [27] calls this process “autocatalytic reactivity” increases. The fact that an LMFBR is its own catalyst for generating power excursions is an inherent safety problem in the reactor [27].

In Cochran’s accident scenario [2], almost immediately after the sodium begins to boil, the cladding on the fuel elements begins to melt. The molten cladding flows up the channels between the fuel assemblies (bundles of fuel rods). Immediately after the cladding melts, the fuel itself melts and molten fuel flows up the channel. When the cladding and fuel flow into a part of the core, which is colder, they refreeze and clog up the flow of sodium in the fuel assemblies. Chunks of cladding and fuel fall to the bottom of the core, clogging it.

The fuel at the top of the reactor core could fall to the bottom of the core under gravity. If enough falls, in re-criticality could occur. The extent of the accident would, of course, depend on how much mechanical energy was released. If enough energy is released (i.e., a powerful explosion occurs), the seal between the reactor head and the reactor vessel could be breached, and the total energy released may be more than the reactor containment can withstand [2].

If, in an accident, molten cladding or molten fuel comes into contact with liquid sodium, a sodium vapor explosion might take place, damaging the rest of the core of the reactor. This is analogous to a steam explosion, like the first explosion in the Chernobyl reactor, which can take place when water is mixed suddenly with some molten metal, due to the rapid transfer of the heat from the metal to the water.

A CDA which does not cause an explosion, but in which the core melts and collects on the floor of the reactor vessel, is likely to result in a melt-through of the reactor vessel. This could lead to a sodium fire, which could eventually breach the secondary containment.

In recent decade, a lot of research and calculations by scientists and engineers around the Bethe and Tait method have taken place. One study that is done by Sha and Walter [23] around a two-dimensional $(r-z)$ integral model for characterizing fast reactor excursions from accident inception through core disassembly was presented.

For predisassembly calculations, which they have taken into account, an Eulerian geometric model is used, and multichannel heat transfer computations were performed. Reactivity feedback due to Doppler broadening, coolant density change and voiding, and fuel movement were taken into account. A Lagrangian coordinate system was used in the disassembly phase, wherein the neutronics balance consists of Doppler broadening and material motion. A unique feature of the model is the ability to accommodate a pointwise energy density-dependent equation of state according to the local sodium inventory that actually exists at the time of disassembly. By providing a consistent basis for establishing the effective reactivity ramp rate, Doppler coefficient, appropriate equation of state, and temperature distribution at the start of core disassembly, much of the arbitrariness normally associated with large accident analyses can be removed. For most accident analyses, this model predicts a significantly lower energy yield during a super-prompt critical nuclear excursion that would be computed by using the conventional modified Bethe–Tait analysis [28].

The original Bethe–Tai analysis [1] was intended only as an order of magnitude estimate of potential energy release from a worst-case disassembly accident. For the purpose of these analyses, many approximations were made by Bethe–Tait for their model to allow them a back-of-the-envelope calculated solution. Their principle assumptions included the following topics:

1. Taking the advantage of the point kinetics formulation analyses.
2. Use of perturbation theory.
3. Eliminating consideration for delayed neutrons.
4. No Doppler feedback.
5. Assumption for a threshold equation of state.
6. Considering spherical shape for reactor core geometry.
7. Reactor was assumed to be completely homogeneous core.
8. Constant fuel density.

The third assumption above was very well justified for the Bethe–Tait model [23] by core dynamic response analyses, only during the prompt critical condition, and Doppler feedback was ignored, because of the core designs in the United States. Their assumption was also based on these early reactor cores that were metal fueled; hence, little Doppler effects and spherical geometry were chosen for the simplicity of finding an analytical solution without any access to a large-scale computing platform, as it is available to us today.

In the Bethe–Tait model [23], reactivity could be added at a constant ramp rate until a threshold energy density is reached, and beyond this time, internal pressures quickly rise and disassembly occurs. In this case, the neutronic transient terminates when the magnitude of the negative disassembly reactivity equals the input reactivity in excess of prompt critical.

Problems

There are no homework problems for this chapter.

References

1. Thomas B. Cochran, Harold A. Feivesion, W. Patterson, G. Pshakin, M.V. Raman, M. Schneider, T. Suzuki, F. von Hipple, Fast breeder reactor programs: history and status. Research Report 8, International Panel on Fissile Materials, February 2010. www.fissilematerials.org
2. T.B. Cochran, *The Plutonium Burner*. Proceeding of the International Conference on Plutonium, Omiya, Japan, 2–4 Nov 1991, pp. 119–151
3. B. Zohuri, *Combined Cycle Driven Efficiency for Next Generation Nuclear Power Plants: An Innovative Design Approach* (Springer, Cham, 2015)
4. B. Zohuri, *Application of Compact Heat Exchangers For Combined Cycle Driven Efficiency In Next Generation Nuclear Power Plants: A Novel Approach* (Springer, Cham, 2015)
5. B. Zohuri, P.J. McDaniel, C.R. de Olivera, Advanced nuclear open air-brayton cycles for highly efficient power conversion. Nucl. Technol. **192**(1), 48–60 (2015)
6. C. Forsberg, P.J. McDaniel, B. Zohuri, *Variable electricity and steam from salt, helium, and sodium cooled base-load reactors with gas turbines and heat storage*. Proceedings of ICAPP 2015, 3–6 May 2015—Nice (France) Paper 15115

7. Zohuri, B., P. McDaniel, A comparison of a recuperated open cycle (air) Brayton power conversion system with the traditional steam Rankine cycle for the next generation nuclear power plant. Nuclear Science October 2015 issue.
8. B. Zohuri, *Innovative Open Air Brayton Combined Cycle Systems for the Next Generation Nuclear Power Plants* (University of New Mexico Publications, 2014)
9. P.J. McDaniel, B. Zohuri, C.R.E. de Oliveira, A combined cycle power conversion system for small modular LMFBRs. ANS Trans., September 2014
10. B. Zohuri, P. McDaniel, C.R.E. de Oliveira, A comparison of a recuperated open cycle (Air) Brayton power conversion system with the traditional steam Rankine cycle for the next generation nuclear power plant. ANS Trans., June 2014
11. P.J. McDaniel, C.R. E. de Oliveira, B. Zohuri, J. Cole, A combined cycle power conversion system for the next generation nuclear power plant. ANS Trans., November 2012.
12. F. Alcaro, S. Dulla, G. Marleau, E.H. Mund, P. Ravetto, Development of dynamic models for neutron transport calculations. Il Nuovo Cimento C **33**, 13–20 (2010)
13. Richard C. Aiken, *Stiff Computation* (Oxford University Press, 1985)
14. A. Aboanber, Stiffness treatment of differential equations for the point reactor dynamic systems. Prog. Nucl. Energy **71**, 248–257 (2014)
15. Fabio Alcaro, Sandra Dulla, Piero Ravetto, Romain Le Tellier, Christophe Suteau, Implementation of the Quasi-Static Method for Neutron Transport. International Conference on Mathematics and Computational Methods Applied to Nuclear Science and Engineering (M&C 2011) Rio de Janeiro, 8–12 May 2011, on CD-ROM, Latin American Section (LAS)/American Nuclear Society (ANS). ISBN 978-85-63688-00-2
16. K.O. Ott, D.A. Meneley, Accuracy of the Quasistatic treatment of spatial reactor kinetics. Nucl. Sci. Eng. **36**, 402–411 (1969)
17. J. Devooght, Quasistatic solutions of reactor kinetics. Ann. Nucl. Energy **7**, 47–58 (1980)
18. J. Devooght, E.H. Mund, Generalized Quasistatic method for space-time kinetics. Nucl. Sci. Eng. **76**, 10–17 (1980)
19. S. Dulla, E.H. Mund, P. Ravetto, The quasi-static method revisited. Prog. Nucl. Energy **50**, 908–920 (2008)
20. P. Picca, S. Dulla, E.H. Mund, P. Ravetto, G. Marleau, Quasi-Static Time-Dependent Computational Tool Using the DRAGON Transport Code, *PHYSOR 2008*, Interlaken, 14–19 Sept 2008
21. S. Goluoglu, H.L. Dodds, A time-dependent, three-dimensional neutron transport methodology. Nucl. Sci. Eng. **139**, 248–261 (2001)
22. S. Yun, J.W. Kim, N.Z. Cho, Monte Carlo space-time reactor kinetics method and its verification with time-dependent SN method, *PHYSOR 2008*, Interlaken, 14–19 Sept 2008
23. H.A. Bethe, J.H. Tait, An estimate of the order of magnitude of the explosion when the core of a fast reactor collapses. UKAEA-RHM (1956)
24. B. Zohuri, Applied technology publication on inherent shutdown heat removal system for fast breeder reactors for Division of Reactor Research and Technology. U.S. Department of Energy)
25. B. Zohuri, *Heat Pipe Design and Technology: Modern Applications for Practical Thermal Management*, 2nd edn. (Springer, Switzerland, 2016)
26. B. Zohuri, *Heat Pipe Design and Technology: A Practical Approach* (CRC and Francis Taylor, 2012)
27. R. Webb, Catastrophic nuclear accident hazards—a warning for Europe, Hinkley Point C Inquiry Document S1982, p. 83
28. W.T. Sha, A.E. Walter, An integrated model for analyzing disruptive accident in fast reactors. Nucl. Sci. Eng. **44**(2), 135–156 (1971)
29. Herbert Kouts, The development of breeder reactors in the United States. Ann. Rev. Energy 8 (1983): 383

Chapter 15
Fission Product Buildup and Decay

Nuclear fission products are the atomic fragments left after a large atomic nucleus undergoes nuclear fission. Typically, a nucleus that has a large atomic mass like uranium could fission by splitting into two smaller nuclei, along with a few neutrons. This process results in the release of heat energy, such as kinetic energy of the nuclei, and gamma rays. The fission products themselves are often unstable and radioactive, due to being relatively neutron rich for their high atomic number, and many of them quickly undergo beta decay. This releases additional energy in the form of beta particles, antineutrinos, and gamma rays. Thus, fission events normally result in beta radiation and antineutrinos, even though these particles are not produced directly by the fission event itself.

15.1 Background Introduction

Early in World War II, the scientific community in the United States, including those Europeans now calling the United States their safe home, pursued the idea that uranium fission and the production of excess neutrons could be the source of extraordinary new weapons. They knew that Lise Meitner's interpretation, in Sweden, of Hahn's experiments would likely be known in Germany. Clearly, there might now be a race commencing for the development and production of a new, super weapon based on the fission of $^{235}U_{92}$ or $^{239}Pu_{94}$.

By early 1942, it was, known that the two naturally occurring isotopes of uranium reacted with neutrons as follows:

B. Zohuri, *Neutronic Analysis For Nuclear Reactor Systems*,
DOI 10.1007/978-3-319-42964-9_15

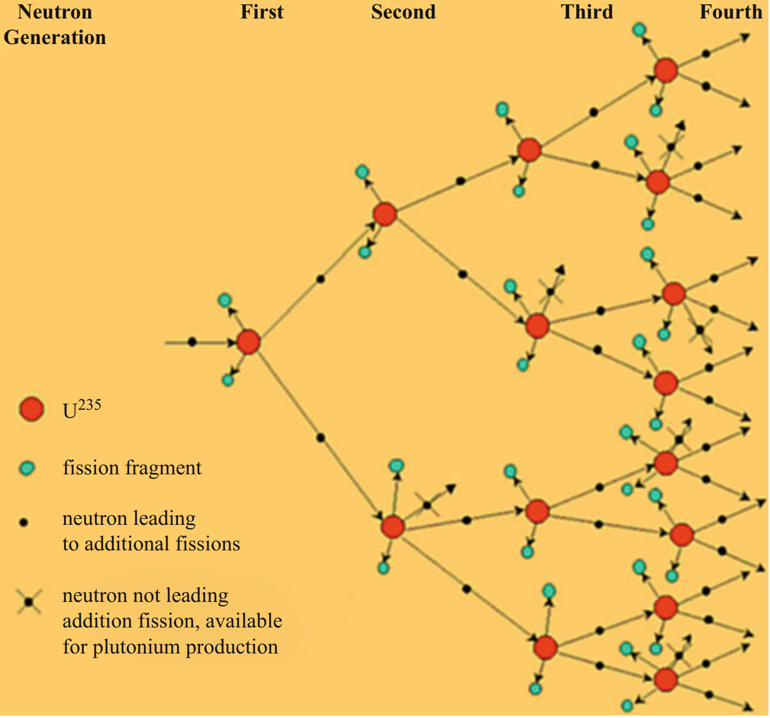

Fig. 15.1 The first generations of a nuclear chain reaction [1]

$$^{235}\mathrm{U}_{92} + {}^{1}\mathrm{n}_0 \rightarrow \text{fission products} + (2.5)^{1}\mathrm{n}_0 + 200\,\mathrm{MeV\ Energy}$$

$$^{238}\mathrm{U}_{92} + {}^{1}\mathrm{n}_0 \rightarrow {}^{239}\mathrm{U}_{92}$$

$$^{239}\mathrm{U}_{92} \rightarrow {}^{239}\mathrm{Np}_{93} + \beta^{-1} \quad \mathrm{t}_{1/2} = 23.5\,\mathrm{min.}$$

$$^{239}\mathrm{Np}_{93} \rightarrow {}^{239}\mathrm{Pu}_{94} + \beta^{-1} \quad \mathrm{t}_{1/2} = 2.33\,\mathrm{days}$$

Each U-235 that undergoes fission produces an average of 2.5 neutrons. In contrast, some U-238 nuclei capture neutrons, become U-239, and subsequently emit two beta particles to produce Pu-239. The plutonium is a fissile element also, and it would produce energy by the same mechanism as the uranium. A flow sheet for uranium fission is shown in Fig. 15.1 [1].

The answers to two questions were critical to the production of plutonium for atomic bombs:

1. Is it possible, using natural uranium (99.3 % U-238 and 0.7 % U-235), to achieve a controlled chain reaction on a large scale? If so, some of the excess neutrons produced by the fission of U-235 would be absorbed by U-238 and produce fissionable Pu-239.

2. How can we separate in a reasonable time period the relatively small quantities of Pu-239 from the unreacted uranium and the highly radioactive fission product elements?

Although fission had been observed on a small scale in many laboratories, no one had carried out a controlled chain reaction that would provide continuous production of plutonium for isolation.

The fission products themselves are often unstable and radioactive, due to being relatively neutron rich for their high atomic number, and many of them quickly undergo beta decay. This releases additional energy in the form of beta particles, antineutrinos, and gamma rays. Thus, fission events normally result in beta radiation and antineutrinos, even though these particles are not produced directly by the fission event itself.

Many of these nuclides have a very short half-life and therefore are very radioactive. For instance, strontium-90, strontium-89, and strontium-94 are all fission products, they are produced in similar quantities, and each nucleus decays by shooting off one beta particle (electron) [1].

Enrico Fermi thought that he could achieve a controlled chain reaction using natural uranium. He had started this work with Leo Szilard at Columbia University, but moved to the University of Chicago in early 1942.

The first nuclear reactor, called a pile, was a daring and sophisticated experiment that required nearly 50 t of machined and shaped uranium and uranium oxide pellets along with 385 t—the equivalent of four railroad coal hoppers—of graphite blocks, machined on site. See Fig. 15.2.

The pile itself was assembled in a squash court under the football field at the University of Chicago from the layered graphite blocks, uranium, and uranium oxide lumps (Fermi's term) arranged roughly in a sphere with an anticipated 13 ft radius. Neutron-absorbing, cadmium-coated control rods were inserted in the pile. By slowly withdrawing the rods, neutron activity within the pile was expected to increase, and at some point, Fermi predicted that there would be one neutron produced for each neutron absorbed by either producing fission or by the control rods [1].

On December 2, 1942, with 57 of the anticipated 75 layers in place, Fermi began the first controlled nuclear chain reaction occurred. At around 3:20 p.m., the reactor went critical; that is, it produced one neutron for every neutron absorbed by the uranium nuclei. Fermi allowed the reaction to continue for the next 27 min before inserting the neutron-absorbing control rods. The energy-releasing nuclear chain reaction stopped as Fermi predicted it would. See Fig. 15.3.

In addition to excess neutrons and energy, the pile also produced a small amount of Pu-239, the other known fissionable material.

The achievement of the first sustained nuclear reaction was the beginning of a new age in nuclear physics and the study of the atom. Humankind could now use the tremendous potential energy contained in the nucleus of the atom. However, while a controlled chain reaction was achieved with natural uranium and could produce plutonium, it would be necessary to separate U-235 from U-238 to build a uranium bomb [1].

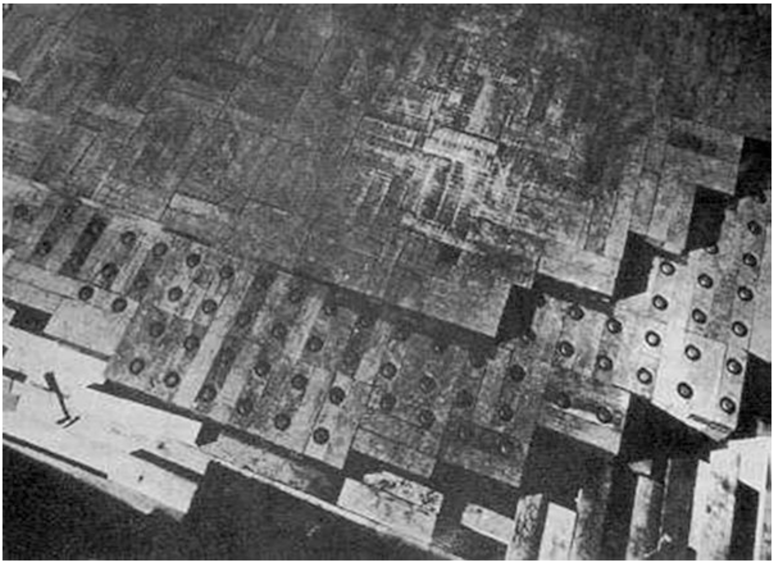

Fig. 15.2 CP-1—graphite blocks with 3 in. diameter uranium cylinders inserted, part of a layer of CP-1, the first nuclear reactor. A layer of graphite blocks without inserted uranium is seen covering the active layer [1]

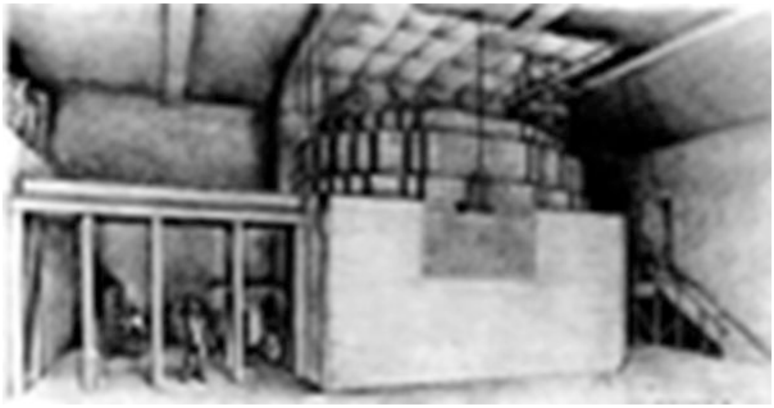

Fig. 15.3 The first controlled chain reaction, Stagg Field, Chicago, Dec. 2, 1942 (Courtesy of the Argonne National Laboratory)

15.2 Nuclear Fission and the Fission Process

As we have learned so far, the fission occurs with certain nuclei of high atomic or mass number and the large value of Z^2, and hence the repulsive force within the nucleus is an important contributory factor. When fission takes place, the exited compound nucleus formed after absorption of a neutron breaks up into two lighter nuclei, and these are called *fission fragments*.

During this process, if the neutron is one of low kinetic energy, which is, known as *slow neutron*, then generally speaking, the two fragment nuclei have unequal masses. This states that symmetrical fission by slow neutrons is rare, and in the majority of slow neutron fissions, the mass ratio of the fragments is approximately 2:3. Anyhow, in most fission process cases, one fission fragment has a substantially heavier mass than the other one. For example, a typical fission reaction is

$$n + \mathrm{U}_{92}^{235} \rightarrow \mathrm{Xe}_{54}^{140} + \mathrm{Sr}_{38}^{94} + 2n + 200\,\mathrm{Me\,V} \tag{15.1}$$

Note that we have mixed out our chemical notations for fission process, so that our readers will get use all kinds of them presented in different books and literatures as well. Bear in your mind that fission fragments are unstable because they have neutron to proton ratios that are too large and only three nuclides that are having sufficient stability to permit storage for a long time. They are, namely, uranium-233, uranium-235, and plutonium-239, fissionable by neutrons of all energies, from thermal values or less to millions of electron volts. U-235 is the only one, which occurs in nature, and the other two are produced artificially from U-238 and thorium-232, respectively, and this can be seen in the below steps.

$$\begin{aligned}
&{}^{232}\mathrm{Th}_{90} + {}^{1}\mathrm{n}_{0} \rightarrow {}^{233}\mathrm{Th}_{90} + \gamma \\
&{}^{233}\mathrm{Th}_{90} \rightarrow {}^{-1}\beta_{0} + {}^{233}\mathrm{Pa}_{91} \\
&{}^{233}\mathrm{Pa}_{91} \rightarrow {}^{-1}\beta_{0} + {}^{233}\mathrm{U}_{92}
\end{aligned}$$

where ${}^{233}\mathrm{Pa}$ is the symbol for protactinium-233.

Figure 15.4 depicts a plot of neutrons versus protons, and it indicates an upward curvature in the line of stable nuclei. This also is indicating that the ratio of neutrons to protons increases above 1:1 as the atomic number becomes larger (e.g., the prominent isotopes of carbon and oxygen are ${}^{12}\mathrm{C}_{6}$ and ${}^{16}\mathrm{O}_{8}$, but for lead and thorium, they are ${}^{207}\mathrm{Pb}_{82}$ and ${}^{232}\mathrm{Th}_{90}$). The dashed line in the Fig. 15.4 is the indication that the ratio of neutron to protons stays the same for nuclear fissions, where it is not for the two to three neutrons that are giving off promptly at the time of fission.

Even though the fission fragments lie above the curve of stable nuclei, less than 1 % of these fragments go through decay process by virtue of the delayed emission of neutrons. This is due to the predomination of decay mode by the beta emission, accompanied by one or more gamma rays.

This decay process moves the resulting nuclide toward the line of stable nuclei as the arrows indicated in Fig. 15.4.

However, more than one decay is normally required to get into the range of stable nuclei.

Given the fission fragment process in Eq. 15.1, we can have the following chemical process as

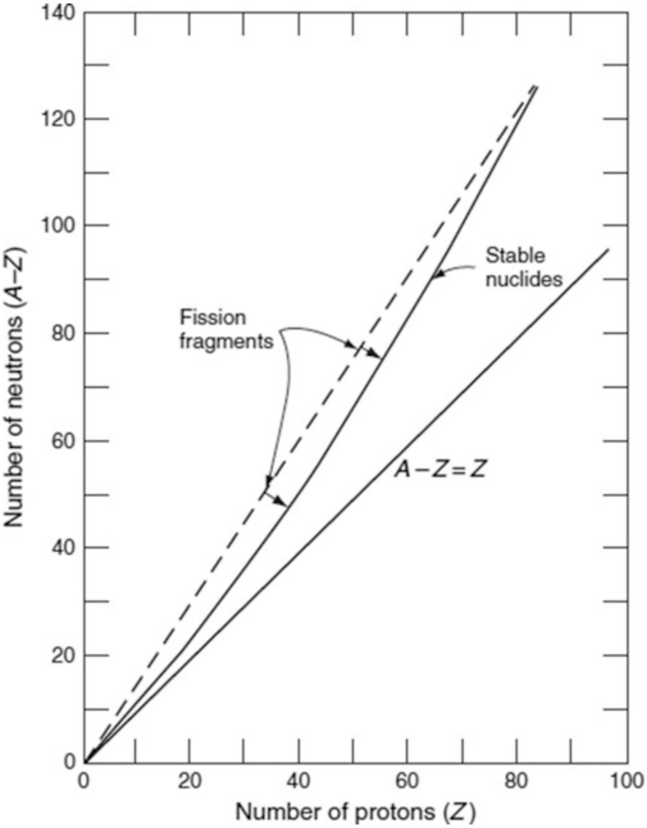

Fig. 15.4 Fission fragment instability (Adopted from Glasstone and Sesonske) [2]

$$\mathrm{Xe}_{54}^{140} \xrightarrow{\beta} \mathrm{Cs}_{55}^{140} \xrightarrow{\beta} \mathrm{Ba}_{56}^{140} \xrightarrow{\beta} \mathrm{La}_{57}^{140} \xrightarrow{\beta} \mathrm{Cs}_{58}^{140} \tag{15.2}$$

and

$$\mathrm{Sr}_{38}^{94} \xrightarrow{\beta} \mathrm{Y}_{39}^{94} \xrightarrow{\beta} \mathrm{Zr}_{40}^{94} \tag{15.3}$$

Each of these decays in Eqs. 15.2 and 15.3 is showing characteristics of half-life, and notably some exception is that the half-lives earlier in the decay chain tend to be shorter than those taking place later on in chain reaction process. The fission fragments taken together with their decay products are classified as fission products.

The detailed study of the slow neutron fission product of uranium-235 reveals that the compound nucleus splits up in more than 40 different ways, yielding over 80 primary fission products or fission fragments. However, the ranges of mass numbers of the fission products are within anywhere, from 72 for possible zinc isotope with atomic number of 30–160 which may be an isotope of terbium with atomic number 65 [2].

Figure 15.4 indicates the mass numbers of the products of thermal fission of uranium-235 and of the fast neutron fission of uranium-238 plot against the corresponding *fission yields*. Note that the fission yield can be defined as the proportion or percentage of the total nuclear fissions that form products of a given mass number.

As we can observe, Fig. 15.5 is plotted in semi-logarithmic scale, and this is because fission yields range from 10^{-5} to over 6 %. It should be noted that as two nuclei result from each fission process, the total yield for all mass numbers adds up to 200 %.

It should also be noted that the reason why mass numbers are considered over the atomic numbers is that most fission fragments are radioactive, decaying by the loss

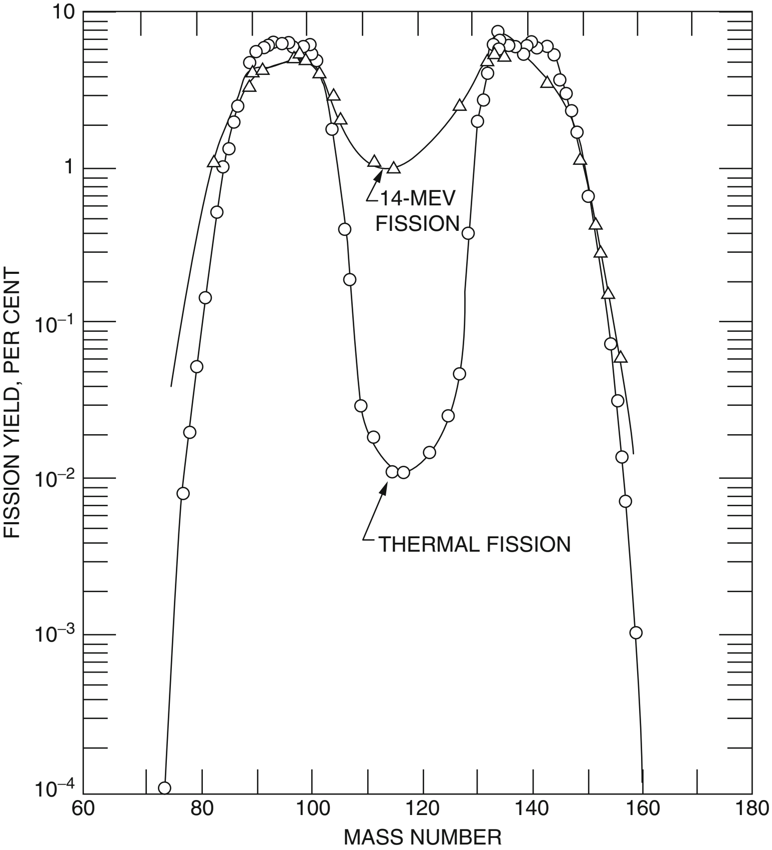

Fig. 15.5 Fission product yield as function of mass number for U^{235} (Adopted from Glasstone and Sesonske) [2]

of a negative beta particles as it was, as shown above. Due to this fact, the atomic numbers, consequently, change with time, but the mass numbers are unaffected by such beta decay. We will elaborate on this matter in the next section.

15.3 Radioactivity and Decay of Fission Product

As we mentioned in the previous section, nearly all, if not all, fission fragments are negative beta emitter, simply because they have neutron/proton ratios that are above the stability range. Figure 15.4 shows the relationship between the fission fragments and the stability curve for nuclei (see Fig. 15.6 as well). Note that in

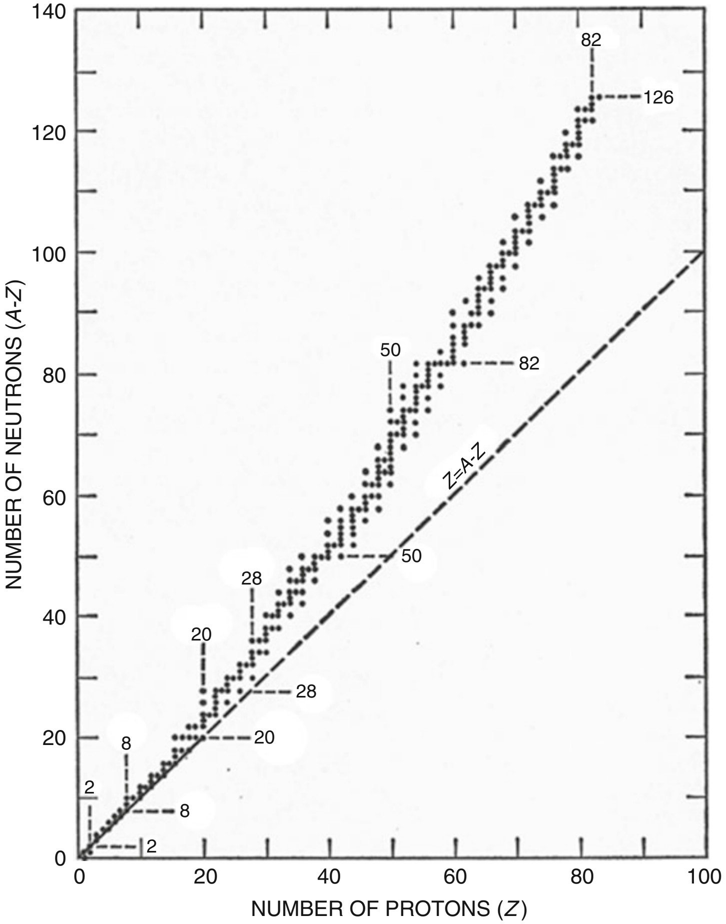

Fig. 15.6 Numbers of neutron and protons in stable nuclei (Adopted from Glasstone and Sesonske) [2]

Fig. 15.6, the short dashed lines indicate magic number of neutrons and protons, and this number is defined because certain nuclei exhibit exponential stability.

The immediate decay products are also usually radioactive, and, although some decay chains are longer, while some are shorter, each fragment on the average is following three stages of decay prior to any stable species found. Since there are some 80 different radioisotopes produced in fission and each is, on the average, the precursor of the other two, there are over 200 radioactive species present among the fission products after a short time [2].

In addition to beta particles, a large proportion of the radioactive fission products emit gamma rays, and these represent the so-called delayed fission gamma radiation. Most of the photons are of moderate energy, less than about 2 MeV, but a few of the fission products expel photons of higher energy. The latter are of interest for some shielding problems and for reactor control. The total energy of the delayed gamma radiation amounts to approximately 7 MeV per fission [2].

Also it should be noted that roughly 8 % of the 200 MeV of energy produced from fission process is attributable to the beta decay of fission products the gamma rays associated with it. Therefore, even following shutdown of a chain reaction, radioactive decay will continue to produce significant amounts of heat. Figure 15.7 shows the decay heat for a reactor that has operated at a power P for a long time.

The heat is approximated by the Wigner–Way formula as follows:

$$P_{\mathrm{d}}(t) = 0.0622 P_0 \left[t^{-0.2} - (t_0 + t)^{-0.2} \right] \tag{15.4}$$

where

$P_{\mathrm{d}}(t)$ = power generation due to beta and gamma rays
P_0 = power before shutdown

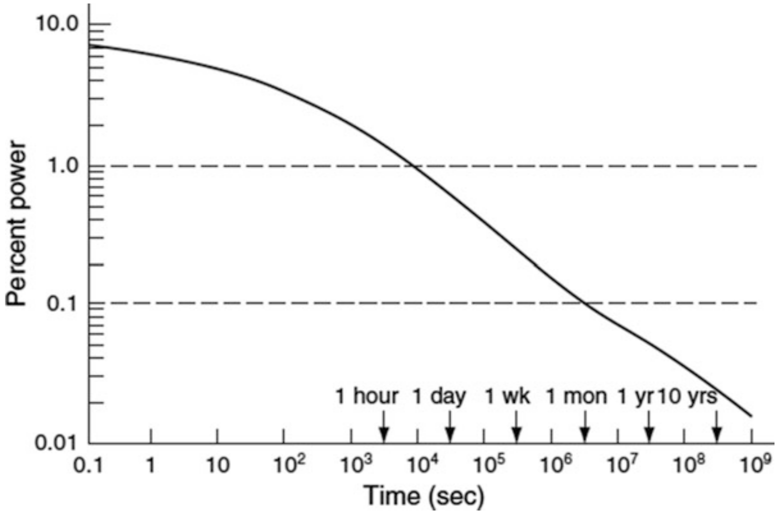

Fig. 15.7 Heat produced by decay of fission products [3]

$t =$ time, in seconds, of power operation before shutdown
$t_0 =$ time, in seconds, elapsed since shutdown

Because of decay heat, cooling must be provided to prevent overheating of reactor fuel for a substantial period of time following power plant shutdown [3].

The law that is governing the decay of a nucleus will allow us to better understand the number of other phenomena associated with reactor physics. This law states that the rate of decay is proportional to the number of nuclei present. Physics of decay for each radioisotope—that is, an isotope that undergoes radioactive decay—allows us to write the following mathematical notation for a simple ordinary differential equation:

$$\frac{d}{dt}N(t) = -\lambda N(t) \tag{15.5}$$

This differential equation indicates that decay has a characteristic decay constant λ. Thus, if the number of nuclei present at time t is $N(t)$ and the rate at which they decay is governed by Eq. 15.5, that is the behavior of radioactive decay.

The solution of this differential equation (i.e., Eq. 15.5) is a simple one and is derived as follows:

$$\begin{cases} \dfrac{dN(t)}{N(t)} = -\lambda dt \\ \displaystyle\int_{N(0)}^{N(t)} \frac{dN(t)}{N(t)} = -\lambda \int_0^t dt \\ \ln[N(t)/N(0)] = -\lambda t \\ N(t) = N(0)\exp(-\lambda t) \end{cases} \tag{15.6a}$$

Therefore, Eq. 15.6a indicates the final solution of Eq. 15.5 is a characteristic exponential rate of decay, which is written as

$$N(t) = N(0)\exp(-\lambda t) \tag{15.6b}$$

where $N(0)$ is the initial number of nuclei and graphical presentation of Eq. 15.6b is depicted in Fig. 15.8, which is nothing more than illustration of an exponential decay of radioactive materials.

The half-life, $t_{1/2}$, is a more intuitive measure of the times over which unstable nuclei decay. As defined earlier in Chap. 1, $t_{1/2}$ is the length of time required for one-half of the nuclei to decay. Thus, it may be obtained by substituting $N(t_{1/2}) = N(0)/2$ into Eq. 15.6b to yield $\ln(1/2) = -0.693 = -\lambda t_{1/2}$, or simply

$$t_{1/2} = 0.693/\lambda \tag{15.7}$$

A second, less-used measure of decay time is the mean time to decay, defined by

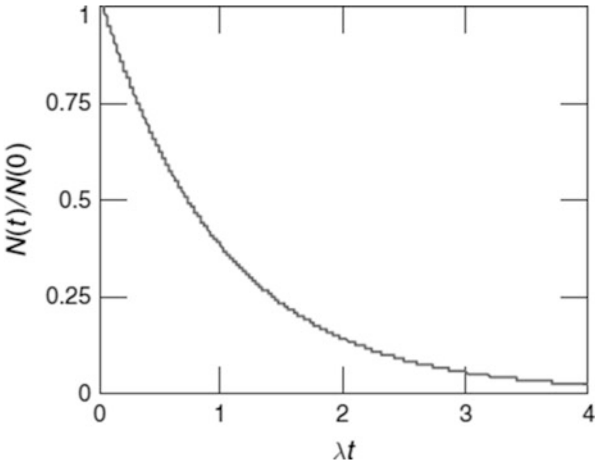

Fig. 15.8 Exponential decay of a radionuclide [3]

$$\bar{t} = \int_0^\infty tN(t)dt \Big/ \int_0^\infty N(t)dt = 1/\lambda \tag{15.8}$$

To calculate the number of nuclei present, we first note that Avogadro's number, $N(0) = 0.6023 \times 10^{24}$, is the number of atoms in 1 g molecular weight, and thus the total number of atoms is just mN_0/A where m is the mass in grams and A is the atomic mass of the isotope. The concentration in atoms/cm^3 is then $\rho N_0/A$, where ρ is the density in grams/cm^3.

For us to be able to describe the behavior of fission products and their rates of conversion of fertile to fissile materials and the number of other phenomena in reactor physics, the basic understanding of the above information is in order.

15.4 Poisons Produced by Fission

So far, we have learned that two fission fragments are produced virtually in every fission. Some of these nuclei and their progeny have substantial absorption cross sections, and their appearance in a nuclear reactor tends to reduce the multiplication factor k. For this given reason, these nuclei are known as *fission-produced poisons*. These play an important role in thermal reactors, because the absorption cross sections decrease rapidly with increasing neutron energy. Control poisons are neutron absorbers that are deliberately included in a reactor core. They may take the form of control rods, of soluble poisons dissolved in liquid coolants, or of the so-called burnable poisons permanently embedded in the fuel or other core constituents. Poisons serve a number of purposes [3].

Control rods are inserted or withdrawn in order to control the value of criticality factor k as it is needed for start-up, shutdown, and changes in power level. They may also be used to keep the reactor critical at a constant power by compensating for fuel depletion, fission product buildup, temperature changes, or other phenomena that affect the multiplication. Control poisons affect both the multiplication and the flux distribution of a core; thus, we must consider both. Now for the purpose of this study, if we focus our attention to reactor of infinite homogeneous type, then we can analyze a good approximation, the only effect of fission product poisons. The impact of this affection on multiplication factor k is on the thermal utilization factor f; therefore, the reactivity equivalent ρ of poisons in a previously critical reactor can be written as

$$\rho = \frac{k'_\infty - k_\infty}{k'_\infty} = \frac{f' - f}{f'} \tag{15.9}$$

where the primed parameters, k'_∞ and f', refer to the poisoned reactor, and in the absence of poison, thermal utilization factor f can be written as

$$f = \frac{\Sigma_{\mathrm{aF}}}{\Sigma_{\mathrm{aF}} + \Sigma_{\mathrm{aM}}} \tag{15.10}$$

where Σ_{aF} and Σ_{aM} are the macroscopic thermal absorption cross sections of the fuel and everything else, except the fuel, respectively. With the presence of poisons in reactor thermal utilization factor $f \rightarrow f'$, Eq. 15.10 becomes

$$f = \frac{\Sigma_{\mathrm{aF}}}{\Sigma_{\mathrm{aF}} + \Sigma_{\mathrm{aM}} + \Sigma_{\mathrm{aP}}} \tag{15.11}$$

where Σ_{aP} is the macroscopic cross section of the poison in the reactor. From Eq. 15.9, the reactivity ρ due to the poison then becomes

$$\rho = \frac{f' - f}{f'} = \frac{\Sigma_{\mathrm{aP}}}{\Sigma_{\mathrm{aF}} + \Sigma_{\mathrm{aM}}} \tag{15.12}$$

Equation 15.13 can be converted to a more convenient form by writing the multiplication factor of the unpoisoned reactor as

$$\begin{aligned} k_\infty = 1 &= \eta T f p \varepsilon \\ &= (\eta T p \varepsilon)\left[\frac{\Sigma_{\mathrm{aF}}}{\Sigma_{\mathrm{aF}} + \Sigma_{\mathrm{aP}}}\right] \\ &= \frac{\eta T f p \varepsilon \Sigma_{\mathrm{aF}}}{(\Sigma_{\mathrm{aF}} + \Sigma_{\mathrm{aP}})} = \frac{p \varepsilon \nu \Sigma_f}{(\Sigma_{\mathrm{aF}} + \Sigma_{\mathrm{aP}})} \end{aligned} \tag{15.13}$$

where Σ_{f} is the macroscopic fission cross section. Solving Eq. 15.13 for $(\Sigma_{\mathrm{aF}} + \Sigma_{\mathrm{aP}})$ and inserting this into Eq. 15.12, we get the following relationship:

$$\rho = -\frac{\Sigma_{\mathrm{aP}}/\Sigma_{\mathrm{f}}}{p\varepsilon v} \tag{15.14}$$

Equation 15.14 is the most suitable form of reactivity ρ for calculation of fission product poisoning.

However, in large reactor operating at a high thermal neutron flux and at constant power, the phenomenon called *xenon instability* can take place, which is the most important fission product poison, and is designated by the chemical symbol of Xe^{135}. Its thermal (2200 m/s) absorption cross section is 2.7×10^6 barns. This isotope is formed as the result of the decay of I^{135} and is produced directly in the fission of U^{235} as well. The I^{135} is not formed in fission but appears as the result of the decay of tellurium-135 or Te^{135}. These process and their half-lives are summarized below:

$$\underbrace{\mathrm{Te}_{42}^{135}}_{\text{fission, } \gamma_{\mathrm{T}}} \underset{11\ \mathrm{s}}{\overset{\beta^-}{\longrightarrow}} \underbrace{\mathrm{I}_{53}^{135}}_{\text{fission, } \gamma_{\mathrm{I}}} \underset{6.7\ \mathrm{h}}{\overset{\beta^-}{\longrightarrow}} \underbrace{\mathrm{Xe}_{54}^{135}}_{\text{fission, } \gamma_{\mathrm{X}}} \underset{9.2\,\mathrm{h}}{\overset{\beta^-}{\longrightarrow}} \mathrm{Cs}_{55}^{135} \underset{2.3\times 10^6\ \text{year}}{\overset{\beta^-}{\longrightarrow}} \mathrm{Ba}_{56}^{135} \tag{15.15}$$

In view of the fact that Te^{135} decays so rapidly to I^{135}, it is possible to assume that the I^{135} is produced directly in fission [4].

Next to Xe^{135} (xenon-135), the most important fission product poison, as it can be seen in the chemical chain reaction below, is Sm^{149} (samrium-149). This is a stable isotope with a capture cross section of 5 × 104 barns for thermal neutrons. Sm149 is not formed directly in fission product, but appears as the result of the decay of Nd^{149} (neodymium-149), and it is the end product of the decay chain reaction as follows:

$$\underbrace{\mathrm{Nd}^{149}}_{\text{fission}} \underset{2.0\ \mathrm{h}}{\overset{\beta^-}{\longrightarrow}} \mathrm{Pm}^{149} \underset{54\ \mathrm{h}}{\overset{\beta^-}{\longrightarrow}} \underbrace{\mathrm{Sm}^{149}}_{\text{stable}} \tag{15.16}$$

Since Nd^{149} decays comparatively rapidly to Pm^{149} (promethium-149), the Pm^{149} may be assumed to be produced directly in fission with yield Pm^{149}.

Although xenon makes the major contribution to fission product poisoning of a nuclear reactor operating at a flux of 10^{13} neutrons/(cm^3)(sec) or more, there are many other nuclides which accumulate during reactor operation and cause a decrease in the reactivity ρ. The method for determining the poisoning of each nuclide is the same, but it is beyond the scope of this book; therefore, we recommend that our reader for further information should refer to the list of references at the end of this chapter.

Problems

Problem 15.1: A thermal reactor using uranium-235 as fissile materials has been operating for some time (about 6.7 h) at an average flux $\phi = 2 \times 10^{14}$ neutron/(cm^2)(s); how long after shutdown will the xenon poisoning reach a maximum and what is the poisoning at this time?

Assume that the time to attain the maximum concentration of xenon (Xe) after shutdown is $t_{\max}$ and it is given by

$$t_{\max} = \frac{1}{\lambda_X - \lambda_I} \ln \frac{\lambda_x}{\lambda_I} \left(1 - \frac{\lambda_X - \lambda_I}{\lambda_I} \cdot \frac{X_0}{I_0} \right) \tag{15.17}$$

where

λ_I = decay constant of iodine-135
λ_X = decay constant of xenon-135
X_0 = xenon concentration at equilibrium
I_0 = iodine concentration at equilibrium

In addition, the *poisoning* $\psi(t)$, in general, of a reactor is defined as the ratio of the number of thermal neutrons absorbed by the poison to those absorbed in fuel; hence, we can write

$$\psi(t_s) = \frac{X(t_s)\sigma_X}{\Sigma_u} \tag{15.18}$$

where

$X(t_s)$ = xenon concentration at time t_s after shutdown
σ_X = absorption cross section of xenon-135
Σ_u = fuel macroscopic absorption cross section

Additionally, the equilibrium concentration, I_0, attained after the reactor that has been operating for some time is obtained by

$$I_0 = \frac{\gamma_I \Sigma_f \phi}{\lambda_I + \sigma_I \phi} \approx \frac{\gamma_I \Sigma_f \phi}{\lambda_I} \tag{15.19}$$

where

Σ_f = macroscopic fission cross section
γ_I = fission yield for iodine-135
ϕ = neutron flux
= absorption cross section of iodine-135

And, similarly, the equilibrium concentration, X_0, of xenon is obtained from the following equation as well:

$$X_0 = \frac{\lambda_\mathrm{I} I_0 + \gamma_\mathrm{X}\Sigma_\mathrm{f}\phi}{\lambda_\mathrm{X}^*} = \frac{\lambda_\mathrm{I}\left(\frac{\gamma_\mathrm{I}\Sigma_\mathrm{f}\phi}{\lambda_\mathrm{I}}\right) + \gamma_\mathrm{X}\Sigma_\mathrm{f}\phi}{\lambda_\mathrm{X}^*} = \frac{(\gamma_\mathrm{I} + \gamma_\mathrm{X})\Sigma_\mathrm{f}\phi}{\lambda_\mathrm{X}^*} \tag{15.20}$$

where $\lambda_\mathrm{X}^* = \lambda_\mathrm{X} + \sigma_\mathrm{X}\phi$ because the absorption cross section of xenon-135 is so high, λ_X^* is appreciably greater than λ_X, and γ_X is fission yield for xenon-135.

We can also write the xenon-135 concentration $X(t_\mathrm{s})$ at time t_s after shutdown as

$$X(t_\mathrm{s}) = \frac{\lambda_\mathrm{I}}{\lambda_\mathrm{X} - \lambda_\mathrm{I}} I_0\left(e^{-\lambda_\mathrm{I} t_\mathrm{s}} - e^{-\lambda_\mathrm{X} t_\mathrm{s}}\right) X_0 e^{-\lambda_\mathrm{X} t_\mathrm{s}}. \tag{15.21}$$

Problem 15.2: Let I and X denote the concentrations of the iodine and xenon isotopes. We then have

$$\frac{d}{dt} I(t) = \gamma_\mathrm{I}\Sigma_\mathrm{f}\phi - \lambda_\mathrm{I} I(t) \tag{15.22}$$

and

$$\frac{d}{dt} X(t) = \gamma_\mathrm{X}\Sigma_\mathrm{f}\phi - \lambda_\mathrm{I} I(t) - \lambda_\mathrm{X} X(t) - \sigma_\mathrm{aX} X(t)\phi \tag{15.23}$$

Note that there is no neutron absorption term, $\sigma_\mathrm{aI} I(t)\phi$, in Eq. 15.22, since even at high flux levels iodine absorption is insignificant compared to its decay.

Considering now, following reactor start-up, both iodine and xenon concentrations build from zero to equilibrium values over a period of several half-lives. Since the half-lives are in hours, after a few days, equilibrium is achieved. Find the final form of both Eqs. 15.22 and 15.23 for $t \to \infty$. Variable definitions are as what is given in Problem 15.1.

Problem 15.3: Let I_0 and X_0 be the concentrations of the iodine and xenon at the time of reactor shutdown. If the reactor is put on a large negative period, to first approximation, we may assume that the shutdown is instantaneous compared to the time spans of hours over which the iodine and xenon concentration evolve. Find the solution of Eqs. 15.22 and 15.23 that are given by Problem 15.2. Variable definitions are as what are given in Problem 15.1.

Problem 15.4: Prove that the following relation is valid if the reactor has been running for several days—long enough for iodine and xenon in order to reach equilibrium:

$$X(t) = \Sigma_{\mathrm{f}}\phi\left[\frac{(\gamma_{\mathrm{I}}+\gamma_{\mathrm{X}})}{\lambda_{\mathrm{X}}+\sigma_{\mathrm{aX}}\phi}e^{-\lambda_{\mathrm{X}}t}+\frac{\gamma_{\mathrm{I}}}{\lambda_{\mathrm{I}}-\lambda_{\mathrm{X}}}\left(e^{-\lambda_{\mathrm{X}}t}-e^{-\lambda_{\mathrm{I}}t}\right)\right] \tag{15.24}$$

Variable definitions are as what is given in Problem 15.1. *Hint*: Use the results that are given by the solution of Problem 15.2 and Problem 15.3.

Problem 15.5: Prove that for a reactor operating at a very high flux level, the maximum xenon-135 concentration takes place at approximately 11.3 h following shutdown.

Variable definitions are as what is given in Problem 15.1. *Hint*: Use the result of the solution for Problem 15.4.

Problem 15.6: Make a logarithmic plot of the effective half-life of xenon-135 over the flux range of $10^{10} \le \phi \le 10^{15}$ $n = \mathrm{cm}^2 = \mathrm{s}$. Use the relation of $\lambda' = \lambda + \sigma_{\mathrm{a}}\phi$, where σ_{a} is absorption cross section, λ radioactive decay constant, and ϕ neutron flux. Note that the effective half-life of xenon is given by $t_{1/2} = 0.693/\lambda$.

Problem 15.7: A thermal reactor fueled with uranium has been operating at a constant power for several days. Make a plot of the ratio of concentration of xenon-135 to uranium-235 atoms in the reactor versus its average flux. Determine the maximum value that this ratio. Note that the effective half-life of xenon is given by $t_{1/2} = 0.693/\lambda$. *Hint*: Use the result of the solution of Problem 15.2 for xenon. Note also that uranium-235 has date of $\gamma_{\mathrm{I}} = 0.0639$ and $\gamma_{\mathrm{X}} = 0.00237$ and $\sigma_{\mathrm{f}}^{25} = 2.65 \times 10^6$ barns.

Problem 15.8: If the rate of formation of neutron designated by q is taken to be constant outside the rod and zero inside, then the fraction of neutrons absorbed in single rod δk may be taken as the total worth of all the rods as it can be seen in the figure below, and it may be written as follows:

$$\begin{aligned}\delta k &= \frac{(\text{Exposed primeter of rod})\, D\nabla^2\phi\ (\text{at rod surface})}{q(\text{Area of source region})}\\ &\approx \frac{4l}{(m-2a)^2}\cdot\frac{1}{h\Sigma_{\mathrm{a}}+\frac{1}{L}\coth\left(\frac{m-2a}{2L}\right)}\end{aligned} \tag{15.25}$$

where

h = linear extrapolation distance
m = poison cell dimension
a = half thickness of cruciform control rod

Fig. P15.8 Poison cell for control rod calculation

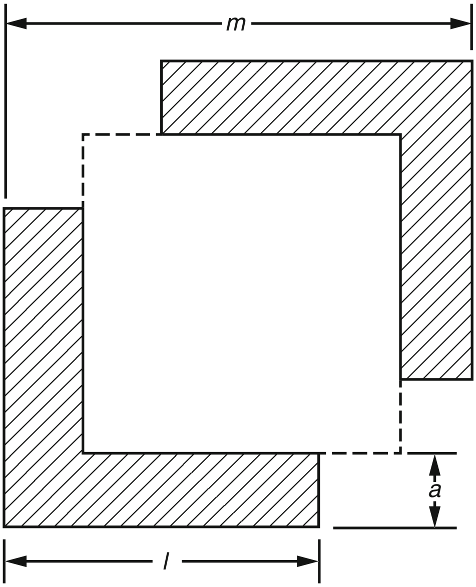

$l =$ half length of arm of cruciform rod
$L =$ diffusion length
$\Sigma_a =$ macroscopic absorption cross section

Now consider that in a water-moderate reactor, in which 32 cruciform control rods are distributed evenly throughout the core, the following dimensions are applicable: $l = 10.0$ cm, $a = 0.336$ cm, and $m = 19.5$ cm. The thermal neutron diffusion length in the core is 1.8 cm, and $\Sigma_a = 0.114\ \text{cm}^{-1}$. Estimate the total worth of the system of control rods.

Problem 15.9: If the rate of formation of neutron designated by q is taken to be constant outside the rod and zero inside, then the fraction of neutrons absorbed in single rod δk may be taken as the total worth of all the rods as it can be seen in the figure below, and it may be written as follows:

References

1. https://en.wikipedia.org/wiki/Nuclear_fission_product
2. S. Glasstone, A. Sesonske, *Nuclear Reactor Engineering* (D Van Nostrand Company, Princeton, 1967)
3. E. Elmer, *Lewis, Fundamentals of Nuclear Reactor Physics* (Academic, Amsterdam, 2008)
4. R. John, *Lamarsh, Introduction to Nuclear Reactor Theory* (Addison Wesley, Reading, 1966)

Chapter 16
Fuel Burnup and Fuel Management

Nuclear fuel is removed from a reactor every few years when it can no longer economically keep a chain reaction going. This "spent" fuel remains radioactive and must be managed. At first, it goes into a pool on-site for cooling and storage. Some utilities are moving their spent fuel after several years in the pool into the US Nuclear Regulatory Commission (NRC) certified dry storage casks. These casks are specially designed to contain the radioactivity and allow hot spent fuel to cool further. In contrast to fossil fuel, the fuel in nuclear reactors cannot be converted since the fuel undergoes changes during its use in the reactor, which require the fuel elements to be exchanged.

16.1 The World's Energy Resources

For the past half century, fossil fuels, namely, coal, oil, and natural gas, have supplied the major portion of the world's energy requirements. It has long been realized, however, that in the not too distance future, these sources of energy will be largely exhausted. At the present time, the total energy consumption, for all countries, is about 1×10^{17} Btu per year. Since the world's population is steadily growing and the power use per capita is increasing as well, the rate of energy utilization by the year 2020 could well be five to ten times the current value. According to one estimate, the known coal, oil, gas, and oil shale, which can be extracted at no more than twice the present cost, would be equivalent to roughly 4×1019 Btu^{10}. This means, about 100 years, the world's economically useful reserves of fossil fuels may approach exhaustion [1].

B. Zohuri, *Neutronic Analysis For Nuclear Reactor Systems*,
DOI 10.1007/978-3-319-42964-9_16

16.2 Today's Global Energy Market

Today's global energy market places many demands on power generation technology including high thermal efficiency, low cost, rapid installation, reliability, environmental compliance, and operation flexibility. The conclusion above, even considering some margin error in it, is inevitable that new sources of power must be found during the next 50 years or so if the earth is to support the growing population with some increase in living standards. Some consideration has been given to few such sources, for example, solar and wind energies as well as nuclear energy. Although solar and wind energies are very attractive, but developing large-scale processes along with a large farm of such systems are still some years away, nuclear energy has been made available and advanced in fission of the heaviest elements or at the stage of research still using fusion of very light nuclei. Technology of fusion process in commercial use with controlled release of such energies using either magnetic confinement of laser drive pellet of deuterium and tritium the two isotope of hydrogen is too far in advanced. Nuclear fission, on the other hand, has already been established as a practical means for production of energy and is getting to be at the point that is economically very competitive with energy produced from fossil fuels in very near future.

The total amount of basic raw materials as a source of fuel for fission power plants, such as uranium and thorium, in the earth's crust to a depth of three miles is very large, possibly something like 10^{12} t. However, much of this is present in minerals containing such a small proportion of the desired element that extraction would be very expensive and not very cost effective. This in particular for high-grade ore reserves that are believed to be in other of 2×10^6 t, therefore we need to reduce the cost of recovery from moderately low-grade ores to at least \$100 or less per pound of metal with advancing technology in this matter.

Development of plant layout and modularization concepts requires an understanding of both primary and secondary systems.

General Electric's steam and gas (STAG) combined cycle power generation equipment has met these demands and surpassed them, taking power plant performance to unprecedented levels.

The development of steam and gas turbine combined cycles has paralleled gas turbine development, resulting in reliable combined cycle plants. Those incorporating GE's advanced gas turbine technology have achieved efficiency levels approaching 58 % due primarily to the higher firing temperatures of advanced technology gas turbines. The MS9001H gas turbine will achieve 60 % efficiency in combined cycle application when it goes into full operation.

In addition to advances in gas turbine technology, steam turbine performance also has evolved. GE's STAG combined cycle power generation product line includes steam cycle options that satisfy a wide range of economic considerations including fuel flexibility, fuel cost, duty cycle, and space limitations.

Heat exchangers, filters, turbines, and other components in the integrated coal gasification combined cycle system must withstand demanding conditions of high temperatures and pressure differentials. Under the highly sulfiding conditions of the high-temperature coal gas, the performance of components degrade significantly with time unless expensive high-alloy materials are used. Deposition of a suitable coating on a low-cost alloy may improve its resistance to such sulfidation attacks and decrease capital and operating costs. A review of the literature indicates that the corrosion reaction is the competition between oxidation and sulfidation reactions. The Fe- and Ni-based high-temperature alloys are susceptible to sulfidation attacks unless they are fortified with high levels of Cr, Al, and Si. To impart corrosion resistance, these elements need not be in the bulk of the alloy and need only be present at the surface layers [1].

16.3 Fuel Utilization and Fuel Burnup

The fuel, which has not been spent, and the generated plutonium may be recovered by *reprocessing* the removed fuel elements. Light-water reactors have a burnup of 45,000–50,000 MW-days per metric ton (MWday/t) of uranium. This means that about 45–50 kg of fissionable material per ton of nuclear fuel used have been fissioned, and 360–400 million kilowatt-hours (kWh) of electricity have been generated at a nuclear power plant efficiency of 34 % [2].

Reprocessing is applied to nuclear fuel reprocessing procedures, where the chemical treatment of nuclear fuel after its use in a reactor to remove the fission products and to recover the unused uranium and the new fissile material plutonium generated during the fission.

In general sense the concept of nuclear fuel utilization should be in contrast with nuclear reactor design, and its relation to the concept of reactor design should be considered as part of the process.

In the present Generation III (GEN-III) nuclear reactors, there exist systems ranging from "burners" of highly enriched uranium, in which there is essentially no conversion of U^{238} to Pu^{239}, to breeders, which produce more fissile nuclei than are consumed. Therefore, if anyone attempts to make use of the nuclear energy available from natural uranium and thorium, a certain amount of breeding of fissile material will be necessary. These days, breeder reactors show better output efficiency than highly developed reactors that use nuclear fuel less effectively [2].

In summary, to understand "burnup," it helps to know more about the uranium that fuels a reactor. Before it is made into fuel, uranium is processed to increase the concentration of atoms that can split in a controlled chain reaction in the reactor. The atoms release energy as they split. This energy produces the heat that is turned into electricity. In general, the higher the concentration of those atoms, the longer the fuel can sustain a chain reaction. In addition, the longer the fuel remains in the reactor, the higher the burnup [2].

In other words, burnup is a way to measure how much uranium is burned in the reactor. It is the amount of energy produced by the uranium. Burnup is expressed in gigawatt-days per metric ton of uranium (GWd/MTU). The average burnup, around

35 GWd/MTU two decades ago, is over 45 GWd/MTU today. Utilities now are able to get more power out of their fuel before replacing it. This means they can operate longer between refueling outages. It also means they use less fuel.

The burnup level affects the fuel's temperature, radioactivity, and physical makeup. It is important to the NRC's review of spent fuel cask designs because each system has limits on temperature and radioactivity. How hot and how radioactive spent fuel is depends on burnup, as well as the fuel's initial makeup and conditions in the core. All these factors must be taken into account in designing and approving dry storage and transport systems for spent fuel [2].

Nuclear fuel is encased in metal cladding. In the reactor, this cladding reacts with cooling water. The reaction forms oxide on the outside (similar to rust) and releases hydrogen. These processes begin slowly and then start to accelerate as the fuel reaches burnup of 45 GWd/MTU. Anything higher is considered high burnup. However, in reality there is no sharp line between low and high burnup. It is a continuum. That means the difference between fuel burned to 45 GWd/MTU and 46 or 47 GWd/MTU can be very small [2].

When spent fuel is placed in a dry storage system and the water is removed, the temperature of the fuel increases and the makeup of the cladding can change. This change can result in the fuel cladding becoming less "ductile," or pliable, as it cools. It was also once thought that the cladding of higher burnup fuel could become brittle enough to create a safety concern. Research now shows that while it may become less ductile, the safety of the public will not be impacted for the systems the NRC has approved [2].

16.4 Fuel Reprocessing

A key, nearly unique, characteristic of nuclear energy is that used fuel may be reprocessed to recover fissile and fertile materials in order to provide fresh fuel for existing and future nuclear power plants. Several European countries, Russia, and Japan have had a policy to reprocess used nuclear fuel, although government policies in many other countries have not yet come around to seeing used fuel as a resource rather than a waste.

Application of chemical processes to separate the valuable substances—the still existing uranium and the newly generated fissile material plutonium—from the fission products, the radioactive waste in the spent nuclear fuel after its use in the reactor. The PUREX process for reprocessing underwent several years of large-scale trial. A spent fuel element has, apart from the structural material, approximately the following composition: 96 % uranium, 3 % fission products (waste), 1 % plutonium, and a small amount of transuranium elements. The recovered uranium and the plutonium can be reused as fuel in a nuclear power plant following appropriate further chemical treatment. The nuclear fuel recoverable in a reprocessing plant with an annual throughput of 350 t corresponds, in the case of use in modern light-water reactors, to an energy quantity of approximately ten million tonnes of hard coal. In the reprocessing, the highly active waste (fission products) is separated and by verification brought into a form suitable for safe ultimate disposal [3].

Details of overall reprocessing are depicted below, which are adopted from the European Nuclear Society (Figs. 16.1 and 16.2).

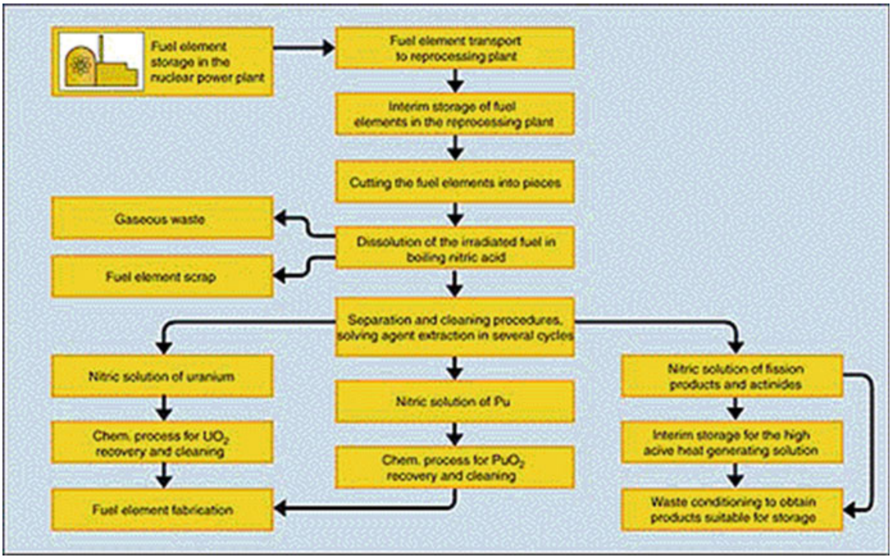

Fig. 16.1 Scheme of the reprocessing of irradiated fuel elements [3]

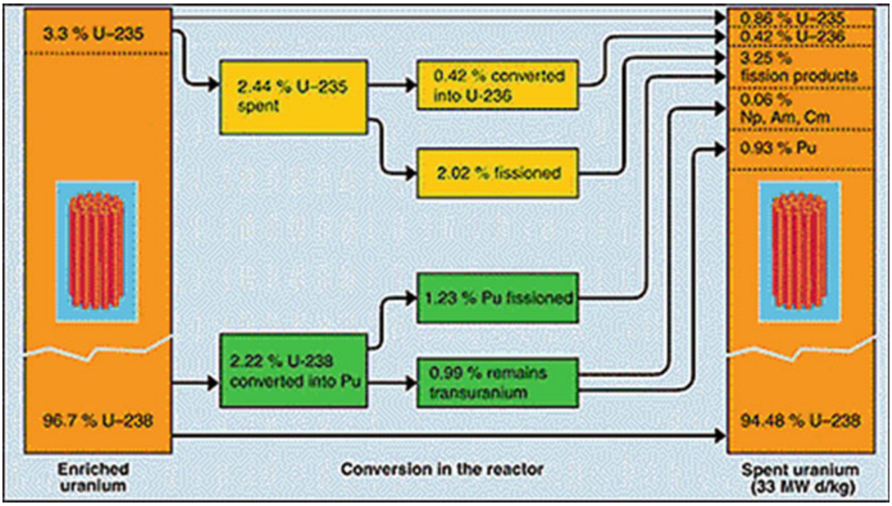

Fig. 16.2 Composition of nuclear fuel for light-water reactors prior and after the use in a reactor [3]

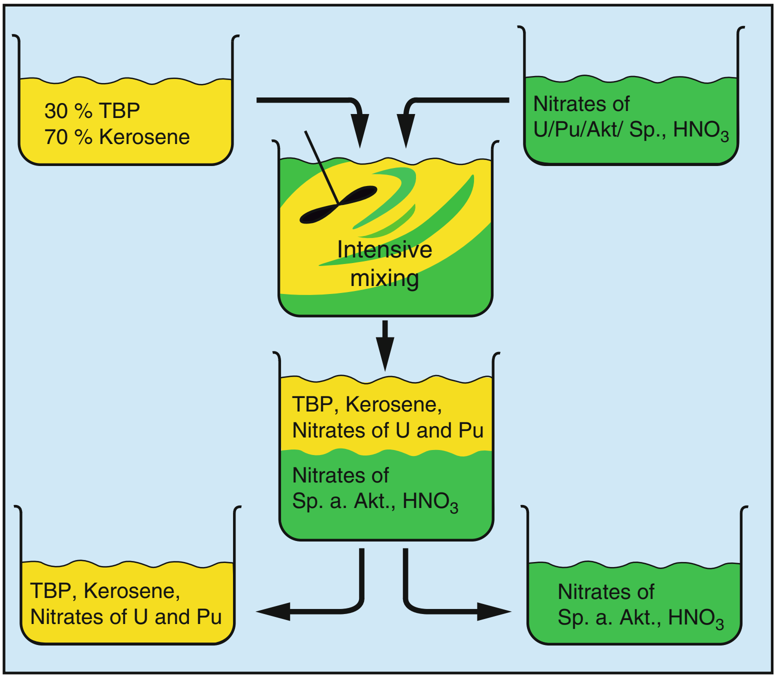

Fig. 16.3 Principle of the PUREX process for the separation of uranium and plutonium from fission products [3]

16.4.1 PUREX Process

The PUREX process is for the reprocessing of spent nuclear fuel to separate uranium and plutonium from the fission products and from one another. Following the dissolution of the irradiated fuel in aqueous nitric acid, uranium and plutonium are transferred to an organic phase by intensive mixing with an organic solvent extraction—30 % tributyl phosphate (TBP) in kerosene is used as an organic solvent—while the fission products remain in the aqueous nitric phase. Further process steps enable the subsequent separation of uranium and plutonium from one another [3] (Fig. 16.3).

16.4.2 Transuranium Elements

Chemical element in the classification of elements, the atomic number of which is greater than 92, that of Uranium. Except for the plutonium isotopes Pu^{244} (half-life about 80 Ma) and Pu^{239} (continuous reformation in uranium by neutron capture in U^{238} by neutrons from the spontaneous fission of U^{238}) detected in very small quantities, all transuranium elements must be produced artificially. See Table 16.1 below [3].

Table 16.1 Transuranium elements

Element name	Symbol	Atomic number
Neptunium	Np	93
Plutonium	Pu	94
Americium	Am	95
Curium	Cm	96
Berkelium	Bk	97
Californium	Cf	98
Einsteinium	Es	99
Fermium	Fm	100
Mendelevium	Md	101
Nobelium	No	102
Lawrencium	Lr	103
Rutherfordium	Rf	104
Dubnium	Db	105
Seaborgium	Sg	106
Bohrium	Bh	107
Hassium	Hs	108
Meitnerium	Mt	109
Darmstadtium	Ds	110
Roentgenium	Rg	111
Copernicium	Cn	112
Still without name		113
Flerovium	Fl	114
Still without name		115
Livermorium	Lv	116
Still without name		117
Still without name		118

16.4.3 Vitrification

The highly active fission product solutions arising in reprocessing must be transferred to a product suitable for ultimate disposal. Vitrification has proven to be a suitable method for this purpose. In the French AVM process, the liquid highly active waste solution is heated to high temperatures that causes the liquid to evaporate, and the resulting granulate is molten at 1100 °C to glass adding glass frit. This process is used in the French large-scale reprocessing plant La Hague. In the process developed by the Karlsruhe research center, liquid highly active waste solution is added directly to the molten glass mass at 1150 °C. The liquid evaporates and the radioactive solids are homogenously embedded in the molten glass mass. In both processes the molten glass mass is filled into 1.3 m high 150 steel containers holding about 400 kg glass products. The heat production due to the radioactive decay of the ingredients of such a container amounts to 1.5 to 2 kW [3].

16.5 Fuel Management for Nuclear Reactors

The heart of a nuclear power plant (NPP) is the reactor core producing power from the fissioning of uranium or plutonium fuel. In reality, a nuclear reactor is composed of individual fuel assemblies having a heterogeneous design. A fuel assembly (FA) consists of discrete components such as fuel rods, spacer grids, control rod channels, etc. Figure 16.4 shows typical fuel assemblies of pressurized water reactors (PWR) and boiling water reactors (BWR), respectively.

A PWR fuel assembly comprises a bottom nozzle into which rods are fixed through the lattice, and to finish the whole assembly, a top nozzle ends it. There are spacing grids between these nozzles. These grids ensure an exact guiding of the fuel rods. The bottom and top nozzles are heavily constructed as they provide much of the mechanical support for the fuel assembly structure.

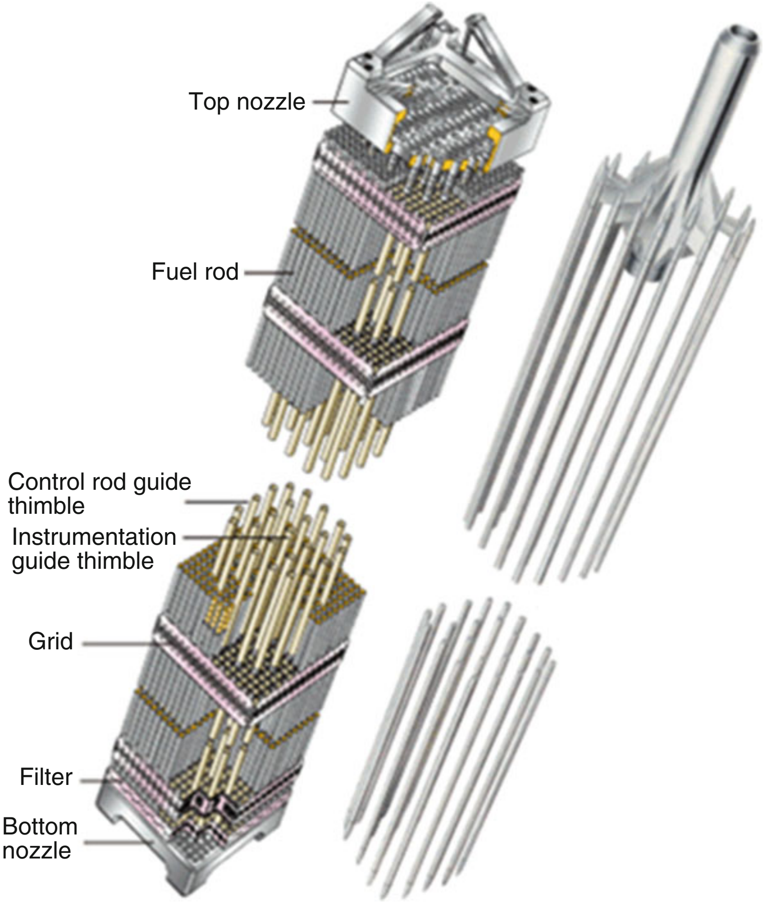

Fig. 16.4 Cutaway of a typical rod cluster control assembly for a PWR. (*Source*: www.world-nuclear.org)

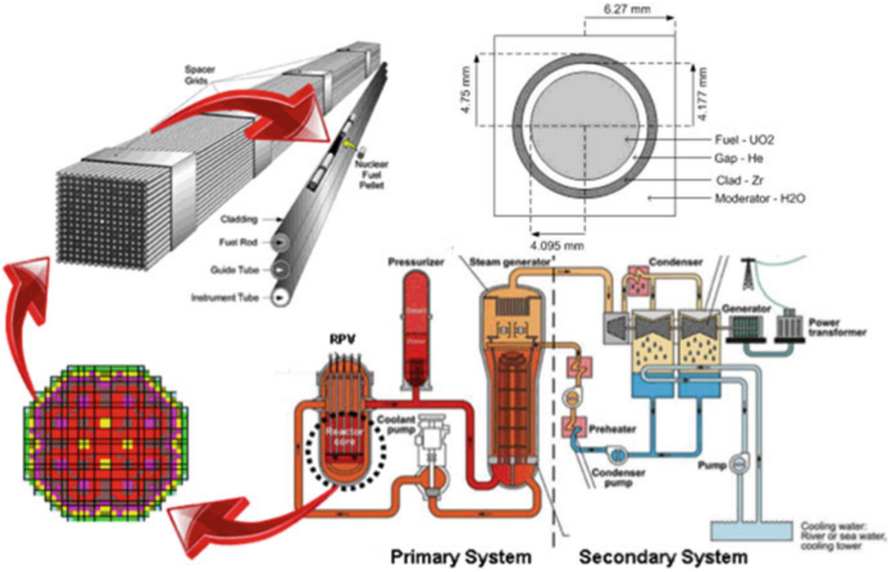

Fig. 16.5 Nuclear reactor, reactor core, fuel loading pattern, fuel assembly, fuel rod, fuel pellet (*Source*: www.world-nuclear.org)

A typical PWR fuel assembly consists of the following subsystems and depicted in Fig. 16.5:

- *Fuel rods*: contain the fuel and burnable poisons
- *Top nozzle*: provides the mechanical support for the fuel assembly structure
- *Bottom nozzle*: provides the mechanical support for the fuel assembly structure
- *Spacing grid*: ensures an exact guiding of the fuel rods
- *Guide thimble tube*: vacant tube for control rods or in-core instrumentation

An 1100 MWe (3300 MWth) nuclear core may contain 157 fuel assemblies composed of over 45,000 fuel rods and some 15 million fuel pellets. Generally, a common fuel assembly contains energy for approximately 4 years of operation at full power. Once loaded, fuel stays in the core for 4 years depending on the design of the operating cycle. During these 4 years, the reactor core have to be refueled.

During refueling, every 12–18 months, some of the fuel—usually one-third or one-quarter of the core—is transferred to the spent fuel pool while the remainder is rearranged to a location in the core better suited to its remaining level of enrichment. The removed fuel (one-third or one-quarter of the core, i.e., 40 assemblies) has to be replaced by fresh fuel assemblies.

Figure 16.6 shows the top view of a reactor core, where the fuel assemblies are arranged in a cylindrical type configuration.

The typical neutron spectrum for light-water reactors (LWRs) is shown in Fig. 16.7.

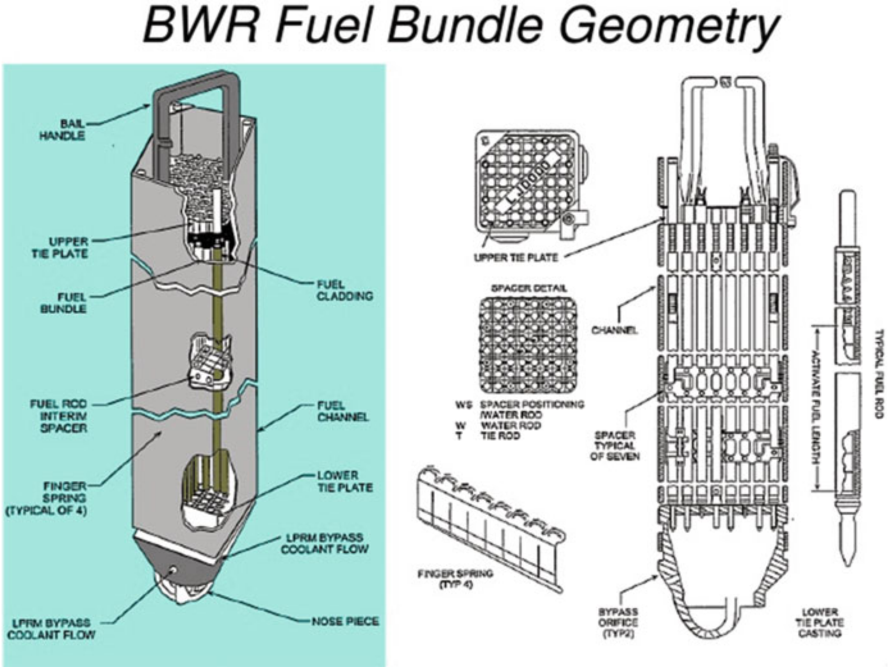

Fig. 16.6 Fuel assembly for a BWR

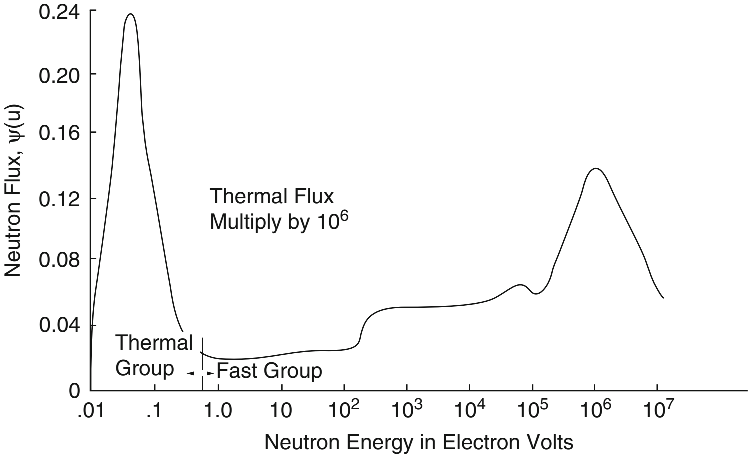

Fig. 16.7 Typical neutron spectrum for an LWR

Now that we have a little history of nuclear reactor core assemblies and their types, we can pay our attention to the subject of fuel management and then talk about the nuclear fuel cycle as well.

For fuel of a given enrichment, the burnup can be extended by suitable fuel loading schedules, generally referred to as "fuel management." A number of such procedures, with their advantages and disadvantages, can be described and will be found in various books and open literatures [4].

Some of the conditions above require changing the location of the fuel elements within the core according to a predetermined schedule. Although these schemes may increase the burnup and the expenditure of fuel, they may add to the cost of reactor operation, especially if a shutdown is necessary for rearranging the fuel [4].

16.6 Nuclear Fuel Cycle

The nuclear fuel cycle includes all activities involved in obtaining and irradiating fuel in nuclear reactors, as well as spent fuel processing and disposing of the fission product wastes produced during irradiation of these reactors. The many activities involved in the fuel cycle may be divided into three categories.

1. The first category involves activities that take place prior to fuel irradiation, when fuel radioactivity levels are relatively low. These activities include milling, conversion to uranium hexafluoride, enrichment in the fissile isotope U^{235} (in the case of all but natural uranium-fueled reactors), and fabrication into fuel elements and assemblies. These activities are designed as head-end fuel management.
2. The second category of activities involves fuel cycle design and irradiation of the fuel assemblies in the reactor. These activities include evaluation of reactivity and control requirements, programming of fuel assemblies in the reactor, power distribution analysis, and core capability evaluation. This category is primarily the responsibility of the nuclear engineer and will be covered in depth in later chapters of the book. It will be referred to as *in-core fuel management*.
3. The third category of fuel management activities includes those activities that involve operations on the highly radioactive spent fuel storage and shipping, reprocessing of the spent fuel to remove fission products and separate transuranium elements, and waste disposal. It will be designed as tail-end fuel management.

There are several features of nuclear fuel that are considerably different from fossil fuel. A unit mass of fissile material fissioned yields nearly four million times as much energy as a unit mass of coal burned. Nuclear fuel is therefore quite valuable. A second feature of nuclear fuel and the nuclear fuel cycle is the presence of radioactivity. Although activity levels in the head end of the fuel cycle are relatively low, they are not insignificant, and care must be taken to prevent the release of radioactivity to the environment. Once any fissioning has taken place in the fuel, activity levels resulting from both fission products and neutron capture products are extremely high, and the release of even a small fraction of this activity to the environment would cause acceptable radioactivity levels to be exceeded.

Another feature of nuclear fuel that differentiates it from other energy sources is that the material produced for use in some types of reactors, and some of the by-products of the reactor operation, could be used to produce crude nuclear explosives. For this reason, access to many phases of the fuel cycle must be carefully controlled, and the probability of a diversion of such material must be reduced to a very low value.

A final feature of nuclear fuel management, as opposed to the management of fossil fuel, is the long time required between mining the ore, irradiation of the fuel in the reactor, and removal of fission product wastes. This process requires a minimum of 2 years and could extend to many decades if spent fuel is stored for an indefinite period prior to the separation of fuel material from fission products, if this separation is performed at all.

Although the nuclear engineer may not be directly involved with the technical details of these activities, he or she should be familiar with how the major fuel processing steps are affected when changes are made in fuel design or reactor operation, as well as how these interactions affect fuel cycle economics.

A cycle is a period of time in which certain events are repeated in the same order and at the same intervals. This is the case with nuclear fuel cycle. Not all fuel cycles are the same, however, and there are a number of different types of fuel cycles that are of interest to us. The differences arise both because of differences in resource availability and differences in the state of technology or national policy objectives in various parts of the world.

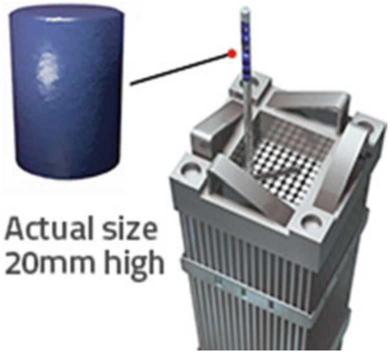

As part of fuel management, the integrated used fuel management is part of the procedure. Used nuclear fuel consists of small uranium fuel pellets stacked inside alloy fuel rods. All the used nuclear fuel produced by the nuclear energy industry in nearly 50 years—if stacked end to end—would cover an area the size of a football field to a depth of less than ten yards.

Under a sustainable, integrated approach for managing the back end of the fuel cycle, used fuel storage at nuclear energy facilities will continue in the near term.

One or more consolidated storage facilities, to be built in willing host communities, will help move used fuel from shutdown and operating reactors and reduce the mounting federal liability for delays in the repository program. Eventually, the government will remove it and place the unusable end product in a deep geologic repository. Before a repository is established, research into used fuel recycling can potentially reduce the quantity, heat, and toxicity of radioactive waste by-products needing repository disposal.

The nuclear energy industry supports completion of the Yucca Mountain project. The industry also supports legislation to create a sustainable, integrated program for federal management of high-level radioactive waste and used nuclear fuel. The industry supports an integrated used nuclear fuel management strategy, consisting of ten basic elements, and they may be found in the references [5].

16.7 Storage and Transportation of High Burnup Fuel

The questions for this section are: [2]

1. *Is it safe to store and transport high burnup fuel*?
   To be certified by the NRC, dry cask designs must meet NRC requirements. For transportation, these are found in 10 CFR Part 71 and for storage, in 10 CFR Part 72. The NRC approves designs only after a full safety review.

   Based on these reviews, the NRC has certified cask designs for the storage and transportation of high burnup spent fuel. Because low burnup spent fuel has been around longer and there is more of it, there are more casks for low than for high burnup spent fuel. There is also a great deal more data on low burnup fuel. Still, there is enough data on high burnup fuel that the NRC has certified high burnup spent fuel storage casks for an initial term of 20 or 40 years. Some systems have also been approved for transporting high burnup spent fuel. Operating experience of dry storage began in 1986 and short-term tests show both low and high burnup spent fuel can be stored and transported safely.
2. *How does the NRC make sure it remains safe*?
   The NRC assures safety by requiring many layers of protection. Cask designs provide several layers, and the fuel cladding itself provides added protection. The regulations are designed to ensure the health and safety of the public is maintained during storage or in a transportation accident. The NRC's regulations ensure the system will remain safe even if the cladding did break. The NRC carefully reviews each cask application to see if it meets the requirements. As part of this review, the NRC does its own analysis to confirm information in the application.
3. *What confirmatory research is being done*?
   The primary focus of research today is to get more data to support the continued certification of storage systems beyond the initial 20- to 40-year license term. Additional research is ongoing to confirm that high burnup fuel will remain safe

> during transport after extended storage. This research is designed to ensure that the existing data on high burnup spent fuel is accurate and can be reproduced.
>
> Cask designers are also involved in research that will assist them in designing casks for higher burnups and additional fuel types. As more data becomes available, the NRC expects to be able to certify more casks. Testing has provided a lot of information on how different types of cladding on spent fuel will behave, and this work continues.
>
> The NRC is conducting tests at the Oak Ridge National Laboratory on high burnup fuel samples under stresses greater than the loads expected during normal transport. These tests have already shown that high burnup fuel is very strong. This information further confirms that long-term storage and eventual transportation of high burnup fuel is safe.

In addition, planning is underway for an important new study, run jointly by the nuclear industry and the Department of Energy, with regulatory oversight by the NRC. In this study, high burnup spent fuel will be loaded into a cask fitted with instruments to provide temperature readings and allow sampling of the gas inside. Those readings, combined with tests on the fuel assemblies and inspection of the cask's interior after years of dry storage, will provide more data. The test is expected to confirm the current understanding of what happens to high burnup spent fuel in a storage cask as it cools over time.

All this work will help cask designers, users, and regulators have a better understanding to ensure high burnup spent fuel will remain safe in dry storage over the long term and during transportation to a centralized storage or disposal facility.

16.8 Nuclear Reactors for Power Production

In the USA, most reactors' design and development for the generation of electrical power was branched from early nuclear navy research, when it was realized that a compact nuclear power plant would have great advantages for submarine-driven nuclear propulsion system. To have such a power plant on board would make it possible for long voyages to cross the oceans at high speeds without the necessity for resurfacing at frequent intervals, and the Argonne National Laboratory was assigned with the task of designing such a reactor. So the first generation of pressurized water reactors (PWR) was born, where the use of highly enriched uranium as the fuel, and water under pressure as the moderator as well as coolant, allowed a small version of this type of high-power reactor. Consequently the first prototype of such a reactor, namely, STR Mark 1, started its operation at Arco, Idaho, in March 1953, and a production version of it was installed on USS Nautilus, the first nuclear power submarine, on May 31, 1953.

As a result of the experience gained in the successful operation of the submarine reactors, the first commercial version of PWR was designed in Shippingport, Pennsylvania, and went into operation in December 2, 1957. The design was based on the water pressure of 13.8 MPa, i.e., 2000 psi, and steam produced in the heat exchanger with a temperature of about 254 °C (490 °F) and a pressure close to 4.14 MPa (600 psi). In order to make such a reactor cost effective and reduce the cost of the power produced, only a small number of the fuel elements are highly enriched in uranium-235 (U^{235}) as an alloy with zirconium, the remainder being of normal uranium as the dioxide. The change in the core design required a bigger real estate for the footprint of a commercialized version of a PWR that was not an issue for a land-based facility. The output power of this reactor was about 60 MW electrical, equivalent to 230 MW thermal, and further enhancement in the core design increased the power to 150 MW electrical and 505 thermal. Pressurized water reactors, using around 2–4 % of enriched uranium dioxide as fuel, are now commonly used in the USA and other countries around the globe for commercial power generation. The most recent plants have electrical capacities in the neighborhood of 1000 MW (3000 MW thermal) which is due to a modification of the pressurized water concept where steam is produced directly by utilizing fission heat to boil water within the reactor core rather than in an external heat exchanger [1].

Later on other reactor designs based on different fuel materials, moderators, and coolants with various electrical and thermal power outputs were born, and examples are thermal reactors such as:

- Boiling water reactor (*BWR*) initiated in 1953
- Water-cooled graphite moderated in 1954
- High-temperature gas-cooled reactor (*HTGR*)
- Liquid metal fast breeder reactors (*LMFBR*)

All commercial reactor power plants of present interest are systems for generating steam utilizing the heat of nuclear fission to boil water and produce steam for turbine, and they are often referred to as "nuclear steam supply systems" or *NSSS*. The steam is expanded in a turbine which drives a generator to produce electricity in the conventional manner. The exhaust steam from the turbine passes on to a condenser where it is converted into liquid water and is returned as feed water to the steam generator of *NSSS*.

The proportion of the heat supplied in a power plant that is actually converted into electrical energy is called the *thermal efficiency* of the system; thus, in a nuclear installation [1],

$$\text{Thermal Efficiency} = \frac{\text{Electrical Energy Generated}}{\text{Heat Produced in the Reactor}} \tag{16.1}$$

The maximum possible value of the thermal efficiency is the *ideal thermodynamic efficiency*, which is given by following relationship:

$$\text{Ideal Thermodynamic Efficiency} = \frac{T_2 - T_1}{T_2} \tag{16.2}$$

where

T_1 is the absolute temperature of the steam entering the turbine (°K, Kelvin) and
T_2 is the temperature at which heat is rejected to the condenser (°K, Kelvin).

The ideal thermodynamic efficiency can be increased by having T_2 as high as possible and T_1 as low as possible. In practice, T_1 is more or less fixed by the ambient temperature; the thermal efficiency of a steam electric plant is then largely determined by the steam temperature, which should be as high as feasible.

Conditions in PWRs and BWRs are such that the steam temperature is lower than in modern fossil-fuel power plants in which the heat is produced by burning coal, oil, or gas. Here, the thermal efficiencies of these reactor plants are only about 33 %, compared with 40 % for the best fossil-fuel facilities. With the HTGRs and fast breeder reactors, however, the thermal efficiencies should equal to those of the best fossil-fuel plants, i.e., about 40 % [1].

16.9 Future Nuclear Power Plant Systems

In response to the difficulties in achieving suitability, a sufficiently high degree of safety, and a competitive economical basis for nuclear power, the US Department of Energy initiated the generation IV program in 1999. Generation IV refers to the broad division of nuclear designs into four categories as follows:

1. Early prototype reactor (Generation I)
2. The large central station nuclear power plants of today (Generation II)
3. The advanced light-water reactors and other systems with inherent safety features that have been designed in recent years (Generation III)
4. The next-generation system to be designed and built two decades from now (Generation IV)

By 2000 international interest in the Generation IV project had resulted in a nine-country coalition that includes:

(a) Argentina
(b) Brazil
(c) Canada
(d) France
(e) Japan
(f) South Africa
(g) South Korea
(h) UK
(i) USA

Those participating are mapping out and collaborating on the research and development of future nuclear energy systems.

Although the Generation IV program is exploring a wide variety of new systems, a few examples serve to illustrate the broad approaches reactor designs are developing to meet their objectives.

The next-generation systems are based on three general classes of reactors:

1. Gas cooled
2. Water cooled
3. Fast spectrum

All these categories and their brief designs are discussed in the next sections.

16.10 Next Generation of Nuclear Power Reactors for Power Production

Experts are projecting worldwide electricity consumption will increase substantially in the coming decades, especially in the development world, accompanying economic growth and social progress that has direct impact on rising electricity prices that have focused fresh attention on nuclear power plants. New, safer and more economical nuclear reactors could not only satisfy many of our future energy needs but could combat global warming as well. Today's existing nuclear power plants on line in the USA provide one-fifth of the nation's total electrical output. See Fig. 16.8.

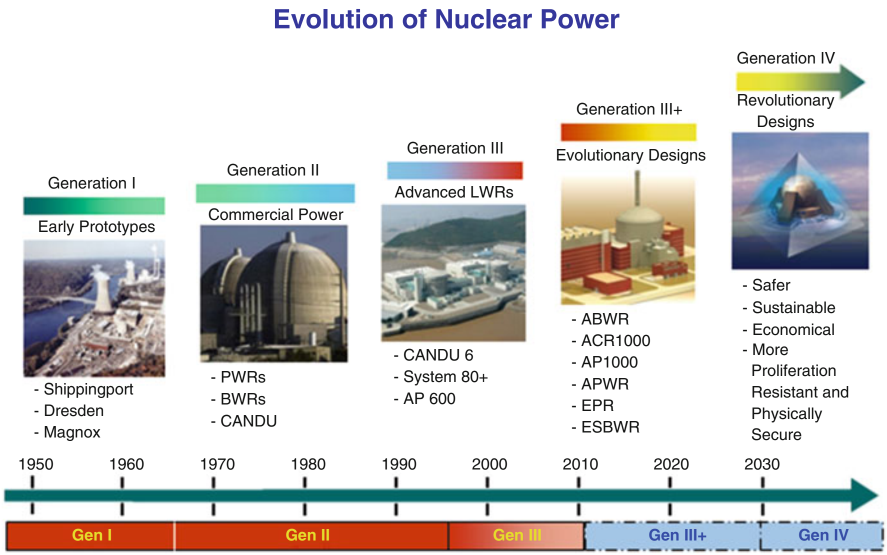

Fig. 16.8 Evolution of nuclear power plants

Taking into account the expected increase in energy demand worldwide and the growing awareness about global warming, climate change issues, and sustainable development, nuclear energy will be needed to meet future global energy demands.

Nuclear power plant technology has evolved as distinct design generations as we mentioned in the previous section and is briefly summarized here again as follows:

- First generation: prototypes and first realizations (~1950–1970)
- Second generation: current operating plants (~1970–2030)
- Third generation: deployable improvements to current reactors (~2000 and beyond)
- Fourth generation: advanced and new reactor systems (2030 and beyond)

The *G*eneration IV *I*nternational *F*orum, or *GIF*, was chartered in July 2001 to lead the collaborative efforts of the world's leading nuclear technology nations to develop next-generation nuclear energy systems to meet the world's future energy needs.

Eight technology goals have been defined for Generation IV systems in four broad areas:

1. Sustainability
2. Economics
3. Safety and reliability
4. Proliferation resistance and physical protection

A large number of countries share these ambitious goals as they aim at responding to the economic, environmental, and social requirements of the twenty-first century. They establish a framework and identify concrete targets for focusing at GIF R&D efforts.

Eight technology goals have been defined for Generation IV systems in four broad areas: sustainability, economics, safety and reliability, and proliferation resistance and physical protection.

The next generation ("Generation IV") of nuclear energy systems is intended to meet the goals, listed in Table 16.2, while being at least as effective as the "third" generation in economic terms.

In principle, the Generation IV systems should be marketable or deployable from 2030 onwards. The systems should also offer a true potential for new applications compatible with an expanded use of nuclear energy, particularly in the fields of hydrogen or synthetic hydrocarbon production, seawater desalination, and process heat production.

It has been recognized that these objectives, widely and officially shared by a large number of countries, should be at the basis of an internationally shared R&D program, which allows keeping open and consolidating the technical options and avoiding any early or premature down selection.

In fact, because the next-generation nuclear energy systems will address needed areas of improvement and offer great potential, many countries share a common interest in advanced R&D that will support their development. The international research community should explore such development benefits from the

Table 16.2 The intended goal of Generation IV nuclear energy systems

Sustainability—1	Generation IV nuclear energy systems will provide sustainable energy generation that meets clean air objectives and provides long-term availability of systems and effective fuel utilization for worldwide energy production
Sustainability—2	Generation IV nuclear energy systems will minimize and manage their nuclear waste and notably reduce the long-term stewardship burden, thereby improving protection for the public health and the environment
Economics—1	Generation IV nuclear energy systems will have a clear life cycle cost advantage over other energy sources
Economics—2	Generation IV nuclear energy systems will have a level of financial risk comparable to other energy projects
Safety and reliability—1	Generation IV nuclear energy system operations will excel in safety and reliability
Safety and reliability—2	Generation IV nuclear systems will have a very low likelihood and degree of reactor core damage
Safety and reliability—3	Generation IV nuclear energy systems will eliminate the need for an off-site emergency response
Proliferation resistance and physical protection	Generation IV nuclear energy systems will increase the assurance that they are very unattractive and the least desirable route for diversion or theft of weapons-usable materials and provide increased physical protection against acts of terrorism

identification of promising research areas and collaborative efforts that. The collaboration on R&D by many nations on the development of advanced next-generation nuclear energy systems will in principle aid the progress toward the realization of such systems by leveraging resources, providing synergistic opportunities, avoiding unnecessary duplication, and enhancing collaboration.

Problems

Problem 16.1: Which weapons material is easier to handle and to create a weapon or improvised nuclear device (IND)?

Problem 16.2: List the effects of a nuclear weapon (NW) blast and identify them in terms of energy release from the device. Which have short-term and which have long-term effects?

Problem 16.3: A 1 mT device explodes at a height of 5000 ft. The equivalent burst height for a 1 kT (kiloton) device is 500 ft, and its equivalent time of arrival is 4 s. What would be the time of arrival of the blast wave from the 1 mT (megaton) device at a distance of ten miles from ground zero?

Problem 16.4: The Acheson–Lilienthal Report and the Baruch Plan have what element in common?

Problem 16.5: Was the nuclear weapon (NW) proliferation threat around the time of Atoms for Peace based on a national or subnational effort?

Problem 16.6: Match the elements of the NPT to the key words in the right-hand column.

Article 1	(a) NW (nuclear weapon)-free zones
Article 2	(b) NWS obligations
Article 3	(c) Carrot
Article 4	(d) Stick
Article 5	(e) NNWS (nonnuclear weapon states) obligations
Article 6	(f) Nuclear disarmament

Problem 16.7: List three levels covered by nuclear safeguards, and indicate the entity responsible for their enforcement.

Problem 16.8: Which of the following countries are under International Atomic Energy Agency (IAEA) Safeguards? Russia, Chile, Japan, Australia, USA, Egypt, Iran, India

Problem 16.9: List the two main objectives of International Atomic Energy Agency (IAEA) Safeguards.

Problem 16.10: List three agreements included in (Information Circular) INFCIRC/under 153.

Problem 16.11: List three measures granted to the International Atomic Energy Agency (IAEA) under the Additional Protocol (AP).

Problem 16.12: List three activities by a state under the International Atomic Energy Agency (IAEA) Additional Protocol (AP) that could put the state into noncompliance.

Problem 16.13: List the six key elements of the International Atomic Energy Agency (IAEA) Safeguards approaches.

Problem 16.14: True or false: U^{233} is defined as an indirect-use material by the International Atomic Energy Agency (IAEA).

Problem 16.15: List the significant quantity (SQ) amounts for the following: HEU, U^{233}, Th, depleted U, Pu^{239}

Problem 16.16: List the critical mass and critical mass reflected by depleted uranium for U^{233}, Pu^{239}, and HEU.

Problem 16.17: Calculate the expected neutron flux from 1 kg of discharged light-water reactor (LWR) fuel (30,000 MWd/t burnup). What is the main neutron contributor? Could Pu^{239} be detected by measuring neutrons alone?

Problem 16.18: Nuclear material accountancy should satisfy what requirement regarding an MUF (material unaccounted for)?

Problem 16.19: Match IAEA assumptions of conversion time with materials below.

Pu^{239} metal	Weeks
HEU in irradiated fuel	Days (7–10)
U containing $< 20\,\%$ U^{235}	Months
Pu in MOX	Weeks
$U^{235}O^2$	
Th	Containing $< 20\,\%$ U^{233}

Problem 16.20: Provide International Atomic Energy Agency (IAEA) timeliness detection goals for:

1. Unirradiated direct-use material
2. Irradiated direct-use material

Problem 16.21: Provide four scenarios for cheating International Atomic Energy Agency (IAEA) Safeguards.

Problem 16.22: List the elements that go into the determination of an MUF.

Problem 16.23: List three general categories of nondestructive assay (NDA) measurements. NDA is a measurement of the nuclear material content.

Problem 16.24: Suppose a nuclear plant were built above the ground, but at a reduced cost, by using inferior materials and shoddy construction. Would that be a violation of the Nonproliferation Treaty?

Problem 16.25: Suppose a nuclear plant were built underground, completely hidden from view. Would that be a violation of the Nonproliferation Treaty?

References

1. B. Zohuri, *Combined Cycle Driven Efficiency for Next Generation Nuclear Power Plants: An Innovative Design Approach* 2015th Edition
2. United Sates Nuclear Regulatory Commission. High burnup spent fuel, 2015 Sept. www.nrc.gov
3. https://www.euronuclear.org/info/encyclopedia/p/purex-process.htm
4. S. Glasstone, A. Sesonske, *Nuclear Reactor Engineering* (D Van Nostrand Company, Princeton, 1967)
5. http://www.nei.org/Issues-Policy/Nuclear-Waste-Management/Integrated-Used-Fuel-Management

Appendix A: Laplace Transforms

To the young engineering student, Laplace transforms seem to be almost a mathematical curiosity. They were developed by Laplace (1749–1827) and Cauchy (1789–1857) as mathematical transforms for mathematicians. Hence, they gave mathematicians a logical reason for studying the complex plane and complex variable theory. However, when it was recognized that they actually provided a mathematical basis for Heaviside's (1850–1925) operational calculus, they became useful to engineers and could be applied to solve real-world problems. Heaviside was an English engineer that suggested solving differential equations by replacing the derivative function by a large D symbol and then treating this "D operator" as if it were similar to an algebraic operator. His operational calculus based on this concept enabled him to simplify systems of differential equations that modeled physical systems and made the prediction of their behavior much more easily understood. Analysis of coupled systems of differential equations, particularly those that contain control loops or feedback operators, is much easier to understand when transformed to the "s" or complex plane. Asymptotic behaviors can be understood without completely solving the time-dependent equations. Unfortunately, the Laplace transform method can only be applied to linear systems, but these have always been the easiest for the human mind to formulate and adequately describe the behavior of the majority of engineered systems.

A.1 Definition of Laplace Transform

The Laplace transform is defined by the following integral equation. If $f(t)$ is a time-dependent function that is piecewise continuous and of exponential order, then its transform $F(s)$ is given by

B. Zohuri, *Neutronic Analysis For Nuclear Reactor Systems*,
DOI 10.1007/978-3-319-42964-9

$$F(s) = \int_0^{\infty} e^{-st} f(t)dt = \pounds\{f(t)\} \tag{A.1}$$

Piecewise continuous simply means that over the t interval of interest, there are only a finite number of discontinuities, and exponential order simply means that the function can be bounded by an exponential function with an exponent that increases no faster than the first power in the variable "t." Most physically realizable functions satisfy these two criteria. Of course we really do not know how $f(t)$ behaves when we transform its differential equation. Normally we will simply apply the transform, and if we get a solution that does not satisfy these criteria, we will conclude the method does not work.

Note that the Laplace of first and second derivatives of a function $f(t)$ demonstrated by $f'(t)$ and $f'(t)$, respectively, is given by the following relationships:

$$\begin{cases} \pounds\{f'(t)\} = sf(s) - F(0) \\ \pounds\{f''(t)\} = s^2 f(s) - sF(0) - F'(0) \end{cases} \tag{A.2}$$

Having defined the Laplace transform, it now seems logical that we would define the inverse Laplace transform. Unfortunately, this requires complex variable math and is probably way beyond the realistic math requirements for this course. Therefore, we will simply try to invert the $F(s)$ functions by inspection. That is, we hopefully recognize the form of $F(s)$ as something we have obtained as a transform of a known function $f(t)$. We can then conclude that the transform process and its inversion are unique. If we know that a particular $F(s)$ is the transform of a known $f(t)$, then $f(t)$ must be the inverse transform of $F(s)$. This leads us to the concept of "transform pairs." Laplace transforms are traditionally used based on having a table of transforms and their inverses in a table, so that when an $F(s)$ is obtained for a system of equations, its inverse can simply be looked up in a table of "transform pairs." We will not even become this sophisticated in this course. We will find a few transforms that will cover the vast majority of cases, and then we will simply use these and combinations of these. In fact, the real power of Laplace transforms lies in the ability of the engineer to apply some analytical tools to the transform function in the s (complex) variable and determine the answers to all reasonable questions about the generic time-dependent behavior of the system.

A.2 Basic Transforms

Some basic transforms that we will use are:

1. *Constant function*
   Consider a function that is simply a constant for all time. Since we are dealing with time-dependent functions, this is sometimes given the symbol $KU(t)$, where

K is a real number and $U(t)$ is the function that has a zero value for all $t < 0$ and is equal to 1.0 for all $t > 0$.
The Laplace transform is given by

$$\pounds\{KU(t)\} = \int_0^\infty Ke^{-st}dt = \frac{K}{s}\int_0^\infty e^{-st}sdt = \frac{K}{s}\int_0^\infty e^{-x}dx = \frac{K}{s} \tag{A.3}$$

2. *Ramp function*
   Consider now a linear function of t. Let $f(t) = Kt$; then its Laplace transform is given by

$$\pounds\{Kt\} = \int_0^\infty Kte^{-st}dt = \frac{K}{s^2}\int_0^\infty ste^{-st}sdt = \frac{K}{s^2}\int_0^\infty xe^{-x}dx = \frac{K}{s^2}\left\{-xe^{-x}\Big|_0^\infty + \int_0^\infty e^{-x}dx\right\} = \frac{K}{s^2} \tag{A.4}$$

3. *Power of t function*
   Now consider an arbitrary power of t given by t^α, then its Laplace transform is given by $f(t) = Kt^\alpha$ as follows:

$$\pounds\{Kt^\alpha\} = \int_0^\infty Kt^\alpha e^{-st}dt = \frac{K}{s^{\alpha+1}}\int_0^\infty (st)^\alpha e^{-st}sdt = \frac{K}{s^{\alpha+1}}\int_0^\infty \alpha x^{\alpha-1}e^{-x}dx = \frac{K}{s^{\alpha+1}}\alpha! \tag{A.5}$$

4. *Exponential function*
   The exponential function, $f(t) = e^{\alpha t}$, has the transform

$$\pounds\{e^{\alpha t}\} = \int_0^\infty e^{\alpha t}e^{-st}dt = \frac{1}{s-\alpha}\int_0^\infty e^{-(s-\alpha)t}sdt = \frac{1}{s-\alpha}\int_0^\infty e^{-x}dx = \frac{1}{s-\alpha} \tag{A.6}$$

5. *Sinusoid function*
   Consider $f(t) = \cos(\omega t)$; then its Laplace transform is given as

$$\begin{aligned}\pounds\{\cos(\omega t)\} &= \int_0^\infty \frac{e^{i\omega t} + e^{-i\omega t}}{2}e^{-st}dt = \frac{1}{2}\int_0^\infty \left(e^{-(s-i\omega)st} + e^{-(s+i\omega)t}\right)dt \\ &= \frac{1}{2}\left\{\frac{1}{s-i\omega} + \frac{1}{s+i\omega}\right\} = \frac{s}{s^2+\omega^2}\end{aligned} \tag{A.7}$$

   Note also that $\pounds\{\sin(\omega t)\} == \frac{\omega}{s^2+\omega^2}$

A.3 Fundamental Properties

1. *Linearity*

$$£\{af(t)\} = \int_0^\infty af(t)e^{-st}dt = a\int_0^\infty f(t)e^{-st}dt = aF(s) \tag{A.8}$$

2. *Superposition*

$$£\{f(t) + g(t)\} = \int_0^\infty f(t)e^{-st}dt + \int_0^\infty g(t)e^{-st}dt = F(s) + G(s) \tag{A.9}$$

3. *Time translation*

$$£\{f(t-a)\} = \int_0^\infty f(t-a)e^{-st}dt = e^{-as}\int_0^\infty e^{-s(t-a)}d(t-a) = e^{-as}F(s) \tag{A.10}$$

4. *Complex differentiation*

$$£\{tf(t)\} = \int_0^\infty tf(t)e^{-st}dt = \frac{dF(s)}{ds} \tag{A.11}$$

5. *Translation in the s variable*

$$£\{e^{at}f(t)\} = \int_0^\infty e^{at}f(t)e^{-st}dt = F(s-a) \tag{A.12}$$

6. *Real differentiation*

$$£\left\{\frac{df(t)}{dt}\right\} = \int_0^\infty \frac{df(t)}{dt}e^{-st}dt = sF(s) - f(0) \tag{A.13}$$

7. *Final value theorem*

$$\lim_{s\to 0} sF(s) = \lim_{t\to\infty} f(t) \tag{A.14}$$

8. *Initial value theorem*

$$\lim_{s\to\infty} sF(s) = \lim_{t\to 0} f(t) \tag{A.15}$$

A.4 Inversion by Complex Variable Residue Theorem

The general inversion formula is given by the following form:

If

$$F(s) = \frac{N(s)}{\prod_{i=1}^{n}(s-p_i)^{m_i}} \tag{A.16}$$

Then

$$F(t) = \sum_{i=1}^{n} \lim_{s \to p_i} \frac{\partial^{m_i - 1}}{\partial s^{m_i - 1}} (s - p_i)^{m_i} F(s) e^{st} \tag{A.17}$$

Examples Simple pole ($n = 1$, $m = 1$)

$$f(t) = \lim_{s \to p_i} (s - p) F(s) e^{st} \tag{A.18}$$

Let $p = 5, f(t) = \lim_{s \to p} (s - 5) F(s) e^{st} = \lim_{s \to 5} \frac{(s-5) N(s) e^{st}}{(s-5)} = n(5) e^{5t}$

Higher-order pole ($n = 1$, $m_i = 2$)

$$f(t) = \lim_{s \to p} \frac{\partial}{\partial s} (s - p)^2 F(s) e^{st} = \lim_{s \to p} \frac{\partial (N(s) e^{st})}{\partial s} = \frac{\partial n(p)}{\partial p} e^{pt} + t n(p) e^{pt}$$

Multiple poles with a zero ($n = 1$, $m_1 = 1$, $m_2 = 1$)

Let $F(s) = \frac{s+\alpha}{(s+\beta)(s+\gamma)}$; then,

$$\begin{aligned} f(t) &= \lim_{s \to -\beta} (s + \beta) \frac{s + \alpha}{(s + \beta)(s + \gamma)} e^{st} + \lim_{s \to -\gamma} (s + \gamma) \frac{s + \alpha}{(s + \beta)(s + \gamma)} e^{st} \\ &= \frac{\alpha - \beta}{\gamma - \beta} e^{-\beta t} + \frac{\alpha - \gamma}{\beta - \gamma} e^{-\gamma t} \end{aligned} \tag{A.19}$$

Appendix B: Transfer Functions and Bode Plots

Bode plots are a very useful way to represent the gain and phase of a system as a function of frequency. This is referred to as the frequency domain behavior of a system. The concept of transfer function representation of nuclear power plants has proved a very fruitful tool both from the point of view of dynamic analysis and from the interpretation of experimental data. Much of the analysis of reactor kinetics and control can be in the form of systems of ordinary differential equations and their boundary conditions by suitable definitions.

B.1 Transfer Functions

As we have seen in Appendix A, the Laplace transformation is a technique that replaces the operation of integration with its general solution and subsequent fitting of boundary conditions with an operation of algebraic manipulation, which, in return, requires at least one boundary and one initial condition to find a solution of an ordinary differential equation for dependent variable $x_i \rightarrow i = 1, 2, \cdots$ in space on the independent variable time t.

The one-sided Laplace transform $\pounds\{f(t)\}$ of a function of time is defined via an integral overall time which has the effect of replacing time dependence with dependence on a new or transform variable s as it was shown in Appendix A, and it was presented as a relationship of the following form:

$$\pounds\{f(t)\} = F(s) = \int_0^\infty e^{-st} f(t) dt \tag{B.1}$$

As it can be seen, the exponential weighting will make this integral converging even for the function of $f(t)$ increasing with variable t. Now we can suppose that s be a real number and s_0 sufficiently large as to dominate any exponential behavior in $f(t)$; then the advantage of the Laplace transform in the case of constant coefficient is

B. Zohuri, *Neutronic Analysis For Nuclear Reactor Systems*,
DOI 10.1007/978-3-319-42964-9

evident since $£\{ax(t)\} = aX(s)$. The application to differential equations comes by considering the transform of the differential via an integration by parts:

$$\int_0^\infty \frac{dx}{dt} e^{-st} dt = [xe^{-st}]_0^\infty + \int_0^\infty sxe^{-st} dt = sX(s) - s_0 \tag{B.2}$$

for all reasonable $x(t)$. Thus, the system of linear equations with constant coefficient reduces to an algebraic system:

$$sX_i - \sum_{i'=1}^{n} a_{ii'} X_{i'} = S_i + x_{i0} \tag{B.3}$$

With the transformed source separated from the summation, we can expect to find the algebraic matrix inverse and they are able to write the following form as

$$X_i = \sum_{i'=1}^{n} G_{ii'}(s)[S_{i'} + x_{i'0}] \tag{B.4}$$

or $X = G(s)\ [S_{i'} + x_0]$ in matrix form.

The right-hand side divides into two noticeable different parts as follows:

1. A driving term due to the source and initial conditions, normally called the excitation function
2. The term $G_{ii'}(s)$ that gives the system behavior modifying the excitation function to yield the system output or response X_i

However, we expect that if a system is going to be *stable*, the inherent response with zero driving terms by itself must display a stable nature and not lead to increasing values of $x(t).G_{ii'}(s)$ relates to the *transfer* function for the *i*th output variable in terms of the *i*th input.

B.2 Sample Transforms

Simple functions of time lead to Laplace transforms that can be found in any books of Laplace transform subject. Utilizing the definition of Dirac delta distribution, we note that $1/s$ is strictly a step function transform, where the time-dependent function rises to 1 at time zero having been zero beforehand. However, this is not strictly a function—defined as being zero everywhere except around $t = 0$ and of such a magnitude that the integral over $\delta(t)$ is normalized to unity. Its transform is readily obtained directly from such a definition with the following notation in mind:

$$\int_{-\infty}^{+\infty} f(t)\delta(t)dt = f(0) \tag{B.5}$$

With the help of this distribution, initial conditions can be stated as equivalent sources. In particular, consider the response of the system for one output s to an impulse source as a describable via the Dirac distribution and no other initial condition. However, we have $X(s) = G(s)\, S(s) \rightarrow G(s)$, where is the *system* function as opposed to $S(s)$ and the initial condition providing a driving term or excitation function. We have the important result that $G(s)$ is the response to an impulse source.

Note as well the general "shifting" relations of any table of Laplace transform with the limiting value relationships useful for steady-state displacement, See Table B.1.

If we are in a situation that the system of equations leads, as it often does, to rational polynomial fractions $g(s)/f(s)$, where both $g(s)$ and $f(s)$ are polynomial functions in respect to variable s, then the inverse transform can generally be found via the method of *partial fractions*. Let $f(s) = 0$; then this leads to roots s_i for $i = 1,2,\ldots$ such that we can write $f(s) = [s - s_1][s - s_2]\cdots[s - s_i]\cdots[s - s_n]$. Three useful results rise from this situation as follows:

(a) If all the roots s_i are distinct, consider the residues R_i where

$$R_i(s) = \frac{g(s)}{f(s)}[s - s_i] \tag{B.5}$$

Then

$$F(s) = \frac{g(s)}{f(s)} = \sum_{i=1}^{n} \frac{R_i}{s - s_i} \tag{B.6}$$

where the $R_i(s)$ are evaluated at $s = s_i$. The results will be distinguished as the sum of a number of time-dependent exponential terms and their coefficients:

$$f(t) = \sum_{i}^{n} R_i e^{s_i t} \tag{B.7}$$

Note that for the same situation of distinct roots, $R_i(s_i) = g(s_i)/f'(s_i)$, where the derivative of $f(s)$ is taken with respect to variable s before substituting $s = s_i$. These results lead to the well-known "cover-up" rule for finding partial fractions, for example:

$$\frac{1}{[s-2][s+3]} = \frac{1}{5}\frac{1}{s-2} - \frac{1}{5}\frac{1}{s+3} \rightarrow \frac{1}{5}\left[e^{2t} - e^{-3t}\right] \tag{B.8}$$

(b) If the roots are repeated, let's say one root repeated once, the expansion in partial fractions is of second order of the form

$$\frac{A_i}{s + s_i} + \frac{B_i}{[s + s_i]^2} + \sum_{i' \neq i} \frac{C_{i'}}{s + s_{i'}} \tag{B.9}$$

While formula for residues are available, it is probably easier to use a direct equation of this form with the original to determine the expansion coefficients A, B, etc.

(c) If the coefficients of the original equations are real, then any complex roots must occur in conjugate pairs of the form:

$$p_i = r_i \pm j\omega_i \text{ with } j = \sqrt{-1} \text{ or in the polar form } A_i e^{\pm j\theta i}$$

Those complex pairs then lead to real trigonometrically functions. It is often convenient to note the implication of a *shift* of the Laplace transform variables as being equivalent to the transform of the unshifted function exponential of the time shift, e.g.,

$$\frac{s}{s^2 + 4s + 5} = \frac{s}{(s+2)^2 + 1} = \frac{s + 2 - 2}{(s+2)^2 + 1} \rightarrow e^{-2t}[\cos t - 2\sin t] \qquad \text{(B.10)}$$

B.3 Fourier Transforms

Now, we need to consider another mathematical transformation, known as Fourier transforms. So far we talked about Laplace transform parameter s as a real number chosen to dominate the real exponentials of the function $f(t)$. More generally, it can be considered a complex number, $s = s_0 + j\omega$, where s is chosen to meet this necessity. If the time dependence of $f(t)$ is such that it does not grow exponentially but remains constant or falls, the s_0 may be put to zero. The Laplace transform with $s = j\omega$ is called the Fourier transform of $f(t)$ and its existence is subject to this restriction on the behavior or $f(t)$.

Suppose a function is to be represented over an interval $-\frac{1}{2}T$ to $\frac{1}{2}T$ and is assumed periodic outside this range. We may try to represent it in a set of the periodic trigonometric functions, $\sin n\omega t$ and $\cos n\omega t$ with $\omega = 2\pi/T$. Thus, we can write

$$f(t) \simeq a_0 + \sum_{n=1}^{\infty} [a_n \cos(n\omega t) + b_n \sin(n\omega t)] \qquad \text{(B.11)}$$

The expansion coefficients will be determined by using the orthogonality properties of the trigonometric functions over the range T, i.e., multiply by one of the expansion functions and integrate over the range; all other functions on the right-hand side when integrated are *zero*.

Table B.1 Short table of Laplace and Fourier transforms

$f(t)$; $\lambda\equiv 1/\tau$	$F(s)$	$F(j\omega)$; $j^2=-1$
$\delta(s)$	1	1
$h(t)$ step function	$\frac{1}{s}$	$\frac{1}{j\omega}=-\frac{j}{\omega}$
$e^{-\lambda t}$ or $e^{-t/\tau}$	$\frac{1}{\lambda+s}$	$\frac{\tau}{1+j\omega\tau}$
$te^{-\lambda t}$	$\frac{1}{(\lambda+s)^2}$	$\left(\frac{\tau}{1+j\omega\tau}\right)^2$
$\sin at$	$\frac{a}{a^2+s^2}$	$\frac{a}{a^2-\omega^2}$
$\cos at$	$\frac{s}{a^2+s^2}$	$\frac{j\omega}{a^2+\omega^2}$
$e^{-\lambda t}f(t)$ $f(t-\tau)$	$f(s+\lambda)$ $e^{s\tau}F(s)$	$F(j\omega+\lambda)$ $e^{-j\omega\tau}F(j\omega)$
$\lim_{t\to 0} f(t)$ $\lim_{t\to\infty} f(t)$	$\lim_{s\to\infty} sF(s)$ $\lim_{s\to 0} sF(s)$	For well-behaved $sF(s)$

Thus,

$$a_0=\frac{1}{T}\int_{-\frac{1}{2}T}^{+\frac{1}{2}T} f(t)dt \qquad \text{Mean value} \tag{B.12}$$

and

$$a_n=\frac{2}{T}\int_{-\frac{1}{2}T}^{+\frac{1}{2}T} \cos n\omega t f(t)dt \qquad \text{Symmetric} \tag{B.13}$$

Last but not least

$$b_n=\frac{2}{T}\int_{-\frac{1}{2}T}^{+\frac{1}{2}T} \sin n\omega t f(t)dt \qquad \text{Anti-Symmetric} \tag{B.14}$$

Having these coefficients available to us, the function is represented in the "best" way. If the initial function is continuous, this representation is indeed exactly an equality. If discontinuous, it is best in the sense of minimizing the integral of the square error over the range. Of course it may call for the infinite terms as $n\to\infty$ to achieve these properties.

A more compact representation comes from using the imaginary exponential forms of the trigonometric functions, $e^{in\omega t}=\cos n\omega t+i\sin n\omega t$. Noting the symmetry involved, we write

$$f(t) \simeq \sum_{n=1}^{\infty} F(n\omega)e^{i\omega t} \tag{B.15}$$

where the complex expansion coefficients $F(n\omega)$ are given by the following mathematical relationship as

$$F(n\omega) = \frac{1}{T}\int_{-\frac{1}{2}T^{+\frac{1}{2}Tf(t)}} e^{-in\omega t}\,dt \tag{B.16}$$

To pass to a continuous representation, the Fourier transform, over an infinite period $T = (2\pi/\omega) \rightarrow \infty$, we let $n\omega$ be the continuous variable ω to obtain

$$F(\omega) = \int_{-\infty}^{+\infty} e^{-i\omega t} f(t)dt \quad \text{and} \quad f(t) = \frac{2}{2\pi}\int_{-\infty}^{+\infty} e^{i\omega t}F(\omega)d\omega \tag{B.17}$$

Equation B.17 shows a formal *inversion* for the Fourier transfer. There is an analogous integral inversion, which is known as Bromwich integral for the Laplace transform though we will not use it for now. Some folks will change the normalization of Eq. B.17 so that the term $\sqrt{2\pi}$ appears symmetrically in both forms. Note that the Fourier transform of a continuous spectrum would have Dirac delta distribution as we described before, added to represent discrete frequency components.

B.4 Transfer Functions

Keep in mind that initial conditions can be written with the source terms of given equation interest to us via the Dirac delta distribution or original problem of Eq. B.1 in the Laplace transform space can be represented as

$$\overline{\mathbf{X}}(s) = G(s)\overline{\mathbf{S}}(s) \tag{B.18}$$

The circumstances are depicted in Fig. B.1 graphically. In this figure, as it is shown, the output of one of the systems may well supply the input for the next element of the system and so on.

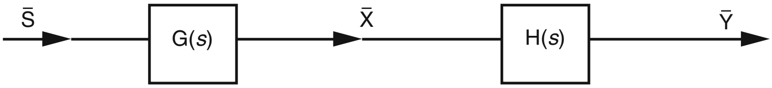

Fig. B.1 Block transfer functions

Given a linear system with constant coefficients, we have an important simplification when we use Laplace or, for that matter, Fourier transforms in such chains of systems. The transform of the overall system is simply the product of the transforms of the individual elements and in particular can be set as the following form:

$$\overline{\mathbf{Y}}(s) = G(s)H(s)\overline{\mathbf{S}}(s) \tag{B.19}$$

This result is also known as convolution or folding theorem, and it is developed as follows for a single variable system. If we have compound systems, where the response of one element becomes the input of the next, how may these be expressed in terms of $G(s)$ or $G(i\omega)$ can be discussed in the following matter.

First of all, we consider the time-dependent solution to an impulse source $g(t)$ called Green's function, and then due to linearity, the response to any source can be obtained by adding integration to all the elementary solutions in the form

$$f(t) = \int_0^t g(t-\tau)s(\tau)d\tau \quad (t \geq 0) \tag{B.20}$$

where the integral is taken up to t, the latest time that a source can affect the responses. If we are in quest of taking the Laplace transform, it is convenient to extend this upper limit to ∞ which we may do artificially by introducing a step function $h(t)$, which is zero before $t = 0$ and unity for $t > 0$. Thus, we can write

$$\begin{aligned} L\{f(t)\} &= \int_0^\infty e^{-st}\left[\int_0^\infty h(t-\tau)g(t-\tau)s(\tau)\right]dt \\ &= \int_0^\infty s(\tau)e^{-st}\left[\int_\tau^\infty e^{-s(t-\tau)}g(t-\tau)dt\right]d\tau G(s)\int_0^\infty e^{-s\tau}S(\tau)d\tau = G(s)S(s) \end{aligned} \tag{B.21}$$

where a change in the order of integration, valid for well-behaved functions g and s, enables the Laplace transform of the convolution integral to be expressed as the product of Laplace transforms. This is in agreement with the results we presented in Eq. B.4, but more generally this is significant as showing that where we have a sequence of elements, the overall transfer function can be obtained simply as the product of the elements in series. However, the transform equation mathematical manipulation when there is an impulse Dirac delta distribution source leads to expressions of the form $F(s) = G(s)$, where $G(s)$ may be called the system transfer function. The more general case will involve arbitrary initial conditions and driving functions, i.e., sources.

In the above situation, the more general case of $G(s)$ is the system response to an impulse source, and we can see that $G(i\omega)$ is the system response to a sinusoidal excitation of unit amplitude at frequency ω, an observation that cause to determine $G(i\omega)$ via experimental process. By letting the value of $s \to i\omega$, we loosely allow the transform $G(s)$ to be interchangeable with the transform function $G(i\omega)$. In particular, we deal with the "linearization" of the model involved, and we also deal with small departures of the output f as a result of small departures of the input s around the steady state. We can also write the transfer function as $G(s) = \delta F(s)/\delta S(s)$. When more than one input variable is presented, a partial differential or thermodynamic notation may be used such as

$$G_1(s) = \left(\frac{\partial f}{\partial s_1}\right)_{s_2, s_3, \cdots} \tag{B.22}$$

Show the remaining input variables s_2,$s_3^{\cdots}$ kept constant in above equation.

B.4 Feedback and Control

Many systems have an *inherent feedback* term in their response. Therefore, the equation $\dot{f} = \lambda f + s$ leads to a Laplace transform of simple lag form as

$$\frac{F}{S} = G(s) = \frac{1}{s - \lambda} \tag{B.23}$$

where we are ignoring the initial conditions. But this itself could be graphed or split up as it was demonstrated in Fig. B.2.

Note that the elementary arguments that λ must be negative for stability which an example of such situation we can mention the dying away of radioactive decay. We may also like to follow a positive feedback convention of the type shown in the figure to represent inherent feedback.

More often the output of a system in response to different loads or excitation function is not satisfactory, and the concepts of automatic control are bound up with the idea of modifying the system output. This takes place by providing a feedback term, a correction excitation signal that depends on the output or rather on the departure of the output from some desired level.

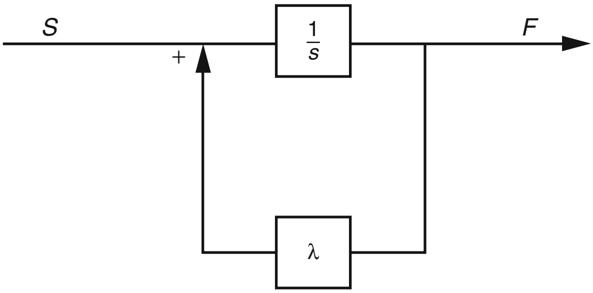

Fig. B.2 Simple inherent feedback

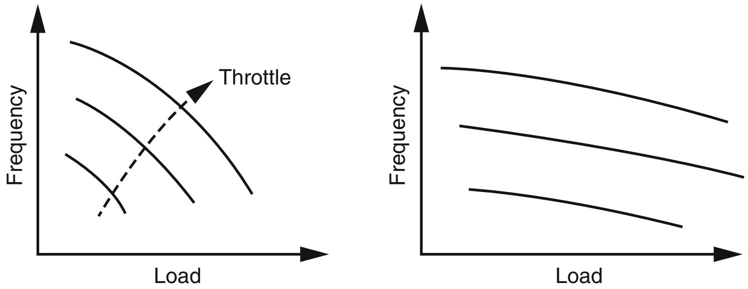

Fig. B.3 Turbine generator droop characteristics and control [1]

Thus, we distinguish between open-loop control and closed-loop control. A good example of open-loop control that we can observe in our day-to-day life is a toaster whose time can be set in advance but which does not respond automatically to the degree of browning the toast [1].

As part of closed loop, we could use the example of a household heating system which is normally supplied with a feedback controller device such as thermostat so that the actual temperature of the rooms or their departure from some desired temperature varies the fuel supply of the furnace.

Other examples of such matter can be seen in turbine industry where the response of a turbine generator to different electrical loads is shown as per Fig. B.3. In this type of example, we have a noticeable droop in the speed at fixed throttle and higher loads without control action and hence an unacceptable drop in electrical frequency as the load varies.

If there is a control for feedback to vary the throttle opening with change of speed, then through a simple proportional controller, we may anticipate to flatten out this undesirable droop. To flatten it still further, using just proportional control would demand for bigger control action or gain for a given speed discrepancy. In that case, we are in the right track to anticipate that there will be a limit to the efficiency of such a simple system. This system can be brought about by the onset of dynamic instability in which a small fluctuation in the response of the system is magnified by means of resonance via too high a gain, to the point of producing even larger swings in the response. For further discussion, refer to Lewins' book [1].

Knowing that the combination of successive forward transfer functions requires the *addition* of phases but the *product* of amplitudes, it becomes useful to plot the amplitudes on a logarithmic scale so that they may be added graphically for this purpose. It is convenient, therefore, to plot the amplitude in decibels as $A(\omega)\ \text{in}\,\text{db} = 20\log_{10}|G(i\omega)|$.

B.5 Graphical Representation (Bode and Nyquist Diagram)

By now we have seen how to build up system transfer function from the basic and elementary transfer function, either by manipulating $G(s)H(s)$, for open response or as in Eq. B.24 for a positive feedback:

$$F(i\omega)S = \frac{G(s)}{1 - KH(s)G(s)}S(i\omega) \tag{B.24}$$

where K is a scalar or gain coefficient and $F(i\omega)$ is defining an equivalent closed-loop transfer function.

Transfer functions or Fourier transform may be represented graphically and also conveniently combined graphically as shown in Fig. B.4 to present two system functions. There exist two representations that are known as Bode diagram (i.e., Fig. B.4) and Nyquist diagram (i.e., Fig. B.5).

In the Bode diagram, the transfer function $G(i\omega)$ is represented in polar format through its amplitude or gain A and phase θ as a complex number $Ae^{i\theta}$. Normally gain and phase are plotted against the frequency either in radians/s or Hertz (cycle/s) on a logarithmic scale. Generally speaking, the angular frequency presented by ω is in radians/s, of course, 2π greater than the cycles in Hertz (Hz).

Figure B.4 shows the simple lag plotted as a Bode diagram. It also shows the important approximate construction technique of the "break frequency" method in which asymptotes of G are established for large and small ω.

These asymptotes intercept at the frequency $\omega_c \equiv 1/\tau$ that is again known as break frequency, and Fig. B.4 shows the departure of the exact result from the asymptote around the break frequency in the example we presented.

Bode diagram is a convenient approach for the compounding of successive transfer functions, and we can find out that the approximation of 6 dB corresponds

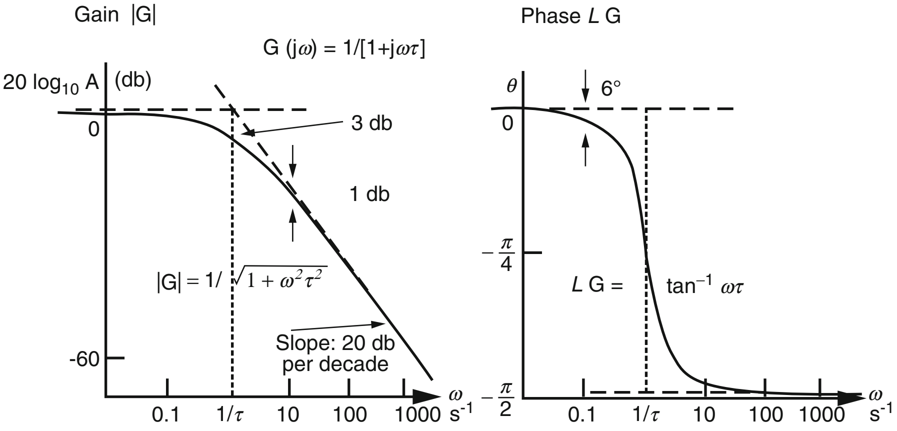

Fig. B.4 The simple lag as Bode diagram with break frequency construction

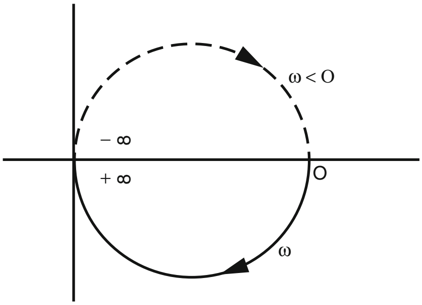

Fig. B.5 Nyquist diagram for simple lag [1]

to a factor of two. On the other hand, the Nyquist diagram is an alternative representation in which $G(i\omega)$ is plotted as an A grand diagram in radial coordinates. Sometimes a polar plot of log A is being more useful, and the same simple lag is given as Nyquist diagram in Fig. B.5. Note that for negative ω, the diagram is completed as a mirror image. For further information, please refer to the book by Lewins [1].

B.6 Root Locus Construction Rules

1. The poles of the transfer function are the poles of the open-loop transfer function, $G(s)H(s)$, when the gain constant K goes to 0.
2. The poles of the transfer function are the zeros of the open-loop transfer function, $G(s)*H(s)$, when the gain constant K goes to infinity. For realizable physical systems, there will always be fewer zeros for the open-loop transfer function than there will be poles. The remaining zeros (hypothetical) are located at infinity.
3. For a positive gain constant, $K > 0$, the real axis to the left of an odd number of poles and zeros contains the locus for the poles of the closed-loop transfer function. For a negative gain constant, $K < 0$, the real axis to the left of an even number of poles and zeros contains the locus of the poles for the closed-loop transfer function.
4. As K grows large, the poles moving toward the zeros at infinity do so along asymptotes given by the following angles with the real axis.

   For $K > 0$, the angles are given by

$$\theta = \frac{(2n+1)\pi}{N_\mathrm{p} - N_\mathrm{z}} \quad N_\mathrm{p} = \text{Number of Poles,} \quad N_\mathrm{z} = \text{Number of zeros} \tag{B.25}$$

   For $K < 0$, the angles are given by

$$\theta = \frac{2n\pi}{N_{\mathrm{p}} - N_{\mathrm{z}}} \tag{B.26}$$

5. The point at which the asymptotes intercept the real axis is given by the following formula:

$$B = \frac{\text{Sum of Pole Real Parts} \; - \text{Sum of Zero Real Parts}}{N_{\mathrm{p}} - N_{\mathrm{z}}} \tag{B.27}$$

6. The actual breakaway points for the locus can be calculated by realizing that the breakaway point must correspond to a double root.

References

1. Lewins, Jeffery, *Nuclear Reactor Kinetics and Control*, 1st edn (Pergamon, New York, 2013).

Index

B. Zohuri, *Neutronic Analysis For Nuclear Reactor Systems*,
DOI 10.1007/978-3-319-42964-9